AN ABSTRACT OF A THESIS

DYNAMICS AND CONTROL OF A FIVE PHASE INDUCTION MACHINE

Sosthenes Francis Karugaba

Master of Science in Electrical Engineering

General and special case expressions for determining the real and reactive powers in a multiphase system have been derived. This has been simplified by the use of the stationary complex reference frame of transformation which transforms a set of m real variables into a set of (m-1) complex vectors (when m is odd). The m^{th} vector is real and is referred to as the zero sequence. For a system with an even number of phases (m is even), the number of complex vectors is (m-2) and there are two zero sequence quantities. The complex vectors are conjugates of each other such that during the analysis only half of them (which are the positive sequence components) are sufficient to give the desired result. In this work, the expressions for determining the real and reactive power of the three, five and seven phase machines have been obtained.

A five phase induction machine has been modeled. The winding function method is used to calculate the self and mutual inductances in the stator windings and the rotor circuits, with constant air gap in which the space harmonics of the stator windings and rotor circuits are accounted for. A n x n complex variable reference frame transformation is carried out to simplify computation of the currents, voltages and torque equations. Computer simulation results of the no-load starting transient have been shown with the response of the machine for a change in the load torque. This approach has made it possible to calculate the rotor bar currents.

A five-phase carrier based PWM (Pulse Width Modulation) induction motor drive has been analyzed. The induction machine windings have been connected in alternate ways to increase the torque produced by the machine. A third harmonic voltage component has been injected to determine the ability of a five phase machine to contribute a third harmonic torque component to the fundamental torque component. It has been found out that with sinusoidally distributed stator winding, the effect of the third harmonic torque component is negligible.

The dynamics of a five-phase induction motor under open phase faults has been discussed. Using stationary reference frame and harmonic balance technique, circuit based models have been used to analyze the open phase, two adjacent phases and two non-adjacent phase faults. Simulation and steady state results have shown that the five phase machine can start and develop torque with one or two of its phases missing. Mall signal analysis has been carried out to determine the stability of the machine at different open phase fault conditions, revealing that despite the missing phases, the machine is stable at relatively high operating speed.

A voltage source inverter has been reconfigured for the purpose of obtaining high speeds in the regions of field weakening operation. The motive being to investigate the possibilities of operating a multiphase induction motor drive in field weakening region under optimum torque production. With a multiphase systems, different winding connections can be obtained apart from the conventional star and delta configurations. Such connections would give higher voltages across the machine's phase winding and thus allowing the for relatively higher torque production in the regions of field weakening operation.

DYNAMICS AND CONTROL OF A FIVE PHASE INDUCTION MACHINE

A Thesis

Presented to

the Faculty of the Graduate School

Tennessee Technological University

by

Sosthenes Francis Karugaba

In Partial Fulfillment

of the Requirements for the Degree

MASTER OF SCIENCE

Electrical Engineering

December 2008

CERTIFICATE OF APPROVAL OF THESIS

DYNAMICS AND CONTROL OF A FIVE PHASE INDUCTION MACHINE

by

Sosthenes Francis Karugaba

Graduate Advisory Committee

Dr. Joseph O. Ojo, Chairperson   Date

Dr. Arun Sekar   Date

Dr. David Gao   Date

Approved for the Faculty

Francis Otuonye

Associate Vice President for

Research and Graduate Studies

Date

DEDICATION

This work is dedicated to my late father Francis Mulokozi, my mother Elizabeth Kokunura, my wife Nafsa, my children Sharon Kokubera and Collin Mwesiga.

ACKNOWLEDGEMENTS

I appreciate the valuable advisement and assistance given to me by the chairperson of my advisory committee and who is also my major professor, Dr. Joseph O. Ojo. His professional guidance and support are left to be admired. I also extend my thanks to Dr. Arun Sekar and Dr. David Gao for their academic enrichment they passed on me during the period of my course of study.

I acknowledge the financial support of the Office of Naval Research (ONR) through the Center for Energy Systems Research (CESR). I appreciate the Director of CESR, Dr. Sastry Munukutla for the support. I thank Sandy Garrison, Etter M. Staggs and Linda Lee for their supporting work. My gratitude goes to the Chairperson of Electrical and Computer Engineering (ECE), Dr. Stephen A. Park, Faculty and Staff, Claudette Venters, Swati Dalvi, Valerie Joshi for their clarifications on several regulations and procedures.

I extend my sincere thanks to the Associate Vice President of Research and Graduate Studies, Dr. Francis Otuonye, the entire staff of graduates School staff, Sheila Kendrick, Becky Stafford and Kathy Reynolds, for their advice and timely response on several occasions.

I appreciate the office of International Students Affairs, Charles Wilkerson and Brenda Gentry for their needful help and support.

I am very grateful to my employer, Dar es Salaam Institute of Technology (DIT), for giving me release to undertake this programme.

I really cherish Ndaga Mwakabuta and Dr. Bakari Mwinyiwiwa for their trust on me, advice, encouragement and tireless efforts they made to me before and in the course of my academic career.

I would like to thank Dr. Zhiqiao Wu, Dr. Juan Munoz, Dr. Emeka S. Obe and Dr. Michael Omoigui for their academic enrichment. I am grateful to Robert (Bob) Peterson, Cornard Murray, David Walker, Andrew Watkins, and Toan Vu for their technical work.

I extend my thanks to Gayathri Murthi, Godwin and Mastidia Mutahangarwa, Praxeda, Filbert, Jovina, Faosta, Liberatus, Melxedeck, Juvenary, Linus, Nicolaus Kaiza, Julius Ernest, Bossi Masamila, Adolph Banyenza, Dina Machuve, Judith Mwakalonge, Veronica Ndaga, Julius Abayateye, Sofia S. Nkya, Frank Mrema, Diego Robalino, Jianfu Fu, Jiaxin Ning, Rohit Satish Kunte, Sharanya Jaganathan, Vadim Zheglov, Ge Wang, Adeola Balogun, Jibril Yusuf, George and Lufaro Chitiyo, Marsha Hobby, Zainab S. Nkya, Audley Bruce Grey, Alex Pama, Anish Joshi, Shounak Abhyankar, Yogesh Barve, all members of MTTA and IJAKUNU for their friendship, moral support and advice.

The love, support, patience and encouragement from my parents and relatives, my wife Nafsa, my children Sharon Kokubera and Collin Mwesiga remain memorable.

TABLE OF CONTENTS

page

LIST OF FIGURES

LIST OF TABLES

page

CHAPTER 1

INTRODUCTION

1.1 Introduction

In general, the induction machines having three-phase windings are normally used, since the standard power supply is three phase. However, when fed by an inverter, there is no need for a fixed number of phases, some other phases being possible and advantageous.

A multiphase machine can operate normally after loss of one or more phases. This improved reliability stems from the fact that only two independently controllable current components are necessary to create a rotating field. In the three-phase machine, this is only possible if the neutral of the motor is connected to the dc link midpoint to allow zero-sequence current component to flow [1.1]. In an m-phase star-connected machine with isolated neutral, there are (m-1) degrees of freedom. It is possible to achieve the rotating magneto- motive force by controlling the remaining phase currents even after losing up to m-3 phases. For example, a five-phase machine can continue to operate if one or even two phases of the supply are lost. When only one phase is lost (open circuited), it does not matter which phase because of the spatial symmetry of the stator windings in the machine, the results are the same regardless of which phase is open.

Much published work has shown that drives with more than three phases have various advantages over conventional three phase drives, such as reduction in amplitude and increase in frequency of pulsating torque, reduction in harmonic currents, increase in current per phase without the need to increase the phase voltage, and reduction in the voltage-level in the dc (direct current) link [2.1, 2.2].

Another important aspect of machines with a higher number of phases is their improved reliability, since they can operate even when one phase is missing [2.1]. An increase in number of phase can result in an increase in torque/ampere relation for the same volume of the machine, such that five-phase machines can develop torque using not only the fundamental, but also using higher harmonics of the air gap field [2.1, 2.3].

The types of multi-phase machines for variable-speed applications are in principle the same as their three-phase counterparts. These include induction and synchronous multiphase machines. Synchronous multiphase machines may be with permanent magnet excitation, with field winding excitation, or of reluctance type.

Three-phase induction and cylindrical synchronous machines are normally designed with distributed stator winding that gives near-sinusoidal magnetomotive force (MMF) distribution and is supplied with sinusoidal currents. The permanent magnet synchronous machine has a trapezoidal flux distribution and rectangular stator current supply. Nevertheless, spatial MMF distribution is never perfectly sinusoidal and some spatial harmonics are inevitably present. For multiphase machines, a near-sinusoidal MMF distribution requires use of more than one slot per pole per phase. As the number of phases increases, it becomes progressively difficult to realize a near-sinusoidal MMF distribution. The minimum number of slots required for this purpose for a three-phase four-pole machine is 24, whereas for the five-phase four-pole machine the minimum number of slots required for production of a near-sinusoidal MMF distribution is 40 [1.2].

Some of the advantages of multiphase machines when compared to their three-phase counterparts are [1.2, 1.3]

- Fundamental stator currents produce a field with a lower space-harmonic content.
- The frequency of the lowest torque ripple component being proportional to $2m$, increases with the number of phases.
- Since only two currents are required for the flux/torque control of an ac machine, regardless of the number of phases, the remaining degrees of freedom can be utilized for other purposes. One such purpose, available only if the machine is with sinusoidal MMF distribution, is the independent control of multi-motor multiphase drive systems with a single power electronic converter supply.
- As a consequence of the improvement in the harmonic content of the MMF, the noise emanated from a machine reduces and the efficiency can be higher than in a three-phase machine.

All multiphase variable-speed drives share a couple of common features.

- For a given machine's output power, utilization of more than three-phases enables splitting of the power across a larger number of inverter legs, thus enabling use of semiconductor switches lower rating.
- Due to a larger number of phases, multiphase machines are characterized with much better fault tolerance than the three-phase machines. Independent flux and torque control requires means for independent control of two currents. This becomes impossible in a three-phase machine if one phase becomes open-circuited, but is not a problem in a multiphase machine as long as no more than $(m-3)$ phases are faulted.

1.2 Control of Variable-speed Multiphase Induction Motor Drives

Methods of speed control of multiphase induction machines are in principle the same as or three-phase induction machines. These methods are namely as constant voltage per hertz $\left(V/f\right)$ control, vector control, and direct torque control (DTC). Constant V/f for the multiphase variable-speed induction motor drive development in conjunction with voltage source inverters operated in the 180^0 conduction mode was presented in [1.4] and [1.5]. In the recent times, the emphasis has shifted to vector control and direct torque control (DTC).

1.2.1 Vector Control of Multiphase Induction Machines

For a symmetrical multiphase induction machine with sinusoidally distributed stator winding, the same vector control schemes for a three-phase induction machine are directly applicable regardless of the number of phases. The only difference is that the co-ordinate transformation has to produce an m-phase set of stator current or stator voltage references, depending on whether current control is stationary or in synchronous rotating reference frame. Indirect rotor flux oriented control (FOC) schemes for multiphase induction machine using these two types of current control.

Assuming the stator winding has a singe neutral point, the scheme of Figure 1.1 utilizes $(m-1)$ stationary current controllers. Either phase currents or phase current components in the stationary reference frame can be controlled an the standard ramp comparison current control method offers the same quality of performance as with three-phase induction motor drives.

The scheme of Figure 1.2 has only two current controllers. However, since an m-phase machine essentially has $(m-1)$ independent currents, utilization of this scheme will suffice only if there are not any winding and /or supply asymmetries within the m-phase stator winding and / or supply. This scheme also requires an adequate method of inverter PWM control to avoid creation of an unwanted low-order stator voltage harmonics that represent voltage $x-y$ components in Equation (2.3) and therefore lead to the flow of large stator $x-y$ current components, as discussed in Chapter 2. In the case of a six-phase induction machine with two isolated neutral points, the scheme of Figure 3 would require four current controllers which would apply to both the control based on the double $q-d$ winding representation and to the control based on the model which in addition to the $q-d$ stator current controllers, one needs to add a pair of $x-y$ current controllers [1.6 - 1.8].

Most literature on control related analysis has considered five-phase or asymmetrical six-phase induction machines. Indirect rotor filed oriented control can be applied to other phase numbers as presented in [1.9 - 1.14] where a 15-phase induction machine is considered. In [1.11 - 1.14], a 15-phase induction machine for electric ship propulsion, configured as a three five-phase stator windings (vector and DTC have been considered in [1.11 - 1.13], while [1.12 - 1.14] used V/f control. Control of a 15-phase induction motor drive is also discussed in [1.7]. Whereas an analysis of possible supply options for a 36.5 MW, 16 Hz, nine-phase variable speed drive aimed at electric ship propulsion is reported in [1.6].

It is concluded in [1.6] that if a good quality of current control is achieved and an appropriate method of PWM for multiphase voltage source inverter (VSI) is applied, the performance of a vector controlled multiphase induction machine will be very much the same as its three-phase counterpart.

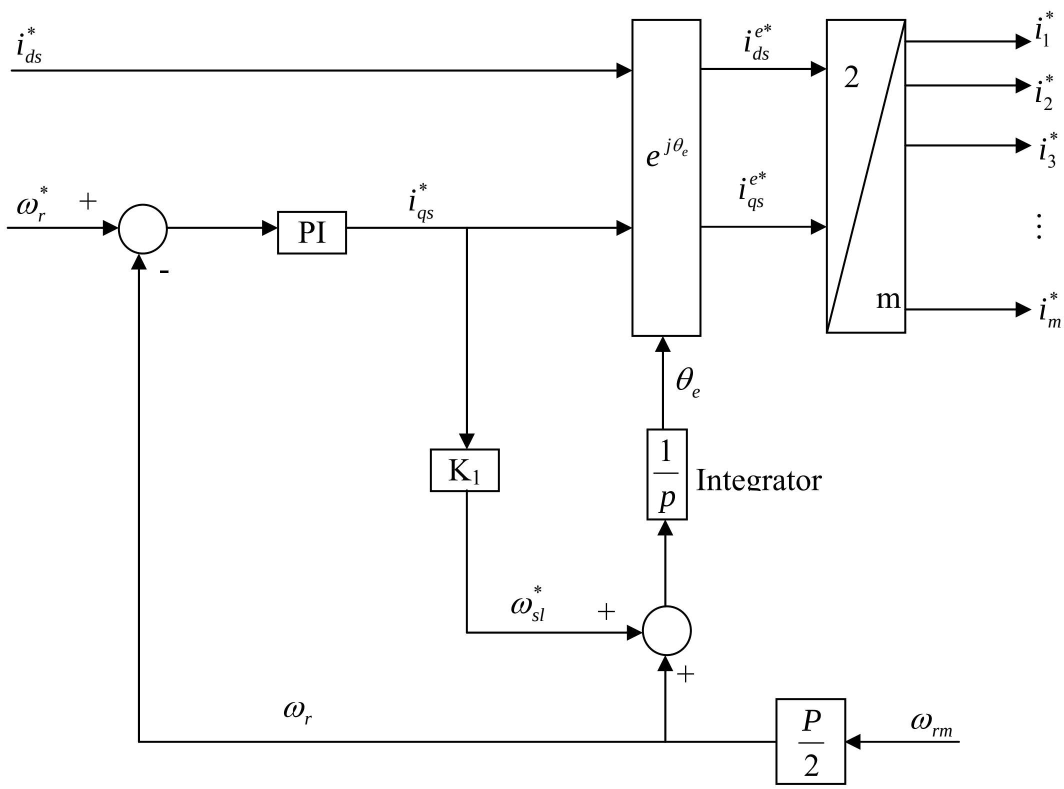

Figure 1.1 Indirect rotor flux oriented controller for m-phase induction motor with sinusoidal distribution of the magneto-motive force and phase current control.

The parameter and symbols shown in Figure 1.1 are defined as follows

$$K_1 = \frac{1}{T_r^* i_{ds}^*} \tag{1.1}$$

$T_r = \frac{L_r}{r_r}$ is the rotor time constant

ω_r is the electrical rotor speed

ω_{rm} is the mechanical rotor speed

ω_{sl}^* is the electrical slip speed

ω_r^* is the reference rotor speed

i_{qs}^* is the reference q-axis stator current

i_{ds}^* is the reference d-axis stator current

PI stands for proportional integral controller

θ_e is the instantaneous rotor flux space vector position

$i_1^*, i_2^*, i_3^*, \cdots, i_m^*$ are the reference stator phase currents

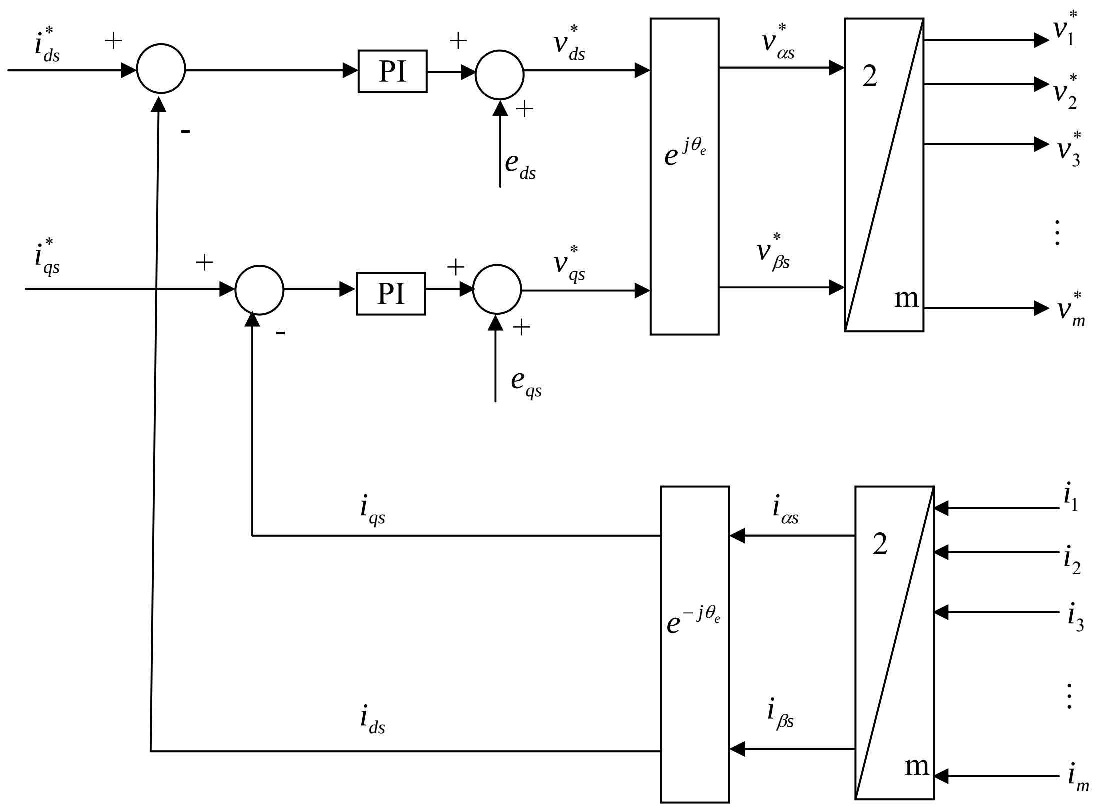

Figure 1.2 Indirect rotor field oriented control of a multiphase induction machine.

The current control of Figure 1.2 is in the rotating reference frame. The stator q and d axis reference currents and rotor flux position are obtained as in Figure 1.1. Some of the defining equations for the system of Figure 1.2 are

$$e_{qs} = \omega_e L_\sigma i_{ds} + \omega_r \frac{L_m}{L_r^{'}} \lambda_{dr}^{'} \tag{1.2}$$

$$e_{ds} = -\omega_e L_\sigma i_{qs} - \frac{r_r^{'} L_m}{L_r^{'2}} \lambda_{dr}^{'} \tag{1.3}$$

where

$$\omega_e = \frac{d\theta_e}{dt} \tag{1.4}$$

$$L_{\sigma} = L_s - \frac{L_m^2}{L_r^{'}} \tag{1.5}$$

where

L_s is the stator self inductance

$L_r^{'}$ is the rotor self inductance referred to stator side

L_m is the magnetizing inductance

$v_1^*, v_2^*, v_3^*, \cdots, v_m^*$ are the reference stator phase voltages

$i_1, i_2, i_3, \cdots, i_m$ are the stator phase currents

v_{α}^* and v_{β}^* are the α and β axis reference stationary voltages, respectively

i_{α} and i_{β} are the α and β axis reference stationary currents, respectively

i_{qs} and i_{ds} are the q and d axis currents, respectively, in the synchronous reference frame

v_{qs}^* and v_{ds}^* are the q and d axis reference voltages, respectively, in the synchronous reference frame

i_{qs}^* and i_{ds}^* are the q and d axis reference currents, respectively, in the synchronous reference frame.

$\lambda_{dr}^{'}$ is the rotor d-axis flux linkage

1.2.2 Direct Torque Control (DTC)

For a three-phase induction machine, two basic approaches of direct torque control (DTC) can be identified [1.6]. The first approach utilizes hysteresis stator flux and torque controllers in conjunction with an optimum stator voltage vector section table leading to a variable switching frequency. In the second approach, an appropriate method of inverter PWM control is applied while keeping the switching frequency constant. These two approaches can be applied to multiphase induction machines achieving the same dynamic performance as for the three-phase induction machines. The important differences are predominantly caused by the existence of additional degrees of freedom in multiphase machines due to the x and y components.

If the multiphase machine is with sinusoidal magneto-motive force distribution, DTC scheme needs to apply sinusoidal voltages to the stator windings of the machine. The unwanted low-order frequency components that would excite the x and y circuits are to be avoided. This can be avoided if the constant switching frequency is used. Since a multiphase induction machine is supplied from a multiphase voltage source inverter. Constant switching frequency DTC of a multiphase induction machine can be realized by using appropriate PWM method that ensures sinusoidal voltage output from the inverter.

In this thesis, indirect rotor flux oriented control (FOC) for a five phase induction machine is presented. The rotor speed is controlled by using a ramp of the reference speed. Using rotor flux oriented control, the five-phase inverter is–reconfigured for improved extended speed drives is presented. It investigates the possibilities of operating a multi-phase induction motor drive in field weakening region under optimum torque production.

1.3 Field Weakening Operation of Induction Motors

Maximum torque production in the field-weakening region is a desired property of vector-controlled induction motors in applications such as traction and spindle drives. Field weakening operation consists of two steps: the choice of the proper flux reference to get maximum toque and producing the necessary currents to meet the flux and torque references. The classical field weakening technique, $\frac{1}{\omega_r}$, in rotor field oriented drives ahs been shown to provide flux reference that are too high, reducing the amount of current available to produce the torque, and therefore, the torque capability of the drive [7.3, 1.15]. In [7.3], the optimal current references for maximum torque were obtained by taking into account both current and voltage limits for the inverter and motor. In [1.15] it was shown that almost optimal flux current references could be obtained by applying $\frac{1}{\omega_r}$ to the stator flux. In these references, only steady state operation has been considered.

Assuming that a proper flux reference is available, dynamic field weakening relies on the dynamic response of both the flux and current regulators. At high speeds, the available voltage will mostly be used to counteract the back emf. Small transient errors in flux regulation could result in insufficient voltage margin to create the desired torque-producing current, dramatically affecting the drive performance.

1.4 Fault Analysis in Multiphase Machines

A good number of research work has been presented on faults in electric machines [5.3]. Various categories of faults have been discussed for multi-phase machines inter-turn short circuits [5.4, 5.5] based on winding function approach. In [2.2] a dq model based on transformation theory for five-phase induction machines has been presented and the analysis of the machine under asymmetrical connections is discussed.

A control strategy of multiphase machines under asymmetric fault conditions due to open phase is presented in [4.7]. The authors used a five-phase synchronous motor with one open phase as a practical example.

So far there is no work that has developed a circuit based model which can be used to predict not only the steady-state and stability of the open-phase five phase induction machine but also the dynamics of the pulsating torque. Although it is known that faulted multi-phase machines can produce significant average torques, not much work has been done to quantify this.

In this work, to determine the steady-state and dynamic stability performance, first a five-phase induction machine with one phase (phase '*a*') open is modeled in stationary reference frame. Then the same analysis is carried out for two phase open, '*a*' and '*b*' (for adjacent phases) and '*a*' and '*c*' (for non-adjacent phases). For the first time, using harmonic balance technique it has been possible to develop a circuit based model that has been used to perform the steady-state and dynamic analysis of a faulted machine. The steady-state speed harmonics and torque pulsations have been calculated and the results compare fairly well with the simulation results based on the full-order dynamic model of the faulted machine.

Furthermore, the small-signal stability study has been made through the small signal analysis whereby the dynamic model obtained from the harmonic balance technique has been used. At low speeds, the machine exhibits instability due to the rotor flux linkages. This instability is eliminated when the machine speeds up close to synchronous speed. This indicates that the machine can still be able to start under one or two open stator phase faults and provide significant torque to meet most load requirements.

1.5 Connections of Multiphase Machines

One of the advantages of a multiphase machine apart from its tolerance is that it can be used in high speed applications. In general, the maximum speed of the machine is limited by the inverter voltage and current limits. High speed operation can be made possible by either employing an inverter with higher voltage or by reducing the counter emf value of the machine using field weakening techniques. Other techniques employed to achieve significant wider speed ranges include reducing the per phase equivalent impedance of the machine, pole amplitude and phase modulation by changing the number of poles. These techniques require additional semiconductor devices in the converter as well as special machine designs. An m-phase machine (where $m > 3$) can be connected in $\frac{m+1}{2}$ different ways. With these available alternatives, the speed range of an m-phase machine can be significantly increased. As the connection pattern changes from one to the other, the impedance of the machine seen by the inverter varies making it possible to achieve higher speeds before the converter rating voltage is reached. In such connection transitions different torque-speed characteristics are realized. In this work, the approach in reconfiguring the inverter in order to achieve wider speed range of operation for the multiphase induction machines is presented.

1.6 Multiphase PWM Voltage Source Inverter

DC/AC voltage source inverters (VSI) are extensively used in motor drives to generate controllable frequency and ac voltage magnitudes using various pulse width modulation (PWM) strategies. The carrier-based PWM is very popular due to its simplicity of implementation, known harmonic waveform characteristics, and low harmonic distortion. Figure 1.3 shows a schematic diagram of five-phase voltage source converter.

The turn on and turn off sequences of a switching device are represented by an existence function which has a value of unity when it is turned on and becomes zero when it is turned off [4.1]. The existence function of a two-level converter comprising of two switching devices is represented by S_{ij}, $i = a, b, c, d, e$ and $j = p, n$ where i represents the load phase to which the device is connected, and j signifies top (p) and bottom (n) device of the converter leg. Hence, S_{ap}, S_{an} which take values of zero or unity are, respectively, the existence functions of the top device and the bottom device of the inverter leg which is connected to phase 'a' of the load.

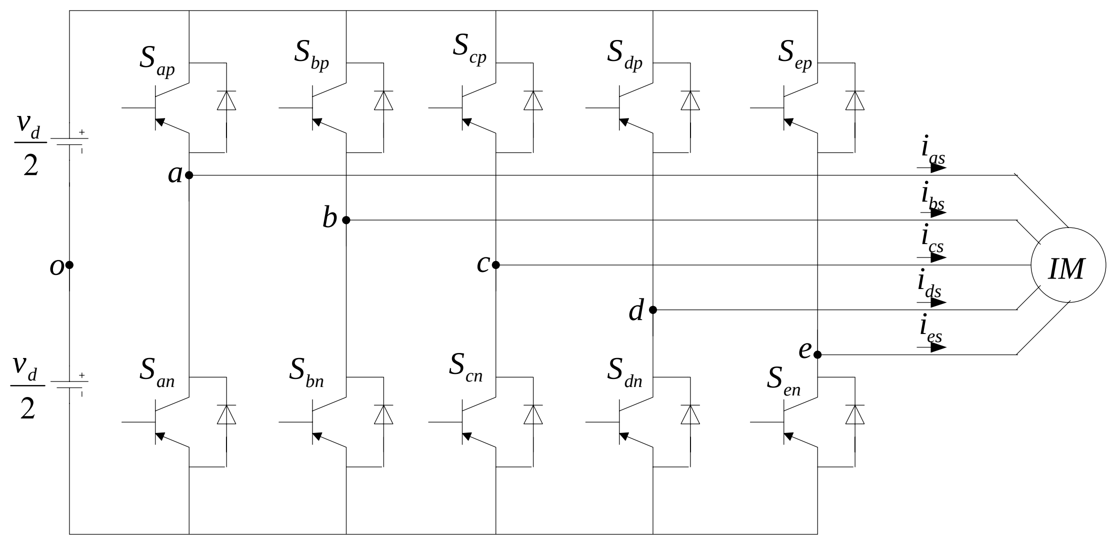

Figure 1.3 Five-phase two-level voltage source inverter supplying a five-phase induction machine

Energy conversion in converters is achieved by the Pulse Width Modulation (PWM) technique [3.5]. The turn on and turn off time of each switching device is calculated from a control scheme and when these PWM pluses are applied, the fundamental voltages embedded in the output PWM voltages are the same as the desired ones. The PWM technique can be generally divided into Carrier-based PWM (CPWM) and Space Vector PWM (SVPWM). In the CPWM method, the modulation signals which contain certain magnitude, frequency and angle information are compared with a high frequency carrier signal to generate the switching pulses. The pulses are “one” when modulation signals are larger than the carrier signal and “zero” when modulation signal are smaller than carrier signal. However, the turn on and turn off times of each device are calculated and then sent to the PWM generator directly in the SVPWM method.

1.7 Scope of the Thesis

The main objective of this research is to explore the advantages of multiphase induction machines. The analysis presented in this Thesis considers a five phase induction machine as an example. An existing 2-pole, three-phase stator winding of a three-phase squirrel cage induction machine was rewound to be a 4-pole, five-phase stator winding of a five-phase squirrel cage induction machine. In some instances, a seven-phase induction machine has been included in order to emphasize the generality.

Chapter 2 presents the theory of multiphase systems in which the reference frame of transformation is presented. General expressions for calculating the real and reactive powers for the three, five and seven phase systems are derived. In addition, vector space modulation for the five phase voltage source inverters is discussed.

The full order model of a five-phase induction machine is discussed in Chapter 3. Computer simulation results are presented. Using two three-phase inverters, open circuit and blocked rotor tests are carried out to determine the machine parameters. The approach of using winding function to determine the self and mutual inductances can be used to analyze the machine performance when there inter-turn and intra-turn faults. Thus, the model would give the actual values of the inductances that are taking part in the machine operation.

Chapter 4 discusses the carrier based PWM scheme for the five-phase induction motor drive. Efforts are made to simulate the machine with different stator winding connections and analyze the capability of producing the third harmonic component torque.

A thorough analysis of the machine dynamics for open phase faults on the stator windings is discussed in Chapter 5. The harmonic balance technique models give way to analyzing the machine performance under open phase faults. It makes it possible to determine the harmonic components of speed and torque.

Rotor flux vector control of five-phase induction machine is discussed in Chapter 6. This precedes the discussion on speed range operation which is presented in Chapter 7.

Chapter 8 includes the conclusion and suggestions for future work on five-phase induction machines and multi-phase systems.

CHAPTER 2

THEORY OF MULTIPHASE SYSTEMS

2.1 Introduction

Multi-phase machines have attracted increased interest in recent years. This is due several advantages that they offer as compared to the conventional three-phase ones. In the presence of a power electronic converter which is needed for variables speed ac drive, the number of phases is essentially not restricted and multiphase machines are nowadays considered as potentially viable solutions for high power and high current applications. Apart from their applications in traction and electric ship propulsion, some investigation is going on for a more-electric aircraft concept, because of their fault tolerance which enables disturbance-free mode of operation in case of loss of one or more phases [2.1].

With such a large number of phases, the analysis of the multiphase machines becomes complicated. In order to include space harmonics, the proper reference frame is required. This will eliminate the time variance of mutual inductance as well as simplifying the model for performance calculation. In this Chapter, a generalized reference frame is presented. Using the complex reference frame transformation, the expressions for the real and reactive powers of the three, five and seven phase systems are derived. It has been shown that depending on the reference frame used, the power is not always invariant. Therefore, it is very important to consider the effect of the multiplying factor if power computation will be part of the analysis.

2.1.1 Transformations

For the purpose of analysis of energy conversion characteristics, an n-phase-stator, m-phase rotor balanced machine can be reduced to an equivalent two-phase machine.

The analysis of the n-m winding machine involves two essential steps [2.2].

(a) establishing the equations of motion in terms of a set of variables, and

(b) eliminating as many of the variables as possible without losing any essential information.

The stationary reference frame `transformations, which prove useful in reducing the variables in the n-m phase machine, are generalized versions of the complex symmetrical component transformation and the real transformation.

A linear complex transformation of variables is defined by

$$\bar{x} = T_x y \tag{2.1}$$

where

$$y = \begin{bmatrix} y_1 & y_2 & \cdots & y_{n-1} & y_n \end{bmatrix}^T \tag{2.2}$$

$$\bar{x} = \begin{bmatrix} \bar{x}_o & \bar{x}_1 & \bar{x}_2 & \cdots & \bar{x}_{m-2} & \bar{x}_{m-1} \end{bmatrix}^T \tag{2.3}$$

Equation (2.2) is a vector of real variables, whereas Equation (2.3) is the complex vector. T_x is the symmetrical component transformation matrix given by [2.2]

$$T_m = \sqrt{\frac{2}{m}}\begin{bmatrix} 1 & 1 & 1 & 1 & \cdots & 1 & 1 & 1 \\ 1 & a^1 & a^2 & a^3 & \cdots & a^{(m-3)} & a^{(m-2)} & a^{(m-1)} \\ 1 & a^2 & a^4 & a^6 & \cdots & a^{2(m-3)} & a^{2(m-2)} & a^{2(m-1)} \\ 1 & a^3 & a^6 & a^9 & \cdots & a^{3(m-3)} & a^{3(m-2)} & a^{3(m-1)} \\ \vdots & \vdots & \vdots & \vdots & \ddots & \vdots & \vdots & \vdots \\ 1 & a^{(m-3)} & a^{2(m-3)} & a^{3(m-3)} & \cdots & a^{(m-3)(m-3)} & a^{(m-3)(m-2)} & a^{(m-3)(m-1)} \\ 1 & a^{(m-2)} & a^{2(m-2)} & a^{3(m-2)} & \cdots & a^{(m-2)(m-3)} & a^{(m-2)(m-2)} & a^{(m-2)(m-1)} \\ 1 & a^{(m-1)} & a^{2(m-1)} & a^{3(m-1)} & \cdots & a^{(m-1)(m-3)} & a^{(m-1)(m-2)} & a^{(m-1)(m-1)} \end{bmatrix} \quad (2.4a)$$

The inverse of the transformation matrix is [2.2]

$$T_m^{-1} = \sqrt{\frac{2}{m}}\begin{bmatrix} 1 & 1 & 1 & 1 & \cdots & 1 & 1 & 1 \\ 1 & a^{-1} & a^{-2} & a^{-3} & \cdots & a^{-(m-3)} & a^{-(m-2)} & a^{-(m-1)} \\ 1 & a^{-2} & a^{-4} & a^{-6} & \cdots & a^{-2(m-3)} & a^{-2(m-2)} & a^{-2(m-1)} \\ 1 & a^{-3} & a^{-6} & a^{-9} & \cdots & a^{-3(m-3)} & a^{-3(m-2)} & a^{-3(m-1)} \\ \vdots & \vdots & \vdots & \vdots & \ddots & \vdots & \vdots & \vdots \\ 1 & a^{-(m-3)} & a^{-2(m-3)} & a^{-3(m-3)} & \cdots & a^{-(m-3)(m-3)} & a^{-(m-3)(m-2)} & a^{-(m-3)(m-1)} \\ 1 & a^{-(m-2)} & a^{-2(m-2)} & a^{-3(m-2)} & \cdots & a^{-(m-2)(m-3)} & a^{-(m-2)(m-2)} & a^{-(m-2)(m-1)} \\ 1 & a^{-(m-1)} & a^{-2(m-1)} & a^{-3(m-1)} & \cdots & a^{-(m-1)(m-3)} & a^{-(m-1)(m-2)} & a^{-(m-1)(m-1)} \end{bmatrix} \quad (2.4b)$$

where

$a = e^{j\frac{2\pi}{m}}$ is the m^{th} root of unity and $\frac{2\pi}{m}$ is the characteristic angle.

The first element in Equation (2.3) is called the zero sequence, and it has a real value. For a multiphase system with even number of phases, there will be two real vectors, the first one and the other at $\frac{m}{2}$, where m is the number of phases.

For $m = 5$, the following identities will apply

$a = e^{j\frac{2\pi}{m}}$ $\quad a^2 = e^{j\frac{4\pi}{m}}$ $\quad a^3 = e^{j\frac{6\pi}{m}} = a^{-2}$ $\quad a^4 = e^{j\frac{8\pi}{m}} = a^{-1}$

$a^6 = e^{j\frac{12\pi}{m}} = a^1$ $\quad a^8 = e^{j\frac{16\pi}{m}} = a^{-2}$ $\quad a^* = e^{-j\frac{2\pi}{m}} = a^{-1}$

$$\left(a^2\right)^* = e^{-j\frac{4\pi}{m}} = a^{-2} \qquad \left(a^3\right)^* = e^{-j\frac{6\pi}{m}} = \left(a^{-2}\right)^* = a^{-2} \qquad \left(a^4\right)^* = e^{-j\frac{8\pi}{m}} = \left(a^{-1}\right)^* = a^1$$

$\left(a^6\right)^* = e^{-j\frac{12\pi}{m}} = \left(a^1\right)^* = a^{-1} \qquad \left(a^8\right)^* = e^{-j\frac{16\pi}{m}} = \left(a^{-2}\right)^* = a^2$ and so on.

The stationary reference frame transformation matrices and their inverses for three, five and seven phase systems are given by Equations (2.4c), (2.4d) and (2.4e), respectively.

$$T_3 = \sqrt{\frac{2}{3}}\begin{bmatrix} 1 & 1 & 1 \\ 1 & a & a^2 \\ 1 & a^2 & a \end{bmatrix} \qquad T_3^{-1} = \sqrt{\frac{2}{3}}\begin{bmatrix} 1 & 1 & 1 \\ 1 & a^{-1} & a^{-2} \\ 1 & a^{-2} & a^{-1} \end{bmatrix} \tag{2.4c}$$

$$T_5 = \sqrt{\frac{2}{5}}\begin{bmatrix} 1 & 1 & 1 & 1 & 1 \\ 1 & a & a^2 & a^{-2} & a^{-1} \\ 1 & a^2 & a^{-1} & a & a^{-2} \\ 1 & a^{-2} & a & a^{-1} & a^2 \\ 1 & a^{-1} & a^{-2} & a^2 & a \end{bmatrix} \qquad T_5^{-1} = \sqrt{\frac{2}{5}}\begin{bmatrix} 1 & 1 & 1 & 1 & 1 \\ 1 & a^{-1} & a^{-2} & a^2 & a^1 \\ 1 & a^{-2} & a & a^{-1} & a^2 \\ 1 & a^2 & a^{-1} & a & a^{-2} \\ 1 & a & a^2 & a^{-2} & a^{-1} \end{bmatrix} \tag{2.4d}$$

$$T_7 = \sqrt{\frac{2}{7}}\begin{bmatrix} 1 & 1 & 1 & 1 & 1 & 1 & 1 \\ 1 & a & a^2 & a^3 & a^{-3} & a^{-2} & a^{-1} \\ 1 & a^2 & a^{-3} & a^{-1} & a & a^3 & a^{-2} \\ 1 & a^3 & a^{-1} & a^2 & a^{-2} & a & a^{-3} \\ 1 & a^{-3} & a^1 & a^{-2} & a^2 & a^{-1} & a^3 \\ 1 & a^{-2} & a^3 & a & a^{-1} & a^{-3} & a^2 \\ 1 & a^{-1} & a^{-2} & a^{-3} & a^3 & a^2 & a^1 \end{bmatrix} \quad T_7^{-1} = \sqrt{\frac{2}{7}}\begin{bmatrix} 1 & 1 & 1 & 1 & 1 & 1 & 1 \\ 1 & a^{-1} & a^{-2} & a^{-3} & a^3 & a^2 & a^1 \\ 1 & a^{-2} & a^3 & a^1 & a^{-1} & a^{-3} & a^2 \\ 1 & a^{-3} & a^1 & a^{-2} & a^2 & a^{-1} & a^3 \\ 1 & a^3 & a^{-1} & a^2 & a^{-2} & a^1 & a^{-3} \\ 1 & a^2 & a^{-3} & a^{-1} & a^1 & a^3 & a^{-2} \\ 1 & a^1 & a^2 & a^3 & a^{-3} & a^{-2} & a^{-1} \end{bmatrix} \tag{2.4e}$$

For an arbitrary reference frame transformation, then the transformation matrices given are multiplied by $e^{j\theta}$, where $\theta = \omega t + \theta_0$, ω is the angular speed of the reference frame and θ_0 is the reference frame initial angle.

The reference frame transformation produces m variables. If the number of phases is odd, then there $\frac{m-1}{2}$ forward rotating complex variable component and $\frac{m-1}{2}$ backward rotating complex components which are the conjugates of the other set if the system is balanced. The remaining component is the zero sequence component. This is in real form. If the number of phases is even, then there are two zero sequence components, the second one occurring at $\frac{m}{2}$. The remaining components are complex conjugates, with $\frac{(m-2)}{2}$ forward rotating and the other $\frac{(m-2)}{2}$ backward rotating.

2.2 Three-phase System

In order to arrive at the general transformation of the multi-phase systems, a brief review of the three-phase system transformation is given first. The y vector of Equation (2.1) can take variables of any form (for example, currents, voltages, flux linkages). As an example of three-phase system, the voltage and current are considered

$$v = \begin{bmatrix} v_{as} & v_{bs} & v_{cs} \end{bmatrix}^T \tag{2.5}$$

$$i = \begin{bmatrix} i_{as} & i_{bs} & i_{cs} \end{bmatrix}^T \tag{2.6}$$

where

v_{as}, v_{bs} and v_{cs} are the phase voltages and i_{as}, i_{bs} and i_{cs} are the phase currents for the three-phase system. In this particular case, $m = 3$ and therefore,

$$a = e^{j\frac{2\pi}{3}}$$

Transforming the phase voltages and currents into a complex form by using the stationary reference frame complex transformation matrix, the following equations are obtained

$$v_{qds} = \sqrt{\frac{2}{3}}\left[v_{as} + av_{bs} + a^2 v_{cs}\right] \tag{2.7}$$

$$i_{qds} = \sqrt{\frac{2}{3}}\left[i_{as} + ai_{bs} + a^2 i_{cs}\right] \tag{2.8}$$

The zero sequence components are give by

$$v_{os} = \sqrt{\frac{2}{3}}\left[v_{as} + v_{bs} + v_{cs}\right] \tag{2.9}$$

$$i_{os} = \sqrt{\frac{2}{3}}\left[i_{as} + i_{bs} + i_{cs}\right] \tag{2.10}$$

2.2.1 Three-phase Power Computation

The three-phase complex power, S, is given by

$$S = v_{qds} i_{qds}^* + v_{os} i_{os}^* \tag{2.11}$$

where

$$i_{qds}^* = \sqrt{\frac{2}{3}}\left[i_{as} + a^{-1} i_{bs} + a^{-2} i_{cs}\right] \tag{2.12}$$

Therefore, the complex power, S_{qd}, due to the qd component is given by

$$S_{qd} = \frac{2}{3}\left[v_{as} + av_{bs} + a^2 v_{cs}\right]\left[i_{as} + a^{-1} i_{bs} + a^{-2} i_{cs}\right] \tag{2.13}$$

$$S_{qd} = \frac{2}{3}\left[\begin{array}{l} v_{as} i_{as} + a^{-1} v_{as} i_{bs} + a^{-2} v_{as} i_{cs} + av_{bs}\, i_{as} + a^{-1} av_{bs}\, i_{bs} + a^{-2} av_{bs}\, i_{cs} \\ + a^2 v_{cs} i_{as} + a^{-1} a^2 v_{cs} i_{bs} + a^{-2} a^2 v_{cs} i_{cs} \end{array}\right] \tag{2.14}$$

$$S_{qd} = \frac{2}{3}\left[\begin{array}{l} v_{as} i_{as} + v_{bs}\, i_{bs} + v_{cs} i_{cs} + a\left(v_{cs} i_{bs} + v_{bs}\, i_{as}\right) \\ + a^2 v_{cs} i_{as} + a^{-2} v_{as} i_{cs} + a^{-1}\left(v_{as} i_{bs} + v_{bs}\, i_{cs}\right) \end{array}\right] \tag{2.14}$$

Substituting for $a = e^{j\frac{2\pi}{3}}$, the following is obtained

$$S_{qd} = \frac{2}{3}\left[\begin{array}{l} v_{as}i_{as} + v_{bs}\, i_{bs} + v_{cs}i_{cs} + e^{j\frac{2\pi}{3}}\left(v_{cs}i_{bs} + v_{bs}\, i_{as}\right) \\ + e^{j\frac{4\pi}{3}} v_{cs}i_{as} + e^{-j\frac{4\pi}{3}} v_{as}i_{cs} + e^{-j\frac{2\pi}{3}}\left(v_{as}i_{bs} + v_{bs}\, i_{cs}\right) \end{array}\right] \tag{2.15}$$

2.2.2 Real Power Computation for a Three-phase System

The active (real power), S_{qd}, due to the qd voltage and current components is obtained by evaluating the real part of Equation (2.15). This result will later be combined with the power due to the zero sequence components to obtain the overall active power in the three-phase system.

Considering the real part of Equation (2.15), the following can be deduced

$$P_{qd} = \mathrm{Re}\left(S_{qd}\right) = \frac{2}{3}\left[\begin{array}{l} v_{as}i_{as} + v_{bs}\, i_{bs} + v_{cs}i_{cs} + \left(v_{cs}i_{bs} + v_{bs}\, i_{as}\right)\cos\left(\frac{2\pi}{3}\right) \\ + \left(v_{cs}i_{as} + v_{as}i_{cs}\right)\cos\left(\frac{4\pi}{3}\right) + \left(v_{as}i_{bs} + v_{bs}\, i_{cs}\right)\cos\left(\frac{2\pi}{3}\right) \end{array}\right] \tag{2.16}$$

$$P_{qd} = \mathrm{Re}\left(S_{qd}\right) = \frac{2}{3}\left[\begin{array}{l} v_{as}i_{as} + v_{bs}\, i_{bs} + v_{cs}i_{cs} - \frac{1}{2}\left(v_{cs}i_{bs} + v_{bs}\, i_{as}\right) + \\ - \frac{1}{2}\left(v_{cs}i_{as} + v_{as}i_{cs}\right) - \frac{1}{2}\left(v_{as}i_{bs} + v_{bs}\, i_{cs}\right) \end{array}\right] \tag{2.17}$$

Since the zero sequence component has a real value, it can contribute to the active power

$$S_{os} = \frac{2}{3}\left[v_{as} + v_{bs} + v_{cs}\right]\left[i_{as} + i_{bs} + i_{cs}\right] \tag{2.18}$$

$$P_{os} = \frac{2}{3}\left[v_{as}i_{as} + v_{bs}i_{bs} + v_{cs}i_{cs} + v_{as}i_{bs} + v_{as}i_{cs} + v_{bs}i_{as} + v_{bs}i_{cs} + v_{cs}i_{as} + v_{cs}i_{bs}\right] \tag{2.19}$$

Combining Equations (2.17) and (2.19) gives

$$P = P_{qds} + P_{os} = \frac{2}{3}\begin{bmatrix} v_{as}i_{as} + v_{bs}\, i_{bs} + v_{cs}i_{cs} - \frac{1}{2}\left(v_{cs}i_{bs} + v_{bs}\, i_{as}\right) + \\ -\frac{1}{2}\left(v_{cs}i_{as} + v_{as}i_{cs}\right) - \frac{1}{2}\left(v_{as}i_{bs} + v_{bs}\, i_{cs}\right) + \\ \begin{bmatrix} v_{as}i_{as} + v_{bs}i_{bs} + v_{cs}i_{cs} + v_{as}i_{bs} + \\ v_{as}i_{cs} + v_{bs}i_{as} + v_{bs}i_{cs} + v_{cs}i_{as} + v_{cs}i_{bs} \end{bmatrix} \end{bmatrix}$$

$$P = P_{qds} + P_{os} = \frac{2}{3}\begin{bmatrix} v_{as}i_{as} + v_{bs}\, i_{bs} + v_{cs}i_{cs} + v_{as}i_{as} + v_{bs}i_{bs} + v_{cs}i_{cs} + \\ -\frac{1}{2}\left(v_{cs}i_{bs} + v_{bs}\, i_{as}\right) + -\frac{1}{2}\left(v_{cs}i_{as} + v_{as}i_{cs}\right) - \frac{1}{2}\left(v_{as}i_{bs} + v_{bs}\, i_{cs}\right) + \\ \left[v_{cs}i_{as} + v_{as}i_{bs} + v_{cs}i_{bs} + v_{as}i_{cs} + v_{bs}i_{as} + v_{bs}i_{cs}\right] \end{bmatrix}$$

$$P = P_{qds} + P_{os} = \frac{2}{3}\begin{bmatrix} 2\left(v_{as}i_{as} + v_{bs}\, i_{bs} + v_{cs}i_{cs}\right) + \left(-\frac{1}{2} + 1\right)v_{cs}i_{bs} + \\ + v_{bs}\, i_{as}\left(-\frac{1}{2} + \frac{1}{4}\right) + v_{cs}i_{as}\left(-\frac{1}{2} + 1\right) + v_{as}i_{cs}\left(-\frac{1}{2} + 1\right) + \\ \left(-\frac{1}{2} + 1\right)v_{as}i_{bs} + \left(-\frac{1}{2} + 1\right)v_{bs}i_{cs} \end{bmatrix}$$

This results into

$$P = P_{qds} + P_{os} = \frac{2}{3}\begin{bmatrix} 2\left(v_{as}i_{as} + v_{bs}\, i_{bs} + v_{cs}i_{cs}\right) + \\ \frac{1}{2}\left[\left(v_{cs} + v_{as}\right)i_{bs} + \left(v_{bs} + v_{cs}\right)i_{as} + \left(v_{as} + v_{bs}\right)i_{cs}\right] \end{bmatrix} \tag{2.20}$$

Equation (2.20) gives a general expression for computing real (active) power by using natural (abc) variables in a three-phase system.

Now, if

$$i_{as} + i_{bs} + i_{cs} = 0 \tag{2.21}$$

$$v_{as} + v_{bs} + v_{cs} = 0 \tag{2.22}$$

Thus

$$v_{as} = -v_{bs} - v_{cs} \tag{2.23}$$

$$v_{bs} = -v_{as} - v_{cs} \tag{2.24}$$

$$v_{cs} = -v_{as} - v_{bs} \tag{2.25}$$

Then by substituting these conditions into Equation (2.20) the following is obtained

$$P = P_{qds} + P_{os} = \frac{2}{3}\left[2(v_{as}i_{as} + v_{bs}\, i_{bs} + v_{cs}i_{cs}) - \frac{1}{2}(v_{bs}i_{bs} + v_{as}i_{as} + v_{cs}\, i_{cs}) \right]$$

$$P = P_{qds} + P_{os} = [v_{as}i_{as} + v_{bs}\, i_{bs} + v_{cs}i_{cs}] \tag{2.26}$$

Therefore, Equation (2.26) is the power equation for a balanced three-phase system. It is important to note that in Equation (2.26), the total three-phase active power is the sum of the individual phase active powers, as expected. Therefore, with the transformation chosen, the power is invariant. In order the power obtained by using the transformed qdo variable to using the reference frame of transformation as given in Equation (2.4a), the general expression for real power will be as given by Equation (2.20) and for a special condition of when Equation (2.21) is true, then the real power will be calculated by using Equation (2.26).

2.2.3 Reactive Power Computation for a Three-phase System

The imaginary part of Equation (2.15) will give the reactive power Q. As it has already been mentioned earlier, the zero sequence components do not contribute to reactive power. Therefore, considering the imaginary part of Equation (2.15) the following is deduced

$$Q = \mathrm{Im}\left(S_{qd}\right) = \frac{2}{3}\left[\begin{array}{l}\left(v_{cs}i_{bs} + v_{bs}\, i_{as}\right)\sin\left(\frac{2\pi}{3}\right) - \left(v_{as}i_{bs} + v_{bs}\, i_{cs}\right)\sin\left(\frac{2\pi}{3}\right) \\ + \left(v_{cs}i_{as} - v_{as}i_{cs}\right)\sin\left(\frac{4\pi}{3}\right)\end{array}\right] \tag{2.27}$$

$$Q = \mathrm{Im}\left(S_{qd}\right) = \frac{2}{3}\left[\left(v_{cs}i_{bs} + v_{bs}\, i_{as} - v_{as}i_{bs} - v_{bs}\, i_{cs}\right)\sin\left(\frac{2\pi}{3}\right) + \left(v_{cs}i_{as} - v_{as}i_{cs}\right)\sin\left(\frac{4\pi}{3}\right)\right] \tag{2.28}$$

$$Q = \mathrm{Im}\left(S_{qd}\right) = \frac{2}{3}\left[\frac{\sqrt{3}}{2}\left(v_{cs}i_{bs} + v_{bs}\, i_{as} - v_{as}i_{bs} - v_{bs}\, i_{cs} - v_{cs}i_{as} + v_{as}i_{cs}\right)\right] \tag{2.29}$$

$$Q = \mathrm{Im}\left(S_{qd}\right) = \frac{2}{3}\left[\frac{\sqrt{3}}{2}\left(v_{as}i_{cs} - v_{cs}i_{as} + v_{bs}\, i_{as} - v_{as}i_{bs} + v_{cs}i_{bs} - v_{bs}\, i_{cs}\right)\right] \tag{2.30}$$

which simplifies into

$$Q = \frac{\sqrt{3}}{3}\left[v_{as}i_{cs} - v_{cs}i_{as} + v_{bs}\, i_{as} - v_{as}i_{bs} + v_{cs}i_{bs} - v_{bs}\, i_{cs}\right] \tag{2.31}$$

Therefore knowing the per phase quantities, the three-phase reactive power can be directly obtained by using Equation (2.31).

2.3 Five-phase System

As opposed to a three-phase system in which there are one complex vector and a zero sequence component, in a five-phase system there are two complex vectors and one zero sequence component.

The real (scalar) voltage and current vectors for the five phase are given as

For the voltage vector

$$v = \left[v_{as} \quad v_{bs} \quad v_{cs} \quad v_{ds} \quad v_{es}\right]^T \tag{2.32}$$

Fro the currents vector

$$i = \begin{bmatrix} i_{as} & i_{bs} & i_{cs} & i_{ds} & i_{es} \end{bmatrix}^T \qquad (2.33)$$

Using Equation (2.1) and (2.4a), the first complex vector (qd) after transformation will be

For the voltages

$$v_{qds} = \sqrt{\frac{2}{5}}\left[v_{as} + av_{bs} + a^2 v_{cs} + a^3 v_{ds} + a^4 v_{es}\right] \qquad (2.34)$$

For the currents

$$i_{qds} = \sqrt{\frac{2}{5}}\left[i_{as} + ai_{bs} + a^2 i_{cs} + a^3 i_{ds} + a^4 i_{es}\right] \qquad (2.37)$$

Using the relations given in section 2.1, the following voltage and current equations are obtained

For the voltages

$$v_{qds} = \sqrt{\frac{2}{5}}\left[v_{as} + av_{bs} + a^2 v_{cs} + a^{-2} v_{ds} + a^{-1} v_{es}\right] \qquad (2.36)$$

For the currents

$$i_{qds} = \sqrt{\frac{2}{5}}\left[i_{as} + ai_{bs} + a^2 i_{cs} + a^{-2} i_{ds} + a^{-1} i_{es}\right] \qquad (2.37)$$

Similarly, using Equations (2.1) and (2.4a), the second complex vector (xy) is given by

For the voltages

$$v_{xys} = \sqrt{\frac{2}{5}}\left[v_{as} + a^2 v_{bs} + a^4 v_{cs} + a^6 v_{ds} + a^8 v_{es}\right] \qquad (2.38)$$

For the currents

$$i_{xys} = \sqrt{\frac{2}{5}}\left[i_{as} + a^2 i_{bs} + a^4 i_{cs} + a^6 i_{ds} + a^8 i_{es}\right] \tag{2.39}$$

Applying the definitions of section 2.1, gives the flowing voltage and current equations

For the voltages

$$v_{xys} = \sqrt{\frac{2}{5}}\left[v_{as} + a^2 v_{bs} + a^{-1} v_{cs} + a^1 v_{ds} + a^{-2} v_{es}\right] \tag{2.40}$$

For the currents

$$i_{xys} = \sqrt{\frac{2}{5}}\left[i_{as} + a^2 i_{bs} + a^{-1} i_{cs} + a^1 i_{ds} + a^{-2} i_{es}\right] \tag{2.41}$$

The zero sequence components, from Equations (2.1) and (2.4a), the transformed voltage and current equations are given by

For the voltages

$$v_{os} = \sqrt{\frac{2}{5}}\left[v_{as} + v_{bs} + v_{cs} + v_{ds} + v_{es}\right] \tag{2.42}$$

For the currents

$$i_{os} = \sqrt{\frac{2}{5}}\left[i_{as} + i_{bs} + i_{cs} + i_{ds} + i_{es}\right] \tag{2.43}$$

2.3.1 Five-phase Power Computation

The complex power in the five-phase system will be given by all the three components. Whereas the qd and xy components contribute to both the real and reactive powers, the zero sequence components contribute only to the real power.

Using the transformed vectors, the five-phase complex power, s, is given by

$$S = v_{qds} i_{qds}^{*} + v_{xys} i_{xys}^{*} + v_{os} i_{os}^{*} \tag{2.44}$$

where

$$i_{qds}^{*} = \sqrt{\frac{2}{5}} \left[i_{as} + a^{-1} i_{bs} + a^{-2} i_{cs} + a^{2} i_{ds} + a^{1} i_{es} \right] \tag{2.45}$$

$$i_{xys}^{*} = \sqrt{\frac{2}{5}} \left[i_{as} + a^{-2} i_{bs} + a^{1} i_{cs} + a^{-1} i_{ds} + a^{2} i_{es} \right] \tag{2.46}$$

$$i_{os}^{*} = i_{os} = \sqrt{\frac{2}{5}} \left[i_{as} + i_{bs} + i_{cs} + i_{ds} + i_{es} \right] \tag{2.47}$$

2.3.1.1 Complex Power Due to qd Components. The complex power due to the qd complex vector components is given by

$$S_{qds} = v_{qds} i_{qds}^{*} \tag{2.48}$$

Substituting for the voltage and current complex vectors, results into

$$S_{qds} = \frac{2}{5} \left[v_{as} + a v_{bs} + a^{2} v_{cs} + a^{-2} v_{ds} + a^{-1} v_{es} \right] \left[i_{as} + a^{-1} i_{bs} + a^{-2} i_{cs} + a^{2} i_{ds} + a^{1} i_{es} \right] \tag{2.49}$$

Equation (2.49) results into

$$S_{qds} = \frac{2}{5} \begin{bmatrix} v_{as} i_{as} + a^{-1} v_{as} i_{bs} + a^{-2} v_{as} i_{cs} + a^{2} v_{as} i_{ds} + a^{1} v_{as} i_{es} + \\ a v_{bs} i_{as} + v_{bs} i_{bs} + a^{-1} v_{bs} i_{cs} + a^{3} v_{bs} i_{ds} + a^{2} v_{bs} i_{es} + \\ a^{2} v_{cs} i_{as} + a^{1} v_{cs} i_{bs} + v_{cs} i_{cs} + a^{4} v_{cs} i_{ds} + a^{3} v_{cs} i_{es} \\ a^{-2} v_{ds} i_{as} + a^{-3} v_{ds} i_{bs} + a^{-4} v_{ds} i_{cs} + v_{ds} i_{ds} + a^{-1} v_{ds} i_{es} + \\ a^{-1} v_{es} i_{as} + a^{-2} v_{es} i_{bs} + a^{-3} v_{es} i_{cs} + a^{1} v_{es} i_{ds} + v_{es} i_{es} \end{bmatrix} \tag{2.50}$$

Applying the identities of section 2.1, gives

$$S_{qds} = \frac{2}{5}\begin{bmatrix} v_{as}i_{as} + a^{-1}v_{as}i_{bs} + a^{-2}v_{as}i_{cs} + a^{2}v_{as}i_{ds} + a^{1}v_{as}i_{es} + \\ av_{bs}i_{as} + v_{bs}i_{bs} + a^{-1}v_{bs}i_{cs} + a^{-2}v_{bs}i_{ds} + a^{2}v_{bs}i_{es} + \\ a^{2}v_{cs}i_{as} + a^{1}v_{cs}i_{bs} + v_{cs}i_{cs} + a^{-1}v_{cs}i_{ds} + a^{-2}v_{cs}i_{es} + \\ a^{-2}v_{ds}i_{as} + a^{2}v_{ds}i_{bs} + a^{1}v_{ds}i_{cs} + v_{ds}i_{ds} + a^{-1}v_{ds}i_{es} + \\ a^{-1}v_{es}i_{as} + a^{-2}v_{es}i_{bs} + a^{2}v_{es}i_{cs} + a^{1}v_{es}i_{ds} + v_{es}i_{es} \end{bmatrix} \tag{2.51}$$

Applying the definitions of section 2.1 to Equation (2.51), gives

$$S_{qds} = \frac{2}{5}\begin{bmatrix} v_{as}i_{as} + e^{-j\frac{2\pi}{5}}v_{as}i_{bs} + e^{-j\frac{4\pi}{5}}v_{as}i_{cs} + e^{j\frac{4\pi}{5}}v_{as}i_{ds} + e^{j\frac{2\pi}{5}}v_{as}i_{es} + \\ e^{j\frac{2\pi}{5}}v_{bs}i_{as} + v_{bs}i_{bs} + e^{-j\frac{2\pi}{5}}v_{bs}i_{cs} + e^{-j\frac{4\pi}{5}}v_{bs}i_{ds} + e^{j\frac{4\pi}{5}}v_{bs}i_{es} + \\ e^{j\frac{4\pi}{5}}v_{cs}i_{as} + e^{j\frac{2\pi}{5}}v_{cs}i_{bs} + v_{cs}i_{cs} + e^{-j\frac{2\pi}{5}}v_{cs}i_{ds} + e^{-j\frac{4\pi}{5}}v_{cs}i_{es} + \\ e^{-j\frac{4\pi}{5}}v_{ds}i_{as} + e^{j\frac{4\pi}{5}}v_{ds}i_{bs} + e^{j\frac{2\pi}{5}}v_{ds}i_{cs} + v_{ds}i_{ds} + e^{-j\frac{2\pi}{5}}v_{ds}i_{es} + \\ e^{-j\frac{2\pi}{5}}v_{es}i_{as} + e^{-j\frac{4\pi}{5}}v_{es}i_{bs} + e^{j\frac{4\pi}{5}}v_{es}i_{cs} + e^{j\frac{2\pi}{5}}v_{es}i_{ds} + v_{es}i_{es} \end{bmatrix} \tag{2.52}$$

2.3.1.2 Real power due to qd components. Evaluating the real part of Equation (2.52) will give the active (real power) due to the qd components. Thus

$$P_{qds} = \frac{2}{5}\begin{bmatrix} v_{as}i_{as} + v_{as}i_{bs}\cos\left(\frac{2\pi}{5}\right) + v_{as}i_{cs}\cos\left(\frac{4\pi}{5}\right) + v_{as}i_{ds}\cos\left(\frac{4\pi}{5}\right) + v_{as}i_{es}\cos\left(\frac{2\pi}{5}\right) + \\ v_{bs}i_{as}\cos\left(\frac{2\pi}{5}\right) + v_{bs}i_{bs} + v_{bs}i_{cs}\cos\left(\frac{2\pi}{5}\right) + v_{bs}i_{ds}\cos\left(\frac{4\pi}{5}\right) + v_{bs}i_{es}\cos\left(\frac{4\pi}{5}\right) + \\ v_{cs}i_{as}\cos\left(\frac{4\pi}{5}\right) + v_{cs}i_{bs}\cos\left(\frac{2\pi}{5}\right) + v_{cs}i_{cs} + v_{cs}i_{ds}\cos\left(\frac{2\pi}{5}\right) + v_{cs}i_{es}\cos\left(\frac{4\pi}{5}\right) + \\ v_{ds}i_{as}\cos\left(\frac{4\pi}{5}\right) + v_{ds}i_{bs}\cos\left(\frac{4\pi}{5}\right) + v_{ds}i_{cs}\cos\left(\frac{2\pi}{5}\right) + v_{ds}i_{ds} + v_{ds}i_{es}\cos\left(\frac{2\pi}{5}\right) + \\ v_{es}i_{as}\cos\left(\frac{2\pi}{5}\right) + v_{es}i_{bs}\cos\left(\frac{4\pi}{5}\right) + v_{es}i_{cs}\cos\left(\frac{4\pi}{5}\right) + v_{es}i_{ds}\cos\left(\frac{2\pi}{5}\right) + v_{es}i_{es} \end{bmatrix} \tag{2.53}$$

Combining the like terms, Equation (2.53) yields

$$P_{qds} = \frac{2}{5}\begin{bmatrix} v_{as}i_{as} + v_{bs}i_{bs} + v_{cs}i_{cs} + v_{ds}i_{ds} + v_{es}i_{es} + \\ \left(v_{as}i_{bs} + v_{as}i_{es} + v_{bs}i_{as} + v_{bs}i_{cs} + v_{cs}i_{bs} + v_{cs}i_{ds} + v_{ds}i_{cs} + v_{ds}i_{es} + v_{es}i_{ds} + v_{es}i_{as}\right)\cos\left(\frac{2\pi}{5}\right) + \\ \left(v_{as}i_{cs} + v_{as}i_{ds} + v_{bs}i_{ds} + v_{bs}i_{es} + v_{cs}i_{as} + v_{cs}i_{es} + v_{ds}i_{as} + v_{ds}i_{bs} + v_{es}i_{bs} + v_{es}i_{cs}\right)\cos\left(\frac{4\pi}{5}\right) \end{bmatrix} \tag{2.54}$$

Equation (2.54) gives the real power due to the qd complex voltage and current components.

2.3.1.3 Reactive power due to qd components. Evaluating the imaginary part of (2.52) will give the reactive (imaginary power) due to the qd components. Thus

$$Q_{qd} = \frac{2}{5}\begin{bmatrix} -v_{as}i_{bs}\sin\left(\frac{2\pi}{5}\right) - v_{as}i_{cs}\sin\left(\frac{4\pi}{5}\right) + v_{as}i_{ds}\sin\left(\frac{4\pi}{5}\right) + v_{as}i_{es}\sin\left(\frac{2\pi}{5}\right) + \\ v_{bs}i_{as}\sin\left(\frac{2\pi}{5}\right) - v_{bs}i_{cs}\sin\left(\frac{2\pi}{5}\right) - v_{bs}i_{ds}\sin\left(\frac{4\pi}{5}\right) + v_{bs}i_{es}\sin\left(\frac{4\pi}{5}\right) + \\ v_{cs}i_{as}\sin\left(\frac{4\pi}{5}\right) + v_{cs}i_{bs}\sin\left(\frac{2\pi}{5}\right) - v_{cs}i_{ds}\sin\left(\frac{2\pi}{5}\right) - v_{cs}i_{es}\sin\left(\frac{4\pi}{5}\right) + \\ -v_{ds}i_{as}\sin\left(\frac{4\pi}{5}\right) + v_{ds}i_{bs}\sin\left(\frac{4\pi}{5}\right) + v_{ds}i_{cs}\sin\left(\frac{2\pi}{5}\right) - v_{ds}i_{es}\sin\left(\frac{2\pi}{5}\right) + \\ -v_{es}i_{as}\sin\left(\frac{2\pi}{5}\right) - v_{es}i_{bs}\sin\left(\frac{4\pi}{5}\right) + v_{es}i_{cs}\sin\left(\frac{4\pi}{5}\right) + v_{es}i_{ds}\sin\left(\frac{2\pi}{5}\right) \end{bmatrix} \tag{2.55}$$

Combining the like terms, Equation (2.55) yields

$$Q_{qds} = \frac{2}{5}\begin{bmatrix} \begin{pmatrix} -v_{as}i_{bs} + v_{as}i_{es} + v_{bs}i_{as} - v_{bs}i_{cs} + v_{cs}i_{bs} - v_{cs}i_{ds} + \\ v_{ds}i_{cs} - v_{ds}i_{es} - v_{es}i_{as} + v_{es}i_{ds} \end{pmatrix}\sin\left(\frac{2\pi}{5}\right) \\ \begin{pmatrix} -v_{as}i_{cs} + v_{as}i_{ds} - v_{bs}i_{ds} + v_{bs}i_{es} + v_{cs}i_{as} - v_{cs}i_{es} + \\ -v_{ds}i_{as} + v_{ds}i_{bs} - v_{es}i_{bs} + v_{es}i_{cs} \end{pmatrix}\sin\left(\frac{4\pi}{5}\right) \end{bmatrix}$$

$$Q_{qds} = \frac{2}{5}\begin{bmatrix} \left(v_{as}i_{es} - v_{es}i_{as} + v_{bs}i_{as} - v_{as}i_{bs} + v_{cs}i_{bs} - v_{bs}i_{cs} + v_{ds}i_{cs} - v_{cs}i_{ds} + v_{es}i_{ds} - v_{ds}i_{es}\right)\sin\left(\frac{2\pi}{5}\right) + \\ \left(v_{as}i_{ds} - v_{ds}i_{as} + v_{cs}i_{as} - v_{as}i_{cs} + v_{bs}i_{es} - v_{es}i_{bs} + v_{es}i_{cs} - v_{cs}i_{es} + v_{ds}i_{bs} - v_{bs}i_{ds}\right)\sin\left(\frac{4\pi}{5}\right) \end{bmatrix} \tag{2.56}$$

Equation (2.56) gives the reactive power due to the qd complex voltage and current components.

2.3.1.4 Complex power due to xy components

2.3.1.4 Complex power due to xy components. The complex power due to the xy complex vector components is given by

$$S_{xys} = v_{xys}i_{xys}^{*} \tag{2.57}$$

Substituting for the voltage and current complex vectors, results into

$$S_{xys} = \frac{2}{5}\left[v_{as} + a^{2}v_{bs} + a^{-1}v_{cs} + a^{1}v_{ds} + a^{-2}v_{es}\right]\left[i_{as} + a^{-2}i_{bs} + a^{1}i_{cs} + a^{-1}i_{ds} + a^{2}i_{es}\right] \tag{2.58}$$

Equation (2.58) results into

$$S_{xys} = \frac{2}{5}\begin{bmatrix} v_{as}i_{as} + a^{-2}v_{as}i_{bs} + a^{1}v_{as}i_{cs} + a^{-1}v_{as}i_{ds} + a^{2}v_{as}i_{es} + \\ a^{2}v_{bs}i_{as} + v_{bs}i_{bs} + a^{3}v_{bs}i_{cs} + a^{1}v_{bs}i_{ds} + a^{4}v_{bs}i_{es} + \\ a^{-1}v_{cs}i_{as} + a^{-3}v_{cs}i_{bs} + v_{cs}i_{cs} + a^{-2}v_{cs}i_{ds} + a^{1}v_{cs}i_{es} + \\ a^{1}v_{ds}i_{as} + a^{-1}v_{ds}i_{bs} + a^{2}v_{ds}i_{cs} + v_{ds}i_{ds} + a^{3}v_{ds}i_{es} + \\ a^{-2}v_{es}i_{as} + a^{-4}v_{es}i_{bs} + a^{-1}v_{es}i_{cs} + a^{-3}v_{es}i_{ds} + v_{es}i_{es} \end{bmatrix} \tag{2.59}$$

Applying the identities of section 2.1, Equation (2.59) gives

$$S_{xys} = \frac{2}{5}\begin{bmatrix} v_{as}i_{as} + a^{-2}v_{as}i_{bs} + a^{1}v_{as}i_{cs} + a^{-1}v_{as}i_{ds} + a^{2}v_{as}i_{es} + \\ a^{2}v_{bs}i_{as} + v_{bs}i_{bs} + a^{-2}v_{bs}i_{cs} + a^{1}v_{bs}i_{ds} + a^{-1}v_{bs}i_{es} \\ a^{-1}v_{cs}i_{as} + a^{2}v_{cs}i_{bs} + v_{cs}i_{cs} + a^{-2}v_{cs}i_{ds} + a^{1}v_{cs}i_{es} \\ a^{1}v_{ds}i_{as} + a^{-1}v_{ds}i_{bs} + a^{2}v_{ds}i_{cs} + v_{ds}i_{ds} + a^{-2}v_{ds}i_{es} \\ a^{-2}v_{es}i_{as} + a^{1}v_{es}i_{bs} + a^{-1}v_{es}i_{cs} + a^{2}v_{es}i_{ds} + v_{es}i_{es} \end{bmatrix} \tag{2.60}$$

Applying the definitions of section 2.1 to Equation (2.60), gives

$$S_{xys} = \frac{2}{5}\begin{bmatrix} v_{as}i_{as} + e^{-j\frac{4\pi}{5}}v_{as}i_{bs} + e^{j\frac{2\pi}{5}}v_{as}i_{cs} + e^{-j\frac{2\pi}{5}}v_{as}i_{ds} + e^{j\frac{4\pi}{5}}v_{as}i_{es} + \\ e^{j\frac{4\pi}{5}}v_{bs}i_{as} + v_{bs}i_{bs} + e^{-j\frac{4\pi}{5}}v_{bs}i_{cs} + e^{j\frac{2\pi}{5}}v_{bs}i_{ds} + e^{-j\frac{2\pi}{5}}v_{bs}i_{es} \\ e^{-j\frac{2\pi}{5}}v_{cs}i_{as} + e^{j\frac{4\pi}{5}}v_{cs}i_{bs} + v_{cs}i_{cs} + e^{-j\frac{4\pi}{5}}v_{cs}i_{ds} + e^{j\frac{2\pi}{5}}v_{cs}i_{es} \\ e^{j\frac{2\pi}{5}}v_{ds}i_{as} + e^{-j\frac{2\pi}{5}}v_{ds}i_{bs} + e^{j\frac{4\pi}{5}}v_{ds}i_{cs} + v_{ds}i_{ds} + e^{-j\frac{4\pi}{5}}v_{ds}i_{es} \\ e^{-j\frac{4\pi}{5}}v_{es}i_{as} + e^{j\frac{2\pi}{5}}v_{es}i_{bs} + e^{-j\frac{2\pi}{5}}v_{es}i_{cs} + e^{j\frac{4\pi}{5}}v_{es}i_{ds} + v_{es}i_{es} \end{bmatrix} \tag{2.61}$$

2.3.1.5 Real power due to xy components. Evaluating the real part of Equation (2.61) will give the active (real power) due to the xy components. Thus

$$P_{xys} = \frac{2}{5}\begin{bmatrix} v_{as}i_{as} + v_{as}i_{bs}\cos\left(\frac{4\pi}{5}\right) + v_{as}i_{cs}\cos\left(\frac{2\pi}{5}\right) + v_{as}i_{ds}\cos\left(\frac{2\pi}{5}\right) + v_{as}i_{es}\cos\left(\frac{4\pi}{5}\right) + \\ v_{bs}i_{as}\cos\left(\frac{4\pi}{5}\right) + v_{bs}i_{bs} + v_{bs}i_{cs}\cos\left(\frac{4\pi}{5}\right) + v_{bs}i_{ds}\cos\left(\frac{2\pi}{5}\right) + v_{bs}i_{es}\cos\left(\frac{2\pi}{5}\right) \\ v_{cs}i_{as}\cos\left(\frac{2\pi}{5}\right) + v_{cs}i_{bs}\cos\left(\frac{4\pi}{5}\right) + v_{cs}i_{cs} + v_{cs}i_{ds}\cos\left(\frac{4\pi}{5}\right) + v_{cs}i_{es}\cos\left(\frac{2\pi}{5}\right) \\ v_{ds}i_{as}\cos\left(\frac{2\pi}{5}\right) + v_{ds}i_{bs}\cos\left(\frac{2\pi}{5}\right) + v_{ds}i_{cs}\cos\left(\frac{4\pi}{5}\right) + v_{ds}i_{ds} + v_{ds}i_{es}\cos\left(\frac{4\pi}{5}\right) \\ v_{es}i_{as}\cos\left(\frac{4\pi}{5}\right) + v_{es}i_{bs}\cos\left(\frac{2\pi}{5}\right) + v_{es}i_{cs}\cos\left(\frac{2\pi}{5}\right) + v_{es}i_{ds}\cos\left(\frac{4\pi}{5}\right) + v_{es}i_{es} \end{bmatrix} \tag{2.62}$$

Combining the like terms, Equation (2.62) yields

$$P_{xys} = \frac{2}{5}\begin{bmatrix} v_{as}i_{as} + v_{bs}i_{bs} + v_{cs}i_{cs} + v_{ds}i_{ds} + v_{es}i_{es} + \\ \left(v_{as}i_{bs} + v_{as}i_{es} + v_{bs}i_{as} + v_{bs}i_{cs} + v_{cs}i_{bs} + v_{cs}i_{ds} + v_{ds}i_{cs} + v_{ds}i_{es} + v_{es}i_{as} + v_{es}i_{ds}\right)\cos\left(\frac{4\pi}{5}\right) \\ + \left(v_{as}i_{cs} + v_{as}i_{ds} + v_{bs}i_{ds} + v_{bs}i_{es} + v_{cs}i_{as} + v_{cs}i_{es} + v_{ds}i_{as} + v_{ds}i_{bs} + v_{es}i_{bs} + v_{es}i_{cs}\right)\cos\left(\frac{2\pi}{5}\right) \end{bmatrix} \tag{2.63}$$

Equation (2.6) gives the real power due to the xy complex voltage and current components.

2.3.1.6 Reactive power due to xy components. Evaluating the imaginary part of Equation (2.61) will give the reactive (imaginary power) due to the xy components. Thus

$$Q_{xys} = \frac{2}{5}\begin{bmatrix} -v_{as}i_{bs}\sin\left(\frac{4\pi}{5}\right) + v_{as}i_{es}\sin\left(\frac{4\pi}{5}\right) + v_{as}i_{cs}\sin\left(\frac{2\pi}{5}\right) - v_{as}i_{ds}\sin\left(\frac{2\pi}{5}\right) + \\ v_{bs}i_{as}\sin\left(\frac{4\pi}{5}\right) - v_{bs}i_{cs}\sin\left(\frac{4\pi}{5}\right) + v_{bs}i_{ds}\sin\left(\frac{2\pi}{5}\right) - v_{bs}i_{es}\sin\left(\frac{2\pi}{5}\right) + \\ -v_{cs}i_{as}\sin\left(\frac{2\pi}{5}\right) + v_{cs}i_{bs}\sin\left(\frac{4\pi}{5}\right) - v_{cs}i_{ds}\sin\left(\frac{4\pi}{5}\right) + v_{cs}i_{es}\sin\left(\frac{2\pi}{5}\right) + \\ v_{ds}i_{as}\sin\left(\frac{2\pi}{5}\right) - v_{ds}i_{bs}\sin\left(\frac{2\pi}{5}\right) + v_{ds}i_{cs}\sin\left(\frac{4\pi}{5}\right) - v_{ds}i_{es}\sin\left(\frac{4\pi}{5}\right) + \\ -v_{es}i_{as}\sin\left(\frac{4\pi}{5}\right) + v_{es}i_{bs}\sin\left(\frac{2\pi}{5}\right) - v_{es}i_{cs}\sin\left(\frac{2\pi}{5}\right) + v_{es}i_{ds}\sin\left(\frac{4\pi}{5}\right) \end{bmatrix} \tag{2.64}$$

Combining the like terms, Equation (2.64) yields

$$Q_{xys} = \frac{2}{5}\begin{bmatrix} \begin{pmatrix} -v_{as}i_{bs} + v_{as}i_{es} + v_{bs}i_{as} - v_{bs}i_{cs} + v_{cs}i_{bs} - v_{cs}i_{ds} + \\ v_{ds}i_{cs} - v_{ds}i_{es} - v_{es}i_{as} + v_{es}i_{ds} \end{pmatrix}\sin\left(\frac{4\pi}{5}\right) + \\ \begin{pmatrix} v_{as}i_{cs} - v_{as}i_{ds} + v_{bs}i_{ds} - v_{bs}i_{es} - v_{cs}i_{as} + v_{cs}i_{es} + \\ v_{ds}i_{as} - v_{ds}i_{bs} + v_{es}i_{bs} - v_{es}i_{cs} \end{pmatrix}\sin\left(\frac{2\pi}{5}\right) \end{bmatrix}$$

$$Q_{xys} = \frac{2}{5}\begin{bmatrix} (v_{bs}i_{as} - v_{as}i_{bs} + v_{as}i_{es} - v_{es}i_{as} + v_{cs}i_{bs} - v_{bs}i_{cs} + v_{ds}i_{cs} - v_{cs}i_{ds} + v_{es}i_{ds} - v_{ds}i_{es})\sin\left(\frac{4\pi}{5}\right) + \\ (v_{as}i_{cs} - v_{cs}i_{as} + v_{ds}i_{as} - v_{as}i_{ds} + v_{bs}i_{ds} - v_{ds}i_{bs} + v_{es}i_{bs} - v_{bs}i_{es} + v_{cs}i_{es} - v_{es}i_{cs})\sin\left(\frac{2\pi}{5}\right) \end{bmatrix} \tag{2.65}$$

Equation (2.65) gives the reactive power due to the xy complex voltage and current components.

2.3.1.7 Real power due to zero sequence components. The zero sequence components are scalar vectors. Therefore, they do not contribute to the reactive power. The power due to the zero sequence is given by

$$S_{os} = v_{os} i_{os}^{*} \tag{2.66}$$

Substituting for the zero sequence voltage and current vectors, gives

$$S_{os} = \frac{2}{5}\left[v_{as} + v_{bs} + v_{cs} + v_{ds} + v_{es}\right]\left[i_{as} + i_{bs} + i_{cs} + i_{ds} + i_{es}\right] \tag{2.67}$$

Equation (2.67) results into

$$P_{os} = \frac{2}{5}\begin{bmatrix} v_{as}i_{as} + v_{bs}i_{bs} + v_{cs}i_{cs} + v_{ds}i_{ds} + v_{es}i_{es} + v_{as}i_{bs} + v_{as}i_{cs} + v_{es}i_{bs} + \\ v_{as}i_{ds} + v_{as}i_{es} + v_{bs}i_{as} + v_{bs}i_{cs} + v_{bs}i_{ds} + v_{bs}i_{es} + v_{ds}i_{es} + v_{es}i_{as} + \\ v_{cs}i_{as} + v_{cs}i_{bs} + v_{cs}i_{ds} + v_{cs}i_{es} + v_{ds}i_{as} + v_{ds}i_{bs} + v_{ds}i_{cs} + v_{es}i_{cs} + v_{es}i_{ds} \end{bmatrix} \tag{2.68}$$

Equation (2.68) gives the value of the real power contributed by the zero sequence components.

2.3.2 Total Power in a Five-phase System

The overall powers in the five-phase systems can be obtained by combining Equations (2.54), (2.63) and (2.68) for the total real power, whereas for the total reactive power, the Equations to be combined are (2.56) and (2.65).

2.3.2.1 Total real power in a five-phase system. This is obtained by adding together the powers given by Equations (2.54), (2.63) and (2.68). Thus

$$P = P_{qds} + P_{xys} + P_{os} \tag{2.69}$$

$$P_{qds} = \frac{2}{5}\left[\begin{array}{l} v_{as}i_{as} + v_{bs}i_{bs} + v_{cs}i_{cs} + v_{ds}i_{ds} + v_{es}i_{es} + \\ \left(v_{as}i_{bs} + v_{as}i_{es} + v_{bs}i_{as} + v_{bs}i_{cs} + v_{cs}i_{bs} + v_{cs}i_{ds} + v_{ds}i_{cs} + v_{ds}i_{es} + v_{es}i_{ds} + v_{es}i_{as}\right)\cos\left(\frac{2\pi}{5}\right) + \\ \left(v_{as}i_{cs} + v_{as}i_{ds} + v_{bs}i_{ds} + v_{bs}i_{es} + v_{cs}i_{as} + v_{cs}i_{es} + v_{ds}i_{as} + v_{ds}i_{bs} + v_{es}i_{bs} + v_{es}i_{cs}\right)\cos\left(\frac{4\pi}{5}\right) + \\ v_{as}i_{as} + v_{bs}i_{bs} + v_{cs}i_{cs} + v_{ds}i_{ds} + v_{es}i_{es} + \\ \left(v_{as}i_{bs} + v_{as}i_{es} + v_{bs}i_{as} + v_{bs}i_{cs} + v_{cs}i_{bs} + v_{cs}i_{ds} + v_{ds}i_{cs} + v_{ds}i_{es} + v_{es}i_{as} + v_{es}i_{ds}\right)\cos\left(\frac{4\pi}{5}\right) \\ + \left(v_{as}i_{cs} + v_{as}i_{ds} + v_{bs}i_{ds} + v_{bs}i_{es} + v_{cs}i_{as} + v_{cs}i_{es} + v_{ds}i_{as} + v_{ds}i_{bs} + v_{es}i_{bs} + v_{es}i_{cs}\right)\cos\left(\frac{2\pi}{5}\right) + \\ \left[\begin{array}{l} v_{as}i_{as} + v_{bs}i_{bs} + v_{cs}i_{cs} + v_{ds}i_{ds} + v_{es}i_{es} + v_{as}i_{bs} + v_{as}i_{cs} + v_{es}i_{bs} + \\ v_{as}i_{ds} + v_{as}i_{es} + v_{bs}i_{as} + v_{bs}i_{cs} + v_{bs}i_{ds} + v_{bs}i_{es} + v_{ds}i_{es} + v_{es}i_{as} + \\ v_{cs}i_{as} + v_{cs}i_{bs} + v_{cs}i_{ds} + v_{cs}i_{es} + v_{ds}i_{as} + v_{ds}i_{bs} + v_{ds}i_{cs} + v_{es}i_{cs} + v_{es}i_{ds} \end{array}\right] \end{array}\right] \tag{2.70}$$

Combining like terms, Equation (2.70) results into

$$P = \frac{2}{5}\left[\begin{array}{l} 3\left[v_{as}i_{as} + v_{bs}i_{bs} + v_{cs}i_{cs} + v_{ds}i_{ds} + v_{es}i_{es}\right] + v_{as}\left(i_{bs} + i_{cs} + i_{ds} + i_{es}\right) + v_{bs}\left(i_{as} + i_{cs} + i_{ds} + i_{es}\right) + \\ v_{cs}\left(i_{as} + i_{bs} + i_{ds} + i_{es}\right) + v_{ds}\left(i_{as} + i_{bs} + i_{cs} + i_{es}\right) + v_{es}\left(i_{as} + i_{bs} + i_{cs} + i_{ds}\right) + \\ \left(\begin{array}{l} v_{as}\left(i_{bs} + i_{cs} + i_{ds} + i_{es}\right) + v_{bs}\left(i_{as} + i_{cs} + i_{ds} + i_{es}\right) + v_{cs}\left(i_{as} + i_{bs} + i_{ds} + i_{es}\right) + \\ v_{ds}\left(i_{as} + i_{bs} + i_{cs} + i_{es}\right) + v_{es}\left(i_{ds} + i_{as} + i_{bs} + i_{cs}\right) \end{array}\right)\cos\left(\frac{2\pi}{5}\right) + \\ \left(\begin{array}{l} v_{as}\left(i_{bs} + i_{cs} + i_{ds} + i_{es}\right) + v_{bs}\left(i_{as} + i_{cs} + i_{ds} + i_{es}\right) + v_{cs}\left(i_{as} + i_{bs} + i_{ds} + i_{es}\right) + \\ v_{ds}\left(i_{as} + i_{bs} + i_{cs} + i_{es}\right) + v_{es}\left(i_{as} + i_{bs} + i_{cs} + i_{ds}\right) \end{array}\right)\cos\left(\frac{4\pi}{5}\right) \end{array}\right] \tag{2.71}$$

Therefore, Equation (2.71) will give the general expression for the real power in a five-phase system.

Now consider a balanced system, such that

$$v_{as} + v_{bs} + v_{cs} + v_{ds} + v_{es} = 0 \tag{2.72}$$

$$i_{as} + i_{bs} + i_{cs} + i_{ds} + i_{es} = 0 \tag{2.73}$$

Thus

$$-i_{as} = i_{bs} + i_{cs} + i_{ds} + i_{es} \tag{2.74}$$

$$-i_{bs} = i_{as} + +i_{cs} + i_{ds} + i_{es} \tag{2.75}$$

$$-i_{cs} = i_{as} + i_{bs} + i_{ds} + i_{es} \tag{2.76}$$

$$-i_{ds} = i_{as} + i_{bs} + i_{cs} + i_{es} \tag{2.77}$$

$$-i_{es} = i_{as} + i_{bs} + i_{cs} + i_{ds} \tag{2.78}$$

Substituting Equations (2.74) trough (7.78) into Equation (2.71), gives

$$P = \frac{\kappa}{5}\left[\left(v_{as}i_{as} + v_{bs}i_{bs} + v_{cs}i_{cs} + v_{ds}i_{ds} + v_{es}i_{es}\right)\right] \tag{2.79}$$

where

$$\kappa = 2 - \cos\left(\frac{2\pi}{5}\right) - \cos\left(\frac{4\pi}{5}\right) = \frac{5}{2} \tag{2.80}$$

Therefore, substituting for the result of Equation (2.80) into Equation (2.79) results into

$$P = \frac{2}{5}\frac{5}{2}\left[\left(v_{as}i_{as} + v_{bs}i_{bs} + v_{cs}i_{cs} + v_{ds}i_{ds} + v_{es}i_{es}\right)\right] \tag{2.81}$$

$$P = \left[v_{as}i_{as} + v_{bs}i_{bs} + v_{cs}i_{cs} + v_{ds}i_{ds} + v_{es}i_{es}\right] \tag{2.82}$$

Equation (2.82) gives the expression for the real power in a balanced five-phase system when the condition given in Equation (2.73) is satisfied. For the general case, the real (active) power will be given by Equation (2.71).

2.3.2.2 Total reactive power in a five-phase system. This is obtained by adding together the powers given by Equations (2.56) and (2.65). Thus

$$Q = Q_{qds} + Q_{xys} \tag{2.83}$$

$$Q = \frac{2}{5}\left[\begin{array}{l} \begin{pmatrix} v_{as}i_{es} - v_{es}i_{as} + v_{bs}i_{as} - v_{as}i_{bs} + v_{cs}i_{bs} - v_{bs}i_{cs} + \\ v_{ds}i_{cs} - v_{cs}i_{ds} + v_{es}i_{ds} - v_{ds}i_{es} \end{pmatrix} \sin\left(\frac{2\pi}{5}\right) + \\ \begin{pmatrix} v_{as}i_{ds} - v_{ds}i_{as} + v_{cs}i_{as} - v_{as}i_{cs} + v_{bs}i_{es} - v_{es}i_{bs} + \\ v_{es}i_{cs} - v_{cs}i_{es} + v_{ds}i_{bs} - v_{bs}i_{ds} \end{pmatrix} \sin\left(\frac{4\pi}{5}\right) + \\ \begin{pmatrix} v_{bs}i_{as} - v_{as}i_{bs} + v_{as}i_{es} - v_{es}i_{as} + v_{cs}i_{bs} - v_{bs}i_{cs} + \\ v_{ds}i_{cs} - v_{cs}i_{ds} + v_{es}i_{ds} - v_{ds}i_{es} \end{pmatrix} \sin\left(\frac{4\pi}{5}\right) + \\ \begin{pmatrix} v_{as}i_{cs} - v_{cs}i_{as} + v_{ds}i_{as} - v_{as}i_{ds} + v_{bs}i_{ds} - v_{ds}i_{bs} + \\ v_{es}i_{bs} - v_{bs}i_{es} + v_{cs}i_{es} - v_{es}i_{cs} \end{pmatrix} \sin\left(\frac{2\pi}{5}\right) \end{array}\right] \tag{2.84}$$

Combining like terms of Equation (2.84) gives

$$Q = \frac{1}{5}\left[\begin{array}{l} \begin{pmatrix} v_{as}i_{es} - v_{es}i_{as} + v_{bs}i_{as} - v_{as}i_{bs} + v_{cs}i_{bs} - v_{bs}i_{cs} + \\ v_{ds}i_{cs} - v_{cs}i_{ds} + v_{es}i_{ds} - v_{ds}i_{es} \end{pmatrix} \left[\sin\left(\frac{2\pi}{5}\right) + \sin\left(\frac{4\pi}{5}\right)\right] + \\ \begin{pmatrix} v_{as}i_{cs} - v_{cs}i_{as} + v_{bs}i_{ds} - v_{ds}i_{bs} + v_{cs}i_{es} - v_{es}i_{cs} + \\ v_{ds}i_{as} - v_{as}i_{ds} + v_{es}i_{bs} - v_{bs}i_{es} \end{pmatrix} \left[\sin\left(\frac{2\pi}{5}\right) - \sin\left(\frac{4\pi}{5}\right)\right] \end{array}\right] \tag{2.85}$$

Equation (2.85) gives the expression for determining the reactive power of a five-phase system.

Thus if the phase voltages and phase currents are known for five-phase system, then the real and reactive powers can be readily obtained by using Equations (2.71) and (2.85), respectively. For a special case when the system voltages and currents are balanced, the real power can be obtained from Equation (2.82).

2.4 Seven-phase System

When the analysis presented in the previous sections is extended to a seven-phase system, the respective power expressions can be obtained. The voltage and current matrices are given as $v = \begin{bmatrix} v_{as} & v_{bs} & v_{cs} & v_{ds} & v_{es} & v_{fs} & v_{gs} \end{bmatrix}^T$ and $i = \begin{bmatrix} i_{as} & i_{bs} & i_{cs} & i_{ds} & i_{es} & i_{fs} & i_{gs} \end{bmatrix}^T$.

The complex transformed voltage vectors and currents used for seven phase are

$$v_{qds} = \sqrt{\frac{2}{7}}\left[v_{as} + av_{bs} + a^2 v_{cs} + a^3 v_{ds} + a^{-3} v_{es} + a^{-2} v_{fs} + a^{-1} v_{gs}\right] \tag{2.86}$$

$$v_{xy1s} = \sqrt{\frac{2}{7}}\left[v_{as} + a^2 v_{bs} + a^{-3} v_{cs} + a^{-1} v_{ds} + av_{es} + a^3 v_{fs} + a^{-2} v_{gs}\right] \tag{2.87}$$

$$v_{xy2s} = \sqrt{\frac{2}{7}}\left[v_{as} + a^3 v_{bs} + a^{-1} v_{cs} + a^2 v_{ds} + a^{-2} v_{es} + av_{fs} + a^{-3} v_{gs}\right] \tag{2.88}$$

$$v_{xy3s} = \sqrt{\frac{2}{7}}\left[v_{as} + a^{-3} v_{bs} + a^1 v_{cs} + a^{-2} v_{ds} + a^2 v_{es} + a^{-1} v_{fs} + a^3 v_{gs}\right] \tag{2.88}$$

$$v_{xy4s} = \sqrt{\frac{2}{7}}\left[v_{as} + a^{-2} v_{bs} + a^3 v_{cs} + a^1 v_{ds} + a^{-1} v_{es} + a^{-3} v_{fs} + a^2 v_{gs}\right] \tag{2.89}$$

$$v_{xy5s} = \sqrt{\frac{2}{7}}\left[v_{as} + a^{-1} v_{bs} + a^{-2} v_{cs} + a^{-3} v_{ds} + a^3 v_{es} + a^2 v_{fs} + a^1 v_{gs}\right] \tag{2.90}$$

$$v_{os} = \sqrt{\frac{2}{7}}\left[v_{as} + v_{bs} + v_{cs} + v_{ds} + v_{es} + v_{fs} + v_{gs}\right] \tag{2.91}$$

The currents are given by

$$i_{qds} = \sqrt{\frac{2}{7}}\left[i_{as} + ai_{bs} + a^2 i_{cs} + a^3 i_{ds} + a^{-3} i_{es} + a^{-2} i_{fs} + a^{-1} i_{gs}\right] \tag{2.92}$$

$$i_{xy1s} = \sqrt{\frac{2}{7}}\left[i_{as} + a^2 i_{bs} + a^{-3} i_{cs} + a^{-1} i_{ds} + ai_{es} + a^3 i_{fs} + a^{-2} i_{gs}\right] \tag{2.93}$$

$$i_{xy2s} = \sqrt{\frac{2}{7}}\left[i_{as} + a^3 i_{bs} + a^{-1} i_{cs} + a^2 i_{ds} + a^{-2} i_{es} + ai_{fs} + a^{-3} i_{gs}\right] \tag{2.94}$$

$$i_{xy3s} = \sqrt{\frac{2}{7}}\left[i_{as} + a^{-3} i_{bs} + a^1 i_{cs} + a^{-2} i_{ds} + a^2 i_{es} + a^{-1} i_{fs} + a^3 i_{gs}\right] \tag{2.95}$$

$$i_{xy4s} = \sqrt{\frac{2}{7}}\left[i_{as} + a^{-2}i_{bs} + a^{3}i_{cs} + a^{1}i_{ds} + a^{-1}i_{es} + a^{-3}i_{fs} + a^{2}i_{gs}\right] \tag{2.96}$$

$$i_{xy5s} = \sqrt{\frac{2}{7}}\left[i_{as} + a^{-1}i_{bs} + a^{-2}i_{cs} + a^{-3}i_{ds} + a^{3}i_{es} + a^{2}i_{fs} + a^{1}i_{gs}\right] \tag{2.97}$$

$$i_{os} = \sqrt{\frac{2}{7}}\left[i_{as} + i_{bs} + i_{cs} + i_{ds} + i_{es} + i_{fs} + i_{gs}\right] \tag{2.98}$$

The conjugates of the currents are given by

$$i^{*}_{qds} = \sqrt{\frac{2}{7}}\left[i_{as} + a^{-1}i_{bs} + a^{-2}i_{cs} + a^{-3}i_{ds} + a^{3}i_{es} + a^{2}i_{fs} + a^{1}i_{gs}\right] \tag{2.100}$$

$$i^{*}_{xy1s} = \sqrt{\frac{2}{7}}\left[i_{as} + a^{-2}i_{bs} + a^{3}i_{cs} + a^{1}i_{ds} + a^{-1}i_{es} + a^{-3}i_{fs} + a^{2}i_{gs}\right] \tag{2.101}$$

$$i^{*}_{xy2s} = \sqrt{\frac{2}{7}}\left[i_{as} + a^{-3}i_{bs} + a^{1}i_{cs} + a^{-2}i_{ds} + a^{2}i_{es} + a^{-1}i_{fs} + a^{3}i_{gs}\right] \tag{2.102}$$

$$i_{os} = \sqrt{\frac{2}{7}}\left[i_{as} + i_{bs} + i_{cs} + i_{ds} + i_{es} + i_{fs} + i_{gs}\right] \tag{2.103}$$

The complex power is given by

$$S = v_{qds}i^{*}_{qds} + v_{xy1s}i^{*}_{xy1s} + v_{xy2s}i^{*}_{xy2s} + v_{os}i^{*}_{os} \tag{2.104}$$

The general expression for the real power in the seven-phase system is given by

$$P = \frac{2}{7}\left\{\begin{array}{l} 4\left[v_{as}i_{as} + v_{bs}i_{bs} + v_{cs}i_{cs} + v_{ds}i_{ds} + v_{es}i_{es} + v_{fs}i_{fs} + v_{gs}i_{gs}\right] + \\ \frac{1}{2}v_{as}\left(i_{bs} + i_{cs} + i_{ds} + i_{es} + i_{fs} + i_{gs}\right) + \frac{1}{2}v_{bs}\left(i_{as} + i_{cs} + i_{ds} + i_{es} + i_{fs} + i_{gs}\right) \\ + \frac{1}{2}v_{cs}\left(i_{as} + i_{bs} + i_{ds} + i_{es} + i_{fs} + i_{gs}\right) + \frac{1}{2}v_{ds}\left(i_{as} + i_{bs} + i_{cs} + i_{es} + i_{fs} + i_{gs}\right) + \\ \frac{1}{2}v_{es}\left(i_{as} + i_{bs} + i_{cs} + i_{ds} + i_{fs} + i_{gs}\right) + \frac{1}{2}v_{fs}\left(i_{as} + i_{bs} + i_{cs} + i_{ds} + i_{es} + i_{gs}\right) + \\ \frac{1}{2}v_{gs}\left(i_{as} + i_{bs} + i_{cs} + i_{ds} + i_{es} + i_{fs}\right) \end{array}\right\} \tag{2.105}$$

Now, if the system is balanced and the machine is star-connected, then

$$i_{as}+i_{bs}+i_{cs}+i_{ds}+i_{es}+i_{fs}+i_{gs}=0 \tag{2.106}$$

Substituting Equation (2.106) into Equation (2.105), results into

$$P=v_{as}i_{as}+v_{bs}i_{bs}+v_{cs}i_{cs}+v_{ds}i_{ds}+v_{es}i_{es}+v_{fs}i_{fs}+v_{gs}i_{gs} \tag{2.107}$$

The general expression for the reactive power in the seven-phase system is given by

$$Q=\frac{2}{7}\left\{\begin{array}{l}
\sin\left(\frac{2\pi}{7}\right)\left(\begin{array}{l}
(v_{as}i_{gs}-v_{gs}i_{as})+(v_{bs}i_{as}-v_{as}i_{bs})+(v_{cs}i_{bs}-v_{bs}i_{cs})+(v_{ds}i_{cs}-v_{cs}i_{ds})+\\
(v_{es}i_{ds}-v_{ds}i_{es})+(v_{fs}i_{es}-v_{es}i_{fs})+(v_{gs}i_{fs}-v_{fs}i_{gs})+(v_{as}i_{ds}-v_{ds}i_{as})+\\
(v_{bs}i_{es}-v_{es}i_{bs})+(v_{cs}i_{fs}-v_{fs}i_{cs})+(v_{ds}i_{gs}-v_{gs}i_{ds})+(v_{es}i_{as}-v_{as}i_{es})+\\
(v_{fs}i_{bs}-v_{bs}i_{fs})+(v_{gs}i_{cs}-v_{cs}i_{gs})+(v_{as}i_{cs}-v_{cs}i_{as})+(v_{bs}i_{ds}-v_{ds}i_{bs})+\\
(v_{cs}i_{es}-v_{es}i_{cs})+(v_{ds}i_{fs}-v_{fs}i_{ds})+(v_{es}i_{gs}-v_{gs}i_{es})+(v_{fs}i_{as}-v_{as}i_{fs})+\\
(v_{gs}i_{bs}-v_{bs}i_{gs})
\end{array}\right)+\\
\sin\left(\frac{4\pi}{7}\right)\left(\begin{array}{l}
(v_{as}i_{fs}-v_{fs}i_{as})+(v_{bs}i_{gs}-v_{gs}i_{bs})+(v_{cs}i_{as}-v_{as}i_{cs})+(v_{ds}i_{bs}-v_{bs}i_{ds})+\\
(v_{es}i_{cs}-v_{cs}i_{es})+(v_{fs}i_{ds}-v_{ds}i_{fs})+(v_{gs}i_{es}-v_{es}i_{gs})+(v_{as}i_{gs}-v_{gs}i_{as})+\\
(v_{bs}i_{as}-v_{as}i_{bs})+(v_{cs}i_{bs}-v_{bs}i_{cs})+(v_{ds}i_{cs}-v_{cs}i_{ds})+(v_{es}i_{ds}-v_{ds}i_{es})+\\
(v_{fs}i_{es}-v_{es}i_{fs})+(v_{gs}i_{fs}-v_{fs}i_{gs})+(v_{as}i_{es}-v_{es}i_{as})+(v_{bs}i_{fs}-v_{fs}i_{bs})+\\
(v_{cs}i_{gs}-v_{gs}i_{cs})+(v_{ds}i_{as}-v_{as}i_{ds})+(v_{es}i_{bs}-v_{bs}i_{es})+(v_{fs}i_{cs}-v_{cs}i_{fs})+\\
(v_{gs}i_{ds}-v_{ds}i_{gs})
\end{array}\right)+\\
\sin\left(\frac{6\pi}{7}\right)\left(\begin{array}{l}
(v_{as}i_{es}-v_{es}i_{as})+(v_{bs}i_{fs}-v_{fs}i_{bs})+(v_{cs}i_{gs}-v_{gs}i_{cs})+(v_{ds}i_{as}-v_{as}i_{ds})+\\
(v_{es}i_{bs}-v_{bs}i_{es})+(v_{fs}i_{cs}-v_{cs}i_{fs})+(v_{gs}i_{ds}-v_{ds}i_{gs})+(v_{as}i_{cs}-v_{cs}i_{as})+\\
(v_{bs}i_{ds}-v_{ds}i_{bs})+(v_{cs}i_{es}-v_{es}i_{cs})+(v_{ds}i_{fs}-v_{fs}i_{ds})+(v_{es}i_{gs}-v_{gs}i_{es})+\\
(v_{fs}i_{as}-v_{as}i_{fs})+(v_{gs}i_{bs}-v_{bs}i_{gs})+(v_{as}i_{gs}-v_{gs}i_{as})+(v_{bs}i_{as}-v_{as}i_{bs})+\\
(v_{cs}i_{bs}-v_{bs}i_{cs})+(v_{ds}i_{cs}-v_{cs}i_{ds})+(v_{es}i_{ds}-v_{ds}i_{es})+(v_{fs}i_{es}-v_{es}i_{fs})+\\
(v_{gs}i_{fs}-v_{fs}i_{gs})
\end{array}\right)
\end{array}\right\} \tag{2.108}$$

2.5 Modulation Technique for Multi-phase Converters

The highest number of power that can be obtained from the conventional electrical power system is three-phase. Due to the advancement in power electronic devices, converters of many phases can be readily available and thus convert the available three-phase to any number of output phases that are require to supply the multi-phase machinery. Figure 2.1 shows a schematic diagram of a five-phase voltage source converter. The switching of the devices are described by switching functions which take the values of one and zero when the devices are turned on or off, respectively.

The switching functions of the top devices are S_{ip} $(i = a, b, c, d, e)$. These are complimentary with the switching functions of the bottom devices. The voltages applied to the load are given by

$$\frac{v_d}{2}\left(2s_{ip} - 1\right) = v_{in} + v_{no} \tag{2.109}$$

The switching function can be averaged and given by

$$s_{ip} = \frac{1}{2}\left(1 + m_{ip}\right) \tag{2.110}$$

where m_{ip} is the modulation signal of the i^{th} inverter leg.

v_{in} is the i^{th} phase voltage and v_{no} is the neutral voltage.

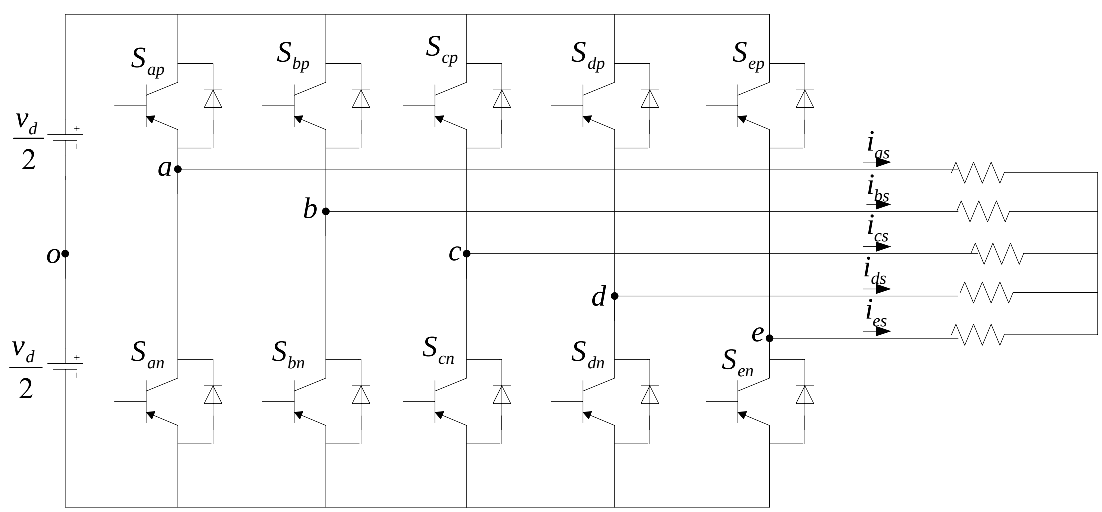

Figure 2.1 Schematic diagram of a five-phase voltage source converter.

To synthesize the desired phase voltages, the modulation signals are compared with a high frequency triangle waveform using the sine-triangle carrier-based pulse width modulation (PWM). The modulation signals are given by

$$m_{ip} = \frac{2}{v_d}\left(v_{in} + v_{no}\right) \tag{2.111}$$

For better performance of the converter, the neutral voltage v_{no} can be selected to take any best form, as it is indeterminate and can take any realistic values [2.2-2.4].

A five-phase voltage source inverter with an input dc voltage given as v_d has 32 switching modes, 30 of which are active and the other two are null modes. The converter is to generate five phase voltages.

The load voltage Equations of the five-phase converter expressed in terms of the existence functions and input DC voltage v_d are given as

$$v_{io} = \frac{v_d}{2}\left(2S_{ip} - 1\right) = v_{in} + v_{no}\,,\ \ i = a,\ b,\ c,\ d,\ e \tag{2.112}$$

$$v_{ao} = \frac{v_d}{2}\left(S_{ap} - S_{an}\right) = \frac{v_d}{2}\left(S_{ap} - \left(1 - S_{ap}\right)\right) = \frac{v_d}{2}\left(2S_{ap} - 1\right) = v_{an} + v_{no} \tag{2.113}$$

Similarly,

$$v_{bo} = \frac{v_d}{2}\left(2S_{bp} - 1\right) = v_{bn} + v_{no} \tag{2.114}$$

$$v_{co} = \frac{v_d}{2}\left(2S_{cp} - 1\right) = v_{cn} + v_{no} \tag{2.115}$$

$$v_{do} = \frac{v_d}{2}\left(2S_{dp} - 1\right) = v_{dn} + v_{no} \tag{2.116}$$

$$v_{eo} = \frac{v_d}{2}\left(2S_{ep} - 1\right) = v_{en} + v_{no} \tag{2.117}$$

$$v_{ao} + v_{bo} + v_{co} + v_{do} + v_{eo} = v_{an} + v_{bn} + v_{cn} + v_{dn} + v_{en} + 5v_{no} \tag{2.118}$$

and

$$v_{ao} + v_{bo} + v_{co} + v_{do} + v_{eo} = \begin{bmatrix} \frac{v_d}{2}\left(2S_{ap} - 1\right) + \frac{v_d}{2}\left(2S_{bp} - 1\right) + \frac{v_d}{2}\left(2S_{cp} - 1\right) \\ + \frac{v_d}{2}\left(2S_{dp} - 1\right) + \frac{v_d}{2}\left(2S_{ep} - 1\right) \end{bmatrix} \tag{2.119}$$

For balanced five-phase system,

$$v_{an} + v_{bn} + v_{cn} + v_{dn} + v_{en} = 0 \tag{2.120}$$

Therefore,

$$v_{ao} + v_{bo} + v_{co} + v_{do} + v_{eo} = 5v_{no} \tag{2.121}$$

$$5v_{no} = \frac{v_d}{2}\left(2S_{ap} - 1\right) + \frac{v_d}{2}\left(2S_{bp} - 1\right) + \frac{v_d}{2}\left(2S_{cp} - 1\right) + \frac{v_d}{2}\left(2S_{dp} - 1\right) + \frac{v_d}{2}\left(2S_{ep} - 1\right) \tag{2.122}$$

From the transformation given in (2.4d), for the five phase balanced variables transformed f_a, f_b, f_c, f_d, f_e, the generalized *qdxy12os* arbitrary reference frame transformed variables expressed in complex-variable form are given by

$$T_5 = \sqrt{\frac{2}{5}} \begin{bmatrix} 1 & 1 & 1 & 1 & 1 \\ 1 & a & a^2 & a^{-2} & a^{-1} \\ 1 & a^2 & a^{-1} & a & a^{-2} \\ 1 & a^{-2} & a & a^{-1} & a^2 \\ 1 & a^{-1} & a^{-2} & a^2 & a \end{bmatrix} \qquad T_5^{-1} = \sqrt{\frac{2}{5}} \begin{bmatrix} 1 & 1 & 1 & 1 & 1 \\ 1 & a^{-1} & a^{-2} & a^2 & a^1 \\ 1 & a^{-2} & a & a^{-1} & a^2 \\ 1 & a^2 & a^{-1} & a & a^{-2} \\ 1 & a & a^2 & a^{-2} & a^{-1} \end{bmatrix} \tag{2.4d}$$

$$f_{os} = \sqrt{\frac{2}{5}}\left[f_{as} + f_{bs} + f_{cs} + f_{ds} + f_{es} \right] \tag{2.123}$$

$$f_{qds} = \sqrt{\frac{2}{5}}\left[f_{as} + af_{bs} + a^2 f_{cs} + a^{-2} f_{ds} + a^{-1} f_{es} \right] \tag{2.124}$$

$$f_{xys1} = \sqrt{\frac{2}{5}}\left[f_{as} + a^2 f_{bs} + a^{-1} f_{cs} + af_{ds} + a^{-1} f_{es} \right] \tag{2.125}$$

$$f_{xys2} = \sqrt{\frac{2}{5}}\left[f_{as} + a^{-2} f_{bs} + af_{cs} + a^{-1} f_{ds} + a^2 f_{es}\right] \tag{2.126}$$

$$f_{xys3} = \sqrt{\frac{2}{5}}\left[f_{as} + a^{-1} f_{bs} + a^{-2} f_{cs} + a^2 f_{ds} + af_{es}\right] \tag{2.127}$$

Substituting Equation (2.122) into Equations (2.113) through (2.117), the phase voltages can be obtained as

$$v_{an} = \frac{v_d}{5}\left(4S_{ap} - S_{bp} - S_{cp} - S_{dp} - S_{ep}\right) \tag{2.128}$$

$$v_{bn} = \frac{v_d}{5}\left(-S_{ap} + 4S_{bp} - S_{cp} - S_{dp} - S_{ep}\right) \tag{2.129}$$

$$v_{cn} = \frac{v_d}{5}\left(-S_{ap} - S_{bp} + 4S_{cp} - S_{dp} - S_{ep}\right) \tag{2.130}$$

$$v_{dn} = \frac{v_d}{5}\left(-S_{ap} - S_{bp} - S_{cp} + 4S_{dp} - S_{ep}\right) \tag{2.131}$$

$$v_{en} = \frac{v_d}{5}\left(-S_{ap} - S_{bp} - S_{cp} - S_{dp} + 4S_{ep}\right) \tag{2.132}$$

Substituting the states into Equations (2.128) through (2.132) gives the respective inverter output phase voltage for each mode as presented in the Table 2.1 below.

Table 2.1 Phase voltages for the five-phase inverter

MODE	S_{ap}	S_{bp}	S_{cp}	S_{dp}	S_{ep}	v_{an}	v_{bn}	v_{cn}	v_{dn}	v_{en}
1	0	0	0	0	0	0	0	0	0	0
2	0	0	0	0	1	-0.2Vd	-0.2Vd	-0.2Vd	-0.2Vd	0.8Vd
3	0	0	0	1	0	-0.2Vd	-0.2Vd	-0.2Vd	0.8Vd	-0.2Vd
4	0	0	0	1	1	-0.4Vd	-0.4Vd	-0.4Vd	0.6Vd	0.6Vd
5	0	0	1	0	0	-0.2Vd	-0.2Vd	0.8Vd	-0.2Vd	-0.2Vd
6	0	0	1	0	1	-0.4Vd	-0.4Vd	0.6Vd	-0.4Vd	0.6Vd
7	0	0	1	1	0	-0.4Vd	-0.4Vd	0.6Vd	0.6Vd	-0.4Vd
8	0	0	1	1	1	-0.6Vd	-0.6Vd	0.4Vd	0.4Vd	0.4Vd
9	0	1	0	0	0	-0.2Vd	0.8Vd	-0.2Vd	-0.2Vd	-0.2Vd
10	0	1	0	0	1	-0.4Vd	0.6Vd	-0.4Vd	-0.4Vd	0.6Vd
11	0	1	0	1	0	-0.4Vd	0.6Vd	-0.4Vd	0.6Vd	-0.4Vd
12	0	1	0	1	1	-0.6Vd	0.4Vd	-0.6Vd	0.4Vd	0.4Vd
13	0	1	1	0	0	-0.4Vd	0.6Vd	0.6Vd	-0.4Vd	-0.4Vd

Table 2.1 continued

MODE	S_{ap}	S_{bp}	S_{cp}	S_{dp}	S_{ep}	v_{an}	v_{bn}	v_{cn}	v_{dn}	v_{en}
14	0	1	1	0	1	-0.6Vd	0.4Vd	0.4Vd	-0.6Vd	0.4Vd
15	0	1	1	1	0	-0.6Vd	0.4Vd	0.4Vd	0.4Vd	-0.6Vd
16	0	1	1	1	1	-0.8Vd	0.2Vd	0.2Vd	0.2Vd	0.2Vd
17	1	0	0	0	0	0.8Vd	-0.2Vd	-0.2Vd	-0.2Vd	-0.2Vd
18	1	0	0	0	1	0.6Vd	-0.4Vd	-0.4Vd	-0.4Vd	0.6Vd
19	1	0	0	1	0	0.6Vd	-0.4Vd	-0.4Vd	0.6Vd	-0.4Vd
20	1	0	0	1	1	0.4Vd	-0.6Vd	-0.6Vd	0.4Vd	0.4Vd
21	1	0	1	0	0	0.6Vd	-0.4Vd	0.6Vd	-0.4Vd	-0.4Vd
22	1	0	1	0	1	0.4Vd	-0.6Vd	0.4Vd	-0.6Vd	0.4Vd
23	1	0	1	1	0	0.4Vd	-0.6Vd	0.4Vd	0.4Vd	-0.6Vd
24	1	0	1	1	1	0.2Vd	-0.8Vd	0.2Vd	0.2Vd	0.2Vd
25	1	1	0	0	0	0.6Vd	0.6Vd	-0.4Vd	-0.4Vd	-0.4Vd
26	1	1	0	0	1	0.4Vd	0.4Vd	-0.6Vd	-0.6Vd	0.4Vd

Table 2.1 continued

MODE	S_{ap}	S_{bp}	S_{cp}	S_{dp}	S_{ep}	v_{an}	v_{bn}	v_{cn}	v_{dn}	v_{en}
27	1	1	0	1	0	0.4Vd	0.4Vd	-0.6Vd	0.4Vd	-0.6Vd
28	1	1	0	1	1	0.2Vd	0.2Vd	-0.8Vd	0.2Vd	0.2Vd
29	1	1	1	0	0	0.4Vd	0.4Vd	0.4Vd	-0.6Vd	-0.6Vd
30	1	1	1	0	1	0.2Vd	0.2Vd	0.2Vd	-0.8Vd	0.2Vd
31	1	1	1	1	0	0.2Vd	0.2Vd	0.2Vd	0.2Vd	-0.8Vd
32	1	1	1	1	1	0	0	0	0	0

Substituting Equations (2.128) through (2.132) into Equations (2.114) through (2.117), the stationary reference frame voltages for each of the four components are calculated. The resulting space vector voltage components for the five-phase voltage source inverter, normalized with respect to the inverter dc link voltage v_d, are shown in Table 2.2. These will generate the space vectors v_{qds} for the fundamental frequency voltages and v_{xy1s} for the third harmonic voltages. It can be easily shown that space vectors v_{xy2s} are the complex conjugates of space vectors v_{xy1s}. Similarly, space vectors v_{xys3} are the complex conjugates of space vectors v_{qds}. Therefore in synthesizing the desired voltage vector, only vectors v_{qds} and v_{xy1} are used.

Table 2.2 Space vector voltage components for the five-phase inverter

MODE	S_{ap}	S_{bp}	S_{cp}	S_{dp}	S_{ep}	v_q (pu)	v_d (pu)	v_{x1} (pu)	v_{y1} (pu)	v_{x2} (pu)	v_{y2} (pu)	v_{x3} (pu)	v_{y3} (pu)	v_{no}
1	0	0	0	0	0	0	0	0	0	0	0	0	0	-0.5
2	0	0	0	0	1	0.0618	-0.1902	-0.1618	-0.1176	-0.1618	0.1176	0.0618	0.1902	-0.3
3	0	0	0	1	0	-0.1618	-0.1176	0.0618	0.1902	0.0618	-0.1902	-0.1618	0.1176	-0.3
4	0	0	0	1	1	-0.1000	-0.3078	-0.1000	0.0727	-0.1	-0.0727	-0.1	0.3078	-0.1
5	0	0	1	0	0	-0.1618	0.1176	0.0618	-0.1902	0.0618	0.1902	-0.1618	-0.1176	-0.3
6	0	0	1	0	1	-0.1000	-0.0727	-0.1000	-0.3078	-0.1	0.3078	-0.1	0.0727	-0.1
7	0	0	1	1	0	-0.3236	0	0.1236	0	0.1236	0	-0.3236	0	-0.1
8	0	0	1	1	1	-0.2618	-0.1902	-0.0382	-0.1176	-0.0382	0.1176	-0.2618	0.1902	0.1
9	0	1	0	0	0	0.0618	0.1902	-0.1618	0.1176	-0.1618	-0.1176	0.0618	-0.1902	-0.3
10	0	1	0	0	1	0.1236	0	-0.3236	0	-0.3236	0	0.1236	0	-0.1
11	0	1	0	1	0	-0.1000	0.0727	-0.1000	0.3078	-0.1	-0.3078	-0.1	-0.0727	-0.1
12	0	1	0	1	1	-0.0382	-0.1176	-0.2618	0.1902	-0.2618	-0.1902	-0.0382	0.1176	0.1
13	0	1	1	0	0	-0.1000	0.3078	-0.1000	-0.0727	-0.1	0.0727	-0.1	-0.3078	-0.1

Table 2.2 continued

MODE	S_{ap}	S_{bp}	S_{cp}	S_{dp}	S_{ep}	v_q (pu)	v_d (pu)	v_{x1} (pu)	v_{y1} (pu)	v_{x2} (pu)	v_{y2} (pu)	v_{x3} (pu)	v_{y3} (pu)	v_{no}
14	0	1	1	0	1	-0.0382	0.1176	-0.2618	-0.1902	-0.2618	0.1902	-0.0382	-0.1176	0.1
15	0	1	1	1	0	-0.2618	0.1902	-0.0382	0.1176	-0.0382	-0.1176	-0.2618	-0.1902	0.1
16	0	1	1	1	1	-0.2000	0	-0.2000	0	-0.2	0	-0.2	0	0.3
17	1	0	0	0	0	0.2000	0	0.2000	0	0.2	0	0.2	0	-0.3
18	1	0	0	0	1	0.2618	-0.1902	0.0382	-0.1176	0.0382	0.1176	0.2618	0.1902	-0.1
19	1	0	0	1	0	0.0382	-0.1176	0.2618	0.1902	0.2618	-0.1902	0.0382	0.1176	-0.1
20	1	0	0	1	1	0.1000	-0.3078	0.1000	0.0727	0.1	-0.0727	0.1	0.3078	0.1
21	1	0	1	0	0	0.0382	0.1176	0.2618	-0.1902	0.2618	0.1902	0.0382	-0.1176	-0.1
22	1	0	1	0	1	0.1000	-0.0727	0.1000	-0.3078	0.1	0.3078	0.1	0.0727	0.1
23	1	0	1	1	0	-0.1236	0	0.3236	0	0.3236	0	-0.1236	0	0.1
24	1	0	1	1	1	-0.0618	-0.1902	0.1618	-0.1176	0.1618	0.1176	-0.0618	0.1902	0.3
25	1	1	0	0	0	0.2618	0.1902	0.0382	0.1176	0.0382	-0.1176	0.2618	-0.1902	-0.1
26	1	1	0	0	1	0.3236	0	-0.1236	0	-0.1236	0	0.3236	0	0.1

Table 2.2 continued

MODE	S_{ap}	S_{bp}	S_{cp}	S_{dp}	S_{ep}	v_q (pu)	v_d (pu)	v_{x1} (pu)	v_{y1} (pu)	v_{x2} (pu)	v_{y2} (pu)	v_{x3} (pu)	v_{y3} (pu)	v_{no}
27	1	1	0	1	0	0.1000	0.0727	0.1000	0.3078	0.1	-0.3078	0.1	-0.0727	0.1
28	1	1	0	1	1	0.1618	-0.1176	-0.0618	0.1902	-0.0618	-0.1902	0.1618	0.1176	0.3
29	1	1	1	0	0	0.1000	0.3078	0.1000	-0.0727	0.1	0.0727	0.1	-0.3078	0.1
30	1	1	1	0	1	0.1618	0.1176	-0.0618	-0.1902	-0.0618	0.1902	0.1618	-0.1176	0.3
31	1	1	1	1	0	-0.0618	0.1902	0.1618	0.1176	0.1618	-0.1176	-0.0618	-0.1902	0.3
32	1	1	1	1	1	0	0	0	0	0	0	0	0	0.5

Figures 2.2 through 2.6 show the voltage space vector diagrams of the five-phase PWM inverter. Whereas Figures 2.2 through 2.5 are obtained directly from Equations (2.114) through (2.117), Figure 2.6 is obtained by using Equation (2.122). The voltage components are normalized with respect to the inverter dc link voltage v_d.

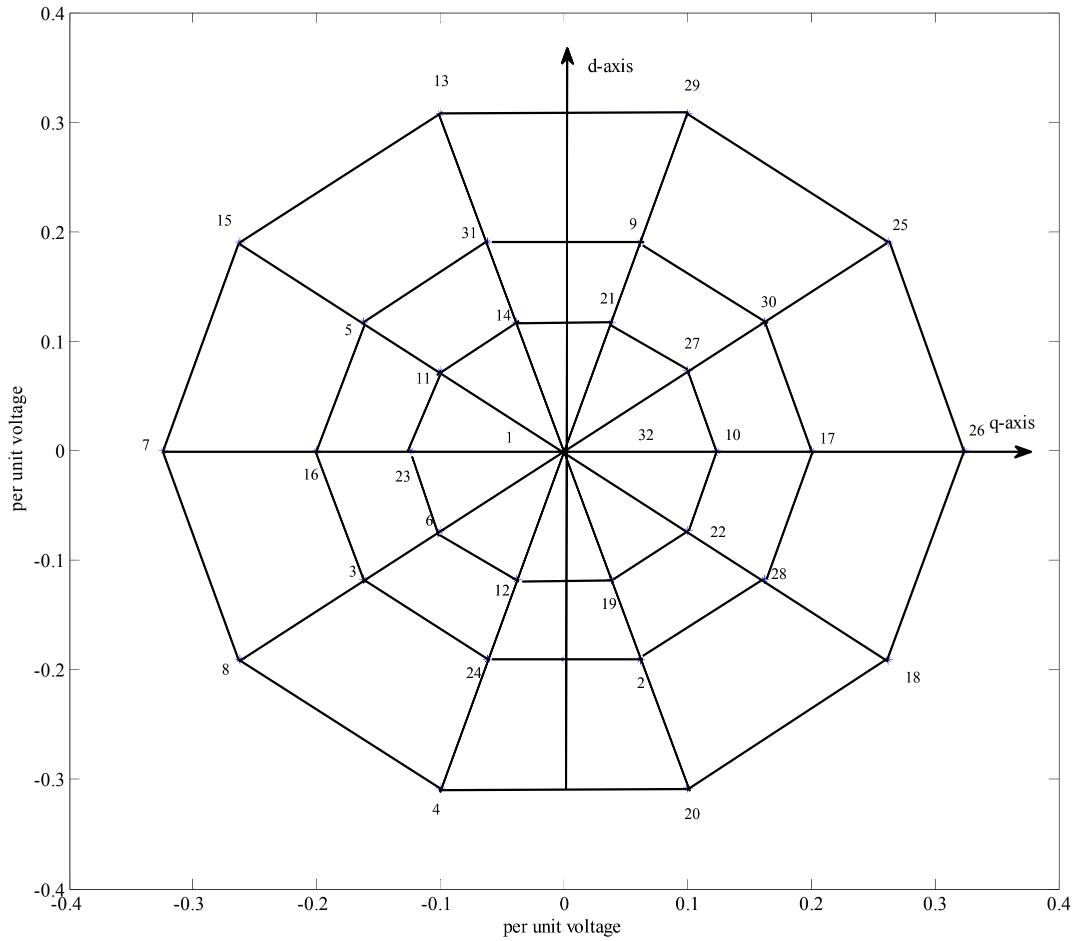

Figure 2.2 Voltage space vector diagram of a five-phase PWM inverter for v_{qds}

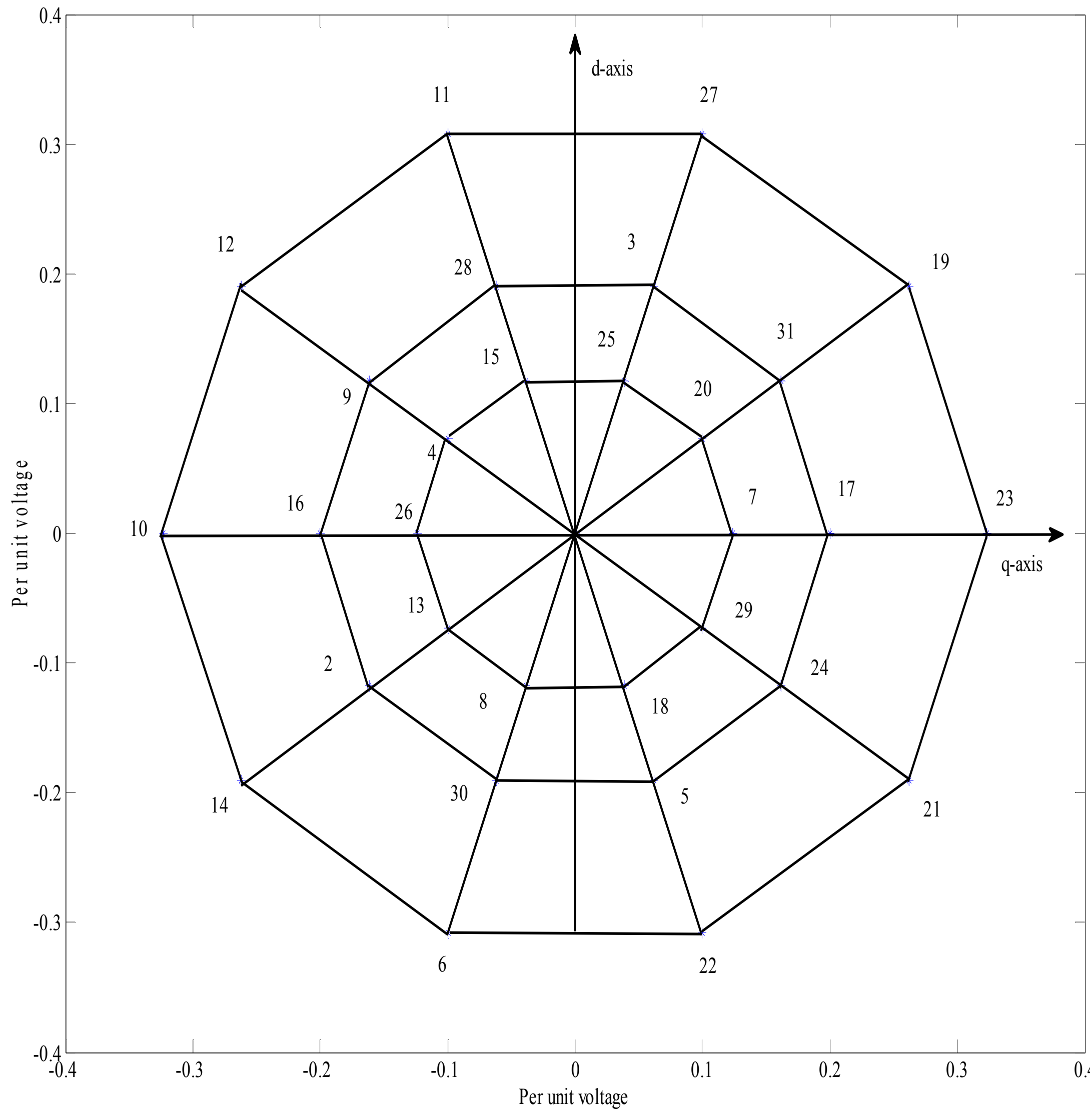

Figure 2.3 Voltage space vector diagram of a five-phase PWM inverter for v_{xy1s}

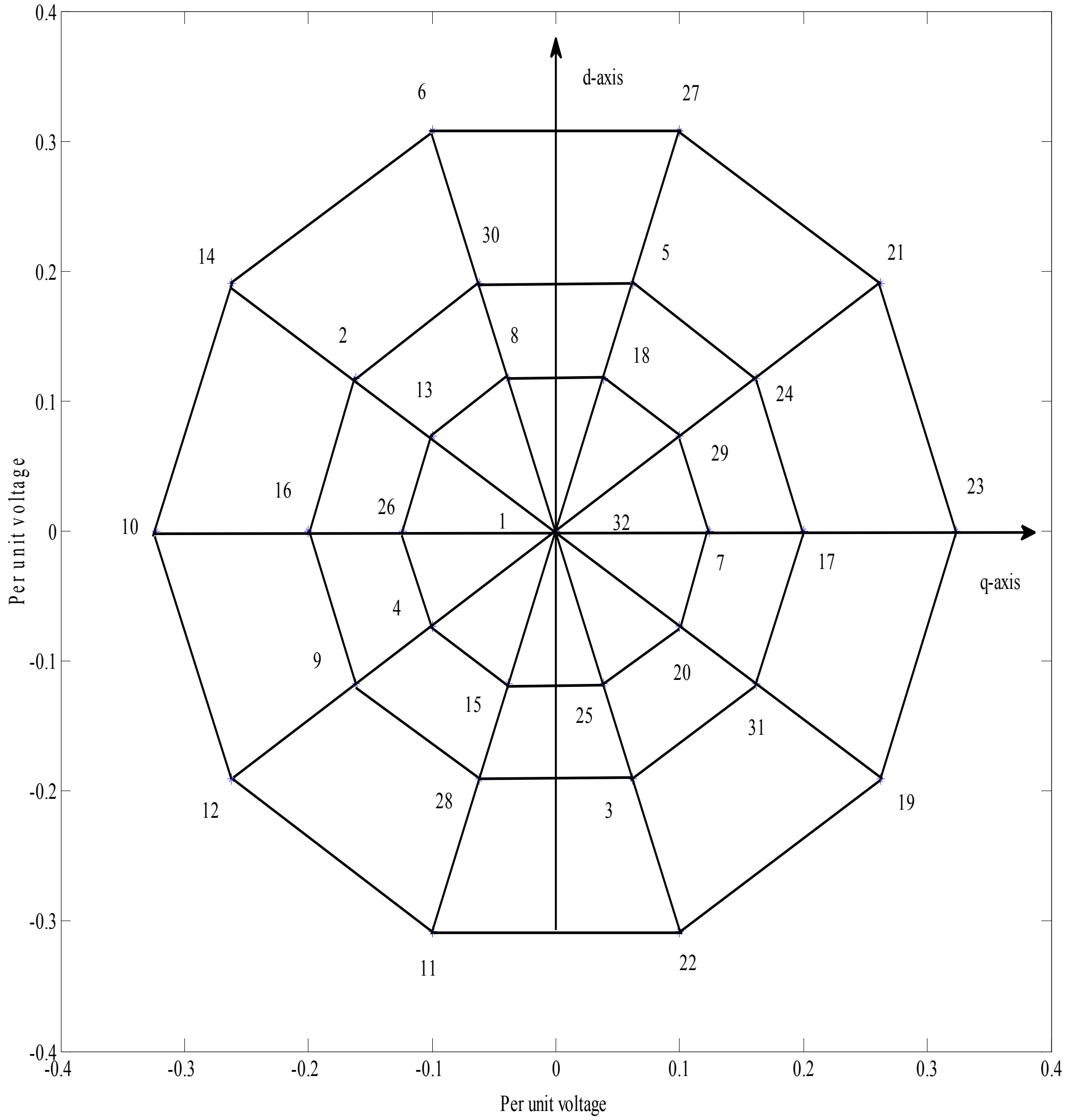

Figure 2.4 Voltage space vector diagram of a five-phase PWM inverter for v_{xy2s}

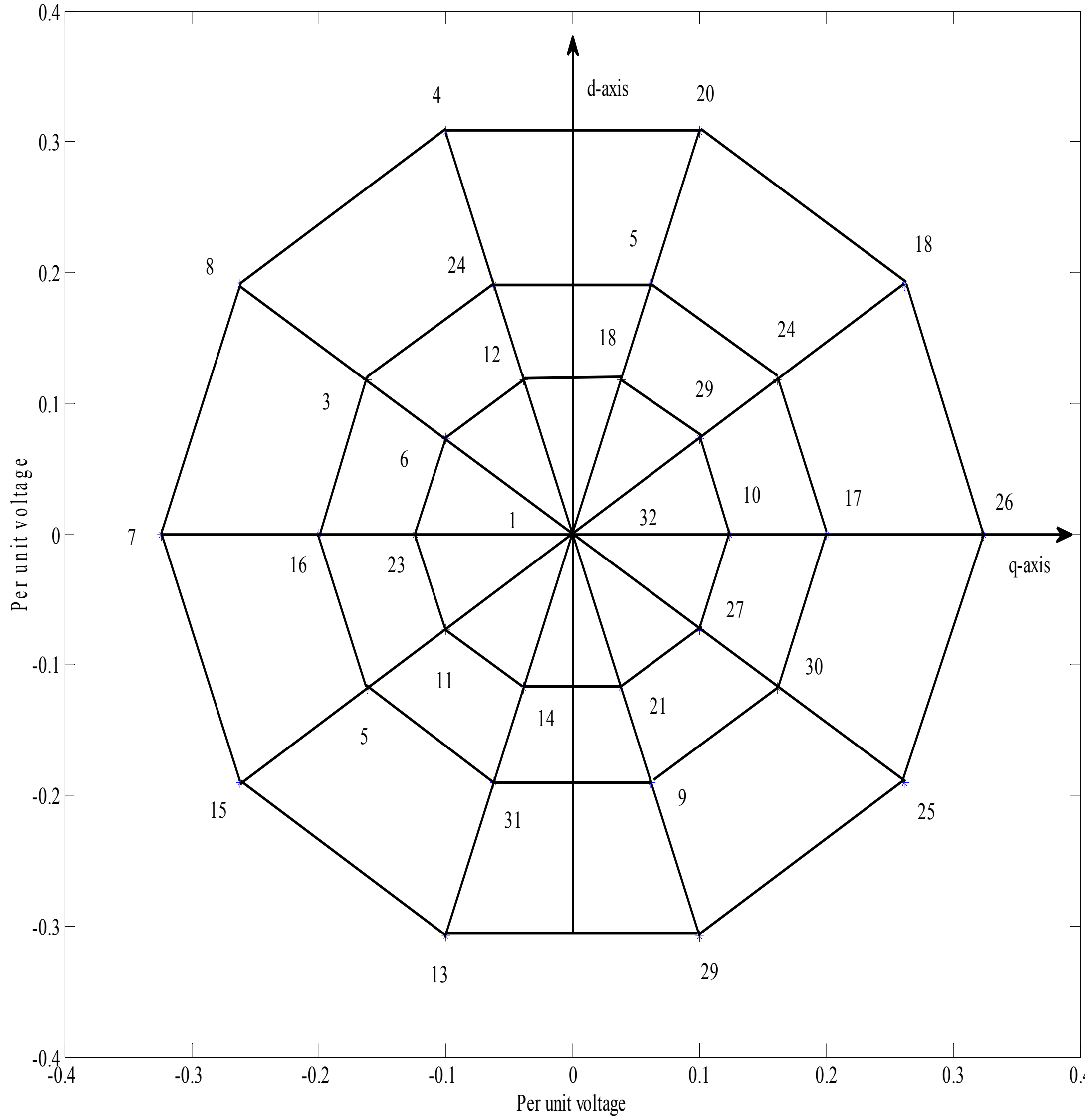

Figure 2.5 Voltage space vector diagram of a five-phase PWM inverter for v_{xy3s}

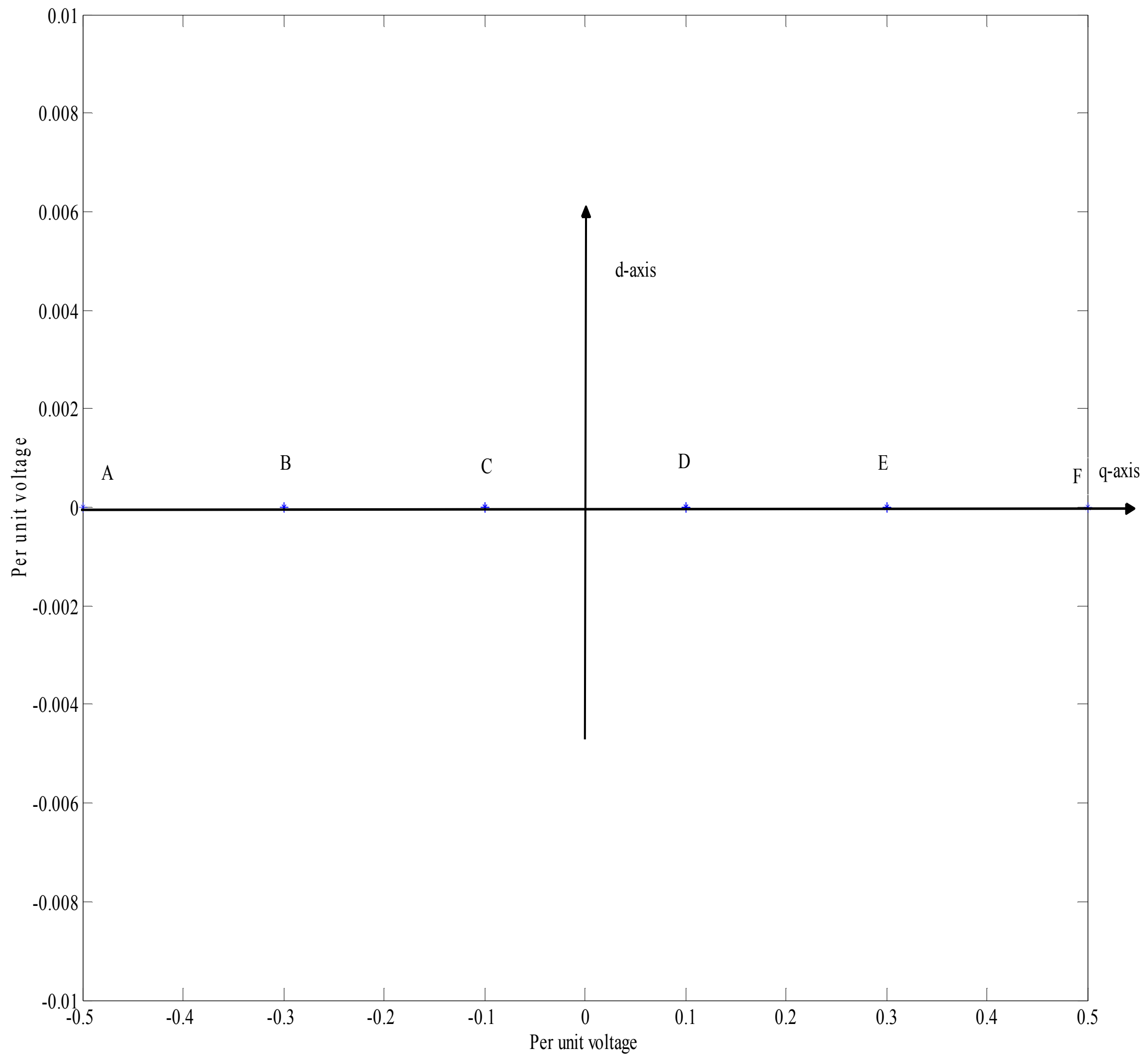

Figure 2.6 Voltage space vector diagram of a five-phase PWM inverter for v_{os}

In Figure (2.6), the letters stand for the modes as follows

$A = 1$, $B = 2,3,5,9,17$, $C = 4,6,7,10,11,13,18,19,21,25$,

$D = 8,12,14,15,20,22,23,26,27,29$, $E = 16,24,28,30,31$, $F = 32$.

Reference voltages in any sector of the space vector are synthesized by time-averaging some four active and two null space vectors as presented in [2.4].

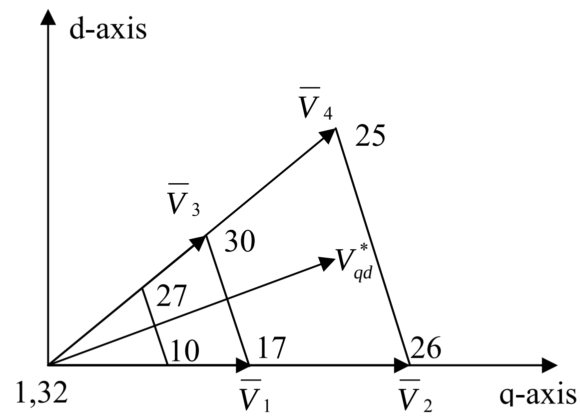

Figure 2.7 Synthesis of the fundamental voltage in sector 1

In sector 1 of the v_{qds} space vector, the active modes are [17(v_{qds1}), 25(v_{qds4}), 26(v_{qds2}), 30(v_{qds3})] and the two null vectors are [1(v_{qds01}) and 32(v_{qds32})]. The corresponding voltage vectors in v_{xy1s} are also selected. Since the qd voltages of the null vectors are zero, the linear equations for determining the averaging times for the vectors are

$$V_{qds} = V_{qds1}t_1 + V_{qds2}t_2 + V_{qds3}t_3 + V_{qds4}t_4 + V_{qds01}t_{01} + V_{qds32}t_{32} \tag{2.133}$$

$$V_{xy1s} = V_{xy1s1}t_1 + V_{xy1s2}t_2 + V_{xy1s3}t_3 + V_{xy1s4}t_4 + V_{xy1s01}t_{01} + V_{xy1s32}t_{32} \tag{2.134}$$

The time ratio between two null states (1 and 32) are defined as $t_{01} = \alpha_c t_c$, $t_{32} = (1-\alpha_c)t_c$ with the variable α_c ranging between zero and unity. With $t_c = 1-(t_1+t_2+t_3+t_4)$, the average neutral voltage corresponding to the selected voltage vectors for sector 1 is

$$V_o = \frac{v_d}{2}\left(\frac{4}{5}(-t_1+t_3)+\frac{2}{5}(t_2-t_4)+\frac{6}{5}(1-2\alpha_c)-\frac{6}{5}(1-2\alpha_c)(t_1+t_2+t_3+t_4)\right) \tag{2.135}$$

$$V_{o1} = \frac{4}{5}(-t_1+t_3) \tag{2.136}$$

$$V_{02} = \frac{2}{5}(t_2-t_4) \tag{2.137}$$

$$V_{00} = (t_1 + t_2 + t_3 + t_4) \tag{2.138}$$

The expressions for times t_1, t_2, t_3, and t_4 obtained from Equations (2.133) and (2.134) are substituted into Equations (2.135) through (2.138) yielding the neutral sequence voltage in terms of V_{qds} and V_{xy1s}. Calculations similar to Equations (2.133-135) are done for all the ten sectors of V_{qds} for which ten expressions are obtained for the average neutral voltages. Using the inverse stationary reference frame transformations (2.4d) the qd voltages in the equations for the ten average neutral voltages are expressed in terms of the phase voltages which can further be expressed in terms of the instantaneous maximum and minimum phase voltages, ($V_{\max}$ and $V_{\min}$, respectively). When the q- and d-axis reference voltages are expressed in terms of phase voltages, the times spent on the voltage vectors can be calculated.

2.6 Conclusion

A theory of multiphase systems has been introduced. The reference frame of transformation has been presented and discussed. The expressions for the real and reactive powers in multiphase systems have been described. The analysis started with the three-phase systems, followed by the five phase system and concluded with the seven phase system. General expressions for real and reactive powers have been derived. A special case when the sum of the phase currents is zero has shown that the total real power of any system is the sum of the individual phase powers, as expected. It has been deduced that using the reference frame of transformation discussed in this Chapter, the power is invariant. Thus, there is no need of multiplying the final result by any factor as it is done when other forms of transformations are considered. This depends on the multiplying factor on the transformation matrix. In this case the multiplying factor is $\sqrt{\frac{2}{m}}$. Thus with the transformed variables, one can easily obtain the actual values of the real and reactive powers. The expressions for powers by using natural variables will ease the power computation if the phase variables are readily available.

A space vector modulation scheme for the five-phase voltage source inverter has been presented. For a five-phase system, there are five vectors (f_{qd}, f_{xy1s}, f_{xy2s}, f_{xy3s} .and f_{os}). Only two of the them (f_{qds} and f_{xy1s}) are sufficient to determine the switching strategy of a five phase voltage source inverter. The other two are the complex conjugates. The fifth one is the zero sequence component, which is essentially a real quantity. In realizing the voltage vector in the space vector diagram, the use of the neutral voltage gives freedom of utilizing the null states in obtaining the switching times for each device.

CHAPTER 3

FULL ORDER MODELING OF A FIVE PHASE INDUCTION MACHINE

3.1 Introduction

The induction machine has been widely used over the last three decades in practically all applications requiring variable speed. This is due to its robustness, versatility and reliability.

In general, the induction machines having three-phase windings are normally used, since the standard power supply is three phase. However, when fed by an inverter, there is no need for a fixed number of phases, some other phases being possible and advantageous.

Much published work has shown that drives with more than three phases have various advantages over conventional three phase drives, such as reduction in amplitude and increase in frequency of pulsating torque, reduction in harmonic currents, increase in current per phase without the need to increase the phase voltage, and reduction in the voltage-level in the dc (direct current) link [3.1, 3.2]

Another important aspect of machines with a higher number of phases is their improved reliability, since they can operate even when one phase is missing [3.1]. An increase in number of phase can result in an increase in torque/Ampere relation for the same volume of the machine, such that five-phase machines can develop torque using not only the fundamental, but also using higher harmonics of the air gap field [3.1, [3.2].

Control strategies and electrical drives for machines with more than three phases have also been presented in several publications [3.2, [3.4]. Hence the analysis, design, and application of such machines as the five phase induction machine requires adequate mathematical models to be established through which their performance and advantages can be evaluated.

Calculation of machine parameters must be done differently from the three phase machines since the distribution of windings is not the same. In this work, therefore a full order model has been used to determine these parameters whereby the higher order harmonics are taken into account. Also, by using the derived expressions, the fundamental and third harmonic components of the machine parameters are determined.

3.2 Coupled Model of a Five-Phase Induction Machine

3.2.1 General Winding Function

The derivation of the general winding function from the fundamental relationships is the subject of this section. With all the assumptions or simplifications removed, a general Equation for the winding function of a winding distribution can be obtained [3.5, [3.6].
A general diagram of an electric machine is given in Figure 3.1 [3.5], in which the air gap length may not be constant. A closed area which includes the stator core, the air gap and the rotor core can be found and its boundary is shown as a dash line in the figure, where AB is in the stator core; O is the central point of stator; OA and OB go through the rotor, the air gap and the stator core and can be considered to be orthogonal to the inner surface of the stator. Based on the Ampere's Law, the magnetic field (H) of the boundary AOB

can be expressed in terms of the current density J, the differential length ∂l and the area ∂s as

$$\oint_C H \cdot dl = \int_S J \cdot ds \tag{3.1}$$

If the turn function of an arbitrary winding 'a' is $n_a(\theta)$, where θ is the angle around the inner surface of the stator, then Equation (3.1) can be written as

$$\oint_C H \cdot dl = n_a(\theta) \cdot i_a \tag{3.2}$$

There are two assumptions that need to be clarified before the next step. The first one is The air gap is so small compared to the stator or the rotor core that the magnetic field in the air gap can be considered to be orthogonal to the inner surface of the stator. This is a very fundamental assumption in electric machine analysis. The second one is The permeability of iron is much greater than that of air, hence the magneto-motive force drops on the stator and the rotor cores can be ignored.

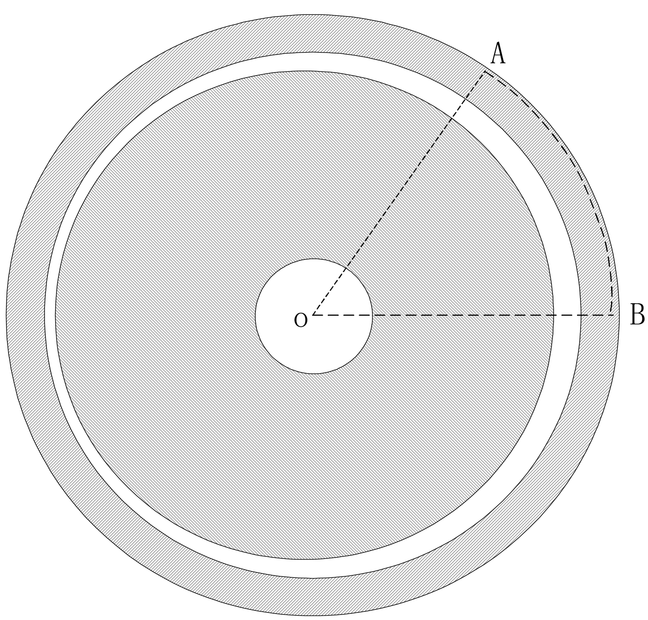

Figure 3.1 General diagram for an electric machine showing non-constant air gap length

A general definition for the air gap is expressed as

$$g(\theta,\theta_{rm}) = g_0\left(1 - a_1\cos(\theta+\gamma) - a_2\cos(\theta-\theta_{rm}+\gamma)\right) \tag{3.3}$$

where a_1 and a_2 are constants, which represent the degree of static and dynamic eccentricity, respectively; θ_{rm} is the rotor mechanical angle; g_0 is the average air gap length and angle γ defines the changes of the distribution of the air gap length around the inner stator surface.

It is clear from (3.3) that the air gap length not only depends on the angle around the stator, but also on the rotor angle, which will be true under almost all possible conditions. The constant air gap length condition can be achieved by setting a_1 and a_2 to be zero. Applying the above two assumptions to Equation (3.2), the integration part of the Equation (3.2) can be restated as

$$\oint_C H\cdot dl = H_a(\theta)\cdot g(\theta,\theta_{rm}) - H_a(0)\cdot g(0,\theta_{rm}) \tag{3.4}$$

where $g(0,\theta_{rm})$ is the air gap length at the starting point and the value of θ at the starting point is assumed to be zero. $H_a(0)$ is the magnetic field at the starting point while $g(\theta,\theta_{rm})$ and $H_a(\theta)$ are the air gap length and magnetic field at θ angle point, respectively.

Substituting (3.4) into (3.2),

$$H_a(\theta)\cdot g(\theta,\theta_{rm}) - H_a(0)\cdot g(0,\theta_{rm}) = n_a(\theta)\cdot i_a \tag{3.5}$$

An expression for the magnetic field around the stator can be found from (3.5) as

$$H_a(\theta) = \frac{n_a(\theta)\cdot i_a + H_a(0)\cdot g(0,\theta_{rm})}{g(\theta,\theta_{rm})} \tag{3.6}$$

The $H_a(\theta)$ and $H_a(0)$ are unknown and must be solved. Hence Gauss's Law is applied to determine the unknown quantity. If a cylinder passing through the air gap is considered, Gauss's Law can be expressed as

$$\int_0^{2\pi} \mu_0 H_a(\theta) r_{is} l_s d\theta = 0 \tag{3.7}$$

where r_{is} is the radius of the inner stator surface; l_s is the length of the machine.

Substituting (3.6) into (3.7),

$$\int_0^{2\pi} \mu_0 r_{is} l_s \frac{n_a(\theta)\cdot i_a + H_a(0)\cdot g(0,\theta_{rm})}{g(\theta,\theta_{rm})} d\theta = 0 \tag{3.8}$$

Rearranging Equation (3.8) gives

$$H_a(0)\cdot g(0,\theta_{rm}) = -\frac{\int_0^{2\pi} \frac{n_a(\theta)}{g(\theta,\theta_{rm})} d\theta}{\int_0^{2\pi} \frac{1}{g(\theta,\theta_{rm})} d\theta} \cdot i_a \tag{3.9}$$

Substituting (9) into (6),

$$H_a(\theta) = \frac{n_a(\theta)\cdot i_a}{g(\theta,\theta_{rm})} - \frac{1}{g(\theta,\theta_{rm})} \frac{\int_0^{2\pi} \frac{n_a(\theta)}{g(\theta,\theta_{rm})} d\theta}{\int_0^{2\pi} \frac{1}{g(\theta,\theta_{rm})} d\theta} \cdot i_a \tag{3.10}$$

Simplification of (10) yields (11),

$$N_a(\theta)\cdot i_a = H_a(\theta)\cdot g(\theta,\theta_{rm}) \tag{3.11}$$

$N_a(\theta)$ is called the winding function. Then the winding function $N_a(\theta)$ is expressed as

$$N_a(\theta) = n_a(\theta) - \frac{\int_0^{2\pi} \frac{n_a(\theta)}{g(\theta, \theta_{rm})} d\theta}{\int_0^{2\pi} \frac{1}{g(\theta, \theta_{rm})} d\theta} \tag{3.12}$$

If the air gap length is constant,

$g(\theta, \theta_{rm}) = g_0$

The winding function in Equation (12) can be simplified as

$$\begin{aligned} N_a(\theta) &= n_a(\theta) - \frac{\int_0^{2\pi} \frac{n_a(\theta)}{g_0} d\theta}{\int_0^{2\pi} \frac{1}{g_0} d\theta} \\ &= n_a(\theta) - \frac{\int_0^{2\pi} n_a(\theta) d\theta}{2\pi} \\ &= n_a(\theta) - \langle n_a(\theta) \rangle \end{aligned} \tag{3.13}$$

where $\langle n_a(\theta) \rangle$ is the average of the turn function. Equation (3.13) is similar to the definition of the winding function traditionally used for constant air gap length.

3.2.2 Calculation of Stator Inductances

The expression for winding inductances is calculated using the winding function and the turn function of the windings. If the winding function of i^{th} winding is expressed as $N_i(\theta)$, where θ is the angle around the stator, then from (3.9) the magnetic field around the stator can be expressed as

$$H_i(\theta) = \frac{N_i(\theta)}{g(\theta, \theta_{rm})} \cdot i_i \tag{3.14}$$

where $g(\theta,\theta_{rm})$ is the air gap function and i_i is the current flowing through the i^{th} winding.

Then the flux density in the air gap can be written as

$$B_i(\theta) = \mu_0 \frac{N_i(\theta)}{g(\theta,\theta_{rm})} \cdot i_i \tag{3.15}$$

Assume the mutual inductance between i^{th} winding and j^{th} winding is the objective and the turn function of j^{th} winding is $n_j(\theta)$. The flux linkage induced in j^{th} winding due to the i^{th} winding current i_i can be expressed as

$$\lambda_{ji} = \mu_0 rl \cdot i_i \cdot \int_0^{2\pi} \frac{1}{g(\theta,\theta_{rm})} \cdot n_j(\theta) \cdot N_i(\theta) \cdot d\theta \tag{3.16}$$

where r is the mean value of radius of the air gap middle line and l is the effective length of the stator core. Since the definition of the mutual inductance is

$$L_{ji} = \frac{\lambda_{ji}}{i_i} \tag{3.17}$$

The general expression for the mutual inductance calculation is

$$L_{ji} = \mu_0 rl \int_0^{2\pi} \frac{1}{g(\theta,\theta_{rm})} \cdot n_j(\theta) \cdot N_i(\theta) \cdot d\theta \tag{3.18}$$

The stator inductances considered include the stator winding self-inductances and the mutual inductances between the stator windings. Since only the uniform air gap condition is considered in this Chapter, the air gap function is a constant

$$g(\theta,\theta_{rm}) = g_0 \tag{3.19}$$

The general expression to calculate the self-inductance of i^{th} winding is

$$L_{ii} = \mu_0 rl \int_0^{2\pi} \frac{1}{g_0} \cdot n_i(\theta) \cdot N_i(\theta) \cdot d\theta \tag{3.20}$$

where $n_i(\theta)$ is the turn function of i^{th} winding; $N_i(\theta)$ is the winding function of i^{th} winding; g_0 is the constant air gap.

3.3 Five Phase Stator Winding Design

3.3.1 Winding Design

An existing 2-pole, three-phase induction machine was rewound to be a 4-pole, five-phase stator winding. The following are the ratings of the original three-phase induction squirrel cage machine

Series No. 5K184AG1720	Power 5 hp
Voltage 208-220/440 V	Current 13.4/6.7 A
Frequency 60 Hz	Speed 3460 rpm.
Stator slots 30	Rotor slots 28.

Since it is possible to have a four-pole five–phase fractional slot-stator winding[3.7]-[3.9], the rewound stator winding is a double-layer five-phase stator fractional slot winding. The stator has thirty (30) slots. The ratings of the five-phase machine are calculated and presented in section 3.4.3.

3.3.2 Winding Configuration

The average number of slots per pole per phase, q, is given by $q = \frac{S_s}{mP} = \frac{30}{20} = \frac{3}{2}$ in which 3 and 2 are the lowest pair of whole numbers, where S_s is the number of stator slots, P is the number of poles and m is the number of stator phases. As each pole phase groups must have an integral number of coils, $q = \frac{3}{2} = 1\frac{1}{2}$, can only be obtained if the 2 (the denominator of q) phase groups under 2 poles have different number of coils totaling up to 3 coils (numerator of q). Now 3 coils for each phase lying under 2 poles can be obtained if we have one (1) pole phase group of one (1) coil and one (1) pole phase group of two (2) coils. This gives an average value of $q = \frac{1\times1+1\times2}{2} = 1\frac{1}{2}$. Two poles make one basic unit of this winding. As this winding has four poles, there are two units of two poles, each covering three slots of each phase. The $(1+1) = 2$ pole phase groups of each phase in a unit must be connected in series and as there are $\frac{4}{2} = 2$ such units, the maximum number of parallel paths is equal to two (2), which is the same as the number of units.

Consider q in the form of $\frac{3}{2}$, where the numerator and denominator have no common factor, we have

(i) number of poles in a unit = 2 (denominator of q)

(ii) number of slots per phase in each unit = 3 (numerator of q)

(iii) number of units $= \dfrac{total\ number\ of\ poles}{poles/unit} = \dfrac{P}{denominator\ of\ q}$

Considering the form $q = 1\frac{1}{2}$, we observe that there are

(i) 2-1=1 group of 1 coil each and

(ii) 1 group of 1+1=2 coils each.

This connection algorithm can be expressed in a general form as

$$q = \frac{S}{mP} = \frac{M}{d} = I + \frac{n}{d}$$

where M and d have no common divisor. Thus for a fractional slot winding

(a) number of poles in a unit is $d = 2$

(b) number of slots per phase in each unit is $M = qd = 3$

(c) number of total slots in each unit is $mM = 5 \times 3 = 15$

(d) number of units $= \frac{P}{d} = \frac{4}{2} = 2$, which is the maximum number of parallel paths.

(e) Each phase, in a unit, contains $d - n$ groups of I coils each and n groups of $I + 1$ coils each

Now, dividing the table in five vertical parts, each having $\frac{15}{5} = 3$ columns and 2 rows, and the mark the cross (X) in the upper left square and move from left to right continuously in every second square, the result is as shown in Table 3.1. The sequence of coil groups is shown in Table 3.2, whereas Table 3.3 shows the distribution of slots in a unit. Figure 3.2 shows a winding layout and Figure 3.3 shows a clock diagram of the stator winding.

Table 3.1 Development of the winding diagram

A			D			B			E			C		
X		X		X		X		X		X		X		X
	X		X		X		X		X		X		X	

Table 3.2 Sequence of coil groups

Phase	A	D	B	E	C	A	D	B	E	C
No. of coils in phase group	2	1	2	1	2	1	2	1	2	1

Table 3.3 Distribution of slots in a unit

Phase		
A	1, 2	9
D	3	10, 11
B	4, 5	12
E	6	13, 14
C	7, 8	15

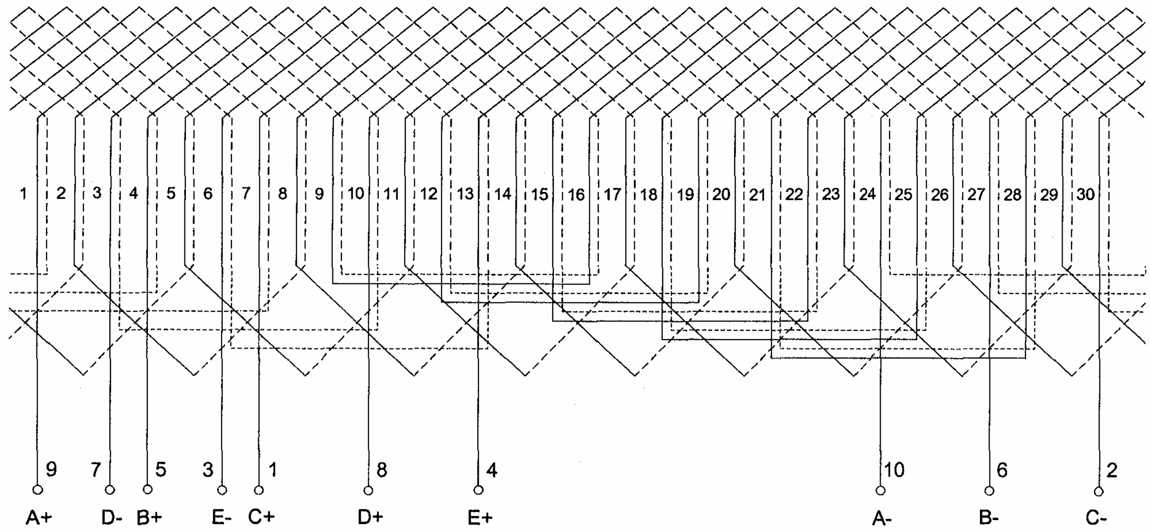

Figure 3.2 Winding diagram for the design of a five-phase induction machine

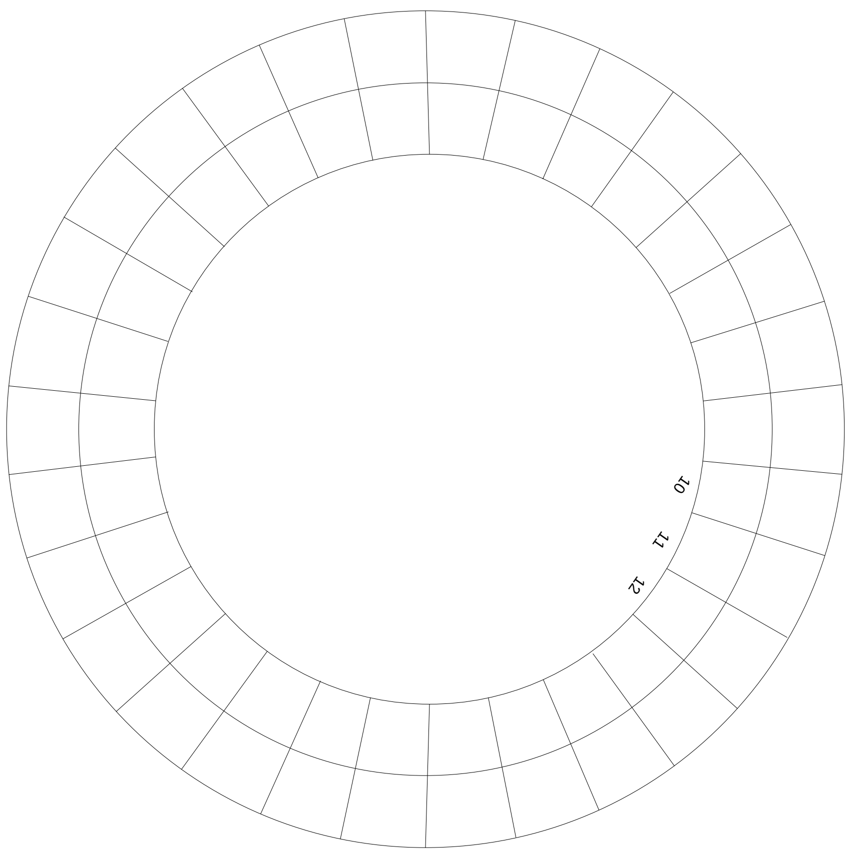

Figure 3.3 Clock diagram for the design of a five-phase induction machine

3.3.3 Conductor Size and Ratings of the Five-Phase Induction Machine

The original three-phase machine had the following specifications on its nameplate

Series No. 5K184AG1720 Power 5 hp

Voltage 208-220/440 V Current 13.4/6.7 A

Frequency 60 Hz Speed 3460 rpm.

The measured dimensions are as follows

Stator core length $L = 71.76\, mm$, Stator inner diameter; $D_{in} = 101.48\, mm$, stator outer diameter $D_{out} = 184.51\, mm$.

Rotor core length $L = 70.40\, mm$, Rotor outer diameter $D_{outrot} = 100.62\, mm$.

From the above data, the calculations for the five phase stator winding were conducted as follows

The following assumptions were made

(a) The average flux density in the air gap is $B_{av} = 0.45 Wb/m^2$

(b) Line-to line voltage is $V_{LL} = 220V$.

(c) Winding factor, $K_{ws} = 0.955$.

(d) Power factor, $pf = 0.85$ and efficiency, $\eta = 0.85\, pu$.

Now, the length of the core is given as $L = 704.mm$.

Pole pitch $\tau = \dfrac{\pi D_{in}}{poles} = \dfrac{\pi \times 101.48}{4} = 79.7\, mm$.

Stator phase voltage (star connection) $E_s = \dfrac{V_{LL}}{\sqrt{3}} = \dfrac{220}{\sqrt{3}} = 127.02\ V$.

Flux per pole $\phi_m = B_{av} L \tau = 2.525 \times 10^{-3}\ Wb$.

Stator turn per phase $T_s = \dfrac{E_s}{4.44 f\phi_m K_{ws}} = 197.73 \approx 198$.

Total conductors $T_{total} = 2mT_s = 1980$.

Conductors per slot $Z_{ss} = \dfrac{T_{otal}}{S_s} = \dfrac{1980}{30} = 66$.

The output power $P = 5\ hp = 5 \times 746W = 3730W$.

Stator current $I_s = \dfrac{P}{m \times E_s \times pf \times \eta} = \dfrac{5 \times 746}{5 \times 127.02 \times 0.85 \times 0.85} = 8.13\,A$.

Area of a stator conductor, $a_s = \dfrac{I_s}{\delta_s} = \dfrac{8.13}{3.5} = 2.323\ mm^2$.

Total copper area in each slot $Z_{ss}a_s = 66 \times 2.323 = 153.32\ mm^2$.

3.3.4 Turn and Winding Functions

The turn and winding functions of the stator winding are shown in Figure 3.4 and Figure 3.5, respectively, where $N_s = 33$ is the number of conductors per layer per slot for the stator winding and $N_s = \dfrac{T_s}{6} = \dfrac{198}{6} = 33$. T_s is the number of turns per phase.

For phase 'a', the self-inductance is

$$L_{aa} = \mu_0 rl \int_0^{2\pi} \frac{1}{g_0} \cdot n_a(\theta) \cdot N_a(\theta) \cdot d\theta \tag{3.21}$$

Since the turn function of phase 'a' is a piecewise linear Equation, the integration can only be done in each linear region and the results of each linear region are added to obtain the final result.

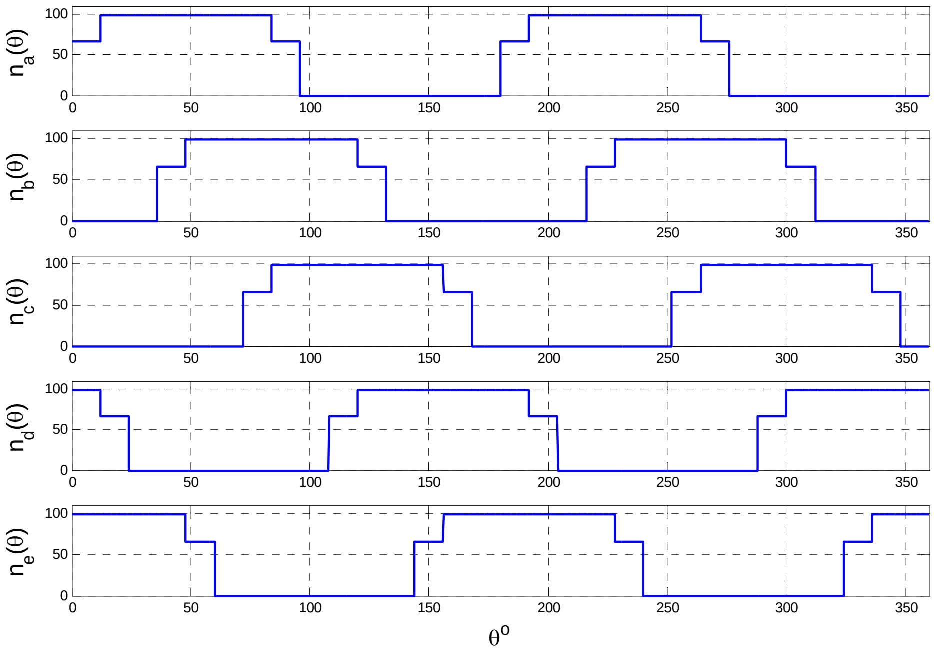

Figure 3.4 The turn functions of the stator winding.

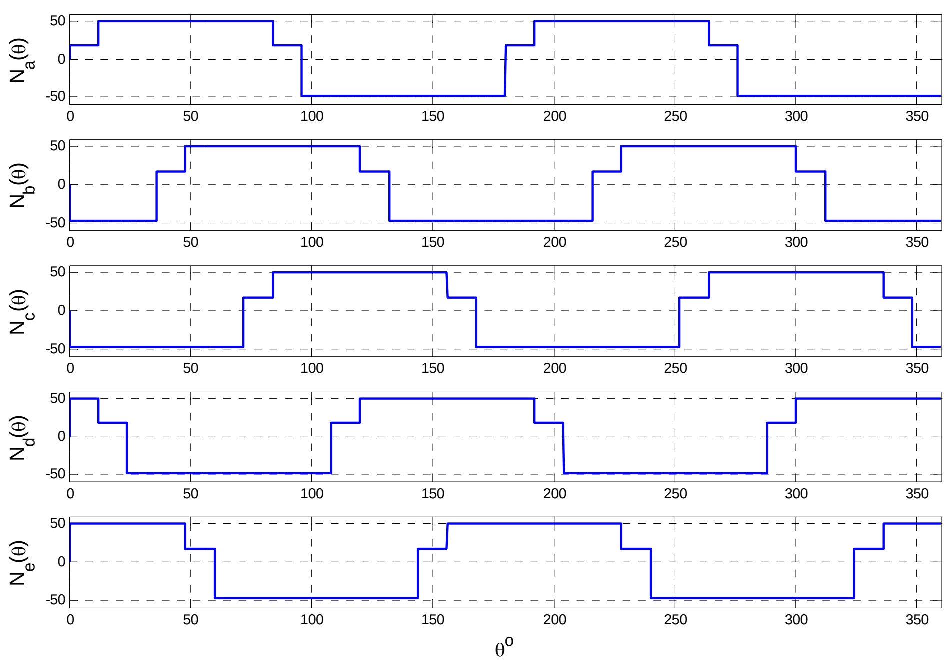

Figure 3.5 The winding functions of the stator winding.

The expression for the self-inductance of phase 'a' can be simplified as

$$L_{aa} = \frac{\mu_0 r l}{g_0} \int_0^{2\pi} n_a(\theta) \cdot \left[n_a(\theta) - \langle n_a(\theta) \rangle \right] \cdot d\theta \tag{3.22}$$

where $\langle n_a(\theta) \rangle$ is the averages of the phase 'a' winding functions.

Similar expressions can be found for phases 'b', 'c', 'd' and 'e' as

$$L_{bb} = \frac{\mu_0 r l}{g_0} \int_0^{2\pi} n_b(\theta) \cdot \left[n_b(\theta) - \langle n_b(\theta) \rangle \right] \cdot d\theta \tag{3.23}$$

$$L_{cc} = \frac{\mu_0 r l}{g_0} \int_0^{2\pi} n_c(\theta) \cdot \left[n_c(\theta) - \langle n_c(\theta) \rangle \right] \cdot d\theta \tag{3.24}$$

$$L_{dd} = \frac{\mu_0 r l}{g_0} \int_0^{2\pi} n_d(\theta) \cdot \left[n_d(\theta) - \langle n_d(\theta) \rangle \right] \cdot d\theta \tag{3.25}$$

$$L_{ee} = \frac{\mu_0 r l}{g_0} \int_0^{2\pi} n_e(\theta) \cdot \left[n_e(\theta) - \langle n_e(\theta) \rangle \right] \cdot d\theta \tag{3.26}$$

where $\langle n_b(\theta) \rangle$, $\langle n_c(\theta) \rangle$, $\langle n_d(\theta) \rangle$ and, $\langle n_e(\theta) \rangle$ are the averages of the phases 'b', 'c', 'd' and 'e' turn functions, respectively.

The self-inductances of three phases have the same value and the value of the self-inductances is

$$\begin{aligned}
&L_{aa} = L_{bb} = L_{cc} = L_{dd} = L_{ee} = \frac{\mu_0 r l}{g_0} \int_0^{2\pi} n_a(\theta) \cdot N_a(\theta) \cdot d\theta \\
&N_a(\theta) = n_a(\theta) - \langle n_a(\theta) \rangle \\
&\langle n_a(\theta) \rangle = \frac{1}{2\pi} \left[\begin{array}{l} \int_0^{\frac{\pi}{15}} (2N_s)^2 d\theta + \int_{\frac{\pi}{15}}^{\frac{7\pi}{15}} (3N_s)^2 d\theta + \int_{\frac{7\cdot\pi}{15}}^{\frac{8\cdot\pi}{15}} (2N_s)^2 d\theta + \int_{\frac{15\pi}{15}}^{\frac{16\pi}{15}} (2N_s)^2 d\theta + \\ \int_{\frac{16\pi}{15}}^{\frac{22\pi}{15}} (3N_s)^2 d\theta + \int_{\frac{22\pi}{15}}^{\frac{23\pi}{15}} (2N_s)^2 d\theta \end{array} \right] \\
&\quad = \frac{22}{15} N_s
\end{aligned} \tag{3.27}$$

$$L_{aa} = \frac{2\mu_0 rl}{g_0}\left[\begin{array}{l}\int_0^{\frac{\pi}{15}}(2N_s)^2 d\theta + \int_{\frac{\pi}{15}}^{\frac{7\pi}{15}}(3N_s)^2 d\theta + \int_{\frac{7\cdot\pi}{15}}^{\frac{8\cdot\pi}{15}}(2N_s)^2 d\theta + \int_{\frac{15\pi}{15}}^{\frac{16\pi}{15}}(2N_s)^2 d\theta + \\ \int_{\frac{16\pi}{15}}^{\frac{22\pi}{15}}(3N_s)^2 d\theta + \int_{\frac{22\pi}{15}}^{\frac{23\pi}{15}}(2N_s)^2 d\theta - 2\pi\left(\frac{22}{15}N_s\right)^2\end{array}\right] \tag{3.28}$$

$$= \frac{892\pi\mu_0 rl}{225 g_0}N_s^2$$

where N_s is the number of conductors per layer per slot for the stator winding. This expression of self-inductance calculation is only good for this particular machine design.

3.3.5 Stator Mutual Inductances

The general expression for the mutual inductance is

$$L_{ij} = \mu_0 rl\int_0^{2\pi}\frac{1}{g_0}\cdot n_i(\theta)\cdot N_j(\theta)\cdot d\theta \tag{3.29}$$

where $n_i(\theta)$ is the turn function of i^{th} winding; $N_j(\theta)$ is the winding function of j^{th} winding, $i, j = a,b,c,d,e$ and $i \neq j$.

The calculation method and process are similar to the one for self-inductance, but the number of linear region is much more than that. Unlike the three-phase machine, the mutual inductances are not the same for the five-phase machine. The mutual inductances between adjacent phases are the same, whereas for the phases which are not adjacent, their mutual inductances are have a different value. The expression for the mutual inductance between phase ‘a’ and phase ‘b’ of the stator winding is

$$L_{ab} = \frac{\mu_0 rl}{g_0}\int_0^{2\pi} n_a(\theta)\cdot N_b(\theta)\cdot d\theta \cdot = \frac{\mu_0 rl}{g_0}\int_0^{2\pi} n_a(\theta)\cdot n_b(\theta)\cdot d\theta - \frac{2\pi\mu_0 rl}{g_0}\langle n_b(\theta)\rangle\langle n_a(\theta)\rangle$$

$$= \frac{\mu_0 rl}{g_0}\left[\int_{\frac{3\pi}{15}}^{\frac{4\pi}{15}} 6d\theta + +\int_{\frac{4\pi}{15}}^{\frac{7\pi}{15}} 9d\theta + \int_{\frac{7\pi}{15}}^{\frac{8\pi}{15}} 6d\theta + \int_{\frac{18\pi}{15}}^{\frac{19\pi}{15}} 6d\theta + \int_{\frac{19\pi}{15}}^{\frac{22\pi}{15}} 9d\theta + \int_{\frac{22\pi}{15}}^{\frac{23\pi}{15}} 6d\theta - 2\pi\left(\frac{22}{15}N_s\right)^2\right]$$

$$= \frac{202}{225}\frac{\pi\mu_0 rl}{g_0}N_s^2$$

Similarly for the remaining adjacent phases, the mutual inductances are

$$L_{ab} = L_{bc} = L_{cd} = L_{de} = L_{ea} = \frac{202}{225}\frac{\pi\mu_0 rl}{g_0}N_s^2 \tag{3.30}$$

The expression for the mutual inductance between phase ‘a’ and phase ‘c’ of the stator winding is

$$L_{ac} = \frac{\mu_0 rl}{g_0}\int_0^{2\pi} n_a(\theta)\cdot N_c(\theta)\cdot d\theta \cdot = \frac{\mu_0 rl}{g_0}\int_0^{2\pi} n_a(\theta)\cdot n_c(\theta)\cdot d\theta - \frac{2\pi\mu_0 rl}{g_0}\langle n_c(\theta)\rangle\langle n_a(\theta)\rangle$$

$$= \frac{\mu_0 rl}{g_0}\left[\int_{\frac{6\pi}{15}}^{\frac{7\pi}{15}} 6d\theta + +\int_{\frac{7\pi}{15}}^{\frac{8\pi}{15}} 6d\theta + \int_{\frac{21\pi}{15}}^{\frac{22\pi}{15}} 6d\theta + \int_{\frac{22\pi}{15}}^{\frac{23\pi}{15}} 6d\theta - 2\pi\left(\frac{22}{15}N_s\right)^2\right] = -\frac{608}{225}\frac{\pi\mu_0 rl}{g_0}N_s^2$$

Similarly for the remaining non-adjacent phases, the mutual inductances are

$$L_{ac} = L_{bd} = L_{ce} = L_{da} = L_{eb} = -\frac{608}{225}\frac{\pi\mu_0 rl}{g_0}N_s^2 \tag{3.31}$$

where $i, j = a, b, c, d, e$ and $i \neq j$. It has to be noted here that $L_{ij} = L_{ji}$.

3.3.6 Calculation of Rotor Inductances

The squirrel cage rotor with n (even or odd) bars and two end rings to short circuit all the bars together is considered as n identical magnetically coupled circuits. Each circuit is composed of two adjunct rotor bars and segments of the end rings connect two adjacent bars together at both ends of the bars. Each bar and end ring segment of the rotor loop is equivalently represented by a serial connection of a resistor and an inductor as shown in Figure 3.6.

The resistance and the inductance of the rotor bar are represented by r_b and l_b, respectively; the resistance and inductance of the partial end winding in the rotor loop are represented by r_e and l_e, respectively. Three rotor loops are shown in Figure 3.7 and the current flowing through the rotor loops are represented by i_{k-1}, i_k and i_{k+1}, respectively. Since every rotor loop is treated as an independent phase, a healthy cage rotor having n rotor bars becomes a n phases balanced system.

The turn function of i^{th} rotor loop is shown in Figure 3.7 (a). Since a constant air gap length is considered in this Chapter, the winding function of the i^{th} rotor loop can be easily found with Figure 3.7 (b).

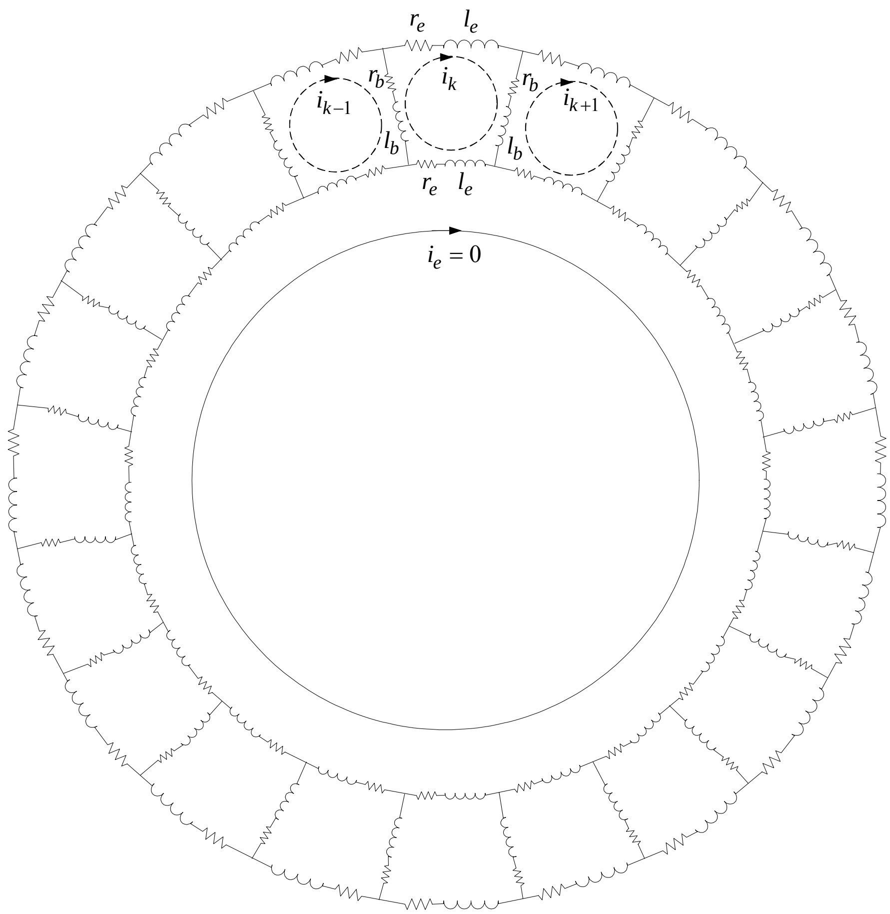

Figure 3.6 Squirrel cage rotor equivalent circuit

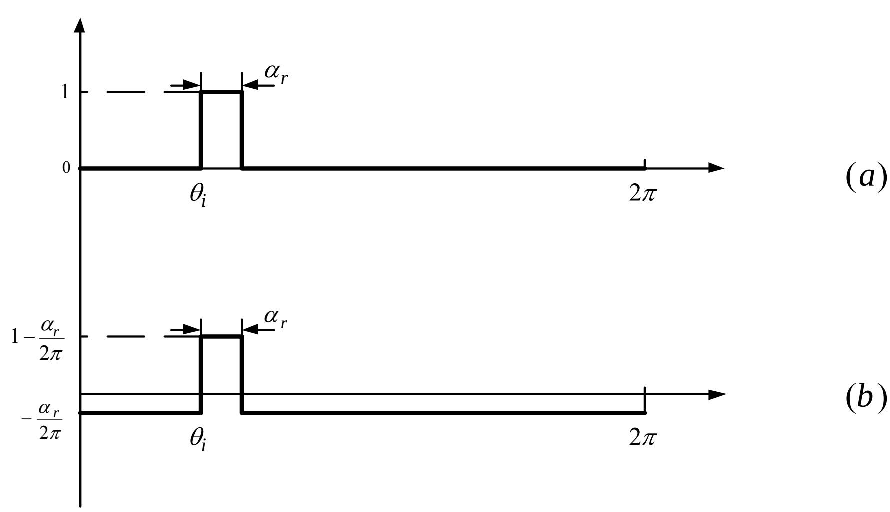

Figure 3.7 Rotor i^{th} rotor loop turn and winding function, (a) turn function, (b) winding function.

The turn function of the i^{th} rotor loop is

$$n_i(\theta) = \begin{cases} 0 & 0 \le \theta \le \theta_i \\ 1 & \theta_i \le \theta \le \theta_i + \alpha_r \\ 0 & \theta_i + \alpha_r \le \theta \le 2\pi \end{cases} \tag{3.32}$$

The winding function can be expressed as

$$N_i(\theta) = \begin{cases} -\dfrac{\alpha_r}{2\pi} & 0 \le \theta \le \theta_i \in \\ 1 - \dfrac{\alpha_r}{2\pi} & \theta_i \le \theta \le \theta_i + \alpha_r \\ -\dfrac{\alpha_r}{2\pi} & \theta_i + \alpha_r \le \theta \le 2\pi \end{cases} \tag{3.33}$$

where α_r is the i^{th} rotor loop pitch. Since a symmetrical equally spaced rotor bar structure is considered in the analysis, all the rotor loops have the same pitch α_r.

None of the turn and winding functions shown in Figure 3.7 take the skew of the rotor into the consideration. If the rotor is skewed, the turn function and winding function are shown in Figure 3.8.

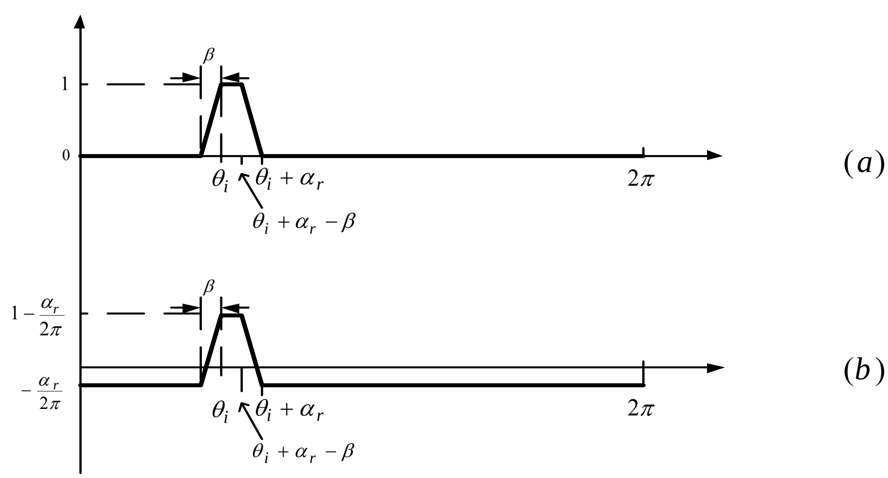

Figure 3.8 Rotor i^{th} rotor loop turn and winding function for skewed rotor, (a) turn function, (b) winding function.

When the skewing factor of the rotor is considered, the expressions for the turn and winding functions become (3.34) and (3.35), respectively

$$n_i(\theta)=\begin{cases}0 & 0\le\theta\le\theta_i-\beta\\ \dfrac{1}{\beta}(\theta-\theta_i+\beta) & \theta_i-\beta\le\theta\le\theta_i\\ 1 & \theta_i\le\theta\le\theta_i+\alpha_r-\beta\\ \dfrac{1}{\beta}(\theta_i+\alpha_r-\theta) & \theta_i+\alpha_r-\beta\le\theta\le\theta_i+\alpha_r\\ 0 & \theta_i+\alpha_r\le\theta\le 2\pi\end{cases} \tag{3.34}$$

$$N_i(\theta)=\begin{cases}-\dfrac{\alpha_r}{2\pi} & 0\le\theta\le\theta_i-\beta\\ \dfrac{1}{\beta}(\theta-\theta_i+\beta)-\dfrac{\alpha_r}{2\pi} & \theta_i-\beta\le\theta\le\theta_i\\ 1-\dfrac{\alpha_r}{2\pi} & \theta_i\le\theta\le\theta_i+\alpha_r-\beta\\ \dfrac{1}{\beta}(\theta_i+\alpha_r-\theta)-\dfrac{\alpha_r}{2\pi} & \theta_i+\alpha_r-\beta\le\theta\le\theta_i+\alpha_r\\ 0-\dfrac{\alpha_r}{2\pi} & \theta_i+\alpha_r\le\theta\le 2\pi\end{cases} \tag{3.35}$$

where $\beta = skew\ factor\cdot\alpha_r$.

Substituting the turn function and winding function of the i^{th} rotor loop into the general expression for the self-inductance given in (3.20), the self-inductance for the i^{th} rotor loop can be determined. Since all the rotor loops have the same self-inductance under the uniform air gap condition, its expression is

$$
\begin{aligned}
L_{rr} &= \frac{\mu_0 rl}{g_0}\int_0^{2\pi} N_i(\theta)\cdot N_i(\theta)d\theta \\
&= \frac{\mu_0 rl}{g_0}\int_0^{2\pi}\left(n_i(\theta)-\frac{\alpha_r}{2\pi}\right)^2 d\theta \\
&= \frac{\mu_0 rl}{g_0}\left(\alpha_r-\frac{\beta}{3}-\frac{\alpha_r^2}{2\pi}\right)
\end{aligned}
\tag{3.36}
$$

The winding functions of the adjacent rotor loops will overlap each other when the rotor is skewed, such that the mutual inductances between i^{th} and $i+1$ th will be different from i^{th} and $i+k^{th}$ $(k=2, n-1)$, where n is the number of rotor bar.

The mutual inductance between i^{th} and $i+1^{th}$ rotor loop is

$$
\begin{aligned}
L_{rm1} &= \frac{\mu_0 rl}{g_0}\left\{
\begin{aligned}
&\int_0^{\theta_i-\beta}\left(-\frac{\alpha_r}{2\pi}\right)^2 d\theta+\int_{\theta_i-\beta}^{\theta_i}\left(-\frac{\alpha_r}{2\pi}\right)\left[\frac{1}{\beta}(\theta-\theta_i+\beta)-\frac{\alpha_r}{2\pi}\right]d\theta \\
&+\int_{\theta_i-\beta}^{\theta_i+\alpha_r-\beta}\left(-\frac{\alpha_r}{2\pi}\right)\cdot\left(1-\frac{\alpha_r}{2\pi}\right)d\theta+\int_{\theta_{i+1}}^{\theta_{i+1}+\alpha_r-\beta}\left(-\frac{\alpha_r}{2\pi}\right)\cdot\left(1-\frac{\alpha_r}{2\pi}\right)d\theta \\
&+\int_{\theta_i+\alpha-\beta}^{\theta_i+\alpha_r}\left[\frac{1}{\beta}(\theta-\theta_i+\beta)-\frac{\alpha_r}{2\pi}\right]\cdot\left[\frac{1}{\beta}(\theta_i+\alpha_r-\theta)-\frac{\alpha_r}{2\pi}\right]d\theta \\
&+\int_{\theta_{i+1}+\alpha_r-\beta}^{\theta_{i+1}+\alpha_r}\left(-\frac{\alpha_r}{2\pi}\right)\left[\frac{1}{\beta}(\theta_i+\alpha_r-\theta)-\frac{\alpha_r}{2\pi}\right]d\theta+\int_{\theta_{i+1}+\alpha_r}^{2\pi}\left(-\frac{\alpha_r}{2\pi}\right)^2 d\theta
\end{aligned}
\right\} \\
&= \frac{\mu_0 rl}{g_0}\left(\frac{\beta}{6}-\frac{\alpha_r^2}{2\pi}\right)
\end{aligned}
\tag{3.37}
$$

All the mutual inductance between i^{th} and $i+k^{th}$ rotor loop have the same value and it can be calculated by

$$
\begin{aligned}
L_{rm2} &= \frac{\mu_0 rl}{g_0}\int_0^{2\pi}\left(n_i(\theta)-\frac{\alpha_r}{2\pi}\right)\cdot\left(n_{i+k}(\theta)-\frac{\alpha_r}{2\pi}\right)d\theta \\
&= \frac{\mu_0 rl}{g_0}\int_0^{2\pi}\left[n_i(\theta)n_{i+k}(\theta)-\frac{\alpha_r}{2\pi}(n_i(\theta)+n_{i+k}(\theta))-\frac{\alpha_r^2}{4\pi^2}\right]d\theta \\
&= \frac{\mu_0 rl}{g_0}\left(-\frac{\alpha_r^2}{2\pi}\right)
\end{aligned}
\tag{3.38}
$$

3.3.7 Calculation of Stator-Rotor Mutual Inductances

Both the stator and the rotor loop winding functions are represented by piecewise linear Equations while the position of the i^{th} rotor loop depends on the rotor angle. Using the expression for the mutual inductance, the mutual inductances between i^{th} rotor loop and the stator winding set are shown in Figure 3.9.

$$L_{ij} = \mu_0 r l \int_0^{2\pi} \frac{1}{g_0} \cdot n_i(\theta) \cdot N_j(\theta) \cdot d\theta \tag{3.39}$$

where $i = a, b, c, d, e$ and $j = 1, 2, \cdots, n$, where n is the rotor bar number.

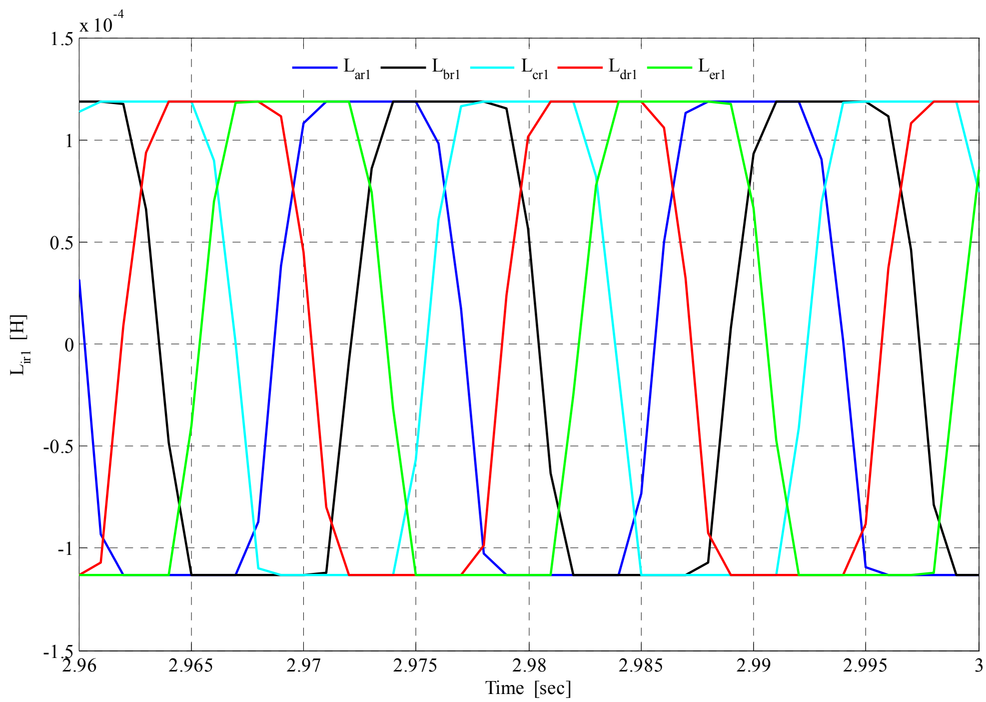

Figure 3.9 Stator rotor mutual inductance.

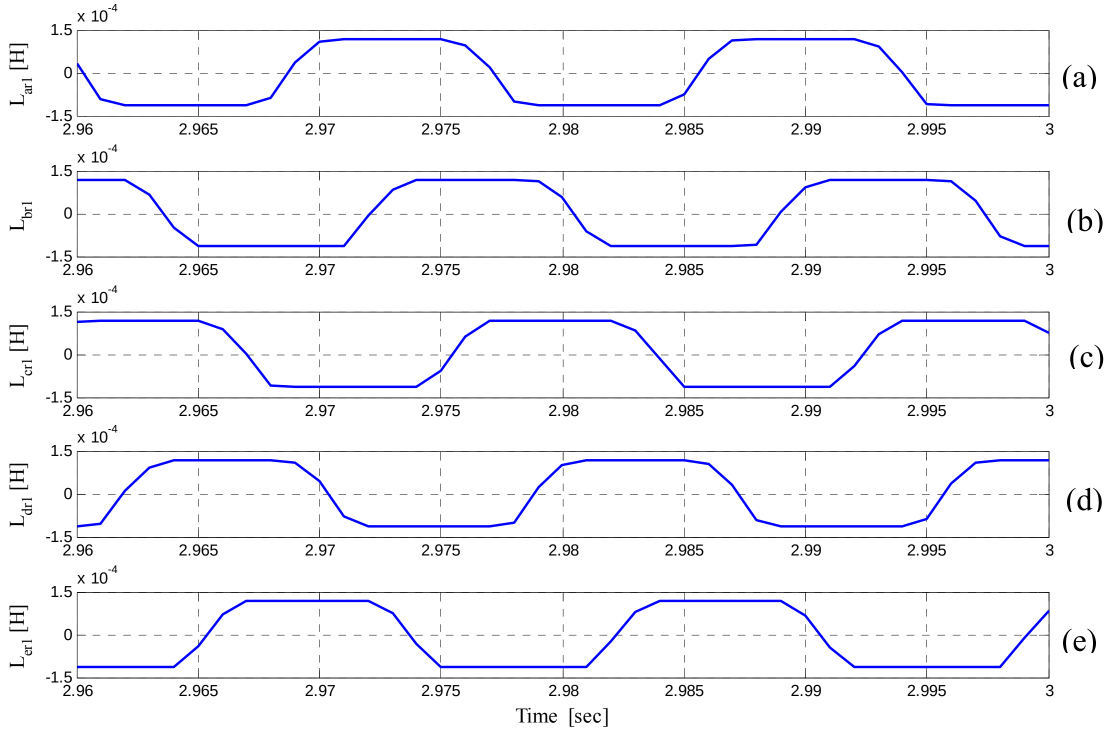

Figure 3.10 Stator-to- rotor bar mutual inductances (a) stator phase ‘a’ to rotor bar number 1 (b) stator phase ‘b’ to rotor bar number 1 (c) stator phase ‘c’ to rotor bar number 1 (d) stator phase ‘d’ to rotor bar number 1 (e) stator phase ‘e’ to rotor bar number 1.

3.4 Model of the Five Phase Stator Winding Machine

Based on the magnetic circuit theory, a full model of the induction machine can be developed. The reason it is called a full model is that this model is not based on any assumptions of stator windings or rotor bars distribution. Hence all the harmonics are included into the model.

The general coupled circuit model can be expressed as

$$v = R \cdot i + \frac{d\lambda}{dt} \tag{3.40}$$

where v, i and λ are the terminal voltage, current and flux linkage in each circuit; R is the matrix of resistance. Applying this general Equation to the five phase stator winding induction machine leads to the full model.

3.4.1 Stator Voltage Equation

For the stator winding, the stator voltage Equation is expressed as

$$v_{abcde} = R_{abcde} i_{abcde} + p\lambda_{abcde} \tag{3.41}$$

where R_{abcde} is a diagonal 5×5 matrix, in which the diagonal value depends on the resistances per phase of the stator' winding; p represents the operator $\frac{d}{dt}$ and

$$v_{abcde} = \begin{pmatrix} v_a \\ v_b \\ v_c \\ v_d \\ v_e \end{pmatrix},\ i_{abcde} = \begin{pmatrix} i_a \\ i_b \\ i_c \\ i_d \\ i_e \end{pmatrix},\ \lambda_{abcde} = \begin{pmatrix} \lambda_a \\ \lambda_b \\ \lambda_c \\ \lambda_d \\ \lambda_e \end{pmatrix} \tag{3.42}$$

The flux linkage can be written as the contribution of two components as

$$\lambda_{abcde} = \lambda_{ss} + \lambda_r \tag{3.43}$$

The first term in Equation (3.43) represents the stator flux linkage due to the stator currents; the second term is the stator flux linkage due to the rotor current.

3.4.2 Stator Flux Linkage Due to the Stator Currents

The stator flux linkage of the stator due to the stator currents can be expressed as

$$\lambda_{ss}=\begin{pmatrix}\lambda_{as}\\ \lambda_{bs}\\ \lambda_{cs}\\ \lambda_{ds}\\ \lambda_{es}\end{pmatrix}\begin{pmatrix}\lambda_{as}\\ \lambda_{bs}\\ \lambda_{cs1}\end{pmatrix}=\begin{pmatrix}L_{ls}+L_{aa} & L_{ab} & L_{ac} & L_{ad} & L_{ae}\\ L_{ba} & L_{ls}+L_{bb} & L_{bc} & L_{bd} & L_{be}\\ L_{ca} & L_{cb} & L_{ls}+L_{cc} & L_{cd} & L_{ce}\\ L_{da} & L_{db} & L_{dc} & L_{ls}+L_{dd} & L_{de}\\ L_{ea} & L_{eb} & L_{ec} & L_{ed} & L_{ls}+L_{ee}\end{pmatrix}i_s \tag{3.44}$$

$$\lambda_{ss}=L_{ss}i_{abcde}$$

3.4.3 Stator Flux Linkage Due to the Rotor Currents

The cage rotor having n rotor bars can be modeled as a n phase system. The total stator flux linkage due to the rotor currents can be written as

$$\lambda_{sr}=\begin{pmatrix}\lambda_{ar}\\ \lambda_{br}\\ \lambda_{cr}\\ \lambda_{dr}\\ \lambda_{er}\end{pmatrix}=\begin{pmatrix}L_{a1} & L_{a2} & \cdots & L_{a(n-1)} & L_{an}\\ L_{b1} & L_{b2} & \cdots & L_{b(n-1)} & L_{bn}\\ L_{c1} & L_{c2} & \cdots & L_{c(n-1)} & L_{cn}\\ L_{d1} & L_{d2} & \cdots & L_{d(n-1)} & L_{dn}\\ L_{e1} & L_{e2} & \cdots & L_{e(n-1)} & L_{en}\end{pmatrix}\cdot\begin{pmatrix}i_{r1}\\ i_{r2}\\ \vdots\\ i_{rn}\end{pmatrix}=L_{sr}\cdot i_r \tag{3.45}$$

where L_{ai} is the mutual inductance between the phase ‘a’ and i^{th} rotor loop, L_{bi} is the mutual inductance between the phase ‘b’ and i^{th} rotor loop, L_{ci} is the mutual inductance between the phase ‘c’ and i^{th} rotor loop, L_{di} is the mutual inductance between the phase ‘d’ and i^{th} rotor loop, L_{ei} is the mutual inductance between the phase ‘e’ and i^{th} rotor loop.

3.4.4 Rotor Voltage Equation

The voltage Equation for the k^{th} rotor loop can be represented as

$$0 = 2(r_b + r_e) \cdot i_k - r_b \cdot i_{k+1} - r_b \cdot i_{k-1} + p\lambda_{rk} \tag{3.46}$$

where r_b is the bar resistance; r_e is the resistance of the segment of end ring; i_k, i_{k-1} and i_{k+1} are the currents of the k^{th}, $k-1^{th}$ and $k+1^{th}$ loop, respectively; λ_{rk} is the flux linkage of the k^{th} rotor loop. This Equation is valid for all the rotor loops, therefore the total rotor voltage Equation can be written in the matrix form as

$$\begin{pmatrix} 0 \\ 0 \\ \vdots \\ 0 \end{pmatrix} = \begin{pmatrix} 2(r_b + r_e) & -r_b & \cdots & -r_b \\ -r_b & 2(r_b + r_e) & \cdots & 0 \\ \vdots & \vdots & \ddots & \vdots \\ -r_b & 0 & \cdots & 2(r_b + r_e) \end{pmatrix} \cdot \begin{pmatrix} i_{r1} \\ i_{r2} \\ \vdots \\ i_{rn} \end{pmatrix} + p \begin{pmatrix} \lambda_{r1} \\ \lambda_{r2} \\ \vdots \\ \lambda_{rn} \end{pmatrix} \tag{3.47}$$

The compact form of the above Equation is

$$0 = R_r \cdot i_r + p\lambda_r \tag{3.48}$$

where R_r is the resistance matrix, i_r is the rotor loop current vector and λ_r is the rotor loop flux linkage vector. The expression for rotor flux linkage can be expressed as

$$\lambda_r = \lambda_{rs} + \lambda_{rr} \tag{3.49}$$

The expression for each term of (3.49) can be written as

$$\lambda_{rs1} = \begin{pmatrix} \lambda_{r1s} \\ \lambda_{r1s} \\ \cdots \\ \lambda_{r(n-1)s} \\ \lambda_{rns} \end{pmatrix} = \begin{pmatrix} L_{ar1} & L_{br1} & L_{cr1} & L_{dr1} & L_{er1} \\ L_{ar2} & L_{br2} & L_{cr2} & L_{dr2} & L_{er2} \\ \cdots & \cdots & \cdots & \cdots & \cdots \\ L_{ar(n-1)} & L_{br(n-1)} & L_{cr(n-1)} & L_{dr(n-1)} & L_{er(n-1)} \\ L_{arn} & L_{brn} & L_{crn} & L_{drn} & L_{ern} \end{pmatrix} \cdot \begin{pmatrix} i_{as} \\ i_{bs} \\ i_{cs} \\ i_{ds} \\ i_{es} \end{pmatrix} \tag{3.50}$$

$$\lambda_{rs1} = L_{rs} \cdot i_{abcdes}$$

$$\lambda_{rr} = \begin{pmatrix} L_{rr} + 2(l_b + l_e) & L_{rm1} - l_b & \cdots & L_{rm1} - l_b \\ L_{rm1} - l_b & L_{rr} + 2(l_b + l_e) & \cdots & L_{rm2} \\ \vdots & \vdots & \ddots & \vdots \\ L_{rm1} - l_b & L_{rm2} & \cdots & L_{rr} + 2(l_b + l_e) \end{pmatrix} \cdot \begin{pmatrix} i_{r1} \\ i_{r2} \\ \vdots \\ i_{rn} \end{pmatrix} = L_{rr} \cdot i_r \qquad (3.51)$$

where L_{irj} is the mutual inductance between the stator i^{th} winding and j^{th} rotor loop, $i = a,b,c,d,e$ and $j = 1,2,\cdots n$, n is the number of rotor loop; L_{rr} is the self-inductance of the rotor loops; L_{rm1} is the mutual inductance between the adjunct rotor loops; L_{rm2} is the mutual inductance between the rotor loops that are not adjunct; l_b and l_e are the leakage inductance of the rotor bar and the segment of end ring, respectively.

3.5 Torque Equation

The electro-magnetic force developed by the machine is the only one that couples the electrical Equation with the mechanical Equation. From the energy point of view, the torque is determined by the instantaneous power transferred in the electromechanical system. The co-energy in a magnetic field is defined as

$$W_c = \sum_{j=1}^{J} i_j \lambda_j - W_f \text{ and } W_f = \int \sum_{j=1}^{J} i_j \cdot d\lambda_j \qquad (3.52)$$

where i_j and λ_j are the current and flux linkage of j^{th} circuit, respectively. W_f is the total field energy in the system. In the five-phase induction machine (with 5 stator windings and *n* rotor bars), there are five stator currents and *n* rotor current. Hence for this particular five-phase induction machine, the total field energy can be expressed as

$$W_f = \frac{1}{2} i_{abcde}{}^T \cdot L_{ss} \cdot i_{abcde} + \frac{1}{2} i_{abcde}{}^T \cdot L_{sr} \cdot i_r + \frac{1}{2} i_r{}^T \cdot L_{rs} \cdot i_{abcde} + \frac{1}{2} i_r{}^T \cdot L_{rr} \cdot i_r \tag{3.53}$$

The electromagnetic torque can be obtained from the magnetic co-energy as

$$T_e = \frac{\partial W_c}{\partial \theta_{rm}} = -\frac{\partial W_f}{\partial \theta_{rm}} \tag{3.54}$$

where θ_{rm} is the mechanical angle of the rotor.

Only terms in Equation (3.53) which are the functions of the rotor angle can contribute the electromagnetic torque. So applying (3.54) to (3.53), the electromagnetic torque can be expressed as

$$T_e = -\frac{1}{2} i_{abcde}{}^T \cdot \frac{\partial L_{sr}}{\partial \theta_{rm}} \cdot i_r - \frac{1}{2} i_r{}^T \cdot \frac{\partial L_{rs}}{\partial \theta_{rm}} \cdot i_{abcde} \tag{3.55}$$

For a linear magnetic circuit,

$$L_{ij} = L_{ji} \tag{3.56}$$

Hence the torque Equation is simplified as

$$T_e = -i_{abcde}{}^T \cdot \frac{\partial L_{sr}}{\partial \theta_{rm}} \cdot i_r \tag{3.57}$$

3.6 Development of the Equivalent Circuit

In this section, we are introducing a letter '*h*' which will stand for the harmonic number. Therefore, the general Equations can be evaluated for any significant harmonic component.

3.6.1 QD Transformation

In order to develop the equivalent circuit for the five phase induction machine, the above voltage, flux and torque Equations are transformed into qd reference frame to eliminate the tome varying quantities. We are adopting an arbitrary reference frame rotating at a speed ω. In the simulation part, the rotor reference frame (ω_r) will be used.

$$v_{qdsh} = T_{sh}(\theta)v_{abcdes} \tag{3.58}$$

$$i_{qdsh} = T_{sh}(\theta)i_{abcdes} \tag{3.59}$$

$$\lambda_{qdsh} = T_{sh}(\theta)\lambda_{abcdes} \tag{3.60}$$

$$v_{qdrh} = T_{rh}(\theta)v_{1234\cdots n} \tag{3.61}$$

$$i_{qdrh} = T_{rh}(\theta)i_{1234\cdots n} \tag{3.62}$$

$$\lambda_{qdrh} = T_{rh}(\theta)\lambda_{1234\cdots n} \tag{3.63}$$

$$v_{abcdes} = \begin{pmatrix} v_{as} \\ v_{bs} \\ v_{cs} \\ v_{ds} \\ v_{es} \end{pmatrix}, \quad i_{abcdes} = \begin{pmatrix} i_{as} \\ i_{bs} \\ i_{cs} \\ i_{ds} \\ i_{es} \end{pmatrix}, \quad \lambda_{abcdes} = \begin{pmatrix} \lambda_{as} \\ \lambda_{bs} \\ \lambda_{cs} \\ \lambda_{ds} \\ \lambda_{es} \end{pmatrix}, \quad v_{1234\cdots n} = \begin{pmatrix} v_1 \\ v_2 \\ \vdots \\ v_{n-1} \\ v_n \end{pmatrix} \tag{3.64}$$

$$i_{1234\cdots n} = \begin{pmatrix} i_1 \\ i_2 \\ \vdots \\ i_{n-1} \\ i_n \end{pmatrix}, \quad \lambda_{1234\cdots n} = \begin{pmatrix} \lambda_1 \\ \lambda_2 \\ \vdots \\ \lambda_{n-1} \\ \lambda_n \end{pmatrix}, \quad v_{qdsh} = \begin{pmatrix} v_{qsh} \\ v_{dsh} \end{pmatrix}, \quad i_{qdsh} = \begin{pmatrix} i_{qsh} \\ i_{dsh} \end{pmatrix} \tag{3.65}$$

$$\lambda_{qdsh} = \begin{pmatrix} \lambda_{qsh} \\ \lambda_{dsh} \end{pmatrix}, \quad v_{qdrh} = \begin{pmatrix} v_{qrh} \\ v_{drh} \end{pmatrix}, \quad i_{qdrh} = \begin{pmatrix} i_{qrh} \\ i_{drh} \end{pmatrix}, \quad \lambda_{qdrh} = \begin{pmatrix} \lambda_{qrh} \\ \lambda_{drh} \end{pmatrix} \tag{3.66}$$

For $h = 1, 3$

$$T_{s1}(\theta) = \frac{2}{5}\begin{bmatrix} \cos(\theta) & \cos\left(\theta - \frac{2\pi}{3}\right) & \cos\left(\theta - \frac{4\pi}{3}\right) & \cos\left(\theta - \frac{6\pi}{3}\right) & \cos\left(\theta - \frac{8\pi}{3}\right) \\ \sin(\theta) & \sin\left(\theta - \frac{2\pi}{3}\right) & \sin\left(\theta - \frac{4\pi}{3}\right) & \sin\left(\theta - \frac{6\pi}{3}\right) & \sin\left(\theta - \frac{8\pi}{3}\right) \end{bmatrix} \tag{3.67}$$

$$T_{s3}(\theta) = \frac{2}{5}\begin{bmatrix} \cos(3\theta) & \cos 3\left(\theta - \frac{2\pi}{3}\right) & \cos 3\left(\theta - \frac{4\pi}{3}\right) & \cos 3\left(\theta - \frac{6\pi}{3}\right) & \cos 3\left(\theta - \frac{8\pi}{3}\right) \\ \sin(3\theta) & \sin 3\left(\theta - \frac{2\pi}{3}\right) & \sin 3\left(\theta - \frac{4\pi}{3}\right) & \sin 3\left(\theta - \frac{6\pi}{3}\right) & \sin 3\left(\theta - \frac{8\pi}{3}\right) \end{bmatrix} \tag{3.68}$$

$$T_{r1}(\theta) = \frac{2}{n}\begin{bmatrix} \cos(\theta - \theta_r) & \cos\left(\theta - \theta_r - \frac{2\pi}{n}\right) & \cos\left(\theta - \theta_r - \frac{4\pi}{n}\right) & \cdots & \cos\left(\theta - \theta_r - \frac{2(n-1)\pi}{n}\right) \\ \sin(\theta - \theta_r) & \sin\left(\theta - \theta_r - \frac{2\pi}{n}\right) & \sin\left(\theta - \theta_r - \frac{4\pi}{n}\right) & \cdots & \sin\left(\theta - \theta_r - \frac{2(n-1)\pi}{n}\right) \end{bmatrix} \tag{3.70}$$

where n is the number of rotor bars.

$$T_{r3}(\theta) = \frac{2}{n}\begin{bmatrix} \cos 3(\theta - \theta_r) & \cos 3\left(\theta - \theta_r - \frac{2\pi}{n}\right) & \cos 3\left(\theta - \theta_r - \frac{4\pi}{n}\right) & \cdots & \cos 3\left(\theta - \theta_r - \frac{2(n-1)\pi}{n}\right) \\ \sin 3(\theta - \theta_r) & \sin 3\left(\theta - \theta_r - \frac{2\pi}{n}\right) & \sin 3\left(\theta - \theta_r - \frac{4\pi}{n}\right) & \cdots & \sin 3\left(\theta - \theta_r - \frac{2(n-1)\pi}{n}\right) \end{bmatrix} \tag{3.71}$$

$$v_{qdsh} = T_{sh}(\theta) r_{sqdh} T_{sh}^{-1}(\theta) i_{qdsh} + T_{sh}(\theta) p T_{sh}^{-1}(\theta) \lambda_{qdsh}$$

$$v_{qdsh} = r_{sqdh} i_{qdsh} + p\lambda_{qdsh} - j\omega\lambda_{qdsh} \tag{3.72}$$

$$v_{qdrh} = T_{rh}(\theta) r_{rqdh} T_{rh}^{-1}(\theta) i_{qdrh} + T_{rh}(\theta) p T_{rh}^{-1} \lambda_{qdrh}$$

$$v_{qdrh} = r_{rqdh} i_{qdrh} + p\lambda_{qdrh} - j(\omega - \omega_r)\lambda_{qdrh} \tag{3.73}$$

The transformed stator and rotor flux linkages are given by Equations (3.74) and (3.75), respectively

$$\lambda_{qdsh} = L_{ssqdh} i_{qdsh} + L_{srqdh} i_{qdrh} \tag{3.74}$$

$$\lambda_{qdrh} = L_{rrqdh} i_{qdrh} + L_{rsqdh} i_{qdsh} \tag{3.75}$$

Substituting the flux Equations into the voltage Equations, we have

$$v_{qdsh} = r_{sqdh} i_{qdsh} + p\left(L_{ssqdh} i_{qdsh} + L_{srqdh} i_{qdrh}\right) - j\omega\left(L_{ssqdh} i_{qdsh} + L_{srqdh} i_{qdrh}\right) \tag{3.76}$$

$$v_{qdrh} = r_{rqdh} i_{qdrh} + p\left(L_{rrqdh} i_{qdrh} + L_{rsqdh} i_{qdsh}\right) - j\left(\omega - \omega_r\right)\left(L_{rrqdh} i_{qdrh} + L_{rsqdh} i_{qdsh}\right) \tag{3.77}$$

When the voltage Equations are referred to the stator side, then we have

$$v_{qdsh} = r_{sqdh} i_{qdsh} + p\left(L_{ssqdh} i_{qdsh} + L_{srqdh} N_{Ih}^{qd} i'_{qdrh}\right) - j\omega\left(L_{ssqdh} i_{qdsh} + L_{srqdh} N_{Ih}^{qd} i'_{qdrh}\right) \tag{3.78}$$

$$N_{Vh}^{qd} v_{qdrh} = \begin{Bmatrix} N_{Vh}^{qd} r_{rqdh} N_{Ih}^{qd} i_{qdrh} + p\left(N_{Vh}^{qd} L_{rrqdh} N_{Ih}^{qd} i'_{qdrh} + N_{Vh}^{qd} L_{rsqdh} i_{qdsh}\right) + \\ - j\left(\omega - \omega_r\right)\left(N_{Vh}^{qd} L_{rrqdh} N_{Ih}^{qd} i'_{qdrh} + N_{Vh}^{qd} L_{rsqdh} i_{qdsh}\right) \end{Bmatrix} \tag{3.79}$$

$$v_{qdsh} = r_{sqdh} i_{qdsh} + L_{ssqdh} p i_{qdsh} + L'_{srqdh} p i'_{qdrh} - j\omega L_{ssqdh} i_{qdsh} - j\omega L'_{srqdh} i'_{qdrh} \tag{3.80}$$

$$v_{qdsh} = \left(r_{sqdh} - j\omega L_{ssqdh}\right) i_{qdsh} + L_{ssqdh} p i_{qdsh} + L'_{srqdh} p i'_{qdrh} - j\omega L'_{srqdh} i'_{qdrh} \tag{3.81}$$

$$v'_{qdrh} = \begin{Bmatrix} r'_{rqdh} i'_{qdrh} + p\left(L'_{rrqdh} i'_{qdrh} + L'_{rsqdh} i_{qdsh}\right) + \\ - j\left(\omega - \omega_r\right)\left(L'_{rrqdh} i'_{qdrh} + L'_{rsqdh} i_{qdsh}\right) \end{Bmatrix} \tag{3.82}$$

$$L'_{srqdh} = L_{srqdh} N_{Ih}^{qd}, \qquad v'_{qdrh} = N_{Vh}^{qd} v_{qdrh}, \qquad r'_{rqdh} = N_{Vh}^{qd} r_{rqdh} N_{Ih}^{qd} \tag{3.83}$$

$$L'_{rrqdh} = N_{Vh}^{qd} L_{rrqdh} N_{Ih}^{qd}, \qquad L'_{rsqdh} = N_{Vh}^{qd} L_{rsqdh} \tag{3.84}$$

The fluxes referred to the stator side become

$$\lambda_{qdsh} = L_{ssqdh} i_{qdsh} + L'_{srqdh} i'_{qdrh}, \qquad \lambda'_{qdrh} = L'_{rrqdh} i'_{qdrh} + L'_{rsqdh} i_{qdsh} \tag{3.85}$$

Dynamic Equations for simulation

$$p\lambda_{qsh} = v_{qsh} - r_{sqh} i_{qsh} - \omega\lambda_{dsh} \tag{3.86}$$

$$p\lambda_{dsh} = v_{dsh} - r_{sdh} i_{dsh} + \omega\lambda_{qsh} \tag{3.87}$$

$$p\lambda'_{qrh} = v'_{qrh} - r'_{rqh} i'_{qrh} - j\left(\omega - \omega_r\right)\lambda'_{drh} \tag{3.88}$$

$$p\lambda'_{drh} = v'_{drh} - r'_{rdh} i'_{drh} + j\left(\omega - \omega_r\right)\lambda'_{qrh} \tag{3.89}$$

In this work, only the fundamental and third harmonic components have been considered. The torque is obtained as follows

$$T_{e1} = \left(\frac{m}{2}\right)\left(\frac{P}{2}\right)\left(\lambda_{ds1} i_{qs1} - \lambda_{qs1} i_{ds1}\right) \tag{3.90}$$

$$T_{e3} = 3\left(\frac{m}{2}\right)\left(\frac{P}{2}\right)\left(\lambda_{ds3} i_{qs3} - \lambda_{qs3} i_{ds3}\right) \tag{3.91}$$

$$T_e = T_{e1} + T_{e3} \tag{3.92}$$

The mechanical Equation is given by

$$p\omega_r = \frac{P}{2J}\left(T_e - T_L\right) \tag{3.93}$$

where ω_r is the rotor speed $\left(rad/\sec\right)$, m is the number of stator phases, P is the number of poles, J is the moment of inertia $\left(kgm^2\right)$ and T_L is the load torque $\left(Nm\right)$.

3.7 Fundamental Component Based Parameter Determination

The primary and secondary m.m.fs, expressed in ampere-turns per pair poles, are [3.8, 3.9]

$$M_{ph} = \frac{2\sqrt{2}}{\pi} k_{bph} k_{pph} m_p N_p I_{ph} = N_p^{'} I_{ph} \tag{3.94}$$

and

$$M_{sph} = \frac{2\sqrt{2}}{\pi} k_{bsh} k_{psh} m_s N_s I_{sh} = N_s^{'} I_{sh} \tag{3.95}$$

where

$$N_p^{'} = \frac{2\sqrt{2}}{\pi} k_{bph} k_{pph} m_p N_p \tag{3.96}$$

$$N_s^{'} = \frac{2\sqrt{2}}{\pi} k_{bsh} k_{psh} m_s N_s \tag{3.97}$$

The vector sum of these two m.m.fs must then be just sufficient to maintain the flux ϕ through the magnetic circuit. Under no-load conditions, it is necessary that

$$N_p^{'} I_{ph} + N_s^{'} I_{sh} = N_p^{'} I_{oh} \tag{3.98}$$

where I_{oh} is the per phase no-load current taken from the line by the primary winding necessary to produce the m.m.f needed to maintain the flux ϕ_h.

Dividing through by $N_p^{'}$, we get

$$I_{ph} + \frac{N_s^{'}}{N_p^{'}} I_{sh} = I_{oh} \tag{3.99}$$

$$\frac{N_s^{'}}{N_p^{'}} I_{sh} = I_{oh} - I_{ph} = I_{sh}^{'} \tag{3.100}$$

$$\frac{I_{sh}^{'}}{I_{ph}} = \frac{N_s^{'}}{N_p^{'}} = \frac{k_{bsh} k_{psh} m_s N_s}{k_{bph} k_{pph} m_p N_p} \tag{3.101}$$

k_{bph} is the distribution (breadth) factor for the primary (stator) winding

k_{pph} is the pitch factor for the primary (stator) winding

m_p is the number of phases for the primary (stator) winding

N_p is the number of series turns per phase for the primary (stator) winding

k_{bsh} is the distribution (breadth) factor for the secondary (rotor) winding

k_{psh} is the pitch factor for the secondary (rotor) winding

m_s is the number of phases for the secondary (rotor) winding

N_s is the number of series turns per phase for the secondary (rotor) winding

At standstill conditions, the e.m.f developed in each phase of the primary (stator) and the secondary (rotor) windings are, respectively, given by

$$E_{ph} = 4.44 k_{bph} k_{pph} f_{ph} N_p \phi_h \tag{3.102}$$

$$E_{sh} = 4.44 k_{bsh} k_{psh} f_{sh} N_s \phi_h \tag{3.103}$$

$$\frac{E_{ph}}{E_{sh}} = \frac{k_{bph} k_{pph} f_{ph} N_p}{k_{bsh} k_{psh} f_{sh} N_s} = \frac{k_{bph} k_{pph} N_p}{k_{bsh} k_{psh} N_s}, \text{ since } f_{sh} = f_{ph} \tag{3.104}$$

where

ϕ_h is the air gap flux

f_{ph} is the hth frequency of the voltages and currents in the primary (stator) winding

f_{sh} is the hth frequency of the voltages and currents in the secondary (rotor) winding

Now, if the primary (stator) and secondary (rotor) turns per phase (N_p and N_s, respectively) are replaced by the corresponding number of conductors per phase (Z_p and $Z_s = 1$), the ratio of the current transformation is

$$\frac{I'_{sh}}{I_{ph}} = \frac{N'_s}{N'_p} = \frac{k_{bsh} k_{psh} m_s Z_s}{k_{bph} k_{pph} m_p Z_p} = \frac{2Z_r}{P k_{bph} k_{pph} m_p Z_p} \tag{3.105}$$

Which is the factor by which the actual rotor current per bar must be multiplied to convert it to equivalent primary (stator) current. The corresponding factor for converting actual rotor e.m.f per phase to equivalent primary (stator) value is

$$\frac{E_{ph}}{E_{sh}} = \frac{k_{bph} k_{pph} N_p}{k_{bsh} k_{psh} N_s} = k_{bph} k_{pph} Z_p \tag{3.106}$$

The parameters of the machine can be determined by using derived expressions as follows

(a) qd Transformed parameters

When the actual time varying parameters have been transformed constant values by using qd transformation, then the appropriate turn transformations for the machine parameters will be

$$N_{Ih}^{qd} = \frac{m_s K_{wsh} N_s}{S_r \sin\left(\frac{hP\pi}{S_r}\right)} \text{, for current transformation} \tag{3.107}$$

$$N_{Vh}^{qd} = \frac{K_{wsh} N_s}{\sin\left(\frac{hP\pi}{S_r}\right)} \text{, for voltage transformation} \tag{3.108}$$

$$N_{Ih}^{qd} N_{Vh}^{qd} = \frac{m_s K_{wsh} N_s}{S_r \sin\left(\frac{hP\pi}{S_r}\right)} \frac{K_{wsh} N_s}{\sin\left(\frac{hP\pi}{S_r}\right)} = \frac{m_s}{S_r}\left(\frac{K_{wsh} N_s}{\sin\left(\frac{hP\pi}{S_r}\right)}\right)^2 \text{, for resistive impedance transformation} \tag{3.109}$$

$$R_{rh}^{'} = \frac{m_s K_{wsh}^2 N_s^2}{S_r \sin^2\left(\frac{hP\pi}{S_r}\right)} R_{rh}^{qd}$$, this is the rotor resistance referred to the stator.

where

S_r is the number of rotor bars

P is the number of poles

h is the harmonic number

R_{rh}^{qd} is the actual hth qd-rotor resistance

(b) Turn transformation of actual parameters

The following turn expressions will be used for transformation of the machine variable when dealing with actual peak values of the variables and parameters [3.8, 3.9]

$$N_{Ih} = \frac{2m_s N_s K_{wsh}}{S_r K_{wrh}}, \text{ for current transformation} \tag{3.110}$$

$$N_{Vh} = \frac{2N_s K_{wsh}}{K_{wrh}}, \text{ for voltage transformation} \tag{3.111}$$

$$N_{Ih}N_{Vh} = \frac{2m_s N_s K_{wsh}}{S_r K_{wrh}} \frac{2N_s K_{wsh}}{K_{wrh}} = \frac{4m_s N_s^2 K_{wsh}^2}{S_r K_{wrh}^2}, \text{ for resistive impedance transformation} \tag{3.112}$$

$$R_{rh}^{'} = \frac{4m_s K_{wsh}^2 N_s^2}{S_r}\left(R_b + \frac{R_e}{2\sin^2\left(\dfrac{hP\pi}{S_r}\right)} \right), \text{ this is the rotor resistance referred to the stator.}$$

where

$$R_{rh} = R_b + \frac{R_e}{2\sin^2\left(\dfrac{hP\pi}{S_r}\right)} \text{ is the actual equivalent rotor resistance}$$

The rotor leakage inductance is given by

$$L_{lrh}^{'} = \frac{4m_s K_{wsh}^2 N_s^2}{S_r}\left(L_b + \frac{L_e}{2\sin^2\left(\dfrac{hP\pi}{S_r}\right)} \right) + L_{mh}\sum_{K\neq 0}\frac{h^2}{\left(\dfrac{KS_r}{P}+h\right)^2}, \quad K = \pm 1, \pm 2, \ldots \tag{3.113}$$

For $K = 1,\ h = 1$

$$L_{lr1}^{'} = \frac{4m_s K_{ws1}^2 N_s^2}{S_r}\left(L_b + \frac{L_e}{2\sin^2\left(\frac{P\pi}{S_r}\right)} \right) + L_{m1}\frac{1}{\left(\frac{S_r}{P}+1\right)^2}, \quad K = \pm 1, \pm 2, ... \tag{3.114}$$

The rotor self inductance is given by

$$L_{rh}^{qd} = \frac{S_r \sin^2\left(\frac{hP\pi}{S_r}\right)}{m_s K_{wsh}^2 N_s^2}\left(L_{rlh}^{'} + L_{mh}\right) \tag{3.115}$$

$$L_{rh}^{'} = L_{rh}^{'qd} = L_{rlh}^{'} + L_{mh} \tag{3.116}$$

Self inductance of a stator phase due to the air gap flux is [3.8, 3.9]

$$L_{ms1} = \frac{\mu_0 r l_e}{g_e}\frac{4}{\pi}\left(\frac{N}{P}\right)^2 \sum_{h=1}^{\infty}\left(\frac{K_{wsh}}{h}\right)^2 \tag{3.117}$$

where g_e is the effective air gap, l_e is the effective length, and N is the total number of turns per phase. To obtain the total self inductance L_{s1}, the leakage inductances should be added to L_{ms1}.

Mutual inductance between two stator phases is [3.8, 3.9]

$$L_{msi} = \frac{\mu_0 r l_e}{g_e}\frac{4}{\pi}\left(\frac{N}{P}\right)^2 \sum_{h=1}^{\infty}\left(\frac{K_{wsh}}{h}\right)^2 \cos\left((i-1)\frac{2\pi}{m_s}\right), \quad i = 1, ...(h \ \ odd) \tag{3.118}$$

The mutual slot leakage inductance should be added to the value given by the above Equation to obtain the total mutual inductances L_{si} $(i = 2,\ 3,\ ...)$ [3.8, 3.9]

$$(n-1)L_{loop} = \frac{\mu_0 r l_e}{g_e}\frac{4}{\pi}\sum_{h=1}^{\infty}\frac{1}{h^2}\sin^2\left(\frac{h\pi}{S_r}\right) \tag{3.119}$$

$$L_{loop} = \frac{\mu_0 r l_e}{g_e}\frac{4}{\pi}\sum_{h=1}^{\infty}\frac{1}{h^2}\sin^2\left(\frac{h\pi}{S_r}\right)\cos(h\theta) \tag{3.120}$$

where θ is the angle between the axes of two rotor loops. The h^{th} term of the above series is the contribution of the h^{th} harmonic to the inductance.

To obtain the total self inductance of a loop, its leakage inductance of the end ring segments and the slot leakage inductance should be added to its air gap self inductance $(n-1)L_{loop}$ [3.8, 3.9]

$$L_{r1} = 2(L_b + L_e) + (n-1)L_{loop} \tag{3.121}$$

$$L_{r2} = -L_b - L_{loop} \tag{3.122}$$

$$L_{ri} = -L_{loop}, \quad i = 3, 4, \ldots \tag{3.123}$$

where L_b is the slot leakage inductance and L_e is the leakage inductance of the ring segments.

If the S_r rotor bars are divided into P basic periods, the above should be modified to

$$L_{r1} = 2(L_b + L_e) + (n-P)L_{loop} \tag{3.124}$$

$$L_{r2} = -L_b - PL_{loop} \tag{3.125}$$

$$L_{ri} = -PL_{loop}, \quad i = 3, 4, \ldots \tag{3.126}$$

3.7.1 Mutual Inductance Between a Rotor Loop and a Stator Phase

The mutual inductance between the i^{th} stator phase and the j^{th} rotor loop can be obtained by [3.8, 3.9]

$$L_{srij} = \frac{\mu_0 r l_e}{g_e} \frac{4}{\pi} \frac{N}{P^2} \sum_{h=1}^{\infty} \frac{K_{wsh}}{h^2} \sin\left(\frac{hP\pi}{S_r}\right) \cos(hP\theta) \qquad (v\ \ odd) \qquad (3.127)$$

Or equivalently

$$L_{srij} = \frac{\mu_0 r l_e}{g_e} \frac{4}{\pi} \frac{N}{P^2} \sum_{h=1}^{\infty} \frac{K_{wsh}}{h^2} \sin\left(\frac{hP'\pi}{S'_r}\right) \cos(hP'\theta') \qquad (v\ \ odd) \qquad (3.128)$$

where θ and θ' are the mechanical and electrical angles between the axes of the stator phase and rotor loop.

3.7.2 Two Axis Equivalent Inductances

The expression for the two-axis inductances can be derived. The stator two-axis inductance is

$$L_{qdsh} = L_{s1} + 2L_{s2} \cos\left(h \frac{2\pi}{m_s}\right) + \cdots \qquad (3.129)$$

Substituting for $L_{si}'s \ \ (i = 1,\ 2,\ \cdots)$

$$\begin{aligned} L_{qdsh} &= L_{ls} + \frac{m_s}{2} \frac{\mu_0 r l_e}{g_e} \frac{4}{\pi} \left(\frac{N}{P}\right)^2 \sum_{\ell} \left(\frac{K_\ell}{\ell}\right)^2 \\ \ell &= Km_s + h, \qquad (K = 0,\ \pm 1,\ \pm 2,\ \cdots) \end{aligned} \qquad (3.130)$$

Defining the h[th] harmonic (stator) magnetizing inductance L_{mh} as [3.8, 3.9]

$$L_{mh} = \frac{m_s}{2} \frac{\mu_0 r l_e}{g_e} \frac{4}{\pi} \left(\frac{N}{P}\right)^2 \left(\frac{K_{wsh}}{h}\right)^2 \qquad (3.131)$$

The L_{qdsh} can be written as

$$L_{qdsh} = L_{ls} + \sum_{\ell} L_{m\ell},\ \ \ell = Km_s + h \quad (K = 0,\ \pm 1,\ \ \pm 2,\ \cdots) \qquad (3.132)$$

It is assumed that the mutual slot leakage is lumped with the leakage inductance L_{ls}.

For squirrel cage rotor with S_r rotor bars or S'_r bars per basic period, since $\frac{S_r}{P} = \frac{S'_r}{P'}$, the rotor two-axis inductance is

$$L_{qdrh} = L_{1r} + 2L_{2r}\cos\left(hP\frac{2\pi}{S_r}\right) + \cdots \tag{3.133}$$

Substituting for L_{ri}'s $(i = 1, 2, \cdots)$

$$L_{qdrh} = 2\left(L_e + \left(1 - \cosh\left(P\frac{2\pi}{S_r}\right)\right)L_b\right) + \frac{S_r}{2}\frac{\mu_0 r l_e}{g_e}\frac{4}{\pi}\sin^2\left(hP\frac{\pi}{S_r}\right)\sum_K \frac{1}{\left(K\frac{S_r}{P} + h\right)^2} \tag{3.134}$$

$(K = 0, \pm 1, \pm 2, \cdots)$

Substituting L_{mh} obtained previously, we have

$$L_{qdrh} = 2\left(L_e + 2\sin^2\left(hP\frac{\pi}{S_r}\right)L_b\right) + \frac{S_r \sin^2\left(hP\frac{\pi}{S_r}\right)}{m_s K_{wsh}^2 N_s^2} L_{mh} \sum_K \frac{h^2}{\left(K\frac{S_r}{P} + h\right)^2} \tag{3.135}$$

$(K = 0, \pm 1, \pm 2, \cdots)$

L_{qdrh} can also be expressed as

$$L_{qdrh} = \frac{S_r \sin^2\left(hP\frac{\pi}{S_r}\right)}{m_s K_{wsh}^2 N_s^2}\left(L'_{lrh} + L_{mh}\right) \tag{3.136}$$

The summation $\sum_K \frac{h^2}{\left(K\frac{S_r}{P} + h\right)^2}$, $(K = 0, \pm 1, \pm 2, \cdots)$ in the above Equations can be evaluated from the following identity

$$\sum_K \frac{h^2}{\left(K\frac{S_r}{P}+h\right)^2} = \left(\frac{hP\frac{\pi}{S_r}}{\sin\left(hP\frac{\pi}{S_r}\right)}\right)^2, \quad (K = 0, \pm 1, \quad \pm 2, \cdots) \tag{3.137}$$

The actual parameters obtained from the full-order modeling whereby the mutual stator-to-rotor bar inductances are calculated during the simulation are shown Table 3.4. Using the turn transformations of section 3.7 (a), these parameters are referred to the stator side as they appear in Table 3.5, and they are close to those determined by sung the fundamental component approach.

Table 3.4 Machine parameters before being referred to the stator side

Parameters	From the Full order model simulation	
	Fundamental component	Third harmonic component
r_s	0.320 Ω	0.320 Ω
r_r	4.87 $\mu\Omega$	24.55 $\mu\Omega$
L_{sr}	1.5 mH	52 mH
L_{rs}	2.7 μH	92.7 μH
L_{rr}	2.332 μH	2.129 μH

Table 3.5 Machine parameters referred to the stator side

Parameters	From the Full order model simulation	
	Fundamental component	Third harmonic component
r_s	0.320 Ω	0.320 Ω
$r_r^{'}$	0.6888 Ω	0.4421 Ω
$L_{sr}^{'}$	0.3185 H	0.0295 H
$L_{rs}^{'}$	0.3185 H	0.0295 H
$L_{rr}^{'}$	0.3297 mH	0.0383 H

3.8 Simulation Results

The simulation results for starting transient and load performance of the five-phase machine are presented in this section. The stator is supplied from a 60 Hz, 230 V line-to-line rms voltages for the fundamental components. To obtain the third harmonic components, the magnitude of the harmonic voltage is taken as 15% of the fundamental. The load torque applied is 8.5 Nm.

Figures 3.11 and 3.12 show the fundamental component of the qd-transformed stator-to-stator mutual inductance and rotor bar self inductance. The qd rotor-bar-to-stator and stator-to-rotor bar mutual inductances are shown in Figures 3.13 and 3.14, respectively; whereas Figure 3.15 shows the qd fundamental component of the rotor bar resistance.

The machine is run at no-load for five seconds at which a load torque of 8.5 Nm is applied. The no-load and load characteristics for different variables are shown in Figures 3.16, 3.17, 3.18, 3.19, 3.20, 3.21, 3.22 and 3.23 for the fundamental components of the no-load speed, load speed, no-load electromagnetic torque, load electromagnetic torque, no-load stator current, load stator current, no-load rotor bar current and load rotor bar current, respectively.

Figures 3.24 and 3.25 show the total electromagnetic torque at no-load and load, respectively. This is obtained by adding the two values of electromagnetic torques, i.e. the fundamental component value and the harmonic component value. The third harmonic components for the stator currents at no-load, stator currents at load, rotor bar currents at no-load, rotor bar currents at load, electromagnetic torque at load and electromagnetic torque at no-load are represented by figures 3.26, 3.27, 3.28, 3.29, 3.30 and 3.31, respectively.

The third harmonic components of the qd rotor bar resistance, qd stator mutual inductance, qd rotor bar self inductance, qd rotor bar-to-stator mutual inductance, and the qd stator-to-rotor mutual inductance are shown in figures 3.32, 3.33, 3.34, 3.35 and 3.36, respectively.

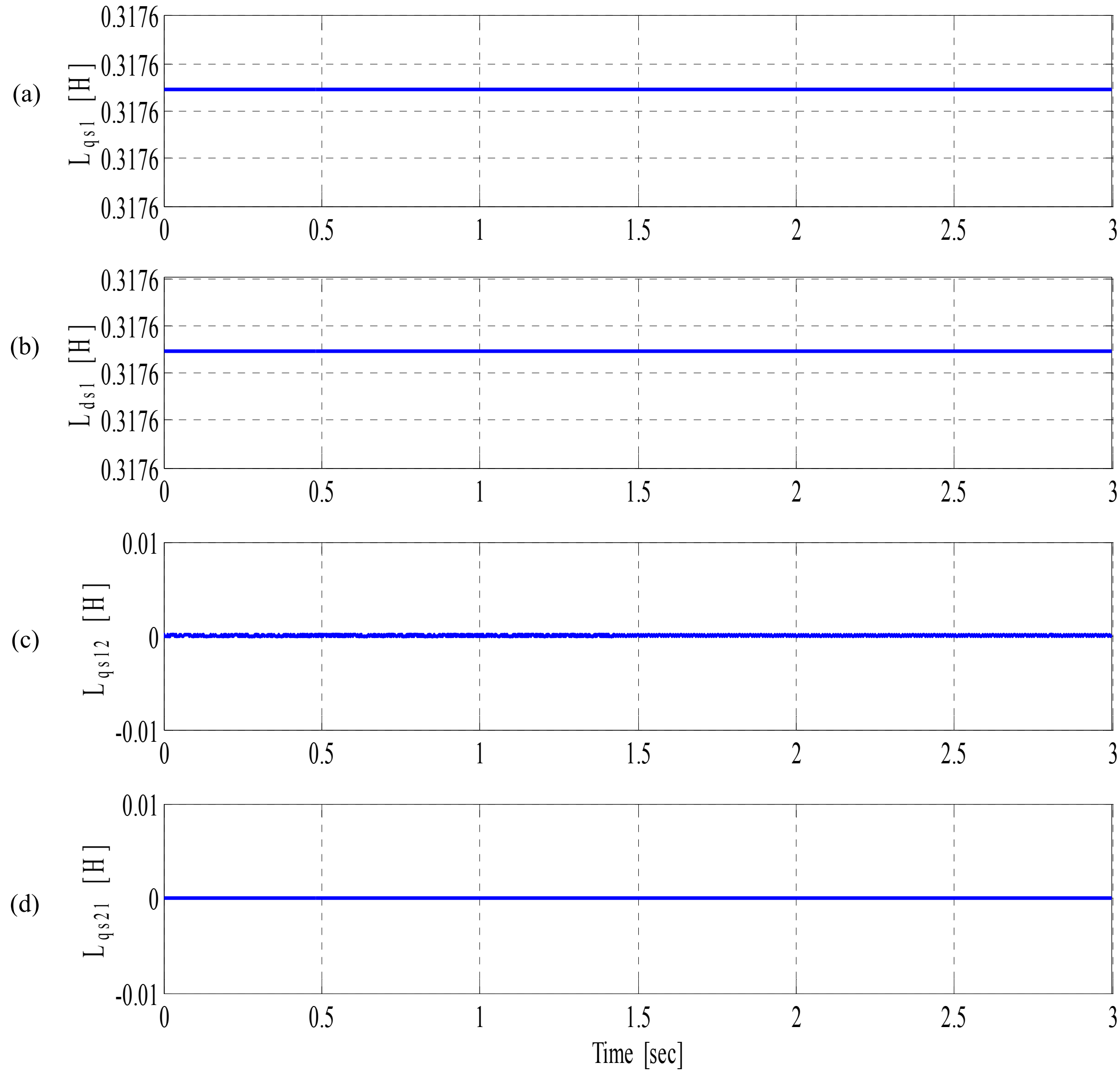

Figure 3.11 Fundamental component of the qd-stator inductance (a) L_{ssq1} (b) L_{ssd1} (c) L_{ssq12} (d) L_{ssd21}

(a)
(b)
(c)
(d)

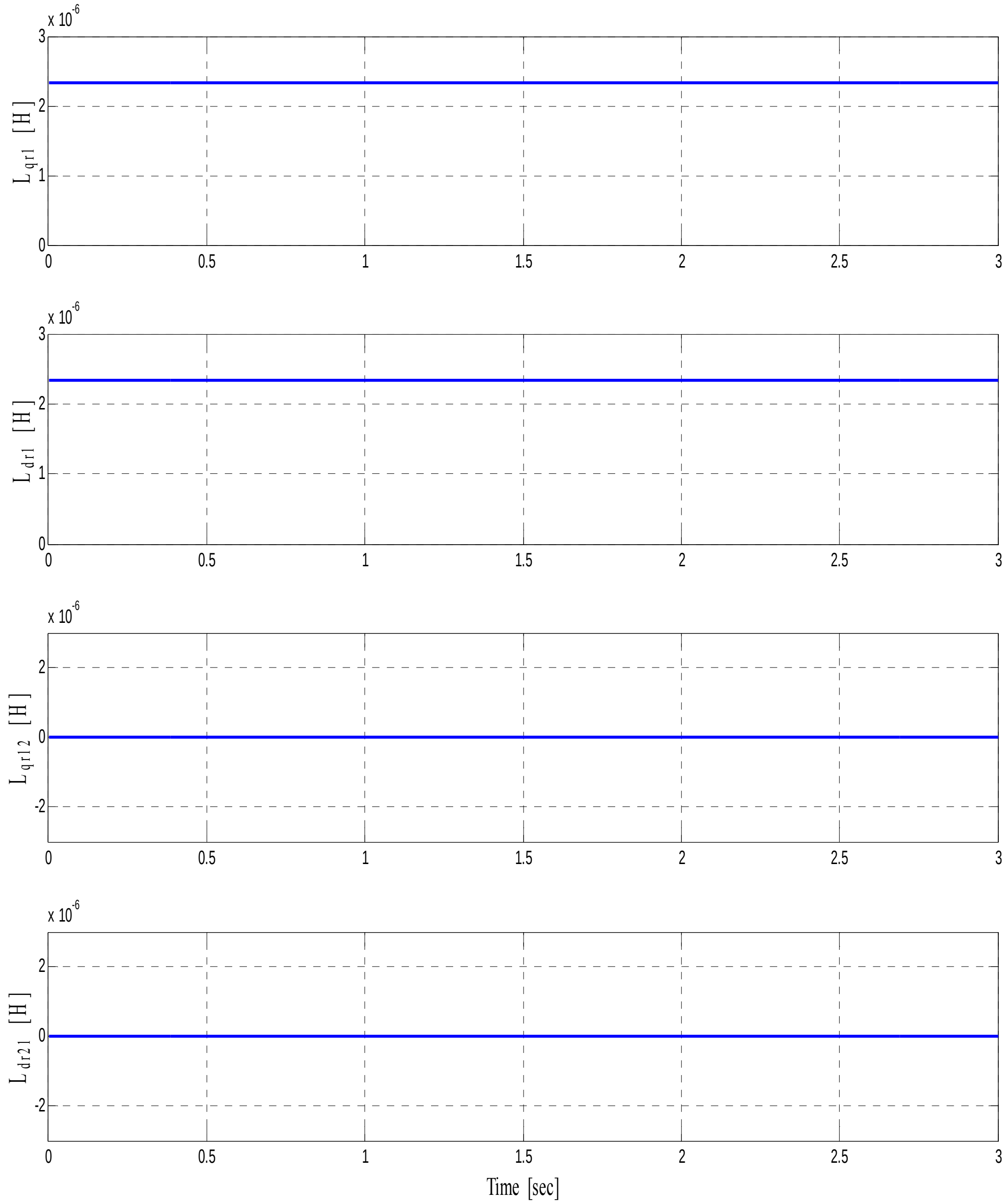

Figure 3.12 Fundamental component of the qd-rotor bar self inductance (a) L'_{rq1} (b) L'_{rd1} **(c)** L'_{rq12} (d) L'_{rd21}

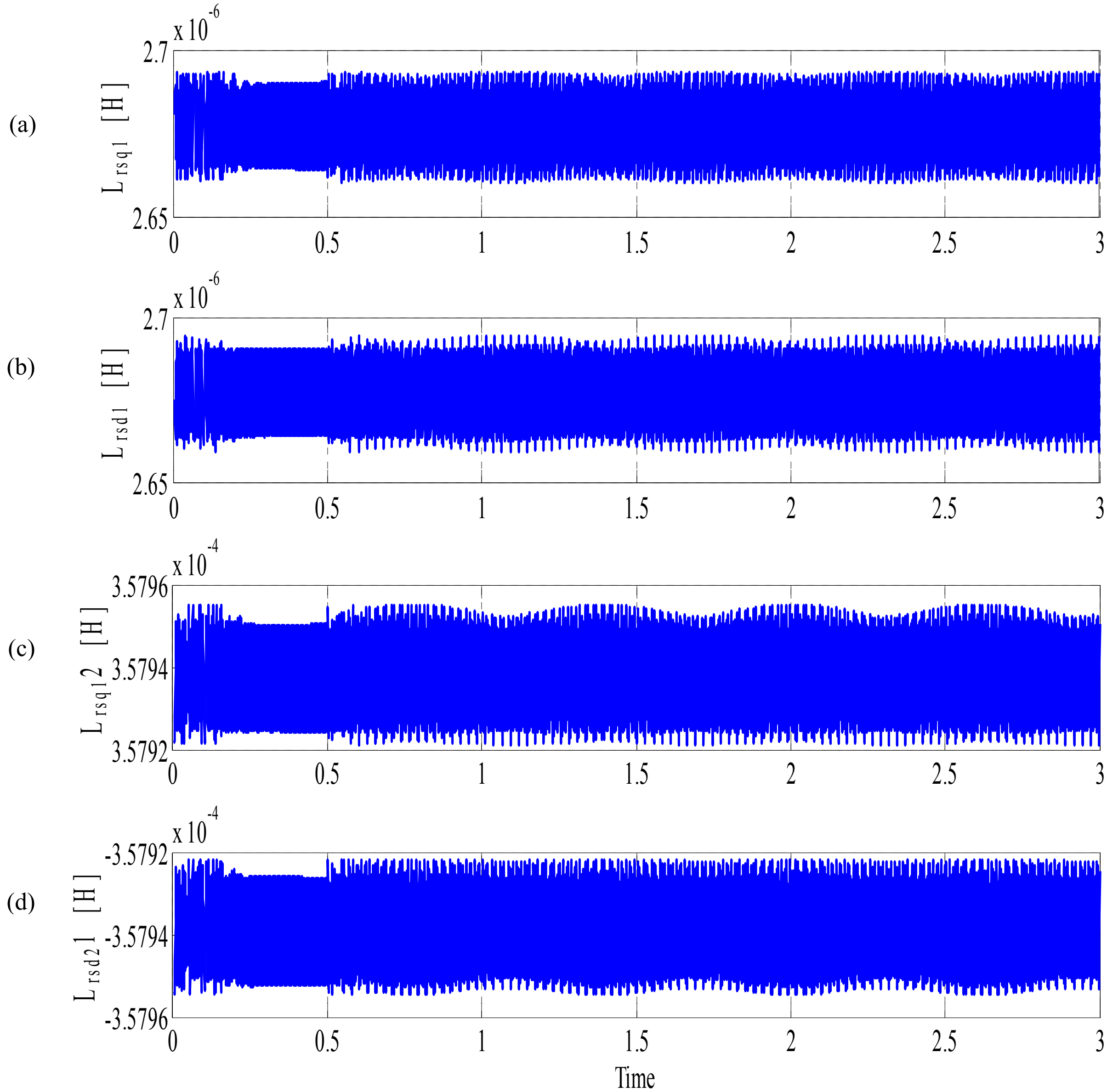

Figure 3.13 Fundamental component of the qd-rotor bar-to-stator mutual inductance (a) L_{rsq1} (b) L_{rsd1} (c) L_{rsq12} (d) L_{rsd21}

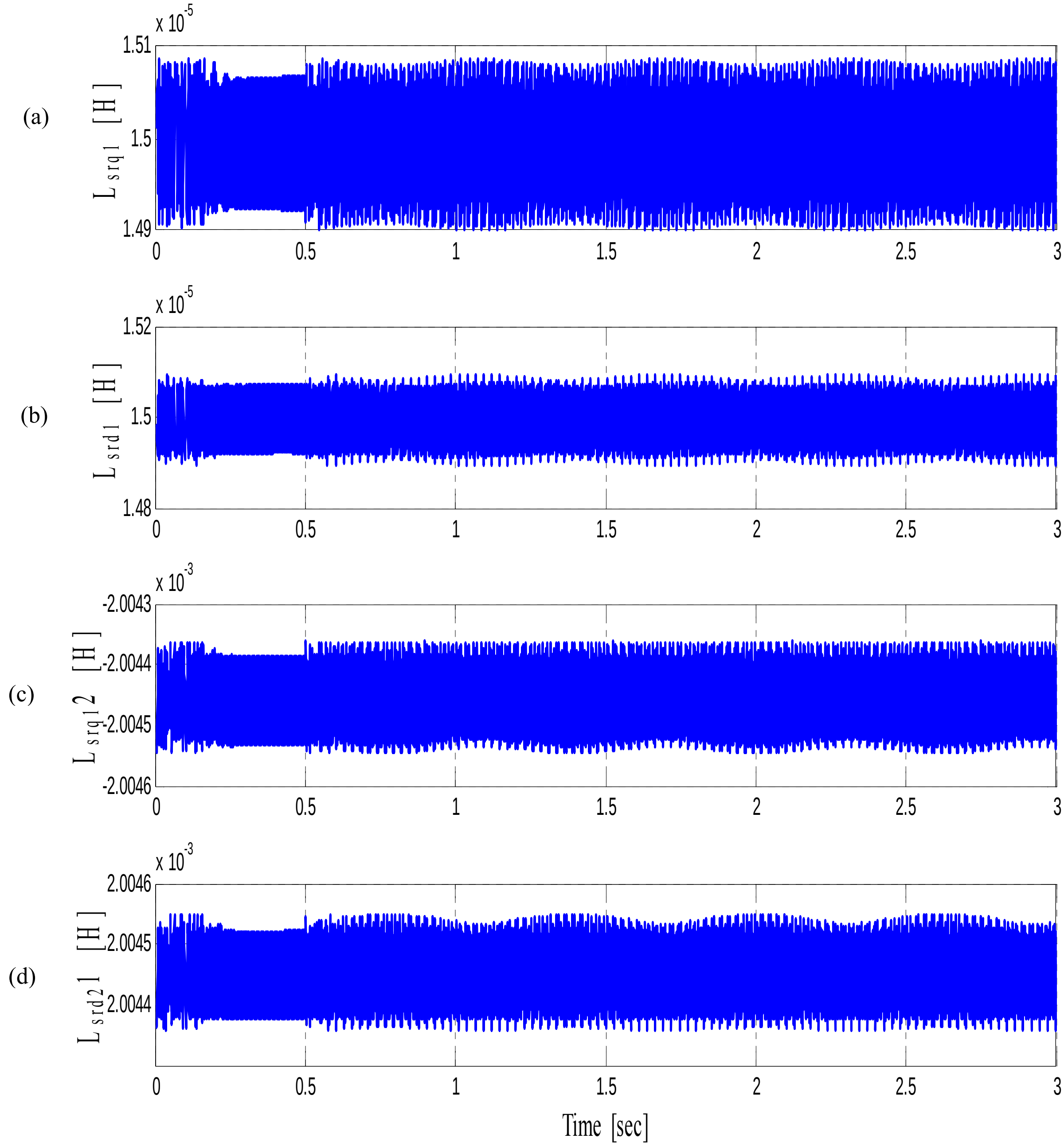

Figure 3.14 Fundamental component of the qd-stator-to-rotor bar mutual inductance (a) L_{srq1} (b) L_{srd1} (c) L_{srq12} (d) L_{srd21}

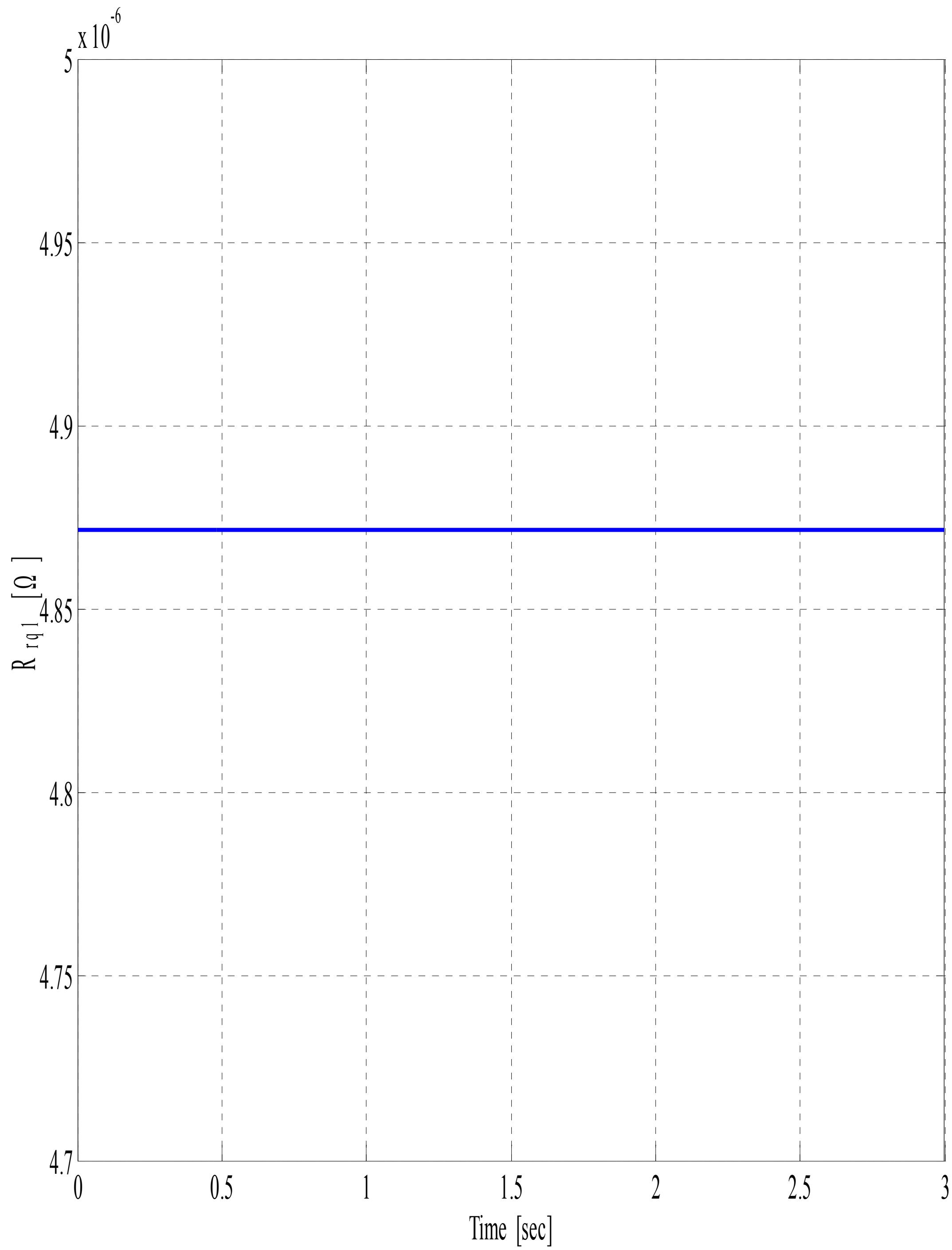

Figure 3.15 Fundamental component of the qd-rotor bar resistance R_{rq1}

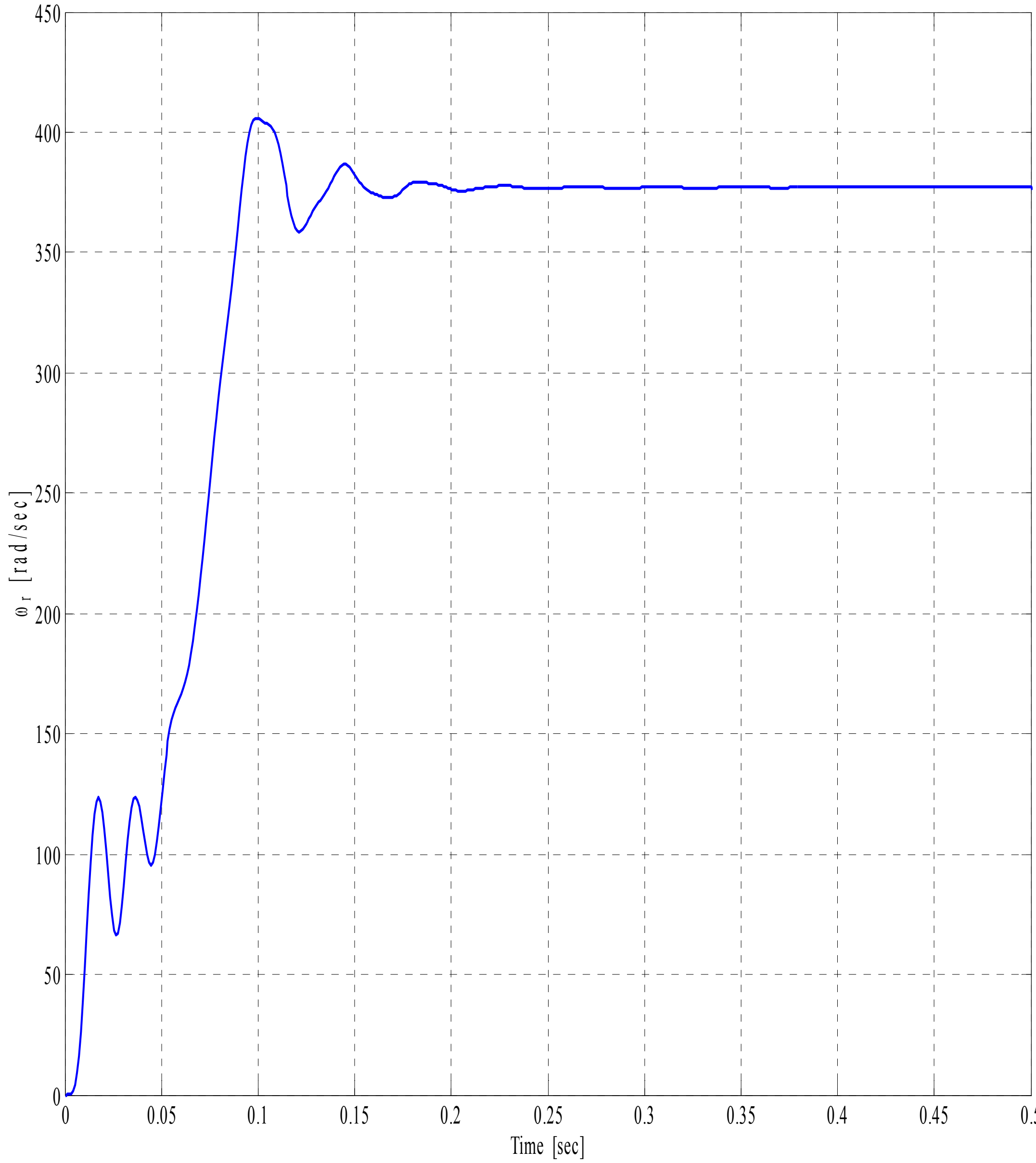

Figure 3.16 Starting transients of the rotor speed at no-load

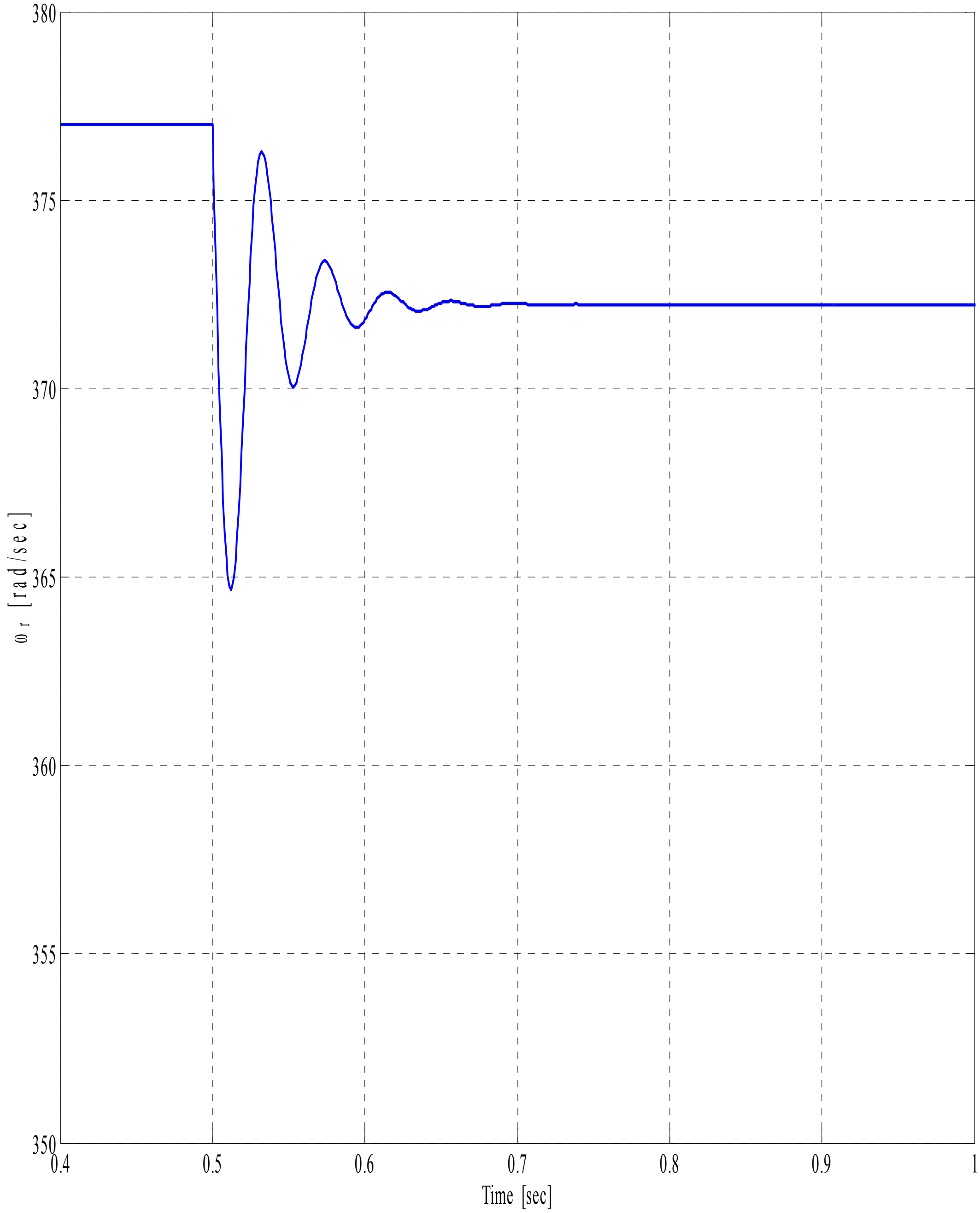

Figure 3.17 Rotor speed at a load torque of 8.5 Nm

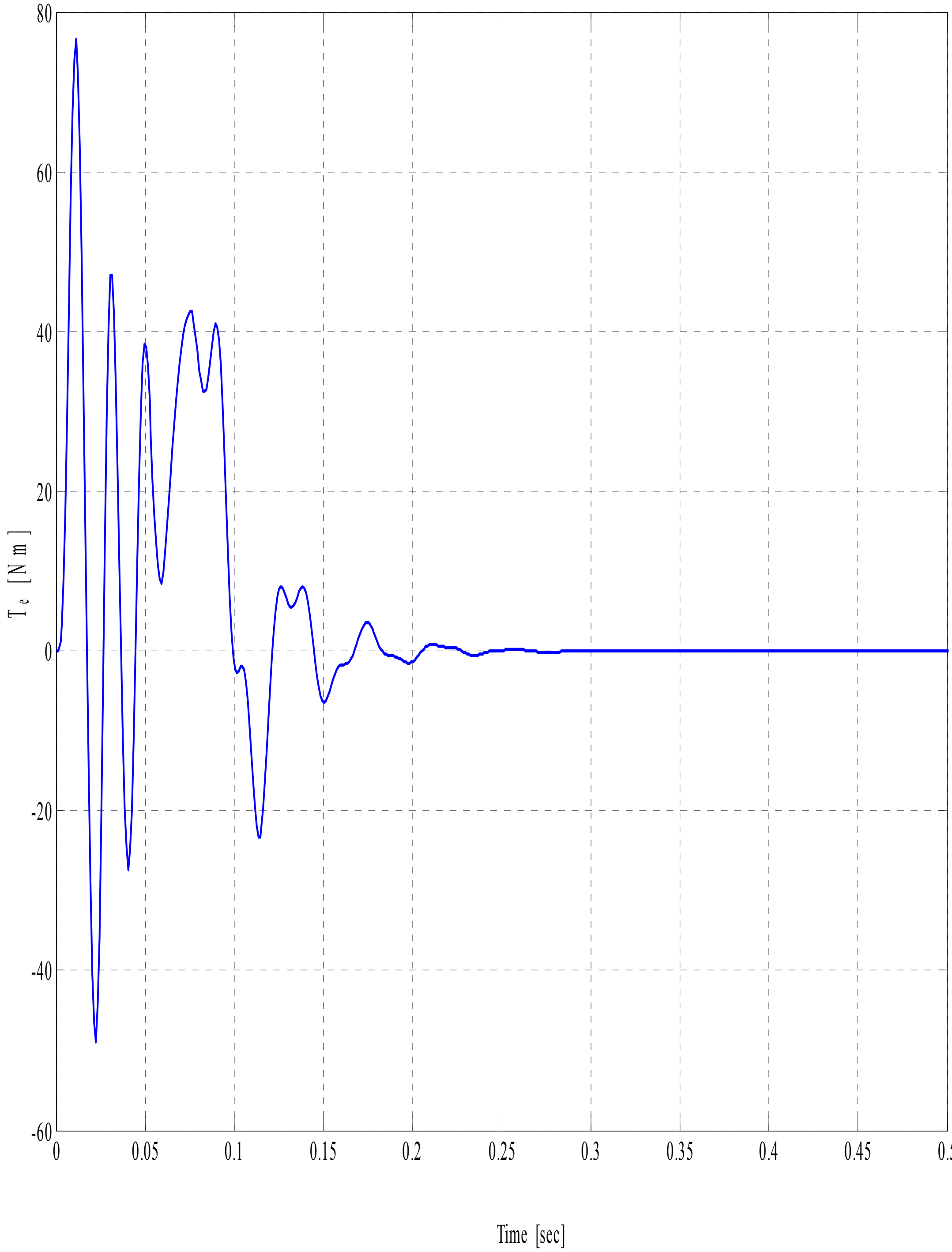

Figure 3.18 Fundamental components of the electromagnetic torque at no-load

Figure 3.19 Fundamental components of the electromagnetic torque at a load torque of 8.5 Nm

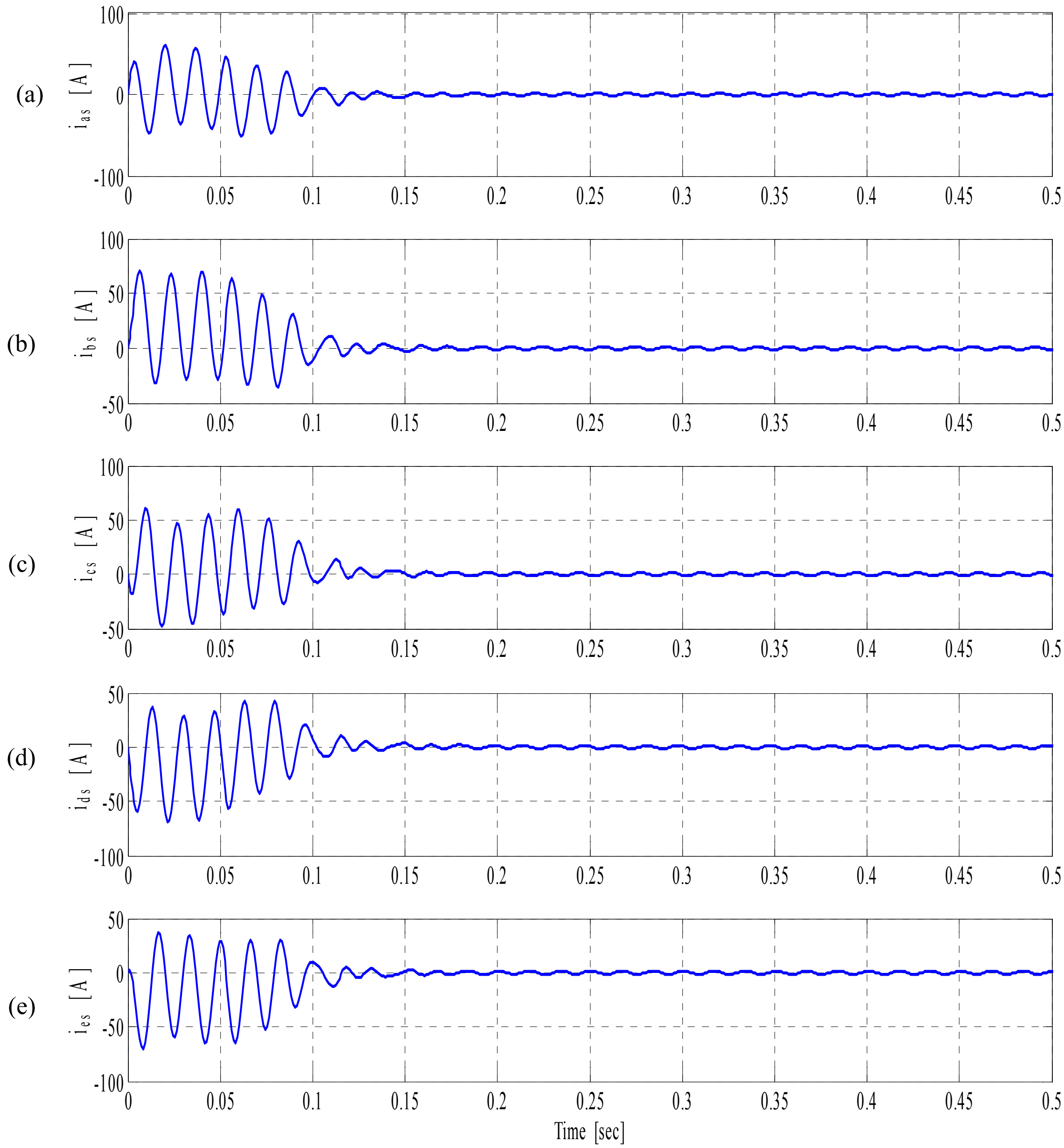

Figure 3.20 Fundamental components of the stator phase currents at no-load (a) phase 'a' (b) phase 'b' (c) phase 'c' (d) phase 'd' (e) phase 'e'

(a)
(b)
(c)
(d)
(e)

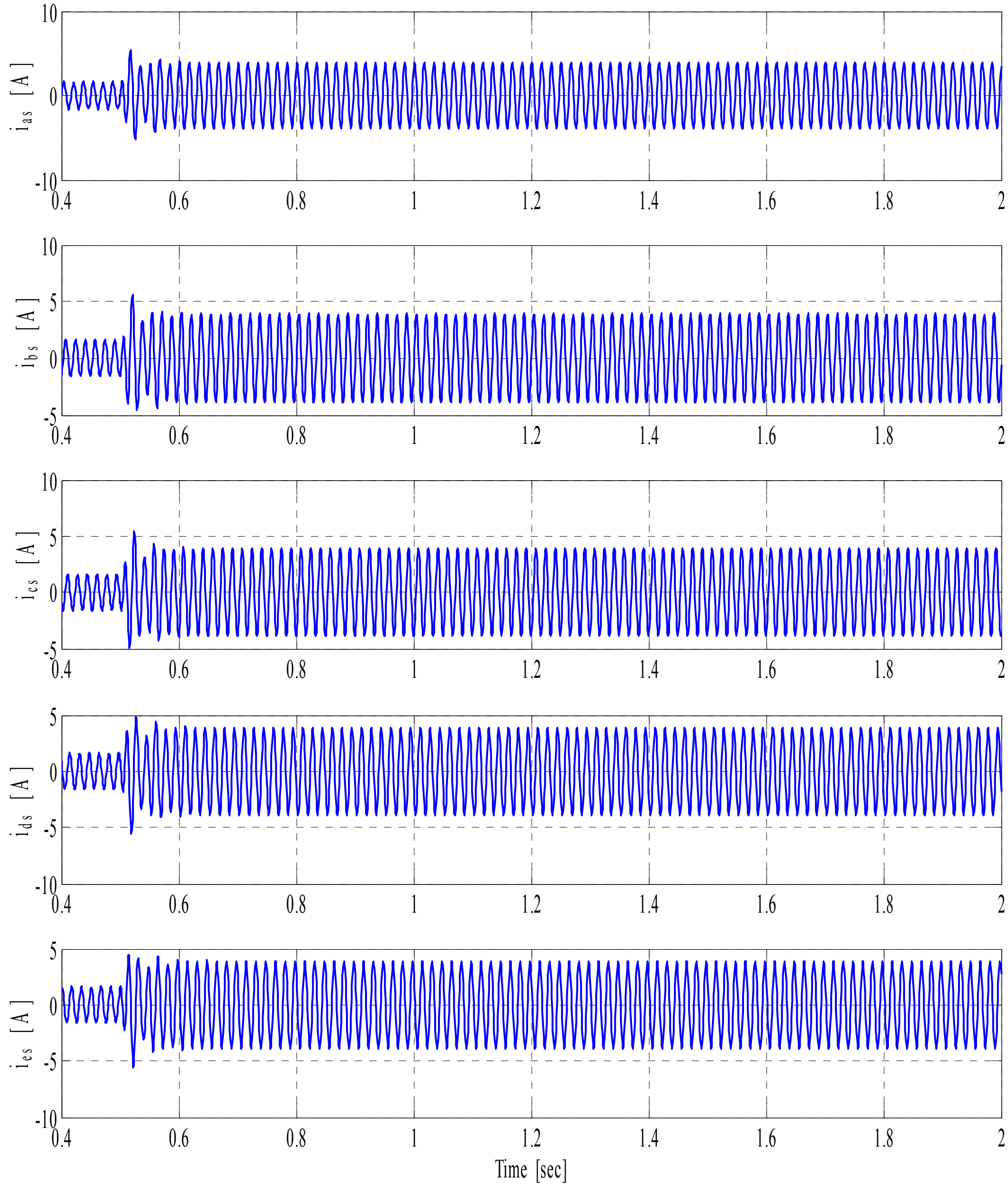

Figure 3.21 Fundamental components of the stator phase currents at a load torque of 8.5 Nm (a) phase ‘a’ (b) phase ‘b’ (c) phase ‘c’ (d) phase ‘d’ (e) phase ‘e’

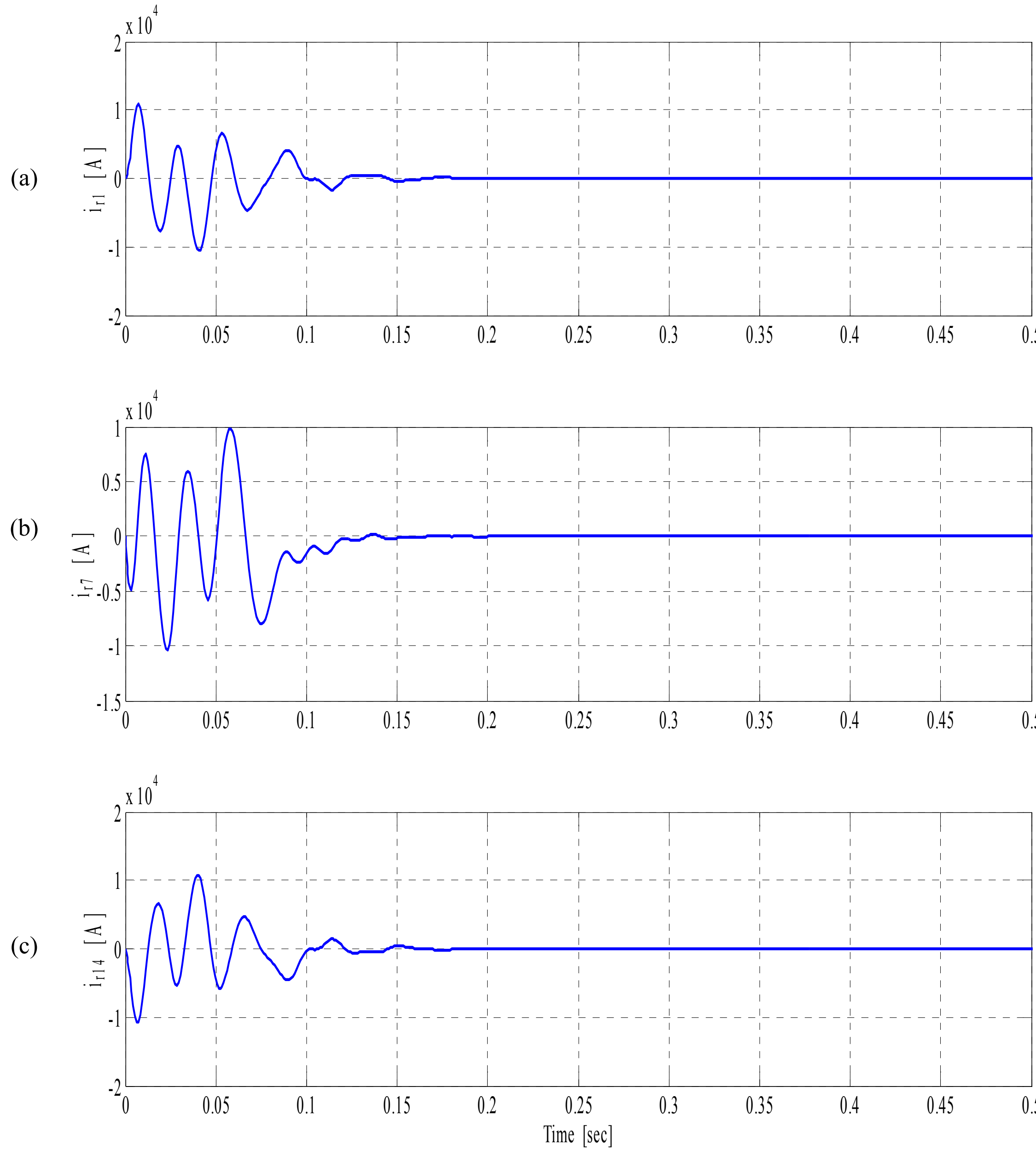

Figure 3.22 Fundamental components of the actual rotor bar currents at no load (a) bar 1 (b) bar 7 and (c) bar 14

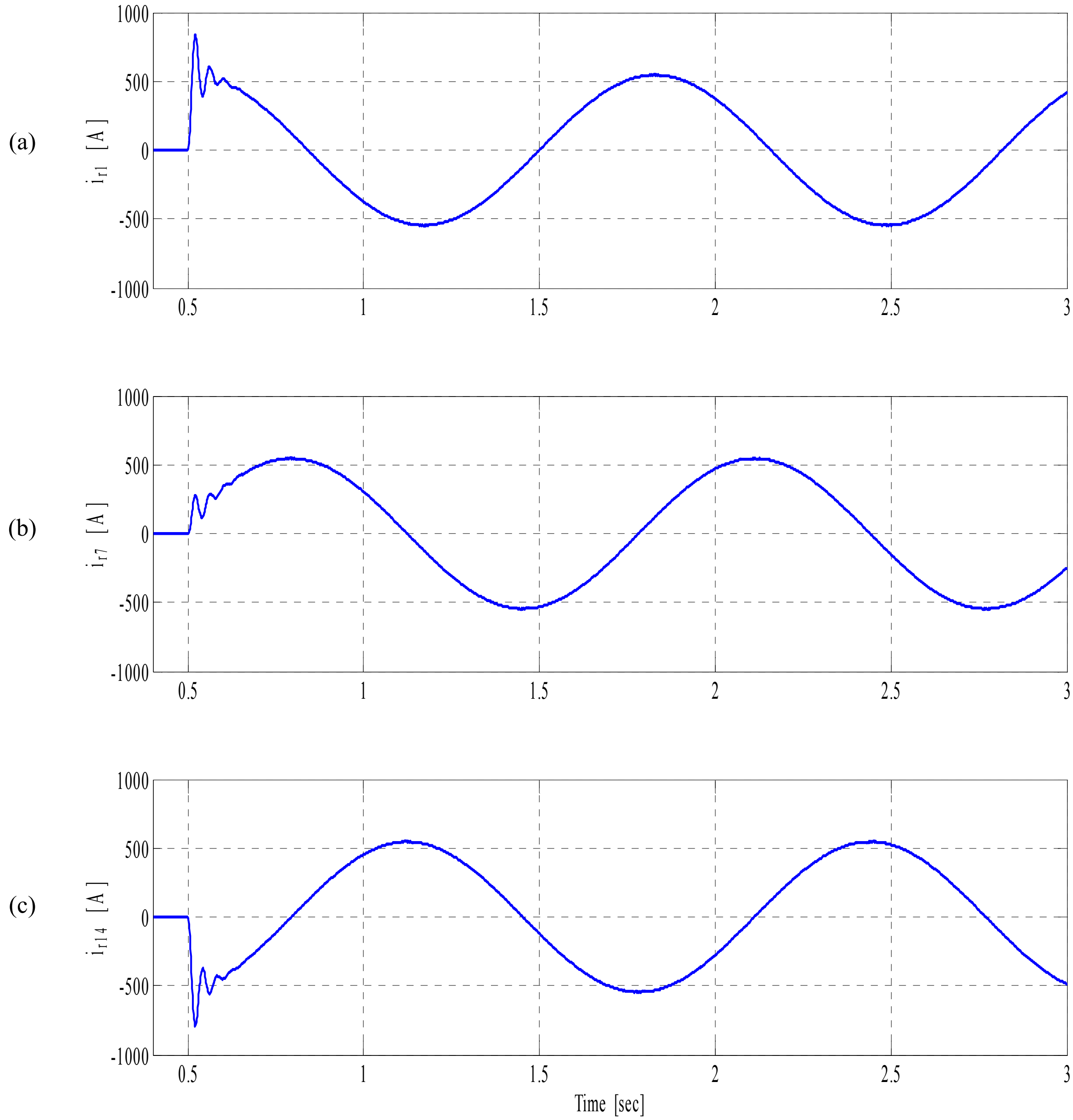

Figure 3.23 Fundamental components of the actual rotor bar currents at a load torque of 8.5 Nm (a) bar 1 (b) bar 7 and (c) bar 14

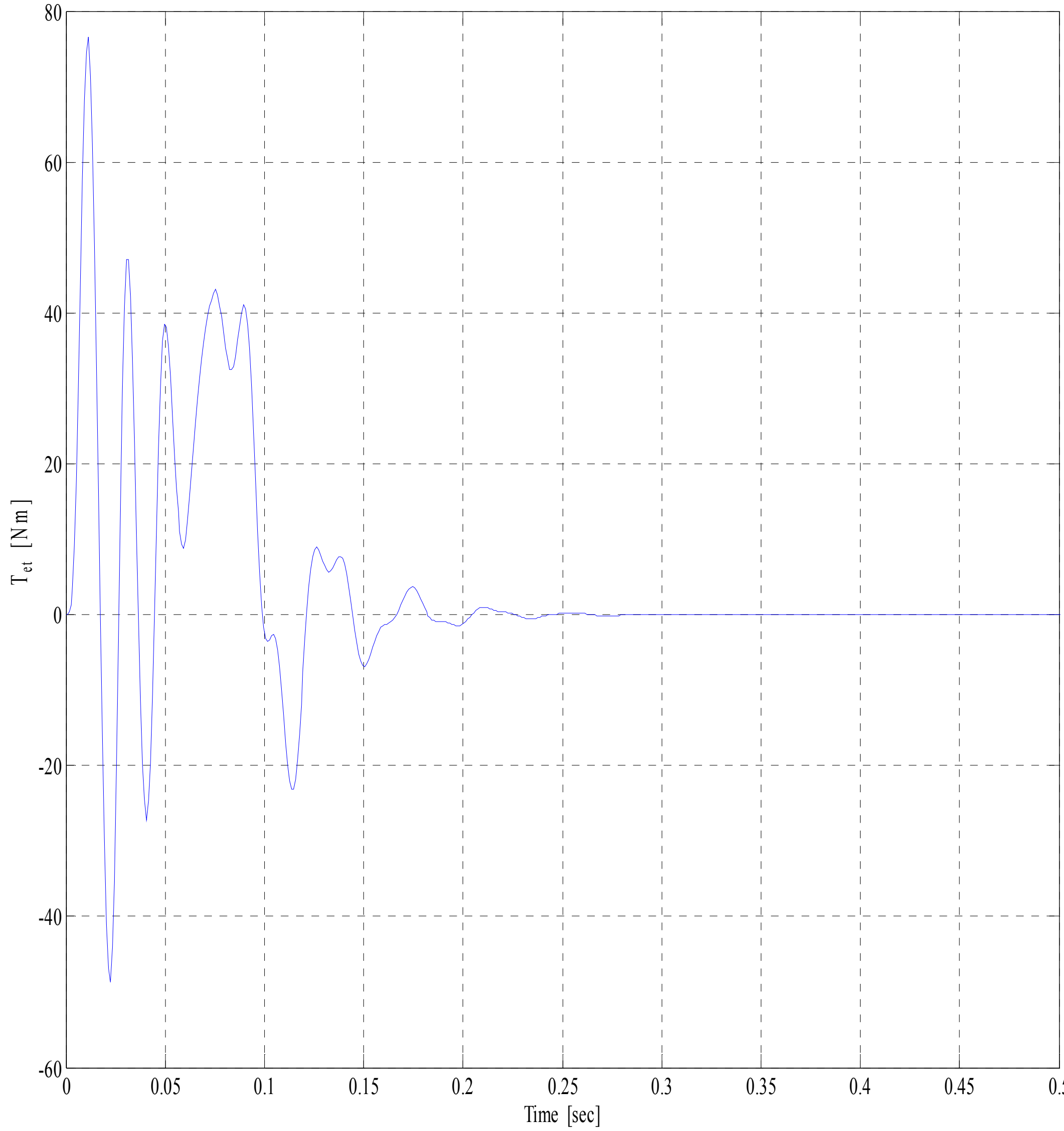

Figure 3.24 Total electromagnetic torque $(T_{e1} + T_{e3})$ at no-load

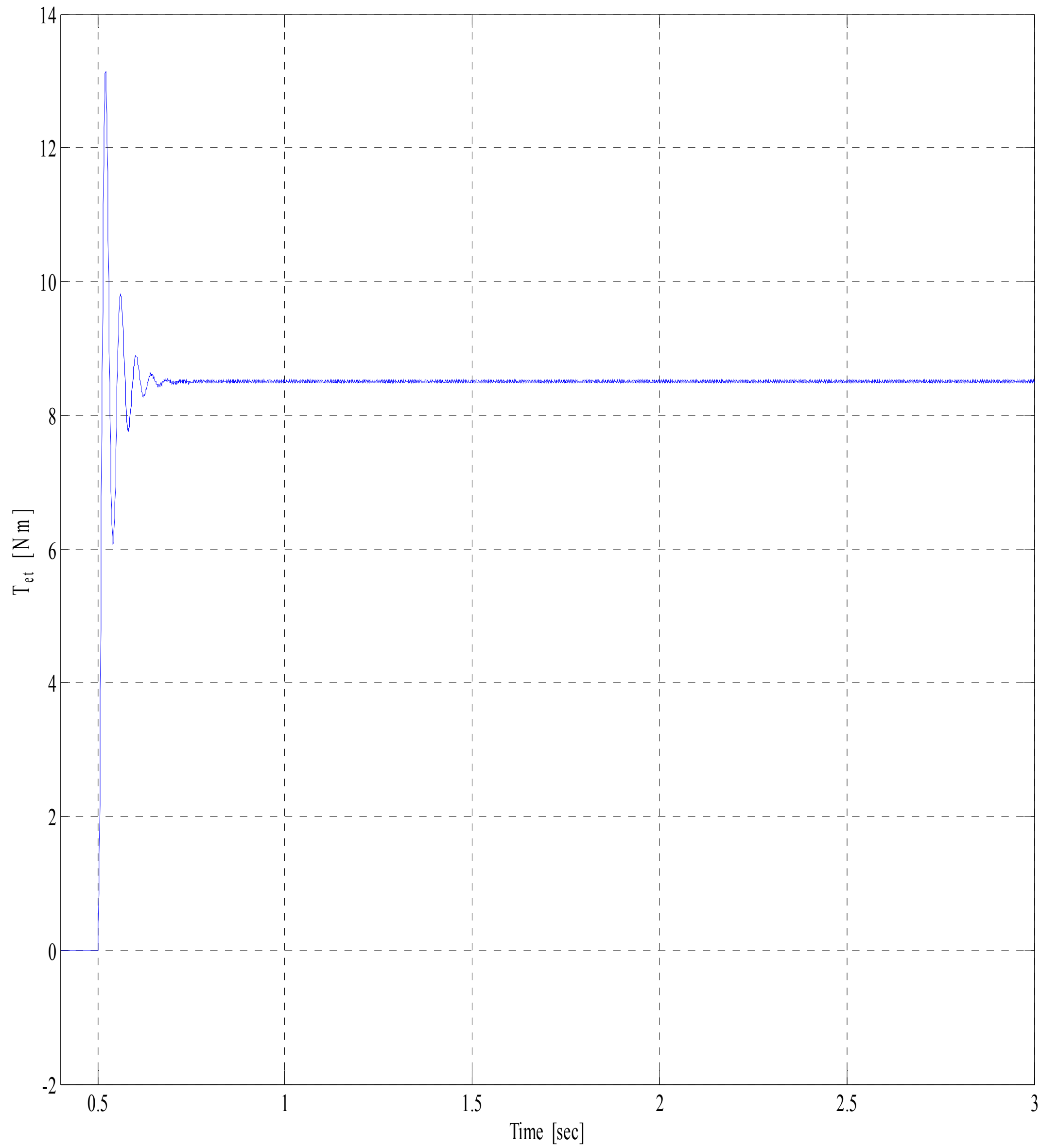

Figure 3.25 Total electromagnetic torque $(T_{e1} + T_{e3})$ at a load torque of 8.5 Nm

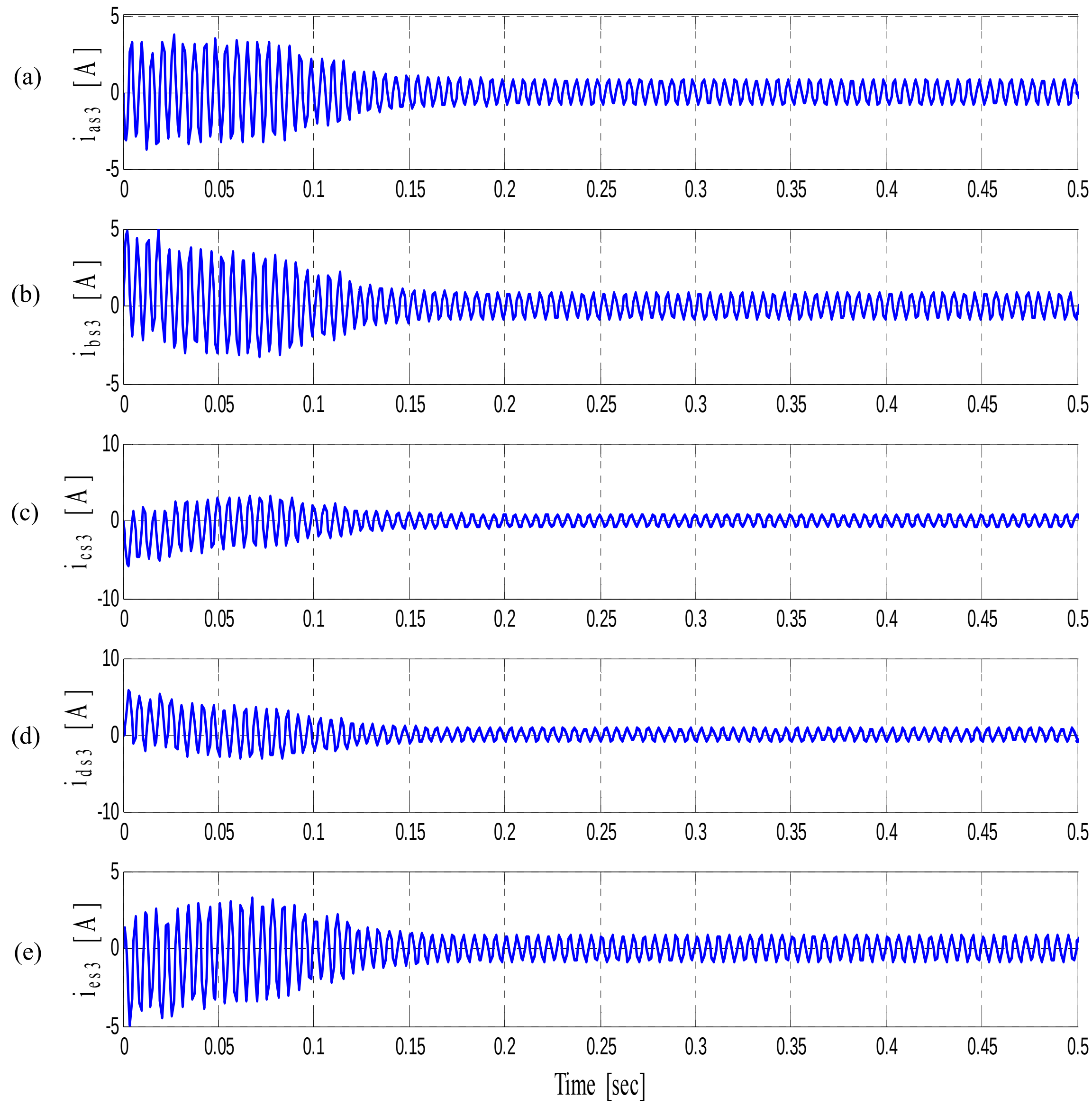

Figure 3.26 Third harmonic components of the stator phase currents at no-load (a) phase 'a' (b) phase 'b' (c) phase 'c' (d) phase 'd' (e) phase 'e'

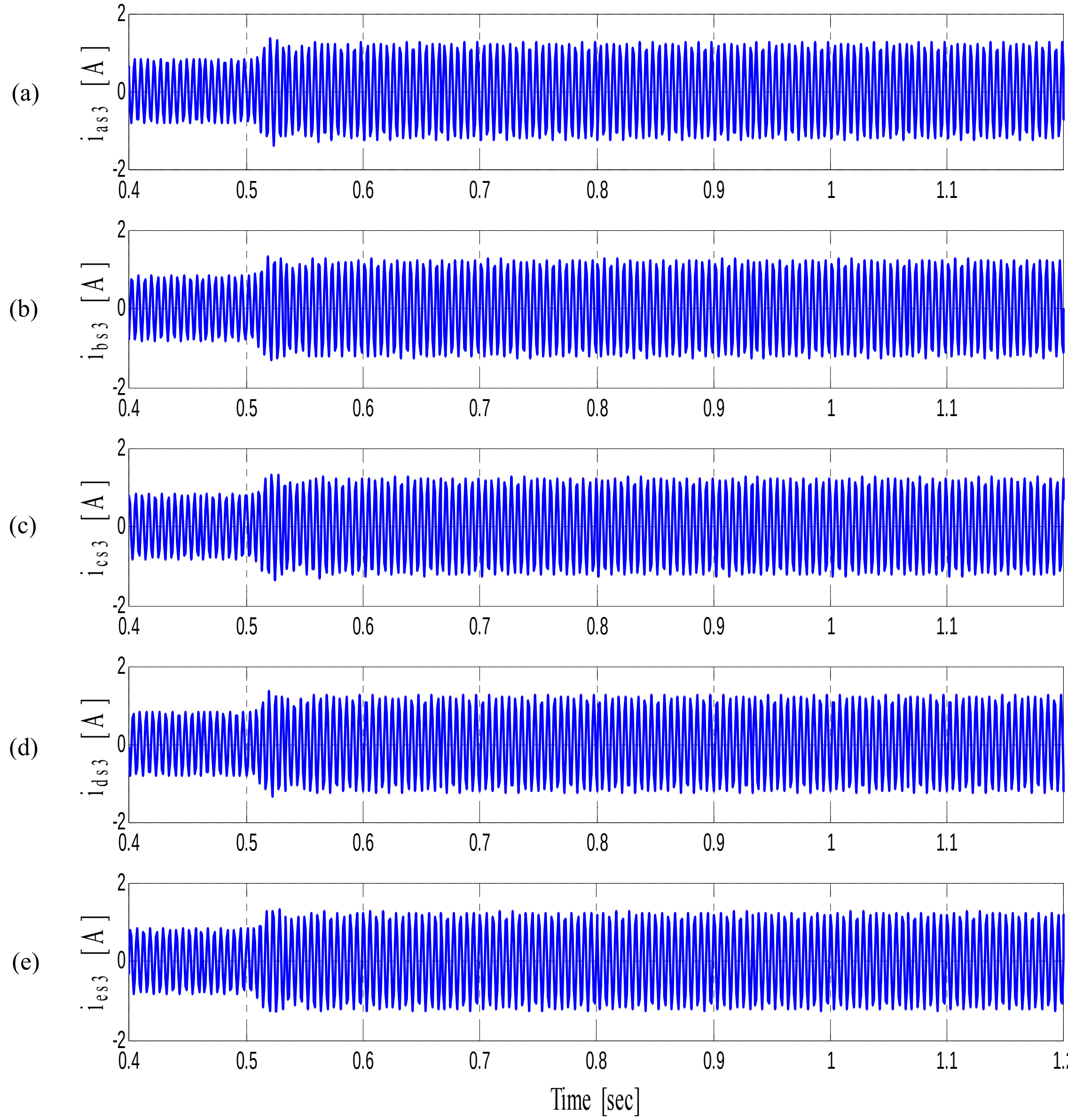

Figure 3.27 Third harmonic components of the stator phase currents at a load torque of 8.5 Nm (a) phase 'a' (b) phase 'b' (c) phase 'c' (d) phase 'd' (e) phase 'e'

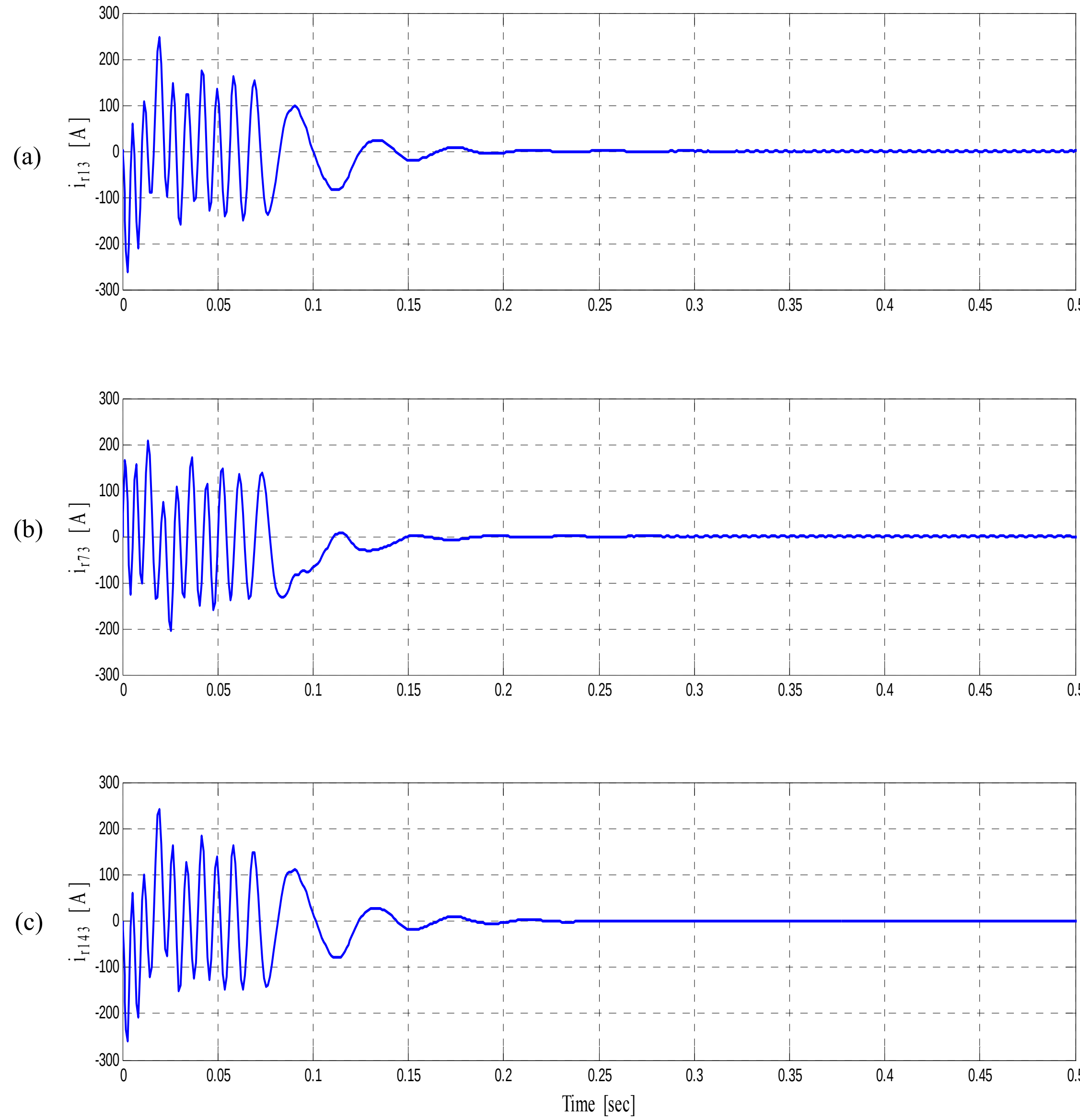

Figure 3.28 Third harmonic components of the actual rotor bar currents at no load (a) bar 1 (b) bar 7 and (c) bar 14

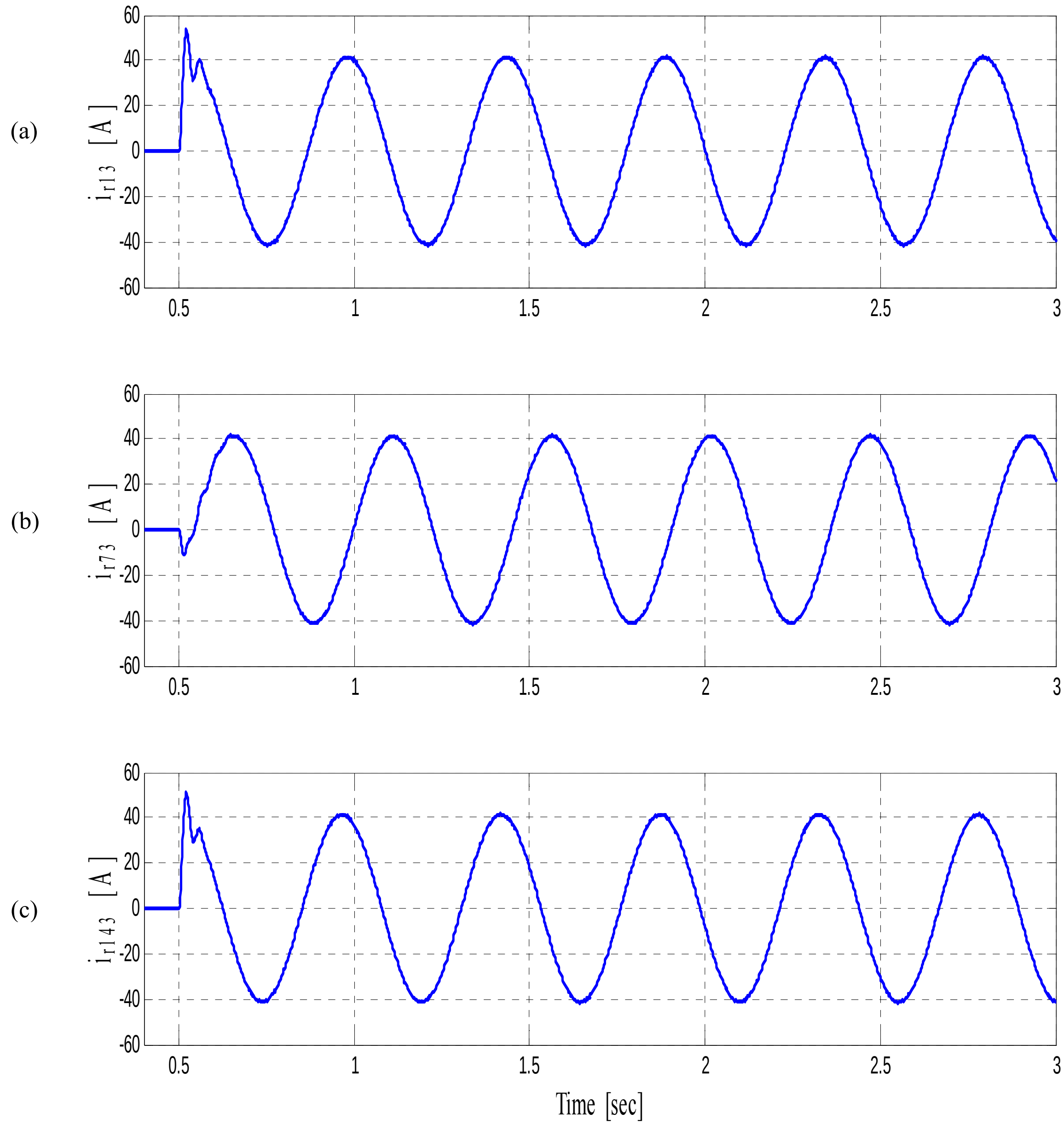

Figure 3.29 Third harmonic components of the actual rotor bar currents at a load torque of 8.5 Nm (a) bar 1 (b) bar 7 and (c) bar 14

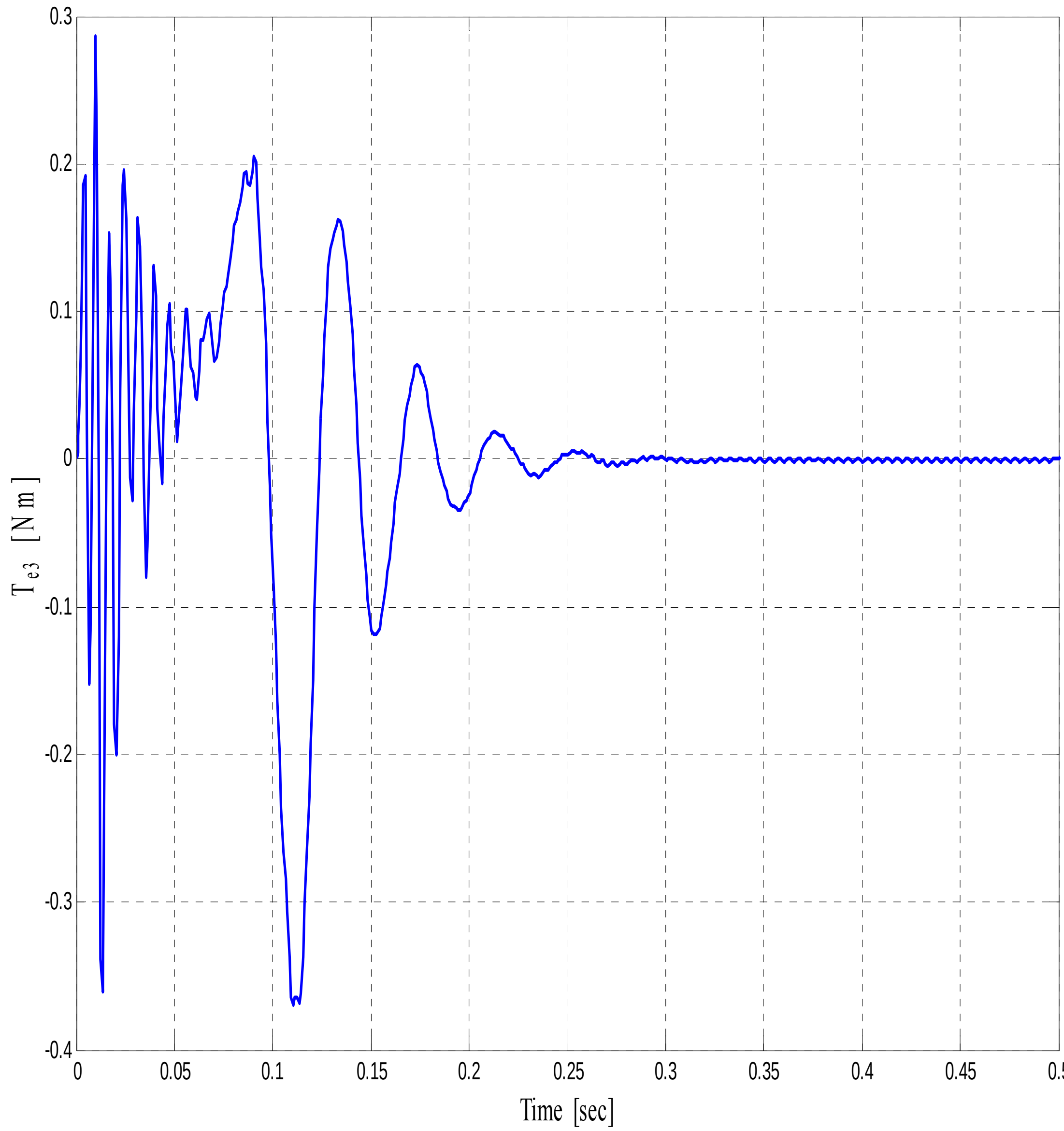

Figure 3.30 Third harmonic component of the electromagnetic torque at no-load

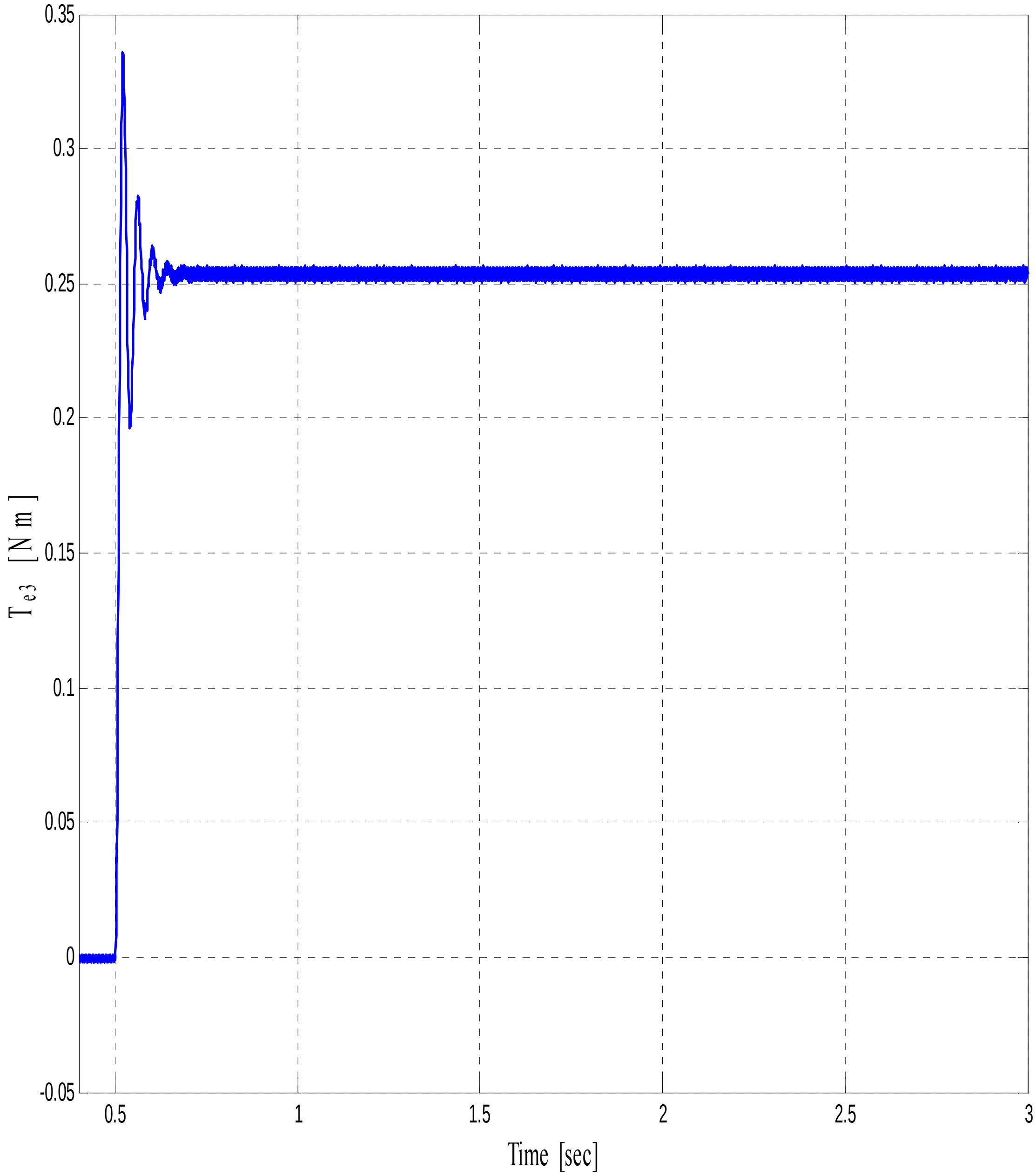

Figure 3.31 Third harmonic component of the electromagnetic torque at a load torque of 8.5 Nm

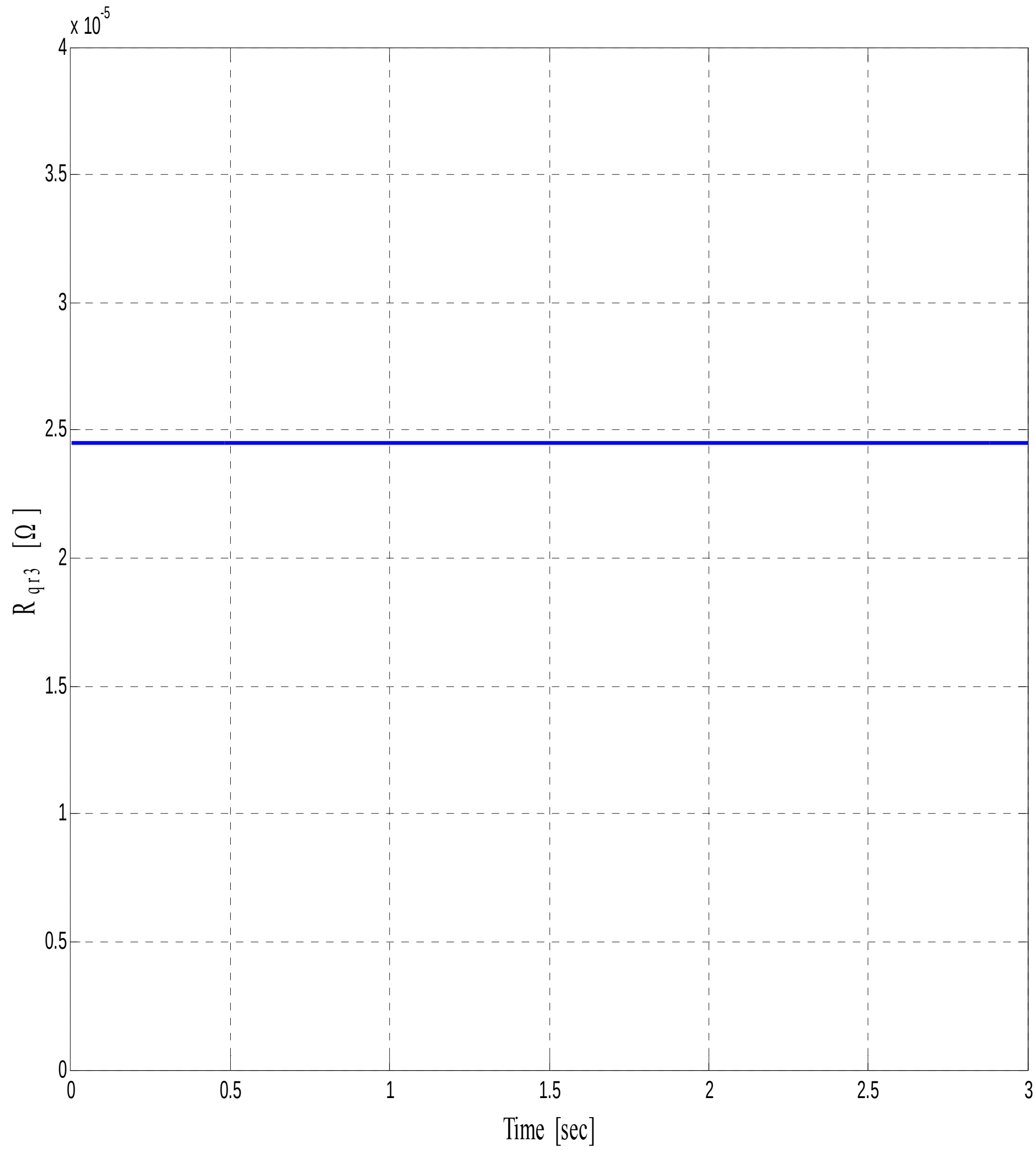

Figure 3.32 Third harmonic component of the qd-rotor bar resistance R_{rq1}

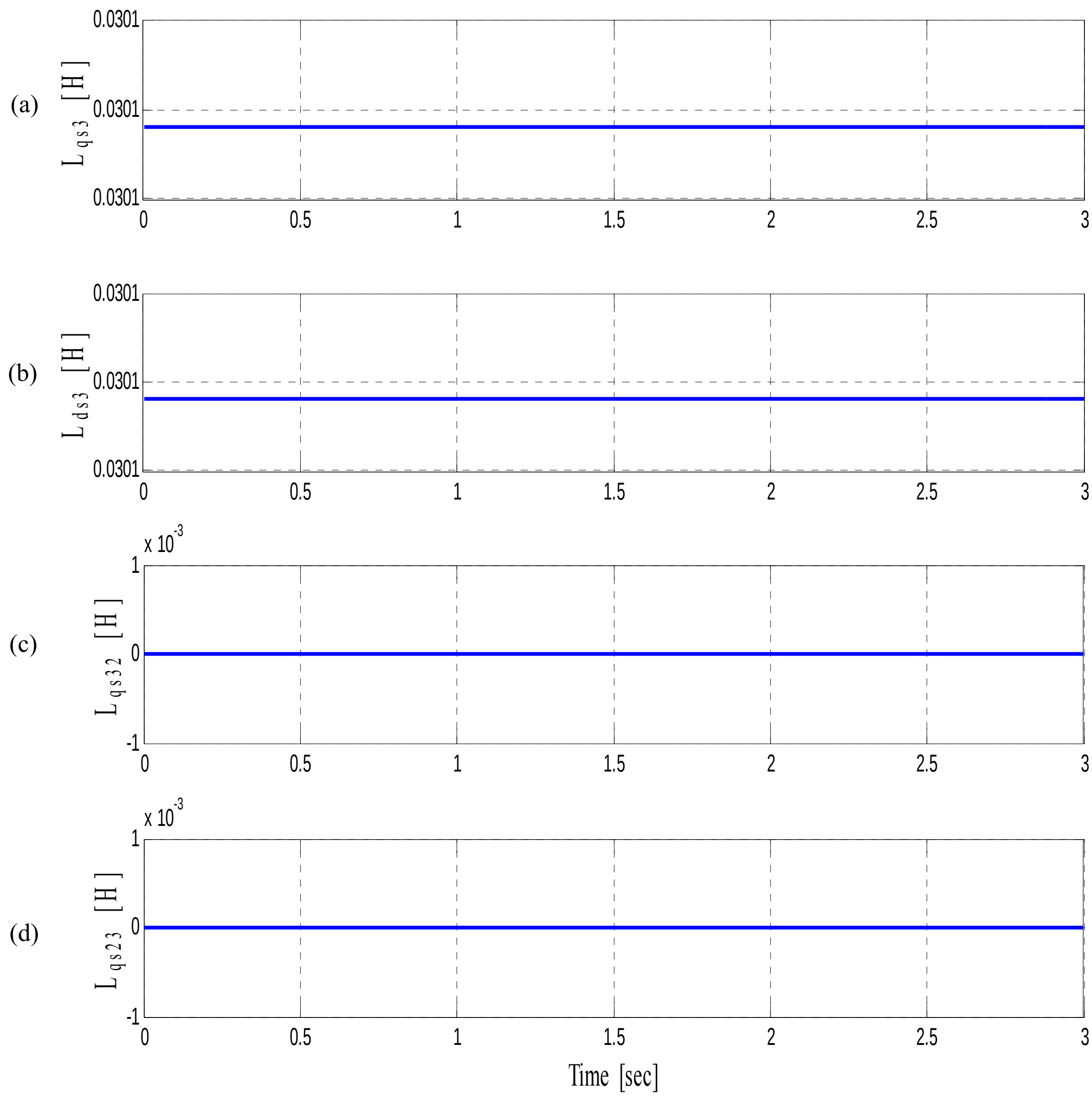

Figure 3.33 Third harmonic component of the qd-stator inductance (a) L_{ssq3} (b) L_{ssd3} (c) L_{ssq32} (e) L_{ssd23}

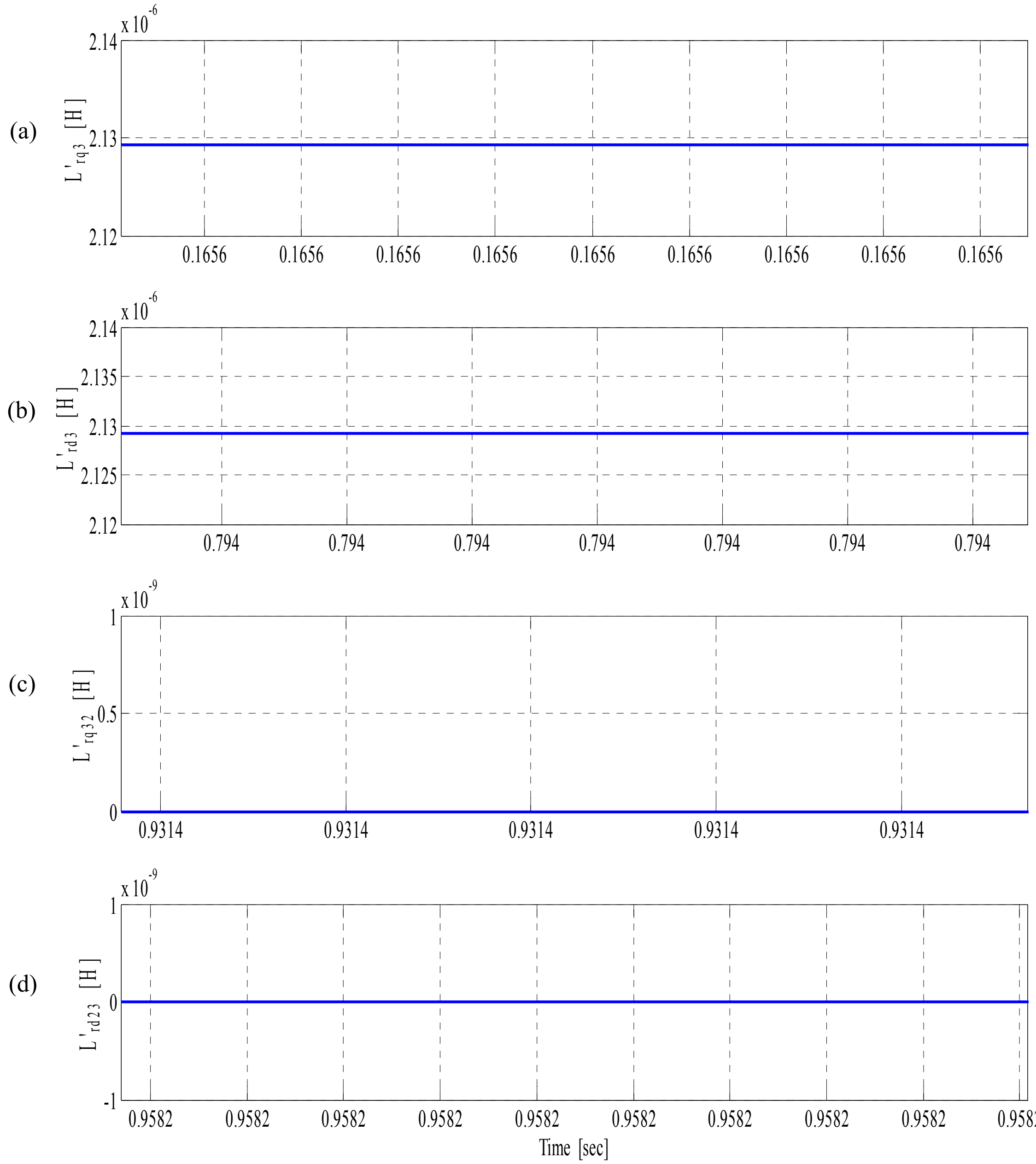

Figure 3.34 Third harmonic component of the qd-rotor bar self inductance (a) L_{rq3} (b) L_{rd3} (c) L_{rq32} (e) L_{rd23}

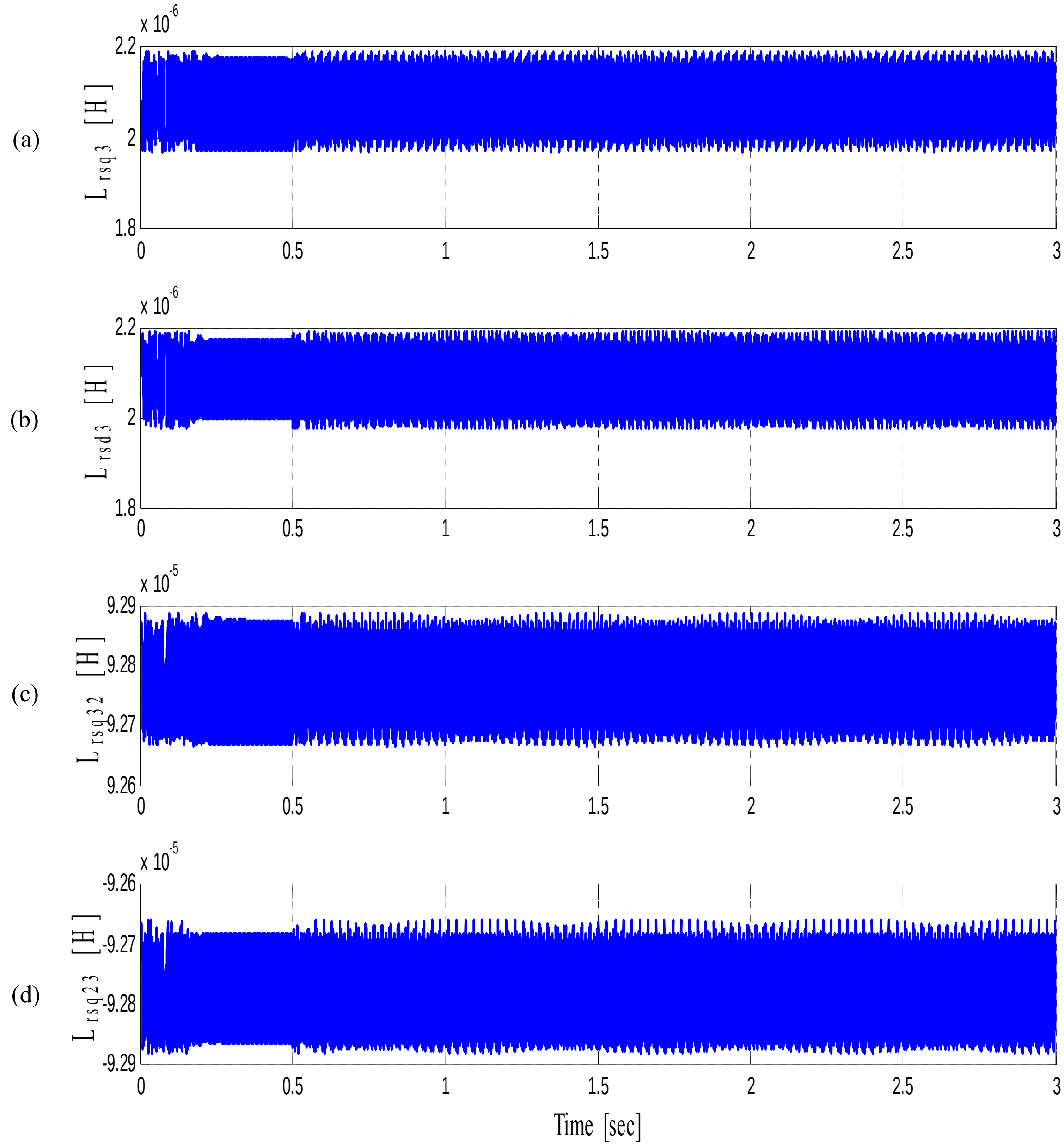

Figure 3.35 Third harmonic component of the qd-rotor bar-to-stator mutual inductance (a) L_{rsq3} (b) L_{rsd3} (c) L_{rsq32} (d) L_{rsd23}

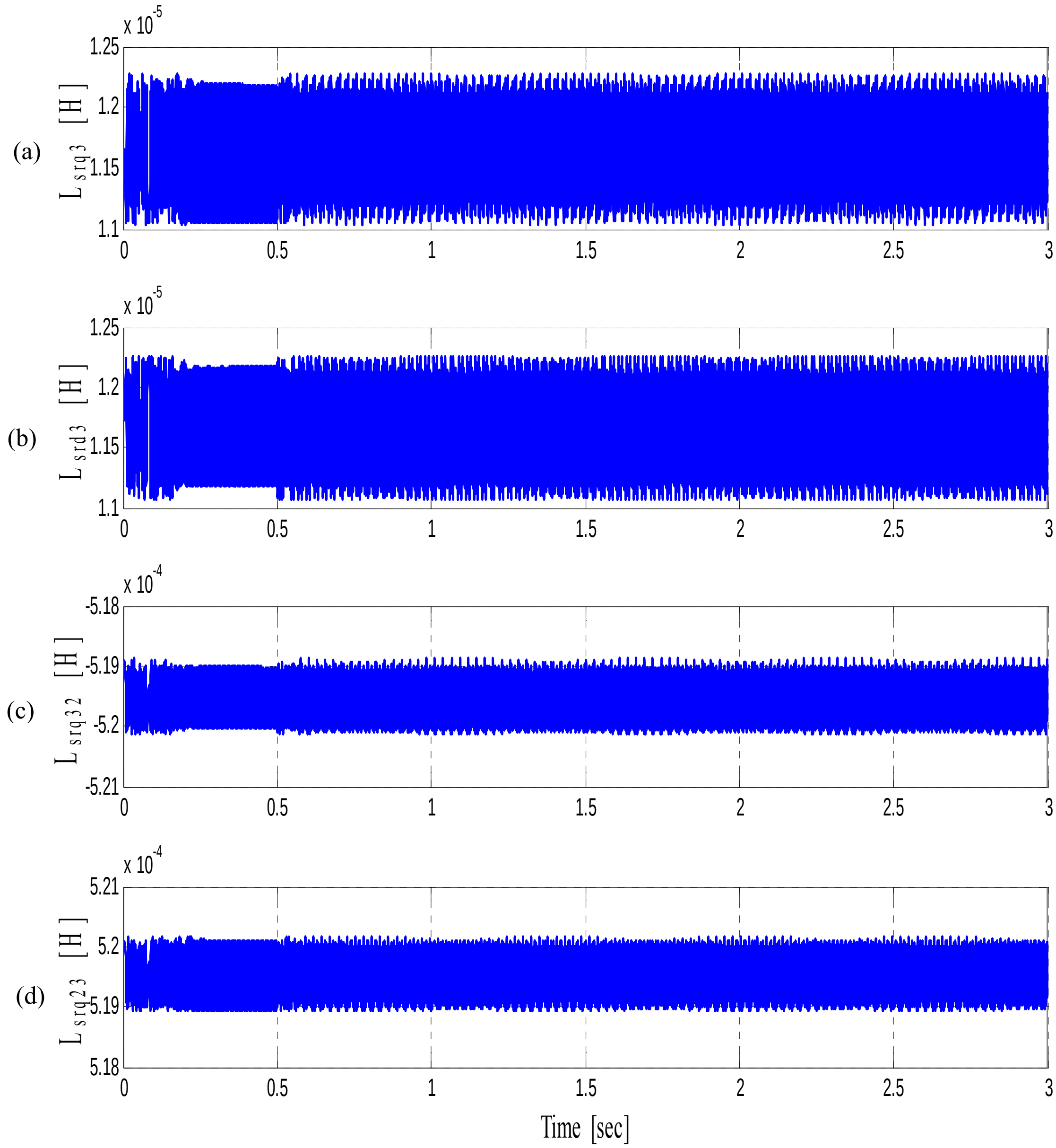

Figure 3.36 Third harmonic component of the qd-stator-to-rotor bar mutual inductance (a) L_{srq3} (b) L_{srd3} (c) L_{srq32} (d) L_{srd23}

3.9 Experimental Determination of Machine Parameters

The machine parameters were identified by performing no load and locked rotor tests. The machine was energized by balanced *abcde* and *acebd* voltages into determine the fundamental and third harmonic components of the machine parameters, respectively.

The no-load test was used to determine the magnetizing inductance as well as the core loss resistance whereas the locked rotor test was used to determine the copper loss resistance and the leakage inductance.

The five-phase induction motor was energized from the five-phases of the two three-phase inverters, one inverter providing only two phases (d and e).

3.9.1 Experimental results

3.9.1.1 No-load test. The five phase induction machine is supplied from two three phase voltage source inverters at no load. The no-load speed is 1800 rpm. The results for the no-load test are shown in Table 3.6

3.9.1.2 Determination of the Magnetizing inductance from the line-to-line voltages. For the determination of the magnetizing inductance, two kinds of measurements were taken. First the line-to-line voltages between adjacent phases were taken as shown in Table 3.7. Secondly, the phase 'a' voltage and phase 'a' current were measured as shown in Table 3.8. The result based on either of the two is plotted in Figure 3.37.

Table 3.6 No-load Tests Power, voltage and current measurements

V_{ae}	V_{be}	V_{ce}	V_{de}	I_{as}	I_{bs}	I_{cs}	I_{ds}	I_{es}	P_{ae}	P_{be}	P_{ce}	P_{de}
95	148	148	97	2.1	1.9	1.8	1.3	1.95	195	110	60	52
84	130	129	86	1.95	1.7	1.55	1.15	1.75	155	95	44	40
75	115	115	76	1.75	1.6	1.40	1.0	1.55	120	80	30	30
65	101	100	67	1.55	1.35	1.25	0.89	1.4	100	65	20	24
55	86	86	56	1.35	1.25	1.1	0.84	1.25	70	56	10	16
47	73	72.5	45	1.15	1.1	1.0	0.75	1.1	60	50	4	10
39	58	57	39	1.0	1.0	1.0	0.65	1.0	45	45	3	6
30	48	48	31	0.5	0.5	0.5	0.5	0.925	30	35	2	4

P_{ij} is the power measured by the wattmeter connected between phase *i* and *j*.

Table 3.7 No-load Tests Line-to-line Voltage and current measurements

V_{ab}	V_{bc}	V_{cd}	V_{de}	I_{as}	I_{bs}	I_{cs}	I_{ds}	I_{es}
150	150	145	152	4.15	3.65	3.2	2.65	3.355
146	146	140	148	3.85	3.4	3	2.45	3.15
140	140	134	143	3.55	3.15	2.75	2.3	3
134	134	128	138	3.3	2.95	2.6	2.15	2.8
128	128	122	130	3.055	2.75	2.45	2.05	2.155
120	120	116	124	2.875	2.575	2.3	1.925	2.475
114	114	110	120	2.7	2.425	2.15	1.825	2.325
108	108	104	116	2.575	2.275	2	1.7	2.2

Table 3.7 Continued

V_{ab}	V_{bc}	V_{cd}	V_{de}	I_{as}	I_{bs}	I_{cs}	I_{ds}	I_{es}
100	100	98	110	2.675	2.125	1.9	1.6	2.05
94	94	92	104	2.225	2	1.75	1.5	1.925
88	88	86	98	2.05	1.85	1.65	1.4	1.8
82	82	80	92	1.95	1.75	1.55	1.3	1.65
78	78	74	88	1.85	1.6	1.45	1.2	1.55
72	72	68	84	1.7	1.5	1.35	1.1	1.45
64	64	62	76	1.55	1.35	1.2	1	1.325
57	57	55	72	1.4	1.25	0.5	0.7	1.225
50	50	48	64	1.275	1.2	0.45	0.625	1.125
44	44	42.5	58	1.15	1.1	0.25	0.6	1.025
38	38	37	50	1.05	1.05	0.25	0.525	0.975
32	32	31.5	42	1	1	0.25	0.55	0.95
28	28	26	36	1	1	0.25	0.575	0.975

Table 3.8 No-load Tests Phase ‘a’ voltage and phase ‘a’ current measurements

V_{an1}	127	4.075	117.5	3.5	107	3.05	96.5	2.675	85.5	2.35	75
I_{as1}	122	3.775	112.5	3.25	102	2.85	91	2.525	80.2	2.2	70

V_{an1}	2.075		65	1.8	54.5	1.55	44	1.275	33	1.1	23	1.05
I_{as1}	1.95		59.5	1.7	49	1.45	38.5	1.2	28.5	1.05	18	1.3

Also from the results of Table 3.8, the core loss resistance, R_{c1} could be determined by using the following relations

$$R_{oc1} = \frac{P_{oc1}}{I_{c1}^2}$$

$$I_{c1} = \sqrt{I_{oc1}^2 - I_{m1}^2}$$

$$I_{m1} = \frac{V_{o1c}}{X_{m1}}$$

$$X_{m1} = 2\pi f L_{m1}$$

where P_{oc1}, I_{oc1} and V_{oc1} are the average values for power, current and voltage, respectively obtained from the no-load tests.

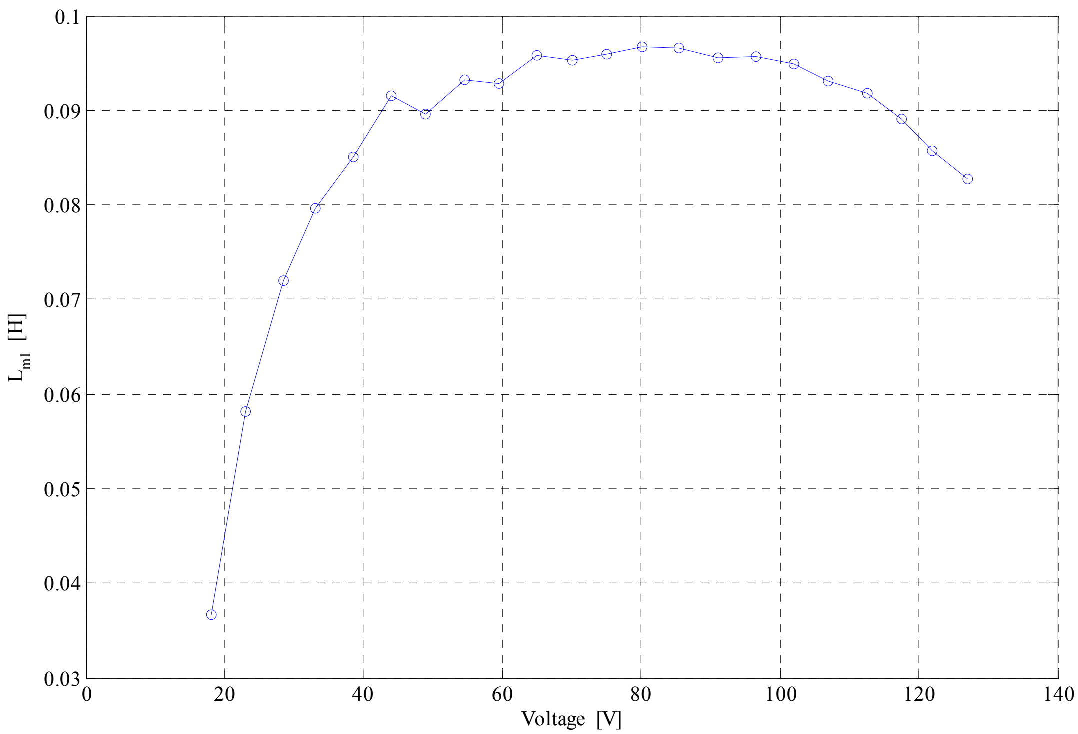

Figure 3.37 Fundamental component of the magnetizing inductance

3.9.1.3 Third harmonic magnetizing inductance calculation. To determine the third harmonic component of the magnetizing inductance, the machine was energized by balanced *acebd* voltages. The phase 'a' voltage and current were measured and the results recorded as shown in Table 3.9.

The inductance is then obtained as

$$X_{m3} = \frac{V_{an3}}{I_{as3}} \qquad\qquad L_{m3} = \frac{X_{m3}}{\omega_s}$$

$\omega_s = 2\pi f_s$, f_s is the supply voltage

Figure 3.38 shows the variation of the third harmonic inductance with the phase 'a' voltage.

3.9.1.4 Locked rotor test. The locked rotor stator line-to-line voltages, current and power were recorded for each measurement and then the average value was calculated for each phase. One stator phase, in this case phase 'e', was made the references such that at every instant, four readings for line-to-line voltages, five readings for the phase currents and four readings for the power were taken as shown in Table 3.10.

Table 3.9 No-load Tests Phase 'a' third harmonic voltage and current measurements

V_{an3}	36	33.5	31	29	27	26	25	24	23	21.5	20.5	19.5	18	15
I_{as3}	7.3	6.65	6.1	5.65	5.35	5.1	4.95	4.75	4.6	4.25	4.05	3.85	3.6	3.2

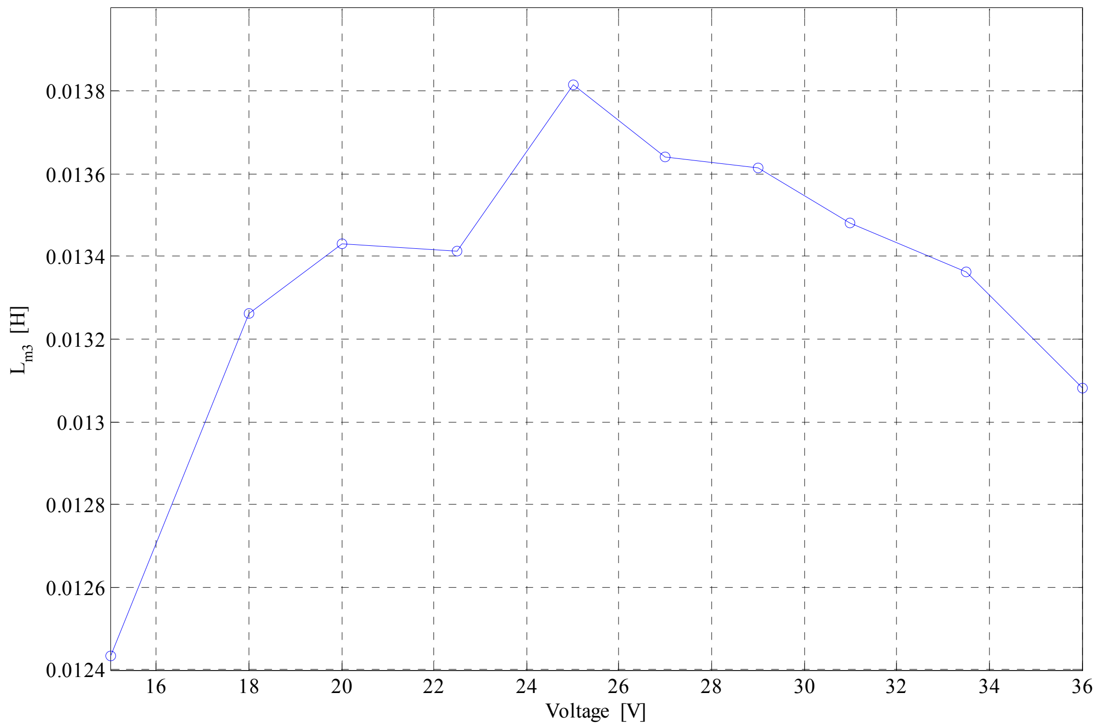

Figure 3.38 Third harmonic component of the magnetizing inductance

Table 3.10 Locked rotor t test Line-to-line voltages, current and power measurements

V_{ae}	V_{be}	V_{ce}	V_{de}	I_{asc}	I_{bsc}	I_{csc}	I_{dsc}	I_{esc}	P_{aesc}	P_{besc}	P_{cesc}	P_{desc}
56	90	85	59	7	7	7	7	7	365	450	132	17
55	86	84	57	6	6	6	6	6	310	395	96	14
40	65	64	44	4.7	4.5	4.55	4.25	4.85	190	210	58	10
30	50	50	34	3.35	3.5	3.4	2.85	3.3	110	120	20	6
25	40	41	27	2.75	2.5	2.4	2.3	2.70	75	70	8	4
15	28	28	20	1.6	1.5	1.4	1.2	1.55	25	25	2	2

Relationship between line-to-line voltage and phase voltage is given by

Adjacent phases $V_{LLadj} = V_{ph}\sqrt{2 - 2\cos\left(\frac{2\pi}{5}\right)}$

Non-adjacent phases $V_{LLnonadj} = V_{ph}\sqrt{2 - 2\cos\left(\frac{4\pi}{5}\right)}$

where V_{ph} is the rms phase voltage.

The parameters are the calculated as follows

$$R_{br} = \frac{P_{br}}{I_{br}^2}, \qquad Z_{br} = \frac{V_{br}}{I_{br}}$$

$$X_{br} = \sqrt{Z_{br}^2 - R_{br}^2}$$

where V_{br} is the blocked rotor stator average phase voltage

I_{br} is the blocked rotor stator average phase current

P_{br} is the blocked rotor stator average phase power

R_{br} is the blocked rotor resistance

Z_{br} is the blocked rotor impedance

X_{br} is the blocked rotor reactance

The equivalent leakage inductance is given by

$L_{br} = \dfrac{X_{br}}{\omega_s}$, $\omega_s = 2\pi f_s$ f_s is the supply frequency.

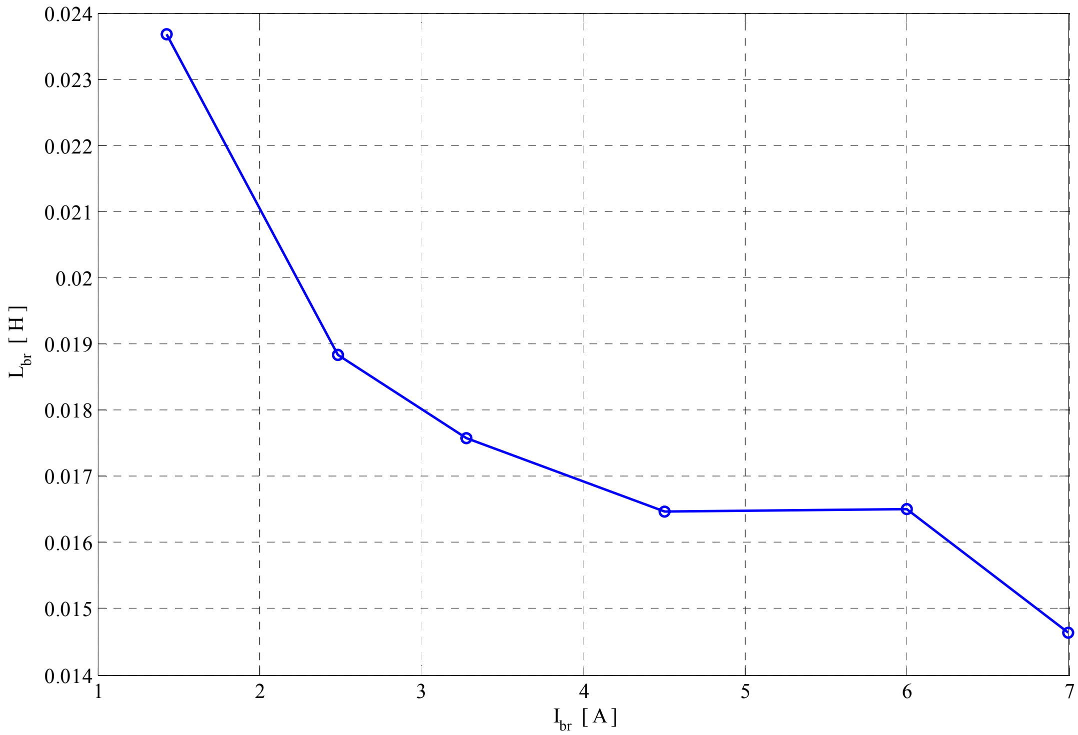

Figure 2.39 Locked Rotor Leakage inductance, L_{br} against stator current, I_{br}

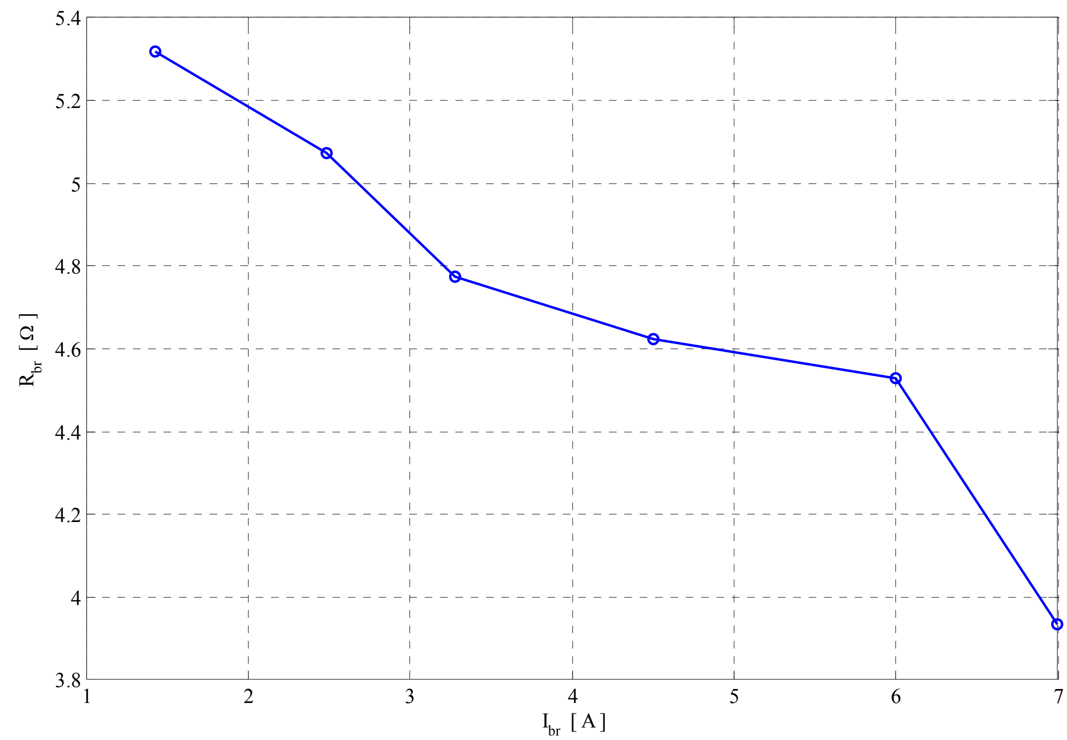

Figure 3.40 Locked Rotor Winding resistance, R_{br} against stator current, I_{br}

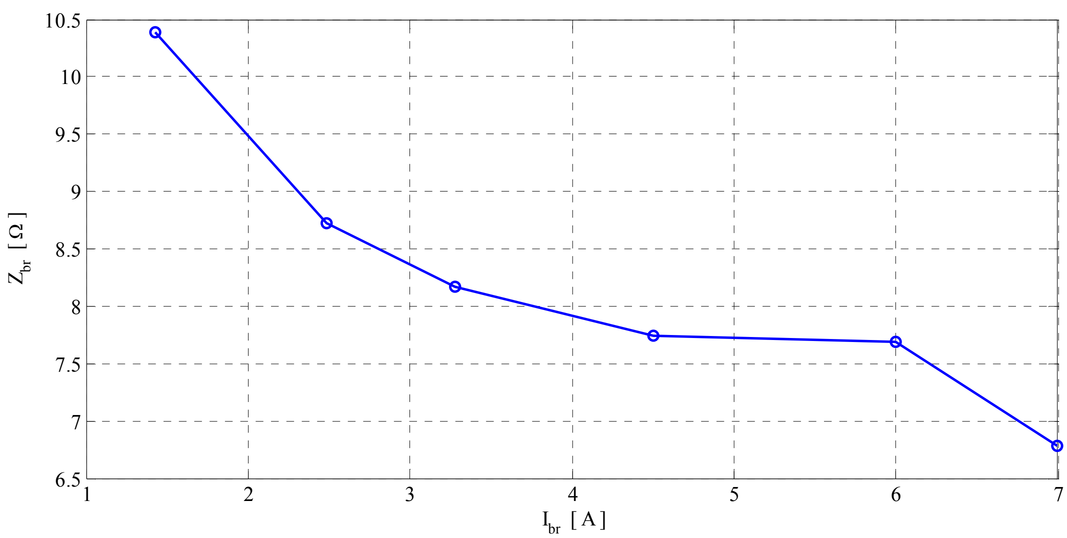

Figure 3.41 Locked Rotor Impedance, Z_{br} against stator current, I_{br}

Table 3.11 Summary of the Test parameters

	Fundamental component			Third harmonic component	
1.	R_{s1}	1.8Ω		R_{s3}	1.8Ω
2.	$R_{r1}^{'}$	2.9086Ω		$R_{r3}^{'}$	1.8669Ω
3.	L_{m1}	$86.7\,mH$		L_{m3}	$13.4\,mH$
4.	L_{ls1}	$8.95\,mH$		L_{ls3}	$1.8669\,mH$
5.	$L_{lr1}^{'}$	$8.95\,mH$		$L_{lr1}^{'}$	$4.9\,mH$
6.	R_{c1}	65.4052Ω			

Figures 3.39, 3.40 and 3.41 show the equivalent leakage inductance, equivalent winding resistance and equivalent impedance, respectively, as they vary with the current in a locked rotor test.

The stator winding resistance was obtained by directly measuring the resistance between two phases and then taking the average value. It was found to be 1.8Ω. Table 3.11 shows the summary of the machine parameters as they were obtained from no-load and locked rotor tests for both the fundamental and harmonic components.

3.10 Conclusion

The analysis and model of a five phase induction machine have been presented. First the stator winding has been redesigned to five phases instead of the previous three phases. Then the turn and winding functions have been calculated. These are used in directly determining the machine parameters. The full-order model in which all higher order harmonics are accounted for has been described and used to determine these parameters. The fundamental and third harmonic parameters of the machine windings have been determined.

The full order model of the five phase induction machine has been presented and simulation results are included in the Chapter. The model takes into account the contribution of the harmonic contents. The fundamental and third harmonic components of machine parameters and variables have been computed and presented for the simulation of the developed model. The derivation for the voltage and current turns ratios have been derived and presented in this Chapter. These ratios are used to transform the machine parameters from one side (rotor) to the other side (stator).

The experimental results for determination of the machine parameters are also included. No-load and blocked rotor tests have been carried out to determine the fundamental and third harmonic components of the five phase machine. The machine is supplied from a balanced five phase supply via two three-phase inverters controlled by the digital signal processor (DSP).

CHAPTER 4

CARRIER BASED PWM SCHEME FOR FIVE PHASE INDUCTION MOTOR DRIVE

4.1 Introduction

DC/AC voltage source inverters (VSI) are extensively used in motor drives to generate controllable frequency and ac voltage magnitudes using various pulse width modulation (PWM) strategies. The carrier-based PWM is very popular due to its simplicity of implementation, known harmonic waveform characteristics, and low harmonic distortion. Figure (4.1) shows a schematic diagram of five-phase voltage source converter.

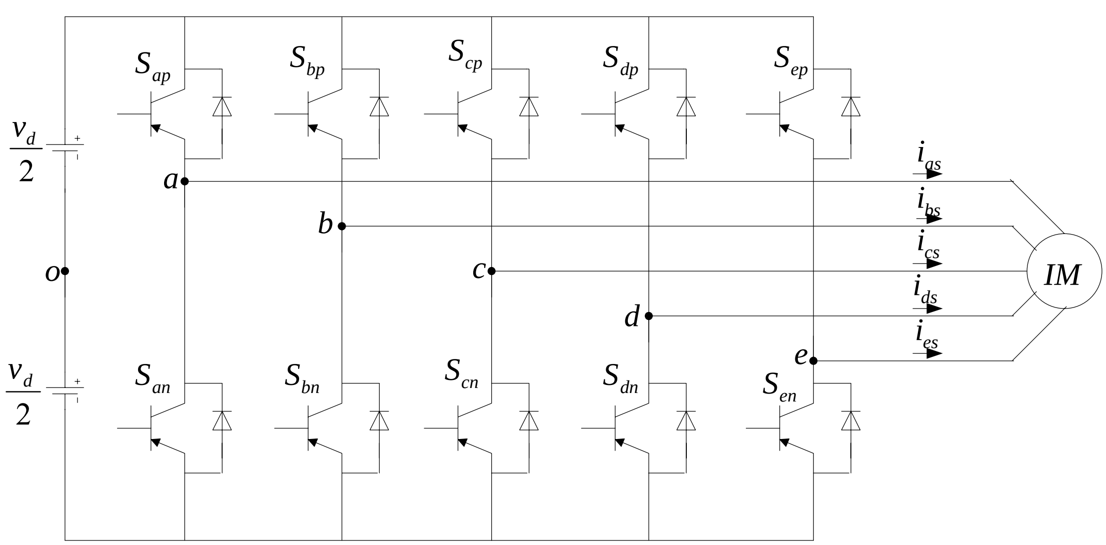

Figure 4.1 Five-phase two-level voltage source inverter supplying a five-phase induction machine

The turn on and turn off sequences of a switching device are represented by an existence function which has a value of unity when it is turned on and becomes zero when it is turned off [4.1]. The existence function of a two-level converter comprising of two switching devices is represented by S_{ij}, $i = a, b, c, d, e$ and $j = p, n$ where i represents the load phase to which the device is connected, and j signifies top (p) and bottom (n) device of the converter leg. Hence, S_{ap}, S_{an} which take values of zero or unity, are, respectively the existence functions of the top device and the bottom device of the inverter leg which is connected to phase 'a' of the load.

The load voltage Equations of the five-phase converter expressed in terms of the existence functions and input DC voltage v_d are given as

$$v_{io} = \frac{v_d}{2}\left(2S_{ip} - 1\right) = v_{in} + v_{no}, \quad i = a,\ b,\ c,\ d,\ e \tag{4.1}$$

$$v_{ao} = \frac{v_d}{2}\left(S_{ap} - S_{an}\right) = \frac{v_d}{2}\left(S_{ap} - \left(1 - S_{ap}\right)\right) = \frac{v_d}{2}\left(2S_{ap} - 1\right) = v_{an} + v_{no} \tag{4.2}$$

Similarly,

$$v_{bo} = \frac{v_d}{2}\left(2S_{bp} - 1\right) = v_{bn} + v_{no} \tag{4.3}$$

$$v_{co} = \frac{v_d}{2}\left(2S_{cp} - 1\right) = v_{cn} + v_{no} \tag{4.4}$$

$$v_{do} = \frac{v_d}{2}\left(2S_{dp} - 1\right) = v_{dn} + v_{no} \tag{4.5}$$

$$v_{eo} = \frac{v_d}{2}\left(2S_{ep} - 1\right) = v_{en} + v_{no} \tag{4.6}$$

$$v_{ao} + v_{bo} + v_{co} + v_{do} + v_{eo} = v_{an} + v_{bn} + v_{cn} + v_{dn} + v_{en} + 5v_{no} \tag{4.7}$$

and

$$v_{ao}+v_{bo}+v_{co}+v_{do}+v_{eo}=\begin{bmatrix}\frac{v_d}{2}\left(2S_{ap}-1\right)+\frac{v_d}{2}\left(2S_{bp}-1\right)+\frac{v_d}{2}\left(2S_{cp}-1\right)\\+\frac{v_d}{2}\left(2S_{dp}-1\right)+\frac{v_d}{2}\left(2S_{ep}-1\right)\end{bmatrix} \tag{4.8}$$

For balanced five-phase system,

$$v_{an}+v_{bn}+v_{cn}+v_{dn}+v_{en}=0 \tag{4.9}$$

Therefore,

$$v_{ao}+v_{bo}+v_{co}+v_{do}+v_{eo}=5v_{no} \tag{4.10}$$

$$5v_{no}=\frac{v_d}{2}\left(2S_{ap}-1\right)+\frac{v_d}{2}\left(2S_{bp}-1\right)+\frac{v_d}{2}\left(2S_{cp}-1\right)+\frac{v_d}{2}\left(2S_{dp}-1\right)+\frac{v_d}{2}\left(2S_{ep}-1\right) \tag{4.11}$$

$v_{an}, v_{bn}, v_{cn}, v_{dn}, v_{en}$ are the desired (reference) phase voltages of the load. The voltage between a reference 'o' of the inverter and the neutral of the load is denoted by v_{no}.

In order to prevent short-circuiting the DC source and satisfy the Kirchhoff's voltage law, S_{ip} and S_{in} cannot be turned on at the same time. Hence Kirchhoff's voltage law constraints the existence function such that $S_{ip}+S_{in}=1$. The existing function is a series of modulation pulses whose magnitude is either unity or zero. A Fourier approximation of this function is given as [4.1]

$$S_{ip}=0.5.\left(1+M_{ip}\right) \tag{4.12}$$

The expressions for the modulation signals are therefore expressed as

$$M_{ip}=\frac{2\left(v_{in}+v_{no}\right)}{v_d},\ i=a,\ b,\ c,\ d,\ e \tag{4.13}$$

The PWM modulation signals for the five top devices of the converter are M_{ip}. Equation (4.13) gives the most general expression for the modulation signals in which reasonable expressions for the zero sequence signal v_{no} can be included. The appropriate zero sequence signal may give rise to minimum switching loss, improved current and/or phase voltage waveforms. These signals are compared with a high frequency triangle carrier waveform to produce the PWM switching pulses which are given to the base drives to turn on and turn off the switching devices. The average neutral voltage, v_{no} is determined below. Equations (4.2-4.6) can be expressed as

$$\frac{v_d}{2}\left(2S_{ip}-1\right)=v_{io} \tag{4.14}$$

$$v_{no}=\frac{v_d}{2}\left(2S_{ip}-1\right)-v_{in} \tag{4.15}$$

$$\frac{2v_{no}}{v_d}=2S_{ip}-1-\frac{2v_{in}}{v_d} \tag{4.16}$$

$$2S_{ip}-1=\frac{2v_{in}}{v_d}+\frac{2v_{no}}{v_d} \tag{4.17}$$

$$2S_{ip}-1=m_{ipp}+m_o \tag{4.18}$$

where $m_{ipp}=\frac{2v_{in}}{v_d}$, $m_o=\frac{2v_{no}}{v_d}$, and $i=a,\ b,\ c,\ d,\ e$.

When the switching function of the top device is unity (when it is turned on), then

$$m_o=1-m_{ipp} \tag{4.19}$$

When the switching function of the top device is zero (when it is turned off), then

$$m_o=-1-m_{ipp} \tag{4.20}$$

There are six feasible solutions for m_o from (4.19) and (4.20) since the Equation is over-determined yielding an infinite number of possibilities. However, m_o must lie within 1 and -1 since the normalized high-frequency triangular signal also lies within this range. A reasonable solution can be obtained by considering the extrema of (4.19) and (4.20). With the following definitions,

$$M_{\max} = Max(m_{ipp}) \qquad\qquad M_{\min} = Min(m_{ipp}) \tag{4.21}$$

where Max and Min, respectively denotes the maximum and minimum value of m_{ipp}. The extrema of the m_o are $(1 - M_{\max})$, $(-1 - M_{\min})$, $(1 - M_{\min})$ and $(-1 - M_{\max})$ of which only the first have magnitudes between the range (1,-1). The two solutions are now linearly weighed to determine the average value of m_o, $\langle m_o \rangle$ where $0 \le \alpha \le 1$ and is given as

$$\langle m_o \rangle = \alpha(-1 - M_{\min}) + (1 - \alpha)(1 - M_{\max}) \tag{4.22}$$

$$\langle m_o \rangle = (1 - 2\alpha) + (\alpha - 1)(M_{\max}) - \alpha M_{\min} \tag{4.23}$$

The values of α gives rise to an infinite number of carrier-base PWM modulation signals [4.1, 4.2]. The generalized discontinuous modulation signals (GDPWM) are obtained when α is given by

$$\alpha = 0.5.[1 + \operatorname{sgn}(\cos(5(\omega_e t + \delta)))] \tag{4.24}$$

$Sgn(x)$ is 1, 0 and -1 when x is positive, zero and negative, respectively. By varying the modulation angle δ, various discontinuous modulation signals are generated. When α = 0.5, this carrier-based modulation schemes corresponds to the known space vector modulation scheme where the null states are time- weighed equally. Figures 4.2 through 4.5 show the modulation signals and corresponding phase 'a' load voltage at different values of α and modulation angle δ. In this result, the peak value of the fundamental voltage is 150 V, and that of the third harmonic voltage is 15 V. The dc voltage is 300 V. Figures 4.2 through 4.7 show the result when only the fundamental component is considered, whereas Figure 4.8 through 4.25 show the results in which both the fundamental voltage and third harmonic voltage have been considered.

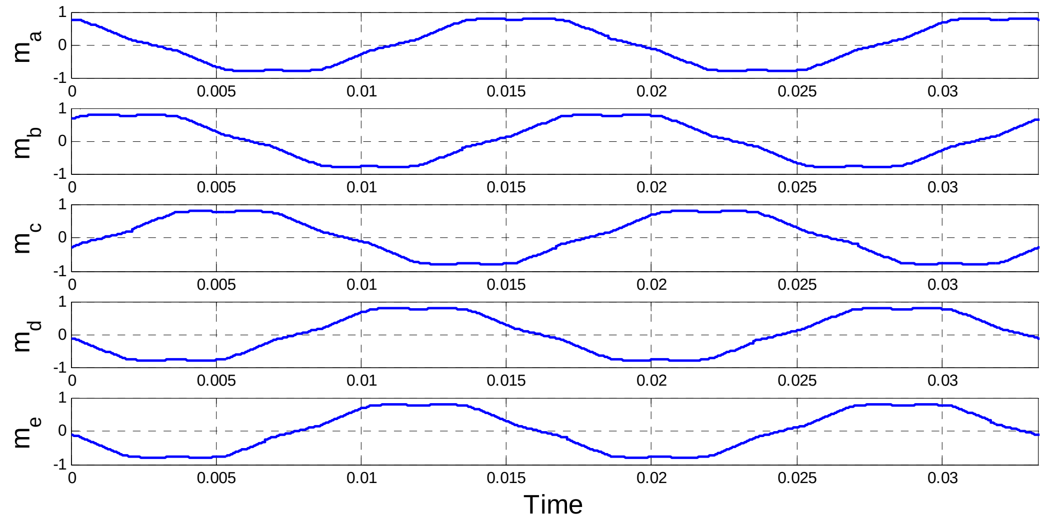

Figure 4.2 Five-phase modulation signals for $\alpha = 0.5$

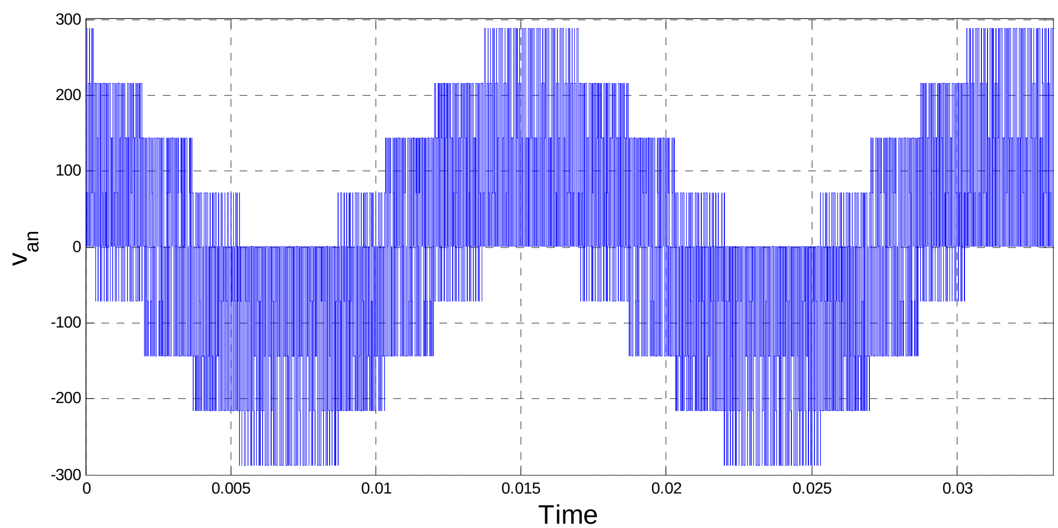

Figure 4.3 Phase ‘a’ load voltage, $\alpha = 0.5$

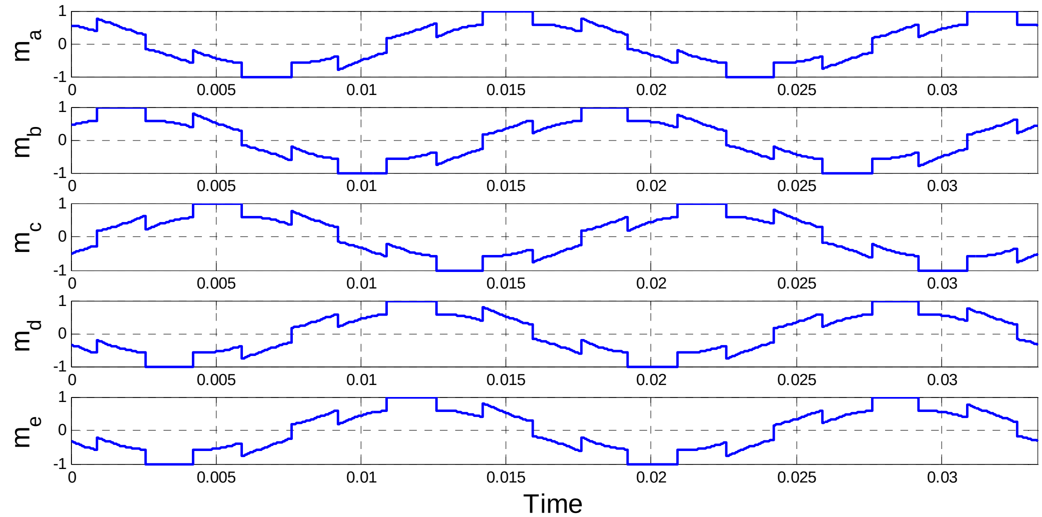

Figure 4.4 Five-phase modulation signals for $\alpha = 0.5[1 + \mathrm{sgn}(\cos(5(\omega_e t + \delta)))]$, $\delta = -36^0$

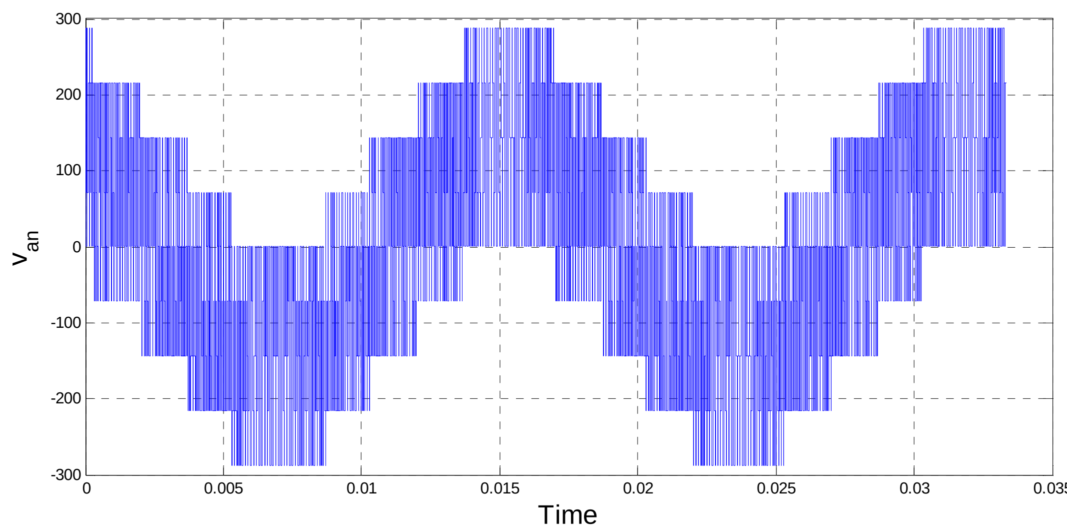

Figure 4.5 Phase 'a' load voltage, $\alpha = 0.5[1 + \mathrm{sgn}(\cos(5(\omega_e t + \delta)))]$, $\delta = -36^0$

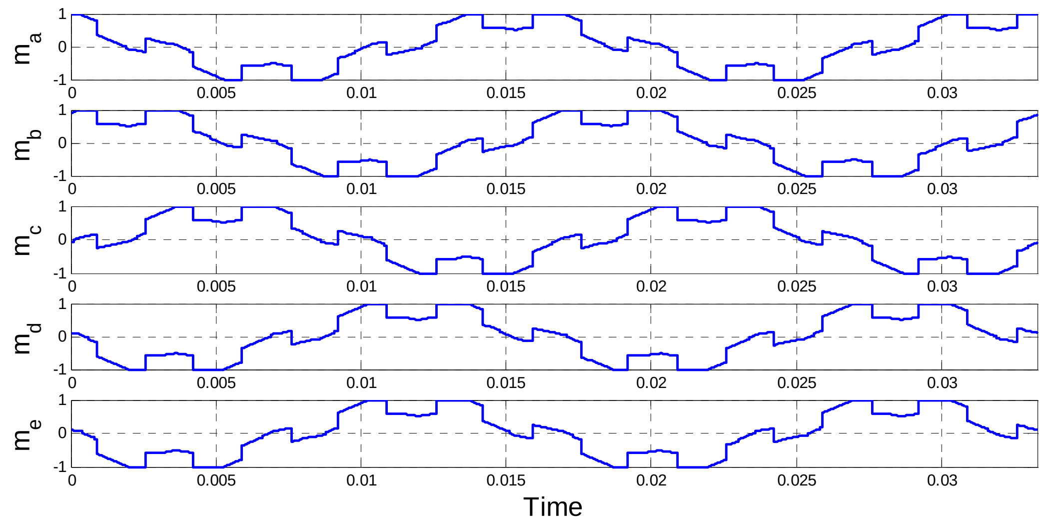

Figure 4.6 Five-phase modulation signals for $\alpha = 0.5[1 + \mathrm{sgn}(\cos(5(\omega_e t + \delta)))]$, $\delta = 0^0$

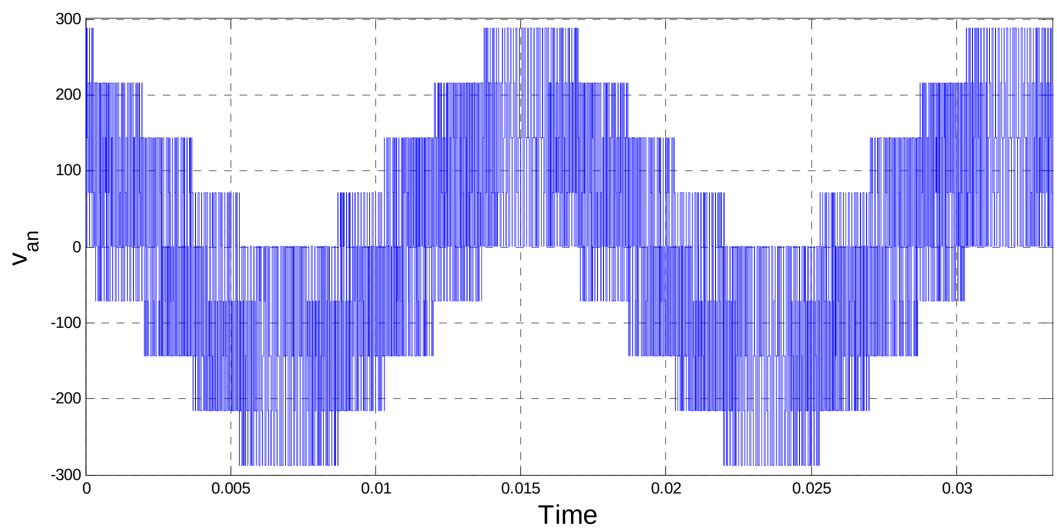

Figure 4.7 Phase 'a' load voltage, $\alpha = 0.5[1 + \mathrm{sgn}(\cos(5(\omega_e t + \delta)))]$, $\delta = 0^0$

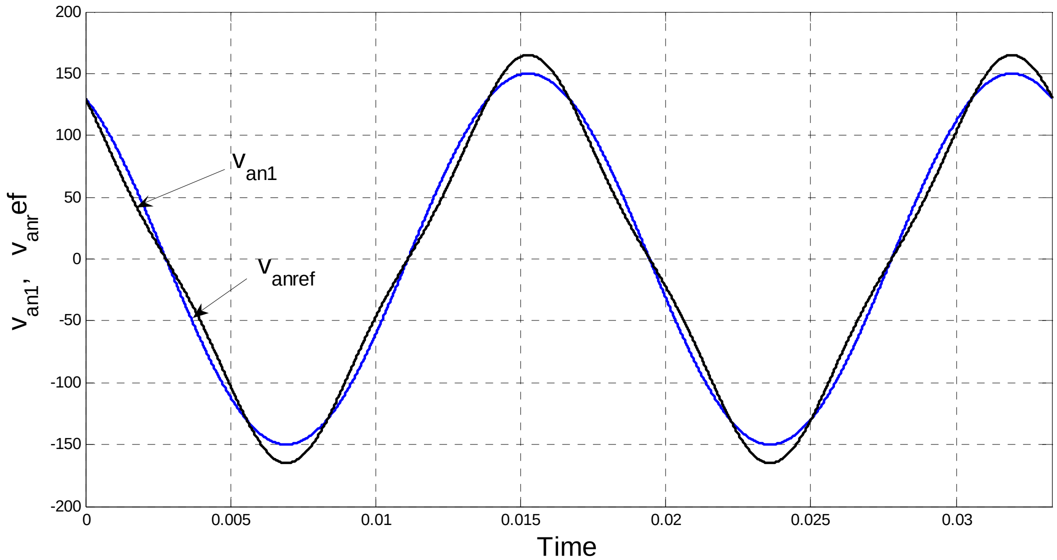

Figure 4.8 Phase 'a' fundamental and reference voltage, $\alpha = 0.5[1 + \text{sgn}(\cos(5(\omega_e t + \delta)))]$, $\delta = -36^0$, $v_{m3} = +15V$

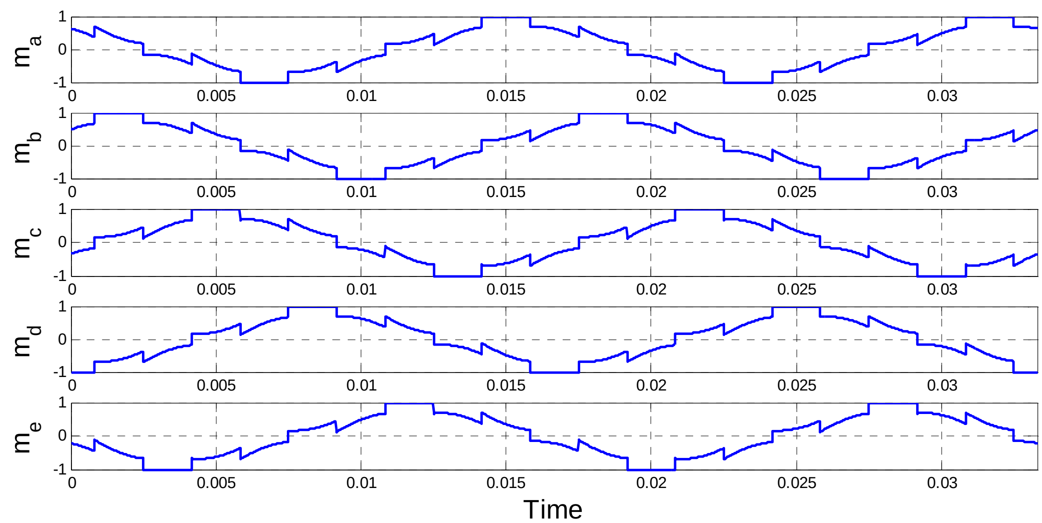

Figure 4.9 Five-phase modulation signals for $\alpha = 0.5[1 + \text{sgn}(\cos(5(\omega_e t + \delta)))]$, $\delta = -36^0$, $v_{m3} = +15V$

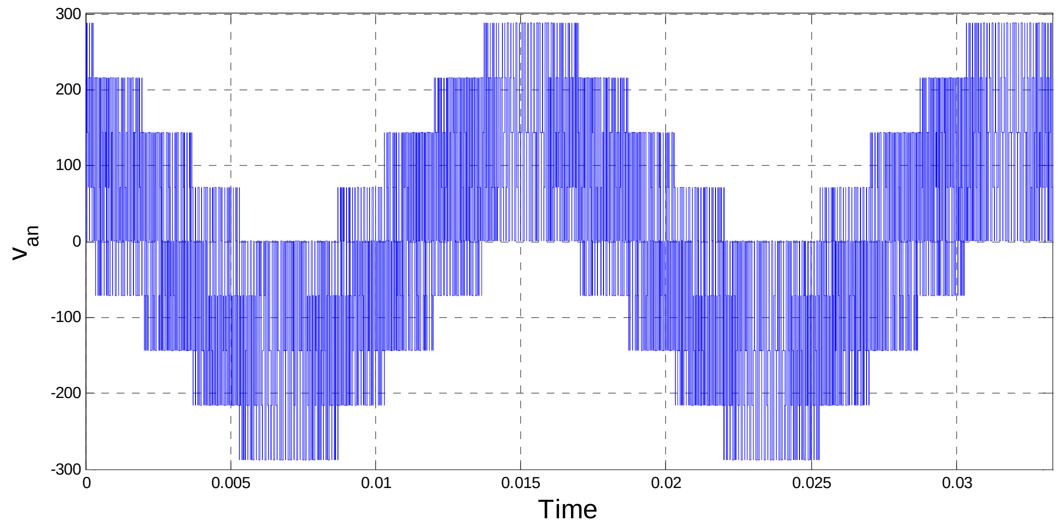

Figure 4.10 Phase 'a' load voltage, $\alpha = 0.5[1+\text{sgn}(\cos(5(\omega_e t+\delta)))]$, $\delta = -36^0$, $v_{m3} = +15V$

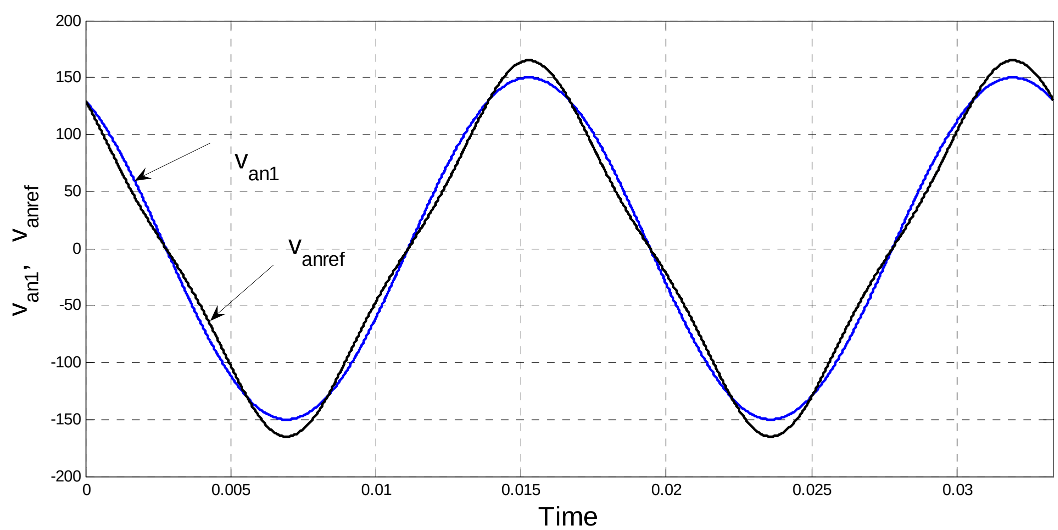

Figure 4.11 Phase 'a' fundamental and reference voltage, $\alpha = 0.5[1+\text{sgn}(\cos(5(\omega_e t+\delta)))]$, $\delta = 0^0$, $v_{m3} = +15V$

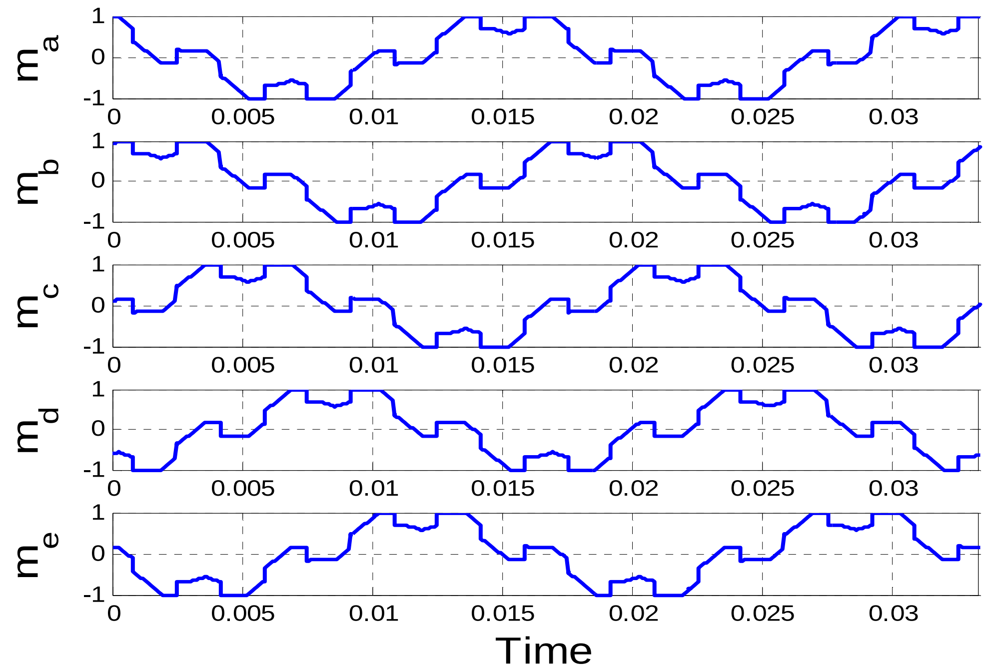

Figure 4.12 Five-phase modulation signals for $\alpha = 0.5[1+\text{sgn}(\cos(5(\omega_e t+\delta)))]$, $\delta = 0^0$, $v_{m3} = +15V$

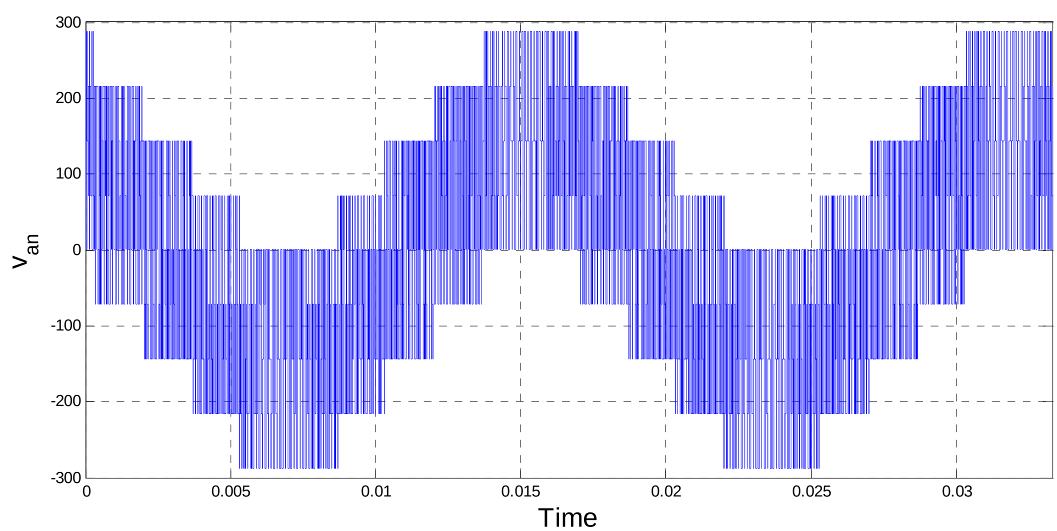

Figure 4.13 Phase 'a' load voltage, $\alpha = 0.5[1+\text{sgn}(\cos(5(\omega_e t+\delta)))]$, $\delta = 0^0$, $v_{m3} = +15V$

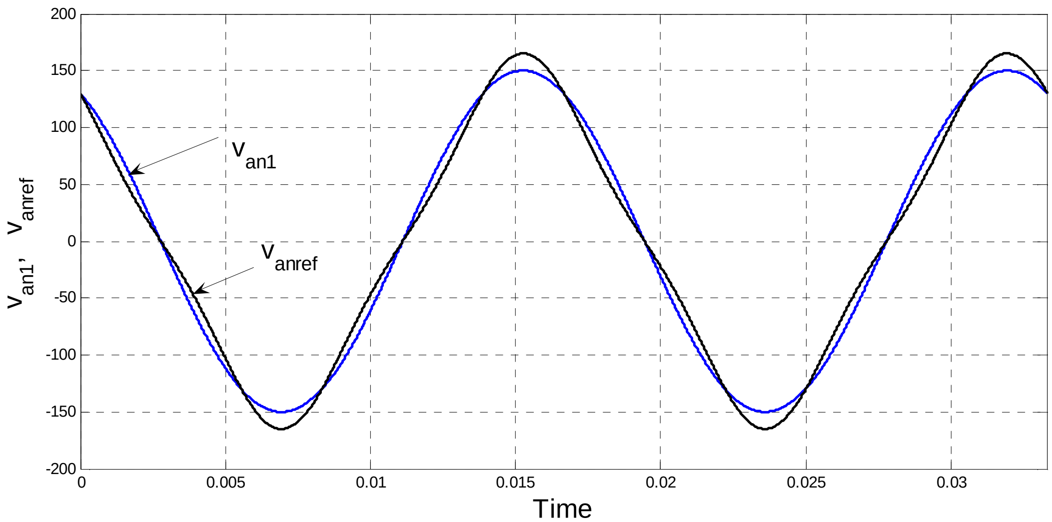

Figure 4.14 Phase ‘a’ fundamental and reference voltage, $\alpha = 0.5$, $v_{m3} = +15V$

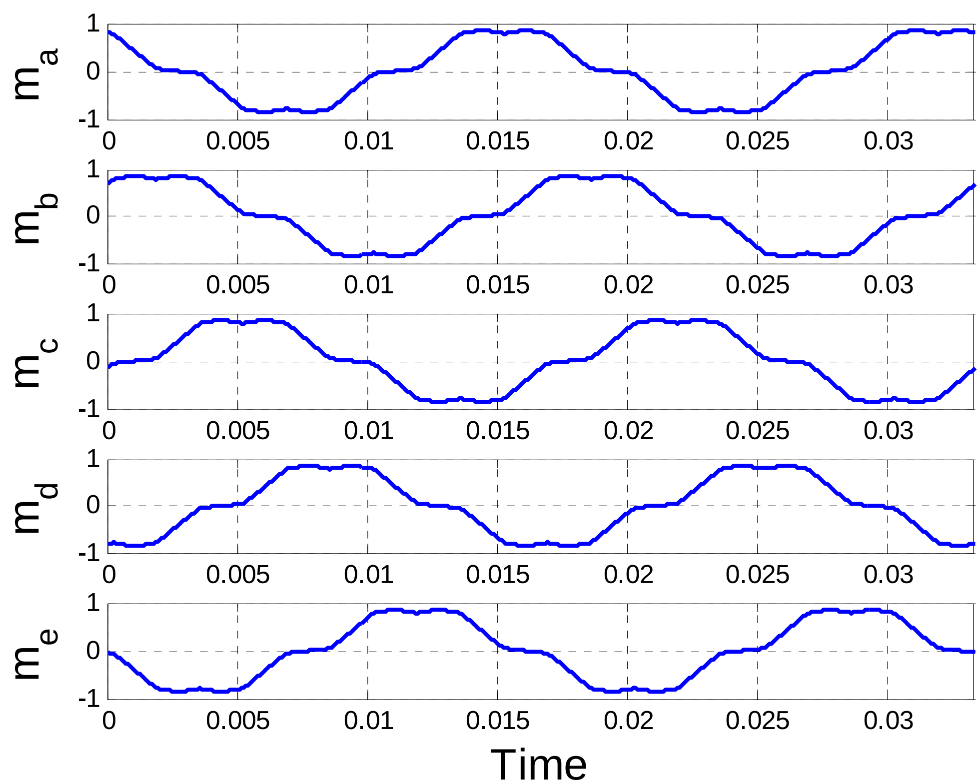

Figure 4.15 Five-phase modulation signals for $\alpha = 0.5$, $v_{m3} = +15V$

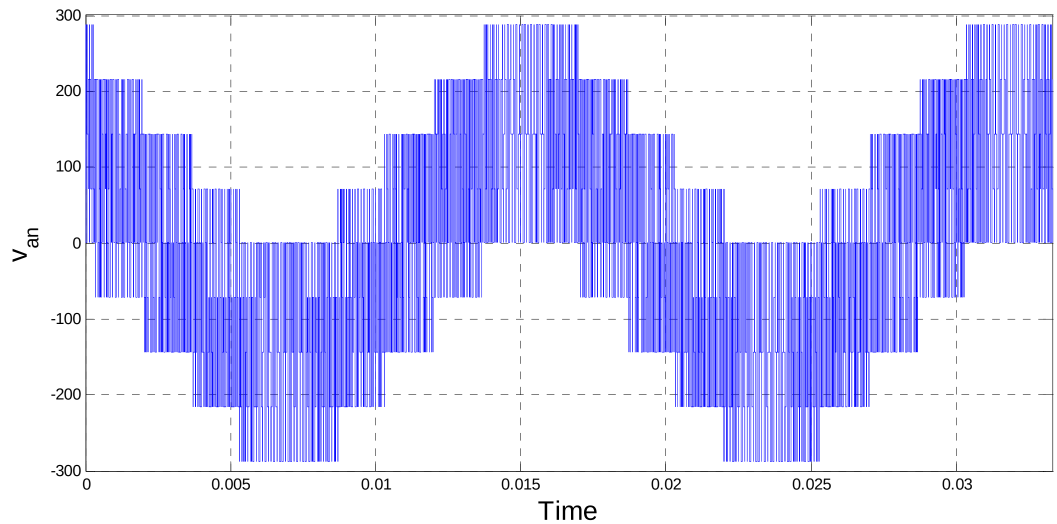

Figure 4.16 Phase ‘a’ load voltage, $\alpha = 0.5$, $v_{m3} = +15V$

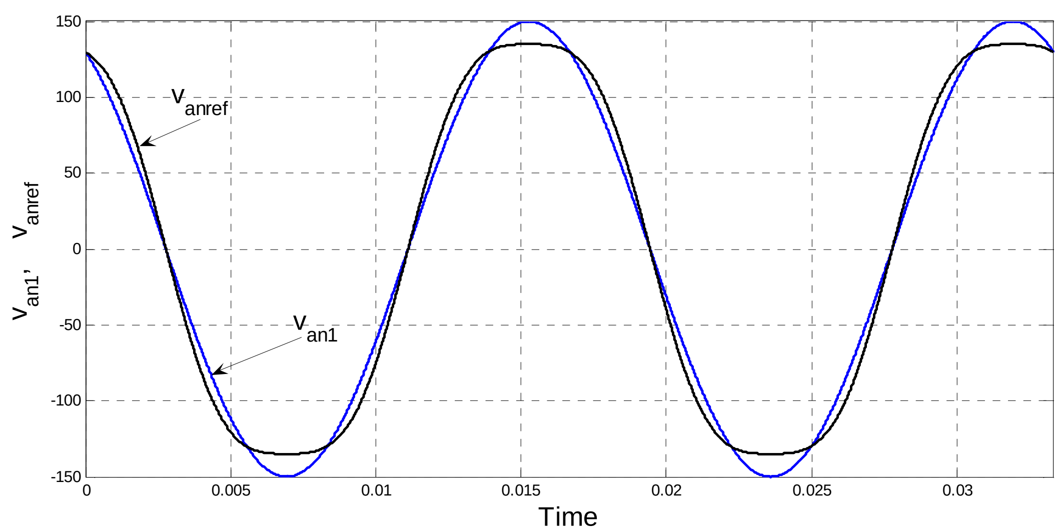

Figure 4.17 Phase ‘a’ fundamental and reference voltage, $\alpha = 0.5$, $v_{m3} = -15V$

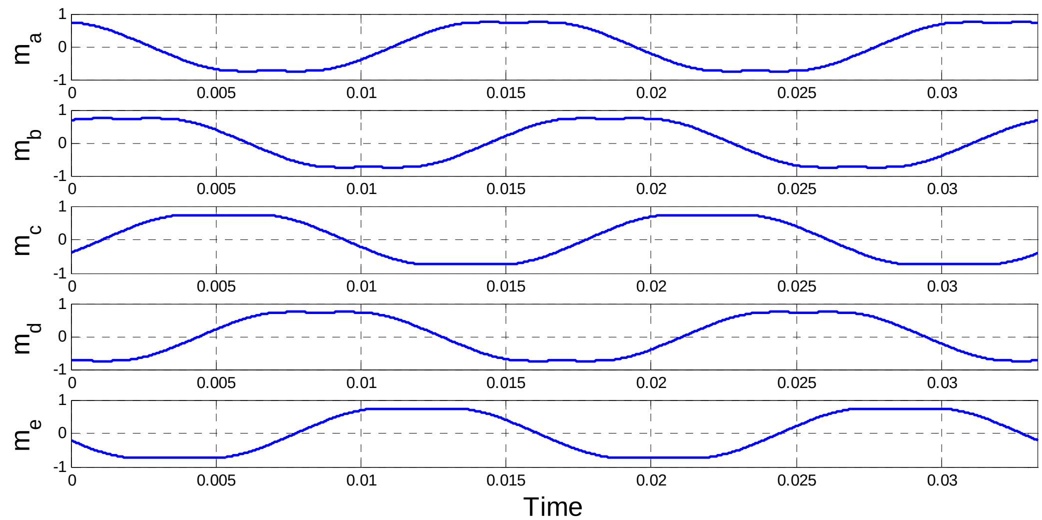

Figure 4.18 Five-phase modulation signals for $\alpha = 0.5$, $v_{m3} = -15V$

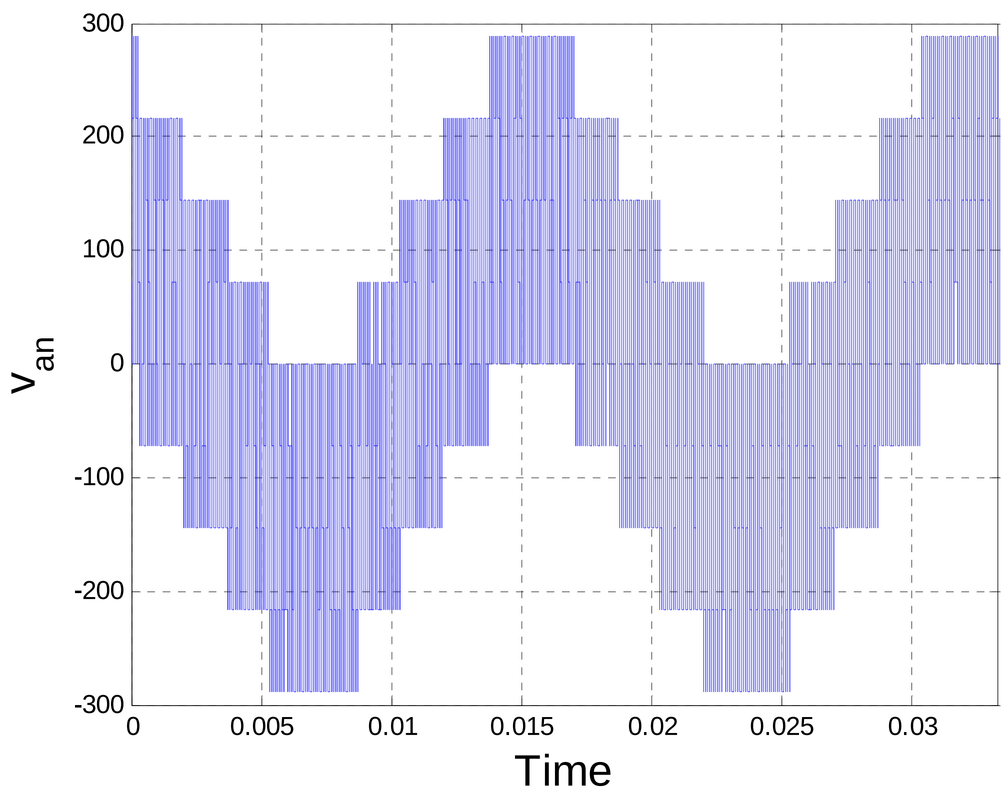

Figure 4.19 Phase 'a' load voltage, $\alpha = 0.5$, $v_{m3} = -15V$

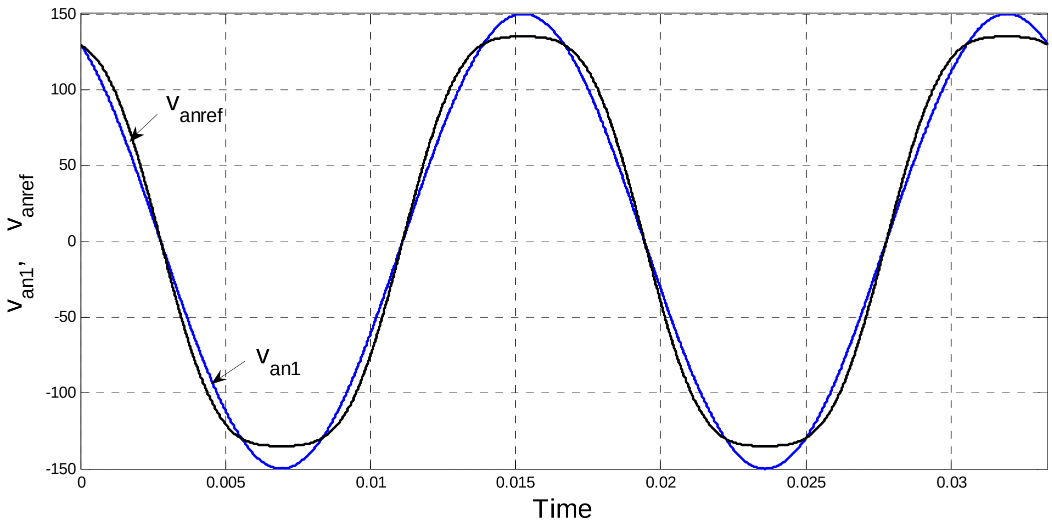

Figure 4.20 Phase ‘a’ fundamental and reference voltage,

$\alpha = 0.5[1+\mathrm{sgn}(\cos(5(\omega_e t+\delta)))]$, $\delta = 0^0$, $v_{m3} = -15V$

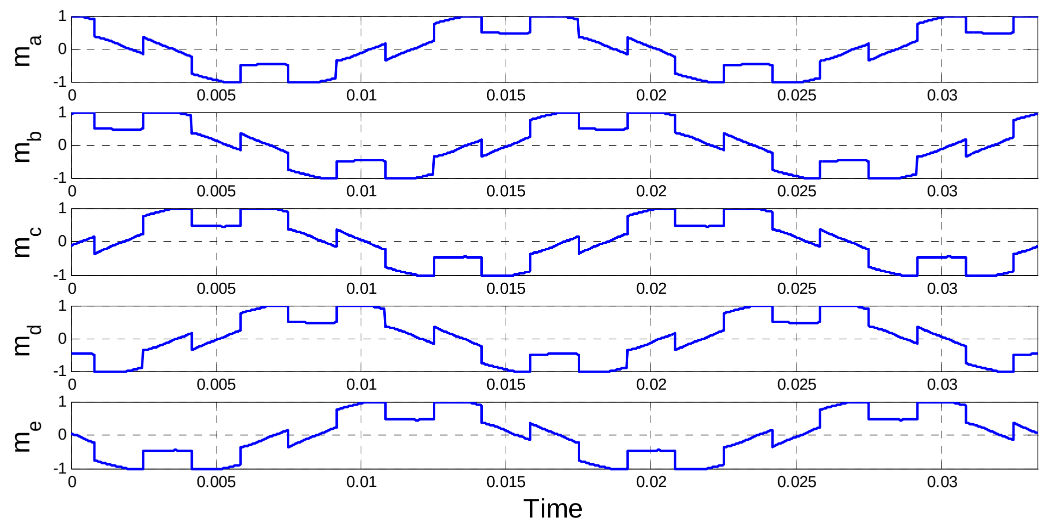

Figure 4.21 Five-phase modulation signals for $\alpha = 0.5[1+\mathrm{sgn}(\cos(5(\omega_e t+\delta)))]$, $\delta = 0^0$, $v_{m3} = -15V$

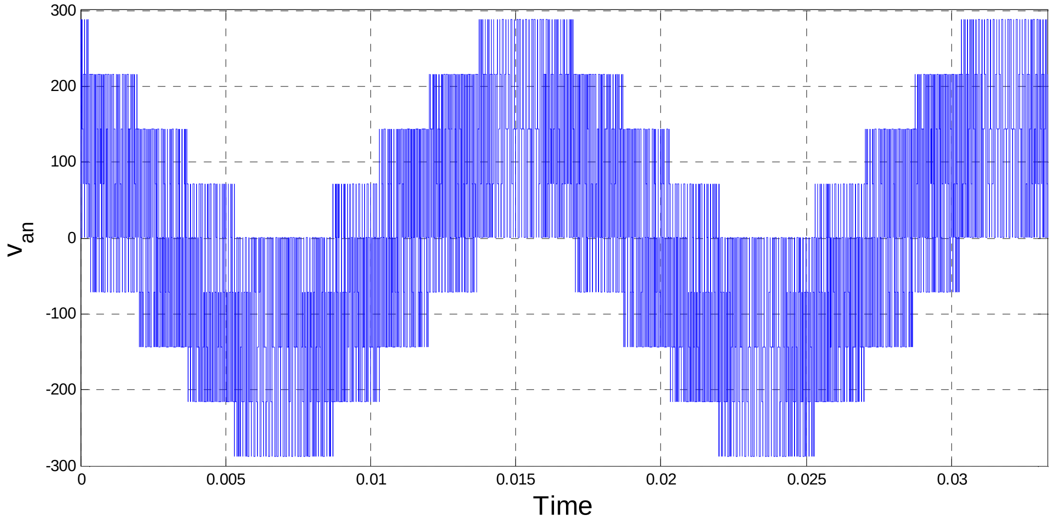

Figure 4.22 Phase 'a' load voltage, $\alpha = 0.5[1 + \mathrm{sgn}(\cos(5(\omega_e t + \delta)))]$, $\delta = 0^0$, $v_{m3} = -15V$

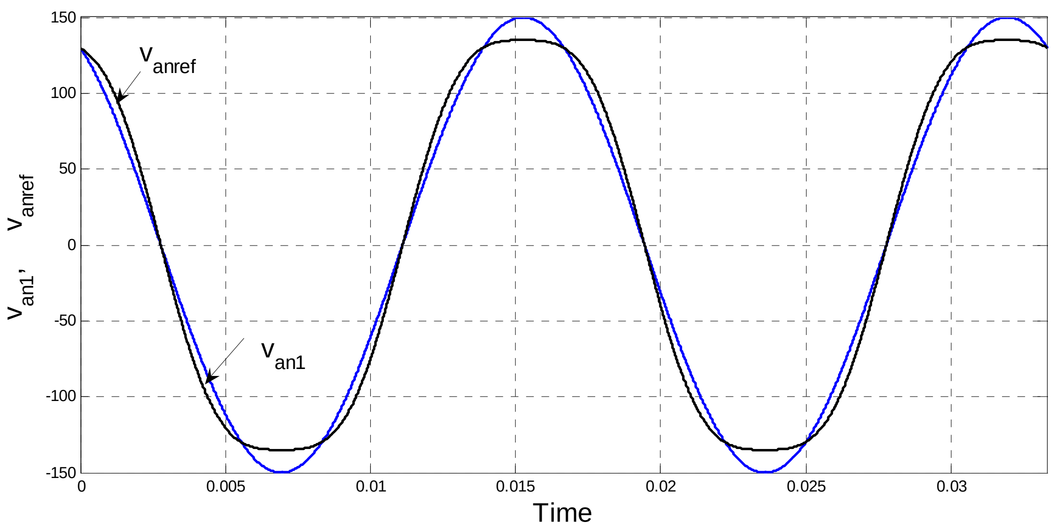

Figure 4.23 Phase 'a' fundamental and reference voltage, $\alpha = 0.5[1 + \mathrm{sgn}(\cos(5(\omega_e t + \delta)))]$, $\delta = -36^0$, $v_{m3} = -15V$

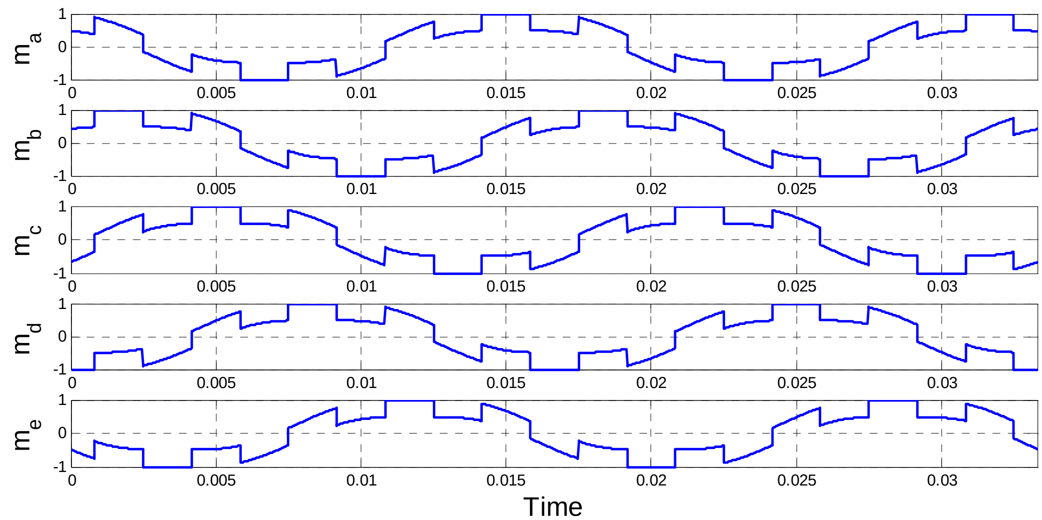

Figure 4.24 Five-phase modulation signals for $\alpha = 0.5[1 + \text{sgn}(\cos(5(\omega_e t + \delta)))]$, $\delta = -36^0$, $v_{m3} = -15V$

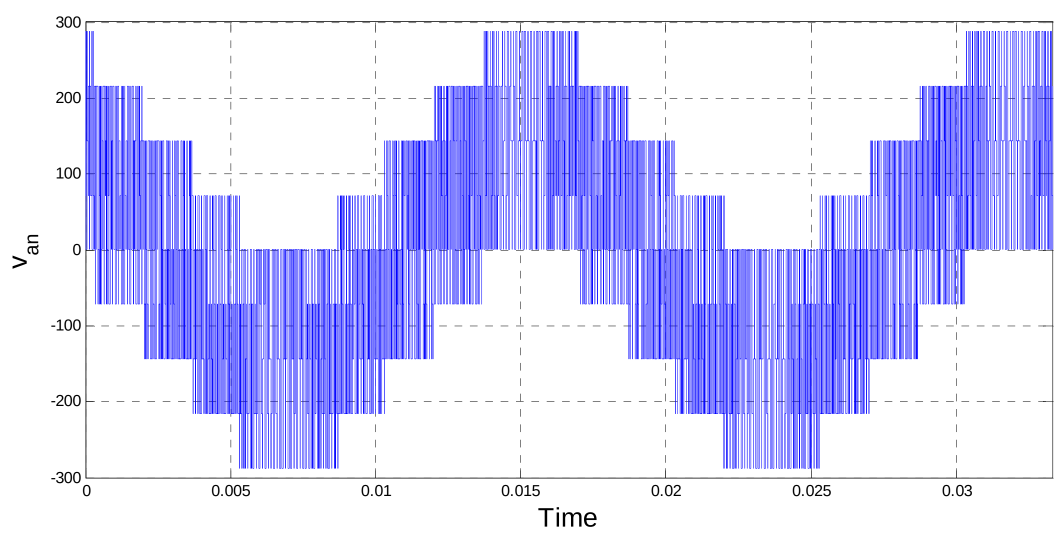

Figure 4.25 Phase 'a' load voltage, $\alpha = 0.5[1 + \text{sgn}(\cos(5(\omega_e t + \delta)))]$, $\delta = -36^0$, $v_{m3} = -15V$

4.2 Simulation Results

The five phase machine is simulated by using three different sets of connections

(a) it is assumed to be star-connected the phase voltages across the machine windings are v_{as}, v_{bs}, v_{cs}, v_{ds} and v_{es}, Figure 35 (a)

(b) It is assumed to be conventionally delta connected the phase voltages across the machine windings are $v_{as} - v_{bs}$, $v_{bs} - v_{cs}$, $v_{cs} - v_{ds}$, $v_{ds} - v_{es}$, and $v_{es} - v_{as}$, Figure 35 (b)

(c) It is assumed to be alternately delta connected the phase voltages across the machine windings are $v_{as} - v_{cs}$, $v_{bs} - v_{ds}$, $v_{cs} - v_{es}$, $v_{ds} - v_{as}$, and $v_{es} - v_{bs}$, Figure 35 (c).

In all simulations, the no-load transients for the electromagnetic torque, stator phase a current, rotor phase current and rotor speed are presented. Then a rated load torque of 8.5 Nm is applied at a time instant of 0.5 seconds, and the results are also presented. The phase a voltage of the machine winding is also shown.

In each different winding connection the machine is supplied directly from the mains (direct online), and then via an inverter. The derived voltage and current relations for the three different stator winding connections as given below.

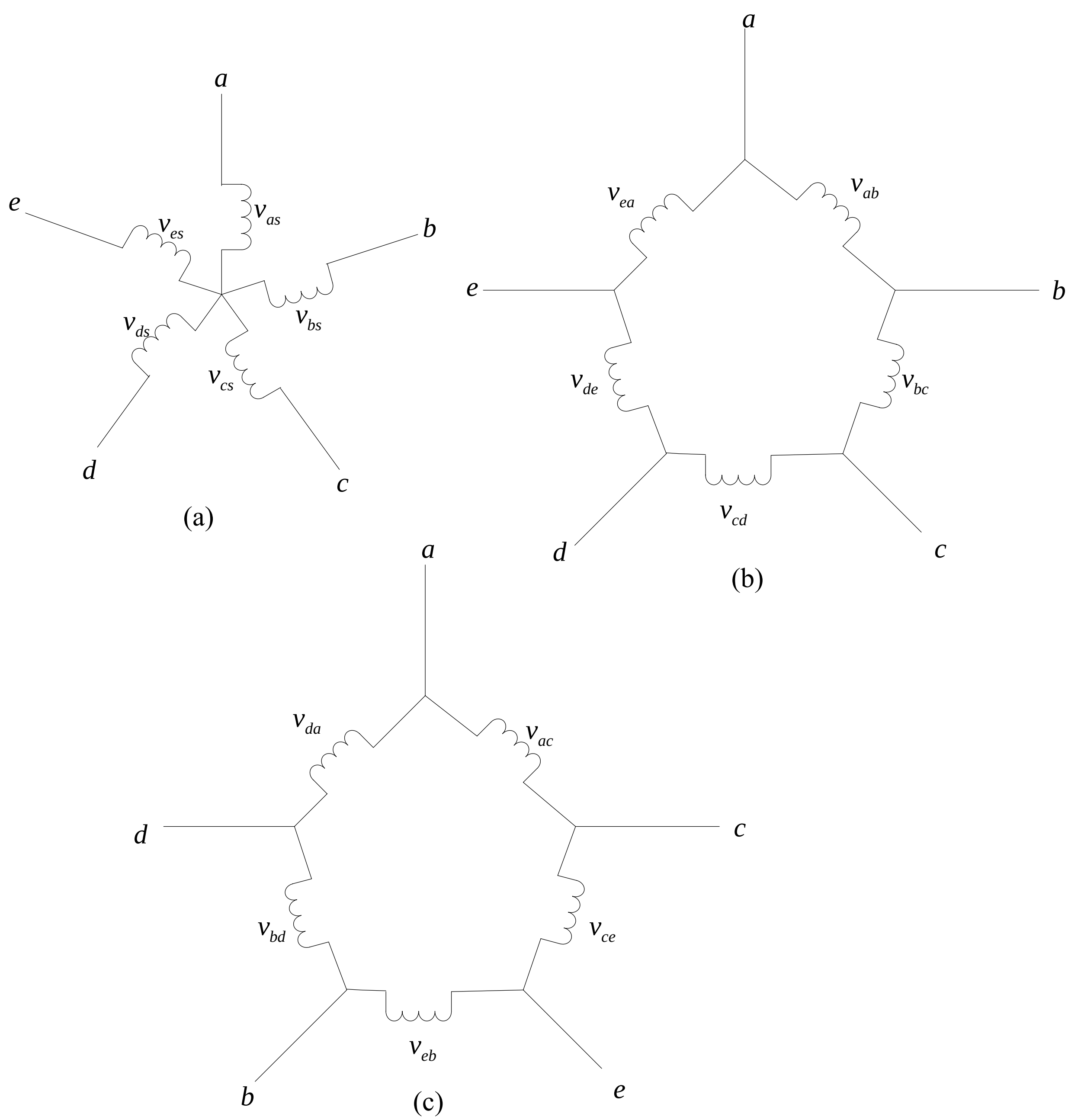

Figure 4.26 Different stator winding connections (a) star (b) normal (conventional) delta and (c) alternate delta.

4.2.1 Conventional Star Connection, Figure 4.26 (a)

Phase voltages are given by

$$v_{as} = V_m \cos(\theta_e), \qquad v_{bs} = V_m \cos\left(\theta_e - \frac{2\pi}{5}\right), \qquad v_{cs} = V_m \cos\left(\theta_e - \frac{4\pi}{5}\right),$$

$$v_{ds} = V_m \cos\left(\theta_e - \frac{6\pi}{5}\right), \qquad v_{es} = V_m \cos\left(\theta_e - \frac{8\pi}{5}\right)$$

Line-to-line voltages are given by

$$v_{ab} = 1.1756 V_m \cos\left(\theta_e + \frac{3\pi}{10}\right), \qquad v_{bc} = 1.1756 V_m \cos\left(\theta_e - \frac{\pi}{10}\right),$$

$$v_{cd} = 1.1756 V_m \cos\left(\theta_e - \frac{5\pi}{10}\right), \qquad v_{de} = 1.1756 V_m \cos\left(\theta_e - \frac{9\pi}{10}\right),$$

$$v_{ea} = 1.1756 V_m \cos\left(\theta_e + \frac{7\pi}{10}\right)$$

Line and phase currents are the same.

$$i_a = I_m \cos(\theta_e + \delta), \quad i_b = I_m \cos\left(\theta_e + \delta - \frac{2\pi}{5}\right), \quad i_c = I_m \cos\left(\theta_e + \delta - \frac{4\pi}{5}\right),$$

$$i_d = I_m \cos\left(\theta_e + \delta - \frac{6\pi}{5}\right), \quad i_e = I_m \cos\left(\theta_e + \delta - \frac{8\pi}{5}\right)$$

4.2.2 Conventional Delta Connection, Figure 4.26 (b)

Phase and line-to-line voltages are the same are given by

$$v_{ab} = v_{as} = 1.1756V_m \cos\left(\theta_e + \frac{3\pi}{10}\right), \quad v_{bc} = v_{bs} = 1.1756V_m \cos\left(\theta_e - \frac{\pi}{10}\right),$$

$$v_{cd} = v_{cs} = 1.1756V_m \cos\left(\theta_e - \frac{5\pi}{10}\right), \quad v_{de} = v_{ds} = 1.1756V_m \cos\left(\theta_e - \frac{9\pi}{10}\right),$$

$$v_{ea} = v_{es} = 1.1756V_m \cos\left(\theta_e + \frac{7\pi}{10}\right)$$

Phase currents are given by

$$i_{ab} = 1.1756I_m \cos\left(\theta_e + \delta + \frac{3\pi}{10}\right), \qquad i_{bc} = 1.1756I_m \cos\left(\theta_e + \delta - \frac{\pi}{10}\right),$$

$$i_{cd} = 1.1756I_m \cos\left(\theta_e + \delta - \frac{5\pi}{10}\right), \qquad i_{de} = 1.1756I_m \cos\left(\theta_e + \delta - \frac{9\pi}{10}\right),$$

$$i_{ea} = 1.1756I_m \cos\left(\theta_e + \delta + \frac{7\pi}{10}\right)$$

Line currents are given by

$$i_a = 1.3820I_m \cos(\theta_e + \delta), \qquad i_b = 1.3820I_m \cos\left(\theta_e + \delta - \frac{4\pi}{10}\right),$$

$$i_c = 1.3820I_m \cos\left(\theta_e + \delta - \frac{8\pi}{10}\right), \qquad i_d = 1.3820I_m \cos\left(\theta_e + \delta + \frac{8\pi}{10}\right),$$

$$i_e = 1.3820I_m \cos\left(\theta_e + \delta + \frac{4\pi}{10}\right)$$

4.2.3 Alternate Delta Connection, Figure 4.26 (c)

Phase and line-to-line voltages are the same and re given by

$$v_{ac} = v_{as} = 1.9021V_m \cos\left(\theta_e + \frac{\pi}{10}\right), \quad v_{bd} = v_{bs} = 1.9021V_m \cos\left(\theta_e - \frac{3\pi}{10}\right),$$

$$v_{ce} = v_{cs} = 1.9021V_m \cos\left(\theta_e - \frac{7\pi}{10}\right), \quad v_{da} = v_{ds} = 1.9021V_m \cos\left(\theta_e + \frac{9\pi}{10}\right),$$

$$v_{eb} = v_{es} = 1.9021V_m \cos\left(\theta_e + \frac{5\pi}{10}\right)$$

Phase currents are given by

$$i_{ac} = 1.9021I_m \cos\left(\theta_e + \delta + \frac{\pi}{10}\right), \qquad i_{bd} = 1.9021I_m \cos\left(\theta_e + \delta - \frac{3\pi}{10}\right),$$

$$i_{ce} = 1.9021I_m \cos\left(\theta_e + \delta - \frac{7\pi}{10}\right), \qquad i_{da} = 1.9021I_m \cos\left(\theta_e + \delta + \frac{9\pi}{10}\right),$$

$$i_{eb} = 1.9021I_m \cos\left(\theta_e + \delta + \frac{5\pi}{10}\right)$$

Line currents are given by

$$i_a = 3.6180I_m \cos(\theta_e + \delta), \qquad i_b = 3.6180I_m \cos\left(\theta_e + \delta - \frac{4\pi}{10}\right),$$

$$i_c = 3.6180I_m \cos\left(\theta_e + \delta - \frac{8\pi}{10}\right), \qquad i_d = 3.6180I_m \cos\left(\theta_e + \delta + \frac{8\pi}{10}\right),$$

$$i_e = 3.6180I_m \cos\left(\theta_e + \delta - \frac{4\pi}{10}\right)$$

4.2.4 Without Third Harmonic Voltage Injection

The five phase induction machine is supplied with fundamental voltage at a fundamental frequency of 60 Hz. Figures (4.27) through (4.38) show different results depending on the machine winding connections.

Figures (4.27) through (4.32) show normal operation without an inverter, whereas Figures (4.33) through (4.38) show the results when a five-phase machine is supplied via an inverter. Figures (4.27), (4.28), (4.33) and (4.34) the machine winding is star connected; Figures (4.29), (4.30), (4.35) and (4.36), the stator winding is delta connected (conventionally) and figures (4.31), (4.32), (4.37) and (4.38) are delta connected (alternately).

The peak value of the fundamental voltage used in this simulation is 187.79 V and the dc voltage is 360 V.

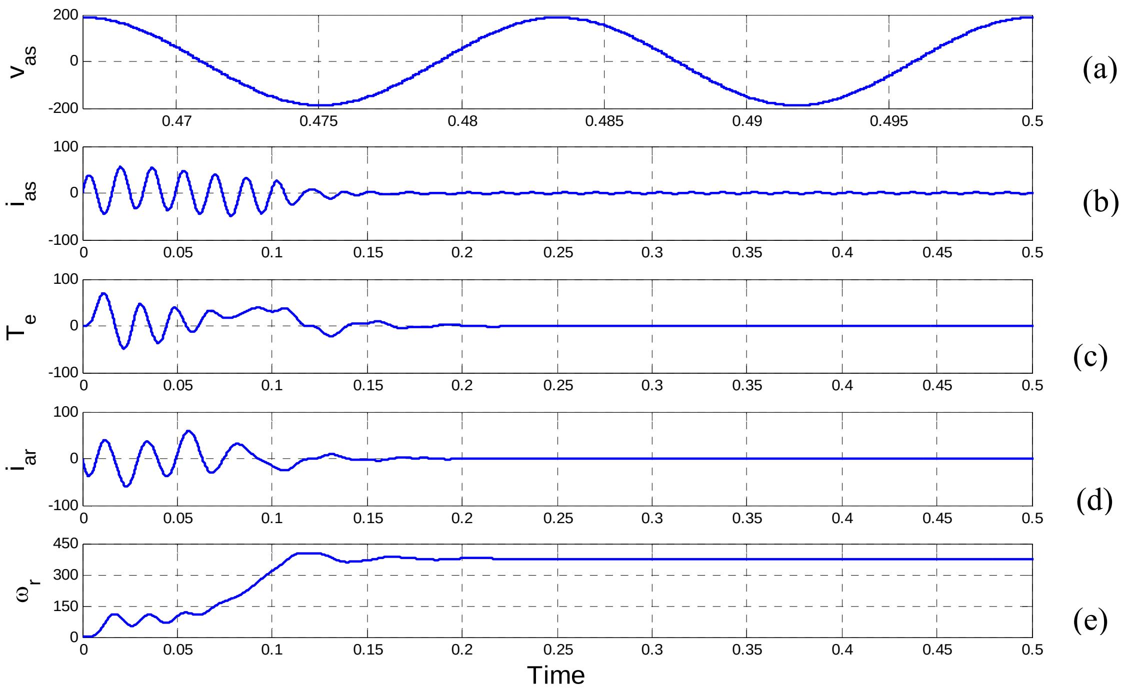

Figure 4.27 Starting transients (a) stator phase ‘a’ voltage, (b) stator phase ‘a’ current, (c) torque, (d) rotor phase ‘a’ current, (e) rotor speed

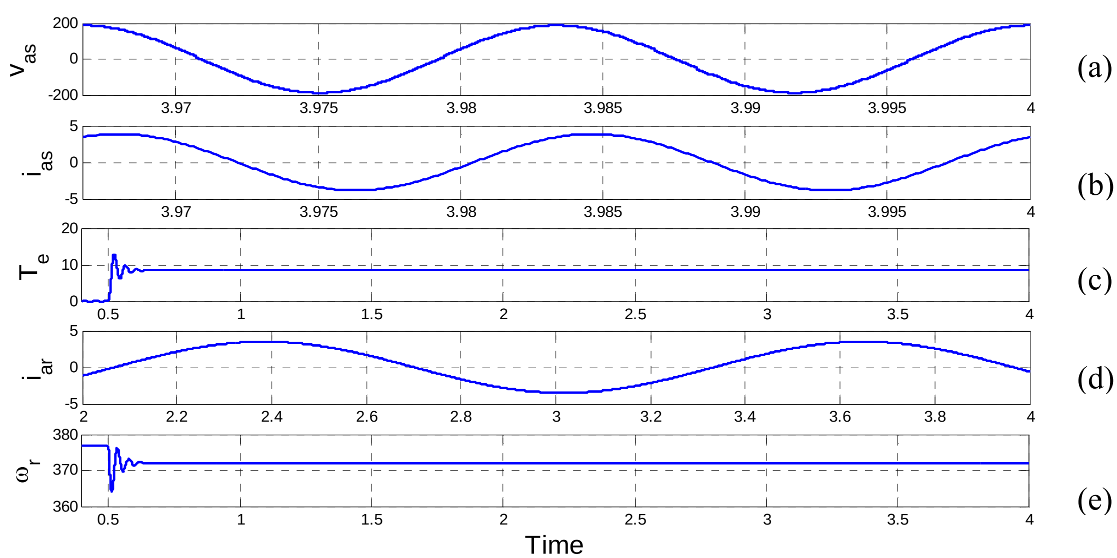

Figure 4.28 Load transients (a) stator phase ‘a’ voltage, (b) stator phase ‘a’ current, (c) torque, (d) rotor phase ‘a’ current, (e) rotor speed

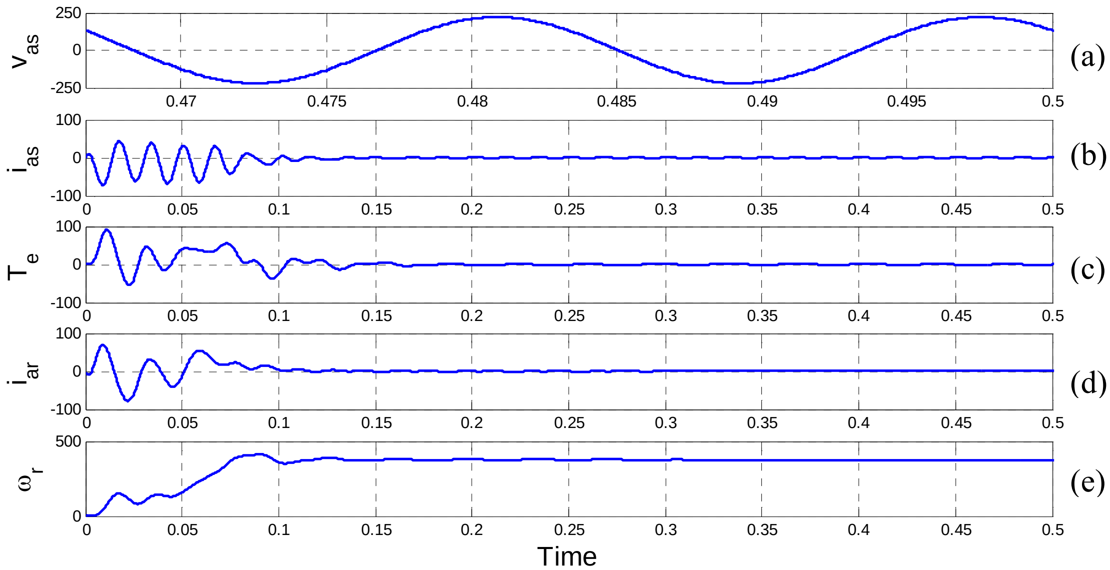

Figure 4.29 Starting transients (a) stator phase ‘a’ voltage, (b) stator phase ‘a’ current, (c) torque, (d) rotor phase ‘a’ current, (e) rotor speed

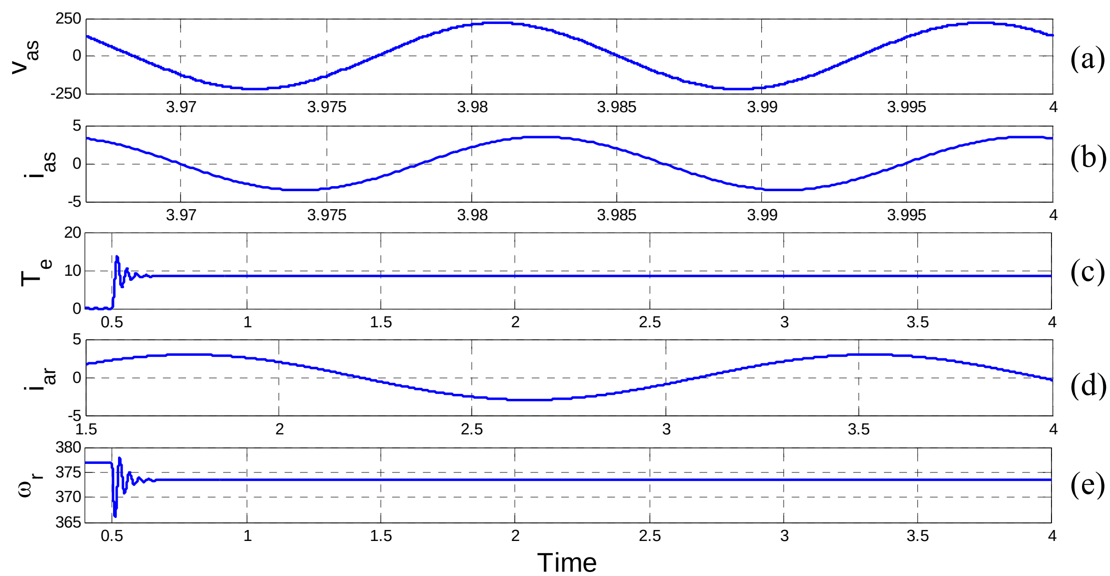

Figure 4.30 Load transients (a) stator phase ‘a’ voltage, (b) stator phase ‘a’ current, (c) torque, (d) rotor phase ‘a’ current, (e) rotor speed

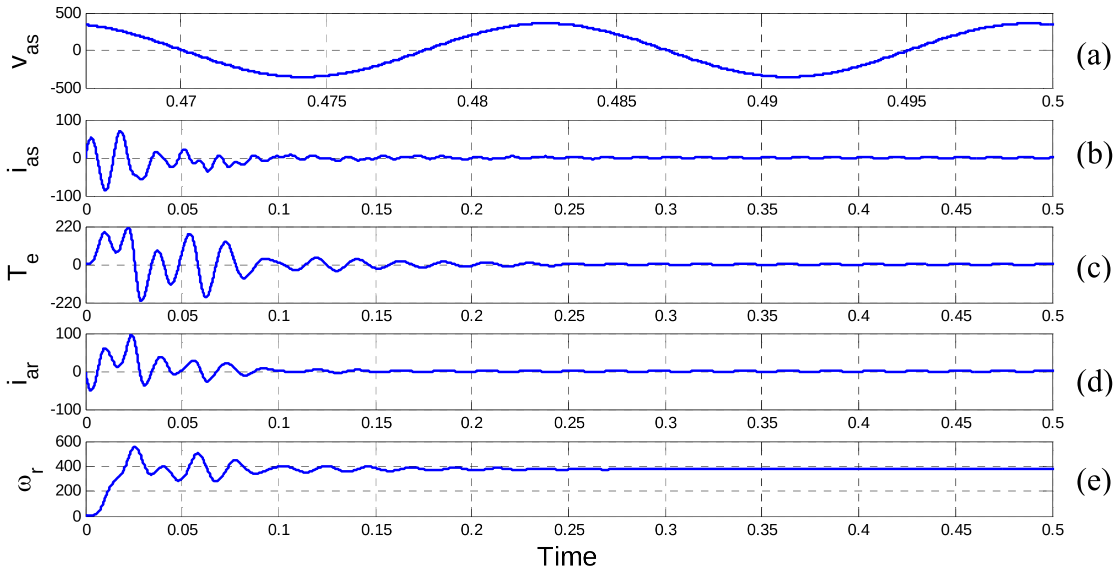

Figure 4.31 Staring transients (a) stator phase 'a' voltage, (b) stator phase 'a' current, (c) torque, (d) rotor phase 'a' current, (e) rotor speed

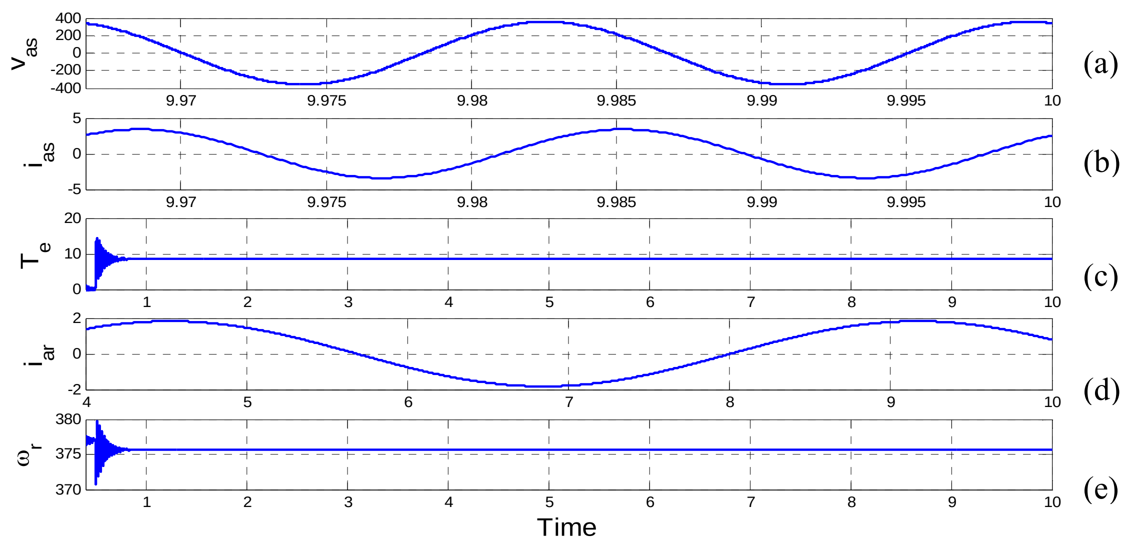

Figure 4.32 Load transients (a) stator phase 'a' voltage, (b) stator phase 'a' current, (c) torque, (d) rotor phase 'a' current, (e) rotor speed

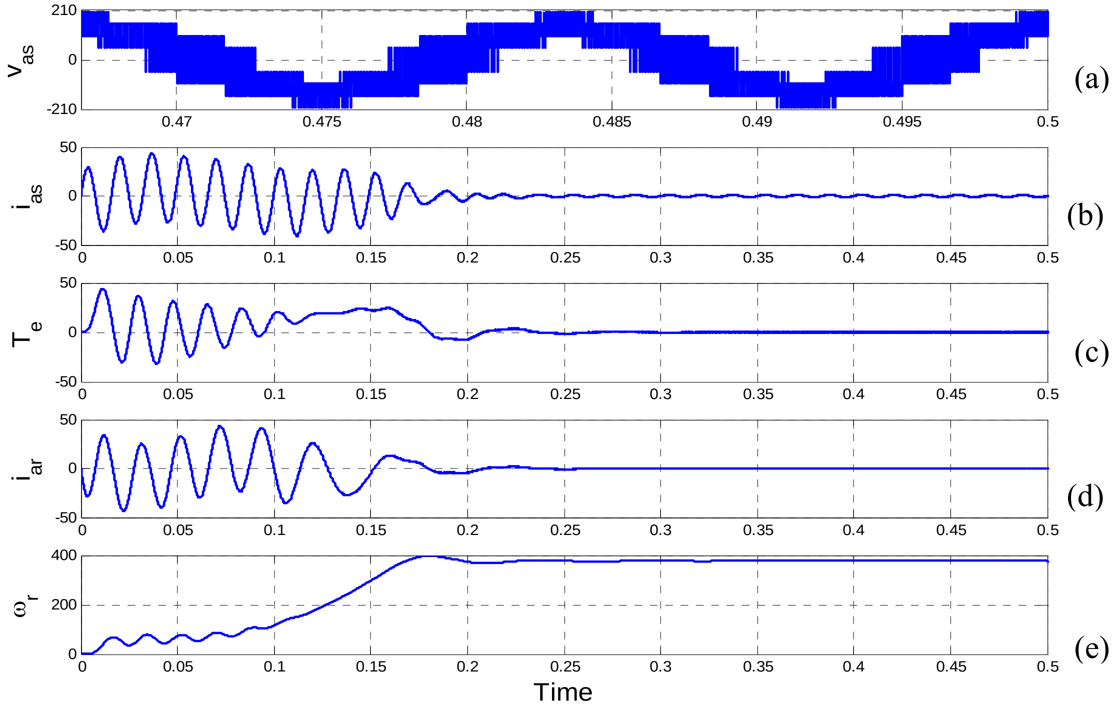

Figure 4.33 Starting transients (a) stator phase ‘a’ voltage, (b) stator phase ‘a’ current, (c) torque, (d) rotor phase ‘a’ current, (e) rotor speed

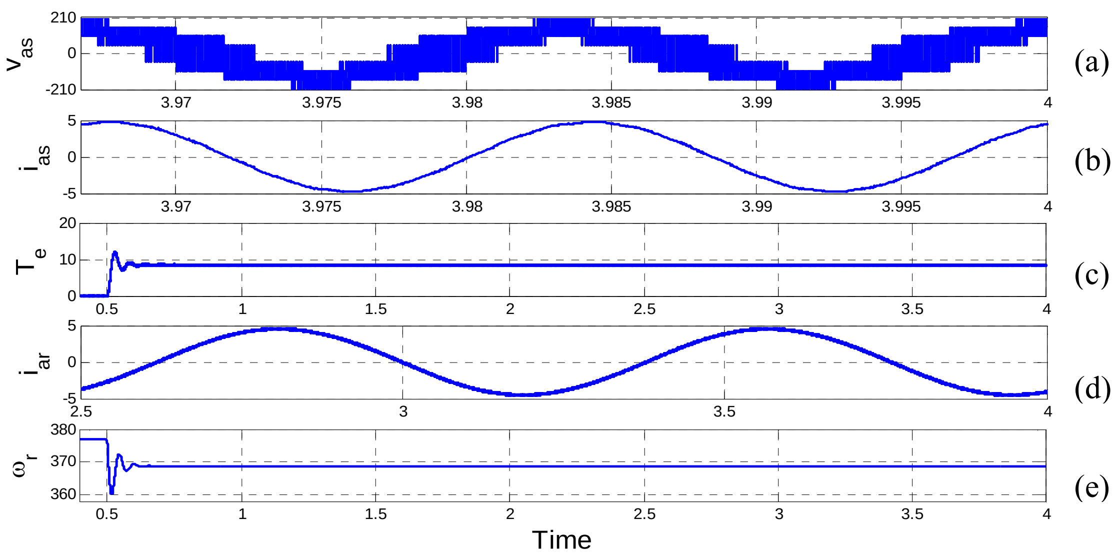

Figure 4.34 Load transients (a) stator phase ‘a’ voltage, (b) stator phase ‘a’ current, (c) torque, (d) rotor phase ‘a’ current, (e) rotor speed

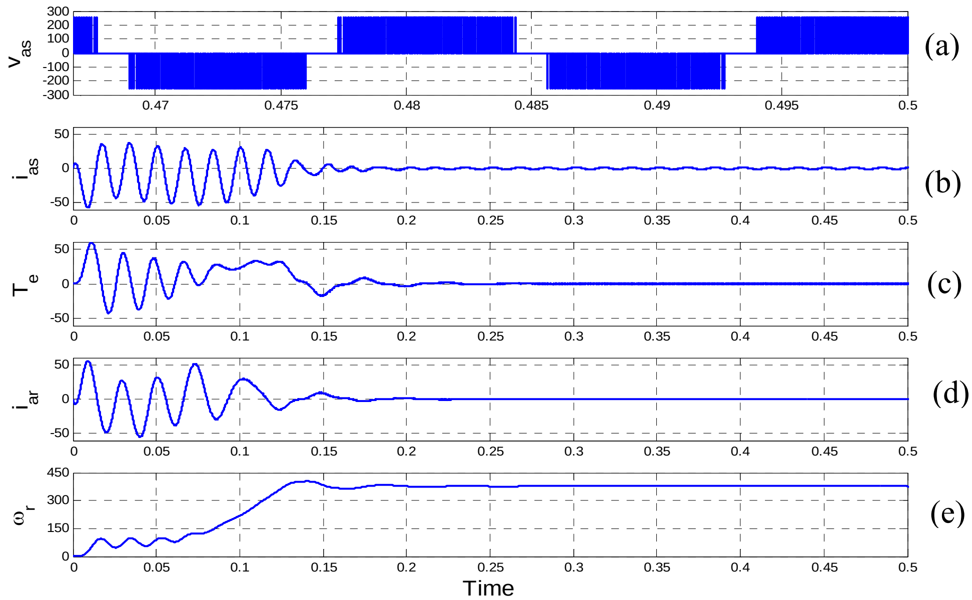

Figure 4.35 Starting transients (a) stator phase ‘a’ voltage, (b) stator phase ‘a’ current, (c) torque, (d) rotor phase ‘a’ current, (e) rotor speed

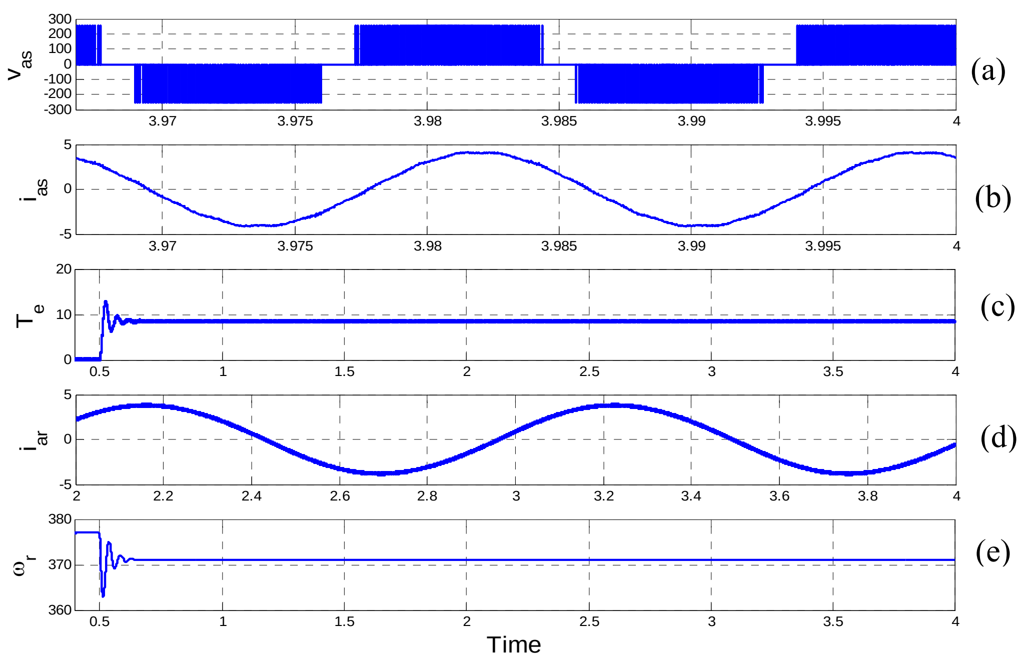

Figure 4.36 Load transients (a) stator phase ‘a’ voltage, (b) stator phase ‘a’ current, (c) torque, (d) rotor phase ‘a’ current, (e) rotor speed

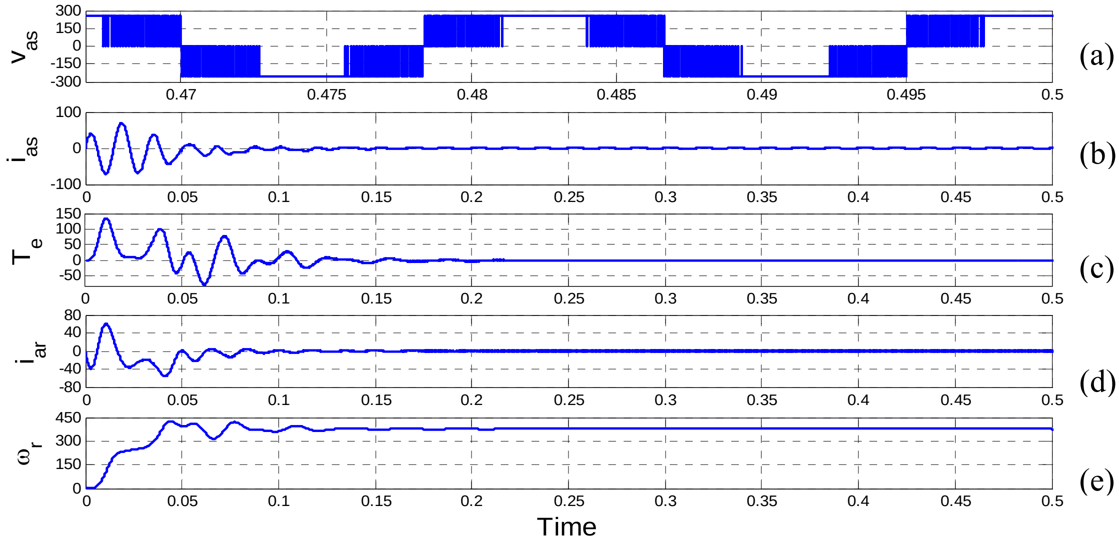

Figure 4.37 Starting transients (a) stator phase ‘a’ voltage, (b) stator phase ‘a’ current, (c) torque, (d) rotor phase ‘a’ current, (e) rotor speed

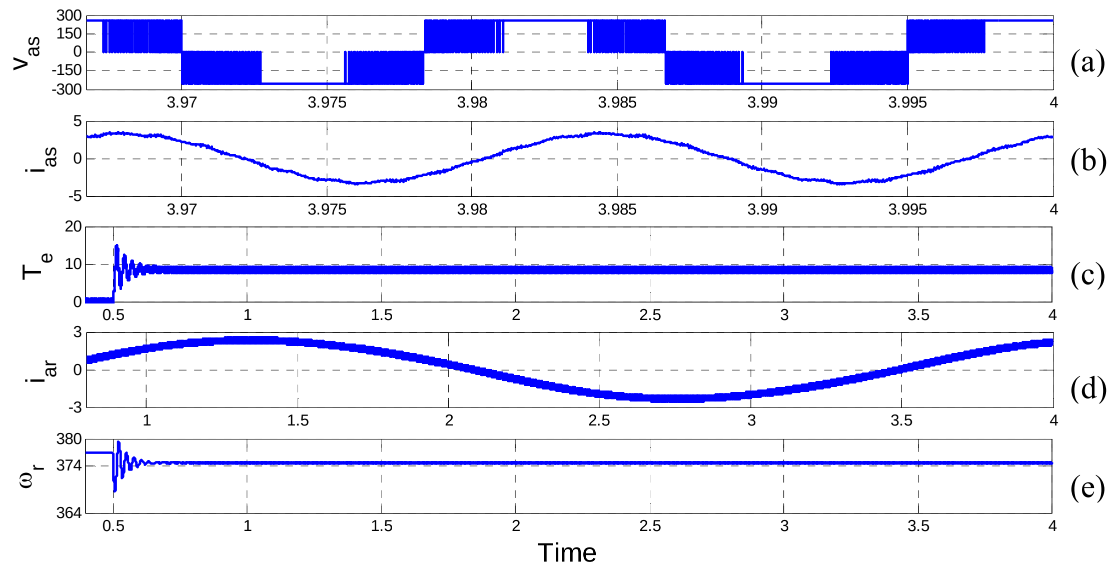

Figure 4.38 Load transients (a) stator phase ‘a’ voltage, (b) stator phase ‘a’ current, (c) torque, (d) rotor phase ‘a’ current, (e) rotor speed

4.2.5 With the Injection of the Third Harmonic Supply Voltage Component

The third harmonic voltage with the 10% magnitude of the fundamental was added to the fundamental voltage. The simulation analyzes the effect of this amount if at all there is any significant in the overall torque caused by third harmonic component. Figures (4.39) through (4.50) show different results depending on the machine winding connections. Figures (4.39) through (4.44) show normal operation without an inverter, whereas Figures (4.45) through (4.50) show the results when a five-phase machine is supplied via an inverter. Figures (4.39), (4.40), (4.45) and (4.46) the machine winding is star connected; Figures (4.41), (4.42), (4.47) and (4.48), the stator winding is delta connected (conventionally) and figures (4.43), (4.44), (4.49) and (4.50) are delta connected (alternately). The peak value of the fundamental voltage used in this simulation is 187.79 V and that of the third harmonic component is 18.779 V. The dc voltage is 360 V.

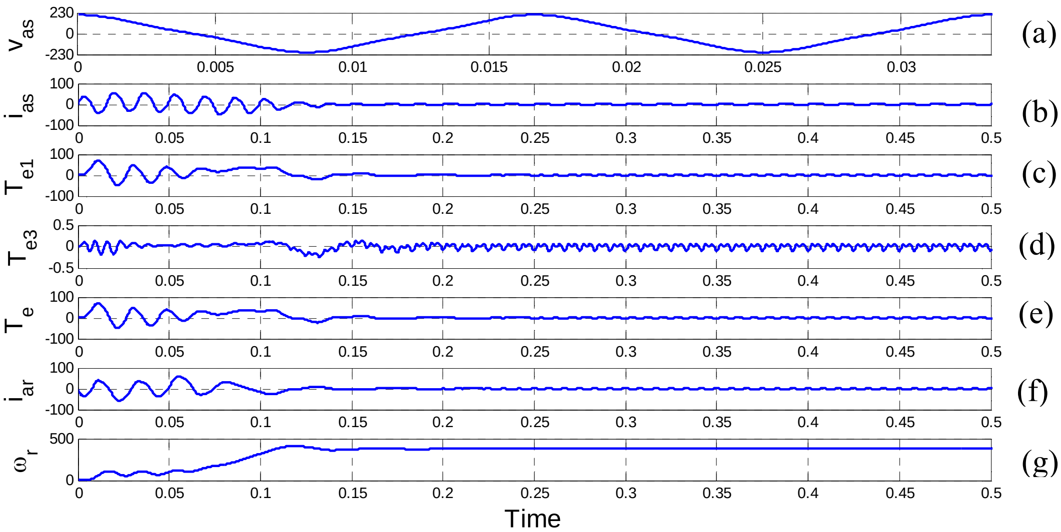

Figure 4.39 Starting transients (a) stator phase ‘a’ voltage, (b) stator phase ‘a’ current, (c) fundamental torque component, (d) third harmonic torque component, (e) total torque, (f) rotor phase ‘a’ current, (g) rotor speed

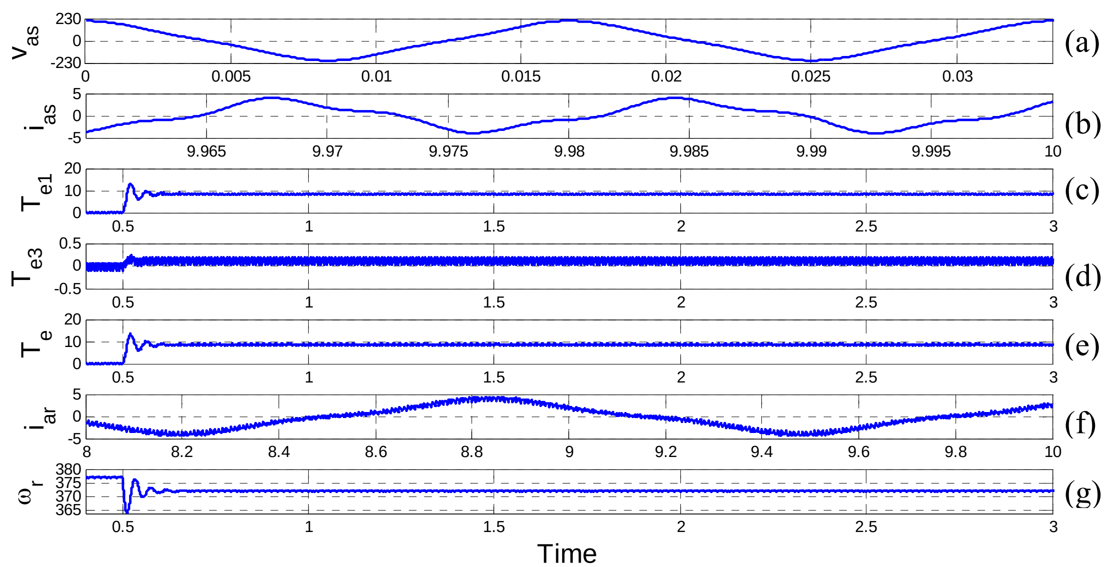

Figure 4.40 Load transients (a) stator phase ‘a’ voltage, (b) stator phase ‘a’ current, (c) fundamental torque component, (d) third harmonic torque component, (e) total torque, (f) rotor phase ‘a’ current, (g) rotor speed

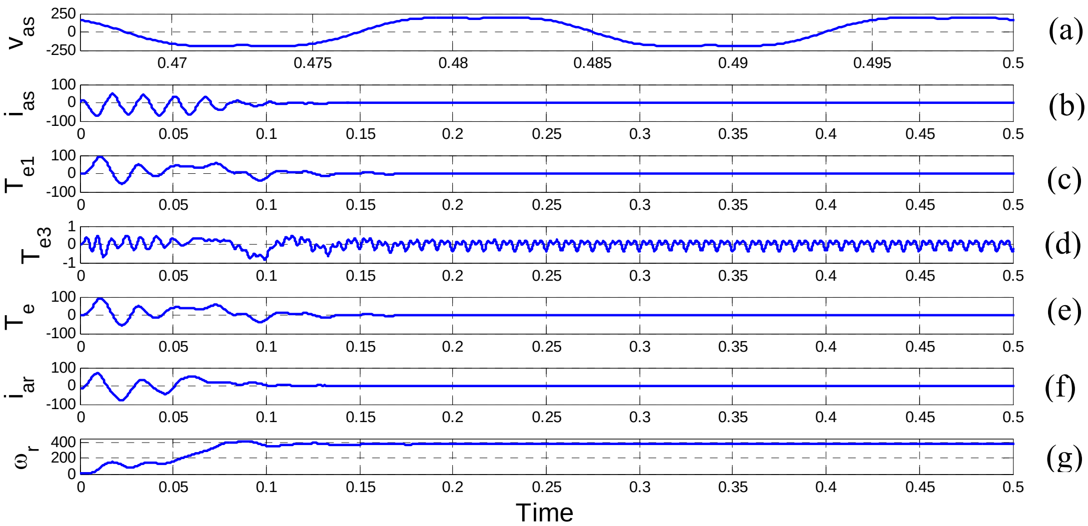

Figure 4.41 Starting transients (a) stator phase ‘a’ voltage, (b) stator phase ‘a’ current, (c) fundamental torque component, (d) third harmonic torque component, (e) total torque, (f) rotor phase ‘a’ current, (g) rotor speed

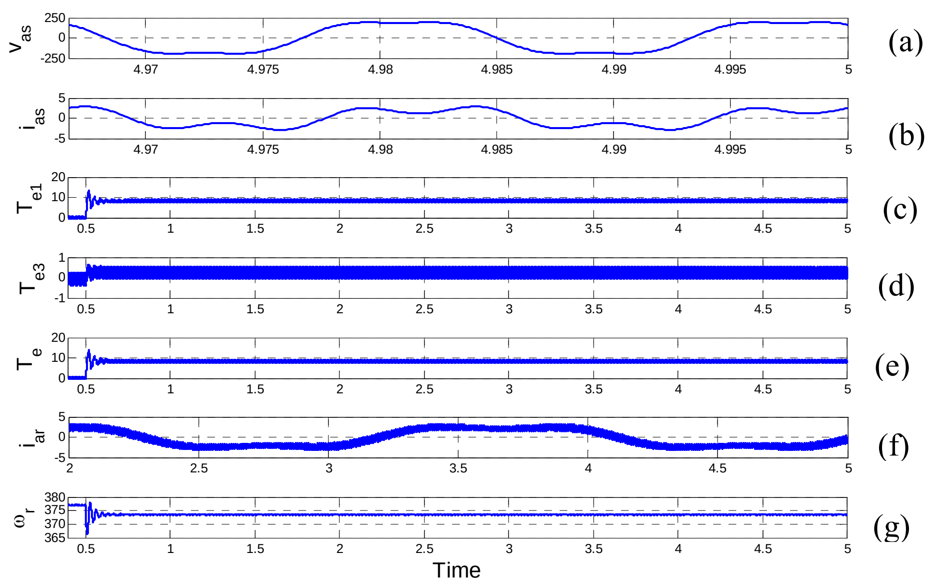

Figure 4.42 Load transients (a) stator phase ‘a’ voltage, (b) stator phase ‘a’ current, (c) fundamental torque component, (d) third harmonic torque component, (e) total torque, (f) rotor phase ‘a’ current, (g) rotor speed

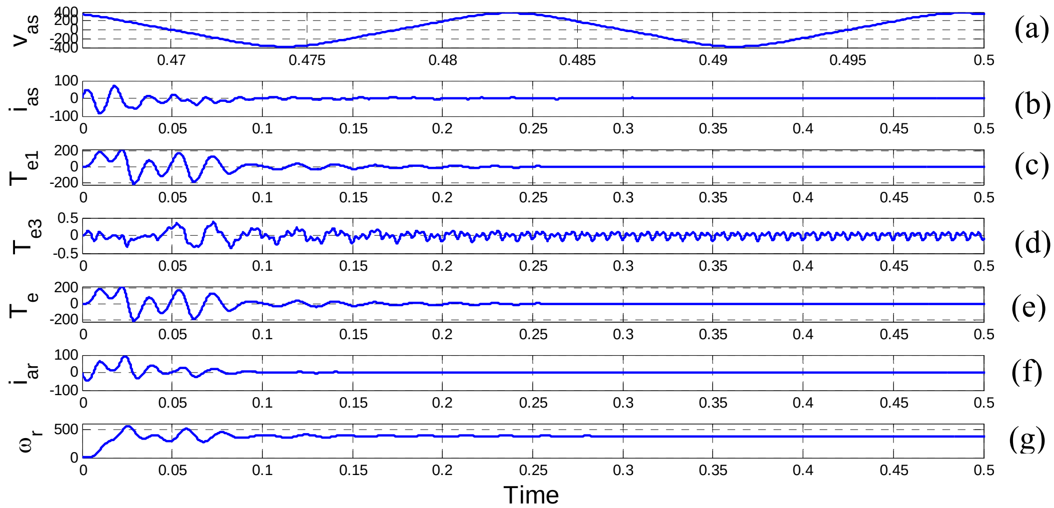

Figure 4.43 Starting transients (a) stator phase ‘a’ voltage, (b) stator phase ‘a’ current, (c) fundamental torque component, (d) third harmonic torque component, (e) total torque, (f) rotor phase ‘a’ current, (g) rotor speed

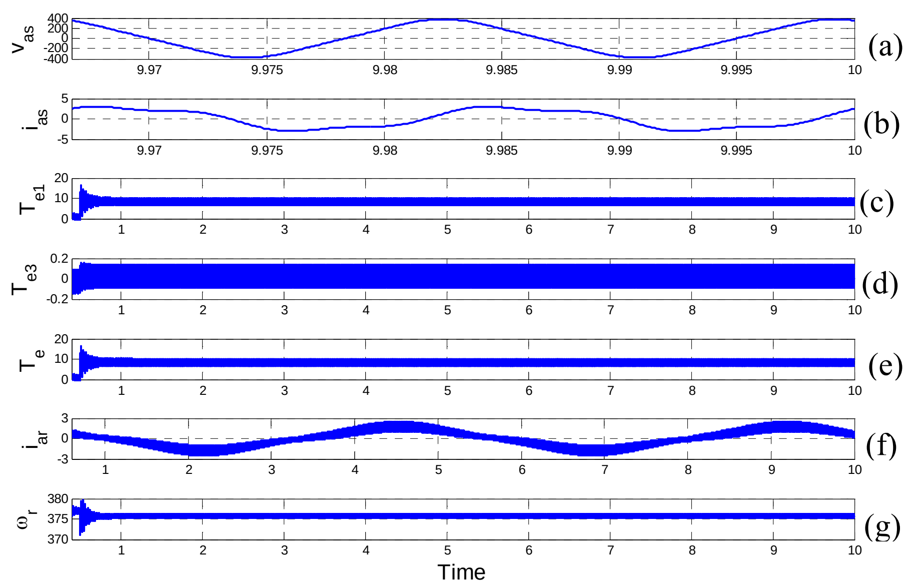

Figure 4.44 Load transients (a) stator phase ‘a’ voltage, (b) stator phase ‘a’ current, (c) fundamental torque component, (d) third harmonic torque component, (e) total torque, (f) rotor phase ‘a’ current, (g) rotor speed

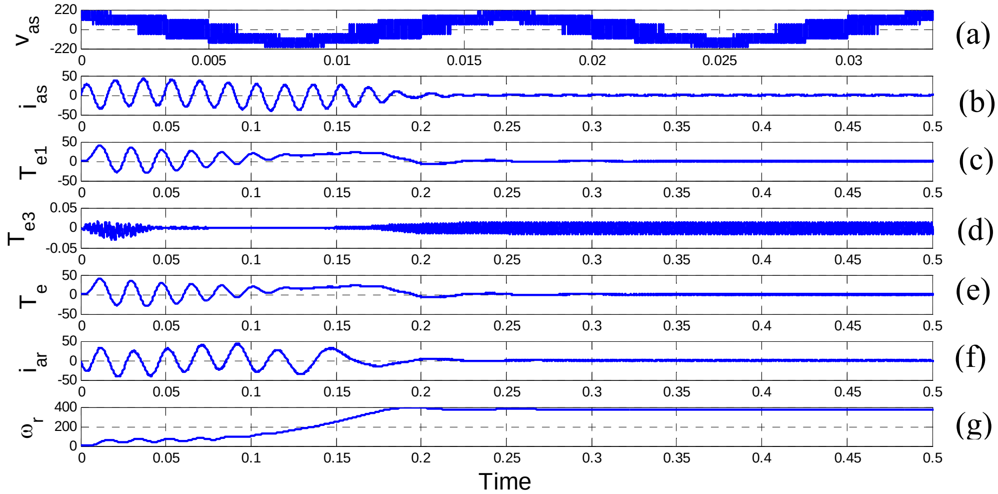

Figure 4.45 Starting transients (a) stator phase ‘a’ voltage, (b) stator phase ‘a’ current, (c) fundamental torque component, (d) third harmonic torque component, (e) total torque, (f) rotor phase ‘a’ current, (g) rotor speed

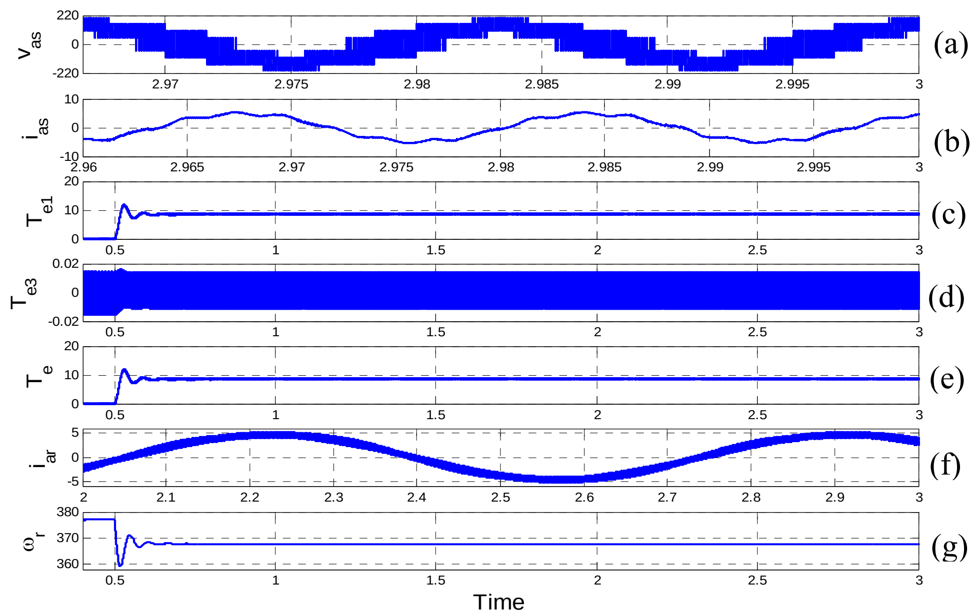

Figure 4.46 Load transients (a) stator phase ‘a’ voltage, (b) stator phase ‘a’ current, (c) fundamental torque component, (d) third harmonic torque component, (e) total torque, (f) rotor phase ‘a’ current, (g) rotor speed.

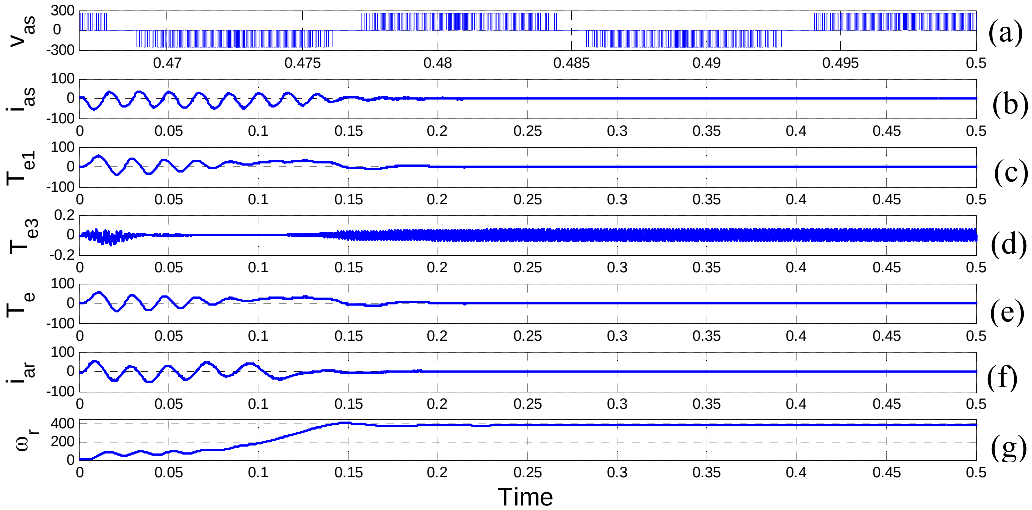

Figure 4.47 Starting transients (a) stator phase ‘a’ voltage, (b) stator phase ‘a’ current, (c) fundamental torque component, (d) third harmonic torque component, (e) total torque, (f) rotor phase ‘a’ current, (g) rotor speed.

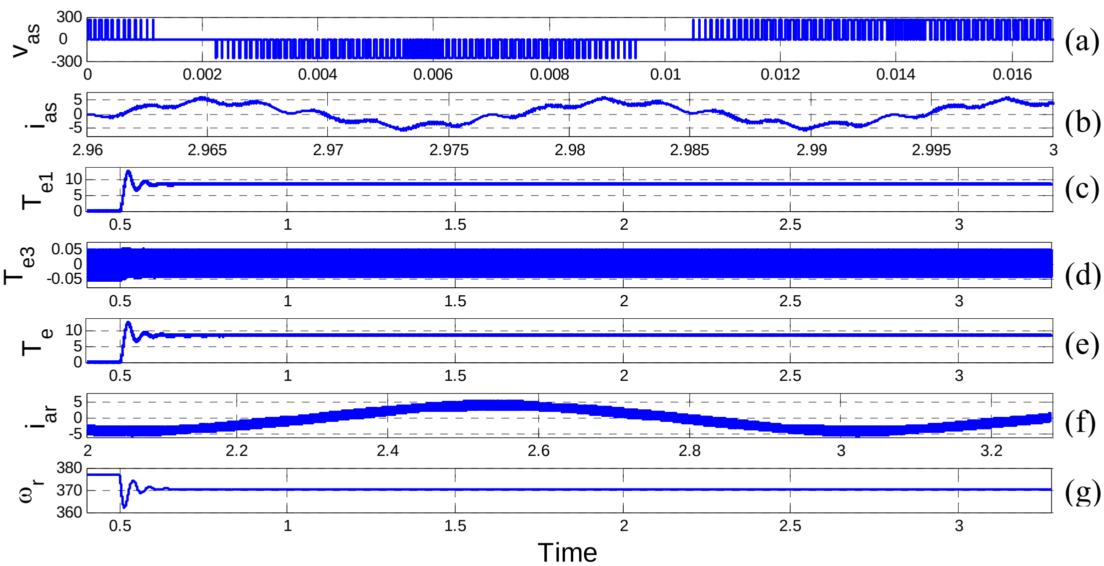

Figure 4.48 Load transients (a) stator phase ‘a’ voltage, (b) stator phase ‘a’ current, (c) fundamental torque component, (d) third harmonic torque component, (e) total torque, (f) rotor phase ‘a’ current, (g) rotor speed

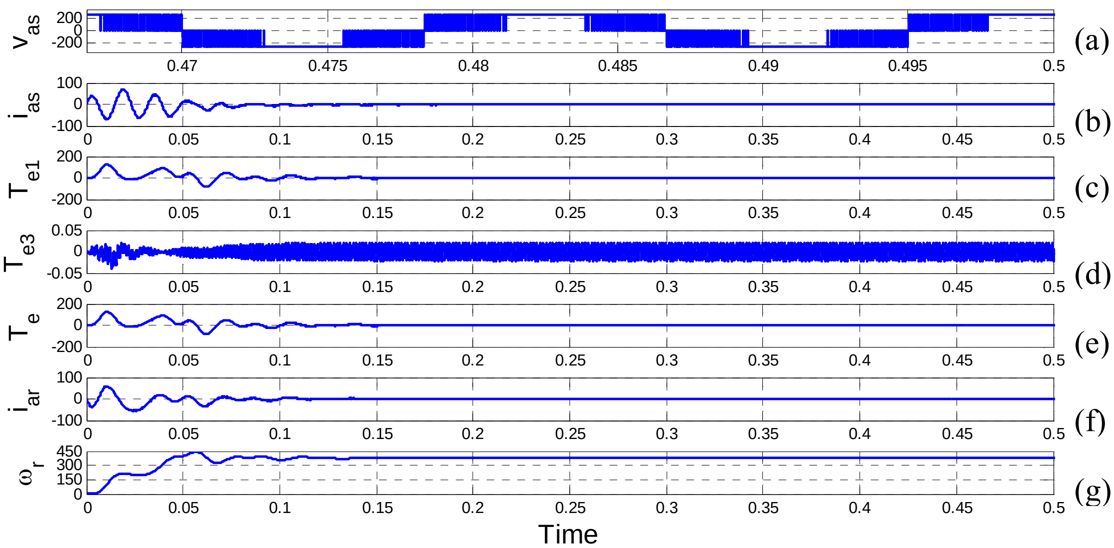

Figure 4.49 Starting transients (a) stator phase ‘a’ voltage, (b) stator phase ‘a’ current, (c) fundamental torque component, (d) third harmonic torque component, (e) total torque, (f) rotor phase ‘a’ current, (g) rotor speed

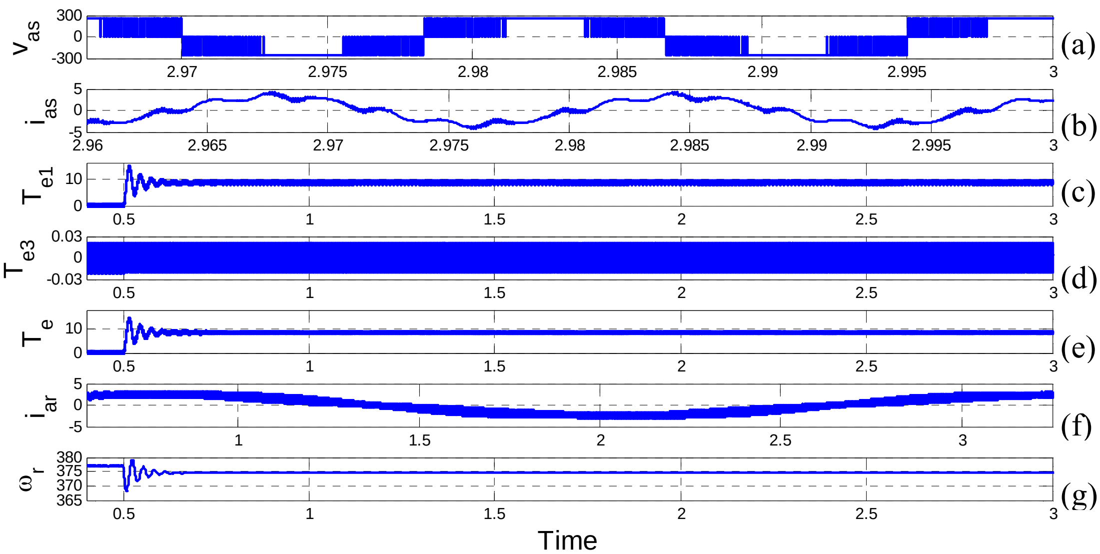

Figure 4.50 Load transients (a) stator phase ‘a’ voltage, (b) stator phase ‘a’ current, (c) fundamental torque component, (d) third harmonic torque component, (e) total torque, (f) rotor phase ‘a’ current, (g) rotor speed

4.3 Conclusion

The five-phase carrier based PWM inverter scheme has been analyzed. It is used in supplying the five-phase induction machine. The simulation of a five phase induction machine has been presented. Both fundamental and third harmonic components have been considered. The harmonic voltage of 10% of the magnitude of the fundamental voltage has been injected. The effect of this injected voltage is shown in the presented results. The third harmonic torque component has a finite value, although not contributing much to the required total torque.

Also three different stator winding connections have been considered, i.e. star connection, conventional delta connection and alternate delta connection. For the delta connections, two values of the peak phase voltage have been realized. The magnitude of the phase voltage for the conventional delta connection is 1.1756 times that of the star connection, whereas for the alternate delta connection, it is 1.9021 times that of the star connection. This means that more voltage can be obtained in the machine windings without a need of increasing the supply voltage.

CHAPTER 5

FIVE PHASE INDUCTION MACHINE UNDER OPEN PHASE FAULTS

5.1 Introduction

The induction machine has been widely used over the last three decades in practically all applications requiring variable speed. This is due to its robustness, versatility and reliability.

In general, the induction machines having three-phase windings are normally used, since the standard power supply is three phase. However, when fed by an inverter, there is no need for a fixed number of phases, some other phases being possible and advantageous.

Much published works have shown that motor drives with more than three phases have various advantages over conventional three phase drives, such as reduction in amplitude and increase in frequency of pulsating torque, reduction in harmonic currents, increase in current per phase without the need to increase the phase voltage, and reduction in the voltage-level in the dc (direct current) link [3.2, 5.1].

Another important aspect of machines with a higher number of phases is their improved reliability, since they can operate even when one phase is missing [5.1]. An increase in number of phases can result in an increase in torque/Ampere relation for the same volume of the machine, such that five-phase machines can develop torque using not only the fundamental, but also using higher harmonics of the air gap field [5.1, 5.2]. A comprehensive review of the advantages of multi-phase electric machines has been presented in [5.3].

A good number of research work has been presented on faults in electric machines [5.4]. Various categories of faults have been discussed for multi-phase machines inter-turn short circuits [5.4, 5.5] based on winding function approach. In [3.2] a dq model based on transformation theory for five-phase induction machines has been presented and the analysis of the machine under asymmetrical connections is discussed.

A control strategy of multiphase machines under asymmetric fault conditions due to open phase is presented in [5.6]. The authors used a five-phase synchronous motor with one open phase as a practical example.

So far there is no work that has developed a circuit based model which can be used to predict not only the steady-state and stability of the open-phase five phase induction machine but also the dynamics of the pulsating torque. Although it is known that faulted multi-phase machines can produce significant average torques, not much work has been done to quantify this.

In this Chapter, to determine the steady-state and dynamic stability performance, first a five-phase induction machine with one phase (phase '*a*') open is modeled in stationary reference frame. Then the same analysis is carried out for two phase open, '*a*' and '*b*' (for adjacent phases) and '*a*' and '*c*' (for non-adjacent phases). For the first time, using harmonic balance technique it has been possible to develop a circuit based model that has been used to perform the steady-state and dynamic analysis of a faulted machine. The steady-state speed harmonics and torque pulsations have been calculated and the results compare fairly well with the simulation results based on the full-order dynamic model of the faulted machine.

Furthermore, the small-signal stability study has been made through the small signal analysis whereby the dynamic model obtained from the harmonic balance technique has been used. At low speeds, the machine exhibits instability due to the rotor flux linkages. This instability is eliminated when the machine speeds up close to synchronous speed. This indicates that the machine can still be able to start under one stator phase fault and provide significant torque to meet most load requirements.

Section 5.2 presents the machine modeling in stationary reference frame. The model of a faulted machine with stator phase 'a' open-circuited is discussed in section 5.3. In section 5.4, a thorough presentation of the harmonic balance technique is described. The steady state and dynamics models are discussed in section 5.5 and finally the conclusions are presented in section 5.6. The approach presented in this work can be extended with ease to any number of open phases for a multi-phase machine.

5.2 Five-Phase Induction Machine Modeling in Stationary Reference Frame

The stator and rotor dynamic Equations in the natural reference frame, followed by transformation of the machine variables to the qd variables in the arbitrary reference frame, are given in Chapter 2 in which the balanced case for the stator voltages was considered. In this case only two components (q and d) of the voltage and current exist, the rest are zero. For the open phase faults analysis, whereby the phase voltages across the stator machine windings are no longer balanced, then the other voltage components do exist after transformation [3.2]. for the sake of clarity, the dynamic Equations for the five phase induction machine will be rewritten as follows

For the stator winding, the stator voltage Equations are expressed as

$$v_{as} = r_s i_{as} + p\lambda_{as} \tag{5.1}$$

$$v_{bs} = r_s i_{bs} + p\lambda_{bs} \tag{5.2}$$

$$v_{cs} = r_s i_{cs} + p\lambda_{cs} \tag{5.3}$$

$$v_{ds}^a = r_s i_{ds}^a + p\lambda_{ds}^a \tag{5.4}$$

$$v_{es} = r_s i_{es} + p\lambda_{es} \tag{5.5}$$

where $v_{as}, v_{bs}, v_{cs}, v_{ds}^a$ and v_{es} are the phase stator voltages, respectively; $i_{as}, i_{bs}, i_{cs}, i_{ds}^a$ and i_{es} are the phase stator currents, respectively; $\lambda_{as}, \lambda_{bs}, \lambda_{cs}, \lambda_{ds}^a$ and λ_{es} are the phase stator flux linkages, respectively; r_s is the stator phase resistance. The superscript '*a*' on phase '*d*' variables will be used throughout this Chapter in order to differentiate it from the d-axis variables.

For the stator winding, the stator voltage Equations are expressed as

$$v_{ar} = r_r i_{ar} + p\lambda_{ar} \tag{5.6}$$

$$v_{br} = r_r i_{br} + p\lambda_{br} \tag{5.7}$$

$$v_{cr} = r_r i_{cr} + p\lambda_{cr} \tag{5.8}$$

$$v_{dr}^a = r_r i_{dr}^a + p\lambda_{dr}^a \tag{5.9}$$

$$v_{er} = r_r i_{er} + p\lambda_{er} \tag{5.10}$$

where $v_{ar}, v_{br}, v_{cr}, v_{dr}^{a}$ and v_{er} are the phase rotor voltages, respectively; $i_{ar}, i_{br}, i_{cr}, i_{dr}^{a}$ and i_{er} are the phase rotor currents, respectively; $\lambda_{ar}, \lambda_{br}, \lambda_{cr}, \lambda_{dr}^{a}$ and λ_{er} are the phase rotor flux linkages, respectively; r_r is the rotor phase resistance

The arbitrary reference frame transformation matrix is given by

$$T(x)=\frac{2}{5}\begin{bmatrix} \cos(x) & \cos(x-\alpha) & \cos(x-2\alpha) & \cos(x+2\alpha) & \cos(x+\alpha) \\ \sin(x) & \sin(x-\alpha) & \sin(x-2\alpha) & \sin(x+2\alpha) & \sin(x+\alpha) \\ \cos(x) & \cos(x-2\alpha) & \cos(x+\alpha) & \cos(x-\alpha) & \cos(x+2\alpha) \\ \sin(x) & \sin(x-2\alpha) & \sin(x+\alpha) & \sin(x-\alpha) & \sin(x+2\alpha) \\ \frac{1}{2} & \frac{1}{2} & \frac{1}{2} & \frac{1}{2} & \frac{1}{2} \end{bmatrix} \tag{5.11}$$

where $\alpha=\frac{2\pi}{5}$, $x=\theta-\theta_x$, θ is the arbitrary reference frame transformation angle. $\theta_x=0^0$ is for the stator stationary reference variable transformation and $\theta_x=\theta_r$ is for the corresponding rotor variable transformation, where θ_r is the electrical rotor angle. Therefore, the machine variables can be transformed to $qdxyoz$ variables as

$$f_{qdxyoz}=T(x)f_{abcdez} \tag{5.12}$$

where

$f_{qdxyoz}=\begin{bmatrix} f_{qz} & f_{dz} & f_{xz} & f_{yz} & f_{oz} \end{bmatrix}^T$ is the variables (voltages, fluxes and currents) matrix in $qdxyo$ reference frame and $f_{abcdez}=\begin{bmatrix} f_{az} & f_{bz} & f_{cz} & f_{dz}^{a} & f_{ez} \end{bmatrix}^T$ is the variable (voltages, fluxes and currents) matrix in natural reference frame; z can replaced with s and r for stator and rotor variables, respectively

For the open stator phase fault, the five-phase induction machine is modeled in stationary reference frame. In this case the reference frame transformation angle is zero, i.e. $\theta = 0^0$. For the general balanced case, the machine model Equations can then be given as follows [5.1].

The stator voltage Equations are

$$v_{qs} = r_s i_{qs} + p\lambda_{qs} \tag{5.13}$$

$$v_{ds} = r_s i_{ds} + p\lambda_{ds} \tag{5.14}$$

$$v_{xs} = r_s i_{xs} + p\lambda_{xs} \tag{5.15}$$

$$v_{ys} = r_s i_{ys} + p\lambda_{ys} \tag{5.16}$$

$$v_{os} = r_s i_{os} + p\lambda_{os} \tag{5.17}$$

where $v_{qs}, v_{ds}, v_{xs}, v_{ys}$ and v_{os} are the q-, d-, x-, y- and o-axis stator voltages, respectively; $i_{qs}, i_{ds}, i_{xs}, i_{ys}$ and i_{os} are the q-, d-, x-, y- and o-axis stator currents, respectively; $\lambda_{qs}, \lambda_{ds}, \lambda_{xs}, \lambda_{ys}$ and λ_{os} are the q-, d-, x-, y- and o-axis stator flux linkages, respectively; r_s is the stator phase resistance

The rotor voltage Equations are

$$v_{qr}^{'} = r_r^{'} i_{qr}^{'} + p\lambda_{qr}^{'} - \omega_r \lambda_{dr}^{'} \tag{5.18}$$

$$v_{dr}^{'} = r_r^{'} i_{dr}^{'} + p\lambda_{dr}^{'} + \omega_r \lambda_{qr}^{'} \tag{5.19}$$

$$v_{xr}^{'} = r_r^{'} i_{xr}^{'} + p\lambda_{xr}^{'} \tag{5.20}$$

$$v_{yr}^{'} = r_r^{'} i_{yr}^{'} + p\lambda_{yr}^{'} \tag{5.21}$$

$$v_{or}^{'} = r_r^{'} i_{or}^{'} + p\lambda_{or}^{'} \tag{5.22}$$

where $v_{qr}^{'}, v_{dr}^{'}, v_{xr}^{'}, v_{yr}^{'}$ and $v_{or}^{'}$ are the q-, d-, x-, y- and o-axis stator voltages, respectively; $i_{qr}^{'}, i_{dr}^{'}, i_{xr}^{'}, i_{yr}^{'}$ and $i_{or}^{'}$ are the q-, d-, x-, y- and o-axis rotor currents, respectively; $\lambda_{qr}^{'}, \lambda_{dr}^{'}, \lambda_{xr}^{'}, \lambda_{yr}^{'}$ and $\lambda_{or}^{'}$ are the *q*-, *d*-, *x*-, *y*- and *o*-axis rotor flux linkages, respectively; $r_r^{'}$ is the rotor phase resistance; p is the differential operator

The stator flux linkages are given by

$$\lambda_{qs} = L_s i_{qs} + L_m i_{qr}^{'} \tag{5.23}$$

$$\lambda_{ds} = L_s i_{ds} + L_m i_{dr}^{'} \tag{5.24}$$

$$\lambda_{xs} = L_{ls} i_{xs} \tag{5.25}$$

$$\lambda_{ys} = L_{ls} i_{ys} \tag{5.26}$$

$$\lambda_{os} = L_{ls} i_{os} \tag{5.27}$$

where L_s and L_{ls} are the stator self and leakage inductances, respectively; L_m is the magnetizing inductance.

The rotor flux linkages are given by

$$\lambda_{qr}^{'} = L_m i_{qs} + L_r^{'} i_{qr}^{'} \tag{5.28}$$

$$\lambda_{dr}^{'} = L_m i_{ds} + L_r i_{dr}^{'} \tag{5.29}$$

$$\lambda_{xr}^{'} = L_{lr} i_{xr}^{'} \tag{5.30}$$

$$\lambda_{yr}^{'} = L_{lr} i_{yr}^{'} \tag{5.31}$$

$$\lambda_{or}^{'} = L_{lr} i_{or}^{'} \tag{5.32}$$

where $L_r^{'}$ and $L_{lr}^{'}$ are the rotor self and leakage inductances, respectively.

The electromagnetic torque T_e is given by

$$T_e = \frac{mP}{4} \frac{L_m}{L_r^{'}} \left(\lambda_{dr}^{'} i_{qs} - \lambda_{qr}^{'} i_{ds} \right) \tag{5.33}$$

The rotor speed is given by

$$\frac{2J}{P} p\omega_r = T_e - T_L \tag{5.34}$$

where m is the number of phases, P is the number of poles, J is the moment of inertia, and T_L is the load torque.

5.3 Model of an Open Phase Faulted Five-Phase Induction Machine

Consider the configuration of Figure 5.1 with a switch connected in series with phase 'a' of the stator winding. Open phase fault occurs when the switch is open such that the supply voltage is disconnected from the machine's phase '*a*'.

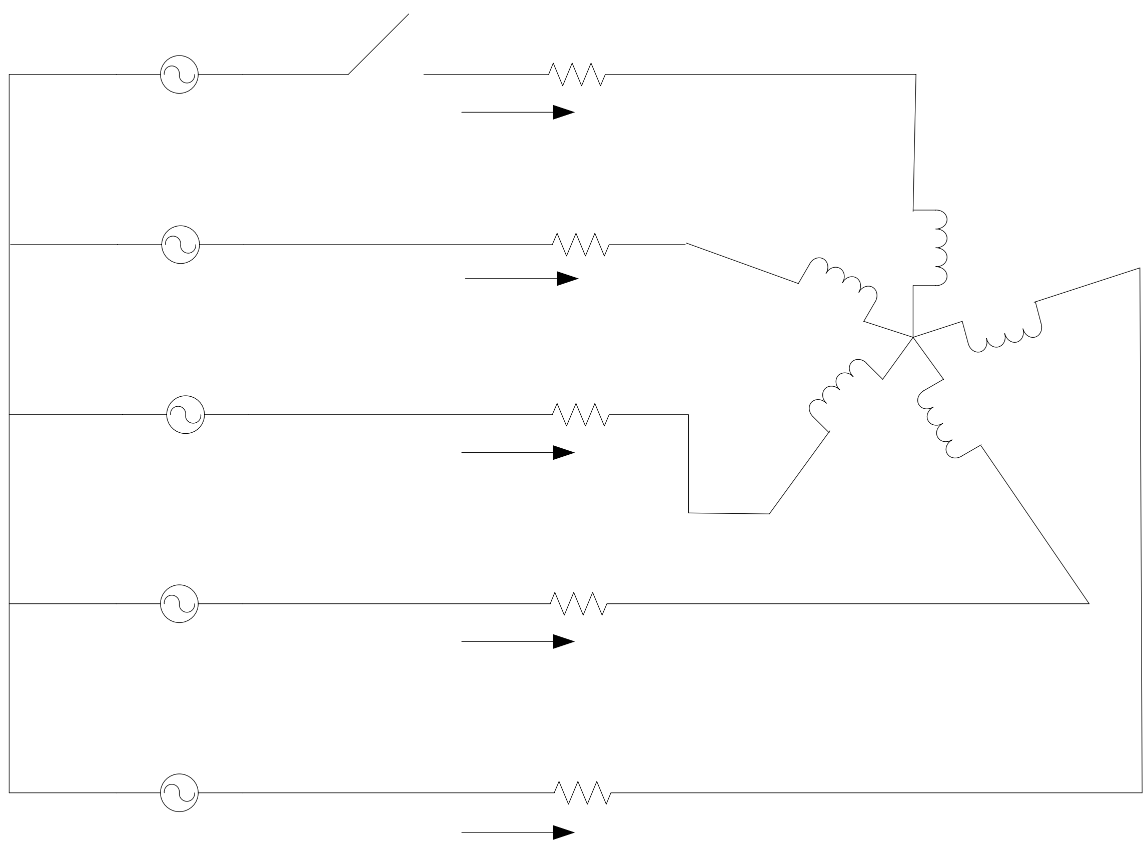

Figure 5.1 Open phase 'a' of the stator for the five phase induction machine.

From the transformation relationships of (5.12), where subscript z is replaced with s for stator variables, it can be deduced that

$$f_{qs} = \frac{2}{5}\left[f_{as} + f_{bs}\cos(\alpha) + f_{cs}\cos(2\alpha) + f_{ds}^{a}\cos(2\alpha) + f_{es}\cos(\alpha)\right] \tag{5.35}$$

$$f_{ds} = \frac{2}{5}\left[- f_{bs}\sin(\alpha) - f_{cs}\sin(2\alpha) + f_{ds}^{a}\sin(2\alpha) + f_{es}\sin(\alpha)\right] \tag{5.36}$$

$$f_{xs} = \frac{2}{5}\left[f_{as} + f_{bs}\cos(2\alpha) + f_{cs}\cos(\alpha) + f_{ds}^{a}\cos(\alpha) + f_{es}\cos(2\alpha)\right] \tag{5.37}$$

$$f_{ys} = \frac{2}{5}\left[- f_{bs}\sin(2\alpha) + f_{cs}\sin(\alpha) - f_{ds}^{a}\sin(\alpha) + f_{es}\sin(2\alpha)\right] \tag{5.38}$$

$$f_{os} = \frac{1}{5}\left[f_{as} + f_{bs} + f_{cs} + f_{ds}^{a} + f_{es}\right] \tag{5.39}$$

When the stator phase ‘a’ is open, the machine voltages become unbalanced. Since phase ‘*a*’ voltage becomes unknown, then the *q*- *x*- and *o*-axis voltages become unknown as they are coupled to v_{as} in Equations (5.35), (5.37) and (5.39), respectively.

The relationship between the q-axis and the x-axis stator variables can be given as

$$f_{qs} - f_{xs} = C \tag{5.40}$$

$$f_{qs} + f_{xs} = \frac{4}{5} f_{as} + \varepsilon_2\left[f_{bs} + f_{cs} + f_{ds}^{a} + f_{es}\right] \tag{5.41}$$

where

$$\begin{aligned} C &= \varepsilon_1\left(f_{bs} - f_{cs} - f_{ds}^{a} + f_{es}\right) \\ \varepsilon_1 &= \frac{2}{5}\left[\cos(\alpha) - \cos(2\alpha)\right] \\ \varepsilon_2 &= \frac{2}{5}\left[\cos(\alpha) + \cos(2\alpha)\right] \end{aligned} \tag{5.42}$$

When the variable f is replaced with the stator phase voltages and currents, Equation (5.40) is used to eliminate the unknown phase 'a' voltage. Also Equation (5.41) is used to get the relationship between the q-axis and x-axis stator currents. Thus, (5.40) and (5.41) turn into

$$v_{qs} - v_{xs} = C \tag{5.43}$$

$$i_{qs} + i_{xs} = \varepsilon_2 \left(i_{bs} + i_{cs} + i_{ds}^{a} + i_{es} \right) \tag{5.44}$$

Kirchhoff's current law (KCL) still holds true such that

$$i_{as} + i_{bs} + i_{cs} + i_{ds}^{a} + i_{es} = 0 \tag{5.45}$$

Now since $i_{as} = 0$, then from Equations (5.44) and (5.45)

$$i_{qs} + i_{xs} = 0 \tag{5.46}$$

When (5.46) is substituted into (5.15), the x-axis stator voltage Equation becomes

$$v_{xs} = -r_s i_{qs} - L_{ls} p i_{qs} \tag{5.47}$$

Substituting (5.47) into (5.43) gives

$$v_{qs} = C - r_s i_{qs} - L_{ls} p i_{qs} \tag{5.48}$$

Equations (5.13) and (5.48) can now be combined to give

$$C = 2 r_s i_{qs} + L_{ls} p i_{qs} + p \lambda_{qs} \tag{5.49}$$

Now, the stator flux linkages and the rotor currents can be eliminated as follows

$$\lambda_{qs} = L_s i_{qs} + \frac{L_m}{L_r^{'}} \left(\lambda_{qr}^{'} - L_m i_{qs} \right) \tag{5.50}$$

$$\lambda_{ds} = L_s i_{ds} + \frac{L_m}{L_r^{'}} \left(\lambda_{dr}^{'} - L_m i_{ds} \right) \tag{5.51}$$

$$i_{qr}^{'} = \frac{1}{L_r^{'}} \left(\lambda_{qr}^{'} - L_m i_{qs} \right) \tag{5.52}$$

$$i'_{dr} = \frac{1}{L'_r}\left(\lambda'_{dr} - L_m i_{ds}\right) \tag{5.53}$$

Substituting (5.50) and (5.51) into (5.49) and (5.14), respectively, and then rearranging, results into

$$pi_{qs} = \frac{1}{L_{ls}L'_r + L_s L'_r - L_m^2}\left(L'_r C - 2r_s L'_r i_{qs} - L_m p\lambda'_{qr}\right) \tag{5.54}$$

$$pi_{ds} = \frac{1}{L_s L'_r - L_m^2}\left(L'_r v_{ds} - r_s L'_r i_{ds} - L_m p\lambda'_{dr}\right) \tag{5.55}$$

Substituting (5.52) and (5.53) into (5.18) and (5.19), respectively leads to

$$p\lambda'_{qr} = v'_{qr} - \frac{r'_r}{L'_r}\left(\lambda'_{qr} - L_m i_{qs}\right) + \omega_r \lambda'_{dr} \tag{5.56}$$

$$p\lambda'_{dr} = v'_{dr} - \frac{r'_r}{L'_r}\left(\lambda'_{dr} - L_m i_{ds}\right) - \omega_r \lambda'_{qr} \tag{5.57}$$

Then from (5.35) phase ‘a’ voltage is given by

$$v_{as} = \frac{5}{2}v_{qs} - \left[v_{bs} + v_{es}\right]\cos(\alpha) - \left[v_{cs} + v^a_{ds}\right]\cos(2\alpha) \tag{5.58}$$

Equations (5.33), (5.34), (5.54), (5.55), (5.56), (5.57) and (5.58) are the defining dynamic Equations for the faulted machine and are used to determine the circuit based model of the open phase faulted five phase induction machine. They are used to simulate the machine for this faulted condition.

In this analysis, the real and reactive powers have been calculated to show the effect of oscillations in the speed and torque. The stator input real and reactive powers are given in terms of the natural reference frame variable as (5.59) and (5.60), respectively, the derivation of which has been presented in Chapter 2. Equation (5.59a) presents the general expression fro the real power, whereas Equation (5.59b) represents the expression for the real power when the system voltages and currents are balanced. Equation (5.60) represents the general expression for the reactive power in all cases.

$$p = \left\{ \begin{array}{l} \dfrac{2}{5}\left[\begin{array}{l} \dfrac{9}{4}\left(v_{as}i_{as} + v_{bs}i_{bs} + v_{cs}i_{cs} + v_{ds}i_{ds} + v_{es}i_{es}\right) \\ \left(\begin{array}{l} v_{as}\left(i_{bs} + i_{cs} + i_{ds} + i_{es}\right) + v_{bs}\left(i_{as} + i_{cs} + i_{ds} + i_{es}\right) + v_{cs}\left(i_{as} + i_{bs} + i_{ds} + i_{es}\right) + \\ v_{ds}\left(i_{as} + i_{bs} + i_{cs} + i_{es}\right) + v_{es}\left(i_{ds} + i_{as} + i_{bs} + i_{cs}\right) \end{array} \right)\cos\left(\dfrac{2\pi}{5}\right) + \\ \left(\begin{array}{l} v_{as}\left(i_{bs} + i_{cs} + i_{ds} + i_{es}\right) + v_{bs}\left(i_{as} + i_{cs} + i_{ds} + i_{es}\right) + v_{cs}\left(i_{as} + i_{bs} + i_{ds} + i_{es}\right) + \\ v_{ds}\left(i_{as} + i_{bs} + i_{cs} + i_{es}\right) + v_{es}\left(i_{as} + i_{bs} + i_{cs} + i_{ds}\right) \end{array} \right)\cos\left(\dfrac{4\pi}{5}\right) \end{array} \right] + \\ \dfrac{1}{5}\left[\begin{array}{l} v_{as}\left(i_{bs} + i_{cs} + i_{ds} + i_{es}\right) + v_{bs}\left(i_{as} + i_{cs} + i_{ds} + i_{es}\right) + \\ v_{cs}\left(i_{as} + i_{bs} + i_{ds} + i_{es}\right) + v_{ds}\left(i_{as} + i_{bs} + i_{cs} + i_{es}\right) + v_{es}\left(i_{as} + i_{bs} + i_{cs} + i_{ds}\right) \end{array} \right] \end{array} \right\} \tag{5.59a}$$

$$p = \left[v_{as}i_{as} + v_{bs}i_{bs} + v_{cs}i_{cs} + v_{ds}i_{ds} + v_{es}i_{es}\right] \tag{5.59b}$$

$$q = \frac{2}{5}\left[\begin{array}{l} \left(\begin{array}{l} v_{as}i_{es} - v_{es}i_{as} + v_{bs}i_{as} - v_{as}i_{bs} + v_{cs}i_{bs} - v_{bs}i_{cs} + \\ v_{ds}i_{cs} - v_{cs}i_{ds} + v_{es}i_{ds} - v_{ds}i_{es} \end{array} \right)\left[\sin\left(\dfrac{2\pi}{5}\right) + \sin\left(\dfrac{4\pi}{5}\right)\right] + \\ \left(\begin{array}{l} v_{as}i_{cs} - v_{cs}i_{as} + v_{bs}i_{ds} - v_{ds}i_{bs} + v_{cs}i_{es} - v_{es}i_{cs} + \\ v_{ds}i_{as} - v_{as}i_{ds} + v_{es}i_{bs} - v_{bs}i_{es} \end{array} \right)\left[\sin\left(\dfrac{2\pi}{5}\right) - \sin\left(\dfrac{4\pi}{5}\right)\right] \end{array} \right] \tag{5.60}$$

5.3.1 Harmonic Balance Technique for One Stator Open Phase Fault

By using the harmonic balance approach, the Equations for the calculation of the steady state and harmonic quantities are derived in this section. The state variables are assumed to have the form of the supply voltages. The supply voltages are represented by

$$\begin{aligned} v_{bs} &= \mathrm{Re}\left(v_{bss}e^{j\theta_e}\right) \\ v_{bss} &= V_m e^{-j\alpha} \end{aligned} \tag{5.61}$$

$$v_{cs} = \mathrm{Re}\left(v_{css} e^{j\theta_e}\right)$$
$$v_{css} = V_m e^{-j2\alpha} \tag{5.62}$$

$$v_{ds}^a = \mathrm{Re}\left(v_{dss}^a e^{j\theta_e}\right)$$
$$v_{dss}^a = V_m e^{j2\alpha} \tag{5.63}$$

$$v_{es} = \mathrm{Re}\left(v_{ess} e^{j\theta_e}\right)$$
$$v_{ess} = V_m e^{j\alpha} \tag{5.64}$$

where V_m is the peak of the phase voltage. In view of the form of the supply phase voltages, the state variables and the input voltages are therefore defined as [5.7]

$$v_{qs} = \mathrm{Re}\left(v_{qss} e^{j\theta_e}\right) \tag{5.65}$$

$$v_{ds} = \mathrm{Re}\left(v_{dss} e^{j\theta_e}\right) \tag{5.67}$$

$$v_{xs} = \mathrm{Re}\left(v_{xss} e^{j\theta_e}\right) \tag{5.68}$$

$$i_{qs} = \mathrm{Re}\left(i_{qss} e^{j\theta_e}\right) \tag{5.69}$$

$$i_{ds} = \mathrm{Re}\left(i_{dss} e^{j\theta_e}\right) \tag{5.70}$$

$$i_{xs} = \mathrm{Re}\left(i_{xss} e^{j\theta_e}\right) \tag{5.71}$$

$$\lambda_{qs} = \mathrm{Re}\left(\lambda_{qss} e^{j\theta_e}\right) \tag{5.72}$$

$$\lambda_{ds} = \mathrm{Re}\left(\lambda_{dss} e^{j\theta_e}\right) \tag{5.73}$$

$$\lambda_{qr}' = \mathrm{Re}\left(\lambda_{qrr}' e^{j\theta_e}\right) \tag{5.74}$$

$$\lambda_{dr}' = \mathrm{Re}\left(\lambda_{drr}' e^{j\theta_e}\right) \tag{5.75}$$

$$i_{qr}' = \mathrm{Re}\left(i_{qrr}' e^{j\theta_e}\right) \tag{5.76}$$

$$i_{dr}' = \mathrm{Re}\left(i_{drr}' e^{j\theta_e}\right) \tag{5.77}$$

where $\theta_e = \omega_e t$, $\omega_e = 2\pi f_e$, f_e is the frequency of the supply voltage, v_{qss}, v_{dss},and v_{xss} are the complex peaks of the q-, d- and x-axis stator voltages, respectively; i_{qss}, i_{dss},and i_{xss} are the respective q-, d- and x-axis complex peaks of the stator phase currents, λ_{qss}, λ_{dss}, and λ_{xss} are the complex peaks of the q-, d- and x-axis stator flux linkages, respectively;. λ'_{qrr}, λ'_{drr},and λ'_{xrr} are the complex peaks of the q-, d- and x-axis rotor flux linkages, respectively; i'_{qrr}, i'_{drr},and i'_{xrr} are the complex peaks of the q-, d- and x-axis rotor phase currents, respectively.

It has to be noted here that $\mathrm{Re}(x)$ refers to the real part of quantity x. In obtaining the model Equations based on the harmonic balance technique, the following relation has been used [5.8, 5.9]

$$\mathrm{Re}(x)\mathrm{Re}(y) = \frac{1}{2}\left[\mathrm{Re}\left(xy^*\right) + \mathrm{Re}(xy)\right] \tag{5.78}$$

Only up to the second order harmonics are considered.

Substituting the stator fluxes and currents into the torque Equation (5.33), results into

$$T_e = \frac{mP}{4}\frac{L_m}{L'_r}\left[\mathrm{Re}\left(\lambda'_{drr}e^{j\theta_e}\right)\mathrm{Re}\left(i_{qss}e^{j\theta_e}\right) - \mathrm{Re}\left(\lambda'_{qrr}e^{j\theta_e}\right)\mathrm{Re}\left(i_{dss}e^{j\theta_e}\right)\right] \tag{5.79}$$

Applying (5.78) on (5.79) and then separating real and imaginary terms gives

$$T_e = \frac{mP}{4}\frac{L_m}{L'_r}\frac{1}{2}\left[\mathrm{Re}\left(\lambda'_{drr}i^*_{qss}\right) + \mathrm{Re}\left(\lambda'_{drr}i_{qss}e^{j2\theta_e}\right) - \mathrm{Re}\left(\lambda'_{qrr}i^*_{dss}\right) - \mathrm{Re}\left(\lambda'_{qrr}i_{dss}e^{j2\theta_e}\right)\right] \tag{5.80}$$

The torque has two components, the average component and the pulsating component given by

$$T_e = T_{eavg} + T_{epuls} \tag{5.81}$$

where

$$T_{eavg} = \frac{mP}{8}\frac{L_m}{L_r^{'}}\left[\mathrm{Re}\left(\lambda_{drr}^{'} I_{qss}^{*}\right) - \mathrm{Re}\left(\lambda_{qrr}^{'} I_{dss}^{*}\right)\right] \tag{5.82}$$

$$T_{epuls} = \frac{mP}{8}\frac{L_m}{L_r^{'}}\left[\mathrm{Re}\left(\lambda_{drr}^{'} I_{qss}\right) - \mathrm{Re}\left(\lambda_{qrr}^{'} I_{dss}\right)\right] \tag{5.83}$$

T_{eavg} is the average torque component, and T_{epuls} is the pulsating torque component which is oscillating at twice the supply frequency.

Using the speed Equation (5.34) and the result of (5.80) it is obvious that the speed will have both the average value and the second order harmonic content. Therefore

$$\omega_r = \omega_{ro} + \mathrm{Re}\left(\omega_{r1} e^{j2\theta_e}\right) \tag{5.84}$$

where ω_{ro} is the average rotor speed and ω_{r1} is the complex peak of the speed harmonic component.

When Equations (5.61) through (5.77) and (5.84) definitions are substituted into Equations (5.54) through (5.58), the following harmonic balance technique model results

Similarly, from Equations (5.54)

$$p\,\mathrm{Re}\left(i_{qss} e^{j\theta_e}\right) = \tau_1\left(L_r^{'}\,\mathrm{Re}\left(\overline{C} e^{j\theta_e}\right) - 2r_s L_r^{'}\,\mathrm{Re}\left(i_{qss} e^{j\theta_e}\right) - L_m\, p\,\mathrm{Re}\left(\lambda_{qrr}^{'} e^{j\theta_e}\right)\right) \tag{5.85}$$

$$\mathrm{Re}\left(p i_{qss} e^{j\theta_e}\right) + \mathrm{Re}\left(j\omega_e i_{qss} e^{j\theta_e}\right) = \tau_1\begin{pmatrix} L_r^{'}\overline{C} e^{j\theta_e} - 2r_s L_r^{'}\,\mathrm{Re}\left(i_{qss} e^{j\theta_e}\right) \\ - L_m\,\mathrm{Re}\left(p\lambda_{qrr}^{'} e^{j\theta_e}\right) - \mathrm{Re}\left(j\omega_e L_m \lambda_{qrr}^{'} e^{j\theta_e}\right)\end{pmatrix} \tag{5.86}$$

$$p i_{qss} + j\omega_e i_{qss} = \tau_1\left(L_r^{'}\overline{C} - 2r_s L_r^{'} i_{qss} - L_m\, p\lambda_{qrr}^{'} - j\omega_e L_m \lambda_{qrr}^{'}\right) \tag{5.87}$$

where

$$\tau_1 = \frac{1}{L_{ls}L_r^{'} + L_s L_r^{'} - L_m^2}$$

$$\overline{C} = \varepsilon_1\left[v_{bss} - v_{css} - v_{dss} + v_{ess}\right]$$

Similarly, from Equations (5.55)

$$p\,\mathrm{Re}\left(i_{dss}e^{j\theta_e}\right)=\tau_2\left\{L_r^{'}\,\mathrm{Re}\left(v_{dss}e^{j\theta_e}\right)-r_s\,\mathrm{Re}\left(i_{dss}e^{j\theta_e}\right)L_r^{'}-L_m\,p\,\mathrm{Re}\left(\lambda_{drr}^{'}e^{j\theta_e}\right)\right\} \tag{5.88}$$

$$\mathrm{Re}\left(pi_{dss}e^{j\theta_e}\right)+\mathrm{Re}\left(j\omega_e i_{dss}e^{j\theta_e}\right)=\tau_2\begin{bmatrix}L_r^{'}\,\mathrm{Re}\left(v_{dss}e^{j\theta_e}\right)-r_s\,\mathrm{Re}\left(i_{dss}e^{j\theta_e}\right)L_r^{'}\\ -L_m\,\mathrm{Re}\left(p\lambda_{drr}^{'}e^{j\theta_e}\right)-L_m\,\mathrm{Re}\left(j\omega_e\lambda_{drr}^{'}e^{j\theta_e}\right)\end{bmatrix} \tag{5.89}$$

$$pi_{dss}+j\omega_e i_{dss}=\tau_2\left(L_r^{'}v_{dss}-r_sL_r^{'}i_{dss}-L_m p\lambda_{drr}^{'}-j\omega_e L_m\lambda_{drr}^{'}\right) \tag{5.90}$$

where

$$\tau_2=\frac{1}{L_sL_r^{'}-L_m^2}$$

from Equation (5.56),

$$p\,\mathrm{Re}\left(\lambda_{qrr}^{'}e^{j\theta_e}\right)=-\frac{r_r^{'}}{L_r^{'}}\begin{pmatrix}\mathrm{Re}\left(\lambda_{qrr}^{'}e^{j\theta_e}\right)\\ -L_m\,\mathrm{Re}\left(I_{qss}e^{j\theta_e}\right)\end{pmatrix}+\left[\omega_{ro}+\mathrm{Re}\left(\omega_{r1}e^{j2\theta_e}\right)\right]\left[\mathrm{Re}\left(\lambda_{drr}^{'}e^{j\theta_e}\right)\right] \tag{5.91}$$

$$\mathrm{Re}\left(p\lambda_{qrr}^{'}e^{j\theta_e}\right)+\mathrm{Re}\left(j\omega_e\lambda_{qrr}^{'}e^{j\theta_e}\right)=\left\{\begin{matrix}-\dfrac{r_r^{'}}{L_r^{'}}\left(\mathrm{Re}\left(\lambda_{qrr}^{'}e^{j\theta_e}\right)-L_m\,\mathrm{Re}\left(I_{qss}e^{j\theta_e}\right)\right)\\ +\begin{bmatrix}\omega_{ro}\,\mathrm{Re}\left(\lambda_{drr}^{'}e^{j\theta_e}\right)+\dfrac{1}{2}\mathrm{Re}\left(\omega_{r1}\lambda_{drr}^{'*}e^{j\theta_e}\right)\\ +\dfrac{1}{2}\mathrm{Re}\left(\omega_{r1}\lambda_{drr}^{'}e^{j3\theta_e}\right)\end{bmatrix}\end{matrix}\right\} \tag{5.92}$$

Considering the fundamental component $\left(e^{j\theta_e}\right)$ and ignoring the third harmonic component, we have

$$p\lambda_{qrr}^{'}+j\omega_e\lambda_{qrr}^{'}=v_{qrr}^{'}-\frac{r_r^{'}}{L_r^{'}}\left(\lambda_{qrr}^{'}-L_m i_{qss}\right)+\omega_{ro}\lambda_{drr}^{'}+\omega_{r1}\lambda_{drr}^{'*} \tag{5.93}$$

Similarly, from Equation (5.57),

$$p\,\mathrm{Re}\left(\lambda_{drr}^{'}e^{j\theta_e}\right)=-\frac{r_r^{'}}{L_r^{'}}\begin{pmatrix}\mathrm{Re}\left(\lambda_{drr}^{'}e^{j\theta_e}\right)\\ -L_m\,\mathrm{Re}\left(i_{dss}e^{j\theta_e}\right)\end{pmatrix}-\left[\omega_{ro}+\mathrm{Re}\left(\omega_{r1}e^{j2\theta_e}\right)\right]\left[\mathrm{Re}\left(\lambda_{qrr}^{'}e^{j\theta_e}\right)\right] \tag{5.94}$$

$$\mathrm{Re}\left(p\lambda_{drr}^{'}e^{j\theta_e}\right)+\mathrm{Re}\left(j\omega_e\lambda_{drr}^{'}e^{j\theta_e}\right)=\begin{Bmatrix}-\dfrac{r_r^{'}}{L_r^{'}}\left(\mathrm{Re}\left(\lambda_{drr}^{'}e^{j\theta_e}\right)-L_m\,\mathrm{Re}\left(I_{dss}e^{j\theta_e}\right)\right)\\ -\omega_{ro}\,\mathrm{Re}\left(\lambda_{qrr}^{'}e^{j\theta_e}\right)-\dfrac{1}{2}\mathrm{Re}\left(\omega_{r1}\lambda_{qrr}^{'*}e^{j\theta_e}\right)\\ -\dfrac{1}{2}\mathrm{Re}\left(\omega_{r1}\lambda_{qrr}^{'}e^{j2\theta_e}\right)\end{Bmatrix} \tag{5.95}$$

Considering the fundamental component $\left(e^{j\theta_e}\right)$ and ignoring the third harmonic component, we have

$$p\lambda_{drr}^{'}+j\omega_e\lambda_{drr}^{'}=v_{drr}^{'}-\frac{r_r^{'}}{L_r^{'}}\left(\lambda_{drr}^{'}-L_m i_{dss}\right)-\omega_{ro}\lambda_{qrr}^{'}-\omega_{r1}\lambda_{qrr}^{'*} \tag{5.96}$$

From Equation (5.58),

$$\mathrm{Re}\left(v_{ass}e^{j\theta_e}\right)=\begin{Bmatrix}\dfrac{5}{2}\mathrm{Re}\left(v_{qss}e^{j\theta_e}\right)-\left[\mathrm{Re}\left(v_{bss}e^{j\theta_e}\right)+\mathrm{Re}\left(v_{ess}e^{j\theta_e}\right)\right]\cos(\alpha)\\ -\left[\mathrm{Re}\left(v_{css}e^{j\theta_e}\right)+\mathrm{Re}\left(v_{dss}e^{j\theta_e}\right)\right]\cos(2\alpha)\end{Bmatrix} \tag{5.97}$$

$$v_{ass}=\frac{5}{2}v_{qss}-\left[v_{bss}+v_{ess}\right]\cos(\alpha)-\left[v_{css}+v_{dss}\right]\cos(2\alpha) \tag{5.98}$$

Performing the same analysis on Equations (5.15) and (5.16), gives

$$p\,\mathrm{Re}\left(i_{xss}e^{j\theta_e}\right)=\frac{1}{L_{ls}}\left[\mathrm{Re}\left(v_{xss}e^{j\theta_e}\right)-r_s\,\mathrm{Re}\left(i_{xss}e^{j\theta_e}\right)\right] \tag{5.99}$$

$$\mathrm{Re}\left(pi_{xss}e^{j\theta_e}\right)+\mathrm{Re}\left(j\omega_e i_{xss}e^{j\theta_e}\right)=\frac{1}{L_{ls}}\left[\mathrm{Re}\left(v_{xss}e^{j\theta_e}\right)-r_s\,\mathrm{Re}\left(i_{xss}e^{j\theta_e}\right)\right] \tag{5.100}$$

$$pi_{xss}+j\omega_e i_{xss}=\frac{1}{L_{ls}}\left[v_{xss}-r_s i_{xss}\right] \tag{5.101}$$

from Equation (5.16)

$$p\,\mathrm{Re}\left(i_{yss}e^{j\theta_e}\right)=\frac{1}{L_{ls}}\left[\mathrm{Re}\left(v_{yss}e^{j\theta_e}\right)-r_s\,\mathrm{Re}\left(i_{yss}e^{j\theta_e}\right)\right] \tag{5.102}$$

$$\mathrm{Re}\left(pi_{yss}e^{j\theta_e}\right)+\mathrm{Re}\left(j\omega_e i_{yss}e^{j\theta_e}\right)=\frac{1}{L_{ls}}\left[\mathrm{Re}\left(v_{yss}e^{j\theta_e}\right)-r_s\,\mathrm{Re}\left(i_{yss}e^{j\theta_e}\right)\right] \tag{5.103}$$

$$pi_{yss} + j\omega_e i_{yss} = \frac{1}{L_{ls}}\left[v_{yss} - r_s i_{yss}\right] \tag{5.104}$$

Substituting Equations (5.80) and (5.84) into Equation (5.34)

$$\frac{2J}{P} p\left[\omega_{ro} + \mathrm{Re}\left(\omega_{r1} e^{j2\theta_e}\right)\right] = \frac{mP}{4}\frac{L_m}{L_r^{'}}\frac{1}{2}\begin{bmatrix} \mathrm{Re}\left(\lambda_{drr}^{'} i_{qss}^{*}\right) + \mathrm{Re}\left(\lambda_{drr}^{'} i_{qss} e^{j2\theta_e}\right) \\ -\mathrm{Re}\left(\lambda_{qrr}^{'} i_{dss}^{*}\right) - \mathrm{Re}\left(\lambda_{qrr}^{'} i_{dss} e^{j2\theta_e}\right) \end{bmatrix} - T_L \tag{5.105}$$

$$\frac{2J}{P}\begin{bmatrix} p\omega_{ro} + \mathrm{Re}\left(p\omega_{r1} e^{j2\theta_e}\right) \\ + \mathrm{Re}\left(j2\omega_e \omega_{r1} e^{j2\theta_e}\right) \end{bmatrix} = \frac{mP}{4}\frac{L_m}{L_r^{'}}\frac{1}{2}\begin{bmatrix} \mathrm{Re}\left(\lambda_{drr}^{'} i_{qss}^{*}\right) + \mathrm{Re}\left(\lambda_{drr}^{'} i_{qss} e^{j2\theta_e}\right) \\ -\mathrm{Re}\left(\lambda_{qrr}^{'} i_{dss}^{*}\right) - \mathrm{Re}\left(\lambda_{qrr}^{'} i_{dss} e^{j2\theta_e}\right) \end{bmatrix} - T_L \tag{5.106}$$

Separating the first and second order harmonic components gives

$$\frac{2J}{P} p\omega_{ro} = T_{eo} - T_L \tag{5.107}$$

$$\frac{2J}{P}\left(p\omega_{r1} + j2\omega_e \omega_{r1}\right) = T_{epuls} \tag{5.108}$$

where T_{eavg} is the average electromagnetic torque and T_{epuls} is the magnitude of the pulsating torque given in Equations (5.82) and (5.83), respectively.

Equations (5.87), (5.90), (5.93), (5.96), (5.98), (5.107), and (5.108) form the dynamic model which is used for steady state performance and stability analysis of the open phase faulted five-phase induction machine.

5.3.2 Steady State and Dynamic Model Analysis

5.3.2.1 Steady state model. The model obtained by harmonic balance technique can be used in analyzing the steady state performance of the faulted machine. In this particular case, the peaks of the state variables are constant and therefore the derivatives of the state variables are zero. Thus at, steady-state, Equations become

$$v_{qss} = \frac{1}{L_{ls}L_r + \alpha_o}\left[L_{ls}r_s L_r^{'} i_{qss} + j\omega_e L_{ls}L_m \lambda_{qrr}^{'} + \alpha_o \overline{C} - \alpha_o r_s i_{qss}\right] \tag{5.109}$$

$$j\omega_e \lambda_{qrr}^{'} = -\frac{r_r^{'}}{L_r^{'}}\left(\lambda_{qrr}^{'} - L_m i_{qss}\right) + \omega_{ro}\lambda_{drr}^{'} + \frac{1}{2}\omega_{r1}\lambda_{drr}^{'*} \tag{5.110}$$

$$j\omega_e \lambda_{drr}^{'} = -\frac{r_r^{'}}{L_r^{'}}\left(\lambda_{drr}^{'} - L_m i_{dss}\right) - \omega_{ro}\lambda_{qrr}^{'} - \frac{1}{2}\omega_{r1}\lambda_{qrr}^{'*} \tag{5.111}$$

$$j\omega_e i_{qss} = \frac{1}{\alpha_o}\left[L_r^{'} V_{qss} - r_s i_{qss} L_r^{'} - j\omega_e L_m \lambda_{qrr}^{'}\right] \tag{5.112}$$

$$j\omega_e i_{dss} = \frac{1}{\alpha_o}\left[L_r^{'} V_{dss} - r_s i_{dss} L_r^{'} - j\omega_e L_m \lambda_{drr}^{'}\right] \tag{5.113}$$

$$j\omega_e i_{yss} = \frac{1}{L_{ls}}\left[v_{yss} - r_s i_{yss}\right] \tag{5.114}$$

$$T_{eavg} = \frac{mP}{8}\frac{L_m}{L_r^{'}}\left[\mathrm{Re}\left(\lambda_{drr}^{'} i_{qss}^{*}\right) - \mathrm{Re}\left(\lambda_{qrr}^{'} i_{dss}^{*}\right)\right] \tag{5.115}$$

$$T_{pul} = \frac{mP}{8}\frac{L_m}{L_r^{'}}\left[\mathrm{Re}\left(\lambda_{drr}^{'} i_{qss}\right) - \mathrm{Re}\left(\lambda_{qrr}^{'} i_{dss}\right)\right] \tag{5.116}$$

$$0 = T_{eavg} - T_L \tag{5.117}$$

$$\omega_{r1} = -\frac{jP}{4J\omega_e}T_{puls} \tag{5.118}$$

Equation (5.110) can be written as

$$0 = \frac{r_r^{'}L_m}{L_r^{'}} i_{qss} - \left(\frac{r_r^{'}}{L_r^{'}}\lambda_{qrr}^{'} + j\omega_e\right)\lambda_{qrr}^{'} + \omega_{ro}\lambda_{drr}^{'} + \frac{1}{2}\omega_{r1}\lambda_{drr}^{'*} \tag{5.119}$$

Equation (5.111) can be written as

$$0 = \frac{r_r^{'}L_m}{L_r^{'}} i_{dss} - \omega_{ro}\lambda_{qrr}^{'} - \frac{1}{2}\omega_{r1}\lambda_{qrr}^{'*} - \left(\frac{r_r^{'}}{L_r^{'}} + j\omega_e\right)\lambda_{drr}^{'} \tag{5.120}$$

Substituting (5.109) into (5.112) for v_{qss} we have

$$j\omega_e i_{qss} = \begin{pmatrix} \frac{L_r^{'2} L_{ls} r_s}{L_{ls} L_r \alpha_o + \alpha_o^2} i_{qss} + \frac{j\omega_e L_{ls} L_m L_r^{'}}{L_{ls} L_r \alpha_o + \alpha_o^2} \lambda_{qrr}^{'} + \frac{L_r^{'} \alpha_o \overline{C}}{L_{ls} L_r \alpha_o + \alpha_o^2} \\ - \frac{L_r^{'} \alpha_o r_s}{L_{ls} L_r \alpha_o + \alpha_o^2} i_{qss} - \frac{r_s L_r^{'}}{\alpha_o} i_{qss} - \frac{j\omega_e L_m}{\alpha_o} \lambda_{qrr}^{'} \end{pmatrix} \quad 5.121$$

$$-\frac{L_r^{'} \alpha_o \overline{C}}{L_{ls} L_r \alpha + \alpha_o^2} = \begin{pmatrix} \frac{L_r^{'2} L_{ls} r_s}{L_{ls} L_r \alpha_o + \alpha_o^2} - \frac{L_r^{'} \alpha_o r_s}{L_{ls} L_r \alpha_o + \alpha_o^2} \\ -\frac{r_s L_r^{'}}{\alpha_o} - j\omega_e \end{pmatrix} i_{qss} + \left(\frac{j\omega_e L_{ls} L_m L_r^{'}}{L_{ls} L_r \alpha + \alpha_o^2} - \frac{j\omega_e L_m}{\alpha_o} \right) \lambda_{qrr}^{'} \quad (5.122)$$

Equation (5.113) can be written as

$$\left(\frac{r_s L_r^{'}}{\alpha_o} + j\omega_e \right) i_{dss} + \frac{j\omega_e L_m}{\alpha_o} \lambda_{drr}^{'} = \frac{L_r^{'} v_{dss}}{\alpha_o} \quad (5.123)$$

Equation (5.114) can be written as

$$\left(\frac{r_s}{L_{ls}} + j\omega_e \right) i_{yss} = \frac{v_{yss}}{L_{ls}} \quad (5.124)$$

The resulting model can be computed normally as for any other steady-state system. Since there is a coupling term due to the speed harmonic content ω_{r1}, then the steady-state model becomes nonlinear and thus requires a nonlinear technique to solve this model iteratively. This approach requires the model Equations to be separated into their real and imaginary parts, and thus introducing more state variables since each of the state variable will be spit into its two components, i.e. the real and imaginary parts as independent state variables. If f_{re} and f_{im} refer to the real and imaginary parts of the quantity f, respectively, then $f = f_{re} + jf_{im}$.

Now, let the quantities of Equations be presented in coordinate form as

$$\lambda_{qrr}^{'} = \lambda_{qrre} + j\lambda_{qrim} \quad (5.109)$$

$$\lambda_{drr}^{'} = \lambda_{drre} + j\lambda_{drim} \tag{5.110}$$

$$i_{qss} = i_{qsre} + ji_{qsim} \tag{5.111}$$

$$i_{dss} = i_{dsre} + ji_{dsim} \tag{5.112}$$

$$i_{yss} = i_{ysre} + ji_{ysim} \tag{5.113}$$

$$c_{sre} + jc_{sim} = -\frac{L_r^{'}\alpha_o \overline{C}}{L_{ls}L_r\alpha_o + \alpha_o^2} \tag{5.114}$$

$$v_{dsre} + jv_{dsim} = \frac{L_r^{'}v_{dss}}{\alpha_o} \tag{5.115}$$

From Equation (5.108) it is obvious that the real part of ω_{r1} is zero $\left(\omega_{r1re} = 0\right)$, hence ω_{r1} is an imaginary quantity. Therefore

$$\omega_{r1} = j\omega_{r1im} \tag{5.116}$$

Substituting these definitions into Equations (k) – (o) and (g) to (j), we have

$$0 = \begin{Bmatrix} \frac{r_r^{'}L_m}{L_r^{'}}i_{qsre} + j\frac{r_r^{'}L_m}{L_r^{'}}i_{qsim} - \frac{r_r^{'}}{L_r^{'}}\lambda_{qrre} - j\omega_e\lambda_{qrre} - j\frac{r_r^{'}}{L_r^{'}}\lambda_{qrim} + \\ \omega_e\lambda_{qrim} + \omega_{ro}\lambda_{drre} + j\omega_{ro}\lambda_{drim} + \frac{1}{2}j\omega_{r1im}\lambda_{drre} + \frac{1}{2}\omega_{r1im}\lambda_{drim} \end{Bmatrix} \tag{5.117}$$

$$0 = \begin{Bmatrix} \frac{r_r^{'}L_m}{L_r^{'}}i_{qsre} - \frac{r_r^{'}}{L_r^{'}}\lambda_{qrre} + \omega_e\lambda_{qrim} + \omega_{ro}\lambda_{drre} + \frac{1}{2}\omega_{r1im}\lambda_{drim} + \\ j\left(\omega_{ro}\lambda_{drim} + \frac{1}{2}\omega_{r1im}\lambda_{drre} + \frac{r_r^{'}L_m}{L_r^{'}}i_{qsim} - \omega_e\lambda_{qrre} - \frac{r_r^{'}}{L_r^{'}}\lambda_{qrim}\right) \end{Bmatrix} \tag{5.118}$$

Separating real and imaginary terms

$$0 = \frac{r_r^{'}L_m}{L_r^{'}}i_{qsre} - \frac{r_r^{'}}{L_r^{'}}\lambda_{qrre} + \omega_e\lambda_{qrim} + \omega_{ro}\lambda_{drre} + \frac{1}{2}\omega_{r1im}\lambda_{drim} \tag{5.119}$$

$$0 = \frac{r_r^{'}L_m}{L_r^{'}}i_{qsim} - \omega_e\lambda_{qrre} - \frac{r_r^{'}}{L_r^{'}}\lambda_{qrim} + \frac{1}{2}\omega_{r1im}\lambda_{drre} + \omega_{ro}\lambda_{drim} \tag{5.120}$$

$$0=\begin{bmatrix}\frac{r_r^{'}L_m}{L_r^{'}}i_{dsre}+j\frac{r_r^{'}L_m}{L_r^{'}}i_{dsim}-\omega_{ro}\lambda_{qrre}-j\omega_{ro}\lambda_{qrim}\\-\frac{1}{2}\omega_{r1}\lambda_{qrre}+j\frac{1}{2}\omega_{r1}\lambda_{qrim}\end{bmatrix}+\begin{pmatrix}-\frac{r_r^{'}}{L_r^{'}}\lambda_{drre}\\-j\omega_e\lambda_{drre}\end{pmatrix}+\begin{pmatrix}-j\frac{r_r^{'}}{L_r^{'}}\lambda_{drim}\\+\omega_e\lambda_{drim}\end{pmatrix}\tag{5.121}$$

$$0=\begin{bmatrix}\frac{r_r^{'}L_m}{L_r^{'}}i_{dsre}-\omega_{ro}\lambda_{qrre}-\frac{1}{2}\omega_{r1}\lambda_{qrre}-\frac{r_r^{'}}{L_r^{'}}\lambda_{drre}+\omega_e\lambda_{drim}+\\j\left(\frac{r_r^{'}L_m}{L_r^{'}}i_{dsim}-\omega_{ro}\lambda_{qrim}+\frac{1}{2}\omega_{r1}\lambda_{qrim}-\omega_e\lambda_{drre}-\frac{r_r^{'}}{L_r^{'}}\lambda_{drim}\right)\end{bmatrix}\tag{5.122}$$

Separating real and imaginary terms

$$0=\frac{r_r^{'}L_m}{L_r^{'}}i_{dsre}-\omega_{ro}\lambda_{qrre}-\frac{1}{2}\omega_{r1}\lambda_{qrre}-\frac{r_r^{'}}{L_r^{'}}\lambda_{drre}+\omega_e\lambda_{drim}\tag{5.123}$$

$$0=\frac{r_r^{'}L_m}{L_r^{'}}i_{dsim}-\omega_{ro}\lambda_{qrim}+\frac{1}{2}\omega_{r1}\lambda_{qrim}-\omega_e\lambda_{drre}-\frac{r_r^{'}}{L_r^{'}}\lambda_{drim}\tag{5.124}$$

$$-\left(\frac{2r_sL_r^{'}\alpha_o}{L_{ls}L_r\alpha_o+\alpha_o^2}+j\omega_e\right)\left(i_{qsre}+ji_{qsim}\right)-\frac{j\omega_eL_m\alpha_o}{L_{ls}L_r\alpha_o+\alpha_o^2}\left(\lambda_{qrre}+j\lambda_{qrim}\right)=c_{sre}+jc_{sim}\tag{5.125}$$

$$\begin{bmatrix}-\frac{2r_sL_r^{'}\alpha_o}{L_{ls}L_r\alpha_o+\alpha^2}i_{qsre}+\frac{\omega_eL_m\alpha_o}{L_{ls}L_r\alpha_o+\alpha^2}\lambda_{qrim}+\omega_ei_{qsim}+\\j\left(-\omega_ei_{qsre}-\frac{2r_sL_r^{'}\alpha_o}{L_{ls}L_r\alpha_o+\alpha_o^2}i_{qsim}-\frac{\omega_eL_m\alpha_o}{L_{ls}L_r\alpha_o+\alpha_o^2}\lambda_{qrre}\right)\end{bmatrix}=c_{sre}+jc_{sim}\tag{5.126}$$

Separating real and imaginary terms

$$-\frac{2r_sL_r^{'}\alpha_o}{L_{ls}L_r\alpha_o+\alpha_o^2}i_{qsre}+\frac{\omega_eL_m\alpha_o}{L_{ls}L_r\alpha_o+\alpha_o^2}\lambda_{qrim}+\omega_ei_{qsim}=c_{sre}\tag{5.127}$$

$$-\omega_ei_{qsre}-\frac{2r_sL_r^{'}\alpha_o}{L_{ls}L_r\alpha_o+\alpha_o^2}i_{qsim}-\frac{\omega_eL_m\alpha_o}{L_{ls}L_r\alpha_o+\alpha_o^2}\lambda_{qrre}=c_{sim}\tag{5.128}$$

$$\left(\frac{r_sL_r^{'}}{\alpha_o}+j\omega_e\right)\left(i_{dsre}+ji_{dsim}\right)+\frac{j\omega_eL_m}{\alpha_o}\left(\lambda_{drre}+j\lambda_{drim}\right)=v_{dsre}+jv_{dsim}\tag{5.129}$$

$$\frac{r_s L_r^{'}}{\alpha_o} i_{dsre} + j\omega_e i_{dsre} + j\frac{r_s L_r^{'}}{\alpha_o} i_{dsim} - \omega_e i_{dsim} + \frac{j\omega_e L_m}{\alpha_o}\lambda_{drre} - \frac{\omega_e L_m}{\alpha_o}\lambda_{drim} = v_{dsre} + jv_{dsim} \quad (5.130)$$

$$\frac{r_s L_r^{'}}{\alpha_o} i_{dsre} - \omega_e i_{dsim} - \frac{\omega_e L_m}{\alpha_o}\lambda_{drim} + j\left(\omega_e i_{dsre} + \frac{r_s L_r^{'}}{\alpha_o} i_{dsim} + \frac{\omega_e L_m}{\alpha_o}\lambda_{drre}\right) = v_{dsre} + jv_{dsim} \quad (5.131)$$

Separating real and imaginary terms

$$\frac{r_s L_r^{'}}{\alpha_o} i_{dsre} - \omega_e i_{dsim} - \frac{\omega_e L_m}{\alpha_o}\lambda_{drim} = v_{dsre} \quad (5.132)$$

$$\omega_e i_{dsre} + \frac{r_s L_r^{'}}{\alpha_o} i_{dsim} + \frac{\omega_e L_m}{\alpha_o}\lambda_{drre} = v_{dsim} \quad (5.133)$$

Therefore the steady-state real Equations are

$$0 = \frac{r_r^{'} L_m}{L_r^{'}} i_{qsre} - \frac{r_r^{'}}{L_r^{'}}\lambda_{qrre} + \omega_e \lambda_{qrim} + \omega_{ro}\lambda_{drre} + \frac{1}{2}\omega_{r1im}\lambda_{drim} \quad (5.134)$$

$$0 = \frac{r_r^{'} L_m}{L_r^{'}} i_{qsim} - \omega_e \lambda_{qrre} - \frac{r_r^{'}}{L_r^{'}}\lambda_{qrim} + \frac{1}{2}\omega_{r1im}\lambda_{drre} + \omega_{ro}\lambda_{drim} \quad (5.135)$$

$$0 = \frac{r_r^{'} L_m}{L_r^{'}} i_{dsre} - \omega_{ro}\lambda_{qrre} - \frac{1}{2}\omega_{r1}\lambda_{qrre} - \frac{r_r^{'}}{L_r^{'}}\lambda_{drre} + \omega_e \lambda_{drim} \quad (5.136)$$

$$0 = \frac{r_r^{'} L_m}{L_r^{'}} i_{dsim} - \omega_{ro}\lambda_{qrim} + \frac{1}{2}\omega_{r1}\lambda_{qrim} - \omega_e \lambda_{drre} - \frac{r_r^{'}}{L_r^{'}}\lambda_{drim} \quad (5.137)$$

$$-\frac{2 r_s L_r^{'} \alpha_o}{L_{ls} L_r \alpha_o + \alpha_o^2} i_{qsre} + \frac{\omega_e L_m \alpha_o}{L_{ls} L_r \alpha_o + \alpha_o^2}\lambda_{qrim} + \omega_e i_{qsim} = c_{sre} \quad (5.138)$$

$$\alpha_3 i_{qsre} + \alpha_4 \lambda_{qrim} + \omega_e i_{qsim} = c_{sre} \quad (5.139)$$

where

$$\alpha_3 = -\frac{2 r_s L_r^{'} \alpha_o}{L_{ls} L_r \alpha_o + \alpha_o^2}$$

$$\alpha_4 = \frac{\omega_e L_m \alpha_o}{L_{ls} L_r \alpha_o + \alpha_o^2}$$

$$-\omega_e i_{qsre} + \alpha_3 i_{qsim} + \alpha_4 \lambda_{qrre} = c_{sim} \tag{5.140}$$

$$\frac{r_s L_r^{'}}{\alpha_o} i_{dsre} - \omega_e i_{dsim} - \frac{\omega_e L_m}{\alpha_o} \lambda_{drim} = v_{dsre} \tag{5.141}$$

$$\omega_e i_{dsre} + \frac{r_s L_r^{'}}{\alpha_o} i_{dsim} + \frac{\omega_e L_m}{\alpha_o} \lambda_{drre} = v_{dsim} \tag{5.142}$$

These Equations can be written in matrix form as

$$b_o = A_o x_o \tag{5.143}$$

where

$$b_o = \begin{bmatrix} 0 \\ 0 \\ 0 \\ 0 \\ c_{sre} \\ c_{sim} \\ v_{dsre} \\ v_{dsim} \end{bmatrix} \tag{5.144}$$

$$A_o = \begin{bmatrix} \frac{r_r^{'} L_m}{L_r^{'}} & 0 & 0 & 0 & -\frac{r_r^{'}}{L_r^{'}} & \omega_e & \omega_{ro} & \frac{1}{2}\omega_{r1im} \\ 0 & \frac{r_r^{'} L_m}{L_r^{'}} & 0 & 0 & -\omega_e & -\frac{r_r^{'}}{L_r^{'}} & \frac{1}{2}\omega_{r1im} & \omega_{ro} \\ 0 & 0 & \frac{r_r^{'} L_m}{L_r^{'}} & 0 & -\frac{1}{2}\omega_{r1im} - \omega_{ro} & 0 & -\frac{r_r^{'}}{L_r^{'}} & \omega_e \\ 0 & 0 & 0 & \frac{r_r^{'} L_m}{L_r^{'}} & 0 & -\frac{1}{2}\omega_{r1im} - \omega_{ro} & -\omega_e & -\frac{r_r^{'}}{L_r^{'}} \\ \alpha_3 & \omega_e & 0 & 0 & 0 & \alpha_4 & 0 & 0 \\ -\omega_e & \alpha_3 & 0 & 0 & \alpha_4 & 0 & 0 & 0 \\ 0 & 0 & \frac{r_s L_r^{'}}{\alpha_o} & -\omega_e & 0 & 0 & 0 & -\frac{\omega_e L_m}{\alpha_o} \\ 0 & 0 & \omega_e & \frac{r_s L_r^{'}}{\alpha_o} & 0 & 0 & \frac{\omega_e L_m}{\alpha_o} & 0 \end{bmatrix}$$

(5.145)

$$x_o = \begin{bmatrix} i_{qsre} \\ i_{qsim} \\ i_{dsre} \\ i_{dsim} \\ \lambda_{qrre} \\ \lambda_{qrim} \\ \lambda_{drre} \\ \lambda_{drim} \end{bmatrix} \tag{5.146}$$

An initial value of ω_{r1} is assumed (in this case 0.6 rad/sec). The rotor speed is varied from 0 to ω_e. At every speed value, the value of ω_{r1} is iterated by using the pulsating torque to calculate the new value of ω_{r1} until the threshold is obtained, then calculation of different state variables continues. If however the speed pulsations are neglected in the voltage Equations, the resulting steady-state Equations are linear and admit closed form solutions.

5.3.2.2 Small signal analysis. To study the dynamics of the faulted system, small signal model is derived from the harmonic balance technique model by causing small changes in the state and control variables.

Equations (5.82), (5.83), (5.87), (5.90), (5.93), (5.96), (5.107) and (5.108) are used in developing a small signal model of the form

$$p\Delta x = A\Delta x + B\Delta u \tag{5.147}$$

where x is the state variable, A is the state matrix given by (5.164), B is the control matrix and u is the control variable. As it is for the case of the steady-state analysis, the resulting equations are split into their real and imaginary parts. Thus, the state matrix (5.164) so obtained consists of real parameters.

The small signal dynamic Equations are

$$p\Delta i_{qsre} = \frac{1}{L_r^{'}\alpha_o + L_{ls}L_r^{'2}}\begin{bmatrix} -\left(2r_s L_r^{'2} + r_r^{'}L_m^2\right)\Delta i_{qsre} + \left(\omega_e L_{ls}L_r^{'2} + \omega_e L_r^{'}\alpha_o\right)\Delta i_{qsim} + \\ L_r^{'2}C_{re} + r_r^{'}L_m\Delta\lambda_{qrre}^{'} - \omega_{ro}L_r^{'}L_m\Delta\lambda_{drre}^{'} - L_r^{'}L_m\lambda_{drre}^{'}\Delta\omega_{ro} \end{bmatrix} \tag{5.148}$$

$$p\Delta i_{qsim} = \frac{1}{L_r^{'}\alpha_o + L_{ls}L_r^{'2}}\begin{bmatrix} -\left(\omega_e L_{ls}L_r^{'2} + \omega_e L_r^{'}\alpha_o\right)\Delta i_{qsre} - \left(2r_s L_r^{'2} + r_r^{'}L_m^2\right)\Delta i_{qsim} + \\ L_r^{'2}C_{im} + r_r^{'}L_m\Delta\lambda_{qrim}^{'} - \omega_{ro}L_r^{'}L_m\Delta\lambda_{drim}^{'} - L_r^{'}L_m\lambda_{drim}^{'}\Delta\omega_{ro} \end{bmatrix} \tag{5.150}$$

$$p\Delta\lambda_{qrre} = \frac{1}{L_r^{'}\alpha_o + L_{ls}L_r^{'2}}\begin{bmatrix} r_r^{'}L_m\left(\alpha_o + L_{ls}L_r^{'}\right)\Delta i_{qsre} - r_r^{'}\left(\alpha_o + L_{ls}L_r^{'}\right)\Delta\lambda_{qrre} \\ + \omega_e L_r^{'}\left(\alpha_o + L_{ls}L_r^{'}\right)\Delta\lambda_{qrim} + \omega_{ro}L_r^{'}\left(\alpha_o + L_{ls}L_r^{'}\right)\Delta\lambda_{drre} \\ + L_r^{'}\left(\alpha_o + L_{ls}L_r^{'}\right)\lambda_{drre}\Delta\omega_{ro} \end{bmatrix} \tag{5.151}$$

$$p\Delta\lambda_{qrim} = \frac{1}{L_r^{'}\alpha_o + L_{ls}L_r^{'2}}\begin{bmatrix} r_r^{'}L_m\left(\alpha_o + L_{ls}L_r^{'}\right)\Delta i_{qsim} - \omega_e L_r^{'}\left(\alpha_o + L_{ls}L_r^{'}\right)\Delta\lambda_{qrre} \\ - r_r^{'}\left(\alpha_o + L_{ls}L_r^{'}\right)\Delta\lambda_{qrim} + \omega_{ro}L_r^{'}\left(\alpha_o + L_{ls}L_r^{'}\right)\Delta\lambda_{drim} \\ + L_r^{'}\left(\alpha_o + L_{ls}L_r^{'}\right)\lambda_{drim}\Delta\omega_{ro} \end{bmatrix} \tag{5.152}$$

$$p\Delta i_{dsre} = \frac{1}{\alpha_o}\begin{bmatrix} v_{dsre} - \left(r_s L_r^{'} + \dfrac{r_r^{'}L_m^2}{L_r^{'}}\right)\Delta i_{dsre} + \omega_e\alpha_o\Delta i_{dsim} + \dfrac{r_r^{'}L_m}{L_r^{'}}\Delta\lambda_{drre}^{'} + \omega_{ro}L_m\Delta\lambda_{qrre}^{'} \\ + L_m\lambda_{qrre}^{'}\Delta\omega_{ro} \end{bmatrix} \tag{5.153}$$

$$p\Delta i_{dsim} = \frac{1}{\alpha_o}\begin{bmatrix} v_{dsim} - \omega_e \alpha_o \Delta i_{dsre} - \left(r_s L_r^{'} + \dfrac{r_r^{'} L_m^2}{L_r^{'}} \right) \Delta i_{dsim} + \dfrac{r_r^{'} L_m}{L_r^{'}} \Delta \lambda_{drim}^{'} \\ + \omega_{ro} L_m \Delta \lambda_{qrim}^{'} + L_m \lambda_{qrim}^{'} \Delta \omega_{ro} \end{bmatrix} \tag{5.154}$$

$$p\Delta \lambda_{drre}^{'} = \frac{r_r^{'} L_m}{L_r^{'}} \Delta i_{dsre} - \omega_{ro} \Delta \lambda_{qrre}^{'} - \lambda_{qrre}^{'} \Delta \omega_{ro} - \frac{r_r^{'}}{L_r^{'}} \Delta \lambda_{drre}^{'} + \omega_e \Delta \lambda_{drim}^{'} \tag{5.155}$$

$$p\Delta \lambda_{drim}^{'} = \frac{r_r^{'} L_m}{L_r^{'}} \Delta i_{dsim} - \omega_{ro} \Delta \lambda_{qrim}^{'} - \lambda_{qrim}^{'} \Delta \omega_{ro} - \frac{r_r^{'}}{L_r^{'}} \Delta \lambda_{drim}^{'} - \omega_e \Delta \lambda_{drre}^{'} \tag{5.156}$$

$$p\Delta \omega_{ro} = \frac{5P^2}{16J} \frac{L_m}{L_r} \begin{bmatrix} \lambda_{drre}^{'} \Delta i_{qsre} + \lambda_{drim}^{'} \Delta i_{qsim} + i_{qsre} \Delta \lambda_{drre}^{'} + i_{qsim} \Delta \lambda_{drim}^{'} \\ - \lambda_{qrre}^{'} \Delta i_{dsre} - \lambda_{qrim}^{'} \Delta i_{dsim} - i_{dsre} \Delta \lambda_{qrre}^{'} - i_{dsim} \Delta \lambda_{qrim}^{'} \end{bmatrix} - \frac{P}{2J} \Delta T_L \tag{5.157}$$

$$\Delta T_{pul} = \frac{5P}{8} \frac{L_m}{L_r} \begin{bmatrix} \lambda_{drre}^{'} \Delta i_{qsre} - \lambda_{drim}^{'} \Delta i_{qsim} + i_{qsre} \Delta \lambda_{drre}^{'} - i_{qsim} \Delta \lambda_{drim}^{'} \\ - i_{dsre} \Delta \lambda_{qrre}^{'} + i_{dsim} \Delta \lambda_{qrim}^{'} - \lambda_{qrre}^{'} \Delta i_{dsre} + \lambda_{qrim}^{'} \Delta i_{dsim} \end{bmatrix} \tag{5.158}$$

$$p\Delta \omega_{r1re} = \frac{P}{2J} \frac{5P}{8} \frac{L_m}{L_r} \begin{bmatrix} \lambda_{drre}^{'} \Delta i_{qsre} - \lambda_{drim}^{'} \Delta i_{qsim} + i_{qsre} \Delta \lambda_{drre}^{'} - i_{qsim} \Delta \lambda_{drim}^{'} \\ - i_{dsre} \Delta \lambda_{qrre}^{'} + i_{dsim} \Delta \lambda_{qrim}^{'} - \lambda_{qrre}^{'} \Delta i_{dsre} + \lambda_{qrim}^{'} \Delta i_{dsim} \end{bmatrix} \tag{5.159}$$

$$p\Delta \omega_{r1im} = -2\omega_e \Delta \omega_{r1} \tag{5.160}$$

$$p\Delta \omega_{ro} = \frac{5P^2}{16J} \frac{L_m}{L_r} \begin{bmatrix} \lambda_{drre}^{'} \Delta i_{qsre} + \lambda_{drim}^{'} \Delta i_{qsim} - \lambda_{qrre}^{'} \Delta i_{dsre} - \lambda_{qrim}^{'} \Delta i_{dsim} \\ - i_{dsre} \Delta \lambda_{qrre}^{'} - i_{dsim} \Delta \lambda_{qrim}^{'} + i_{qsre} \Delta \lambda_{drre}^{'} + i_{qsim} \Delta \lambda_{drim}^{'} \end{bmatrix} - \frac{P}{2J} \Delta T_L \tag{5.161}$$

$$p\Delta \omega_{r1re} = \frac{P}{2J} \frac{5P}{8} \frac{L_m}{L_r} \begin{bmatrix} \lambda_{drre}^{'} \Delta i_{qsre} - \lambda_{drim}^{'} \Delta i_{qsim} - \lambda_{qrre}^{'} \Delta i_{dsre} + \lambda_{qrim}^{'} \Delta i_{dsim} \\ - i_{dsre} \Delta \lambda_{qrre}^{'} + i_{dsim} \Delta \lambda_{qrim}^{'} + i_{qsre} \Delta \lambda_{drre}^{'} - i_{qsim} \Delta \lambda_{drim}^{'} \end{bmatrix} \tag{5.162}$$

Thus, the matrices of Equation (5.144) can be deduced form (5.148) through (5.162) as

$$p\Delta x = \begin{bmatrix} \Delta i_{qsre} \\ \Delta i_{qsim} \\ \Delta i_{dsre} \\ \Delta i_{dsim} \\ \Delta \lambda_{qrre} \\ \Delta \lambda_{qrim} \\ \Delta \lambda_{drre} \\ \Delta \lambda_{drim} \\ \Delta \omega_{ro} \\ \Delta \omega_{r1re} \\ \Delta \omega_{r1im} \end{bmatrix} \tag{5.163}$$

$$A = \begin{bmatrix} \beta_1 & \beta_2 & 0 & 0 & \beta_3 & 0 & \beta_4 & 0 & \beta_5 & 0 & 0 \\ \beta_6 & \beta_7 & 0 & 0 & 0 & \beta_8 & 0 & \beta_9 & \beta_{10} & 0 & 0 \\ 0 & 0 & \beta_{11} & \beta_{12} & \beta_{13} & 0 & \beta_{14} & 0 & \beta_{15} & 0 & 0 \\ 0 & 0 & \beta_{16} & \beta_{17} & 0 & \beta_{18} & 0 & \beta_{19} & \beta_{20} & 0 & 0 \\ \beta_{21} & 0 & 0 & 0 & \beta_{22} & \beta_{23} & \beta_{24} & 0 & \beta_{25} & 0 & 0 \\ 0 & \beta_{26} & 0 & 0 & \beta_{27} & \beta_{28} & 0 & \beta_{29} & \beta_{30} & 0 & 0 \\ 0 & 0 & \beta_{31} & 0 & \beta_{32} & 0 & \beta_{33} & \beta_{34} & \beta_{35} & 0 & 0 \\ 0 & 0 & 0 & \beta_{36} & 0 & \beta_{37} & \beta_{38} & \beta_{39} & \beta_{40} & 0 & 0 \\ \beta_{41} & \beta_{42} & \beta_{43} & \beta_{44} & \beta_{45} & \beta_{46} & \beta_{47} & \beta_{48} & 0 & 0 & 0 \\ \beta_{49} & \beta_{50} & \beta_{51} & \beta_{52} & \beta_{53} & \beta_{54} & \beta_{55} & \beta_{56} & 0 & 0 & 0 \\ 0 & 0 & 0 & 0 & 0 & 0 & 0 & 0 & 0 & 0 & -2\omega_e \end{bmatrix} \tag{5.164}$$

The stability of the faulted five phase machine is studied through the calculation of the eigen values of the resulting state matrix. The entries of (5.164) can be easily obtained from Equations (5.148) through (5.162).

where

$$a_o = \frac{1}{\alpha_o L_r^{'} + L_{ls} L_r^{'2}}, \quad a_1 = -\left(2 r_s L_r^{'2} + r_r L_m^2\right), \qquad a_2 = \omega_e \left(L_{ls} L_r^{'2} + \alpha_o L_r^{'}\right),$$

$$a_3 = r_r L_m \qquad a_4 = -\omega_{ro} L_r^{'} L_m, \qquad a_5 = -L_r^{'} L_m \lambda_{drre}, \qquad a_6 = -L_r^{'} L_m \lambda_{drim},$$

$$a_7 = -\frac{1}{\alpha_o}\left(r_s L_r^{'} + \frac{r_r^{'} L_m^2}{L_r^{'}}\right) \qquad a_8 = \omega_e, \qquad a_9 = \frac{1}{\alpha_o}\omega_{ro} L_m, \qquad a_{10} = \frac{1}{\alpha_o} L_m \lambda_{qrre},$$

$$a_{11} = \frac{1}{\alpha_o L_r^{'}} r_r^{'} L_m, \qquad a_{12} = \frac{1}{\alpha_o} L_m \lambda_{qrim} \qquad a_{13} = r_r^{'} L_m \left(\alpha_o + L_{ls} L_r^{'}\right),$$

$$a_{14} = -r_r^{'}\left(\alpha_o + L_{ls} L_r^{'}\right), \qquad a_{15} = \omega_e L_r^{'}\left(\alpha_o + L_{ls} L_r^{'}\right), a_{16} = \omega_{ro} L_r^{'}\left(\alpha_o + L_{ls} L_r^{'}\right),$$

$$a_{17} = L_r^{'}\left(\alpha_o + L_{ls} L_r^{'}\right)\lambda_{drre}, \qquad a_{18} = L_r^{'}\left(\alpha_o + L_{ls} L_r^{'}\right)\lambda_{drim}, \qquad a_{19} = \frac{5P^2 L_m}{16 J L_r^{'}}, \beta_1 = a_o a_1,$$

$$\beta_2 = a_o a_2, \quad \beta_3 = a_o a_3, \quad \beta_4 = a_o a_4, \quad \beta_5 = a_o a_5 \quad \beta_6 = -\beta_2, \quad \beta_7 = \beta_1,$$

$$\beta_8 = \beta_3, \quad \beta_9 = \beta_4, \quad \beta_{10} = a_o a_6 \quad \beta_{11} = a_7, \quad \beta_{12} = a_8, \quad \beta_{13} = a_9,$$

$$\beta_{14} = a_{10}, \quad \beta_{15} = a_{11} \quad \beta_{16} = -\beta_{12}, \quad \beta_{17} = \beta_{11}, \quad \beta_{18} = \beta_{13}, \quad \beta_{19} = \beta_{12},$$

$$\beta_{20} = \beta_{15} \quad \beta_{21} = a_o a_{13}, \quad \beta_{22} = a_o a_{14}, \quad \beta_{23} = a_o a_{15}, \quad \beta_{24} = a_o a_{16}, \quad \beta_{25} = a_o a_{17}$$

$$\beta_{26} = \beta_{21}, \quad \beta_{27} = -\beta_{23}, \quad \beta_{28} = \beta_{22}, \quad \beta_{29} = \beta_{24}, \quad \beta_{30} = a_o a_{18} \quad \beta_{31} = \frac{r_r^{'} L_m}{L_r},$$

$$\beta_{32} = -\omega_{ro}, \quad \beta_{33} = -\frac{r_r^{'}}{L_r^{'}}, \quad \beta_{34} = \omega_e, \quad \beta_{35} = \lambda_{qrre}^{'} \quad \beta_{36} = \beta_{31}, \quad \beta_{37} = \beta_{32},$$

$$\beta_{38} = -\beta_{34}, \quad \beta_{39} = \beta_{33}, \quad \beta_{40} = -\lambda_{qrim}^{'} \quad \beta_{41} = a_{19}\lambda_{drre}^{'}, \ \beta_{42} = a_{19}\lambda_{drim}^{'},$$

$$\beta_{43} = -a_{19}\lambda_{qrre}^{'}, \quad \beta_{44} = -a_{19}\lambda_{qrim}^{'} \quad \beta_{45} = -a_{19} i_{dsre}, \quad \beta_{46} = -a_{19} i_{dsim},$$

$$\beta_{47} = a_{19} i_{qsre}, \quad \beta_{48} = a_{19} i_{qsim} \quad \beta_{49} = \beta_{41}, \quad \beta_{50} = -\beta_{42}, \quad \beta_{51} = \beta_{43},$$

$$\beta_{52} = -\beta_{44}, \quad \beta_{53} = \beta_{45}, \quad \beta_{54} = -\beta_{46} \quad \beta_{55} = \beta_{47}, \quad \beta_{56} = -\beta_{48}$$

5.3.3 Results and Discussion

The validity of the various models presented in Sections 5.2-5.3.3 has been investigated through the computer simulation of the full-order model of the machine with stator phase ‘a’ open-circuited. The steady-state model is used to calculate the state variables and then the results are compared.

Figure 5.2 through Figure 5.4 present the simulation of the free acceleration starting process of the machine. The phase voltage is applied to the remaining four phases (b, c, d, and e) and Equation (5.58) is used to determine stator phase ‘a’ voltage. Figure 5.2(a) and (b) show the rotor speed and electromagnetic torque, respectively, showing the characteristics similar to those of the healthy induction machine. In Figure 5.3(a) the stator phase ‘a’ current is zero as expected. The stator phase voltages are shown in Figure 5.4 with the starting transients of the open phase ‘a’ as it develops the voltage is clearly displayed in Figure 5.4(a).

When the rotor speed is in steady state, the load torque is changed from 0 to 11 Nm to show the effect of the speed harmonics. The dynamic responses of the machine to load changes are shown in Figure 5.5(a) and (b) for the rotor speed and electromagnetic torque, respectively. In Figure 5.6 through Figure 5.9, the waveforms of the variables are shown after the speed has reached steady-state average value. It is evident from Figure 5.6(a) and (b) that the speed and torque consist of the harmonics at twice the frequency of the supply voltages as predicted by the harmonic balance technique model. The unbalance caused by the open phase fault is clearly indicated in the stator phase load currents, Figure 5.7. Figure 5.8 (a) shows that when the machine is loaded, the open phase ‘a’ voltage is affect as it is reduced. This is due to the fact that the voltage waveform is induced by the other phases and the rotor circuits. The real power and reactive power also contain second order oscillations as shown in Figure 5.9 (a) and (b).

Figure 5.10(a) and Figure 5.10 (b) show the peak values of the rotor speed and torque pulsations, respectively as a function of the rotor speed. In Figure 5.6 (a) the average rotor speed is approximately 364.6 rad/sec, the peak value of the speed oscillations is about 0.04 rad/sec. In Figure 5.6(b) the average torque is 11 Nm and the peak of the torque oscillations is about 2.5 Nm. These speed and torque values are fairly comparable to those in Figure 5.10(a) and Figure 5.10(b), respectively.

Figure 5.11 presents the torque-speed characteristics at both normal and open-phase faulted conditions. First the normal operation of the machine is computer simulated and the steady-state torque curve is superimposed on the simulated curve. Then the same procedure is followed for the open phase faulted condition. Under this operation, the torque envelope is obtained by adding the peak of the pulsation torque to, and subtracting it from the average value obtained from the harmonic balance technique. Comparing the results of the dynamic computer simulation and the steady state calculations for both cases, the harmonic balance technique gives average and peak values of the torque that compare fairly with simulation results.

Figure 5.12 and Figure 5.13 present the small-signal dynamics of the system when the rotor speed is changing. The result of Figure 5.12 is obtained when the rotor speed is varied from 0 to 377 rad/sec. The machine shows instability at low speeds. This is contributed by both the speed harmonics and the q-axis rotor flux linkage λ'_{qrr}. In Figure 5.13, when the rotor speed is varied from 11. 78 rad/sec to 377 rad/sec, the instability due to the q-axis rotor flux linkage disappears. Thus the machine is stable at a relatively high speed. This may be due to the fact that at low speed (below 11.78 rad/sec), the machine is has not developed enough torque due to the loss of phase. But it quickly recovers beyond 1.78 rad/sec. This observation can be seen in Figure 5.2 in which it is clear that the machine takes a longer time to reach the steady-state speed.

The speed and torque oscillations are also shown in Figure 5.14 (a) and Figure 5.14(b), respectively. The results of which compare well with those presented in Figure 5.6(a) and Figure 5.6(b), respectively, as well as Figure 5.10(a) and Figure 5.10(b), respectively.

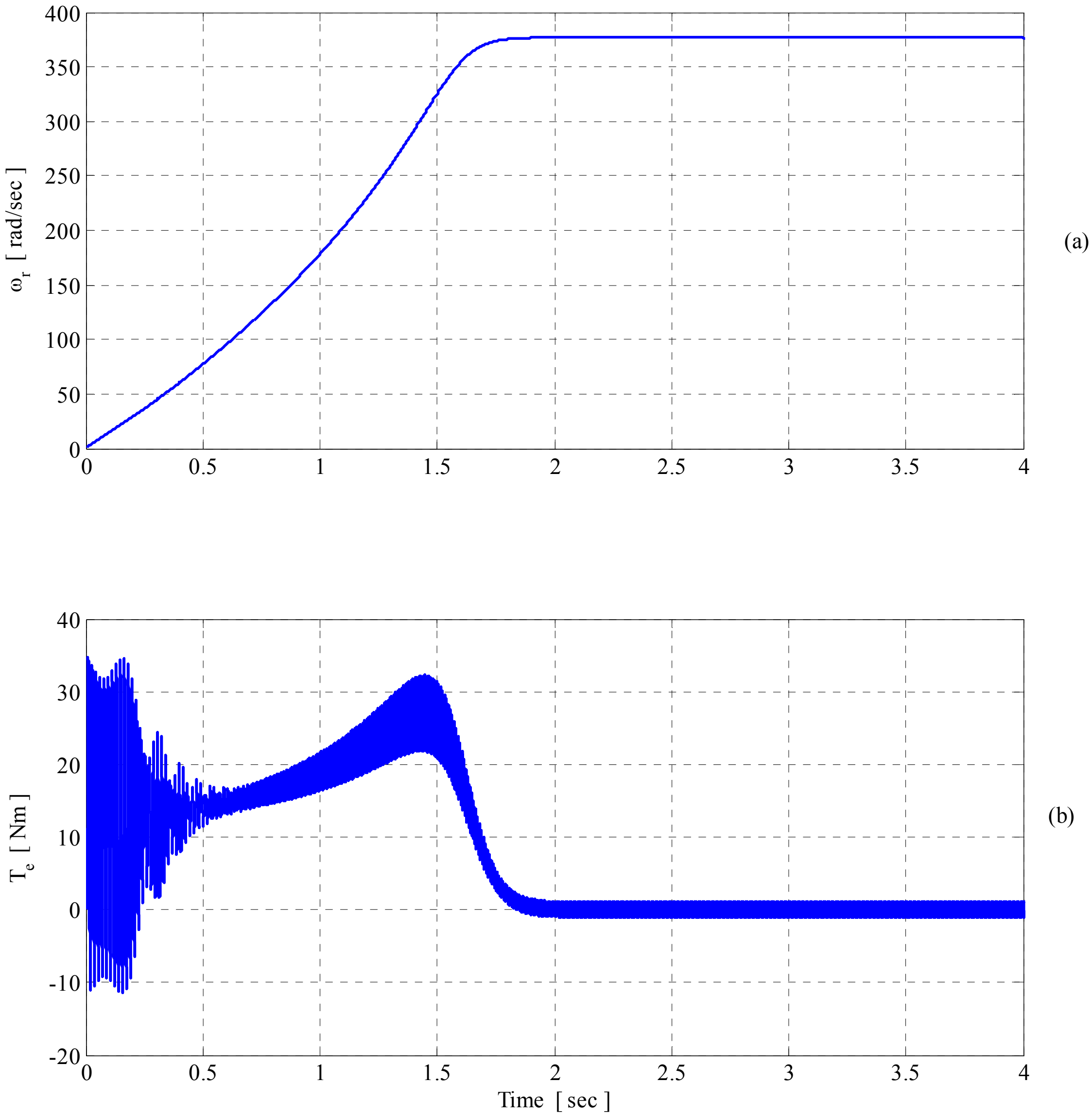

Figure 5.2 Starting transients (a) rotor speed and (b) electromagnetic torque

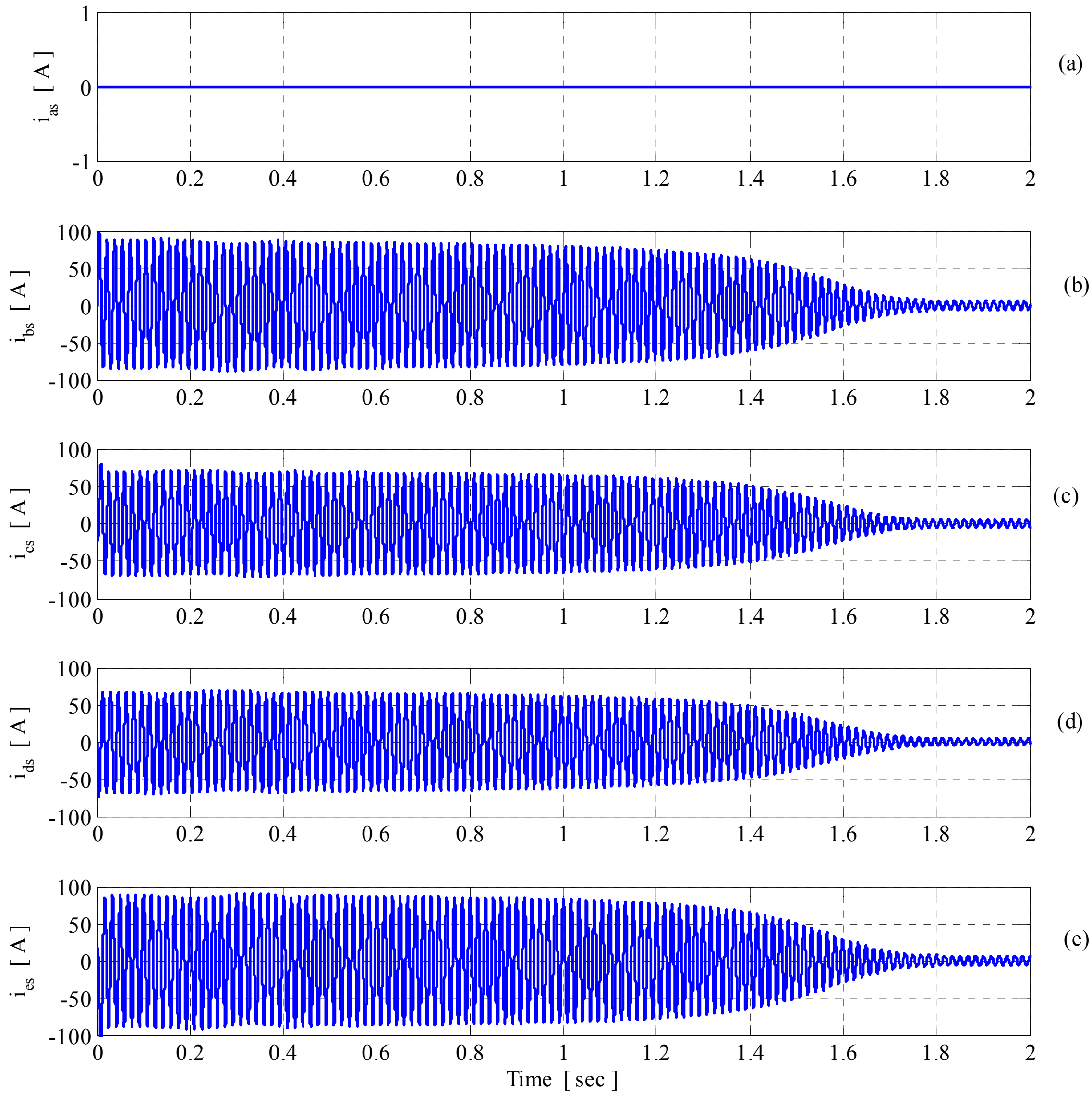

Figure 5.3 Starting transients Stator phase currents (a) phase ‘a’ (b) phase ‘b’ (c) phase ‘c’ (d) phase ‘d’ (e) phase ‘e’

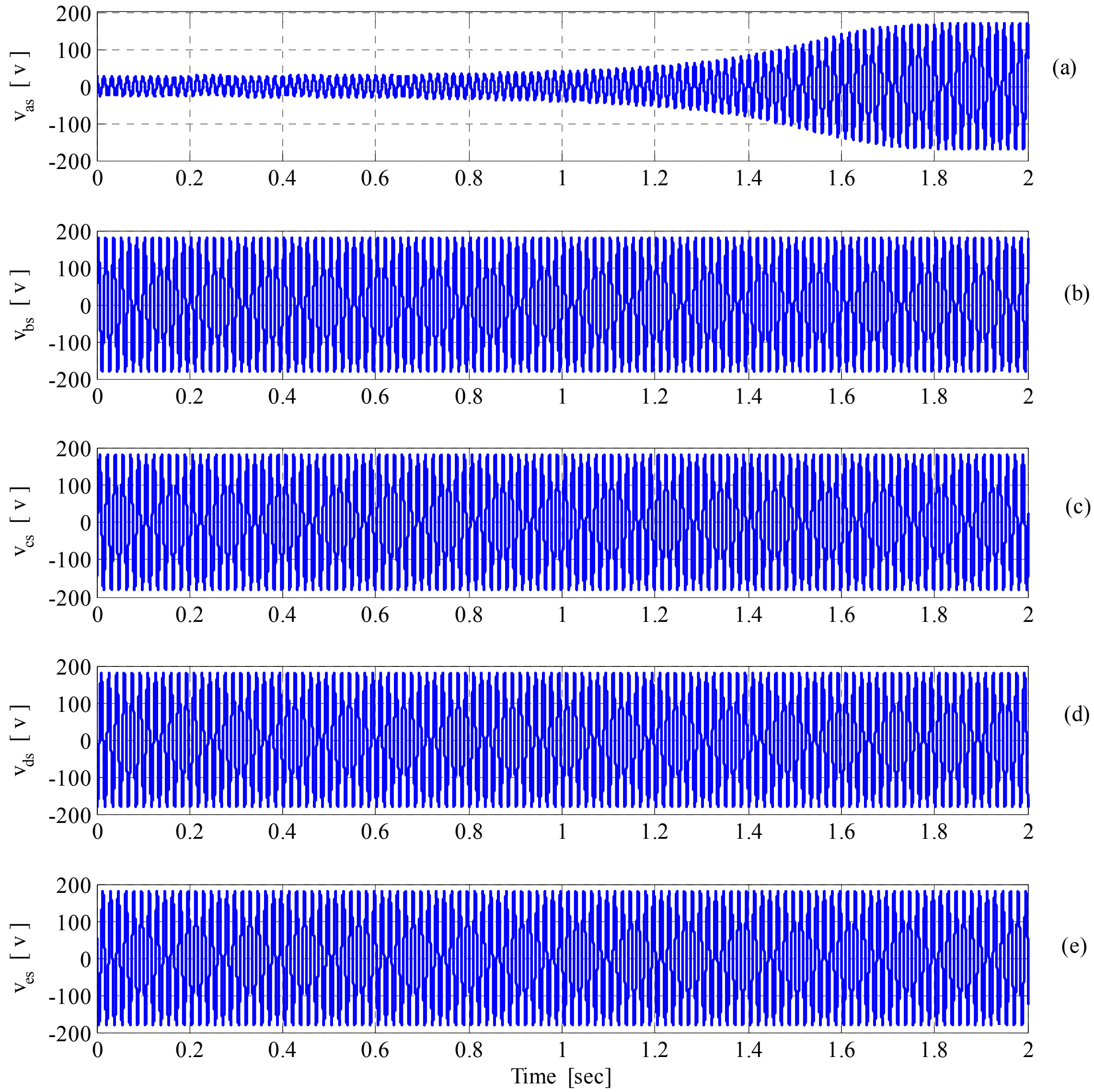

Figure 5.4 Starting transients stator phase voltages (a) phase ‘a’ (b) phase ‘b’ (c) phase ‘c’ (d) phase ‘d’ (e) phase ‘e’

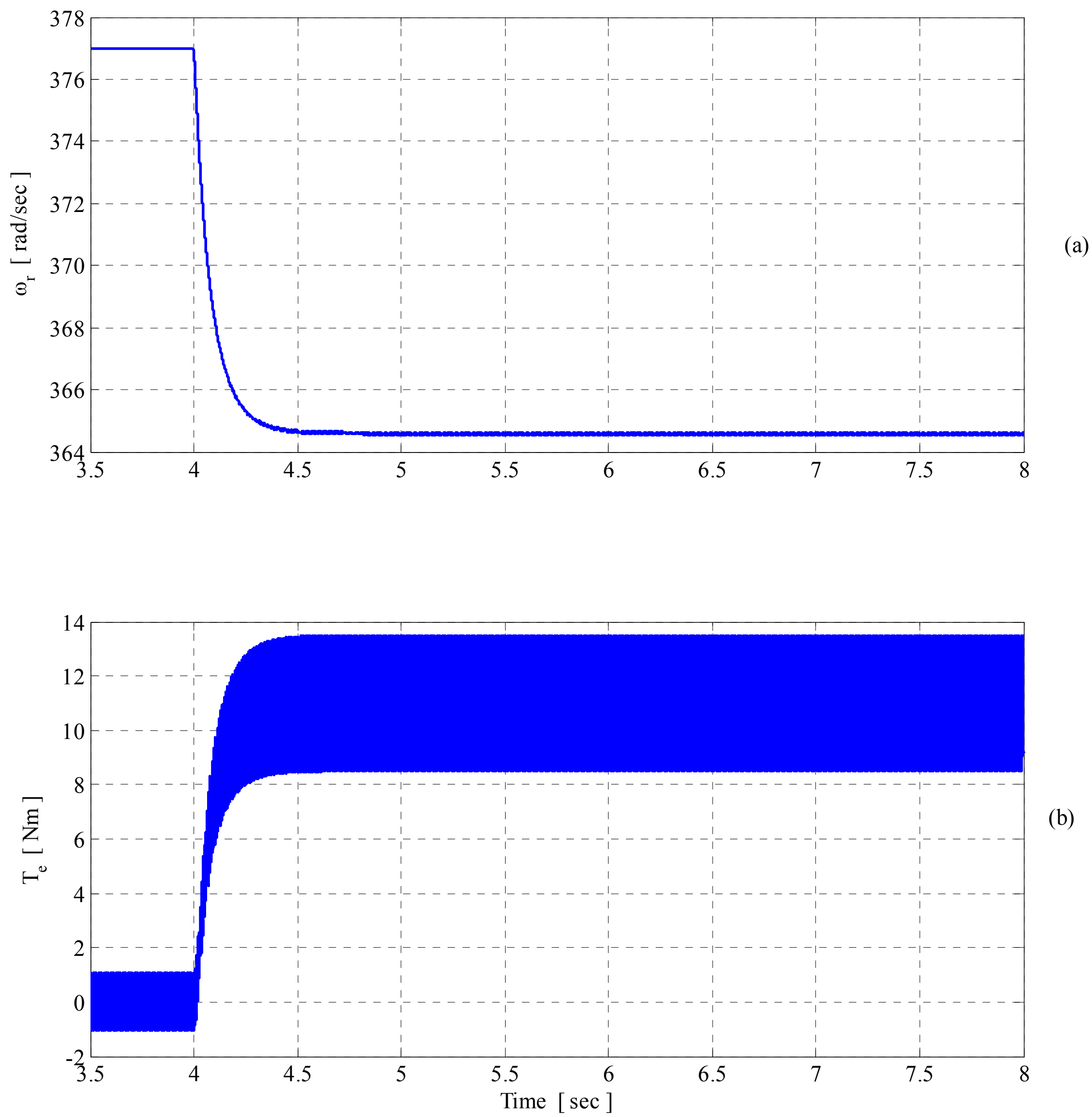

Figure 5.5 Simulation Dynamics of (a) rotor speed and (b) electromagnetic torque due to a load torque change of 11 Nm applied at 4 seconds.

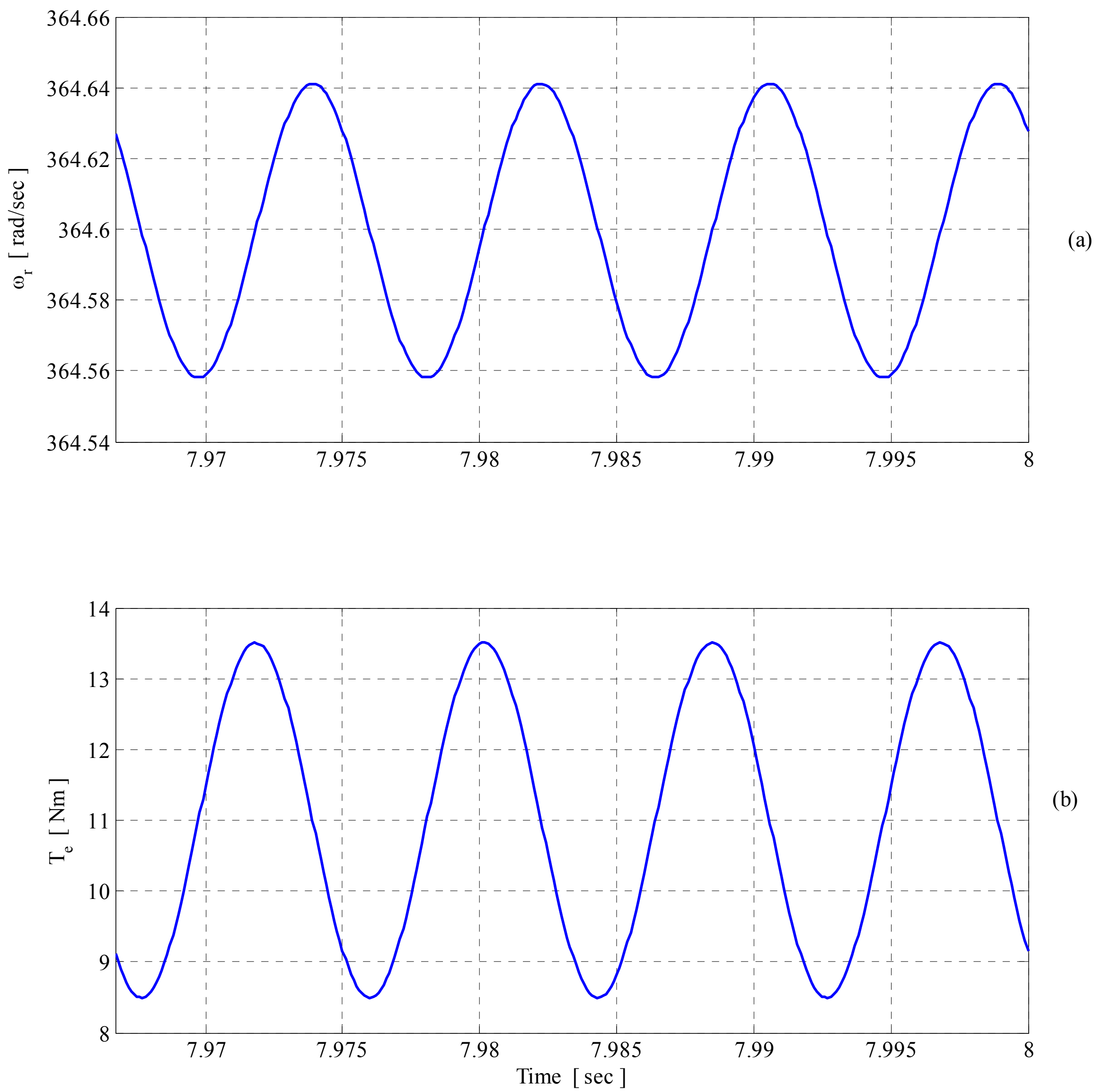

Figure 5.6 Simulation Steady-state (a) rotor speed and (b) electromagnetic torque at a load torque of 11 Nm.

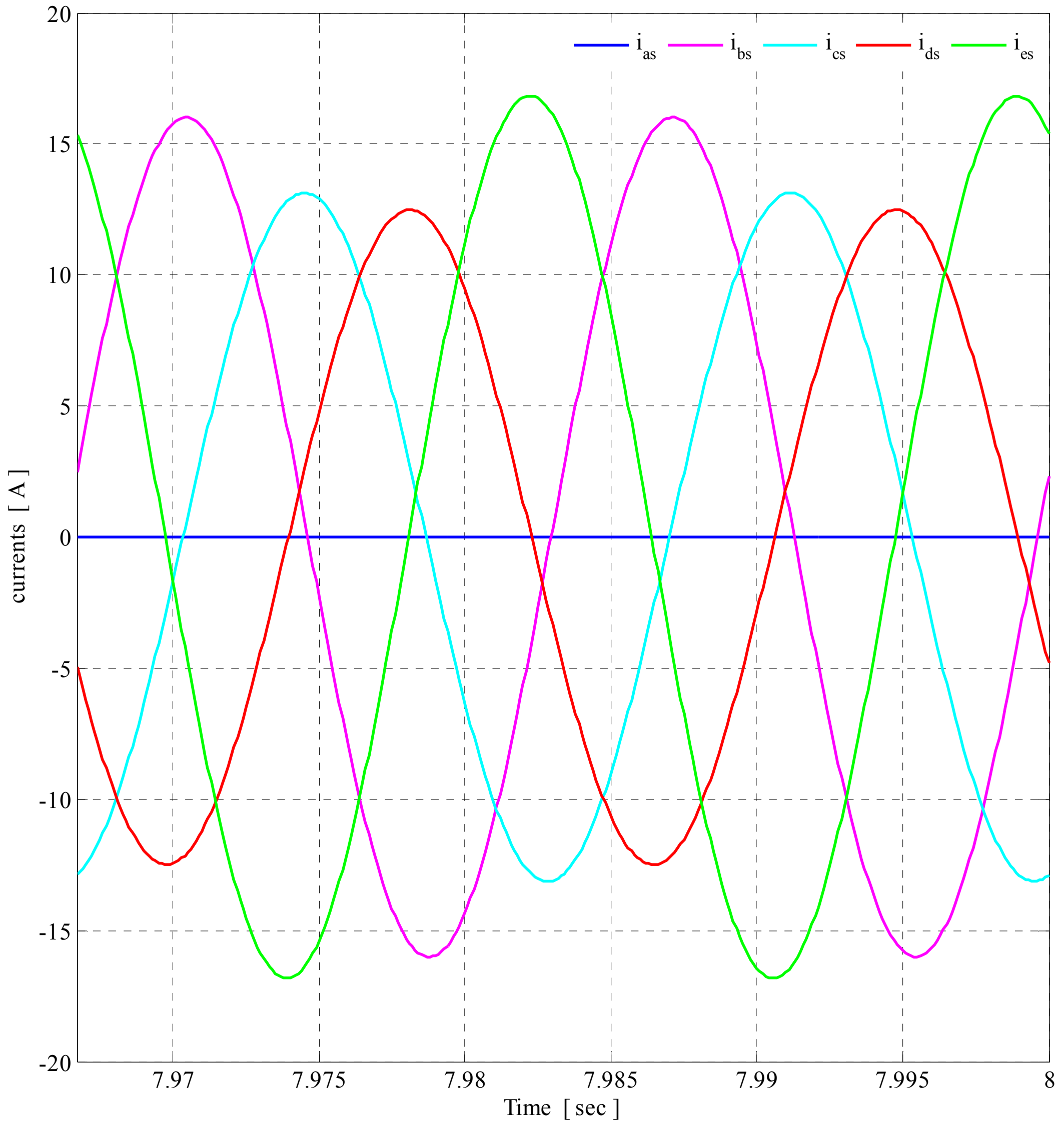

Figure 5.7 Simulation Steady-state stator phase currents at a load torque of 11 Nm.

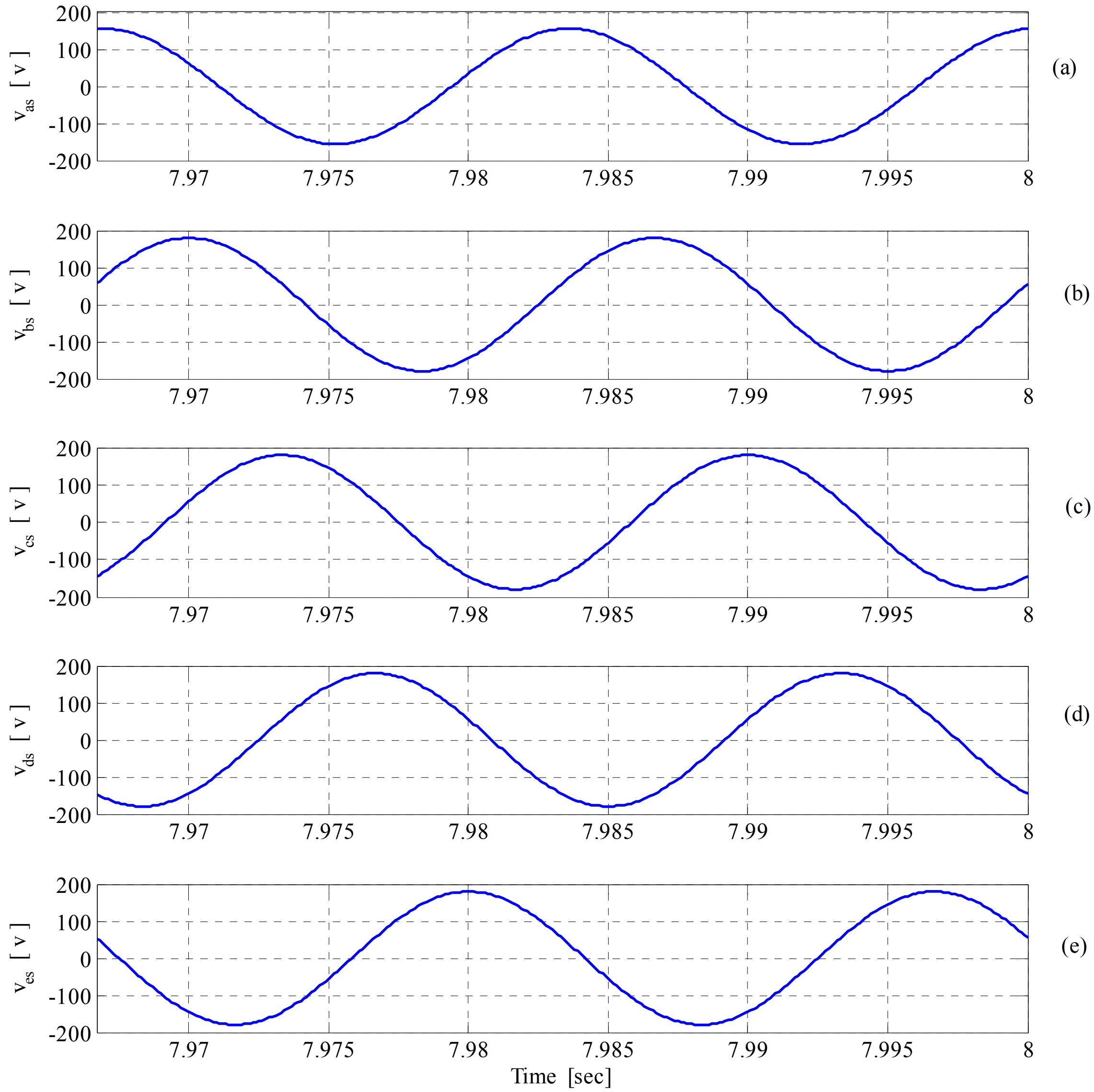

Figure 5.8 Simulation Steady-state stator phase voltages at a load torque of 11 Nm (a) phase 'a' (b) phase 'b' (c) phase 'c' (d) phase 'd' (e) phase 'e'

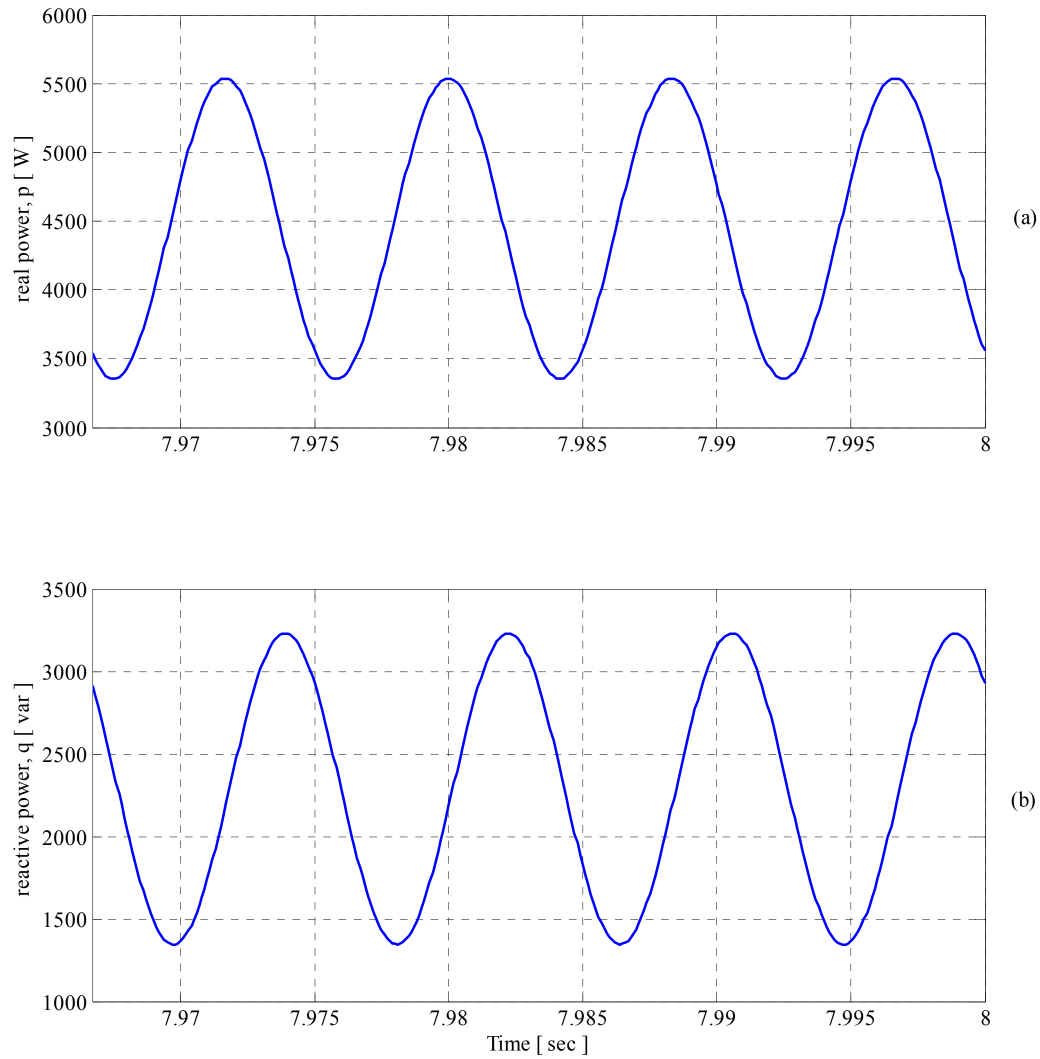

Figure 5.9 Simulation Steady-state stator input five-phase power (a) Real power and (b) Reactive power at a load torque of 11 Nm.

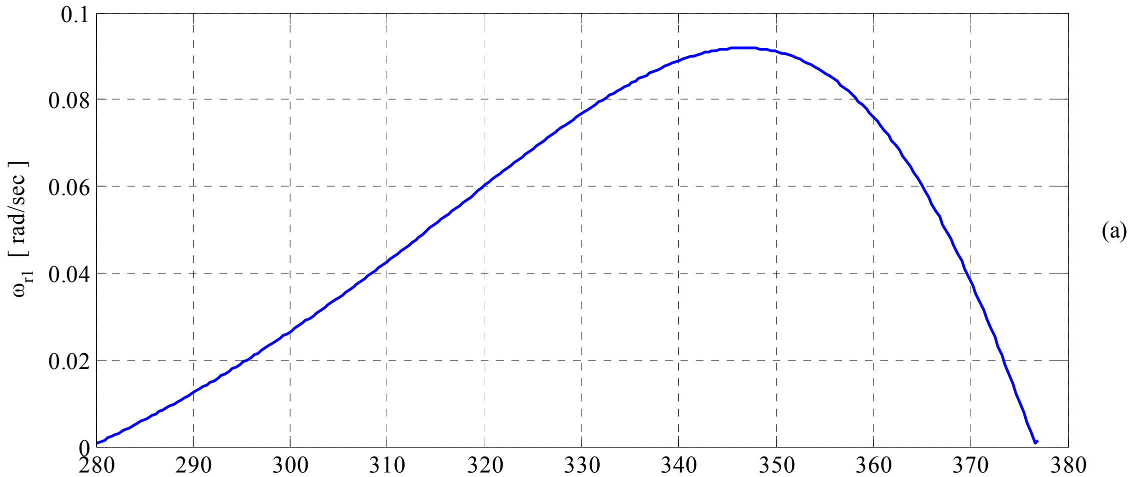

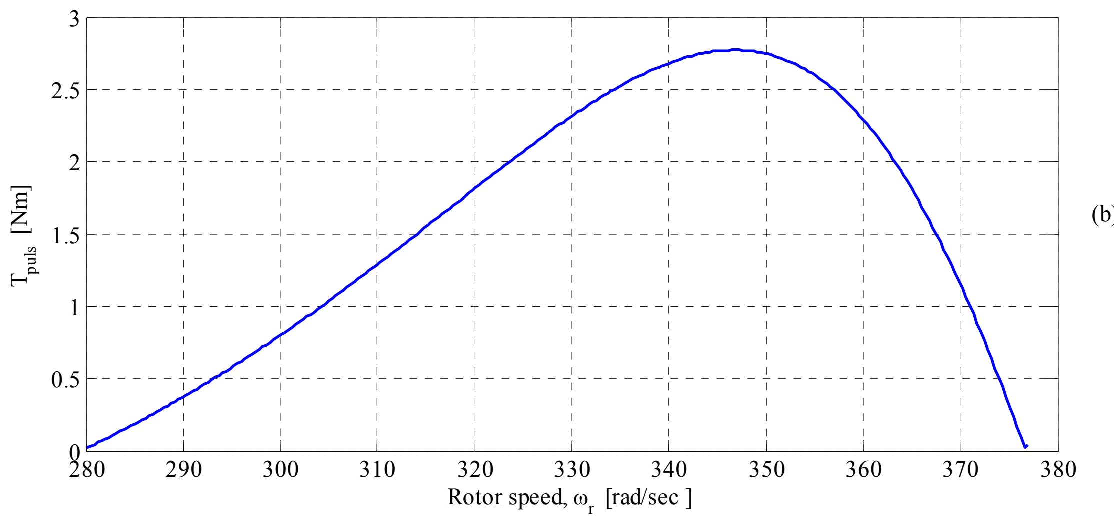

Figure 5.10. Steady-state calculation results (a) Peak value of the speed harmonic component and (b) Peak value of the torque pulsation

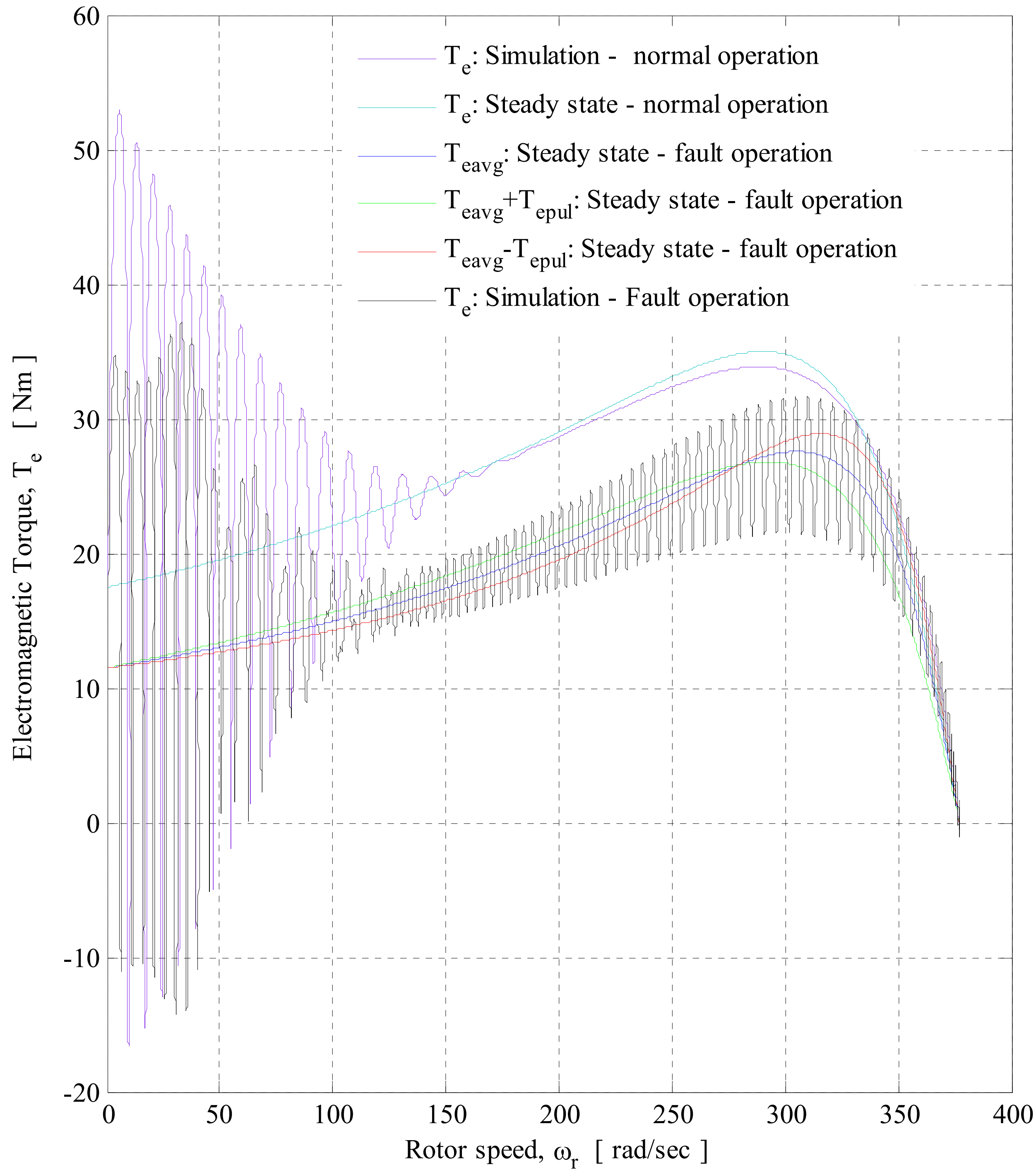

Figure 5.11. Various torque components of the five-phase induction machine under balanced and a stator phase open based on computer simulation and steady-state calculations.

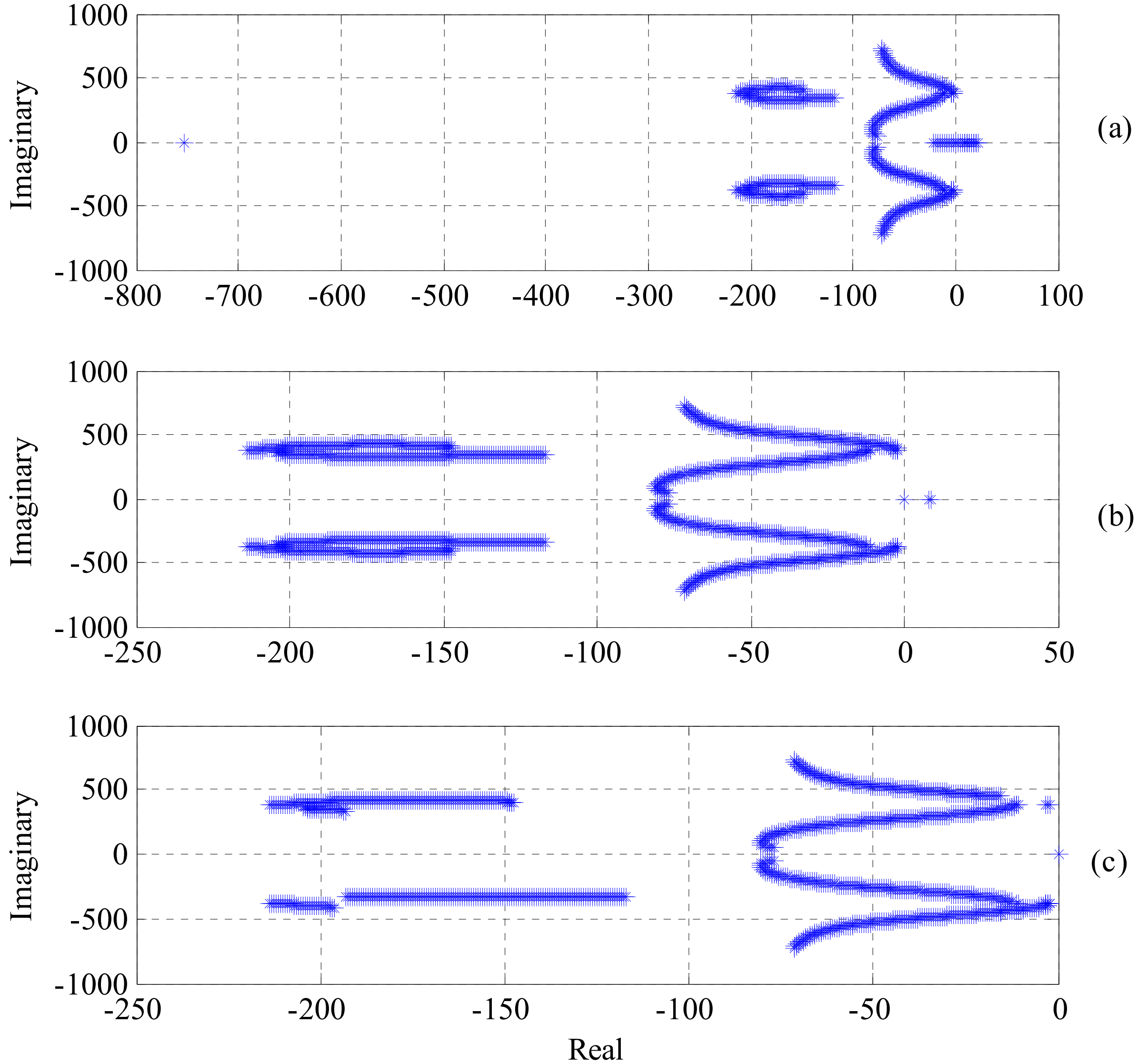

Figure 5.12. Small signal stability analysis (a) all state variables included (b) speed harmonics are not included (c) both speed harmonics and q-axis rotor flux linkage state variables are not included. (Rotor speed is varied from 0 to 377 rad/sec)

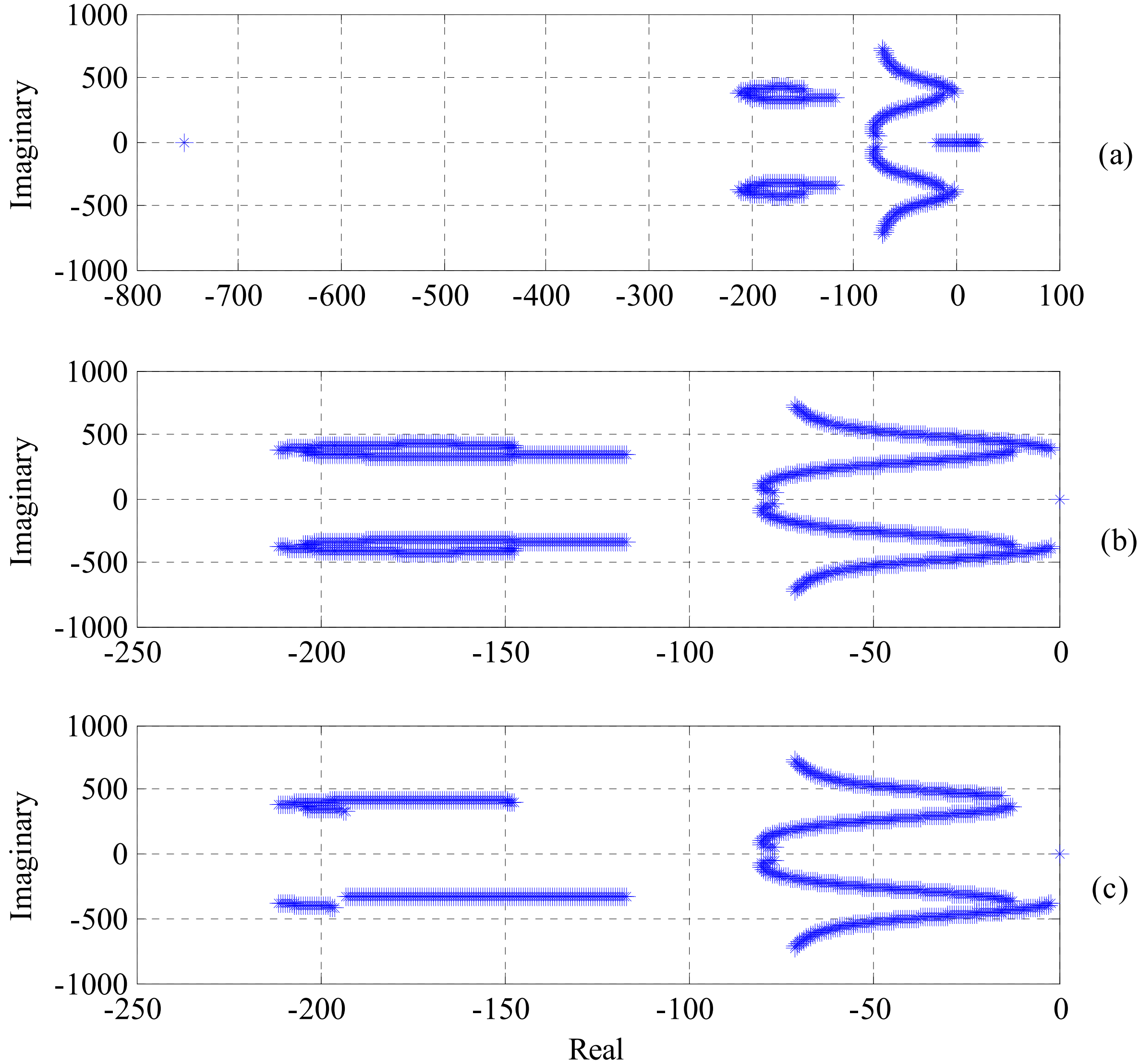

Figure 5.13. Small signal stability analysis (a) all state variables included (b) speed harmonics are not included (c) both speed harmonics and q-axis rotor flux linkage state variables are not included. (Rotor speed is varied from 11.78 to 377 rad/sec)

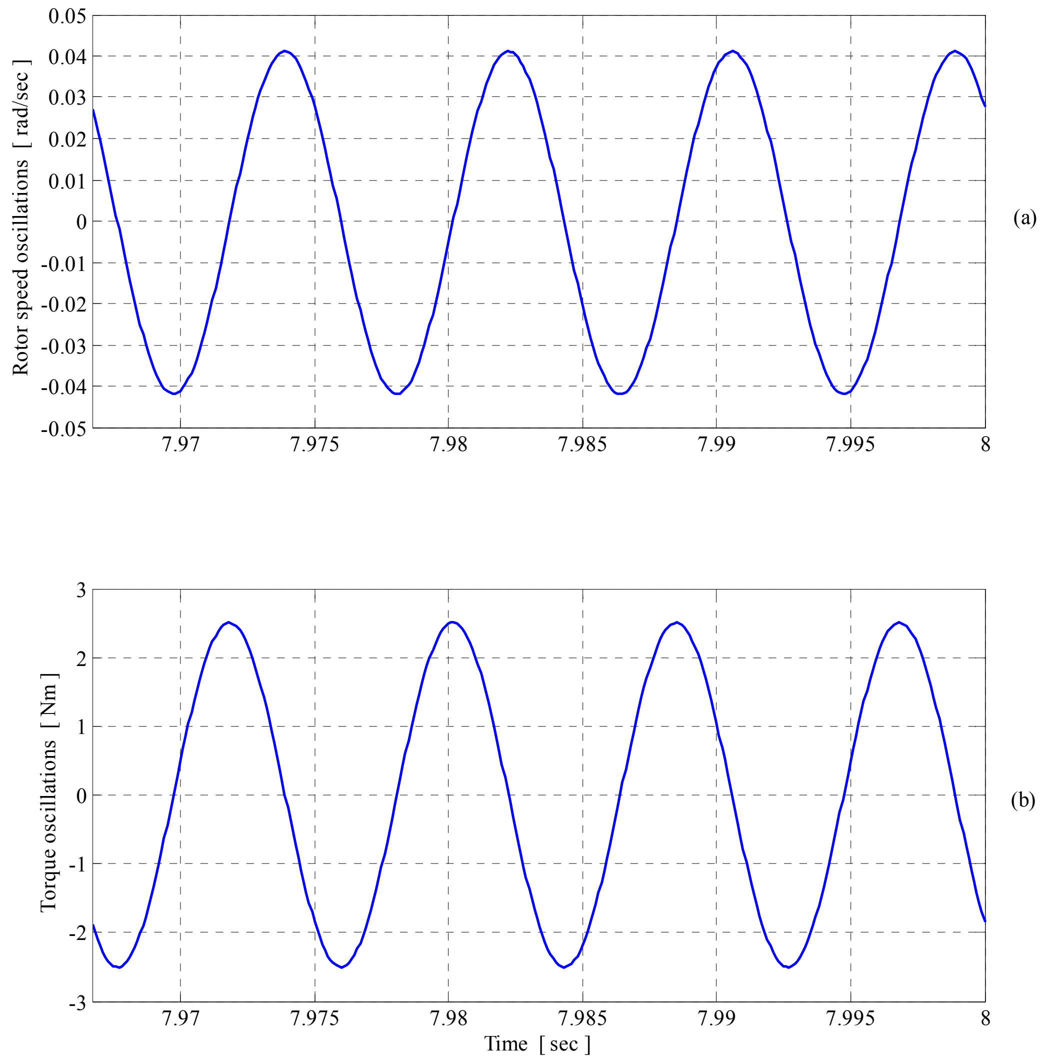

Figure 5.14 Simulation Steady-state (a) rotor speed oscillations and (b) electromagnetic torque oscillations at a load torque of 11 Nm.

5.4 Two Adjacent Phases ('a' and 'b') Open Circuited

The operation with two adjacent phases ('*a*' and '*b*') open on fault is depicted in Figure 5.15. When the two phases are open, the phase voltages across the machine phase windings '*a*' and '*b*' become unknown. Under this condition, all the *qdxyos* transformed voltages become unknown.

The following Equations will apply when the two stator phases "a" and "b" are open

$$i_{as} = 0 \tag{5.165}$$

$$i_{bs} = 0 \tag{5.166}$$

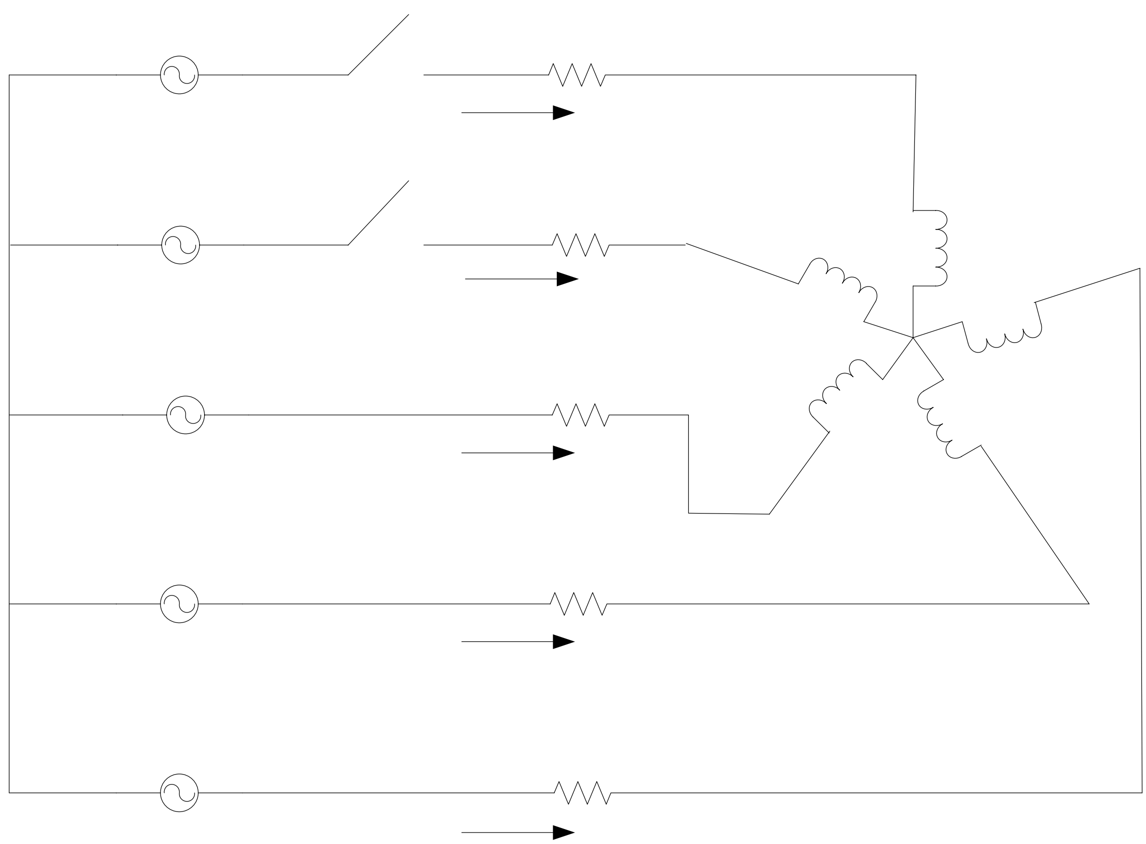

Figure 5.15 Open phases '*a*' and '*b*' of the stator for the five phase induction machine.

KCL requires that

$$i_{as} + i_{bs} + i_{cs} + i_{ds}^{a} + i_{es} = 0 \tag{5.167}$$

Therefore

$$i_{cs} + i_{ds}^{a} + i_{es} = 0 \tag{5.168}$$

Using Equations (5.35) and (5.37), the *q*- and *x*- axis voltages are related by

$$v_{qs} - v_{xs} = \frac{2}{5}\begin{bmatrix} \left[\cos\left(\frac{2\pi}{5}\right) - \cos\left(\frac{4\pi}{5}\right)\right]v_{bs} + \left[\cos\left(\frac{4\pi}{5}\right) - \cos\left(\frac{2\pi}{5}\right)\right]v_{cs} + \\ \left[\cos\left(\frac{4\pi}{5}\right) - \cos\left(\frac{2\pi}{5}\right)\right]v_{ds}^{a} + \left[\cos\left(\frac{2\pi}{5}\right) - \cos\left(\frac{4\pi}{5}\right)\right]v_{es} \end{bmatrix} \tag{5.169}$$

$$v_{qs} - v_{xs} = \frac{2}{5}\begin{bmatrix} \left[\cos\left(\frac{2\pi}{5}\right) - \cos\left(\frac{4\pi}{5}\right)\right]v_{bs} - \left[\cos\left(\frac{2\pi}{5}\right) - \cos\left(\frac{4\pi}{5}\right)\right]v_{cs} \\ -\left[\cos\left(\frac{2\pi}{5}\right) - \cos\left(\frac{4\pi}{5}\right)\right]v_{ds}^{a} + \left[\cos\left(\frac{2\pi}{5}\right) - \cos\left(\frac{4\pi}{5}\right)\right]v_{es} \end{bmatrix} \tag{5.170}$$

$$v_{qs} - v_{xs} = \frac{2}{5}\left(\cos\left(\frac{2\pi}{5}\right) - \cos\left(\frac{4\pi}{5}\right)\right)\left(v_{bs} - v_{cs} - v_{ds}^{a} + v_{es}\right) \tag{5.171}$$

From Equations (5.39), (5.167) and (5.168) it can be shown by KCL that

$$i_{os} = \frac{1}{5}\left(i_{as} + i_{bs} + i_{cs} + i_{ds}^{a} + i_{es}\right) = 0 \tag{5.172}$$

$$i_{os} = \frac{1}{5}\left(i_{cs} + i_{ds}^{a} + i_{es}\right) = 0 \tag{5.173}$$

Therefore,

$$i_{os} = 0 \tag{5.174}$$

This leads to

$$\lambda_{os} = L_{ls} i_{os} = 0 \tag{5.175}$$

$$v_{os} = r_s i_{os} + p\lambda_{os} = 0 \tag{5.176}$$

Using Equations (5.39) and (5.176) guives

$$v_{as} + v_{bs} = -\left(v_{cs} + v_{ds}^{a} + v_{es}\right) \tag{5.177}$$

Equation (5.35) is re-written as (5.178)

$$v_{as} = \frac{5}{2}v_{qs} - \left[\cos\left(\frac{2\pi}{5}\right)v_{bs} + \cos\left(\frac{4\pi}{5}\right)v_{cs} + \cos\left(\frac{4\pi}{5}\right)v_{ds}^{a} + \cos\left(\frac{2\pi}{5}\right)v_{es}\right] \tag{5.178}$$

Substituting for v_{as} from (5.178) into (5.177) gives

$$v_{bs} = \frac{1}{\left(1 - \cos\left(\frac{2\pi}{5}\right)\right)}\begin{bmatrix} -\frac{5}{2}v_{qs} - \left(1 - \cos\left(\frac{4\pi}{5}\right)\right)v_{cs} \\ -\left(1 - \cos\left(\frac{4\pi}{5}\right)\right)v_{ds}^{a} - \left(1 - \cos\left(\frac{2\pi}{5}\right)\right)v_{es} \end{bmatrix} \tag{5.179}$$

$$v_{bs} = xv_{qs} + yv_{cs} + zv_{ds}^{a} + \gamma v_{es} \tag{5.180}$$

where

$$x = -\frac{5}{2}\frac{1}{1 - \cos\frac{2\pi}{5}}$$

$$y = \frac{1}{1 - \cos\frac{2\pi}{5}}\left(\cos\frac{4\pi}{5} - 1\right)$$

$$z = \frac{1}{1 - \cos\frac{2\pi}{5}}\left(\cos\frac{4\pi}{5} - 1\right)$$

$$\gamma = \frac{1}{1 - \cos\frac{2\pi}{5}}\left(\cos\frac{2\pi}{5} - 1\right)$$

Substituting for v_{bs} from (5.180) into (5.171) gives

$$\left[1 - \frac{2}{5}\begin{pmatrix} \cos\left(\frac{2\pi}{5}\right) \\ -\cos\left(\frac{4\pi}{5}\right) \end{pmatrix}x\right]v_{qs} - v_{xs} = \frac{2}{5}\left(\cos\left(\frac{2\pi}{5}\right) - \cos\left(\frac{4\pi}{5}\right)\right)\begin{pmatrix} (y-1)v_{cs} + (z-1)v_{ds}^{a} \\ + (\gamma + 1)v_{es} \end{pmatrix} \tag{5.181}$$

$$\left[1-\frac{2}{5}\alpha x\right]v_{qs}-v_{xs}=\frac{2}{5}\alpha\left((y-1)v_{cs}+(z-1)v_{ds}^{a}+(\gamma+1)v_{es}\right) \tag{5.182}$$

$$\left[1-\frac{2}{5}\alpha x\right]v_{qs}-v_{xs}=\frac{2}{5}\alpha(y-1)v_{cs}+\frac{2}{5}\alpha(z-1)v_{ds}^{a}+\frac{2}{5}\alpha(\gamma+1)v_{es} \tag{5.183}$$

$$av_{qs}-v_{xs}=bv_{cs}+cv_{ds}^{a}+dv_{es} \tag{5.184}$$

where

$$\alpha=\cos\frac{2\pi}{5}-\cos\frac{4\pi}{5}$$

$$a=1-\frac{2}{5}\alpha x$$

$$b=\frac{2}{5}\alpha(y-1)$$

$$c=\frac{2}{5}\alpha(z-1)$$

$$d=\frac{2}{5}\alpha(\gamma+1)$$

Substituting (5.180) into (5.177) results into

$$v_{as}=\frac{5}{2}v_{qs}-\left[xv_{qs}+yv_{cs}+zv_{ds}^{a}+\gamma v_{es}\right]\cos\frac{2\pi}{5}-v_{cs}\cos\frac{4\pi}{5}-v_{ds}^{a}\cos\frac{4\pi}{5}-v_{es}\cos\frac{2\pi}{5} \tag{5.185}$$

$$v_{as}=\begin{bmatrix}\left(\frac{5}{2}-x\cos\frac{2\pi}{5}\right)v_{qs}-\left(y\cos\frac{2\pi}{5}+\cos\frac{4\pi}{5}\right)v_{cs}-\left(z\cos\frac{2\pi}{5}+\cos\frac{4\pi}{5}\right)v_{ds}^{a}\\ -\left(\gamma\cos\frac{2\pi}{5}+\cos\frac{2\pi}{5}\right)v_{es}\end{bmatrix} \tag{5.186}$$

$$v_{as}=t_1v_{qs}+t_2v_{cs}+t_3v_{ds}^{a}+t_4v_{es} \tag{5.187}$$

where

$$t_1=\left(\frac{5}{2}-x\cos\frac{2\pi}{5}\right)$$

$$t_2 = -\left(y\cos\frac{2\pi}{5} + \cos\frac{4\pi}{5} \right)$$

$$t_3 = -\left(z\cos\frac{2\pi}{5} + \cos\frac{4\pi}{5} \right)$$

$$t_4 = -\left(\gamma\cos\frac{2\pi}{5} + \cos\frac{2\pi}{5} \right)$$

The d-axis voltage is given by

$$v_{ds} = \frac{2}{5}\left(-v_{bs}\sin\frac{2}{5}\pi - v_{cs}\sin\frac{4}{5}\pi + v_{ds}^{a}\sin\frac{4}{5}\pi + v_{es}\sin\frac{2}{5}\pi \right) \tag{5.188}$$

Substituting (5.180) into (5.188) gives

$$v_{ds} = \frac{2}{5}\left(-\left(xv_{qs} + yv_{cs} + zv_{ds}^{a} + \gamma v_{es} \right)\sin\frac{2}{5}\pi - v_{cs}\sin\frac{4}{5}\pi + v_{ds}^{a}\sin\frac{4}{5}\pi + v_{es}\sin\frac{2}{5}\pi \right)$$

$$v_{ds} = -\frac{2}{5}xv_{qs}\sin\frac{2}{5}\pi + \frac{2}{5}\begin{pmatrix} -yv_{cs}\sin\frac{2}{5}\pi - zv_{ds}^{a}\sin\frac{2}{5}\pi - \gamma v_{es}\sin\frac{2}{5}\pi \\ -v_{cs}\sin\frac{4}{5}\pi + v_{ds}^{a}\sin\frac{4}{5}\pi + v_{es}\sin\frac{2}{5}\pi \end{pmatrix}$$

$$v_{ds} = \left[-\frac{2}{5}x\sin\frac{2}{5}\pi v_{qs} + \frac{2}{5}\begin{pmatrix} -\left(y\sin\frac{2}{5}\pi + \sin\frac{4}{5}\pi \right)v_{cs} - \left(z\sin\frac{2}{5}\pi - \sin\frac{4}{5}\pi \right)v_{ds}^{a} \\ -\left(\gamma\sin\frac{2}{5}\pi - \sin\frac{2}{5}\pi \right)v_{es} \end{pmatrix} \right] \tag{5.189}$$

$$v_{ds} = t_5 v_{qs} + t_6 v_{cs} + t_7 v_{ds}^{a} + t_8 v_{es} \tag{5.190}$$

where

$$t_5 = -\frac{2}{5}x\sin\frac{2}{5}\pi$$

$$t_6 = -\frac{2}{5}\left(y\sin\frac{2}{5}\pi + \sin\frac{4}{5}\pi \right)$$

$$t_7 = -\frac{2}{5}\left(z\sin\frac{2}{5}\pi - \sin\frac{4}{5}\pi\right)$$

$$t_8 = -\frac{2}{5}\left(\gamma\sin\frac{2}{5}\pi - \sin\frac{2}{5}\pi\right)$$

The y-axis voltage is given by

$$v_{ys} = \frac{2}{5}\left(-v_{bs}\sin\frac{4\pi}{5} + v_{cs}\sin\frac{2\pi}{5} - v_{ds}^{a}\sin\frac{2\pi}{5} + v_{es}\sin\frac{4\pi}{5}\right) \tag{5.191}$$

Substituting (5.180) into (5.191) results into

$$v_{ys} = \begin{bmatrix} -\frac{2}{5}x\sin\frac{4\pi}{5}v_{qs} - \frac{2}{5}\left(y\sin\frac{4\pi}{5} - \sin\frac{2\pi}{5}\right)v_{cs} \\ -\frac{2}{5}\left(z\sin\frac{4\pi}{5} + \sin\frac{2\pi}{5}\right)v_{ds}^{a} - \frac{2}{5}\left(\gamma\sin\frac{4\pi}{5} - \sin\frac{4\pi}{5}\right)v_{es} \end{bmatrix} \tag{5.192}$$

$$v_{ys} = t_9 v_{qs} + t_{10} v_{cs} + t_{11} v_{ds}^{a} + t_{12} v_{es} \tag{5.193}$$

where

$$t_9 = -\frac{2}{5}x\sin\frac{4\pi}{5}$$

$$t_{10} = -\frac{2}{5}\left(y\sin\frac{4\pi}{5} - \sin\frac{2\pi}{5}\right)$$

$$t_{11} = -\frac{2}{5}\left(z\sin\frac{4\pi}{5} + \sin\frac{2\pi}{5}\right)$$

$$t_{12} = -\frac{2}{5}\left(\gamma\sin\frac{4\pi}{5} - \sin\frac{4\pi}{5}\right)$$

Since $i_{xs} = -i_{qs}$, then

$$v_{xs} = -r_s i_{qs} - L_{ls} p i_{qs} \tag{5.194}$$

Substituting (5.194) into (5.184) gives

$$a v_{qs} + r_s i_{qs} + L_{ls} p i_{qs} = b v_{cs} + c v_{ds}^{a} + d v_{es} \tag{5.195}$$

Substituting for the stator and the rotor current, the q-axis stator voltage Equation becomes

$$pi_{qs} = \frac{1}{L_s L_r - L_m^2}\left(L_r v_{qs} - r_s i_{qs} L_r - L_m p\lambda_{qr}\right) \tag{5.196}$$

Substituting for pi_{qs} from (5.196) into (5.195) gives

$$av_{qs} + \frac{L_{ls} L_r}{L_s L_r - L_m^2} v_{qs} + r_s i_{qs} - \frac{L_{ls}}{L_s L_r - L_m^2}\left(r_s i_{qs} L_r + L_m p\lambda_{qr}\right) = bv_{cs} + cv_{ds}^a + dv_{es}$$

$$\left(a + \frac{L_{ls} L_r}{L_s L_r - L_m^2}\right) v_{qs} = bv_{cs} + cv_{ds}^a + dv_{es} - r_s i_{qs} + \frac{L_{ls}}{L_s L_r - L_m^2}\left(r_s i_{qs} L_r + L_m p\lambda_{qr}\right)$$

$$v_{qs} = \frac{1}{\left(a + \frac{L_{ls} L_r}{L_s L_r - L_m^2}\right)}\left[bv_{cs} + cv_{ds}^a + dv_{es} - r_s i_{qs} + \frac{L_{ls}}{L_s L_r - L_m^2}\left(r_s i_{qs} L_r + L_m p\lambda_{qr}\right)\right] \tag{5.197}$$

Therefore, with v_{as}, v_{cs}, v_{qs}, v_{ds} and v_{ys} known, then the faulted condition can be simulated by using the following dynamic Equations

The q-axis stator dynamic Equation is

$$pi_{qs} = \frac{1}{L_s L_r - L_m^2}\left(L_r v_{qs} - r_s i_{qs} L_r - L_m p\lambda_{qr}\right) \tag{5.198}$$

The d-axis stator dynamic Equation is

$$pi_{ds} = \frac{1}{\left(L_s L_r - L_m^2\right)}\left(L_r v_{ds} - r_s i_{ds} L_r - L_m p\lambda_{dr}\right) \tag{5.199}$$

The y-axis stator dynamic Equation is

$$pi_{ys} = \frac{1}{L_{ls}}\left(v_{ys} - r_s i_{ys}\right) \tag{5.200}$$

The phase currents are obtained as

$$i_{as} = i_{qs} + i_{xs} \tag{5.201}$$

$$i_{bs} = -i_{qs} - i_{xs} \tag{5.202}$$

$$i_{cs} = \left[\frac{5}{2\left(\sin\frac{2\pi}{5} - \sin\frac{4\pi}{5}\right)} + \frac{5}{4\sin\frac{4\pi}{5}}\right] i_{ds} - \frac{5}{4\sin\frac{4\pi}{5}} i_{ys} \tag{5.203}$$

$$i_{ds}^{a} = -\frac{5}{2\left(\sin\frac{2\pi}{5} - \sin\frac{4\pi}{5}\right)} i_{ds} \tag{5.204}$$

$$i_{es} = \frac{5}{4\sin\frac{4\pi}{5}}\left(i_{ys} - i_{ds}\right) \tag{5.205}$$

5.4.1 Harmonic Balance Technique for the Two Adjacent Open Phase Faults

The same approach that has been used in section 5.3.1 applies here as well.

Let

$$\sigma_1 = \frac{1}{\left(a + \frac{L_{ls} L_r}{L_s L_r - L_m^2}\right)}$$

Then Equation (5.197) can be written as

$$v_{qs} = \sigma_1 \left[b v_{cs} + c v_{ds}^{a} + d v_{es} - r_s i_{qs} + \frac{L_{ls}}{L_s L_r - L_m^2}\left(r_s i_{qs} L_r + L_m p \lambda_{qr}\right)\right] \tag{5.206}$$

Using Equations (5.61) through (5.84), the following harmonic balance technique dynamic model is obtained

The q-axis stator voltage is given by

$$v_{qss} = \sigma_1 \left[bv_{css} + cv_{dss}^a + dv_{ess} - r_s i_{qss} + \frac{L_{ls}}{L_s L_r - L_m^2}\left(r_s L_r i_{qss} + L_m p\lambda_{qrr} + j\omega_e L_m \lambda_{qrr} \right) \right] \quad (5.207)$$

The q-axis stator voltage Equation is given by

$$pi_{qss} + j\omega_e i_{qss} = \frac{1}{L_s L_r - L_m^2}\left(L_r v_{qss} - r_s L_r i_{qss} - L_m p\lambda_{qrr} - j\omega_e L_m \lambda_{qrr} \right) \quad (5.208)$$

The d-axis stator voltage Equation is given by

$$pi_{dss} + j\omega_e i_{dss} = \frac{1}{\left(L_s L_r - L_m^2 \right)}\left(L_r v_{dss} - r_s i_{dss} L_r - L_m p\lambda_{drr} - j\omega_e L_m \lambda_{drr} \right) \quad (5.209)$$

The d-axis stator voltage Equation is given by

$$pi_{yss} + j\omega_e i_{yss} = \frac{1}{L_{ls}}\left(v_{yss} - r_s i_{yss} \right) \quad (5.210)$$

The q-axis rotor voltage Equation is given by

$$p\lambda_{qrr} + j\omega_e \lambda_{qrr} = v_{qrr} - \frac{r_r}{L_r}\left(\lambda_{qrr} - L_m i_{qss} \right) + \omega_{ro}\lambda_{drr} + \frac{1}{2}\omega_{r1}\lambda_{drr}^* \quad (5.211)$$

The q-axis rotor voltage Equation is given by

$$p\lambda_{drr} + j\omega_e \lambda_{drr} = v_{drr} - \frac{r_r}{L_r}\left(\lambda_{drr} - L_m i_{dss} \right) - \omega_{ro}\lambda_{qrr} - \frac{1}{2}\omega_{r1}\lambda_{qrr}^* \quad (5.212)$$

5.4.2 Steady State and Dynamic Model Analysis for Two Adjacent Open Phases

5.4.2.1 Steady state model. At steady state, the derivatives of the peaks are zero. Therefore, the above Equations (5.206) through (5.212) become

$$-\sigma_1\left(bv_{css} + cv_{dss}^a + dv_{ess} \right) = -v_{qss} + \left(\frac{r_s L_r L_{ls}}{L_s L_r - L_m^2} - r_s \right)\sigma_1 i_{qss} + \frac{j\omega_e L_m L_{ls}\sigma_1}{L_s L_r - L_m^2}\lambda_{qrr} \quad (5.213)$$

$$0=\frac{L_r}{L_sL_r-L_m^2}v_{qss}-\left(\frac{r_sL_r}{L_sL_r-L_m^2}+j\omega_e\right)i_{qss}-\frac{j\omega_eL_m}{L_sL_r-L_m^2}\lambda_{qrr} \tag{5.214}$$

$$0=\frac{L_r}{L_sL_r-L_m^2}v_{dss}-\left(\frac{r_sL_r}{L_sL_r-L_m^2}+j\omega_e\right)i_{dss}-\frac{j\omega_eL_m}{L_sL_r-L_m^2}\lambda_{drr} \tag{5.215}$$

$$0=\frac{1}{L_{ls}}v_{yss}-\left(\frac{r_s}{L_{ls}}+j\omega_e\right)i_{yss} \tag{5.216}$$

$$-v_{qrr}=\frac{r_rL_m}{L_r}i_{qss}-\left(\frac{r_r}{L_r}+j\omega_e\right)\lambda_{qrr}+\omega_{ro}\lambda_{drr}+\frac{1}{2}\omega_{r1}\lambda_{drr}^{*} \tag{5.217}$$

$$-v_{drr}=-\omega_{ro}\lambda_{qrr}-\frac{1}{2}\omega_{r1}\lambda_{qrr}^{*}-\left(\frac{r_r}{L_r}+j\omega_e\right)\lambda_{drr}+\frac{r_rL_m}{L_r}i_{dss} \tag{5.218}$$

The d-axis and y-axis stator voltages, respectively, given by (5.219) and (5.220)

$$t_6v_{css}+t_7v_{dss}^a+t_8v_{ess}=-t_5v_{qss}+v_{dss} \tag{5.219}$$

$$t_{10}v_{css}+t_{11}v_{dss}^a+t_{12}v_{ess}=-t_9v_{qss}+v_{yss} \tag{5.220}$$

Equations (5.213) through (5.220) can be represented in matrix form as

$$A_1x_1=b_1 \tag{5.221}$$

$$x_1=A_1^{-1}b_1 \tag{5.222}$$

where the matrices b_1 and x_1 are, respectively, given by Equations (5.223) and (5.224), with

$b_{111}=-\sigma_1\left(bv_{css}+cv_{dss}^a+dv_{ess}\right)$, $b_{171}=t_6v_{css}+t_7v_{dss}^a+t_8v_{ess}$, $b_{181}=t_{10}v_{css}+t_{11}v_{dss}^a+t_{12}v_{ess}$

$$b_1=\begin{bmatrix}b_{111} & 0 & 0 & 0 & -v_{qrr} & -v_{drr} & b_{171} & b_{181}\end{bmatrix}^T \tag{5.223}$$

$$x_1=\begin{bmatrix}v_{qss} & v_{dss} & v_{yss} & i_{qss} & i_{dss} & i_{yss} & \lambda_{qrr} & \lambda_{drr}\end{bmatrix}^T \tag{5.224}$$

The matrix A_1 is given by Equation (5.225).

$$A_1 = \begin{bmatrix} -1 & 0 & 0 & \left(\dfrac{r_s L_r L_{ls}}{L_s L_r - L_m^2} - r_s\right)\sigma_1 & 0 & 0 & \dfrac{j\omega_e L_m L_{ls}\sigma_1}{L_s L_r - L_m^2} & 0 \\ \dfrac{L_r}{L_s L_r - L_m^2} & 0 & 0 & -\left(\dfrac{r_s L_r}{L_s L_r - L_m^2} + j\omega_e\right) & 0 & 0 & -\dfrac{j\omega_e L_m}{L_s L_r - L_m^2} & 0 \\ 0 & \dfrac{L_r}{L_s L_r - L_m^2} & 0 & 0 & -\left(\dfrac{r_s L_r}{L_s L_r - L_m^2} + j\omega_e\right) & 0 & 0 & -\dfrac{j\omega_e L_m}{L_s L_r - L_m^2} \\ 0 & 0 & \dfrac{1}{L_{ls}} & 0 & 0 & -\left(\dfrac{r_s}{L_{ls}} + j\omega_e\right) & 0 & 0 \\ 0 & 0 & 0 & \dfrac{r_r L_m}{L_r} & 0 & 0 & -\left(\dfrac{r_r}{L_r} + j\omega_e\right) & \omega_{ro} \\ 0 & 0 & 0 & 0 & \dfrac{r_r L_m}{L_r} & 0 & -\omega_{ro} & -\left(\dfrac{r_r}{L_r} + j\omega_e\right) \\ -t_5 & 1 & 0 & 0 & 0 & 0 & 0 & 0 \\ -t_9 & 0 & 1 & 0 & 0 & 0 & 0 & 0 \end{bmatrix} \tag{5.225}$$

When the speed harmonic component is taken into account, then the Equations have to be separate into their real and imaginary parts. The resulting systems of steady-state Equations will be solved by iteration to obtain the results.

Now let,

$$v_{qss} = v_{qsre} + jv_{qsim} \tag{5.226}$$

$$v_{dss} = v_{dsre} + jv_{dsim} \tag{5.227}$$

$$v_{yss} = v_{ysre} + jv_{ysim} \tag{5.228}$$

$$v_{dss}^{a} = v_{dsre}^{a} + jv_{dsim}^{a} \tag{5.229}$$

$$v_{css} = v_{csre} + jv_{csim} \tag{5.230}$$

$$v_{ess} = v_{esre} + jv_{esim} \tag{5.231}$$

$$\omega_{r1} = j\omega_{r1im}$$

Substituting these Equations (5.109) through (5.116) and (5.226) through (5.231) into Equations (5.213) through (5.220), the steady state model comprising of the real Equations is obtained as

From Equation (5.213),

$$-\sigma_1\begin{bmatrix} b(v_{csre} + jv_{csim}) + c(v_{dsre}^{a} + jv_{dsim}^{a}) \\ + d(v_{esre} + jv_{esim}) \end{bmatrix} = \begin{bmatrix} -v_{qsre} - jv_{qsim} + \left(\dfrac{r_s L_r L_{ls}}{L_s L_r - L_m^2} - r_s\right)\sigma_1\left(i_{qsre} + ji_{qsim}\right) \\ + \dfrac{j\omega_e L_m L_{ls}\sigma_1}{L_s L_r - L_m^2}\left(\lambda_{qrre} + j\lambda_{qrim}\right) \end{bmatrix}$$

$$-\sigma_1\begin{bmatrix} b(v_{csre} + jv_{csim}) + c(v_{dsre}^{a} + jv_{dsim}^{a}) \\ + d(v_{esre} + jv_{esim}) \end{bmatrix} = \begin{bmatrix} \begin{pmatrix} -v_{qsre} \\ -jv_{qsim} \end{pmatrix} + \left(\dfrac{r_s L_r L_{ls}}{L_s L_r - L_m^2} - r_s\right)\sigma_1\begin{pmatrix} i_{qsre} \\ + ji_{qsim} \end{pmatrix} \\ + \dfrac{\omega_e L_m L_{ls}\sigma_1}{L_s L_r - L_m^2}\begin{pmatrix} -\lambda_{qrim} \\ + j\lambda_{qrre} \end{pmatrix} \end{bmatrix} \tag{5.232}$$

Separating real and imaginary parts,

$$-\sigma_1\left[bv_{csre}+cv_{dsre}^{a}+dv_{esre}\right]=-v_{qsre}+\left(\frac{r_sL_rL_{ls}}{L_sL_r-L_m^2}-r_s\right)\sigma_1 i_{qsre}-\frac{\omega_eL_mL_{ls}\sigma_1}{L_sL_r-L_m^2}\lambda_{qrim} \qquad (5.233)$$

$$-\sigma_1\left[bv_{csim}+cv_{dsim}^{a}+dv_{esim}\right]=\left[-v_{qsim}+\left(\frac{r_sL_rL_{ls}}{L_sL_r-L_m^2}-r_s\right)\sigma_1 i_{qsim}+\frac{\omega_eL_mL_{ls}\sigma_1}{L_sL_r-L_m^2}\lambda_{qrre}\right] \qquad (5.234)$$

From Equation (5.214),

$$0=\frac{L_r}{L_sL_r-L_m^2}\left(v_{qsre}+jv_{qsim}\right)-\left(\frac{r_sL_r}{L_sL_r-L_m^2}+j\omega_e\right)\left(i_{qsre}+ji_{qsim}\right)-\frac{j\omega_eL_m}{L_sL_r-L_m^2}\left(\lambda_{qrre}+j\lambda_{qrim}\right)$$

$$0=\left[\begin{array}{l}\frac{L_r}{L_sL_r-L_m^2}\left(v_{qsre}+jv_{qsim}\right)-\left(\frac{r_sL_r}{L_sL_r-L_m^2}i_{qsre}+j\omega_e i_{qsre}\right)\\ -\left(\frac{jr_sL_r}{L_sL_r-L_m^2}i_{qsim}-\omega_e i_{qsim}\right)-\frac{j\omega_eL_m}{L_sL_r-L_m^2}\lambda_{qrre}+\frac{\omega_eL_m}{L_sL_r-L_m^2}\lambda_{qrim}\end{array}\right] \qquad (5.235)$$

Separating the real and imaginary parts

$$0=\frac{L_r}{L_sL_r-L_m^2}v_{qsre}-\frac{r_sL_r}{L_sL_r-L_m^2}i_{qsre}+\omega_e i_{qsim}+\frac{\omega_eL_m}{L_sL_r-L_m^2}\lambda_{qrim} \qquad (5.236)$$

$$0=\frac{L_r}{L_sL_r-L_m^2}v_{qsim}-\omega_e i_{qsre}-\frac{r_sL_r}{L_sL_r-L_m^2}i_{qsim}-\frac{\omega_eL_m}{L_sL_r-L_m^2}\lambda_{qrre} \qquad (5.237)$$

From Equation (5.215),

$$0=\frac{L_r}{L_sL_r-L_m^2}\left(v_{dsre}+jv_{dsim}\right)-\left(\frac{r_sL_r}{L_sL_r-L_m^2}+j\omega_e\right)\left(i_{dsre}+ji_{dsim}\right)-\frac{j\omega_eL_m}{L_sL_r-L_m^2}\left(\lambda_{drre}+j\lambda_{drim}\right)$$

$$0=\left[\begin{array}{l}\frac{L_r}{L_sL_r-L_m^2}\left(v_{dsre}+jv_{dsim}\right)-\left(\frac{r_sL_r}{L_sL_r-L_m^2}i_{dsre}+j\omega_e i_{dsre}\right)\\ -\left(\frac{jr_sL_r}{L_sL_r-L_m^2}i_{dsim}-\omega_e i_{dsim}\right)-\frac{j\omega_eL_m}{L_sL_r-L_m^2}\lambda_{drre}+\frac{\omega_eL_m}{L_sL_r-L_m^2}\lambda_{drim}\end{array}\right] \qquad (5.238)$$

Separating the real and imaginary parts

$$0=L_{22}v_{dsre}-r_sL_{22}i_{dsre}+\omega_e i_{dsim}+L_{11}\lambda_{drim} \qquad (5.239)$$

$$0 = L_{22} v_{dsim} - \omega_e i_{dsre} - r_s L_{22} i_{dsim} - L_{11} \lambda_{drre} \tag{5.240}$$

From Equation (5.216),

$$0 = \frac{1}{L_{ls}}\left(v_{ysre} + jv_{ysim}\right) - \left(\frac{r_s}{L_{ls}} + j\omega_e\right)\left(i_{ysre} + ji_{ysim}\right)$$

$$0 = \frac{1}{L_{ls}}\left(v_{ysre} + jv_{ysim}\right) - \left(\frac{r_s}{L_{ls}} i_{ysre} + j\omega_e i_{ysre}\right) - \left(\frac{jr_s}{L_{ls}} i_{ysim} - \omega_e i_{ysim}\right) \tag{5.241}$$

Separating the real and imaginary parts

$$0 = L_{33} v_{ysre} - L_{44} i_{ysre} + \omega_e i_{ysim} \tag{5.242}$$

$$0 = L_{33} v_{ysim} - \omega_e i_{ysre} - L_{44} i_{ysim} \tag{5.243}$$

From Equation (5.217),

$$-v_{qrre} - jv_{qrim} = \begin{bmatrix} \frac{r_r L_m}{L_r}\left(i_{qsre} + ji_{qsim}\right) - \left(\frac{r_r}{L_r} + j\omega_e\right)\left(\lambda_{qrre} + j\lambda_{qrim}\right) \\ + \omega_{ro}\left(\lambda_{drre} + j\lambda_{drim}\right) + \frac{1}{2} j\omega_{r1im}\left(\lambda_{drre} - j\lambda_{drim}\right) \end{bmatrix}$$

$$-v_{qrre} - jv_{qrim} = \begin{bmatrix} \frac{r_r L_m}{L_r}\left(i_{qsre} + ji_{qsim}\right) - \left(\frac{r_r}{L_r}\lambda_{qrre} + j\omega_e \lambda_{qrre}\right) - \left(\frac{jr_r}{L_r}\lambda_{qrim} - \omega_e \lambda_{qrim}\right) \\ + \omega_{ro}\lambda_{drre} + j\omega_{ro}\lambda_{drim} + j\frac{1}{2}\omega_{r1im}\lambda_{drre} + \frac{1}{2}\omega_{r1im}\lambda_{drim} \end{bmatrix} \tag{5.244}$$

Separating the real and imaginary parts

$$-v_{qrre} = L_{55} i_{qsre} - L_{66}\lambda_{qrre} + \omega_e \lambda_{qrim} + \omega_{ro}\lambda_{drre} + \frac{1}{2}\omega_{r1im}\lambda_{drim} \tag{5.245}$$

$$-v_{qrim} = L_{55} i_{qsim} - \omega_e \lambda_{qrre} - L_{66}\lambda_{qrim} + \omega_{ro}\lambda_{drim} + \frac{1}{2}\omega_{r1im}\lambda_{drre} \tag{5.246}$$

From Equation (5.218),

$$-v_{drre}-jv_{drim}=\begin{bmatrix}-\omega_{ro}\left(\lambda_{qrre}+j\lambda_{qrim}\right)-\frac{1}{2}j\omega_{r1}\left(\lambda_{qrre}-j\lambda_{qrim}\right)-\left(\frac{r_r}{L_r}+j\omega_e\right)\left(\lambda_{drre}+j\lambda_{drim}\right)\\+\frac{r_rL_m}{L_r}\left(i_{dsre}+ji_{dsim}\right)\end{bmatrix}$$

$$-v_{drre}-jv_{drim}=\begin{bmatrix}-\omega_{ro}\lambda_{qrre}-j\omega_{ro}\lambda_{qrim}-\left(j\frac{1}{2}\omega_{r1}\lambda_{qrre}+\frac{1}{2}\omega_{r1}\lambda_{qrim}\right)\\-\left(\frac{r_r}{L_r}\lambda_{drre}+j\omega_e\lambda_{drre}\right)-\left(\frac{jr_r}{L_r}\lambda_{drim}-\omega_e\lambda_{drim}\right)+\frac{r_rL_m}{L_r}\begin{pmatrix}i_{dsre}\\+ji_{dsim}\end{pmatrix}\end{bmatrix}\tag{5.247}$$

Separating the real and imaginary parts

$$-v_{drre}=-\omega_{ro}\lambda_{qrre}-\frac{1}{2}\omega_{r1}\lambda_{qrim}-L_{66}\lambda_{drre}+\omega_e\lambda_{drim}+L_{55}i_{dsre}\tag{5.248}$$

$$-v_{drim}=-\omega_{ro}\lambda_{qrim}-\frac{1}{2}\omega_{r1}\lambda_{qrre}-\omega_e\lambda_{drre}-L_{66}\lambda_{drim}+L_{55}i_{dsim}\tag{5.249}$$

From Equation (5.219),

$$\begin{bmatrix}t_6\left(v_{csre}+jv_{csim}\right)+t_7\left(v_{dsre}^a+jv_{dsim}^a\right)\\+t_8\left(v_{esre}+jv_{esim}\right)\end{bmatrix}=-t_5\left(v_{qsre}+jv_{qsim}\right)+v_{dsre}+jv_{dsim}\tag{5.250}$$

Separating the real and imaginary parts

$$t_6v_{csre}+t_7v_{dsre}^a+t_8v_{esre}=-t_5v_{qsre}+v_{dsre}\tag{5.251}$$

$$t_6v_{csim}+t_7v_{dsim}^a+t_8v_{esim}=-t_5v_{qsim}+v_{dsim}\tag{5.252}$$

From Equation (5.220),

$$\begin{bmatrix}t_{10}\left(v_{csre}+jv_{csim}\right)+t_{11}\left(v_{dsre}^a+jv_{dsim}^a\right)\\+t_{12}\left(v_{esre}+jv_{esim}\right)\end{bmatrix}=-t_9\left(v_{qsre}+jv_{qsim}\right)+v_{ysre}+jv_{ysim}\tag{5.253}$$

Separating the real and imaginary parts

$$t_{10}v_{csre}+t_{11}v_{dsre}^a+t_{12}v_{esre}=-t_9v_{qsre}+v_{ysre}\tag{5.254}$$

$$t_{10}v_{csim}+t_{11}v_{dsim}^a+t_{12}v_{esim}=-t_9v_{qsim}+v_{ysim}\tag{5.255}$$

These Equations can be written in matrix form as

$$A_2 x_2 = b_2 \tag{5.256}$$

$$x_2 = A_2^{-1} b_2 \tag{5.257}$$

where b_2 and x_2 are give by Equations (5.258) and (5.259), respectively, with

$$b_{211} = -\sigma_1 \left(b v_{csre} + c v_{dsre}^{a} + d v_{esre} \right)$$

$$b_{221} = -\sigma_1 \left(b v_{csim} + c v_{dsim}^{a} + d v_{esim} \right)$$

$$b_{2131} = t_6 v_{csre} + t_7 v_{dsre}^{a} + t_8 v_{esre}$$

$$b_{2141} = t_6 v_{csim} + t_7 v_{dsim}^{a} + t_8 v_{esim}$$

$$b_{2151} = t_{10} v_{csre} + t_{11} v_{dsre}^{a} + t_{12} v_{esre}$$

$$b_{2161} = t_{10} v_{csim} + t_{11} v_{dsim}^{a} + t_{12} v_{esim}$$

Let,

$$L_{oo} = \left(r_s L_{22} L_{ls} - r_s \right) \sigma_1 \qquad L_{11} = \frac{\omega_e L_m}{L_s L_r - L_m^2}$$

$$L_{22} = \frac{L_r}{L_s L_r - L_m^2} \qquad L_{33} = \frac{1}{L_{ls}}$$

$$L_{44} = \frac{r_s}{L_{ls}} \qquad L_{55} = \frac{r_r L_m}{L_r} \qquad L_{66} = \frac{r_r}{L_r}$$

Then the matrix A_2 is given by

$$b_2 = \begin{bmatrix} b_{211} & b_{221} & 0 & 0 & 0 & 0 & 0 & 0 & -v_{qrre} & -v_{qrim} & -v_{drre} & -v_{drim} & b_{2131} & b_{2141} & b_{2151} & b_{2161} \end{bmatrix}^T \tag{5.258}$$

$$x_2 = \begin{bmatrix} v_{qsre} & v_{qsim} & v_{dsre} & v_{dsim} & v_{ysre} & v_{ysim} & i_{qsre} & i_{qsim} & i_{dsre} & i_{dsim} & i_{ysre} & i_{ysim} & \lambda_{qrre} & \lambda_{qrim} & \lambda_{drre} & \lambda_{drim} \end{bmatrix}^T \tag{5.259}$$

$$A_2 = \begin{bmatrix}
-1 & 0 & 0 & 0 & 0 & 0 & L_{oo} & 0 & 0 & 0 & 0 & 0 & 0 & -L_{11}L_{ls}\sigma_1 & 0 & 0 \\
0 & -1 & 0 & 0 & 0 & 0 & 0 & L_{oo} & 0 & 0 & 0 & 0 & L_{11}L_{ls}\sigma_1 & 0 & 0 & 0 \\
L_{22} & 0 & 0 & 0 & 0 & 0 & -r_s L_{22} & \omega_e & 0 & 0 & 0 & 0 & 0 & L_{11} & 0 & 0 \\
0 & L_{22} & 0 & 0 & 0 & 0 & -\omega_e & -r_s L_{22} & 0 & 0 & 0 & 0 & -L_{11} & 0 & 0 & 0 \\
0 & 0 & L_{22} & 0 & 0 & 0 & 0 & 0 & -r_s L_{22} & \omega_e & 0 & 0 & 0 & 0 & 0 & L_{11} \\
0 & 0 & 0 & L_{22} & 0 & 0 & 0 & 0 & -\omega_e & -r_s L_{22} & 0 & 0 & 0 & 0 & -L_{11} & 0 \\
0 & 0 & 0 & 0 & L_{33} & 0 & 0 & 0 & 0 & 0 & -L_{44} & \omega_e & 0 & 0 & 0 & 0 \\
0 & 0 & 0 & 0 & 0 & L_{33} & 0 & 0 & 0 & 0 & -\omega_e & -L_{44} & 0 & 0 & 0 & 0 \\
0 & 0 & 0 & 0 & 0 & 0 & L_{55} & 0 & 0 & 0 & 0 & 0 & -L_{66} & \omega_e & \omega_{ro} & \frac{1}{2}\omega_{r1im} \\
0 & 0 & 0 & 0 & 0 & 0 & 0 & L_{55} & 0 & 0 & 0 & 0 & -\omega_e & -L_{66} & \frac{1}{2}\omega_{r1im} & \omega_{ro} \\
0 & 0 & 0 & 0 & 0 & 0 & 0 & 0 & L_{55} & 0 & 0 & 0 & -\omega_{ro} & -\frac{1}{2}\omega_{r1im} & -L_{66} & \omega_e \\
0 & 0 & 0 & 0 & 0 & 0 & 0 & 0 & 0 & L_{55} & 0 & 0 & -\frac{1}{2}\omega_{r1} & -\omega_{ro} & -\omega_e & -L_{66} \\
-t_5 & 0 & 1 & 0 & 0 & 0 & 0 & 0 & 0 & 0 & 0 & 0 & 0 & 0 & 0 & 0 \\
0 & -t_5 & 0 & 1 & 0 & 0 & 0 & 0 & 0 & 0 & 0 & 0 & 0 & 0 & 0 & 0 \\
-t_9 & 0 & 0 & 0 & 1 & 0 & 0 & 0 & 0 & 0 & 0 & 0 & 0 & 0 & 0 & 0 \\
0 & -t_9 & 0 & 0 & 0 & 1 & 0 & 0 & 0 & 0 & 0 & 0 & 0 & 0 & 0 & 0
\end{bmatrix} \tag{5.260}$$

5.4.2.2 Small signal analysis for two adjacent open stator phases. Substituting Equations (5.109) through (5.1116), (5.226) through (5.231) into Equations (5.207) through (5.212) and using Equations (5.159) through (5.162), the following real dynamic model equations are obtained

From Equation (5.207)

$$v_{qsre} + jv_{qsim} = \sigma_1 \begin{bmatrix} b\left(v_{csre} + jv_{csim}\right) + c\left(v^a_{dsre} + jv^a_{dsim}\right) + d\left(v_{esre} + jv_{esim}\right) \\ - r_s\left(i_{qsre} + ji_{qsim}\right) + \dfrac{L_{ls} r_s L_r}{L_s L_r - L_m^2}\left(i_{qsre} + ji_{qsim}\right) \\ + \dfrac{L_{ls} L_m}{L_s L_r - L_m^2}\left(p\lambda_{qrre} + jp\lambda_{qrim} + j\omega_e \lambda_{qrre} - \omega_e \lambda_{qrim}\right) \end{bmatrix} \tag{5.261}$$

Separating real and imaginary terms

$$v_{qsre} = \sigma_1 \left[bv_{csre} + cv^a_{dsre} + dv_{esre} - r_s i_{qsre} + \frac{L_{ls}}{L_s L_r - L_m^2} \begin{pmatrix} r_s L_r i_{qsre} + L_m p\lambda_{qrre} \\ - \omega_e L_m \lambda_{qrim} \end{pmatrix} \right] \tag{5.262}$$

$$v_{qsim} = \sigma_1 \left[bv_{csim} + cv^a_{dsim} + dv_{esim} - r_s i_{qsim} + \frac{L_{ls}}{L_s L_r - L_m^2} \begin{pmatrix} r_s L_r i_{qsim} + L_m p\lambda_{qrim} \\ + \omega_e L_m \lambda_{qrre} \end{pmatrix} \right] \tag{5.263}$$

From Equation (5.208)

$$\begin{bmatrix} pi_{qsre} - \omega_e i_{qsim} \\ + j\left(pi_{qsim} + \omega_e i_{qsre}\right) \end{bmatrix} = \frac{1}{L_s L_r - L_m^2} \begin{bmatrix} L_r\left(v_{qsre} + jv_{qsim}\right) - r_s L_r\left(i_{qsre} + ji_{qsim}\right) \\ - L_m p\left(\lambda_{qrre} + j\lambda_{qrim}\right) - \omega_e L_m\left(j\lambda_{qrre} - \lambda_{qrim}\right) \end{bmatrix} \tag{5.264}$$

Separating real and imaginary terms

$$pi_{qsre} - \omega_e i_{qsim} = \frac{1}{L_s L_r - L_m^2}\left[L_r v_{qsre} - r_s L_r i_{qsre} - L_m p\lambda_{qrre} + \omega_e L_m \lambda_{qrim}\right] \tag{5.265}$$

$$pi_{qsim} + \omega_e i_{qsre} = \frac{1}{L_s L_r - L_m^2}\left[L_r v_{qsim} - r_s L_r i_{qsim} - L_m p\lambda_{qrim} - \omega_e L_m \lambda_{qrre}\right] \tag{5.266}$$

From Equation (5.209)

$$\begin{bmatrix} pi_{dsre} - \omega_e i_{dsim} \\ + j\omega_e i_{dsre} + jpi_{dsim} \end{bmatrix} = \frac{1}{\left(L_s L_r - L_m^2\right)} \begin{pmatrix} L_r \left(v_{dsre} + jv_{dsim}\right) - r_s L_r \left(i_{dsre} + ji_{dsim}\right) \\ - L_m p\left(\lambda_{drre} + j\lambda_{drim}\right) - \omega_e L_m \left(j\lambda_{drre} - \lambda_{drim}\right) \end{pmatrix} \tag{5.267}$$

Separating real and imaginary terms

$$pi_{dsre} - \omega_e i_{dsim} = \frac{1}{\left(L_s L_r - L_m^2\right)} \left(L_r v_{dsre} - r_s L_r i_{dsre} - L_m p\lambda_{drre} + \omega_e L_m \lambda_{drim}\right) \tag{5.268}$$

$$\omega_e i_{dsre} + pi_{dsim} = \frac{1}{\left(L_s L_r - L_m^2\right)} \left(L_r v_{dsim} - r_s L_r i_{dsim} - L_m p\lambda_{drim} - \omega_e L_m \lambda_{drre}\right) \tag{5.269}$$

From Equation (5.210)

$$\left(pi_{ysre} - \omega_e i_{ysim}\right) + j\left(\omega_e i_{ysre} + pi_{ysim}\right) = \frac{1}{L_{ls}} \left(\left(v_{ysre} + jv_{ysim}\right) - r_s \left(i_{ysre} + ji_{ysim}\right)\right) \tag{5.270}$$

Separating real and imaginary terms

$$pi_{ysre} - \omega_e i_{ysim} = \frac{1}{L_{ls}} \left(v_{ysre} - r_s i_{ysre}\right) \tag{5.271}$$

$$\omega_e i_{ysre} + pi_{ysim} = \frac{1}{L_{ls}} \left(v_{ysim} - r_s i_{ysim}\right) \tag{5.272}$$

From Equation (5.211)

$$\begin{bmatrix} p\lambda_{qrre} - \omega_e \lambda_{qrim} \\ jp\lambda_{qrim} + j\omega_e \lambda_{qrre} \end{bmatrix} = \begin{bmatrix} v_{qrr} - \frac{r_r}{L_r} \left(\left(\lambda_{qrre} + j\lambda_{qrim}\right) - L_m \left(i_{qsre} + ji_{qsim}\right)\right) \\ + \omega_{ro} \left(\lambda_{drre} + j\lambda_{drim}\right) + \frac{1}{2} \omega_{r1im} \left(j\lambda_{drre} + \lambda_{drim}\right) \end{bmatrix} \tag{5.273}$$

Separating real and imaginary terms

$$p\lambda_{qrre} - \omega_e \lambda_{qrim} = v_{qrre} - \frac{r_r}{L_r} \lambda_{qrre} + \frac{r_r L_m}{L_r} i_{qsre} + \omega_{ro} \lambda_{drre} + \frac{1}{2} \omega_{r1im} \lambda_{drim} \tag{5.274}$$

$$p\lambda_{qrim} + \omega_e \lambda_{qrre} = v_{qrim} - \frac{r_r}{L_r} \left(\lambda_{qrim} - L_m i_{qsim}\right) + \omega_{ro} \lambda_{drim} + \frac{1}{2} \omega_{r1im} \lambda_{drre} \tag{5.275}$$

From Equation (5.212)

$$\begin{bmatrix} p\lambda_{drre} - \omega_e \lambda_{drim} \\ + jp\lambda_{drim} + j\omega_e \lambda_{drre} \end{bmatrix} = \begin{bmatrix} v_{drr} - \frac{r_r}{L_r}\left(\left(\lambda_{drre} + j\lambda_{drim}\right) - L_m\left(i_{dsre} + ji_{dsim}\right)\right) \\ -\omega_{ro}\left(\lambda_{qrre} + j\lambda_{qrim}\right) - \frac{1}{2}\omega_{r1im}\frac{1}{2}\omega_{r1im}\left(j\lambda_{qrre} + \lambda_{qrim}\right) \end{bmatrix} \tag{5.276}$$

Separating real and imaginary terms

$$p\lambda_{drre} - \omega_e \lambda_{drim} = v_{drre} - \frac{r_r}{L_r}\left(\lambda_{drre} - L_m i_{dsre}\right) - \omega_{ro}\lambda_{qrre} - \frac{1}{2}\omega_{r1im}\lambda_{qrim} \tag{5.277}$$

$$p\lambda_{drim} + \omega_e \lambda_{drre} = v_{drim} - \frac{r_r}{L_r}\left(\lambda_{drim} - L_m i_{dsim}\right) - \omega_{ro}\lambda_{qrim} - \frac{1}{2}\omega_{r1im}\lambda_{qrre} \tag{5.278}$$

From Equations (5.265), (5.266), (5.268), (5.269), (5.271), (5.272), (5.274), (5.275), (5.277), (5.298), and (5.278), can be rearrange and written as

$$p\Delta i_{qsre} + L_{77}\, p\Delta\lambda_{qrre} = -r_s L_{22}\Delta i_{qsre} + \omega_e \Delta i_{qsim} + L_{11}\Delta\lambda_{qrim} + L_{22}\Delta v_{qsre} \tag{5.279}$$

$$p\Delta i_{qsim} + L_{77}\, p\Delta\lambda_{qrim} = -\omega_e \Delta i_{qsre} - r_s L_{22}\Delta i_{qsim} - L_{11}\Delta\lambda_{qrre} + L_{22}\Delta v_{qsim} \tag{5.280}$$

$$p\Delta i_{dsre} + L_{77}\, p\Delta\lambda_{drre} = -r_s L_{22}\Delta i_{dsre} + \omega_e \Delta i_{dsim} + L_{11}\Delta\lambda_{drim} + L_{22}\Delta v_{dsre} \tag{5.281}$$

$$p\Delta i_{dsim} + L_{77}\, p\Delta\lambda_{drim} = -\omega_e \Delta i_{dsre} - r_s L_{22}\Delta i_{dsim} - L_{11}\Delta\lambda_{drre} + L_{22}\Delta v_{dsim} \tag{5.282}$$

$$p\Delta i_{ysre} = -\frac{r_s}{L_{ls}}\Delta i_{ysre} + \omega_e \Delta i_{ysim} + \frac{1}{L_{ls}}\Delta v_{ysre} \tag{5.283}$$

$$p\Delta i_{ysim} = -\omega_e \Delta i_{ysre} + \frac{1}{L_{ls}}\Delta v_{ysim} - \frac{r_s}{L_{ls}}\Delta i_{ysim} \tag{5.284}$$

$$p\Delta\lambda_{qrre} = \begin{bmatrix} \frac{r_r L_m}{L_r}\Delta i_{qsre} - \frac{r_r}{L_r}\Delta\lambda_{qrre} + \omega_e \Delta\lambda_{qrim} + \omega_{ro}\Delta\lambda_{drre} \\ + \frac{1}{2}\omega_{r1im}\Delta\lambda_{drim} + \lambda_{drre}\Delta\omega_{ro} + \frac{1}{2}\lambda_{drim}\Delta\omega_{r1im} + \Delta v_{qrre} \end{bmatrix} \tag{5.285}$$

$$p\Delta\lambda_{qrim} = \begin{bmatrix} \frac{r_r L_m}{L_r}\Delta i_{qsim} - \omega_e \Delta\lambda_{qrre} - \frac{r_r}{L_r}\Delta\lambda_{qrim} + \frac{1}{2}\omega_{r1im}\Delta\lambda_{drre} \\ + \omega_{ro}\Delta\lambda_{drim} + \lambda_{drim}\Delta\omega_{ro} + \frac{1}{2}\lambda_{drre}\Delta\omega_{r1im} + \Delta v_{qrim} \end{bmatrix} \tag{5.286}$$

$$p\Delta\lambda_{drre} = \begin{bmatrix} \frac{r_r L_m}{L_r}\Delta i_{dsre} - \omega_{ro}\Delta\lambda_{qrre} - \frac{1}{2}\omega_{r1im}\Delta\lambda_{qrim} - \frac{r_r}{L_r}\Delta\lambda_{drre} \\ +\omega_e\Delta\lambda_{drim} - \lambda_{qrre}\Delta\omega_{ro} - \frac{1}{2}\lambda_{qrim}\Delta\omega_{r1im} + \Delta v_{drre} \end{bmatrix} \tag{5.287}$$

$$p\Delta\lambda_{drim} = \begin{bmatrix} \frac{r_r L_m}{L_r}\Delta i_{dsim} - \frac{1}{2}\omega_{r1im}\Delta\lambda_{qrre} - \omega_{ro}\Delta\lambda_{qrim} - \omega_e\Delta\lambda_{drre} \\ -\frac{r_r}{L_r}\Delta\lambda_{drim} - \lambda_{qrim}\Delta\omega_{ro} - \frac{1}{2}\lambda_{qrre}\Delta\omega_{r1im} + \Delta v_{drim} \end{bmatrix} \tag{5.288}$$

where

$$L_{77} = \frac{L_m}{L_s L_r - L_m^2}$$

Substituting (5.285) into (5.279) for $p\Delta\lambda_{qrre}$, results into

$$p\Delta i_{qsre} + L_{77}\begin{bmatrix} \left(\frac{r_r L_m}{L_r} + \frac{r_s L_{22}}{L_{77}}\right)\Delta i_{qsre} - \frac{\omega_e}{L_{77}}\Delta i_{qsim} - \frac{r_r}{L_r}\Delta\lambda_{qrre} \\ +\left(\omega_e - \frac{L_{11}}{L_{77}}\right)\Delta\lambda_{qrim} + \omega_{ro}\Delta\lambda_{drre} \\ +\frac{1}{2}\omega_{r1im}\Delta\lambda_{drim} + \lambda_{drre}\Delta\omega_{ro} + \frac{1}{2}\lambda_{drim}\Delta\omega_{r1im} \end{bmatrix} = \begin{pmatrix} -L_{77}\Delta v_{qrre} \\ +L_{22}\Delta v_{qsre} \end{pmatrix} \tag{5.289}$$

$$p\Delta i_{qsre} = \begin{bmatrix} -\left(\frac{r_r L_{77} L_m}{L_r} + r_s L_{22}\right)\Delta i_{qsre} + \omega_e\Delta i_{qsim} + \frac{r_r L_{77}}{L_r}\Delta\lambda_{qrre} \\ -\left(\omega_e L_{77} - L_{11}\right)\Delta\lambda_{qrim} - \omega_{ro} L_{77}\Delta\lambda_{drre} \\ -\frac{1}{2}\omega_{r1im} L_{77}\Delta\lambda_{drim} - \lambda_{drre} L_{77}\Delta\omega_{ro} - \frac{1}{2}\lambda_{drim} L_{77}\Delta\omega_{r1im} \end{bmatrix} + \begin{pmatrix} -L_{77}\Delta v_{qrre} \\ +L_{22}\Delta v_{qsre} \end{pmatrix} \tag{5.290}$$

Substituting (5.286) into (5.280) for $p\Delta\lambda_{qrim}$, results into

$$p\Delta i_{qsim} + \begin{bmatrix} \omega_e \Delta i_{qsre} + \left(\dfrac{r_r L_{77} L_m}{L_r} + r_s L_{22} \right) \Delta i_{qsim} \\ -\left(\omega_e L_{77} - L_{11}\right) \Delta\lambda_{qrre} - \dfrac{r_r L_{77}}{L_r} \Delta\lambda_{qrim} + \dfrac{1}{2} \omega_{r1im} L_{77} \Delta\lambda_{drre} \\ + \omega_{ro} L_{77} \Delta\lambda_{drim} + \lambda_{drim} L_{77} \Delta\omega_{ro} + \dfrac{1}{2} \lambda_{drre} L_{77} \Delta\omega_{r1im} \end{bmatrix} = \begin{pmatrix} -L_{77} \Delta v_{qrim} \\ + L_{22} \Delta v_{qsim} \end{pmatrix} \quad (5.291)$$

$$p\Delta i_{qsim} = \begin{bmatrix} -\omega_e \Delta i_{qsre} - \left(\dfrac{r_r L_{77} L_m}{L_r} + r_s L_{22} \right) \Delta i_{qsim} \\ + \left(\omega_e L_{77} - L_{11}\right) \Delta\lambda_{qrre} + \dfrac{r_r L_{77}}{L_r} \Delta\lambda_{qrim} - \dfrac{1}{2} \omega_{r1im} L_{77} \Delta\lambda_{drre} \\ - \omega_{ro} L_{77} \Delta\lambda_{drim} - \lambda_{drim} L_{77} \Delta\omega_{ro} - \dfrac{1}{2} \lambda_{drre} L_{77} \Delta\omega_{r1im} \end{bmatrix} + \begin{pmatrix} -L_{77} \Delta v_{qrim} \\ + L_{22} \Delta v_{qsim} \end{pmatrix} \quad (5.292)$$

Substituting (5.287) into (5.281) for $p\Delta\lambda_{drre}$, results into

$$p\Delta i_{dsre} + \begin{bmatrix} \left(\dfrac{r_r L_{77} L_m}{L_r} + r_s L_{22} \right) \Delta i_{dsre} - \omega_e \Delta i_{dsim} - \omega_{ro} L_{77} \Delta\lambda_{qrre} \\ -\dfrac{1}{2} \omega_{r1im} L_{77} \Delta\lambda_{qrim} - \dfrac{r_r L_{77}}{L_r} \Delta\lambda_{drre} + \left(\omega_e L_{77} - L_{11}\right) \Delta\lambda_{drim} \\ - L_{77} \lambda_{qrre} \Delta\omega_{ro} - \dfrac{1}{2} L_{77} \lambda_{qrim} \Delta\omega_{r1im} \end{bmatrix} = \begin{pmatrix} -L_{77} \Delta v_{drre} \\ + L_{22} \Delta v_{dsre} \end{pmatrix} \quad (5.293)$$

$$p\Delta i_{dsre} = \begin{bmatrix} -\left(\dfrac{r_r L_{77} L_m}{L_r} + r_s L_{22} \right) \Delta i_{dsre} + \omega_e \Delta i_{dsim} + \omega_{ro} L_{77} \Delta\lambda_{qrre} \\ +\dfrac{1}{2} \omega_{r1im} L_{77} \Delta\lambda_{qrim} + \dfrac{r_r L_{77}}{L_r} \Delta\lambda_{drre} - \left(\omega_e L_{77} - L_{11}\right) \Delta\lambda_{drim} \\ + L_{77} \lambda_{qrre} \Delta\omega_{ro} + \dfrac{1}{2} L_{77} \lambda_{qrim} \Delta\omega_{r1im} \end{bmatrix} + \begin{pmatrix} -L_{77} \Delta v_{drre} \\ + L_{22} \Delta v_{dsre} \end{pmatrix} \quad (5.294)$$

Substituting (5.288) into (5.282) for $p\Delta\lambda_{drim}$, results into

$$p\Delta i_{dsim} + \begin{bmatrix} \omega_e \Delta i_{dsre} + \left(\dfrac{r_r L_{77} L_m}{L_r} + r_s L_{22}\right)\Delta i_{dsim} - \dfrac{1}{2}\omega_{r1im} L_{77} \Delta\lambda_{qrre} \\ -\omega_{ro} L_{77} \Delta\lambda_{qrim} - \left(\omega_e L_{77} - L_{11}\right)\Delta\lambda_{drre} \\ -\dfrac{r_r L_{77}}{L_r}\Delta\lambda_{drim} - L_{77}\lambda_{qrim}\Delta\omega_{ro} - \dfrac{1}{2} L_{77}\lambda_{qrre}\Delta\omega_{r1im} \end{bmatrix} = \begin{pmatrix} -L_{77}\Delta v_{drim} \\ +L_{22}\Delta v_{dsim} \end{pmatrix} \quad (5.294)$$

$$p\Delta i_{dsim} = \begin{bmatrix} -\omega_e \Delta i_{dsre} - \left(\dfrac{r_r L_{77} L_m}{L_r} + r_s L_{22}\right)\Delta i_{dsim} + \dfrac{1}{2}\omega_{r1im} L_{77} \Delta\lambda_{qrre} \\ +\omega_{ro} L_{77} \Delta\lambda_{qrim} + \left(\omega_e L_{77} - L_{11}\right)\Delta\lambda_{drre} \\ +\dfrac{r_r L_{77}}{L_r}\Delta\lambda_{drim} + L_{77}\lambda_{qrim}\Delta\omega_{ro} + \dfrac{1}{2} L_{77}\lambda_{qrre}\Delta\omega_{r1im} \end{bmatrix} + \begin{pmatrix} -L_{77}\Delta v_{drim} \\ +L_{22}\Delta v_{dsim} \end{pmatrix} \quad (5.296)$$

Let

$$a_{11} = -\left(\frac{r_r L_{77} L_m}{L_r} + r_s L_{22}\right) \qquad a_{17} = \frac{r_r L_{77}}{L_r} \qquad a_{18} = \left(\omega_e L_{77} - L_{11}\right)$$

Then Equations (5.290) and (5.292) (5.294) and (5.29) can be written as

$$p\Delta i_{qsre} = \begin{bmatrix} a_{11}\Delta i_{qsre} + \omega_e \Delta i_{qsim} + a_{17}\Delta\lambda_{qrre} - a_{18}\Delta\lambda_{qrim} - \omega_{ro} L_{77}\Delta\lambda_{drre} \\ -\dfrac{1}{2}\omega_{r1im} L_{77}\Delta\lambda_{drim} - \lambda_{drre} L_{77}\Delta\omega_{ro} - \dfrac{1}{2}\lambda_{drim} L_{77}\Delta\omega_{r1im} \\ -L_{77}\Delta v_{qrre} + L_{22}\Delta v_{qsre} \end{bmatrix} \quad (5.297)$$

$$p\Delta i_{qsim} = \begin{bmatrix} -\omega_e \Delta i_{qsre} - a_{11}\Delta i_{qsim} + a_{18}\Delta\lambda_{qrre} + a_{17}\Delta\lambda_{qrim} - \dfrac{1}{2}\omega_{r1im} L_{77}\Delta\lambda_{drre} \\ -\omega_{ro} L_{77}\Delta\lambda_{drim} - \lambda_{drim} L_{77}\Delta\omega_{ro} - \dfrac{1}{2}\lambda_{drre} L_{77}\Delta\omega_{r1im} \\ -L_{77}\Delta v_{qrim} + L_{22}\Delta v_{qsim} \end{bmatrix} \quad (5.298)$$

$$p\Delta i_{dsre} = \begin{bmatrix} -a_{11}\Delta i_{dsre} + \omega_e \Delta i_{dsim} + \omega_{ro} L_{77}\Delta\lambda_{qrre} + \dfrac{1}{2}\omega_{r1im} L_{77}\Delta\lambda_{qrim} + a_{17}\Delta\lambda_{drre} \\ -a_{18}\Delta\lambda_{drim} + L_{77}\lambda_{qrre}\Delta\omega_{ro} + \dfrac{1}{2} L_{77}\lambda_{qrim}\Delta\omega_{r1im} - L_{77}\Delta v_{drre} + L_{22}\Delta v_{dsre} \end{bmatrix} \quad (5.299)$$

$$p\Delta i_{dsim} = \begin{bmatrix} -\omega_e \Delta i_{dsre} - a_{11}\Delta i_{dsim} + \dfrac{1}{2}\omega_{r1im} L_{77}\Delta\lambda_{qrre} + \omega_{ro} L_{77}\Delta\lambda_{qrim} + a_{18}\Delta\lambda_{drre} \\ + a_{17}\Delta\lambda_{drim} + L_{77}\lambda_{qrim}\Delta\omega_{ro} + \dfrac{1}{2} L_{77}\lambda_{qrre}\Delta\omega_{r1im} - L_{77}\Delta v_{drim} + L_{22}\Delta v_{dsim} \end{bmatrix} \quad (5.300)$$

Equations (5.161) and (5.162) can be written as (5.301) and (5.302), respectively

$$p\Delta\omega_{ro} = \begin{bmatrix} \varepsilon_o \lambda'_{drre}\Delta i_{qsre} + \varepsilon_o \lambda'_{drim}\Delta i_{qsim} - \varepsilon_o \lambda'_{qrre}\Delta i_{dsre} - \varepsilon_o \lambda'_{qrim}\Delta i_{dsim} \\ -\varepsilon_o i_{dsre}\Delta\lambda'_{qrre} - \varepsilon_o i_{dsim}\Delta\lambda'_{qrim} + \varepsilon_o i_{qsre}\Delta\lambda'_{drre} + \varepsilon_o i_{qsim}\Delta\lambda'_{drim} - \dfrac{P}{2J}\Delta T_L \end{bmatrix} \quad (5.301)$$

$$p\Delta\omega_{r1re} = \begin{bmatrix} \varepsilon_o \lambda'_{drre}\Delta i_{qsre} - \varepsilon_o \lambda'_{drim}\Delta i_{qsim} - \varepsilon_o \lambda'_{qrre}\Delta i_{dsre} + \varepsilon_o \lambda'_{qrim}\Delta i_{dsim} \\ -\varepsilon_o i_{dsre}\Delta\lambda'_{qrre} + \varepsilon_o i_{dsim}\Delta\lambda'_{qrim} + \varepsilon_o i_{qsre}\Delta\lambda'_{drre} - \varepsilon_o i_{qsim}\Delta\lambda'_{drim} \end{bmatrix} \quad (5.302)$$

where

$$\varepsilon_o = \frac{5P^2}{16J}\frac{L_m}{L_r}$$

From Equations (5.160), (5.283), (5.284), (5.285), (5.286), (5.287), (5.288), (5.286) , (5.297), (5.298), (5.299), (5.300), (5.301) , and (5.302), the A matrix for small signal analysis is as presented in Equation , (5.303).

$$
A=\begin{bmatrix}
a_{11} & \omega_e & 0 & 0 & 0 & 0 & a_{17} & -a_{18} & -\omega_{ro}L_{77} & -\frac{1}{2}\omega_{r1im}L_{77} & -\lambda_{drre}L_{77} & 0 & -\frac{1}{2}\lambda_{drim}L_{77} \\
-\omega_e & a_{11} & 0 & 0 & 0 & 0 & a_{18} & a_{17} & -\frac{1}{2}\omega_{r1im}L_{77} & -\omega_{ro}L_{77} & -\lambda_{drim}L_{77} & 0 & -\frac{1}{2}\lambda_{drre}L_{77} \\
0 & 0 & a_{11} & \omega_e & 0 & 0 & \omega_{ro}L_{77} & \frac{1}{2}\omega_{r1im}L_{77} & a_{17} & -a_{18} & L_{77}\lambda_{qrre} & 0 & \frac{1}{2}L_{77}\lambda_{qrim} \\
0 & 0 & -\omega_e & a_{11} & 0 & 0 & \frac{1}{2}\omega_{r1im}L_{77} & \omega_{ro}L_{77} & a_{18} & a_{17} & L_{77}\lambda_{qrim} & 0 & \frac{1}{2}L_{77}\lambda_{qrre} \\
0 & 0 & 0 & 0 & -\frac{r_s}{L_{ls}} & \omega_e & 0 & 0 & 0 & 0 & 0 & 0 & 0 \\
0 & 0 & 0 & 0 & -\omega_e & -\frac{r_s}{L_{ls}} & 0 & 0 & 0 & 0 & 0 & 0 & 0 \\
\frac{r_r L_m}{L_r} & 0 & 0 & 0 & 0 & 0 & -\frac{r_r}{L_r} & \omega_e & \omega_{ro} & \frac{1}{2}\omega_{r1im} & \lambda_{drre} & 0 & \frac{1}{2}\lambda_{drim} \\
0 & \frac{r_r L_m}{L_r} & 0 & 0 & 0 & 0 & -\omega_e & -\frac{r_r}{L_r} & \frac{1}{2}\omega_{r1im} & \omega_{ro} & \lambda_{drim} & 0 & \frac{1}{2}\lambda_{drre} \\
0 & 0 & \frac{r_r L_m}{L_r} & 0 & 0 & 0 & -\omega_{ro} & -\frac{1}{2}\omega_{r1im} & -\frac{r_r}{L_r} & \omega_e & -\lambda_{qrre} & 0 & -\frac{1}{2}\lambda_{qrim} \\
0 & 0 & 0 & \frac{r_r L_m}{L_r} & 0 & 0 & -\frac{1}{2}\omega_{r1im} & -\omega_{ro} & -\omega_e & -\frac{r_r}{L_r} & -\lambda_{qrim} & 0 & -\frac{1}{2}\lambda_{qrre} \\
\varepsilon_o\lambda'_{drre} & \varepsilon_o\lambda'_{drim} & -\varepsilon_o\lambda'_{qrre} & -\varepsilon_o\lambda'_{qrim} & 0 & 0 & -\varepsilon_o i_{dsre} & -\varepsilon_o i_{dsim} & \varepsilon_o i_{qsre} & \varepsilon_o i_{qsim} & 0 & 0 & 0 \\
\varepsilon_o\lambda'_{drre} & -\varepsilon_o\lambda'_{drim} & -\varepsilon_o\lambda'_{qrre} & \varepsilon_o\lambda'_{qrim} & 0 & 0 & -\varepsilon_o i_{dsre} & \varepsilon_o i_{dsim} & \varepsilon_o i_{qsre} & -\varepsilon_o i_{qsim} & 0 & 0 & 0 \\
0 & 0 & 0 & 0 & 0 & 0 & 0 & 0 & 0 & 0 & 0 & 0 & -2\omega_e
\end{bmatrix}
\tag{5.303}
$$

5.4.3 Results and Discussion for Two Adjacent Open Phase Fault

The validity of the models presented in section 5.4 - 5.4.2 has been investigated through the computer simulation of the full-order model of the machine with stator phases '*a*' and '*b*' open-circuited. The steady-state model is used to calculate the state variables and then the results are compared.

Figure 5.16 through Figure 5.19 present the simulation of the free acceleration starting process of the machine. The phase voltage is applied to the remaining three phases (c, d, and e) and Equations (5.187) and (5.180) are used to determine stator phase '*a*' and '*b*' voltages, respectively. Figure 5.16(a) and (b) show the rotor speed and electromagnetic torque, respectively, showing the characteristics similar to those of the healthy induction machine. In Figure 5.17(a) the stator phase '*a*' and '*b*' currents are zero as expected. The stator phase voltages are shown in Figure 5.18 with the starting transients of the open phases '*a*' and '*b*' as they develops the voltages are clearly displayed in Figure 5.18(a) and (b), respectively.

When the rotor speed is in steady state, the load torque is changed from 0 to 11 Nm to show the effect of the speed harmonics. The dynamic responses of the machine to load changes are shown in Figure 5.19(a) and (b) for the rotor speed and electromagnetic torque, respectively. In Figure 5.20 through Figure 5.23, the waveforms of the variables are shown after the speed has reached steady-state average value. It is evident from Figure 5.20(a) and (b) that the speed and torque consist of the harmonics at twice the frequency of the supply voltages as predicted by the harmonic balance technique model. The unbalance caused by the open phase fault is clearly indicated in the stator phase load currents, Figure 5.21. Figure 5.22 (a) and (b) show that when the machine is loaded, the open phase 'a' and 'b' voltages are affected as they are reduced. This is due to the fact that the voltage waveforms are induced by the other phases and the rotor circuits.

Figure 5.24(a) and Figure 5.24 (b) show the peak values of the rotor speed and torque pulsations, respectively as a function of the rotor speed. In Figure 5.24 (a) the average rotor speed is approximately 361.58 rad/sec, the peak value of the speed oscillations is about 0.06 rad/sec. In Figure 5.24(b) the average torque is 11 Nm and the peak of the torque oscillations is about 1.75 Nm. These speed and torque values are fairly comparable to those in Figure 5.20(a) and Figure 5.20(b), respectively.

Figure 5.26 presents the torque-speed characteristics at both normal and two open-phase faulted conditions. First the normal operation of the machine is computer simulated and the steady-state torque curve is superimposed on the simulated curve. Then the same procedure is followed for the open phase faulted condition. Under this operation, the torque envelope is obtained by adding the peak of the pulsation torque to, and subtracting it from the average value obtained from the harmonic balance technique. Comparing the results of the dynamic computer simulation and the steady state calculations for both cases, the harmonic balance technique gives average and peak values of the torque that compare fairly with simulation results.

The stator input and reactive powers at steady state are shown in figure 5.27(a) and Figure 5.27(b), respectively. The speed and torque oscillations are also shown in figure 5.28 (a) and Figure 5.28(b), respectively. The results of which compare well with those presented in Figure 5.20(a) and Figure 5.20(b), respectively, as well as Figure 5.24(a) and Figure 5.24(b), respectively.

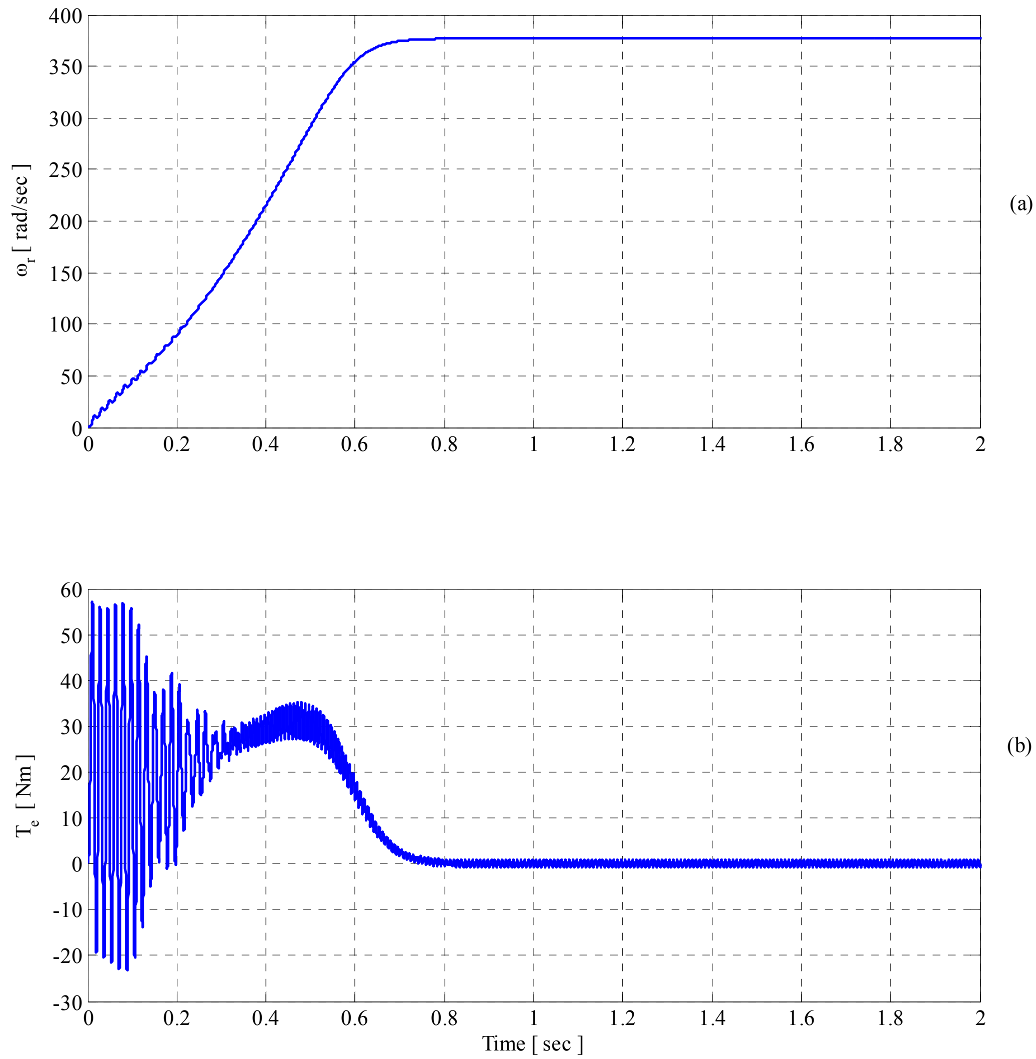

Figure 5.16 Stator phases 'a' and 'b' open starting transients (a) rotor speed and (b) electromagnetic torque

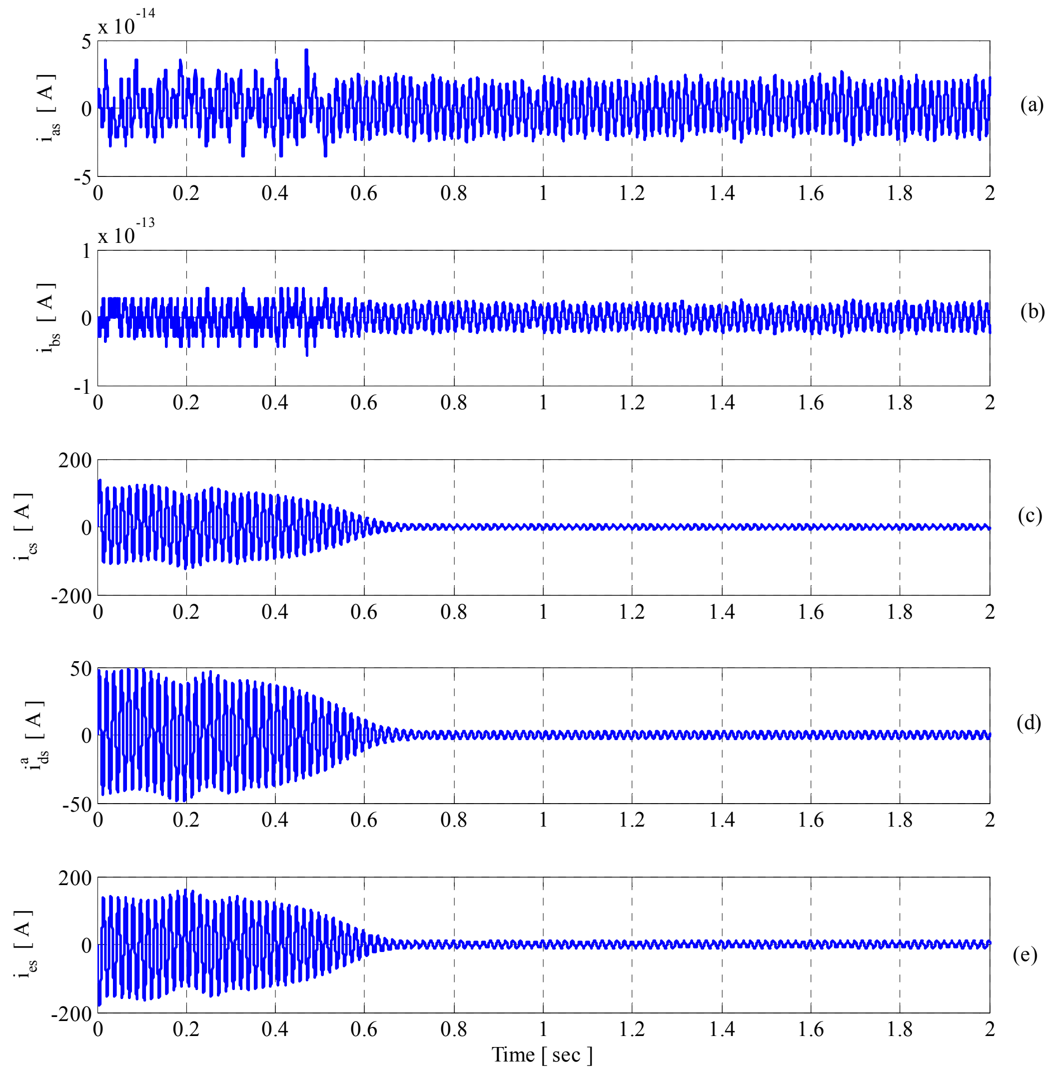

Figure 5.17 Stator phases ‘a’ and ‘b’ open Starting transients Stator phase currents (a) phase ‘a’ (b) phase ‘b’ (c) phase ‘c’ (d) phase ‘d’ (e) phase ‘e’

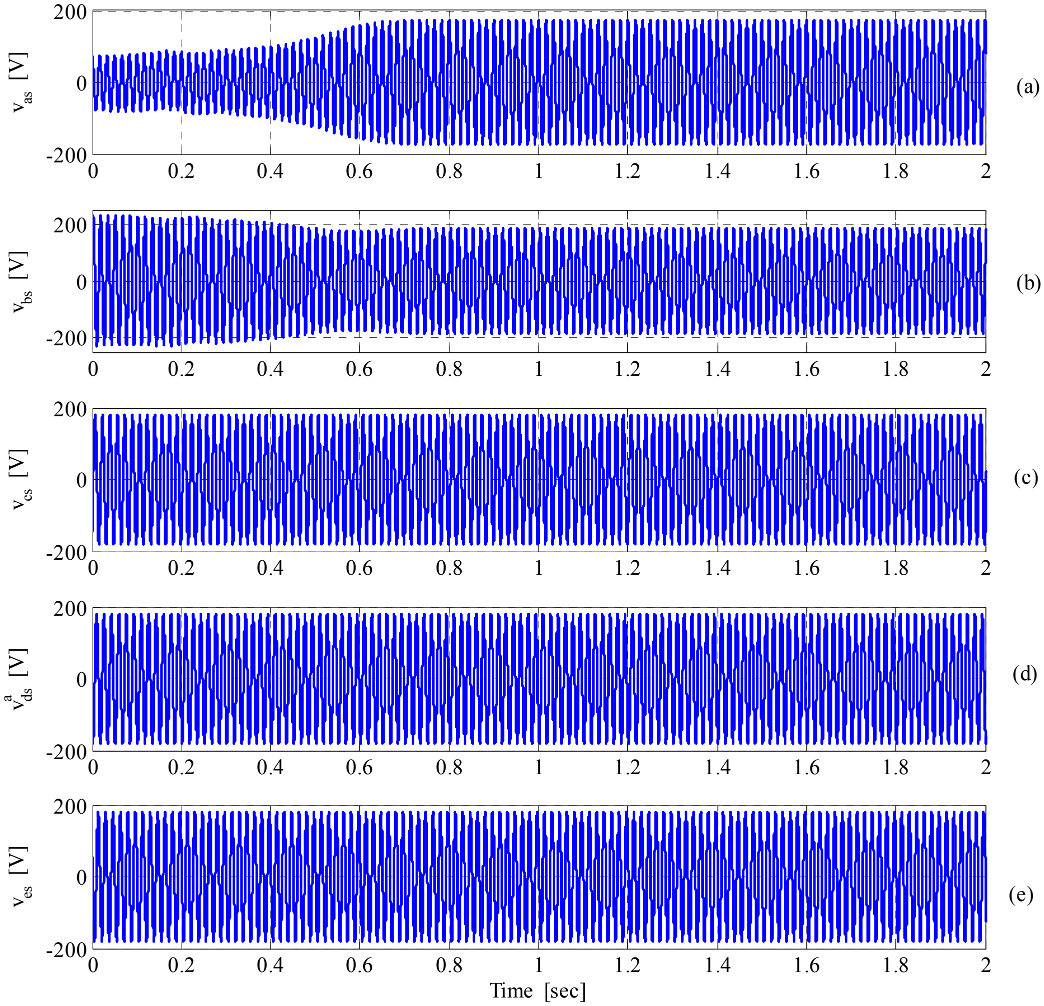

Figure 5.18 Stator phases ‘a’ and ‘b’ open Starting transients stator phase voltages (a) phase ‘a’ (b) phase ‘b’ (c) phase ‘c’ (d) phase ‘d’ (e) phase ‘e’

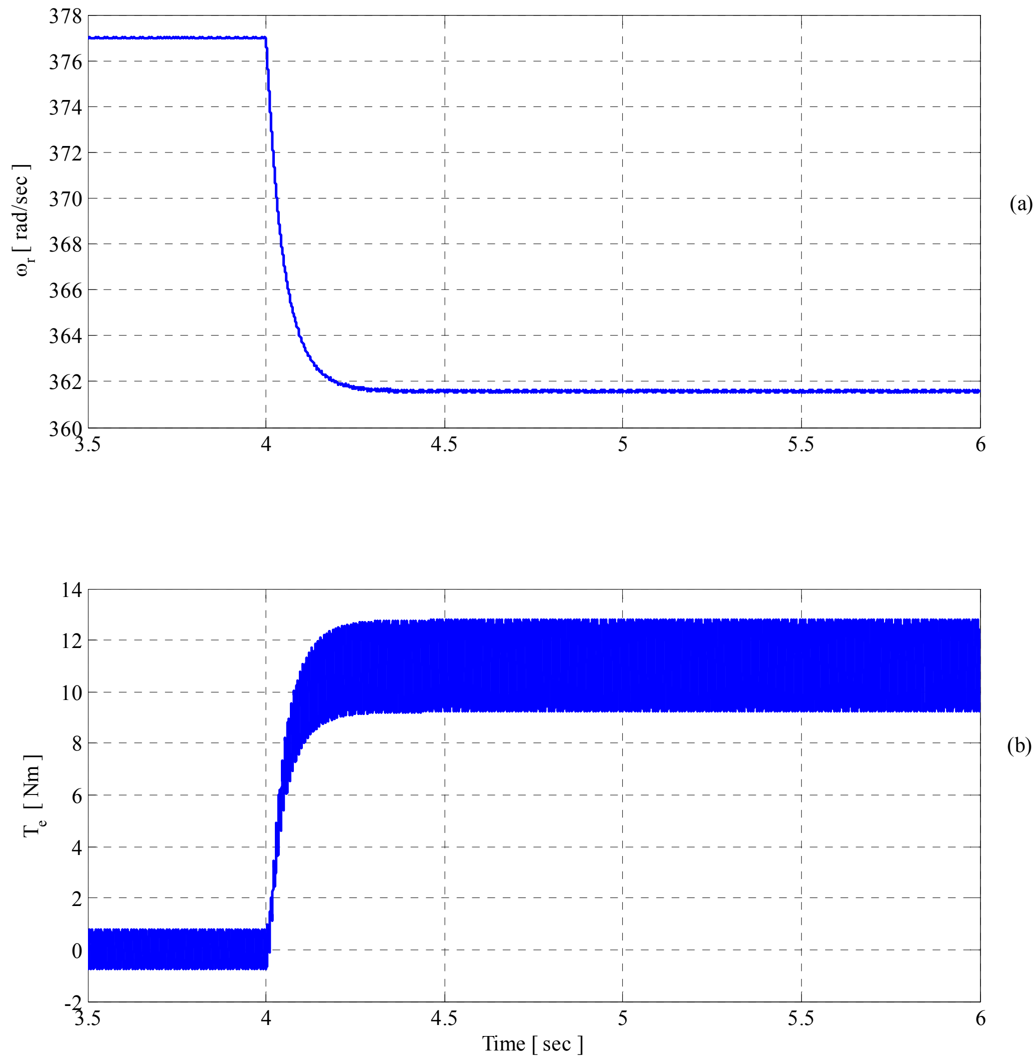

Figure 5.19. Stator phases ‘a’ and ‘b’ open Simulation Dynamics of (a) rotor speed and (b) electromagnetic torque due to a load torque change of 11 Nm applied at 4 seconds.

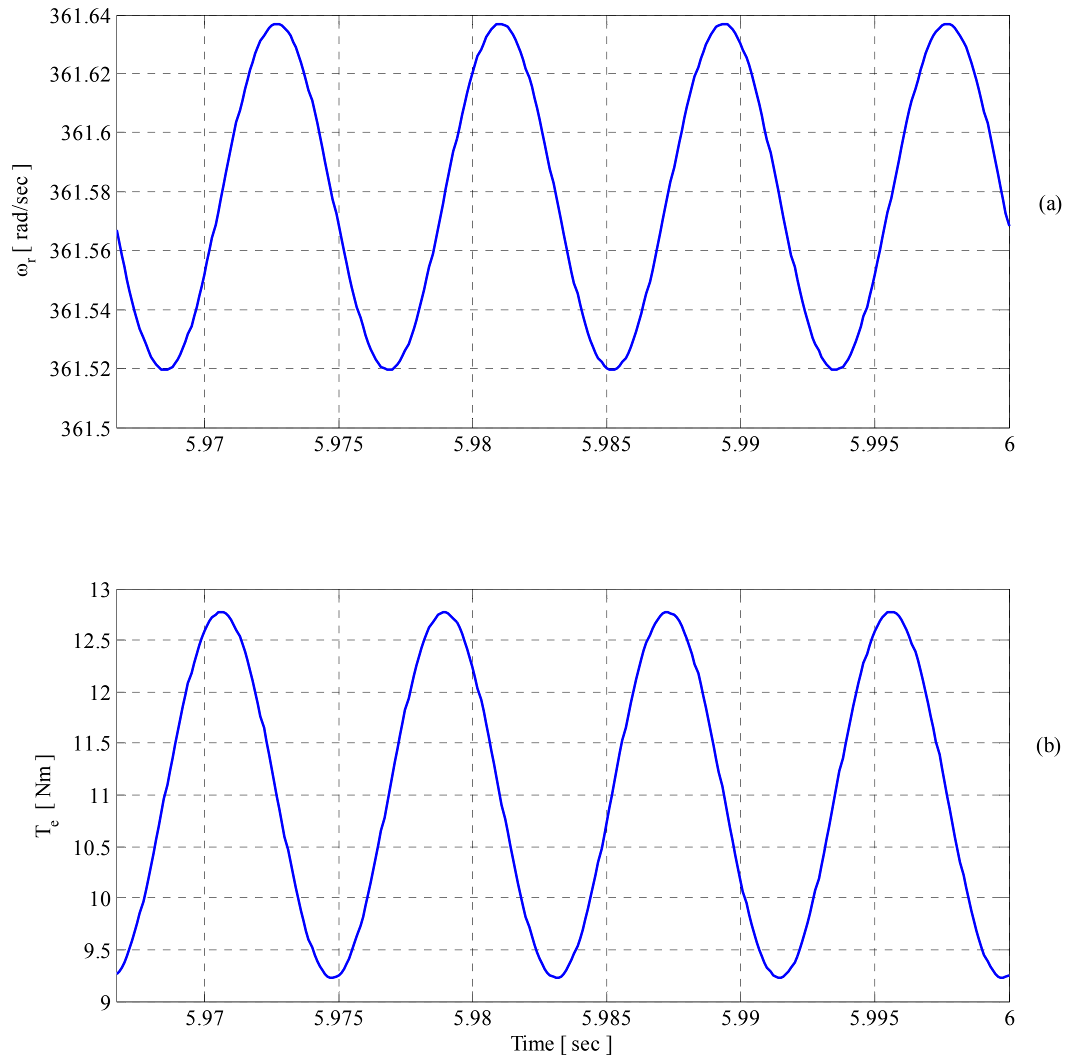

Figure 5.20. Stator phases 'a' and 'b' open Simulation Steady-state (a) rotor speed and (b) electromagnetic torque at a load torque of 11 Nm, showing the presence of the harmonic (oscillating) components.

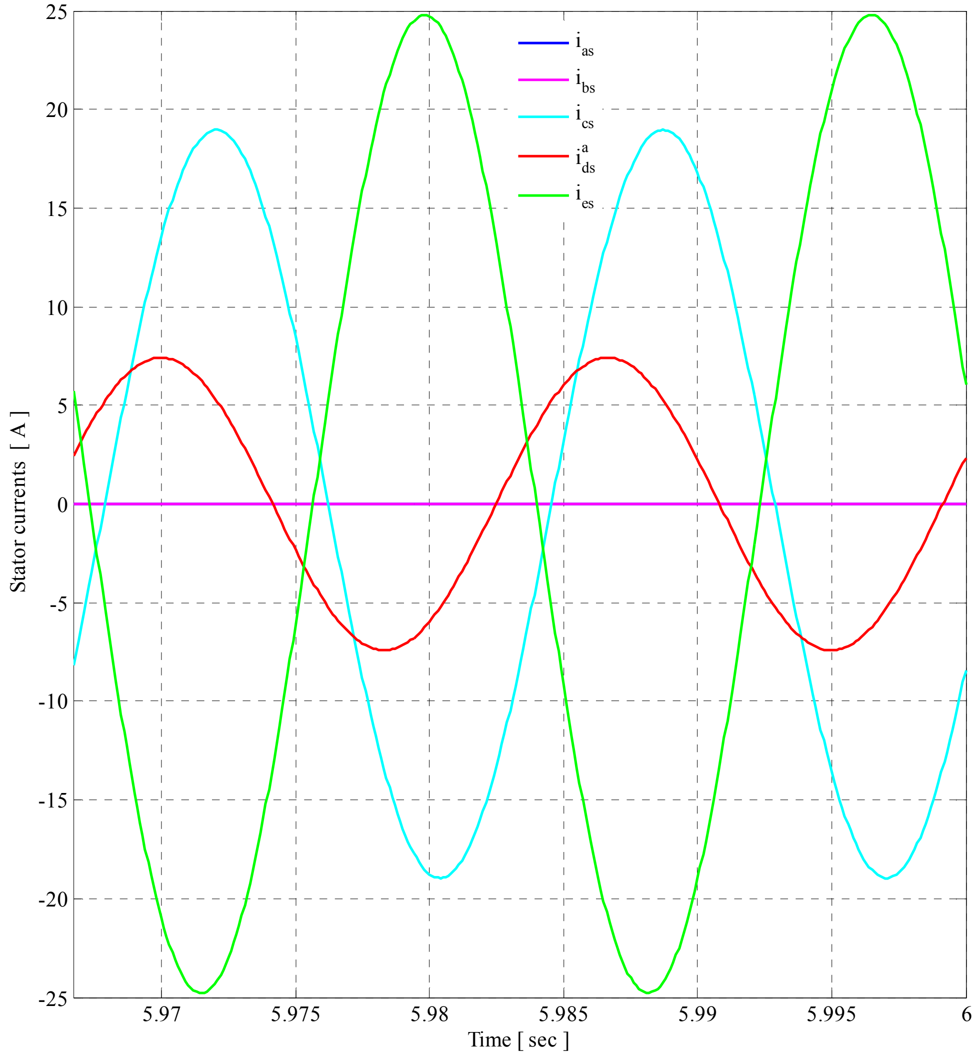

Figure 5.21. Stator phases 'a' and 'b' open Simulation Steady-state stator phase currents at a load torque of 11 Nm.

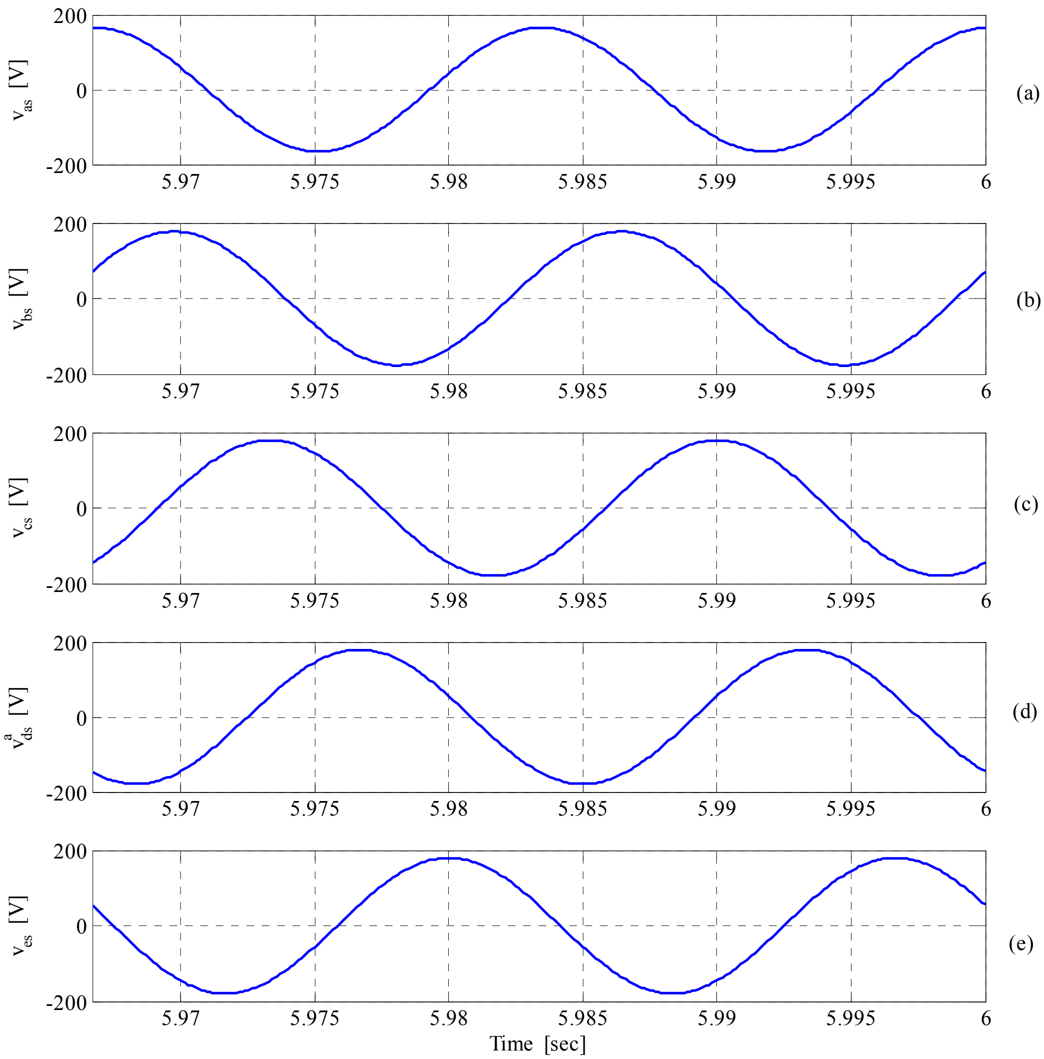

Figure 5.22. Stator phases ‘a’ and ‘b’ open Simulation Steady-state stator phase voltages at a load torque of 11 Nm (a) phase ‘a’ (b) phase ‘b’ (c) phase ‘c’ (d) phase ‘d’ (e) phase ‘e’

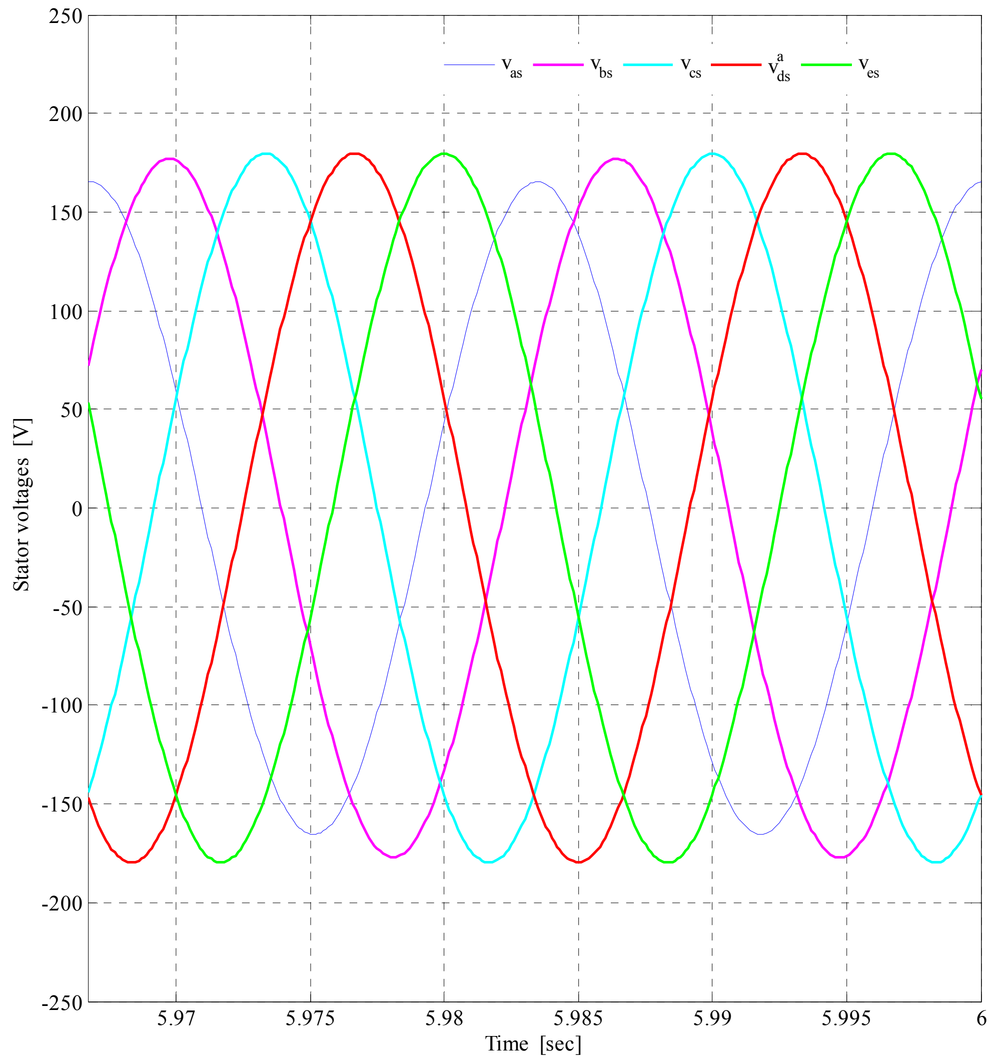

Figure 5.23. Stator phases 'a' and 'b' open Simulation Steady-state stator phase voltages at a load torque of 11 Nm showing the unbalance

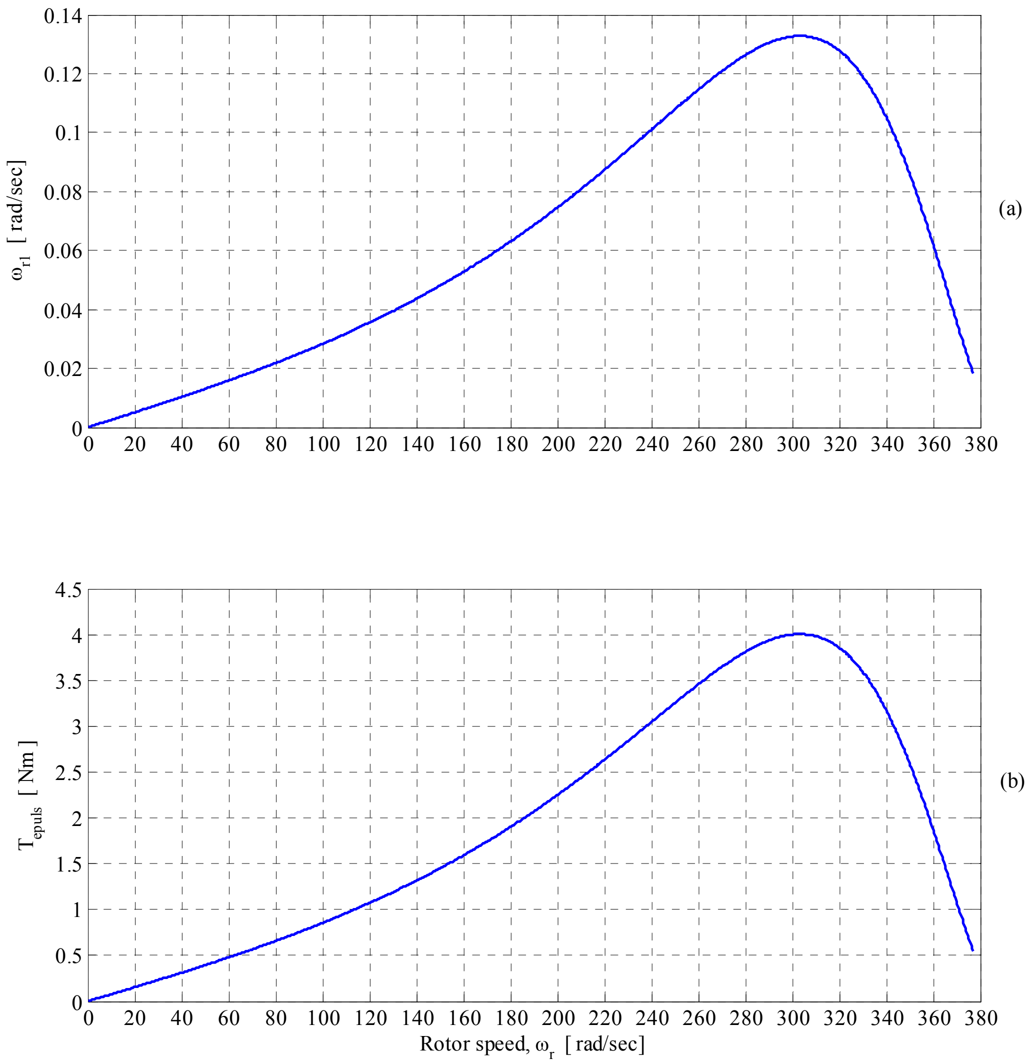

Figure 5.24. Steady-state calculation results (a) Peak value of the speed harmonic component (b) Peak value of the torque pulsation

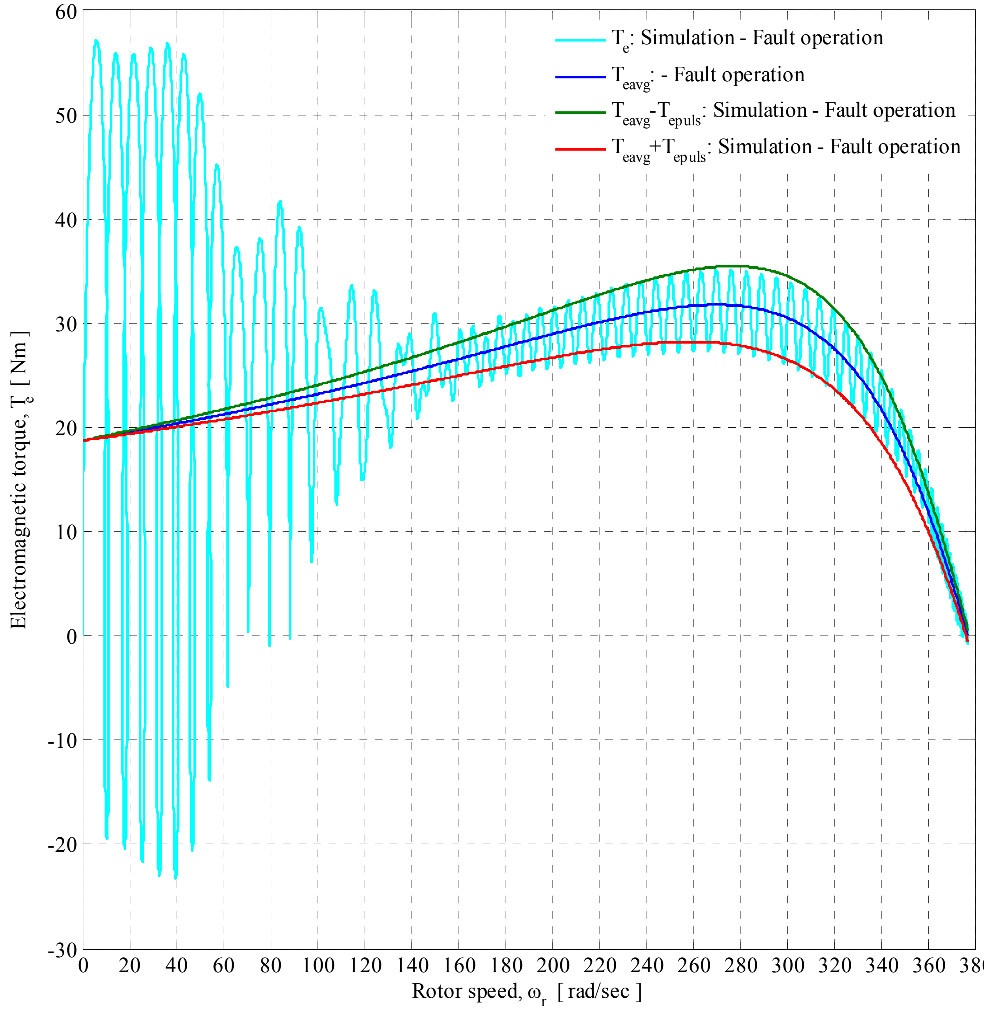

Figure 5.25 Faulted machine Various torque components of the five-phase induction machine under unbalanced stator phases 'a' and 'b' open based on computer simulation and steady-state calculations.

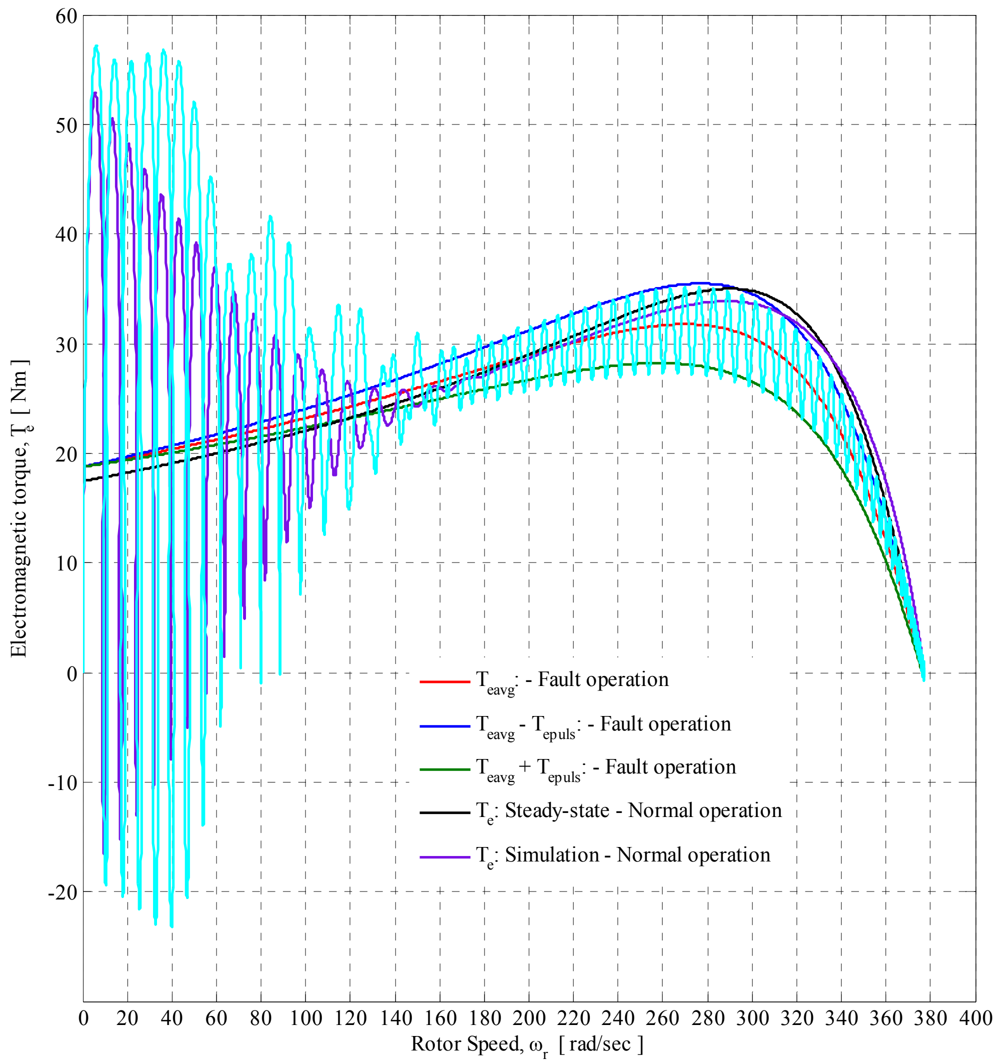

Figure 5.26 Various torque components of the five-phase induction machine under balanced and a stator phases ‘a’ and ‘b’ open based on computer simulation and steady state calculations.

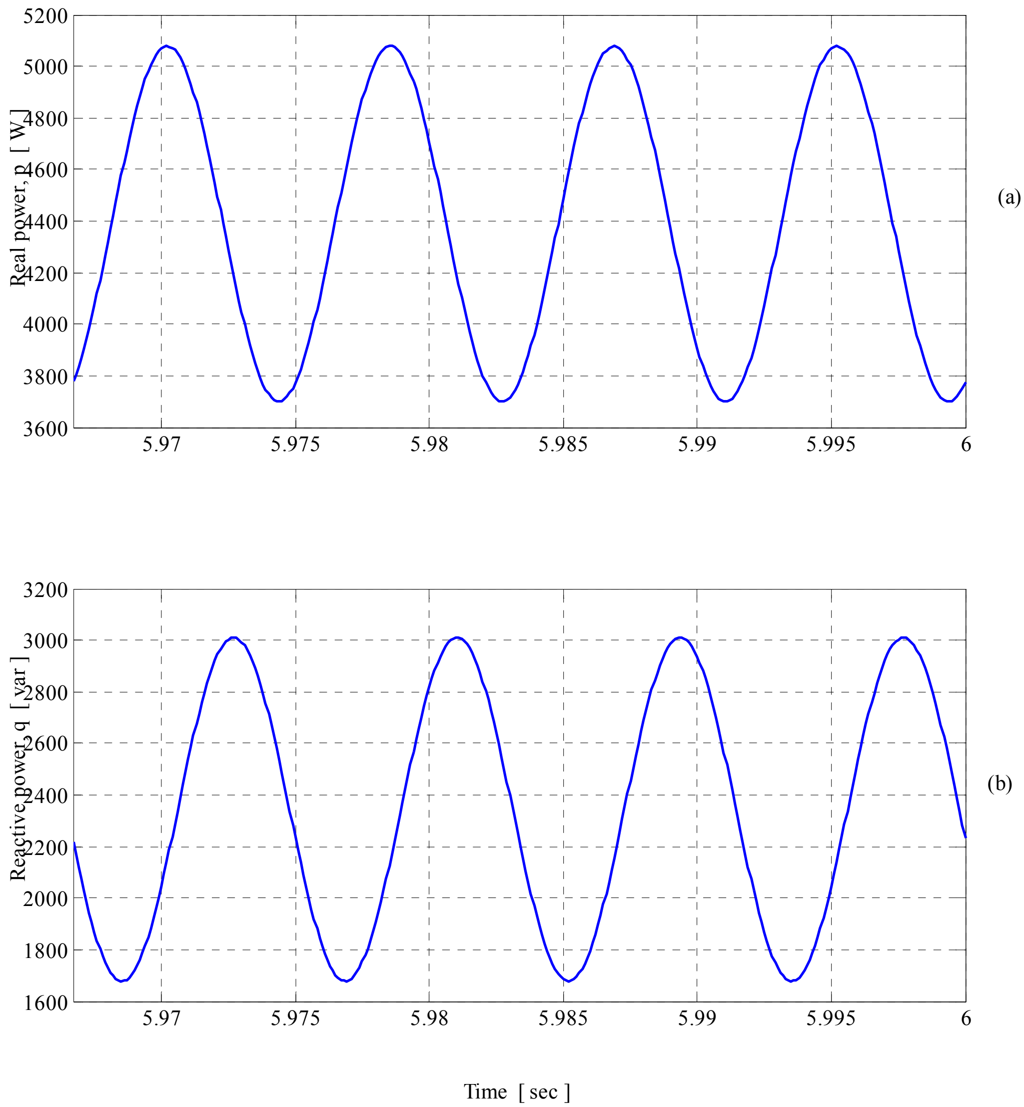

Figure 5.27 Simulation Steady-state stator input five-phase power (a) Real power and (b) Reactive power at a load torque of 11 Nm.

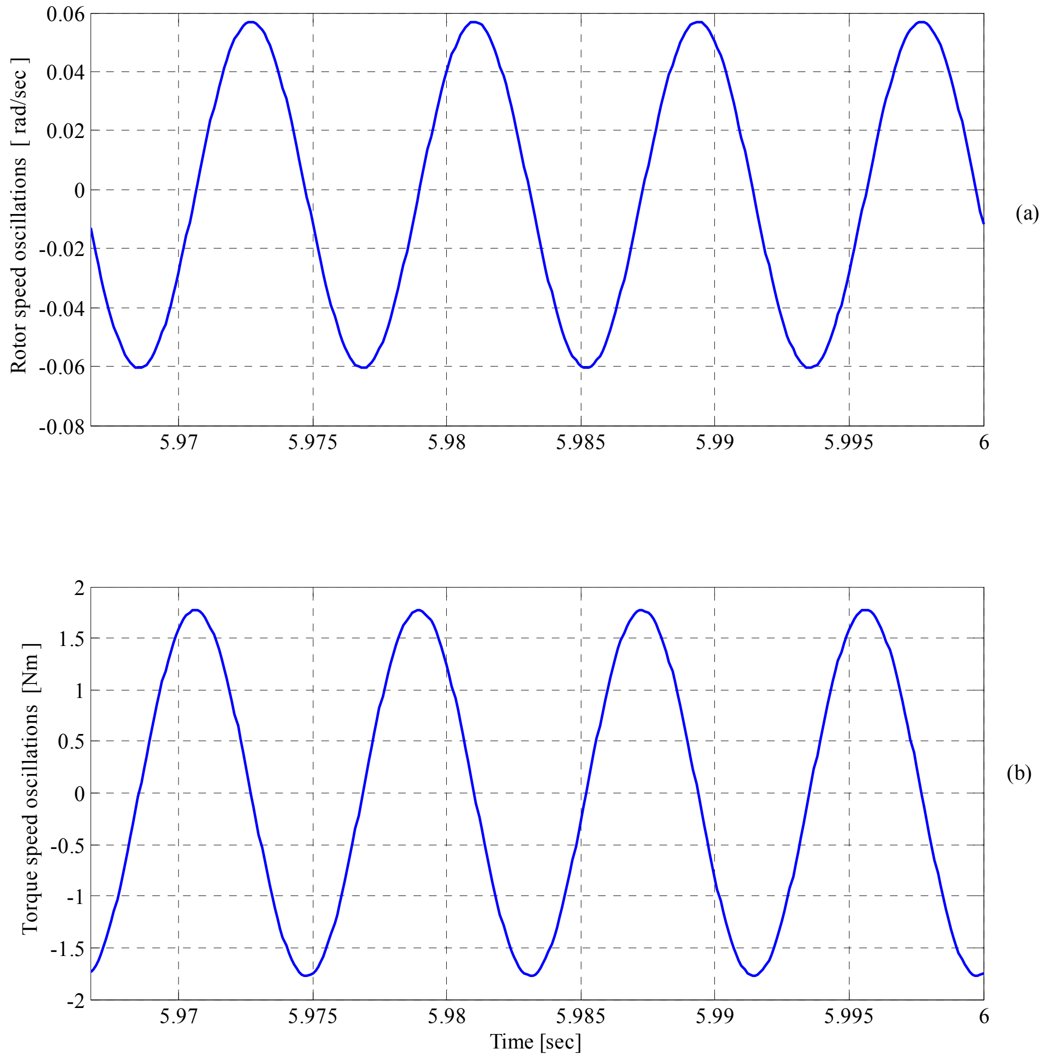

Figure 5.28 Simulation Steady-state (a) rotor speed oscillations and (b) electromagnetic torque oscillations at a load torque of 11 Nm.

5.5 Two Non-adjacent Phases (‘*a*’ and ‘*c*’) Open Circuited

The operation with two non-adjacent phases (‘*a*’ and ‘*c*’) open on fault is depicted in Figure 5.29. When the two phases are open, the phase voltages across the machine phase windings ‘*a*’ and ‘*c*’ become unknown. Under this condition, all the *qdxyos* transformed voltages become unknown.

The following Equations will apply when the two stator phases “a” and “c” are open

$$i_{as} = 0 \tag{5.304}$$

$$i_{cs} = 0 \tag{5.304}$$

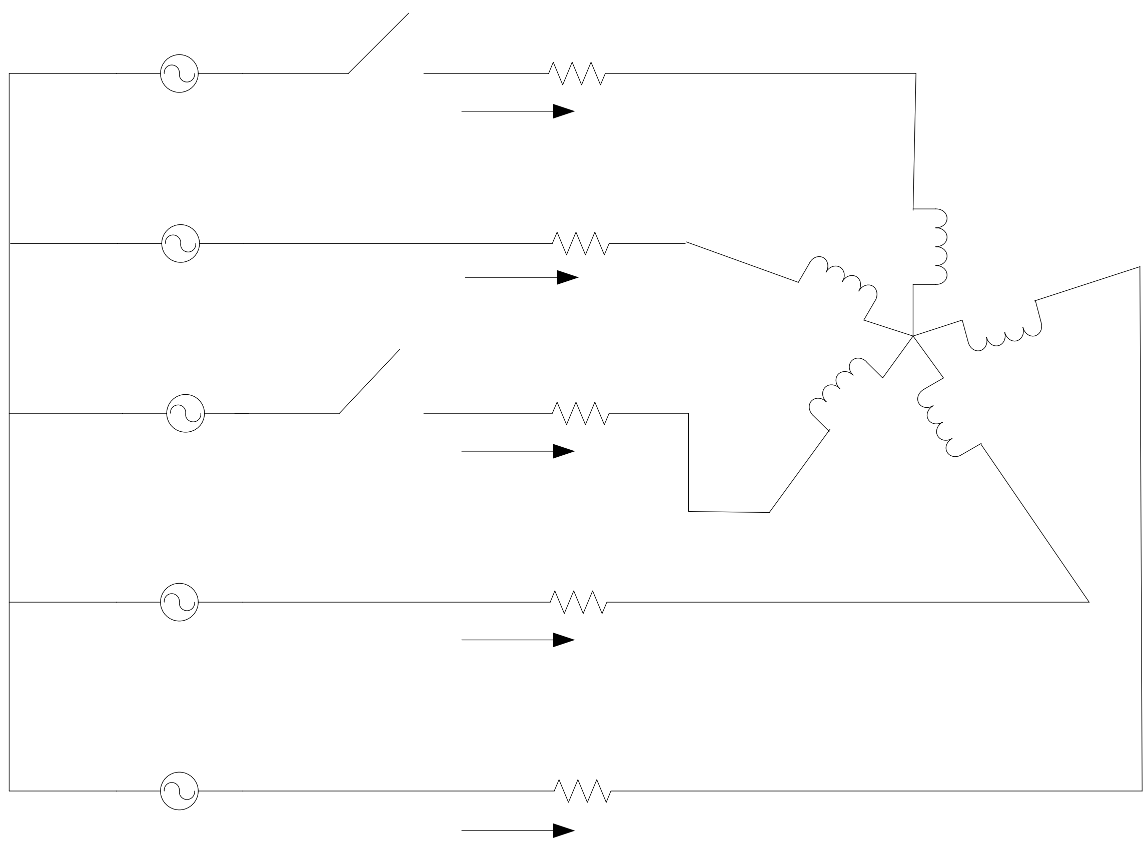

Figure 5.29 Open phases ‘*a*’ and ‘*c*’ of the stator for the five-phase induction machine.

KCL requires that

$$i_{as} + i_{bs} + i_{cs} + i_{ds}^{a} + i_{es} = 0 \tag{5.306}$$

Therefore

$$i_{bs} + i_{ds}^{a} + i_{es} = 0 \tag{5.307}$$

$$i_{os} = \frac{1}{5}\left(i_{as} + i_{bs} + i_{cs} + i_{ds}^{a} + i_{es}\right) = 0$$

$$i_{os} = \frac{1}{5}\left(i_{bs} + i_{ds}^{a} + i_{es}\right) = 0$$

$$i_{os} = 0 \tag{5.308}$$

Which leads to

$$\lambda_{os} = L_{ls} i_{os} = 0 \tag{5.309}$$

$$v_{os} = r_s i_{os} + p\lambda_{os} = 0 \tag{5.310}$$

Equation (5.39), therefore, can be written as

$$v_{as} + v_{cs} = -\left(v_{bs} + v_{ds}^{a} + v_{es}\right) \tag{5.311}$$

From Equation (5.35)

$$v_{as} = \frac{5}{2} v_{qs} - \left[\cos\left(\frac{2\pi}{5}\right) v_{bs} + \cos\left(\frac{4\pi}{5}\right) v_{cs} + \cos\left(\frac{4\pi}{5}\right) v_{ds}^{a} + \cos\left(\frac{2\pi}{5}\right) v_{es}\right] \tag{5.312}$$

Substituting for v_{as} from (5.312) into (5.311) gives

$$\frac{5}{2} v_{qs} - \begin{bmatrix} \cos\left(\frac{2\pi}{5}\right) v_{bs} + \cos\left(\frac{4\pi}{5}\right) v_{cs} \\ + \cos\left(\frac{4\pi}{5}\right) v_{ds}^{a} + \cos\left(\frac{2\pi}{5}\right) v_{es} \end{bmatrix} + v_{bs} = -\left(v_{cs} + v_{ds}^{a} + v_{es}\right)$$

$$v_{cs} = \frac{1}{\left(1-\cos\left(\frac{4\pi}{5}\right)\right)}\begin{bmatrix} -\frac{5}{2}v_{qs} - \left(1-\cos\left(\frac{2\pi}{5}\right)\right)v_{bs} \\ -\left(1-\cos\left(\frac{4\pi}{5}\right)\right)v_{ds}^{a} - \left(1-\cos\left(\frac{2\pi}{5}\right)\right)v_{es} \end{bmatrix} \tag{5.313}$$

$$v_{cs} = x_1 v_{qs} + y_1 v_{bs} + z_1 v_{ds}^{a} + \gamma_1 v_{es} \tag{5.314}$$

where

$$x_1 = -\frac{5}{2}\frac{1}{1-\cos\frac{4\pi}{5}}$$

$$y_1 = \frac{-1}{1-\cos\frac{4\pi}{5}}\left(1-\cos\frac{2\pi}{5}\right)$$

$$z_1 = \frac{-1}{1-\cos\frac{4\pi}{5}}\left(1-\cos\frac{4\pi}{5}\right)$$

$$\gamma_1 = \frac{-1}{1-\cos\frac{4\pi}{5}}\left(1-\cos\frac{2\pi}{5}\right)$$

Substituting for v_{cs} from (5.314) into (5.171) gives

$$\left[1+\frac{2}{5}\begin{pmatrix} \cos\left(\frac{2\pi}{5}\right) \\ -\cos\left(\frac{4\pi}{5}\right) \end{pmatrix} x_1\right] v_{qs} - v_{xs} = \frac{2}{5}\left(\cos\left(\frac{2\pi}{5}\right) - \cos\left(\frac{4\pi}{5}\right)\right)\begin{pmatrix} (1-y_1)v_{bs} - (z_1+1)v_{ds}^{a} \\ +(1-\gamma_1)v_{es} \end{pmatrix} \tag{5.315}$$

$$\left[1+\frac{2}{5}\alpha x\right] v_{qs} - v_{xs} = \frac{2}{5}\alpha\left((1-y)v_{bs} - (z+1)v_{ds}^{a} + (1-\gamma)v_{es}\right) \tag{5.316}$$

$$\left[1+\frac{2}{5}\alpha x\right] v_{qs} - v_{xs} = \frac{2}{5}\alpha(1-y)v_{bs} - \frac{2}{5}\alpha(z+1)v_{ds}^{a} + \frac{2}{5}\alpha(1-\gamma)v_{es} \tag{5.317}$$

$$a_1 v_{qs} - v_{xs} = b_1 v_{bs} + c_1 v_{ds}^{a} + d_1 v_{es} \tag{5.318}$$

where

$$\alpha_1 = \left(\cos\left(\frac{2\pi}{5}\right) - \cos\left(\frac{4\pi}{5}\right)\right)$$

$$a_1 = 1 + \frac{2}{5}\alpha_1 x_1$$

$$b_1 = \frac{2}{5}\alpha_1 (1 - y_1)$$

$$c_1 = -\frac{2}{5}\alpha_1 (z_1 + 1)$$

$$d_1 = \frac{2}{5}\alpha_1 (1 - \gamma_1)$$

Substituting for from (5.318) into (5.312) results into

$$v_{as} = \frac{5}{2}v_{qs} - \left[x_1 v_{qs} + y_1 v_{bs} + z_1 v_{ds}^a + \gamma_1 v_{es}\right]\cos\frac{4\pi}{5} - v_{bs}\cos\frac{2\pi}{5} - v_{ds}^a \cos\frac{4\pi}{5} - v_{es}\cos\frac{2\pi}{5}$$
(5.319)

$$v_{as} = \begin{bmatrix} \left(\frac{5}{2} - x_1 \cos\frac{4\pi}{5}\right)v_{qs} - \left(y_1 \cos\frac{4\pi}{5} + \cos\frac{2\pi}{5}\right)v_{bs} \\ -\left(z_1 \cos\frac{4\pi}{5} + \cos\frac{4\pi}{5}\right)v_{ds}^a - \left(\gamma_1 \cos\frac{4\pi}{5} + \cos\frac{2\pi}{5}\right)v_{es} \end{bmatrix} \tag{5.320}$$

$$v_{as} = s_1 v_{qs} + s_2 v_{bs} + s_3 v_{ds}^a + s_4 v_{es} \tag{5.321}$$

where

$$s_1 = \left(\frac{5}{2} - x_1 \cos\frac{4\pi}{5}\right)$$

$$s_2 = -\left(y_1 \cos\frac{4\pi}{5} + \cos\frac{2\pi}{5}\right)$$

$$s_3 = -\left(z_1 \cos\frac{4\pi}{5} + \cos\frac{4\pi}{5}\right)$$

$$s_4 = -\left(\gamma_1 \cos\frac{4\pi}{5} + \cos\frac{2\pi}{5}\right)$$

The d-axis voltage is given by

$$v_{ds} = \frac{2}{5}\left(-v_{bs}\sin\frac{2}{5}\pi - v_{cs}\sin\frac{4}{5}\pi + v_{ds}^{a}\sin\frac{4}{5}\pi + v_{es}\sin\frac{2}{5}\pi\right) \tag{5.322}$$

Substituting (5.314) into (5.322) gives

$$v_{ds} = \frac{2}{5}\left(-\left(x_1 v_{qs} + y_1 v_{bs} + z_1 v_{ds}^{a} + \gamma_1 v_{es}\right)\sin\frac{4}{5}\pi - v_{bs}\sin\frac{2}{5}\pi + v_{ds}^{a}\sin\frac{4}{5}\pi + v_{es}\sin\frac{2}{5}\pi\right)$$

$$v_{ds} = -\frac{2}{5}xv_{qs}\sin\frac{4}{5}\pi + \frac{2}{5}\begin{pmatrix} -yv_{bs}\sin\frac{4}{5}\pi - zv_{ds}^{a}\sin\frac{4}{5}\pi - \gamma v_{es}\sin\frac{4}{5}\pi \\ -v_{bs}\sin\frac{2}{5}\pi + v_{ds}^{a}\sin\frac{4}{5}\pi + v_{es}\sin\frac{2}{5}\pi \end{pmatrix}$$

$$v_{ds} = -\frac{2}{5}x\sin\frac{4}{5}\pi v_{qs} + \frac{2}{5}\begin{pmatrix} -\left(y\sin\frac{4}{5}\pi + \sin\frac{2}{5}\pi\right)v_{bs} - \left(z\sin\frac{4}{5}\pi - \sin\frac{4}{5}\pi\right)v_{ds}^{a} \\ -\left(\gamma\sin\frac{4}{5}\pi - \sin\frac{2}{5}\pi\right)v_{es} \end{pmatrix} \tag{5.323}$$

$$v_{ds} = s_5 v_{qs} + s_6 v_{bs} + s_7 v_{ds}^{a} + s_8 v_{es} \tag{5.324}$$

where

$$s_5 = -\frac{2}{5}x_1\sin\frac{4}{5}\pi$$

$$s_6 = -\frac{2}{5}\left(y_1\sin\frac{4}{5}\pi + \sin\frac{2}{5}\pi\right)$$

$$s_7 = -\frac{2}{5}\left(z_1\sin\frac{4}{5}\pi - \sin\frac{4}{5}\pi\right)$$

$$s_8 = -\frac{2}{5}\left(\gamma_1\sin\frac{4}{5}\pi - \sin\frac{2}{5}\pi\right)$$

The y-axis voltage is given by

$$v_{ys} = \frac{2}{5}\left(- v_{bs} \sin\frac{4\pi}{5} + v_{cs} \sin\frac{2\pi}{5} - v_{ds}^{a} \sin\frac{2\pi}{5} + v_{es} \sin\frac{4\pi}{5} \right) \tag{5.325}$$

Substituting (5.314) into (5.325) results into

$$v_{ys} = \begin{bmatrix} \frac{2}{5} x_1 \sin\frac{2\pi}{5} v_{qs} + \frac{2}{5}\left(y_1 \sin\frac{2\pi}{5} - \sin\frac{4\pi}{5} \right) v_{bs} + \frac{2}{5}\left(z_1 \sin\frac{2\pi}{5} - \sin\frac{2\pi}{5} \right) v_{ds}^{a} \\ + \frac{2}{5}\left(\gamma_1 \sin\frac{2\pi}{5} + \sin\frac{4\pi}{5} \right) v_{es} \end{bmatrix} \tag{5.326}$$

$$v_{ys} = s_9 v_{qs} + s_{10} v_{bs} + s_{11} v_{ds}^{a} + s_{12} v_{es} \tag{5.327}$$

where

$$s_9 = \frac{2}{5} x_1 \sin\frac{2\pi}{5}$$

$$s_{10} = \frac{2}{5}\left(y_1 \sin\frac{2\pi}{5} - \sin\frac{4\pi}{5} \right)$$

$$s_{11} = \frac{2}{5}\left(z_1 \sin\frac{2\pi}{5} - \sin\frac{2\pi}{5} \right)$$

$$s_{12} = \frac{2}{5}\left(\gamma_1 \sin\frac{2\pi}{5} + \sin\frac{4\pi}{5} \right)$$

Since $i_{xs} = -i_{qs}$, then

$$v_{xs} = -r_s i_{qs} - L_{ls} p i_{qs} \tag{5.328}$$

Substituting (5.328) into (5.318) gives

$$a_1 v_{qs} + r_s i_{qs} + L_{ls} p i_{qs} = b_1 v_{bs} + c_1 v_{ds} + d_1 v_{es} \tag{5.329}$$

Substituting for $p i_{qs}$ from (5.196) into (5.329) gives

$$a_1 v_{qs} + \frac{L_{ls} L_r}{L_s L_r - L_m^2} v_{qs} + r_s i_{qs} - \frac{L_{ls}}{L_s L_r - L_m^2}\left(r_s i_{qs} L_r + L_m p \lambda_{qr} \right) = b_1 v_{bs} + c_1 v_{ds} + d_1 v_{es} \tag{5.330}$$

$$v_{qs} = \frac{1}{\left(a_1 + \frac{L_{ls}L_r}{L_sL_r - L_m^2}\right)}\left[b_1 v_{bs} + c_1 v_{ds} + d_1 v_{es} - r_s i_{qs} + \frac{L_{ls}}{L_sL_r - L_m^2}\begin{pmatrix} r_s i_{qs} L_r \\ + L_m p\lambda_{qr} \end{pmatrix}\right] \tag{5.331}$$

Therefore, with v_{as}, v_{cs}, v_{qs}, v_{ds} and v_{ys} known, then the faulted condition can be simulated by using dynamic Equations (5.198) through (5.200).

The phase currents are obtained as

$$i_{as} = i_{qs} + i_{xs} \tag{5.332}$$

$$i_{bs} = -i_{qs} - i_{xs} - \frac{5}{2}\left[\frac{\sin\frac{4\pi}{5} i_{ds}}{\sin^2\frac{4\pi}{5} + \sin^2\frac{2\pi}{5}} - \frac{3}{2}\frac{\sin\frac{2\pi}{5} i_{ys}}{\sin^2\frac{4\pi}{5} + \sin^2\frac{2\pi}{5}}\right] \tag{5.333}$$

$$i_{cs} = -i_{qs} - i_{xs} \tag{5.334}$$

$$i_{ds}^a = \frac{5}{2}\frac{\sin\frac{4\pi}{5} i_{ds} - \sin\frac{2\pi}{5} i_{ys}}{\sin^2\frac{4\pi}{5} + \sin^2\frac{2\pi}{5}} \tag{5.335}$$

$$i_{es} = -\frac{5}{4}\frac{\sin\frac{2\pi}{5} i_{ys}}{\sin^2\frac{4\pi}{5} + \sin^2\frac{2\pi}{5}} \tag{5.336}$$

5.5.1 Harmonic Balance Technique for the Two Non-adjacent Stator Open Phases

The same approach that has been used in section 5.3.1 applies here as well.

$$v_{ds} = s_5 v_{qs} + s_6 v_{bs} + s_7 v_{ds}^a + s_8 v_{es} \tag{22}$$

$$v_{ys} = s_9 v_{qs} + s_{10} v_{bs} + s_{11} v_{ds}^a + s_{12} v_{es} \tag{24}$$

Let

$$\sigma_2 = \frac{1}{\left(a_1 + \frac{L_{ls}L_r}{L_sL_r - L_m^2}\right)}$$

Then Equation (5.331) can be written as

$$v_{qs} = \sigma_2\left[b_1 v_{bs} + c_1 v_{ds}^a + d_1 v_{es} - r_s i_{qs} + \frac{L_{ls}}{L_sL_r - L_m^2}\left(r_s i_{qs} L_r + L_m p\lambda_{qr}\right)\right] \tag{5.337}$$

Using Equations (5.61) through (5.84), the following harmonic balance technique dynamic model is obtained

The q-axis stator voltage is given by

$$v_{qss} = \sigma_2\left[b_1 v_{bss} + c_1 v_{dss}^a + d_1 v_{ess} - r_s i_{qss} + \frac{L_{ls}}{L_sL_r - L_m^2}\begin{pmatrix} r_s L_r i_{qss} + L_m p\lambda_{qrr} \\ + j\omega_e L_m \lambda_{qrr} \end{pmatrix}\right] \tag{5.338}$$

The rest of the harmonic balance technique model Equations are as given in Equations (5.208) through (5.212).

5.5.2 Steady State and Dynamic Model Analysis for Two Adjacent Open Phases

5.5.2.1 Steady state model. At steady state, the derivatives of the peaks are zero. Therefore, the steady state model is given by Equations (5.339) and (5.214) through (5.218) become

$$-\sigma_2\left(b_1 v_{bss} + c_1 v_{dss}^a + d_1 v_{ess}\right) = -v_{qss} + \left(\frac{r_s L_r L_{ls}}{L_sL_r - L_m^2} - r_s\right)\sigma_2 i_{qss} + \frac{j\omega_e L_m L_{ls}\sigma_2}{L_sL_r - L_m^2}\lambda_{qrr} \tag{5.339}$$

The d-axis and y-axis stator voltages re, respectively given by (5.340) and (5.341)

$$s_6 v_{bss} + s_7 v_{dss}^a + s_8 v_{ess} = -s_5 v_{qss} + v_{dss} \tag{5.340}$$

$$s_{10} v_{bss} + s_{11} v_{dss}^a + s_{12} v_{ess} = -s_9 v_{qss} + v_{yss} \tag{5.341}$$

In matrix form, the steady-state harmonic balance technique model can be represented as

$$A_3 x_3 = b_3 \tag{5.342}$$

$$x_3 = A_3^{-1} b_3 \tag{5.343}$$

where the matrices b_3 and x_3 are, respectively, given by Equations (5.344) and (5.345), with

$$b_{311} = -\sigma_2 \left(b_1 v_{bss} + c_1 v_{dss}^a + d_1 v_{ess} \right)$$

$$b_{371} = s_6 v_{bss} + s_7 v_{dss}^a + s_8 v_{ess}$$

$$b_{381} = s_{10} v_{bss} + s_{11} v_{dss}^a + s_{12} v_{ess}$$

$$b_3 = \begin{bmatrix} b_{311} & 0 & 0 & 0 & -v_{qrr} & -v_{drr} & b_{371} & b_{381} \end{bmatrix}^T \tag{5.344}$$

$$x_3 = \begin{bmatrix} v_{qss} & v_{dss} & v_{yss} & i_{qss} & i_{dss} & i_{yss} & \lambda_{qrr} & \lambda_{drr} \end{bmatrix}^T \tag{5.345}$$

The matrix A_3 is given by Equation (5.346).

$$A_3 = \begin{bmatrix} -1 & 0 & 0 & \left(\frac{r_s L_r L_{ls}}{L_s L_r - L_m^2} - r_s\right)\sigma_2 & 0 & 0 & \frac{j\omega_e L_m L_{ls}\sigma_2}{L_s L_r - L_m^2} & 0 \\ \frac{L_r}{L_s L_r - L_m^2} & 0 & 0 & -\left(\frac{r_s L_r}{L_s L_r - L_m^2} + j\omega_e\right) & 0 & 0 & -\frac{j\omega_e L_m}{L_s L_r - L_m^2} & 0 \\ 0 & \frac{L_r}{L_s L_r - L_m^2} & 0 & 0 & -\left(\frac{r_s L_r}{L_s L_r - L_m^2} + j\omega_e\right) & 0 & 0 & -\frac{j\omega_e L_m}{L_s L_r - L_m^2} \\ 0 & 0 & \frac{1}{L_{ls}} & 0 & 0 & -\left(\frac{r_s}{L_{ls}} + j\omega_e\right) & 0 & 0 \\ 0 & 0 & 0 & \frac{r_r L_m}{L_r} & 0 & 0 & -\left(\frac{r_r}{L_r} + j\omega_e\right) & \omega_{ro} \\ 0 & 0 & 0 & 0 & \frac{r_r L_m}{L_r} & 0 & -\omega_{ro} & -\left(\frac{r_r}{L_r} + j\omega_e\right) \\ -t_5 & 1 & 0 & 0 & 0 & 0 & 0 & 0 \\ -t_9 & 0 & 1 & 0 & 0 & 0 & 0 & 0 \end{bmatrix} \tag{5.346}$$

When the speed harmonic component is taken into account, then the Equations have to be separate into their real and imaginary parts. The resulting systems of steady-state equations will be solved by iteration to obtain the results.

Substituting Equations (5.109) through (5.116) and (5.226) through (5.231) into Equation (5.339), gives

$$-\sigma_2\begin{bmatrix} b_1\left(v_{bsre}+jv_{bsim}\right)+c_1\left(v_{dsre}^a+jv_{dsim}^a\right) \\ +d_1\left(v_{esre}+jv_{esim}\right) \end{bmatrix}=\begin{bmatrix} -v_{qsre}-jv_{qsim}+\left(\dfrac{r_sL_rL_{ls}}{L_sL_r-L_m^2}-r_s\right)\sigma_2\left(i_{qsre}+ji_{qsim}\right) \\ +\dfrac{j\omega_eL_mL_{ls}\sigma_2}{L_sL_r-L_m^2}\left(\lambda_{qrre}+j\lambda_{qrim}\right) \end{bmatrix} \tag{5.347}$$

$$-\sigma_2\begin{bmatrix} b_1\left(v_{bsre}+jv_{bsim}\right)+c_1\left(v_{dsre}^a+jv_{dsim}^a\right) \\ +d_1\left(v_{esre}+jv_{esim}\right) \end{bmatrix}=\begin{bmatrix} -v_{qsre}-jv_{qsim}+\left(\dfrac{r_sL_rL_{ls}}{L_sL_r-L_m^2}-r_s\right)\sigma_2\left(i_{qsre}+ji_{qsim}\right) \\ +\dfrac{\omega_eL_mL_{ls}\sigma_2}{L_sL_r-L_m^2}\left(-\lambda_{qrim}+j\lambda_{qrre}\right) \end{bmatrix} \tag{5.348}$$

Separating real and imaginary parts,

$$-\sigma_2\left[b_1v_{bsre}+c_1v_{dsre}^a+d_1v_{esre}\right]=-v_{qsre}+\left(\frac{r_sL_rL_{ls}}{L_sL_r-L_m^2}-r_s\right)\sigma_2 i_{qsre}-\frac{\omega_eL_mL_{ls}\sigma_2}{L_sL_r-L_m^2}\lambda_{qrim} \tag{5.349}$$

$$-\sigma_2\left[b_1v_{bsim}+c_1v_{dsim}^a+d_1v_{esim}\right]=-v_{qsim}+\left(\frac{r_sL_rL_{ls}}{L_sL_r-L_m^2}-r_s\right)\sigma_2 i_{qsim}+\frac{\omega_eL_mL_{ls}\sigma_2}{L_sL_r-L_m^2}\lambda_{qrre} \tag{5.350}$$

From Equation (5.214),

$$0=\frac{L_r}{L_sL_r-L_m^2}\left(v_{qsre}+jv_{qsim}\right)-\left(\frac{r_sL_r}{L_sL_r-L_m^2}+j\omega_e\right)\left(i_{qsre}+ji_{qsim}\right)-\frac{j\omega_eL_m}{L_sL_r-L_m^2}\left(\lambda_{qrre}+j\lambda_{qrim}\right)$$

$$0=\left[\begin{array}{l}\frac{L_r}{L_sL_r-L_m^2}\left(v_{qsre}+jv_{qsim}\right)-\left(\frac{r_sL_r}{L_sL_r-L_m^2}i_{qsre}+j\omega_e i_{qsre}\right)-\left(\frac{jr_sL_r}{L_sL_r-L_m^2}i_{qsim}-\omega_e i_{qsim}\right)\\ -\frac{j\omega_e L_m}{L_sL_r-L_m^2}\lambda_{qrre}+\frac{\omega_e L_m}{L_sL_r-L_m^2}\lambda_{qrim}\end{array}\right] \tag{5.351}$$

Separating the real and imaginary parts

$$0=\frac{L_r}{L_sL_r-L_m^2}v_{qsre}-\frac{r_sL_r}{L_sL_r-L_m^2}i_{qsre}+\omega_e i_{qsim}+\frac{\omega_e L_m}{L_sL_r-L_m^2}\lambda_{qrim} \tag{5.352}$$

$$0=\frac{L_r}{L_sL_r-L_m^2}v_{qsim}-\omega_e i_{qsre}-\frac{r_sL_r}{L_sL_r-L_m^2}i_{qsim}-\frac{\omega_e L_m}{L_sL_r-L_m^2}\lambda_{qrre} \tag{5.353}$$

From Equation (5.215),

$$0=\frac{L_r}{L_sL_r-L_m^2}\left(v_{dsre}+jv_{dsim}\right)-\left(\frac{r_sL_r}{L_sL_r-L_m^2}+j\omega_e\right)\left(i_{dsre}+ji_{dsim}\right)-\frac{j\omega_e L_m}{L_sL_r-L_m^2}\left(\lambda_{drre}+j\lambda_{drim}\right)$$

$$0=\left[\begin{array}{l}\frac{L_r}{L_sL_r-L_m^2}\left(v_{dsre}+jv_{dsim}\right)-\left(\frac{r_sL_r}{L_sL_r-L_m^2}i_{dsre}+j\omega_e i_{dsre}\right)-\left(\frac{jr_sL_r}{L_sL_r-L_m^2}i_{dsim}-\omega_e i_{dsim}\right)\\ -\frac{j\omega_e L_m}{L_sL_r-L_m^2}\lambda_{drre}+\frac{\omega_e L_m}{L_sL_r-L_m^2}\lambda_{drim}\end{array}\right] \tag{5.354}$$

Separating the real and imaginary parts

$$0=L_{22}v_{dsre}-r_sL_{22}i_{dsre}+\omega_e i_{dsim}+L_{11}\lambda_{drim} \tag{5.355}$$

$$0=L_{22}v_{dsim}-\omega_e i_{dsre}-r_sL_{22}i_{dsim}-L_{11}\lambda_{drre} \tag{5.356}$$

From Equation (5.216),

$$0=\frac{1}{L_{ls}}\left(v_{ysre}+jv_{ysim}\right)-\left(\frac{r_s}{L_{ls}}+j\omega_e\right)\left(i_{ysre}+ji_{ysim}\right)$$

$$0=\frac{1}{L_{ls}}\left(v_{ysre}+jv_{ysim}\right)-\left(\frac{r_s}{L_{ls}}i_{ysre}+j\omega_e i_{ysre}\right)-\left(\frac{jr_s}{L_{ls}}i_{ysim}-\omega_e i_{ysim}\right) \tag{5.357}$$

Separating the real and imaginary parts

$$0 = L_{33} v_{ysre} - L_{44} i_{ysre} + \omega_e i_{ysim} \tag{5.358}$$

$$0 = L_{33} v_{ysim} - \omega_e i_{ysre} - L_{44} i_{ysim} \tag{5.359}$$

From Equation (5.217),

$$-v_{qrre} - jv_{qrim} = \begin{bmatrix} \frac{r_r L_m}{L_r}\left(i_{qsre} + ji_{qsim}\right) - \left(\frac{r_r}{L_r} + j\omega_e\right)\left(\lambda_{qrre} + j\lambda_{qrim}\right) \\ + \omega_{ro}\left(\lambda_{drre} + j\lambda_{drim}\right) + \frac{1}{2} j\omega_{r1im}\left(\lambda_{drre} - j\lambda_{drim}\right) \end{bmatrix}$$

$$-v_{qrre} - jv_{qrim} = \begin{bmatrix} \frac{r_r L_m}{L_r}\left(i_{qsre} + ji_{qsim}\right) - \left(\frac{r_r}{L_r}\lambda_{qrre} + j\omega_e \lambda_{qrre}\right) - \left(\frac{jr_r}{L_r}\lambda_{qrim} - \omega_e \lambda_{qrim}\right) \\ + \omega_{ro}\lambda_{drre} + j\omega_{ro}\lambda_{drim} + j\frac{1}{2}\omega_{r1im}\lambda_{drre} + \frac{1}{2}\omega_{r1im}\lambda_{drim} \end{bmatrix} \tag{5.360}$$

Separating the real and imaginary parts

$$-v_{qrre} = L_{55} i_{qsre} - L_{66}\lambda_{qrre} + \omega_e \lambda_{qrim} + \omega_{ro}\lambda_{drre} + \frac{1}{2}\omega_{r1im}\lambda_{drim} \tag{5.361}$$

$$-v_{qrim} = L_{55} i_{qsim} - \omega_e \lambda_{qrre} - L_{66}\lambda_{qrim} + \omega_{ro}\lambda_{drim} + \frac{1}{2}\omega_{r1im}\lambda_{drre} \tag{5.362}$$

From Equation (5.218),

$$-v_{drre} - jv_{drim} = \begin{bmatrix} -\omega_{ro}\left(\lambda_{qrre} + j\lambda_{qrim}\right) - \frac{1}{2} j\omega_{r1}\left(\lambda_{qrre} - j\lambda_{qrim}\right) - \left(\frac{r_r}{L_r} + j\omega_e\right)\left(\lambda_{drre} + j\lambda_{drim}\right) \\ + \frac{r_r L_m}{L_r}\left(i_{dsre} + ji_{dsim}\right) \end{bmatrix}$$

$$-v_{drre} - jv_{drim} = \begin{bmatrix} -\omega_{ro}\lambda_{qrre} - j\omega_{ro}\lambda_{qrim} - \left(j\frac{1}{2}\omega_{r1}\lambda_{qrre} + \frac{1}{2}\omega_{r1}\lambda_{qrim}\right) - \left(\frac{r_r}{L_r}\lambda_{drre} + j\omega_e \lambda_{drre}\right) \\ -\left(\frac{jr_r}{L_r}\lambda_{drim} - \omega_e \lambda_{drim}\right) + \frac{r_r L_m}{L_r}\left(i_{dsre} + ji_{dsim}\right) \end{bmatrix} \tag{5.363}$$

Separating the real and imaginary parts

$$-v_{drre} = -\omega_{ro}\lambda_{qrre} - \frac{1}{2}\omega_{r1}\lambda_{qrim} - L_{66}\lambda_{drre} + \omega_e\lambda_{drim} + L_{55}i_{dsre} \tag{5.364}$$

$$-v_{drim} = -\omega_{ro}\lambda_{qrim} - \frac{1}{2}\omega_{r1}\lambda_{qrre} - \omega_e\lambda_{drre} - L_{66}\lambda_{drim} + L_{55}i_{dsim} \tag{5.365}$$

From Equation (5.340),

$$s_6\left(v_{bsre} + jv_{bsim}\right) + s_7\left(v^a_{dsre} + jv^a_{dsim}\right) + s_8\left(v_{esre} + jv_{esim}\right) = -s_5\left(v_{qsre} + jv_{qsim}\right) + v_{dsre} + jv_{dsim} \tag{5.366}$$

Separating the real and imaginary parts

$$s_6v_{bsre} + s_7v^a_{dsre} + s_8v_{esre} = -s_5v_{qsre} + v_{dsre} \tag{5.367}$$

$$s_6v_{bsim} + s_7v^a_{dsim} + s_8v_{esim} = -s_5v_{qsim} + v_{dsim} \tag{5.368}$$

From Equation (5.341),

$$s_{10}\left(v_{bsre} + jv_{bsim}\right) + s_{11}\left(v^a_{dsre} + jv^a_{dsim}\right) + s_{12}\left(v_{esre} + jv_{esim}\right) = -s_9\left(v_{qsre} + jv_{qsim}\right) + v_{ysre} + jv_{ysim} \tag{5.369}$$

Separating the real and imaginary parts

$$s_{10}v_{bsre} + s_{11}v^a_{dsre} + s_{12}v_{esre} = -s_9v_{qsre} + v_{ysre} \tag{5.370}$$

$$s_{10}v_{bsim} + s_{11}v^a_{dsim} + s_{12}v_{esim} = -s_9v_{qsim} + v_{ysim} \tag{5.371}$$

These Equations can be written in matrix form as

$$A_4x_4 = b_4 \tag{5.372}$$

$$x_4 = A_4^{-1}b_4 \tag{5.373}$$

where b_4 and x_4 are, respectively, given by Equations (5.374) and (5.375), with

$$b_{411} = -\sigma_2\left(b_1v_{bsre} + c_1v^a_{dsre} + d_1v_{esre}\right)$$

$$b_{421} = -\sigma_2\left(b_1v_{bsim} + c_1v^a_{dsim} + d_1v_{esim}\right)$$

$$b_{4131} = s_6 v_{bsre} + s_7 v_{dsre}^a + s_8 v_{esre}$$

$$b_{4141} = s_6 v_{bsim} + s_7 v_{dsim}^a + s_8 v_{esim}$$

$$b_{4151} = s_{10} v_{bsre} + s_{11} v_{dsre}^a + s_{12} v_{esre}$$

$$b_{4161} = s_{10} v_{bsim} + s_{11} v_{dsim}^a + s_{12} v_{esim}$$

Let

$$L_{o1} = \left(r_s L_{22} L_{ls} - r_s\right)\sigma_2 \qquad L_{11} = \frac{\omega_e L_m}{L_s L_r - L_m^2} \qquad L_{22} = \frac{L_r}{L_s L_r - L_m^2}$$

$$L_{33} = \frac{1}{L_{ls}} \qquad L_{44} = \frac{r_s}{L_{ls}} \qquad L_{55} = \frac{r_r L_m}{L_r} \qquad L_{66} = \frac{r_r}{L_r}$$

The matrix A_4 is given by Equation (5.376).

$$b_4 = \begin{bmatrix} b_{411} & b_{421} & 0 & 0 & 0 & 0 & 0 & 0 & -v_{qrre} & -v_{qrim} & -v_{drre} & -v_{drim} & b_{4131} & b_{4141} & b_{4151} & b_{4161} \end{bmatrix}^T \tag{5.374}$$

$$x_4 = \begin{bmatrix} v_{qsre} & v_{qsim} & v_{dsre} & v_{dsim} & v_{ysre} & v_{ysim} & i_{qsre} & i_{qsim} & i_{dsre} & i_{dsim} & i_{ysre} & i_{ysim} & \lambda_{qrre} & \lambda_{qrim} & \lambda_{drre} & \lambda_{drim} \end{bmatrix}^T \tag{5.375}$$

$$A_4 = \begin{bmatrix}
-1 & 0 & 0 & 0 & 0 & 0 & L_{o1} & 0 & 0 & 0 & 0 & 0 & 0 & -L_{11}L_{ls}\sigma_2 & 0 & 0 \\
0 & -1 & 0 & 0 & 0 & 0 & 0 & L_{o1} & 0 & 0 & 0 & 0 & L_{11}L_{ls}\sigma_2 & 0 & 0 & 0 \\
L_{22} & 0 & 0 & 0 & 0 & 0 & -r_s L_{22} & \omega_e & 0 & 0 & 0 & 0 & 0 & L_{11} & 0 & 0 \\
0 & L_{22} & 0 & 0 & 0 & 0 & -\omega_e & -r_s L_{22} & 0 & 0 & 0 & 0 & -L_{11} & 0 & 0 & 0 \\
0 & 0 & L_{22} & 0 & 0 & 0 & 0 & 0 & -r_s L_{22} & \omega_e & 0 & 0 & 0 & 0 & 0 & L_{11} \\
0 & 0 & 0 & L_{22} & 0 & 0 & 0 & 0 & -\omega_e & -r_s L_{22} & 0 & 0 & 0 & 0 & -L_{11} & 0 \\
0 & 0 & 0 & 0 & L_{33} & 0 & 0 & 0 & 0 & 0 & -L_{44} & \omega_e & 0 & 0 & 0 & 0 \\
0 & 0 & 0 & 0 & 0 & L_{33} & 0 & 0 & 0 & 0 & -\omega_e & -L_{44} & 0 & 0 & 0 & 0 \\
0 & 0 & 0 & 0 & 0 & 0 & L_{55} & 0 & 0 & 0 & 0 & 0 & -L_{66} & \omega_e & \omega_{ro} & \frac{1}{2}\omega_{r1im} \\
0 & 0 & 0 & 0 & 0 & 0 & 0 & L_{55} & 0 & 0 & 0 & 0 & -\omega_e & -L_{66} & \frac{1}{2}\omega_{r1im} & \omega_{ro} \\
0 & 0 & 0 & 0 & 0 & 0 & 0 & 0 & L_{55} & 0 & 0 & 0 & -\omega_{ro} & -\frac{1}{2}\omega_{r1im} & -L_{66} & \omega_e \\
0 & 0 & 0 & 0 & 0 & 0 & 0 & 0 & 0 & L_{55} & 0 & 0 & -\frac{1}{2}\omega_{r1} & -\omega_{ro} & -\omega_e & -L_{66} \\
-t_5 & 0 & 1 & 0 & 0 & 0 & 0 & 0 & 0 & 0 & 0 & 0 & 0 & 0 & 0 & 0 \\
0 & -t_5 & 0 & 1 & 0 & 0 & 0 & 0 & 0 & 0 & 0 & 0 & 0 & 0 & 0 & 0 \\
-t_9 & 0 & 0 & 0 & 1 & 0 & 0 & 0 & 0 & 0 & 0 & 0 & 0 & 0 & 0 & 0 \\
0 & -t_9 & 0 & 0 & 0 & 1 & 0 & 0 & 0 & 0 & 0 & 0 & 0 & 0 & 0 & 0
\end{bmatrix}$$

(5.376)

5.5.3 Results and Discussion for Two Non-adjacent Open Phase Fault

The validity of the models presented in section 5.5 - 5.5.2 has been investigated through the computer simulation of the full-order model of the machine with stator phases '*a*' and '*c*' open-circuited. The steady-state model is used to calculate the state variables and then the results are compared.

Figure 5.30 through Figure 5.33 present the simulation of the free acceleration starting process of the machine. The phase voltage is applied to the remaining three phases (b, d, and e) and Equations (5.321) and (5.314) are used to determine stator phase '*a*' and '*c*' voltages, respectively. Figure 5.30(a) and (b) show the rotor speed and electromagnetic torque, respectively, showing the characteristics similar to those of the healthy induction machine. In Figure 5.31(a) the stator phase '*a*' and '*c*' currents are zero as expected. The stator phase voltages are shown in Figure 5.32 with the starting transients of the open phases '*a*' and '*c*' as they develops the voltages are clearly displayed in Figure 5.32(a) and (b), respectively.

When the rotor speed is in steady state, the load torque is changed from 0 to 11 Nm to show the effect of the speed harmonics. The dynamic responses of the machine to load changes are shown in Figure 5.33(a) and (b) for the rotor speed and electromagnetic torque, respectively. In Figure 5.34 through Figure 5.37, the waveforms of the variables are shown after the speed has reached steady-state average value. It is evident from Figure 5.34(a) and (b) that the speed and torque consist of the harmonics at twice the frequency of the supply voltages as predicted by the harmonic balance technique model. The unbalance caused by the two open phases fault is clearly indicated in the stator phase load currents, Figure 5.35. Figure 5.36 (a) and (b) show that when the machine is loaded, the open phase '*a*' and '*c*' voltages are affected as they are reduced. This is due to the fact that the voltage waveforms are induced by the other phases and the rotor circuits.

Figure 5.38(a) and Figure 5.38 (b) show the peak values of the rotor speed and torque pulsations, respectively as a function of the rotor speed. In Figure 5.34 (a) the average rotor speed is approximately 359.95 rad/sec, the peak value of the speed oscillations is about 0.15 rad/sec. In Figure 5.34(b) the average torque is 11 Nm and the peak of the torque oscillations is about 5 Nm. These speed and torque values are fairly comparable to those in Figure 5.38(a) and Figure 5.38(b), respectively.

Figure 5.40 presents the torque-speed characteristics at both normal and two open-phase faulted conditions. First the normal operation of the machine is computer simulated and the steady-state torque curve is superimposed on the simulated curve. Then the same procedure is followed for the open phase faulted condition. Under this operation, the torque envelope is obtained by adding the peak of the pulsation torque to, and subtracting it from the average value obtained from the harmonic balance technique. Comparing the results of the dynamic computer simulation and the steady state calculations for both cases, the harmonic balance technique gives average and peak values of the torque that compare fairly with simulation results.

The stator input and reactive powers at steady state are shown in figure 5.41(a) and Figure 5.41(b), respectively. The speed and torque oscillations are also shown in figure 5.42 (a) and Figure 5.42(b), respectively. The results of which compare well with those presented in Figure 5.34(a) and Figure 5.34(b), respectively, as well as Figure 5.38(a) and Figure 5.38(b), respectively.

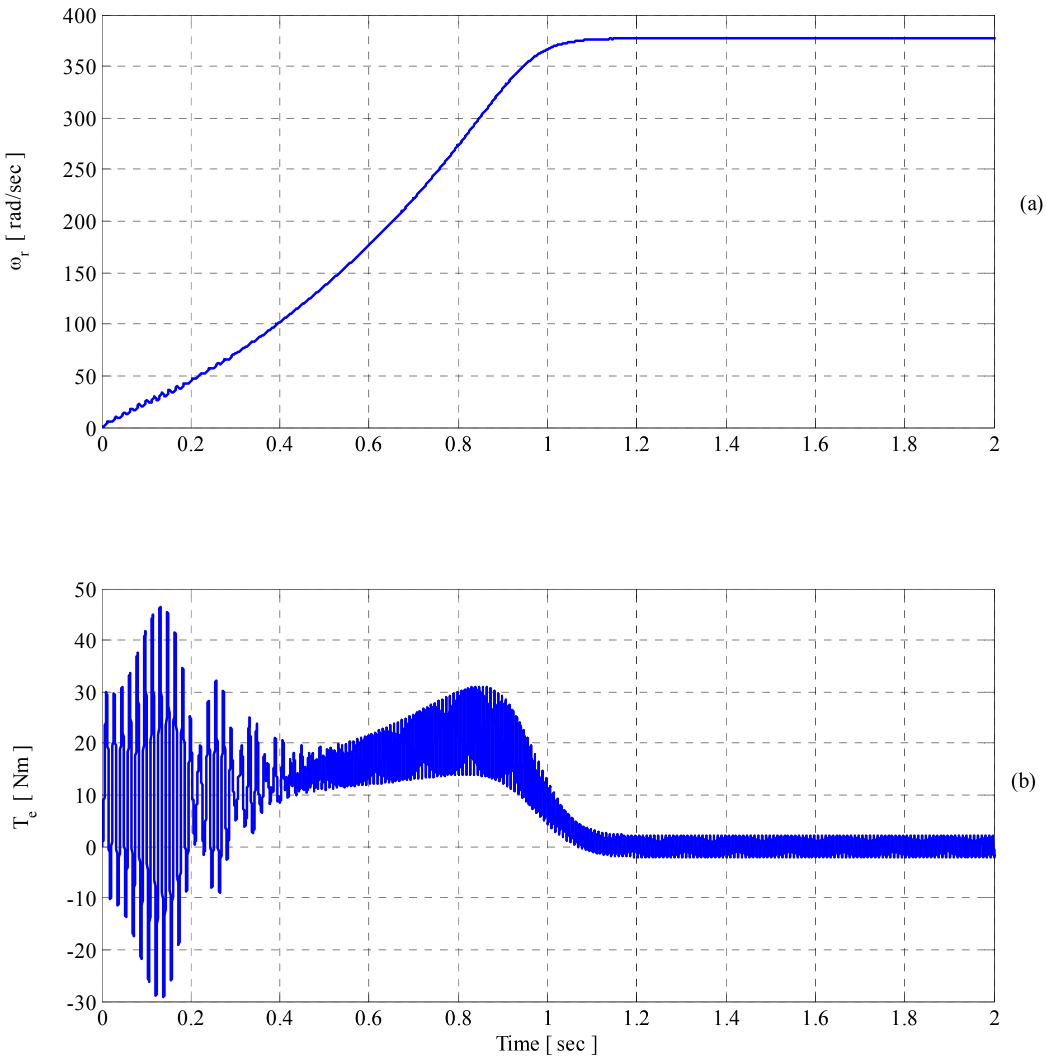

Figure 5.30 Starting transients (a) rotor speed and (b) electromagnetic torque

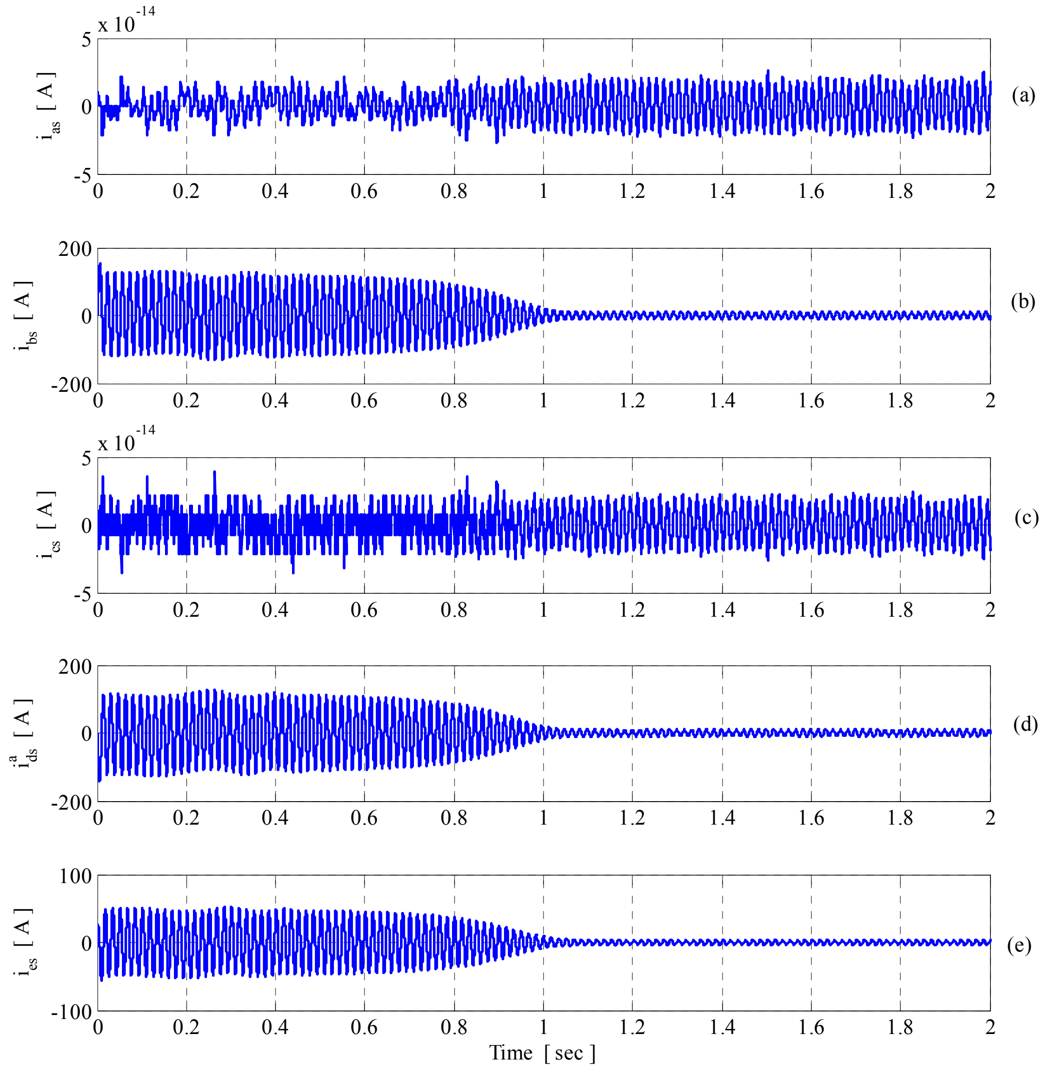

Figure 5.31 Starting transients Stator phase currents (a) phase ‘a’ (b) phase ‘b’ (c) phase ‘c’ (d) phase ‘d’ (e) phase ‘e’

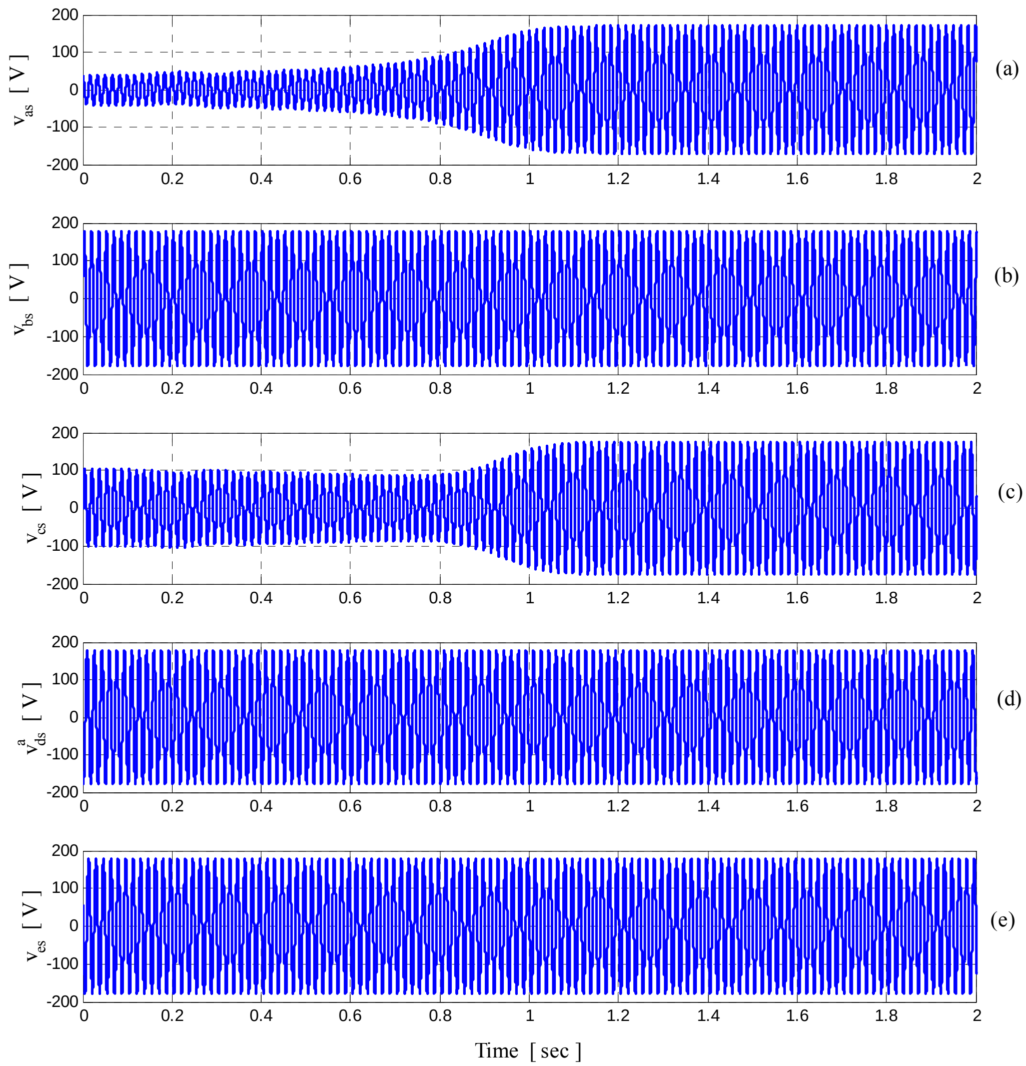

Figure 5.32 Starting transients stator phase voltages (a) phase ‘a’ (b) phase ‘b’ (c) phase ‘c’ (d) phase ‘d’ (e) phase ‘e’

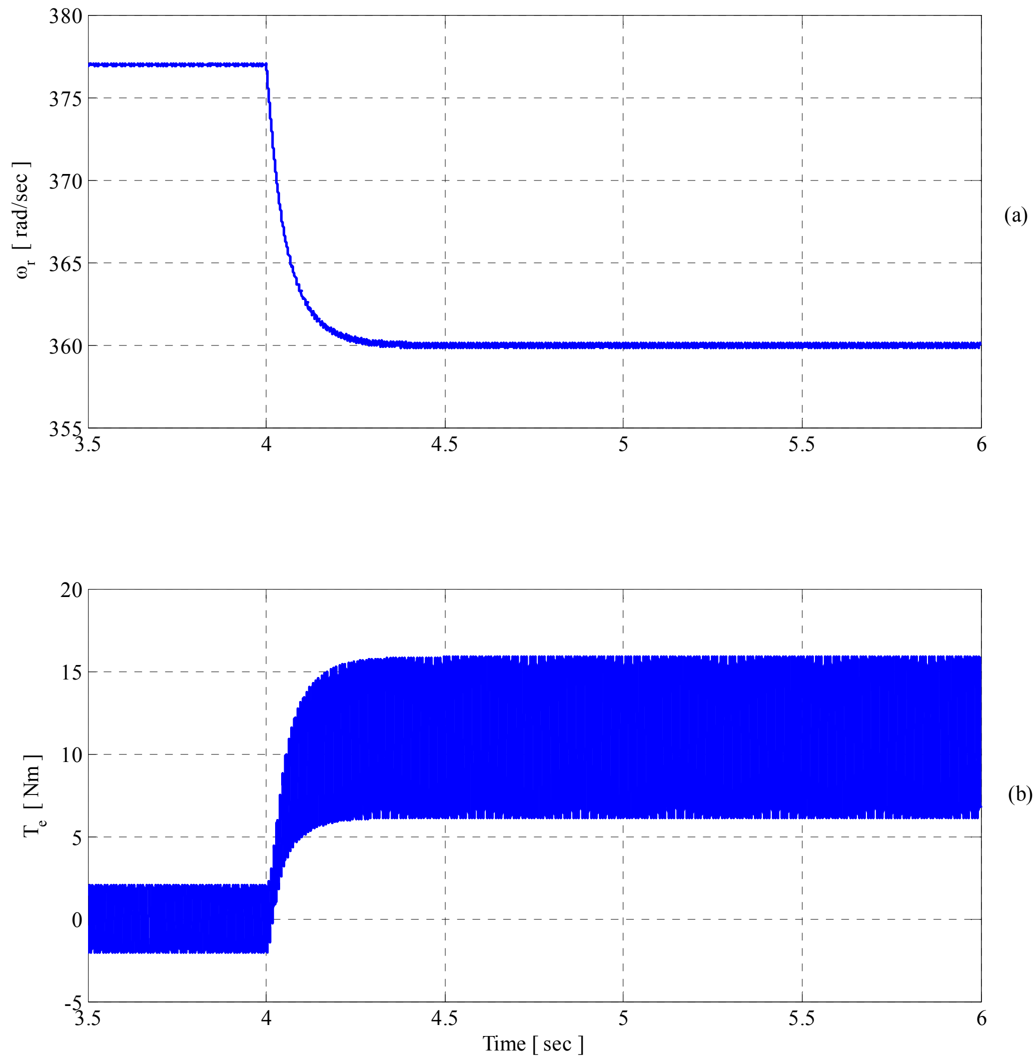

Figure 5.33 Simulation Dynamics of (a) rotor speed and (b) electromagnetic torque due to a load torque change of 11 Nm applied at 4 seconds.

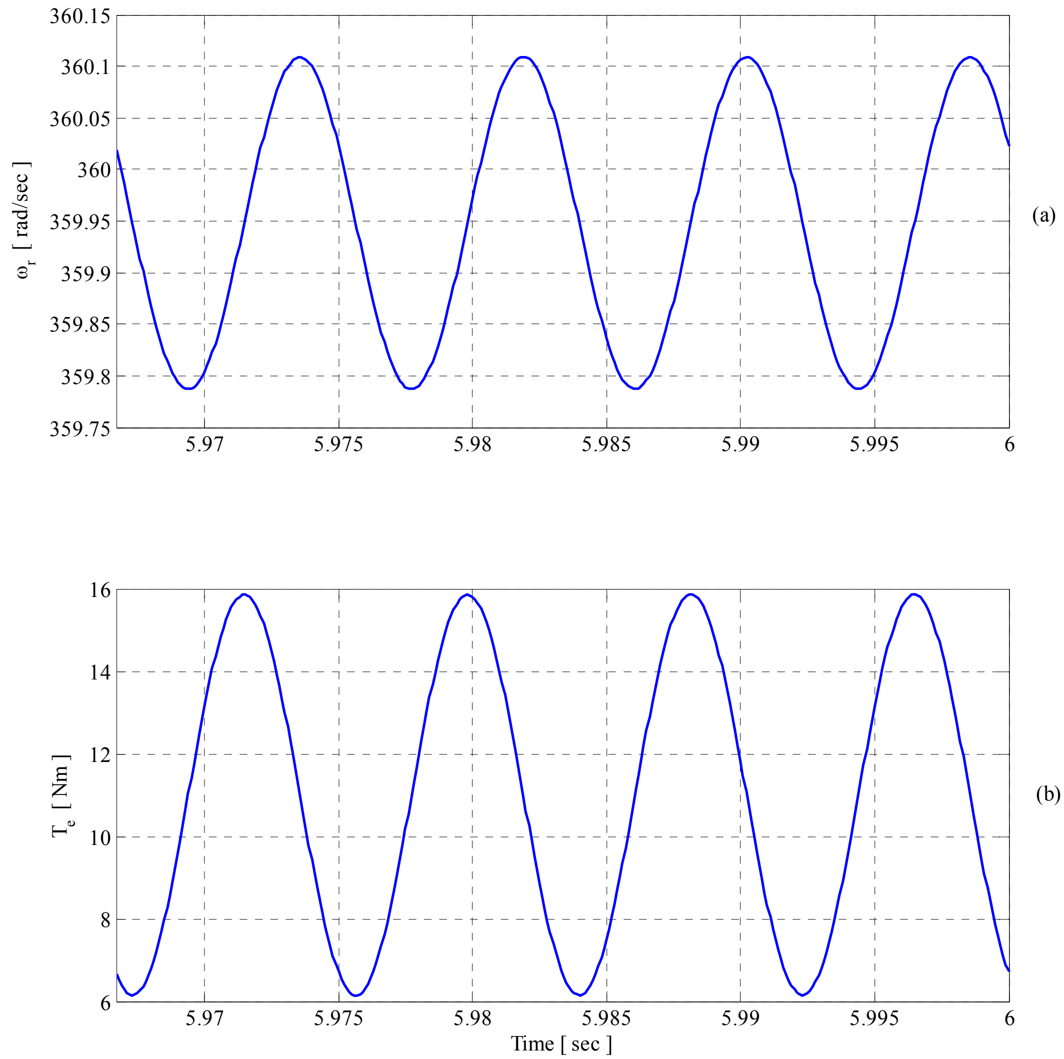

Figure 5.34 Simulation Steady-state (a) rotor speed and (b) electromagnetic torque at a load torque of 11 Nm.

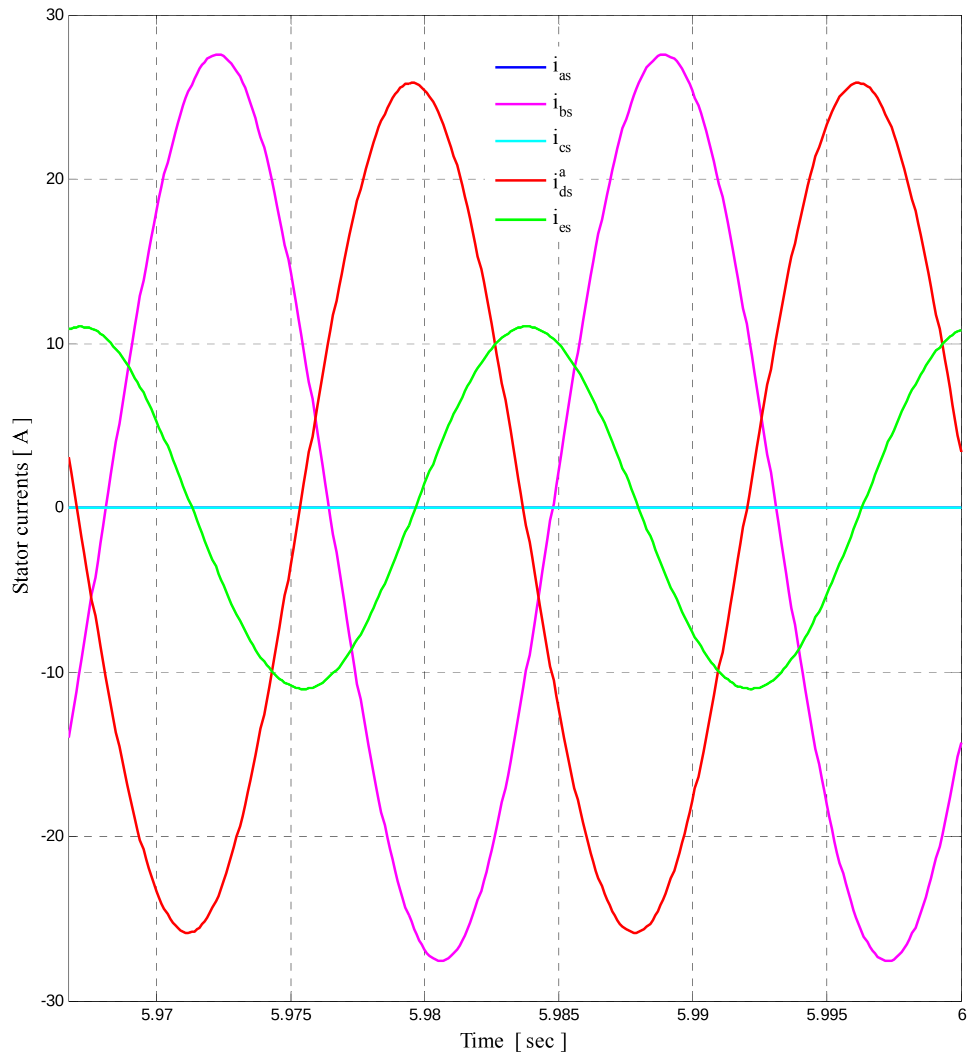

Figure 5.35 Simulation Steady-state stator phase currents at a load torque of 11 Nm.

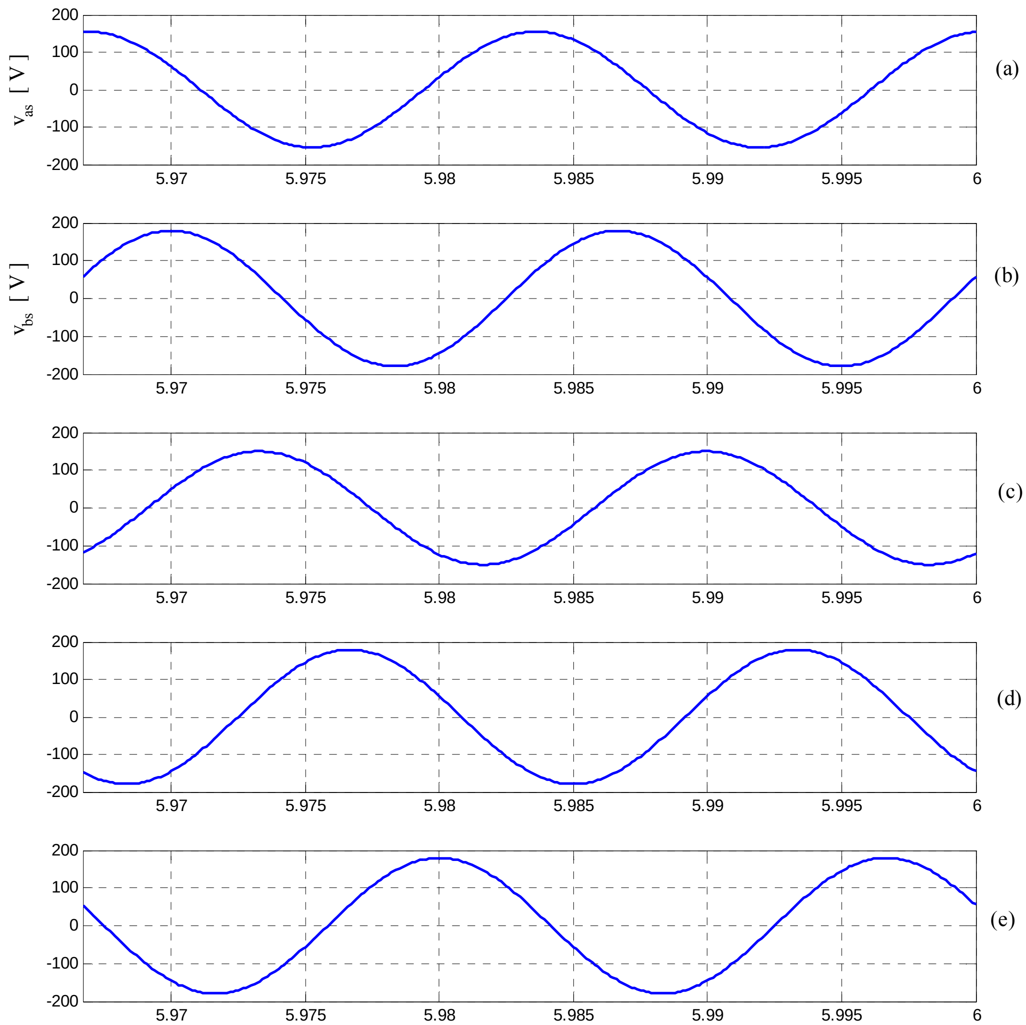

Figure 5.36 Simulation Steady-state stator phase voltages at a load torque of 11 Nm (a) phase ‘a’ (b) phase ‘b’ (c) phase ‘c’ (d) phase ‘d’ (e) phase ‘e’

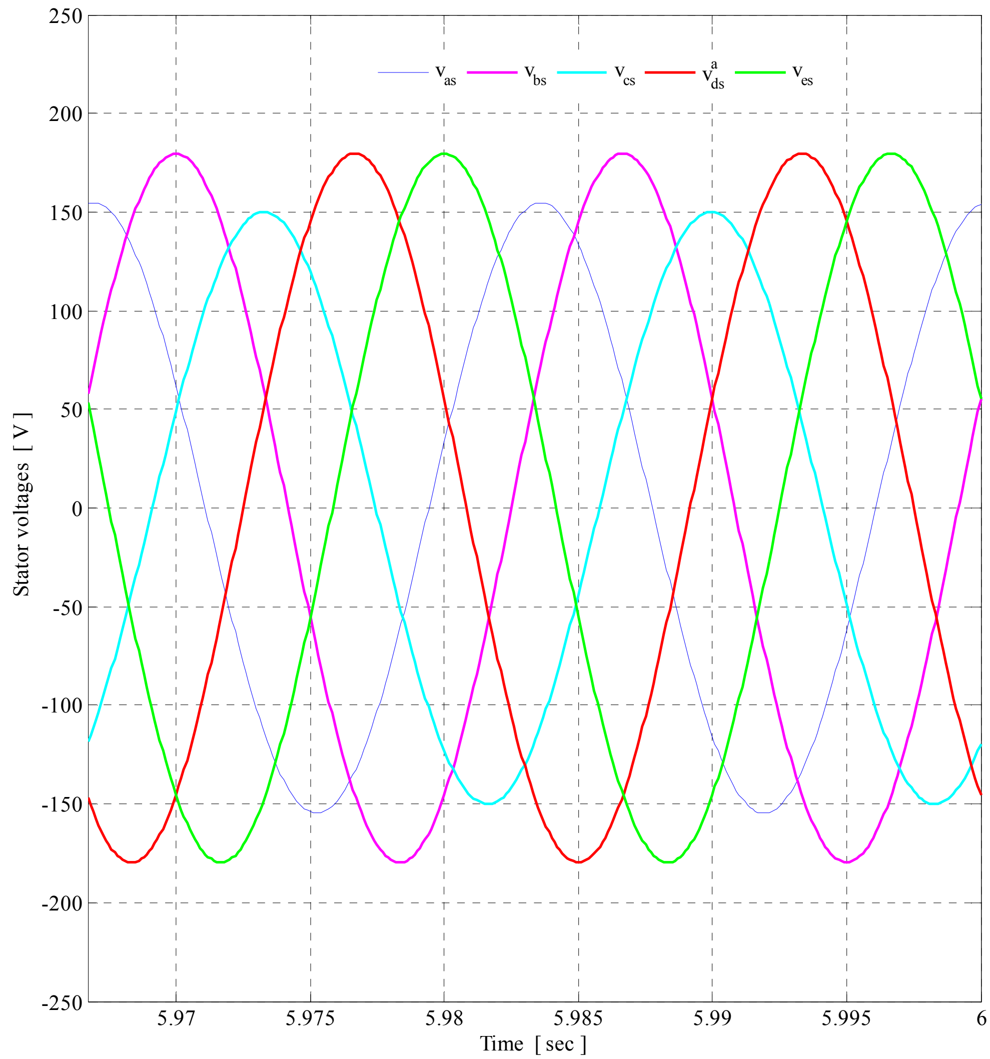

Figure 5.37 Stator phases '*a*' and '*c*' open Simulation Steady-state stator phase voltages at a load torque of 11 Nm showing the unbalance

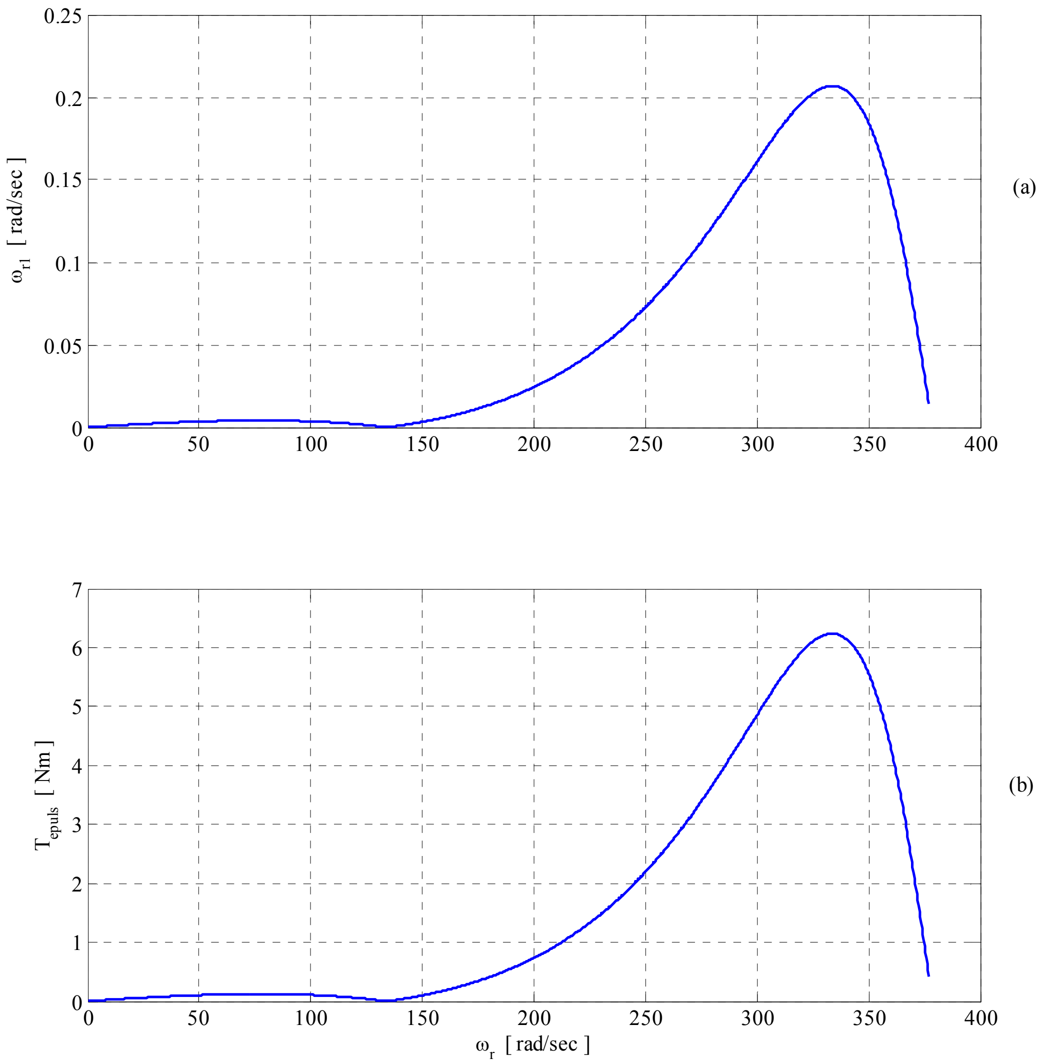

Figure 5.38 Phases '*a*' and '*c*' open circuited Steady-state calculation results (a) Peak value of the speed harmonic component and (b) Peak value of the torque pulsation

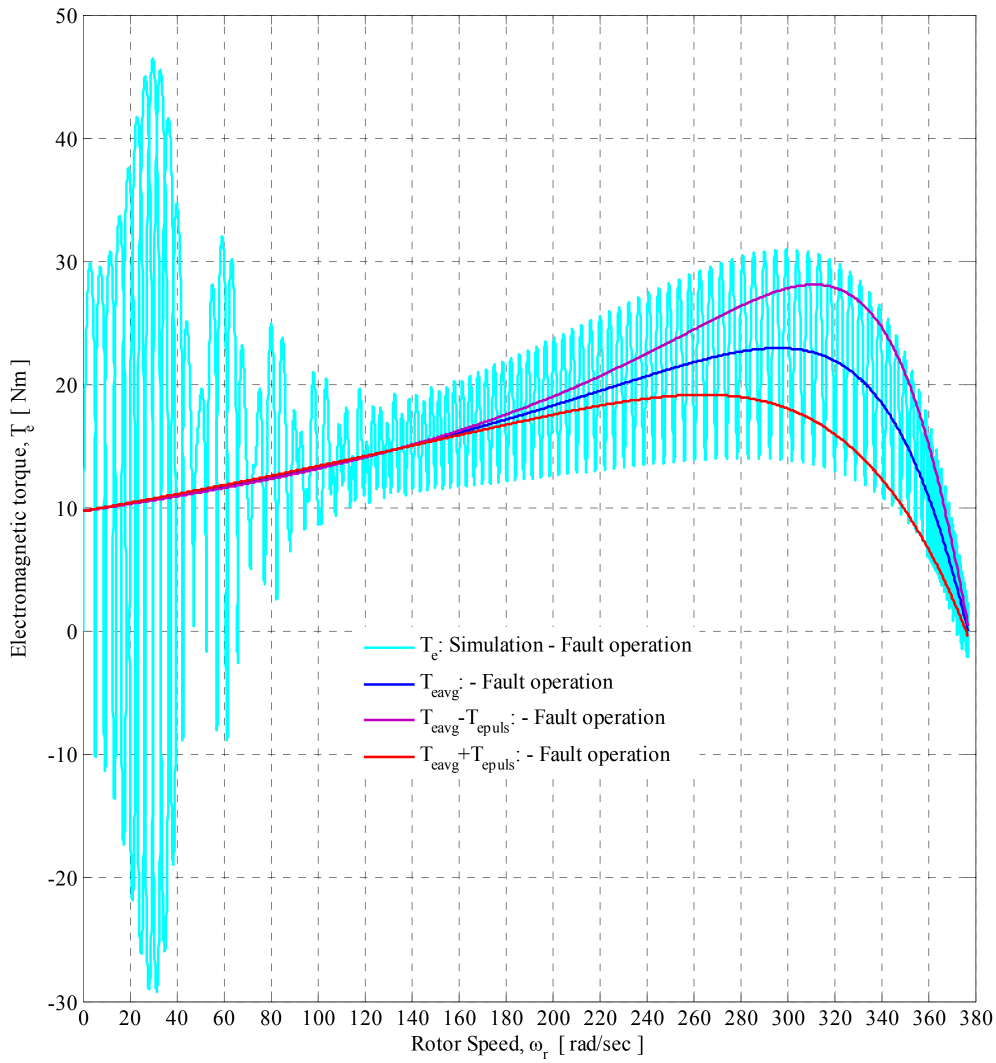

Figure 5.39 Various torque components of the five-phase induction machine under unbalanced stator phases '*a*' and '*c*' open circuited based on computer simulation and steady-state calculations.

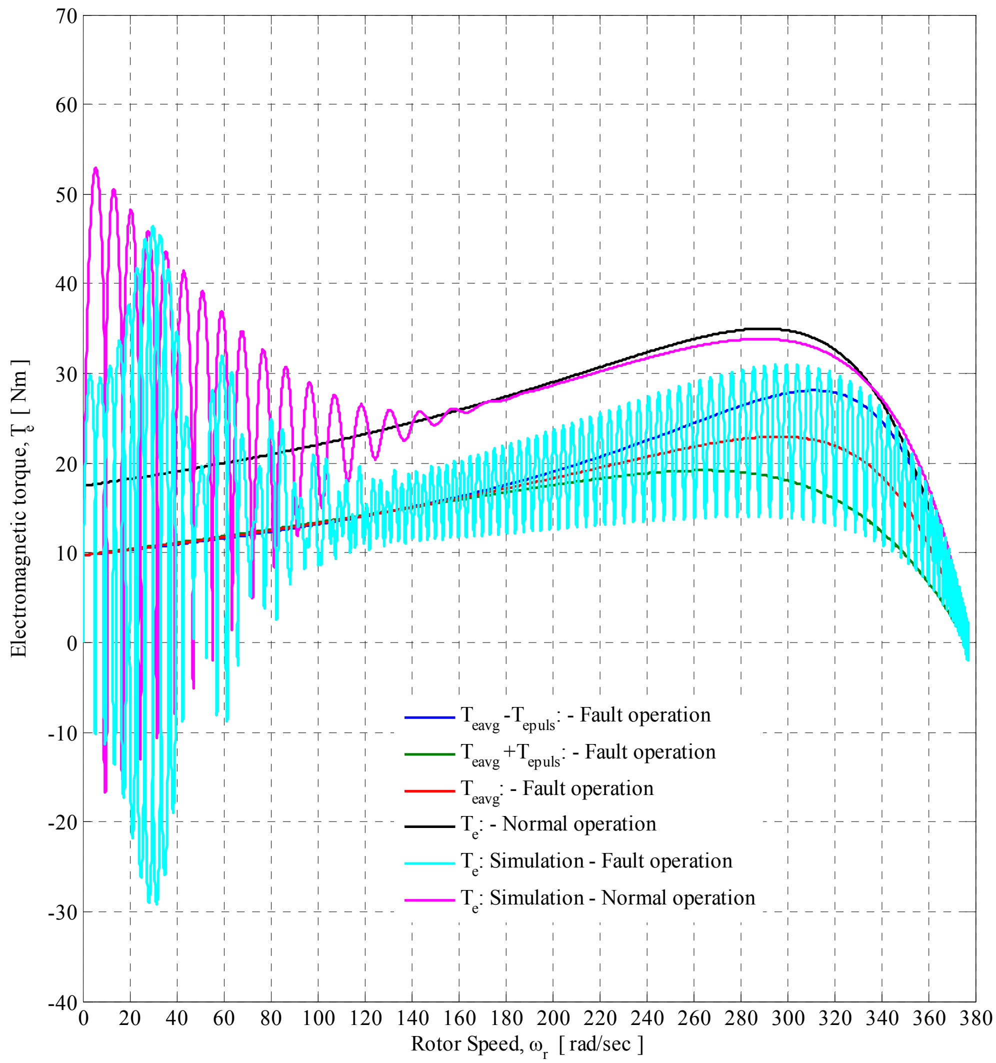

Figure 5.40 Various torque components of the five-phase induction machine under balanced and a stator phases '*a*' and '*c*' open based on computer simulation and steady-state calculations.

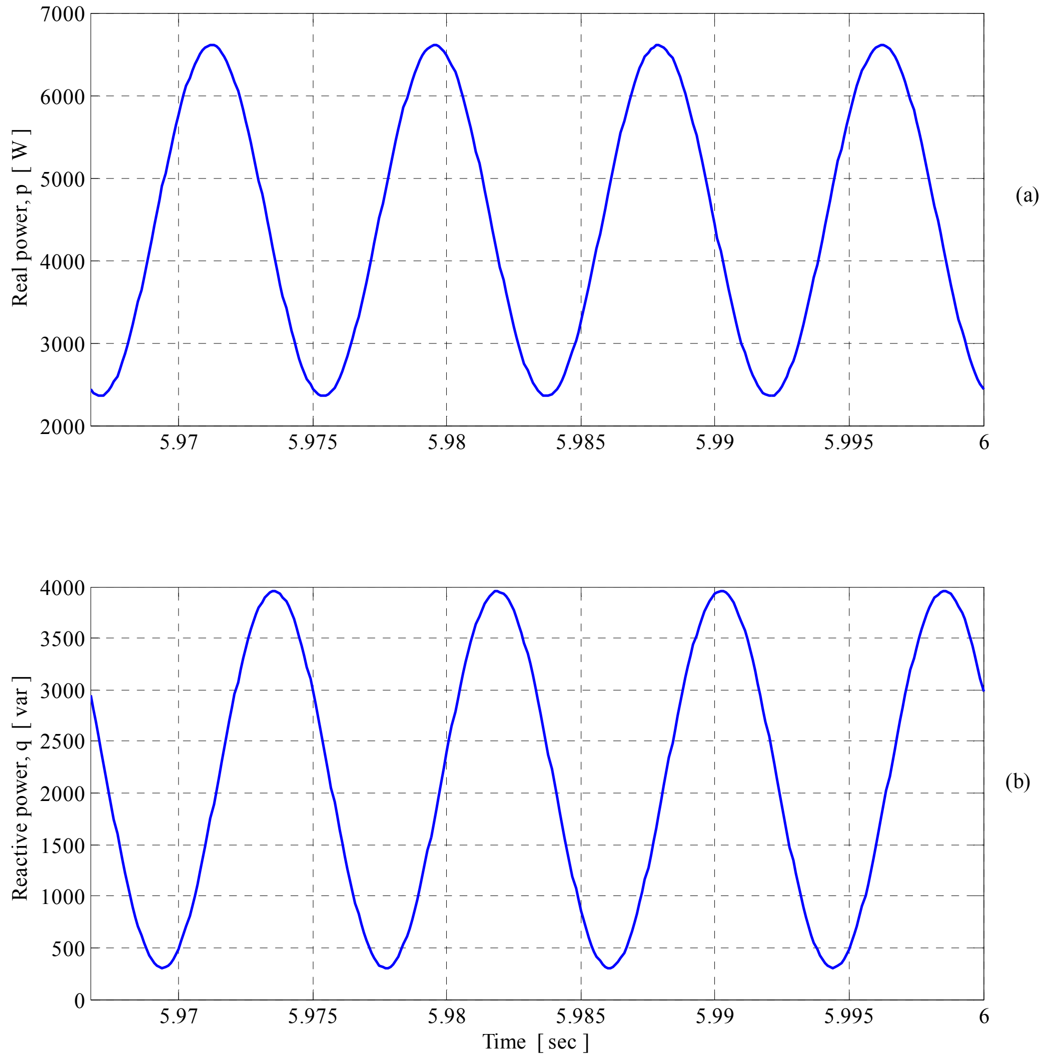

Figure 5.41 Simulation Steady-state stator input five-phase power (a) Real power and (b) Reactive power at a load torque of 11 Nm.

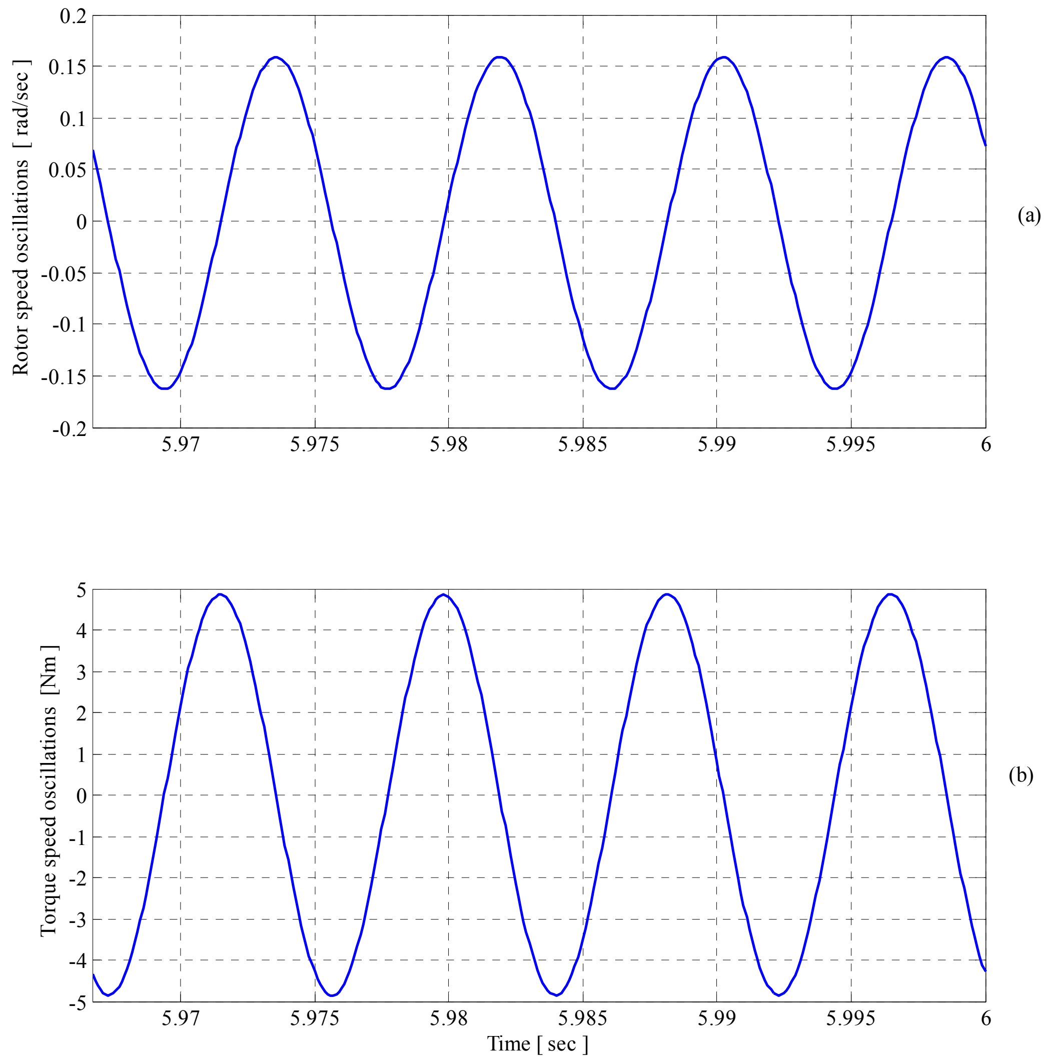

Figure 5.42 Simulation Steady-state (a) rotor speed oscillations and (b) electromagnetic torque oscillations at a load torque of 11 Nm.

5.6 Conclusion

This Chapter has presented a steady state and dynamic model of the open phase faults for a five phase induction motor for one phase, two adjacent phases as well as two non-adjacent phases. Circuit based models have been developed which can help to predict not only the starting transients and steady-state performance and pulsating components but also the dynamics such as the small-signal stability of the faulted machine. This is made possible by the application of the harmonic balance technique on the full-order differential Equation model of the faulted machine in stationary reference frame. The resulting Equations are also used in determining the stability of the five-phase induction motor under open-phase faults. Simulation results and steady state results have been presented, in which it has been possible to calculate the speed harmonic components as well as the torque pulsations. Small signal analysis has been performed to predict the stability of the faulted machine. At low rotor speeds, the machine exhibits instability due to the rotor flux linkage. If the speed harmonics are neglected, the resulting model is stable at relatively high speed operating conditions.

The analysis presented in this work has shown that with one or two phases missing, the five-phase machine is able to start and generate a high percentage of rated torque as demonstrated in the presented results. The analytical methodologies presented in this work have great promise in the study of the transient, steady state and dynamic responses of various faults of multi-phase electric machinery.

CHAPTER 6

ROTOR FLUX VECTOR CONTROL OF A FIVE PHASE INDUCTION MACHINE

6.1 1 Introduction

Induction machines are widely used in the industrial drive system as a means of converting electric power to mechanical power. The do offer a high performance as well as independent control on torque and flux linkages, which is similar to that of the DC machine. It is also possible to drive the induction machines above their rated speed through flux weakening [6.1, 6.2]. The vector control is referred for controlling both amplitude and phase of the AC excitation. Vector control of the voltages and currents results in the control of the spatial orientation of the electromagnetic fields in the machine, which leads to field orientation. The control schemes available for induction motor drives are the scalar control, direct torque control, adaptive control and vector (field) oriented control.

The rotor flux oriented control is usually employed although it is possible to implement stator flux oriented control and magnetizing (air gap) flux oriented control [6.3]. Both the stator and rotor flux linkages are necessary for vector control scheme.

The field-oriented control of induction machine systems can be categorized in two groups. One, as direct field oriented control with flux sensors for determining the flux magnitudes and phase angle. The second classification is indirect field oriented control in which the magnitude and space angle are obtained from the stator currents and rotor speed. The space angle is the sum of the rotor angle (obtained from the rotor peed) and the calculated slip (obtained from the reference values).

In this Chapter, the Equations for the vector control of a five-phase induction machine are derived using both the fundamental and harmonic components of the state and machine variables and parameters. Control Simulation results using the fundamental model are presented.

6.2 Vector Control of an Induction machine

The induction machine Equations transformed to the qd reference frame for the fundamental components are presented as follows

$$v_{qs1} = r_{s1} i_{qs1} + p\lambda_{qs1} + \omega_{e1}\lambda_{ds1} \tag{6.1}$$

$$v_{ds1} = r_s i_{ds1} + p\lambda_{ds1} - \omega_{e1}\lambda_{qs1} \tag{6.2}$$

$$v'_{qr1} = r'_{r1} i'_{qr1} + p\lambda'_{qr1} + (\omega_{e1} - \omega_{r1})\lambda'_{dr1} \tag{6.3}$$

$$v'_{dr1} = r'_{r1} i'_{dr1} + p\lambda'_{dr1} - (\omega_{e1} - \omega_{r1})\lambda'_{qr1} \tag{6.4}$$

For the third harmonic components, the voltage Equations are given by

$$v_{qs3} = r_s i_{qs3} + p\lambda_{qs3} + 3\omega_{e3}\lambda_{ds3} \tag{6.5}$$

$$v_{ds3} = r_s i_{ds3} + p\lambda_{ds3} - 3\omega_{e3}\lambda_{qs3} \tag{6.6}$$

$$v'_{qr3} = r'_{r3} i'_{qr3} + p\lambda'_{qr3} + 3(\omega_{e3} - \omega_r)\lambda'_{dr3} \tag{6.7}$$

$$v'_{dr3} = r'_{r3} i'_{dr3} + p\lambda'_{dr3} - 3(\omega_{e3} - \omega_r)\lambda'_{qr3} \tag{6.8}$$

The torque Equation of an induction machine in terms of rotor flux linkages and stator currents is given as

$$T_{e1} = \left(\frac{m}{2}\right)\left(\frac{P}{2}\right)\frac{L_{m1}}{L_{r1}}\left(\lambda'_{dr1} i_{qs1} - \lambda'_{qr1} i_{ds1}\right) \tag{6.9}$$

For the third harmonic components, the torque Equation is given by

$$T_{e3} = 3\left(\frac{m}{2}\right)\left(\frac{P}{2}\right)\frac{L_{m3}}{L_{r3}}\left(\lambda'_{dr3} i_{qs3} - \lambda'_{qr3} i_{ds3}\right) \tag{6.10}$$

The fundamental components of the stator and rotor qd flux linkages are obtained as shown by the following Equations (6.11) to (6.18)

$$\lambda_{qs1} = L_{s1} i_{qs1} + L_{m1} i'_{qr1} \tag{6.11}$$

$$\lambda_{ds1} = L_{s1} i_{ds1} + L_{m1} i'_{dr1} \tag{6.12}$$

$$\lambda'_{qr1} = L_{m1} i_{qs1} + L'_{r1} i'_{qr1} \tag{6.13}$$

$$\lambda'_{dr1} = L_{m1} i_{ds1} + L'_{r1} i'_{dr1} \tag{6.14}$$

For the third harmonic components, the flux linkages are given by

$$\lambda_{qs3} = L_{s3} i_{qs3} + L_{m3} i'_{qr3} \tag{6.15}$$

$$\lambda_{ds3} = L_{s3} i_{ds3} + L_{m3} i'_{dr3} \tag{6.16}$$

$$\lambda'_{qr3} = L_{m3} i_{qs3} + L'_{r3} i'_{qr3} \tag{6.17}$$

$$\lambda'_{dr3} = L_{m3} i_{ds3} + L'_{r3} i'_{dr3} \tag{6.18}$$

where

p is the differential operator

v_{qs1} is the fundamental component of the q-axis stator voltage.

v_{ds1} is the fundamental component of the d-axis stator voltage.

i_{qs1} is the fundamental component of the q-axis stator current.

i_{ds1} is the fundamental component of the d-axis stator current.

λ_{qs1} is the fundamental component of the q-axis stator flux linkage.

λ_{ds1} is the fundamental component of the d-axis stator flux linkage.

$v_{qr1}^{'}$ is the fundamental component of the q-axis rotor voltage.

$v_{dr1}^{'}$ is the fundamental component of the d-axis rotor voltage.

$i_{qr1}^{'}$ is the fundamental component of the q-axis rotor current.

$i_{dr1}^{'}$ is the fundamental component of the d-axis rotor current.

$\lambda_{qr1}^{'}$ is the fundamental component of the q-axis rotor flux linkage

$\lambda_{dr1}^{'}$ is the fundamental component of the d-axis rotor flux linkage

v_{qs3} is the third harmonic component of the q-axis stator voltage.

v_{ds3} is the third harmonic component of the d-axis stator voltage.

i_{qs3} is the third harmonic component of the q-axis stator current.

i_{ds3} is the third harmonic component of the d-axis stator current.

λ_{qs3} is the third harmonic component of the q-axis stator flux linkage.

λ_{ds3} is the third harmonic component of the d-axis stator flux linkage.

$v_{qr3}^{'}$ is the third harmonic component of the q-axis rotor voltage.

$v_{dr3}^{'}$ is the third harmonic component of the d-axis rotor voltage.

$i_{qr3}^{'}$ is the third harmonic component of the q-axis rotor current.

$i_{dr3}^{'}$ is the third harmonic component of the d-axis rotor current.

$\lambda_{qr3}^{'}$ is the third harmonic component of the q-axis rotor flux linkage.

$\lambda_{dr3}^{'}$ is the third harmonic component of the d-axis rotor flux linkage.

T_{e1} is the fundamental component of the electromagnetic torque.

T_{e3} is the third harmonic of the electromagnetic torque.

ω_{e1} is the fundamental component frequency of the reference frame of transformation.

ω_{e3} is the third harmonic component frequency of the reference frame of transformation

m is the number of stator phases.

P is the number of stator poles.

Now, the stator currents and rotor flux linkages are chosen as state variables, the stator flux linkages and rotor currents can be expressed in terms of state variables by eliminating the stator flux linkages and rotor currents.

From Equations (6.13) and (6.17), respectively, the q-axis fundamental and third harmonic rotor currents can be obtained as Equations (6.19) and (6.20)

$$i_{qr}^{'} = \frac{1}{L_r^{'}}\left(\lambda_{qr}^{'} - L_m i_{qs}\right) \tag{6.19}$$

$$i_{qr3}^{'} = \frac{1}{L_{r3}^{'}}\left(\lambda_{qr3}^{'} - L_{m3} i_{qs3}\right) \tag{6.20}$$

Similarly, Equations (6.14) and (6.18), respectively give the d-axis fundamental and third harmonic rotor currents as presented in Equation (6.21) and (6.22)

$$i_{dr}^{'} = \frac{1}{L_r^{'}}\left(\lambda_{dr}^{'} - L_m i_{ds}\right) \tag{6.21}$$

$$i_{dr3}^{'} = \frac{1}{L_{r3}^{'}}\left(\lambda_{dr3}^{'} - L_{m3} i_{ds3}\right) \tag{6.22}$$

Substituting for $i_{qr1}^{'}$ and $i_{dr1}^{'}$ from Equations (6.19) and (6.21) into Equations (6.11) and (6.12), respectively, the following expressions for the fundamental components of q-axis and d-axis stator flux linkages are obtained

$$\lambda_{qs1} = L_{s1} i_{qs1} + \frac{L_{m1}}{L_{r1}^{'}}\left(\lambda_{qr1}^{'} - L_{m1} i_{qs1}\right)$$

$$\lambda_{qs1} = \left(L_{s1} - \frac{L_{m1}^2}{L_{r1}^{'}}\right) i_{qs1} + \frac{L_{m1}}{L_{r1}^{'}} \lambda_{qr1}^{'} \tag{6.23}$$

$$\lambda_{ds1} = \left(L_{s1} - \frac{L_{m1}^2}{L_{r1}^{'}}\right) i_{ds1} + \frac{L_{m1}}{L_{r1}^{'}} \lambda_{dr1}^{'} \tag{6.24}$$

Substituting for $i_{qr3}^{'}$ and $i_{dr3}^{'}$ from Equations (6.20) and (6.22) into Equations (6.15) and (6.16), respectively, the following expressions for the third harmonic components of q-axis and d-axis stator flux linkages are obtained

$$\lambda_{qs3} = L_{s3} i_{qs3} + \frac{L_{m3}}{L_{r3}^{'}}\left(\lambda_{qr3}^{'} - L_{m3} i_{qs3}\right)$$

$$\lambda_{qs3} = \left(L_{s3} - \frac{L_{m3}^2}{L_{r3}^{'}}\right) i_{qs3} + \frac{L_{m3}}{L_{r3}^{'}} \lambda_{qr3}^{'} \tag{6.25}$$

$$\lambda_{ds3} = \left(L_{s3} - \frac{L_{m3}^2}{L_{r3}^{'}}\right) i_{ds3} + \frac{L_{m3}}{L_{r3}^{'}} \lambda_{dr3}^{'} \tag{6.26}$$

Substituting for the qd stator flux linkages from Equations (6.23) and (6.24) into Equations (6.1) and (6.2) gives the following results for the fundamental component stator voltage Equations

$$v_{qs1} = r_{s1} i_{qs1} + \left(L_{s1} - \frac{L_{m1}^2}{L_{r1}^{'}}\right) p i_{qs1} + \omega_{e1}\left(L_{s1} - \frac{L_{m1}^2}{L_{r1}^{'}}\right) i_{ds1} + \frac{L_{m1}}{L_{r1}^{'}} p \lambda_{qr1}^{'} + \omega_{e1} \frac{L_{m1}}{L_{r1}^{'}} \lambda_{dr1}^{'}$$

$$v_{qs1} = r_{s1} i_{qs1} + L_{\sigma 1} p i_{qs1} + \omega_{e1} L_{\sigma 1} i_{ds1} + \frac{L_{m1}}{L_{r1}^{'}} p \lambda_{qr1}^{'} + \omega_{e1} \frac{L_{m1}}{L_{r1}^{'}} \lambda_{dr1}^{'} \tag{6.27}$$

$$v_{ds1} = r_{s1} i_{ds1} + L_{\sigma 1} p i_{ds1} - \omega_{e1} L_{\sigma 1} i_{qs1} + \frac{L_{m1}}{L_{r1}^{'}} p \lambda_{dr1}^{'} - \omega_{e1} \frac{L_{m1}}{L_{r1}^{'}} \lambda_{qr1}^{'} \tag{6.28}$$

Similarly, Substituting for the qd stator flux linkages from Equations (6.25) and (6.26) into Equations (6.5) and (6.6), the following results for the third harmonic component stator voltage Equations are obtained

$$v_{qs3} = r_{s3} i_{qs3} + \left(L_{s3} - \frac{L_{m3}^2}{L_{r3}^{'}} \right) p i_{qs3} + 3\omega_{e3} \left(L_{s3} - \frac{L_{m3}^2}{L_{r3}^{'}} \right) i_{ds3} + \frac{L_{m3}}{L_{r3}^{'}} p \lambda_{qr3}^{'} + 3\omega_{e3} \frac{L_m}{L_r^{'}} \lambda_{dr3}^{'}$$

$$v_{qs3} = r_{s3} i_{qs3} + L_{\sigma 3} p i_{qs3} + 3\omega_{e3} L_{\sigma 3} i_{ds3} + \frac{L_{m3}}{L_{r3}^{'}} p \lambda_{qr3}^{'} + 3\omega_{e3} \frac{L_{m3}}{L_{r3}^{'}} \lambda_{dr3}^{'} \tag{6.29}$$

$$v_{ds3} = r_{s3} i_{ds3} + L_{\sigma 3} p i_{ds3} - 3\omega_{e3} L_{\sigma 3} i_{qs3} + \frac{L_{m3}}{L_{r3}^{'}} p \lambda_{dr3}^{'} - 3\omega_{e3} \frac{L_{m3}}{L_{r3}^{'}} \lambda_{qr3}^{'} \tag{6.30}$$

Equations (6.27) and (6.28) can be re-written as

$$L_{\sigma 1} p i_{qs1} = v_{qs1} - r_{s1} i_{qs1} - \omega_{e1} L_{\sigma 1} i_{ds1} - \frac{L_{m1}}{L_{r1}^{'}} p \lambda_{qr1}^{'} - \omega_{e1} \frac{L_{m1}}{L_{r1}^{'}} \lambda_{dr1}^{'} \tag{6.31}$$

$$L_{\sigma 1} p i_{ds1} = v_{ds1} - r_{s1} i_{ds1} + \omega_{e1} L_{\sigma 1} i_{qs1} - \frac{L_{m1}}{L_{r1}^{'}} p \lambda_{dr1}^{'} + \omega_{e1} \frac{L_{m1}}{L_{r1}^{'}} \lambda_{qr1}^{'} \tag{6.32}$$

Equations (6.29) and (6.30) can be re-written as

$$L_{\sigma 3} p i_{qs3} = v_{qs3} - r_{s3} i_{qs3} - 3\omega_{e3} L_{\sigma} i_{ds3} - \frac{L_{m3}}{L_{r3}^{'}} p \lambda_{qr3}^{'} - 3\omega_{e3} \frac{L_{m3}}{L_{r3}^{'}} \lambda_{dr3}^{'} \tag{6.33}$$

$$L_{\sigma 3} p i_{ds3} = v_{ds3} - r_{s3} i_{ds3} + 3\omega_{e3} L_{\sigma 3} i_{qs3} - \frac{L_{m3}}{L_{r3}^{'}} p \lambda_{dr3}^{'} + 3\omega_{e} \frac{L_{m3}}{L_{r3}^{'}} \lambda_{qr3}^{'} \tag{6.34}$$

for a squirrel cage induction machine

$v_{qr1}^{'} = 0$ and $v_{dr1}^{'} = 0$

$v_{qr3}^{'} = 0$ and $v_{dr3}^{'} = 0$

Therefore Equation (6.3) becomes

$$0 = \frac{r_{r1}^{'}}{L_{r1}}\left(\lambda_{qr1}^{'} - L_{m1}i_{qs1}\right) + p\lambda_{qr1}^{'} + \left(\omega_{e1} - \omega_r\right)\lambda_{dr1}^{'}$$

$$p\lambda_{qr1}^{'} = -\frac{r_{r1}^{'}}{L_{r1}}\lambda_{qr1}^{'} + \frac{r_{r1}^{'}L_{m1}}{L_{r1}}i_{qs1} - \left(\omega_{e1} - \omega_r\right)\lambda_{dr1}^{'} \tag{6.35}$$

Equation (6.4) becomes

$$0 = \frac{r_{r1}^{'}}{L_{r1}}\left(\lambda_{dr1}^{'} - L_{m1}i_{ds1}\right) + p\lambda_{dr1}^{'} - \left(\omega_{e1} - \omega_r\right)\lambda_{qr1}^{'}$$

$$p\lambda_{dr1}^{'} = -\frac{r_{r1}^{'}}{L_{r1}}\lambda_{dr1}^{'} + \frac{r_{r1}^{'}L_{m1}}{L_{r1}}i_{ds1} + \left(\omega_{e1} - \omega_r\right)\lambda_{qr1}^{'} \tag{6.36}$$

Equation (6.7) becomes

$$0 = \frac{r_{r3}^{'}}{L_{r3}}\left(\lambda_{qr3}^{'} - L_{m3}i_{qs3}\right) + p\lambda_{qr3}^{'} + 3\left(\omega_{e3} - \omega_r\right)\lambda_{dr3}^{'}$$

$$p\lambda_{qr3}^{'} = -\frac{r_{r3}^{'}}{L_{r3}}\lambda_{qr3}^{'} + \frac{r_{r3}^{'}L_{m3}}{L_{r3}}i_{qs3} - 3\left(\omega_{e3} - \omega_r\right)\lambda_{dr3}^{'} \tag{6.37}$$

Equation (6.8) becomes

$$0 = \frac{r_{r3}^{'}}{L_{r3}}\left(\lambda_{dr3}^{'} - L_{m3}i_{ds3}\right) + p\lambda_{dr3}^{'} - 3\left(\omega_{e3} - \omega_r\right)\lambda_{qr3}^{'}$$

$$p\lambda_{dr3}^{'} = -\frac{r_{r3}^{'}}{L_{r3}}\lambda_{dr3}^{'} + \frac{r_{r3}^{'}L_{m3}}{L_{r3}}i_{ds3} + 3\left(\omega_{e3} - \omega_r\right)\lambda_{qr3}^{'} \tag{6.38}$$

Substituting Equations (6.35) and (6.36) into Equations (6.31) and (6.32), respectively results into

$$L_{\sigma 1} p i_{qs1} = v_{qs1} - r_{s1} i_{qs1} - \omega_{e1} L_{\sigma 1} i_{ds1} - \frac{L_{m1}}{L_{r1}^{'}} \begin{pmatrix} -\dfrac{r_{r1}^{'}}{L_{r1}} \lambda_{qr1}^{'} + \dfrac{r_{r1}^{'} L_{m1}}{L_{r1}} i_{qs1} \\ -(\omega_{e1} - \omega_{r}) \lambda_{dr1}^{'} \end{pmatrix} - \omega_{e1} \frac{L_{m1}}{L_{r1}^{'}} \lambda_{dr1}^{'}$$

$$L_{\sigma 1} p i_{qs1} = v \begin{bmatrix} {}_{qs1} - \left(r_{s1} + \dfrac{r_{r1}^{'} L_{m1}^{2}}{L_{r1}^{'2}} \right) i_{qs1} - \omega_{e1} L_{\sigma 1} i_{ds1} + \dfrac{r_{r1}^{'} L_{m1}}{L_{r1}^{'2}} \lambda_{qr1}^{'} \\ + \left(\dfrac{L_{m1}}{L_{r1}^{'}} \omega_{e1} - \dfrac{L_{m1}}{L_{r1}^{'}} \omega_{r} - \omega_{e1} \dfrac{L_{m1}}{L_{r1}^{'}} \right) \lambda_{dr1}^{'} \end{bmatrix}$$

$$L_{\sigma 1} p i_{qs1} = v_{qs1} - \left(r_{s1} + \frac{r_{r1}^{'} L_{m1}^{2}}{L_{r1}^{'2}} \right) i_{qs1} - \omega_{e1} L_{\sigma 1} i_{ds1} + \frac{r_{r1}^{'} L_{m1}}{L_{r1}^{'2}} \lambda_{qr1}^{'} - \omega_{r} \frac{L_{m1}}{L_{r1}^{'}} \lambda_{dr1}^{'}$$

$$L_{\sigma 1} p i_{qs1} = v_{qs1} - r_{\sigma 1} i_{qs1} + \frac{r_{r1}^{'} L_{m1}}{L_{r1}^{'2}} \lambda_{qr1}^{'} - \omega_{e1} L_{\sigma 1} i_{ds1} - \omega_{r} \frac{L_{m1}}{L_{r1}^{'}} \lambda_{dr1}^{'} \tag{6.39}$$

$$L_{\sigma 1} p i_{ds1} = v_{ds1} - r_{s1} i_{ds1} + \omega_{e1} L_{\sigma 1} i_{qs1} - \frac{L_{m1}}{L_{r1}^{'}} \begin{pmatrix} -\dfrac{r_{r1}^{'}}{L_{r1}} \lambda_{dr1}^{'} + \dfrac{r_{r1}^{'} L_{m1}}{L_{r1}} i_{ds1} \\ +(\omega_{e1} - \omega_{r}) \lambda_{qr1}^{'} \end{pmatrix} + \omega_{e1} \frac{L_{m1}}{L_{r1}^{'}} \lambda_{qr1}^{'}$$

$$L_{\sigma 1} p i_{ds1} = \begin{pmatrix} v_{ds1} - r_{s1} i_{ds1} + \omega_{e1} L_{\sigma 1} i_{qs1} + \dfrac{r_{r1}^{'} L_{m1}}{L_{r1}^{'2}} \lambda_{dr1}^{'} - \dfrac{r_{r1}^{'} L_{m1}^{2}}{L_{r1}^{'2}} i_{ds1} - \dfrac{L_{m1}}{L_{r1}^{'}} \omega_{e1} \lambda_{qr1}^{'} \\ + \dfrac{L_{m1}}{L_{r1}^{'}} \omega_{r} \lambda_{qr1}^{'} + \omega_{e1} \dfrac{L_{m1}}{L_{r1}^{'}} \lambda_{qr1}^{'} \end{pmatrix}$$

$$L_{\sigma 1} p i_{ds1} = v_{ds1} - \left(r_{s1} + \frac{r_{r1}^{'} L_{m1}^{2}}{L_{r1}^{'2}} \right) i_{ds1} + \omega_{e1} L_{\sigma 1} i_{qs1} + \frac{r_{r1}^{'} L_{m1}}{L_{r1}^{'2}} \lambda_{dr1}^{'} + \frac{L_{m1}}{L_{r1}^{'}} \omega_{r} \lambda_{qr1}^{'}$$

$$L_{\sigma 1} p i_{ds1} = v_{ds1} - r_{\sigma 1} i_{ds1} + \frac{r_{r1}^{'} L_{m1}}{L_{r1}^{'2}} \lambda_{dr1}^{'} + \omega_{e1} L_{\sigma 1} i_{qs1} + \omega_{r} \frac{L_{m1}}{L_{r1}^{'}} \lambda_{qr1}^{'} \tag{6.40}$$

Substituting Equations (6.37) and (6.38) into Equations (6.33) and (6.34), respectively results into

$$L_{\sigma 3} p i_{qs3} = v_{qs3} - r_{s3} i_{qs3} - \omega_{e3} L_{\sigma 3} i_{ds3} - \frac{L_{m3}}{L_{r3}^{'}} \begin{pmatrix} -\dfrac{r_{r3}^{'}}{L_{r3}} \lambda_{qr3}^{'} + \dfrac{r_{r3}^{'} L_{m3}}{L_{r3}} i_{qs3} \\ -3(\omega_{e3} - \omega_{r}) \lambda_{dr3}^{'} \end{pmatrix} - 3\omega_{e3} \frac{L_{m3}}{L_{r3}^{'}} \lambda_{dr3}^{'}$$

$$L_{\sigma 3} p i_{qs3} = v_{qs3} - \left(r_{s3} + \frac{r_{r3}^{'} L_{m3}^{2}}{L_{r3}^{'2}} \right) i_{qs3} - 3\omega_{e3} L_{\sigma 3} i_{ds3} + \frac{r_{r3}^{'} L_{m3}}{L_{r3}^{'2}} \lambda_{qr3}^{'} + 3 \begin{pmatrix} \frac{L_{m3}}{L_{r3}^{'}} \omega_{e3} - \frac{L_{m3}}{L_{r3}^{'}} \omega_{r} \\ - \omega_{e3} \frac{L_{m3}}{L_{r3}^{'}} \end{pmatrix} \lambda_{dr3}^{'}$$

$$L_{\sigma 3} p i_{qs3} = v_{qs3} - \left(r_{s3} + \frac{r_{r3}^{'} L_{m3}^{2}}{L_{r3}^{'2}} \right) i_{qs3} - 3\omega_{e3} L_{\sigma 3} i_{ds3} + \frac{r_{r3}^{'} L_{m3}}{L_{r3}^{'2}} \lambda_{qr3}^{'} - 3\omega_{r} \frac{L_{m3}}{L_{r3}^{'}} \lambda_{dr3}^{'}$$

$$L_{\sigma 3} p i_{qs3} = v_{qs3} - r_{\sigma 3} i_{qs3} + \frac{r_{r3}^{'} L_{m3}}{L_{r3}^{'2}} \lambda_{qr3}^{'} - 3\omega_{e3} L_{\sigma 3} i_{ds3} - 3\omega_{r} \frac{L_{m3}}{L_{r3}^{'}} \lambda_{dr3}^{'} \tag{6.41}$$

$$L_{\sigma 3} p i_{ds3} = v_{ds3} - r_{s3} i_{ds3} + 3\omega_{e3} L_{\sigma 3} i_{qs3} - \frac{L_{m3}}{L_{r3}^{'}} \begin{pmatrix} - \frac{r_{r3}^{'}}{L_{r3}} \lambda_{dr3}^{'} + \frac{r_{r3}^{'} L_{m3}}{L_{r3}} i_{ds3} \\ + 3(\omega_{e3} - \omega_{r}) \lambda_{qr3}^{'} \end{pmatrix} + 3\omega_{e} \frac{L_{m3}}{L_{r3}^{'}} \lambda_{qr3}^{'}$$

$$L_{\sigma 3} p i_{ds3} = \begin{pmatrix} v_{ds3} - r_{s3} i_{ds3} + 3\omega_{e3} L_{\sigma 3} i_{qs3} + \frac{r_{r3}^{'} L_{m3}}{L_{r3}^{'2}} \lambda_{dr3}^{'} - \frac{r_{r3}^{'} L_{m3}^{2}}{L_{r3}^{'2}} i_{ds3} \\ -3 \frac{L_{m3}}{L_{r3}^{'}} \omega_{e3} \lambda_{qr3}^{'} + 3 \frac{L_{m3}}{L_{r3}^{'}} \omega_{r} \lambda_{qr3}^{'} + 3\omega_{e3} \frac{L_{m3}}{L_{r3}^{'}} \lambda_{qr3}^{'} \end{pmatrix}$$

$$L_{\sigma 3} p i_{ds3} = v_{ds3} - \left(r_{s3} + \frac{r_{r3}^{'} L_{m3}^{2}}{L_{r3}^{'2}} \right) i_{ds3} + 3\omega_{e3} L_{\sigma 3} i_{qs3} + \frac{r_{r3}^{'} L_{m3}}{L_{r3}^{'2}} \lambda_{dr3}^{'} + 3 \frac{L_{m3}}{L_{r3}^{'}} \omega_{r} \lambda_{qr3}^{'}$$

$$L_{\sigma 3} p i_{ds3} = v_{ds3} - r_{\sigma 3} i_{ds3} + \frac{r_{r3}^{'} L_{m3}}{L_{r3}^{'2}} \lambda_{dr3}^{'} + 3\omega_{e3} L_{\sigma 3} i_{qs3} + 3\omega_{r} \frac{L_{m3}}{L_{r3}^{'}} \lambda_{qr3}^{'} \tag{6.42}$$

where

$$L_{\sigma 1} = L_{s1} - \frac{L_{m1}^{2}}{L_{r1}^{'}} \text{ and } r_{\sigma 1} = r_{s1} + \frac{r_{r1}^{'} L_{m1}^{2}}{L_{r1}^{'2}}, \; L_{\sigma 3} = L_{s3} - \frac{L_{m3}^{2}}{L_{r3}^{'}} \text{ and } r_{\sigma 3} = r_{s3} + \frac{r_{r3}^{'} L_{m3}^{2}}{L_{r3}^{'2}}$$

Aligning the rotor flux linkage with the d-axis of the synchronous reference frame, the q-axis rotor flux linkage and its derivative are zero. Thus

$$\lambda_{qr1}^{'} = 0 \tag{6.43}$$

$$p\lambda_{qr1}^{'} = 0 \tag{6.44}$$

$$\lambda_{r1}^{'} = \lambda_{dr1}^{'} \tag{6.45}$$

where $\lambda_{r1}^{'}$ is the fundamental component of the rotor flux linkage.

$$\lambda_{qr3}^{'} = 0 \tag{6.46}$$

$$p\lambda_{qr3}^{'} = 0 \tag{6.47}$$

$$\lambda_{r3}^{'} = \lambda_{dr3}^{'} \tag{6.48}$$

where $\lambda_{r3}^{'}$ is the harmonic component of the rotor flux linkage.

Substituting Equations (6.43) - (6.48) into Equations (6.9) - (6.10), and (6.35) – (6.42), results into

For the fundamental components

$$T_{e1} = \frac{mP}{4}\frac{L_{m1}}{L_{r1}}\lambda_{dr1}^{'} i_{qs1} \tag{6.49}$$

$$0 = \frac{r_{r1}^{'} L_{m1}}{L_{r1}} i_{qs1} - (\omega_{e1} - \omega_r)\lambda_{dr1}^{'} \tag{6.50}$$

$$p\lambda_{dr1}^{'} = -\frac{r_{r1}^{'}}{L_{r1}}\lambda_{dr1}^{'} + \frac{r_{r1}^{'} L_{m1}}{L_{r1}} i_{ds1} \tag{6.51}$$

$$L_{\sigma 1} p i_{qs1} = v_{qs1} - r_{\sigma 1} i_{qs1} - \omega_{e1} L_{\sigma 1} i_{ds1} - \omega_r \frac{L_{m1}}{L_{r1}^{'}}\lambda_{dr1}^{'} \tag{6.52}$$

$$L_{\sigma 1} p i_{ds1} = v_{ds1} - r_{\sigma 1} i_{ds1} + \frac{r_{r1}^{'} L_{m1}}{L_{r1}^{'2}}\lambda_{dr1}^{'} + \omega_{e1} L_{\sigma 1} i_{qs1} \tag{6.53}$$

For the third harmonic components

$$T_{e3} = 3\frac{mP}{4}\frac{L_{m3}}{L_{r3}}\lambda_{dr3}^{'} i_{qs3} \tag{6.54}$$

$$0 = \frac{r_{r3}^{'} L_{m3}}{L_{r3}} i_{qs3} - 3(\omega_{e3} - \omega_r)\lambda_{dr3}^{'} \tag{6.55}$$

$$p\lambda_{dr3}^{'} = -\frac{r_{r3}^{'}}{L_{r3}}\lambda_{dr3}^{'} + \frac{r_{r3}^{'}L_{m3}}{L_{r3}}i_{ds3} \tag{6.56}$$

$$L_{\sigma 3}\, pi_{qs3} = v_{qs3} - r_{\sigma 3}i_{qs3} - 3\omega_{e3}L_{\sigma 3}i_{ds3} - 3\omega_r \frac{L_{m3}}{L_{r3}^{'}}\lambda_{dr3}^{'} \tag{6.57}$$

$$L_{\sigma 3}\, pi_{ds3} = v_{ds3} - r_{\sigma 3}i_{ds3} + \frac{r_{r3}^{'}L_{m3}}{L_{r3}^{'2}}\lambda_{dr3}^{'} + 3\omega_{e3}L_{\sigma 3}i_{qs3} \tag{6.58}$$

Equation (6.50) yields the expression of the fundamental component of the slip frequency required for rotor field orientation control given by

$$\left(\omega_{e1} - \omega_r\right) = \frac{r_{r1}^{'}L_{m1}}{L_{r1}}\frac{i_{qs1}}{\lambda_{dr1}^{'}} \tag{6.59}$$

Equation (6.55) yields the expression of the third harmonic component of the slip frequency required for rotor field orientation control given by

$$\left(\omega_{e3} - \omega_r\right) = \frac{r_{r3}^{'}L_{m3}}{3L_{r3}}\frac{i_{qs3}}{\lambda_{dr3}^{'}} \tag{6.60}$$

The input-output linearization method is used to design the control scheme of the m-phase induction machine as follows [6.1]

Equations (6.51) - (6.53) can be re-arranged and written as

$$L_{\sigma 1}\, pi_{qs1} + r_{\sigma 1}i_{qs1} = v_{qs1} - \omega_{e1}L_{\sigma 1}i_{ds1} - \omega_r \frac{L_{m1}}{L_{r1}^{'}}\lambda_{dr1}^{'} = \sigma_{qs1} \tag{6.61}$$

$$L_{\sigma 1}\, pi_{ds1} + r_{\sigma 1}i_{ds1} = v_{ds1} + \omega_{e1}L_{\sigma 1}i_{qs1} + \frac{r_{r1}^{'}L_{m1}}{L_{r1}^{'2}}\lambda_{dr1}^{'} = \sigma_{ds1} \tag{6.62}$$

$$p\lambda_{dr1}^{'} + \frac{r_{r1}^{'}}{L_{r1}}\lambda_{dr1}^{'} = \frac{r_{r1}^{'}L_{m1}}{L_{r1}}i_{ds1} = \sigma_{dr1} \tag{6.63}$$

Equations (6.56) - (6.58) can be re-arranged and written as

$$L_{\sigma 3} p i_{qs3} + r_{\sigma 3} i_{qs3} = v_{qs3} - 3\omega_{e3} L_{\sigma 3} i_{ds3} - 3\omega_r \frac{L_{m3}}{L_{r3}^{'}} \lambda_{dr3}^{'} = \sigma_{qs3} \tag{6.64}$$

$$L_{\sigma 3} p i_{ds3} + r_{\sigma 3} i_{ds3} = v_{ds3} + \omega_{e3} L_{\sigma 3} i_{qs3} + \frac{r_{r3}^{'} L_{m3}}{L_{r3}^{'2}} \lambda_{dr3}^{'} = \sigma_{ds3} \tag{6.65}$$

$$p\lambda_{dr3}^{'} + \frac{r_{r3}^{'}}{L_{r3}} \lambda_{dr3}^{'} = \frac{r_{r3}^{'} L_{m3}}{L_{r3}} i_{ds3} = \sigma_{dr3} \tag{6.66}$$

Now, the rotor electrical speed, ω_r, is given by

$$\frac{2J}{P} p\omega_r = T_e - T_L \tag{6.67}$$

where

T_e is the total electromagnetic torque due to the two torque components, i.e. $T_e = T_{e1} + T_{e3}$

J is the ,moment of inertia and T_L is the load torque.

Substituting Equations (6.49) and (6.54) into Equation (6.67), the following is obtained

$$\frac{2J}{P} p\omega_r = \frac{mP}{4}\left(\frac{L_{m1}}{L_{r1}} \lambda_{dr1}^{'} i_{qs1} + 3\frac{L_{m3}}{L_{r3}} \lambda_{dr3}^{'} i_{qs3} \right) - T_L$$

$$p\omega_r = \frac{P}{2J}\left[\frac{mP}{4}\left(\frac{L_{m1}}{L_{r1}} \lambda_{dr1}^{'} i_{qs1} + 3\frac{L_{m3}}{L_{r3}} \lambda_{dr3}^{'} i_{qs3} \right) - T_L \right] = \sigma_\omega \tag{6.68}$$

where

σ_{qs1} is the output of the q-axis fundamental component of current controller

σ_{ds1} is the output of the d-axis fundamental component of current controller

σ_{dr1} is the output of the rotor fundamental component of flux linkage controller

σ_ω is the output of the speed controller

σ_{qs3} is the output of the q-axis third harmonic component of current controller

σ_{ds3} is the output of the d-axis third harmonic component of current controller

σ_{dr3} is the output of the rotor third harmonic component of flux linkage controller

The controller outputs are related to the reference and actual quantities as follows

For the fundamental components

$$\sigma_{qs1} = K_{qs1}\left(i_{qs1}^{*} - i_{qs1}\right) \tag{6.69}$$

$$\sigma_{ds1} = K_{ds1}\left(i_{ds1}^{*} - i_{ds1}\right) \tag{6.70}$$

$$\sigma_{dr1} = K_{dr1}\left(\lambda_{dr1}^{'*} - \lambda_{dr1}^{'}\right) \tag{6.71}$$

for the rotor speed

$$\sigma_{\omega} = K_{\omega}\left(\omega_{r}^{*} - \omega_{r}\right) \tag{6.72}$$

For the third harmonic components

$$\sigma_{qs3} = K_{qs3}\left(i_{qs3}^{*} - i_{qs3}\right) \tag{6.73}$$

$$\sigma_{ds3} = K_{ds3}\left(i_{ds3}^{*} - i_{ds3}\right) \tag{6.74}$$

$$\sigma_{dr3} = K_{dr3}\left(\lambda_{dr3}^{'*} - \lambda_{dr3}^{'}\right) \tag{6.75}$$

where

K_{qs1}, K_{ds1}, K_{dr1} and K_{ω} are the transfer functions of the controller for q-axis fundamental component of current, d-axis fundamental component of current, fundamental component of rotor flux linkage and rotor speed, respectively.

K_{qs3}, K_{ds3}, and K_{dr3} are the transfer functions of the controller for q-axis third harmonic component of current, d-axis third harmonic component of current, and third harmonic component of rotor flux linkage, respectively.

From Equations (6.61) and (6.62), the fundamental components of the qd reference stator voltages are given by

$$v_{qs1}^{*} = \sigma_{qs1} + \omega_{e1} L_{\sigma 1} i_{ds1} + \omega_r \frac{L_{m1}}{L_{r1}^{'}} \lambda_{dr1}^{'} \tag{6.76}$$

$$v_{ds1}^{*} = \sigma_{ds1} - \omega_{e1} L_{\sigma 1} i_{qs1} - \frac{r_{r1}^{'} L_{m1}}{L_{r1}^{'2}} \lambda_{dr1}^{'} \tag{6.77}$$

From Equations (6.64) and (6.65), the third harmonic components of the qd reference stator voltages are given by

$$v_{qs3}^{*} = \sigma_{qs3} + 3\omega_{e3} L_{\sigma 3} i_{ds3} + 3\omega_r \frac{L_{m3}}{L_{r3}^{'}} \lambda_{dr3}^{'} \tag{6.78}$$

$$v_{ds3}^{*} = \sigma_{ds3} - 3\omega_{e3} L_{\sigma 3} i_{qs3} - \frac{r_{r3}^{'} L_{m3}}{L_{r3}^{'2}} \lambda_{dr3}^{'} \tag{6.79}$$

From Equation (6.63) the fundamental component of the reference d-axis stator current is given by

$$i_{ds1}^{*} = \frac{L_{r1}}{r_{r1}^{'} L_{m1}} \sigma_{dr1} \tag{6.80}$$

From Equation (6.66) the third harmonic component of the reference d-axis stator current is given by

$$i_{ds3}^{*} = \frac{L_{r3}}{r_{r3}^{'} L_{m3}} \sigma_{dr3} \tag{6.81}$$

Now if the two slips are equal, then the relationship between the two torque producing currents i_{qs1} and i_{qs3} is given as

$$\left(\omega_{e3} - \omega_r\right) = \left(\omega_{e1} - \omega_r\right) \tag{6.82}$$

$$\frac{r_{r1}^{'} L_{m1}}{L_{r1}} \frac{i_{qs1}}{\lambda_{dr1}^{'}} = \frac{r_{r3}^{'} L_{m3}}{3L_{r3}} \frac{i_{qs3}}{\lambda_{dr3}^{'}} \tag{6.83}$$

$$i_{qs3} = 3\frac{r_{r1}^{'}}{r_{r3}^{'}}\frac{L_{m1}}{L_{m3}}\frac{L_{r3}}{L_{r1}}\frac{\lambda_{dr3}^{'}}{\lambda_{dr1}^{'}}i_{qs1}$$

From Equations (6.68) and (6.84), the reference q-axis current is given by

$$i_{qs}^{*} = \frac{\frac{2J}{P}\sigma_{\omega} + T_L}{\frac{mP}{4}\frac{L_{m1}}{L_{r1}}\left(\lambda_{dr1} + \frac{9r_{r1}}{r_{r3}}\frac{\lambda_{dr3}^{2}}{\lambda_{dr1}}\right)} \tag{6.84}$$

where

v_{qs1}^{*} is the fundamental component of the q-axis reference stator voltage.

v_{ds1}^{*} is the fundamental component of the d-axis reference stator voltage.

v_{qs3}^{*} is the third harmonic component of the q-axis reference stator voltage.

v_{ds3}^{*} is the third harmonic component of the d-axis reference stator voltage.

i_{ds1}^{*} is the fundamental component of the d-axis reference stator current.

i_{ds3}^{*} is the third harmonic component of the d-axis reference stator current.

i_{qs}^{*} is the q-axis reference stator current.

6.3 Controller Design

As it has been derived in Equations (6.61) – (6.63) and (6.68), there are four controllers a controller for flux control, two controllers for the q- and d-axis currents and a controller for the rotor speed. The pole placement method called the Butterworth method is used in the design of controllers, in which the parameters are selected to locate the eigen-values of the transfer function uniformly in the left half of the s-plane, on a circle of radius ω_o, with its center at the origin. The poles are evenly distributed around the circle [3.5].

The design steps using the Butterworth method are firstly, the transfer function of the controller is obtained; then the denominator of the transfer function is compared with the Butterworth polynomial by equaling the coefficient of each term. Since the Butterworth polynomial is expressed only in term of ω_o , if the value of ω_o is selected, all the controller parameters can be obtained.

The value of ω_o determines the dynamic response of the controller. It should be noticed that in a control system with multiple controllers, the values of ω_o for different controllers must be properly designed.

6.4 PI Controller Design Based on Fundamental Components

The four controllers discussed in the previous section are designed. Only the fundamental components are considered at this stage. In this section, the subscripts '1' and '3' for the respective fundamental and third harmonic components will be dropped. Therefore, all variables and parameters in the Equations presented in this section are for the fundamental quantities.

The transfer function for a PI (proportional integral) controller is expressed as

$$K_x = K_{px} + \frac{K_{ix}}{p} \tag{6.85}$$

The Butterworth second order polynomial is give as shown in Equation (6.45). This characteristic Equation will be used to compare the characteristics Equation for different controller transfer functions in order to determine the appropriate value of ω_o to tune the respective controllers

$$p^2 + \sqrt{2}\omega_o p + \omega_o^2 = 0 \tag{6.86}$$

6.4.1 Stator Q-axis Current and D-axis Controller Design

The transfer functions for a PI q-axis current controller is expressed as in Equations

$$K_{qs} = K_{pq} + \frac{K_{iq}}{p} \tag{6.87}$$

$$L_\sigma p i_{qs} + r_\sigma i_{qs} = \left(K_{pq} + \frac{K_{iq}}{p} \right)\left(i_{qs}^* - i_{qs} \right)$$

$$\left(L_\sigma p + r_\sigma + K_{pq} + \frac{K_{iq}}{p} \right) i_{qs} = \left(K_{pq} + \frac{K_{iq}}{p} \right) i_{qs}^*$$

$$\frac{i_{qs}}{i_{qs}^*} = \frac{K_{pq} + \frac{K_{iq}}{p}}{L_\sigma p + r_\sigma + K_{pq} + \frac{K_{iq}}{p}}$$

$$\frac{i_{qs}}{i_{qs}^*} = \frac{pK_{pq} + K_{iq}}{L_\sigma p^2 + \left(r_\sigma + K_{pq} \right) p + K_{iq}}$$

$$\frac{i_{qs}}{i_{qs}^*} = \frac{\frac{1}{L_\sigma}\left(pK_{pq} + K_{iq} \right)}{p^2 + \frac{1}{L_\sigma}\left(r_\sigma + K_{pq} \right) p + \frac{K_{iq}}{L_\sigma}} \tag{6.88}$$

The characteristic Equation of the transfer function in Equation (6.88) is

$$p^2 + \frac{1}{L_\sigma}\left(r_\sigma + K_{pq}\right)p + \frac{K_{iq}}{L_\sigma} = 0 \tag{6.89}$$

Comparing Equation (6.89) with Equation (6.86), the following is obtained

$$\frac{1}{L_\sigma}\left(r_\sigma + K_{pq}\right) = \sqrt{2}\omega_o$$

$$K_{pq} = \sqrt{2}\omega_{oq}L_\sigma - r_\sigma \tag{6.90}$$

$$K_{iq} = \omega_{oq}^2 L_\sigma \tag{6.91}$$

Similarly, the stator d-axis current controller is given by

$$\frac{i_{ds}}{i_{ds}^*} = \frac{\frac{1}{L_\sigma}\left(pK_{pd} + K_{id}\right)}{p^2 + \frac{1}{L_\sigma}\left(r_\sigma + K_{pd}\right)p + \frac{K_{id}}{L_\sigma}} \tag{6.92}$$

The characteristic Equation is

$$p^2 + \frac{1}{L_\sigma}\left(r_\sigma + K_{pd}\right)p + \frac{K_{id}}{L_\sigma} = 0 \tag{6.93}$$

Therefore,

$$K_{pd} = \sqrt{2}\omega_{od}L_\sigma - r_\sigma \tag{6.94}$$

$$K_{id} = \omega_{od}^2 L_\sigma \tag{6.95}$$

6.4.2 Flux Controller Design

The transfer function for a PI flux controller is expressed as

$$K_{dr} = K_{pr} + \frac{K_{ir}}{p} \tag{6.96}$$

$$p\lambda_{dr}^{'} + \frac{r_r^{'}}{L_r^{'}}\lambda_{dr}^{'} = \left(K_{pr} + \frac{K_{ir}}{p}\right)\left(\lambda_{dr}^{'*} - \lambda_{dr}^{'}\right)$$

$$\left(p + \frac{r_r^{'}}{L_r^{'}} + K_{pr} + \frac{K_{ir}}{p}\right)\lambda_{dr}^{'} = \left(K_{pr} + \frac{K_{ir}}{p}\right)\lambda_{dr}^{'*}$$

$$\frac{\lambda_{dr}^{'}}{\lambda_{dr}^{'*}} = \frac{K_{pr} + \frac{K_{ir}}{p}}{p + \frac{r_r^{'}}{L_r^{'}} + K_{pr} + \frac{K_{ir}}{p}}$$

$$\frac{\lambda_{dr}^{'}}{\lambda_{dr}^{'*}} = \frac{pK_{pr} + K_{ir}}{p^2 + \left(\frac{r_r^{'}}{L_r^{'}} + K_{pr}\right)p + K_{ir}} \tag{6.97}$$

The characteristic Equation is

$$p^2 + \left(\frac{r_r^{'}}{L_r^{'}} + K_{pr}\right)p + K_{ir} = 0 \tag{6.98}$$

Comparing Equation (6.98) with Equation (6.86), the following is obtained

$$\frac{r_r^{'}}{L_r^{'}} + K_{pr} = \sqrt{2}\omega_{or}$$

$$K_{pr} = \sqrt{2}\omega_{or} - \frac{r_r^{'}}{L_r^{'}} \tag{6.99}$$

$$K_{ir} = \omega_{or}^2 \tag{6.100}$$

6.4.3 Speed Controller Design

The speed controller is designed as follows

$$K_{\omega} = K_{p\omega} + \frac{K_{i\omega}}{p} \tag{6.101}$$

$$p\omega_r = \left(K_{p\omega} + \frac{K_{i\omega}}{p} \right)\left(\omega_r^* - \omega_r\right)$$

$$\left(p + K_{p\omega} + \frac{K_{i\omega}}{p} \right)\omega_r = \left(K_{p\omega} + \frac{K_{i\omega}}{p} \right)\omega_r^*$$

$$\frac{\omega_r}{\omega_r^*} = \frac{K_{p\omega} + \dfrac{K_{i\omega}}{p}}{p + K_{p\omega} + \dfrac{K_{i\omega}}{p}}$$

$$\frac{\omega_r}{\omega_r^*} = \frac{pK_{p\omega} + K_{i\omega}}{p^2 + pK_{p\omega} + K_{i\omega}} \tag{6.102}$$

The characteristic Equation is

$$p^2 + pK_{p\omega} + K_{i\omega} = 0 \tag{6.103}$$

Comparing Equation (6.103) with Equation (6.86), the following is obtained

$$K_{p\omega} = \sqrt{2}\omega_{o\omega} \tag{6.104}$$

$$K_{i\omega} = \omega_{o\omega}^2 \tag{6.105}$$

Figure 6.1 shows the controller block diagram for the five-phase induction motor drive. The Equations shown in Figure 6.1 are explained as follows

The q-axis stator reference voltage, v_{qs}^*, is given by

$$v_{qs}^{*} = \sigma_{qs} + \omega_e L_\sigma i_{ds} + \omega_r \frac{L_m}{L_r^{'}} \lambda_{dr}^{'} \tag{6.106}$$

The d-axis stator reference voltage, v_{ds}^{*}, is given by

$$v_{ds}^{*} = \sigma_{ds} - \omega_e L_\sigma i_{qs} - \frac{r_r^{'} L_m}{L_r^{'2}} \lambda_{dr}^{'} \tag{6.107}$$

The d-axis stator reference current, i_{ds}^{*}, is given by

$$i_{ds}^{*} = \frac{L_r}{r_r^{'} L_m} \sigma_{dr} \tag{6.108}$$

The d-axis stator reference current, i_{ds}^{*}, is given by

$$i_{qs}^{*} = \frac{\frac{2J}{P}\sigma_\omega + T_L}{\frac{mP}{4}\frac{L_m}{L_r}\lambda_{dr}^{'}} \tag{6.109}$$

The slip speed is, ω_{sl}, is given by

$$\omega_{sl} = \frac{r_r^{'} L_m}{L_r} \frac{i_{qs}}{\lambda_{dr}^{'}} \tag{6.110}$$

The stator flux linkages are estimated as follows

$$\left.\begin{aligned} \lambda_{qs} &= \int \left(v_{qs} - r_s i_{qs}\right) dt \\ \lambda_{ds} &= \int \left(v_{ds} - r_s i_{ds}\right) dt \end{aligned}\right\} \tag{6.111}$$

Then the rotor flux linkages are obtained as

$$\left.\begin{aligned} \lambda_{qr} &= L_{rm}\left(\lambda_{qs} - L_\sigma i_{qs}\right) \\ \lambda_{dr} &= L_{rm}\left(\lambda_{ds} - L_\sigma i_{ds}\right) \end{aligned}\right\} \qquad L_{rm} = \frac{L_r}{L_m} \tag{6.112}$$

The stator voltage frequency is given by the slip speed and the rotor speed as

$$\omega_e = \omega_r + \omega_{sl} \tag{6.113}$$

This frequency is used to transform the stationary quantities to the synchronously rotating reference frame.

M_{qs}^* and M_{ds}^* are q-axis and d-axis modulation indices.

v_{dc} is the inverter dc supply.

The block diagram of Figure 6.1 consists of two cascaded control loops. The outer control loop regulates the rotor speed and the rotor flux linkage independently. The output of the rotor speed and the flux linkage controllers form the reference signals, i_{qs}^* and i_{ds}^*, for the inner loop q-axis and d-axis stator currents controllers, respectively. The inner current control loop regulates independently the q-axis and d-axis stator current components, i_{qs} and i_{ds}. The instantaneous five-phase stator currents are sampled and transformed to q-d components i_{qs} and i_{ds} in the synchronous reference frame. These actual d-q current signals are then compared with their reference signals to generate the error signals, which are passed through two PI controllers to form the output signals σ_{qs} and σ_{ds}. These two voltage signals are compensated by the corresponding cross coupling terms to form the q-d voltage signals v_{qs}^* and v_{ds}^*. They are then used by the PWM module to generate the IGBT (Insulated Gate Bipolar Transistor) gate control signals to drive the IGBT converter.

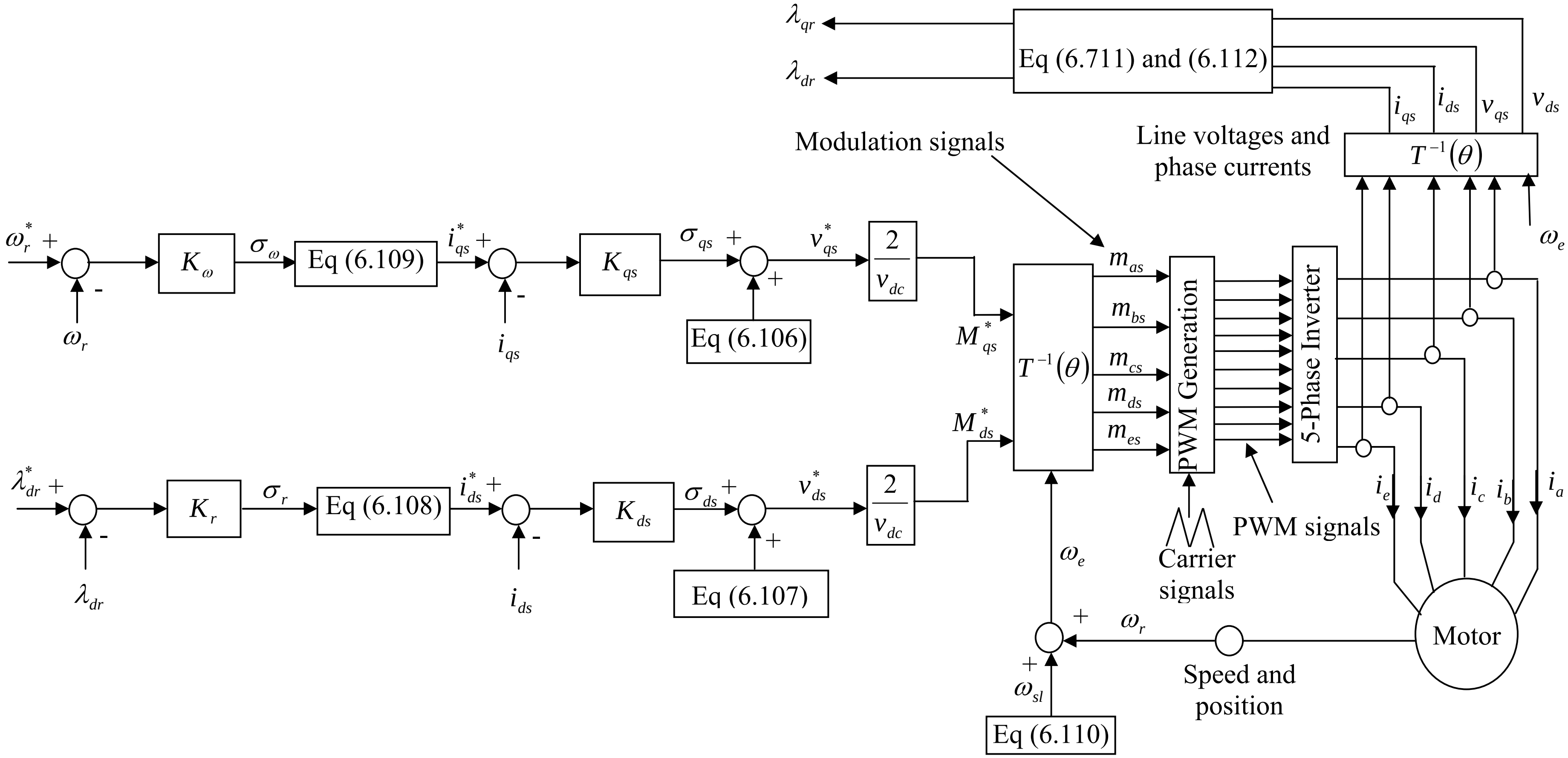

Figure 6.1 Control Block Diagram for the five-phase induction motor drive

6.5 Controller Simulation Results

The rotor reference d-axis flux is chosen to be 0.275 Wb. This will produce the d-axis current using the flux controller output. From the speed controller output and the d-axis rotor flux, the reference q-axis current required to produce the desired torque is obtained.

Figure 6.2 shows the controller simulation for the five phase induction machine. Figure 6.2(a) shows the q-axis stator actual current and the reference current. Figure 6.2(b) shows the d-axis stator actual current and the reference current. Figure 6.2(c) shows the d-axis rotor actual current and the reference current. Figure 6.2(d) shows the actual rotor speed. Figure 6.2(e) shows the reference rotor speed. The reference speed is varied linearly from 0 to 450 rad/sec for 1.5 sec and then made constant at 40 rad/sec for 1.5 sec. At 3 sec it is varied linearly from 450 rad/sec to 0 rad/sec for 1.5 sec, then made constant at 0 rad/sec until the simulation time is for 4.5 sec. At this point it varies linearly until -250 rad/sec for the next for 1.5 sec and it stay constant for 1.5 sec before increasing linearly following the same procedure. It can be seen from the graphs of Figure 6.1 that the actual values are able to track the reference values.

Figure 6.3 shows the stator q-axis and d-axis flux linkages as the response due to change in reference speed. Shown also are the q-axis and d-axis rotor flux, the slip speed and the stator frequency. It can be noted that the controller is effective in the sense that the variables are giving the values as expected.

Figure 6.4 shows the stator q-axis voltage, stator d-axis voltage, electromagnetic torque, rotor q-axis current and rotor d-axis current. The q-axis voltage increases from zero to the maximum value where it has to remain constant as it has already reached its maximum limit. The stator reference and actual phase currents are shown in Figure 6.5. These currents are obtained by performing the inverse transformation fro the qd variables to the abcde variables by using proper reference frame of transformation.

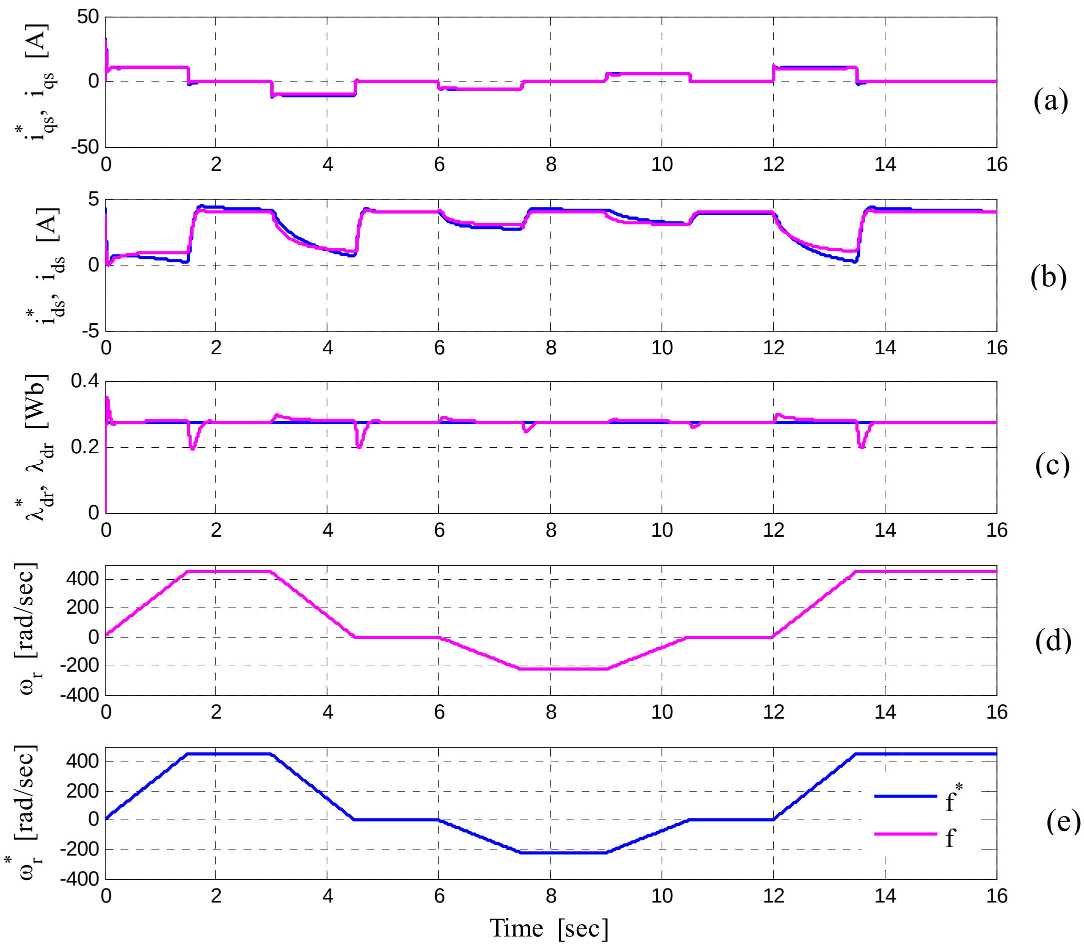

Figure 6.2 Controller simulation (a) Stator q-axis current (b) Stator d-axis current (c) Rotor d-axis flux (d) Actual rotor speed (e) Reference rotor speed

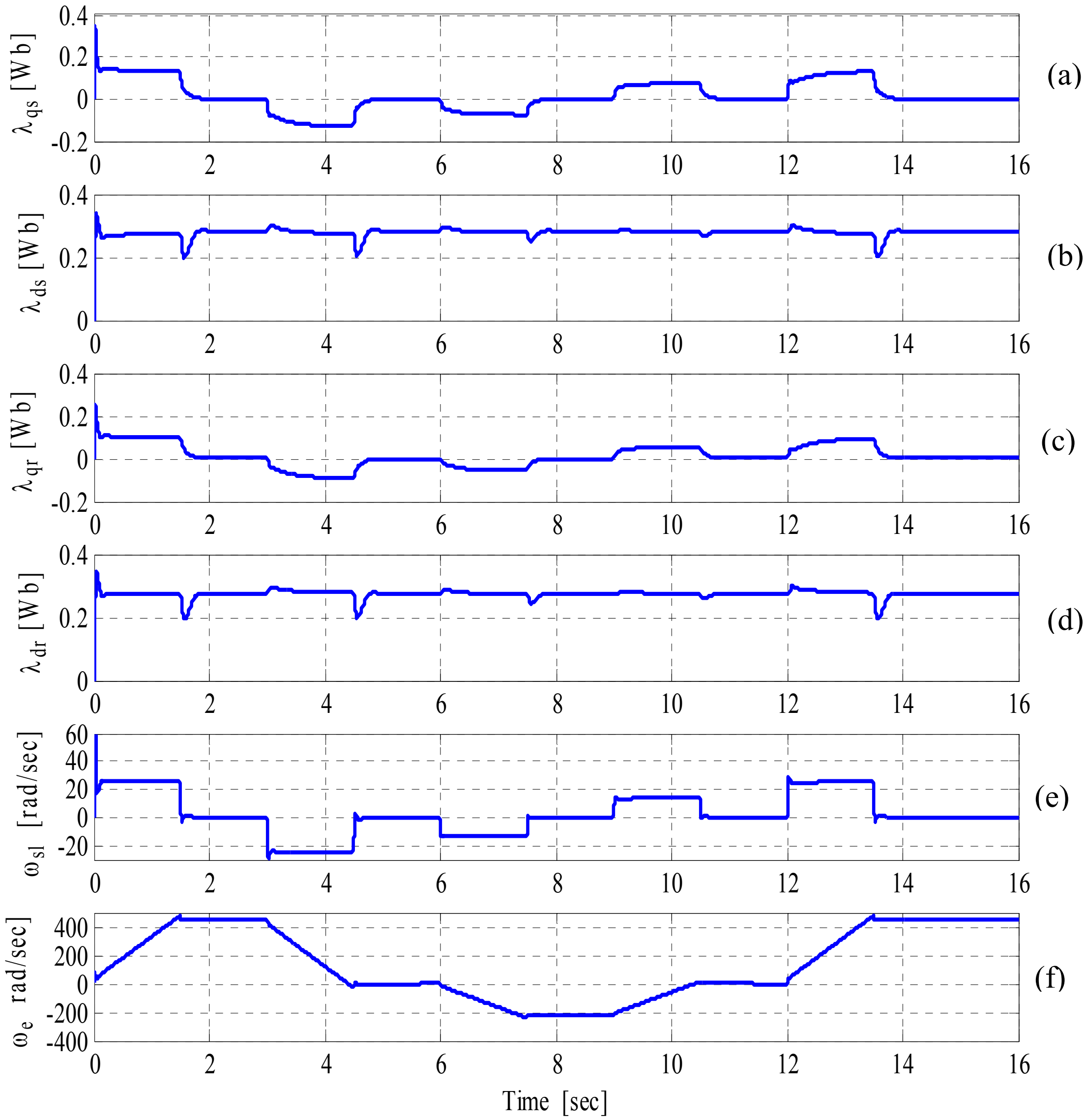

Figure 6.3 (a) stator q-axis flux linkage (b) stator d-axis flux linkage (c) rotor q-axis flux linkage (d) rotor d-axis flux linkage (e) slip speed and (f) stator frequency.

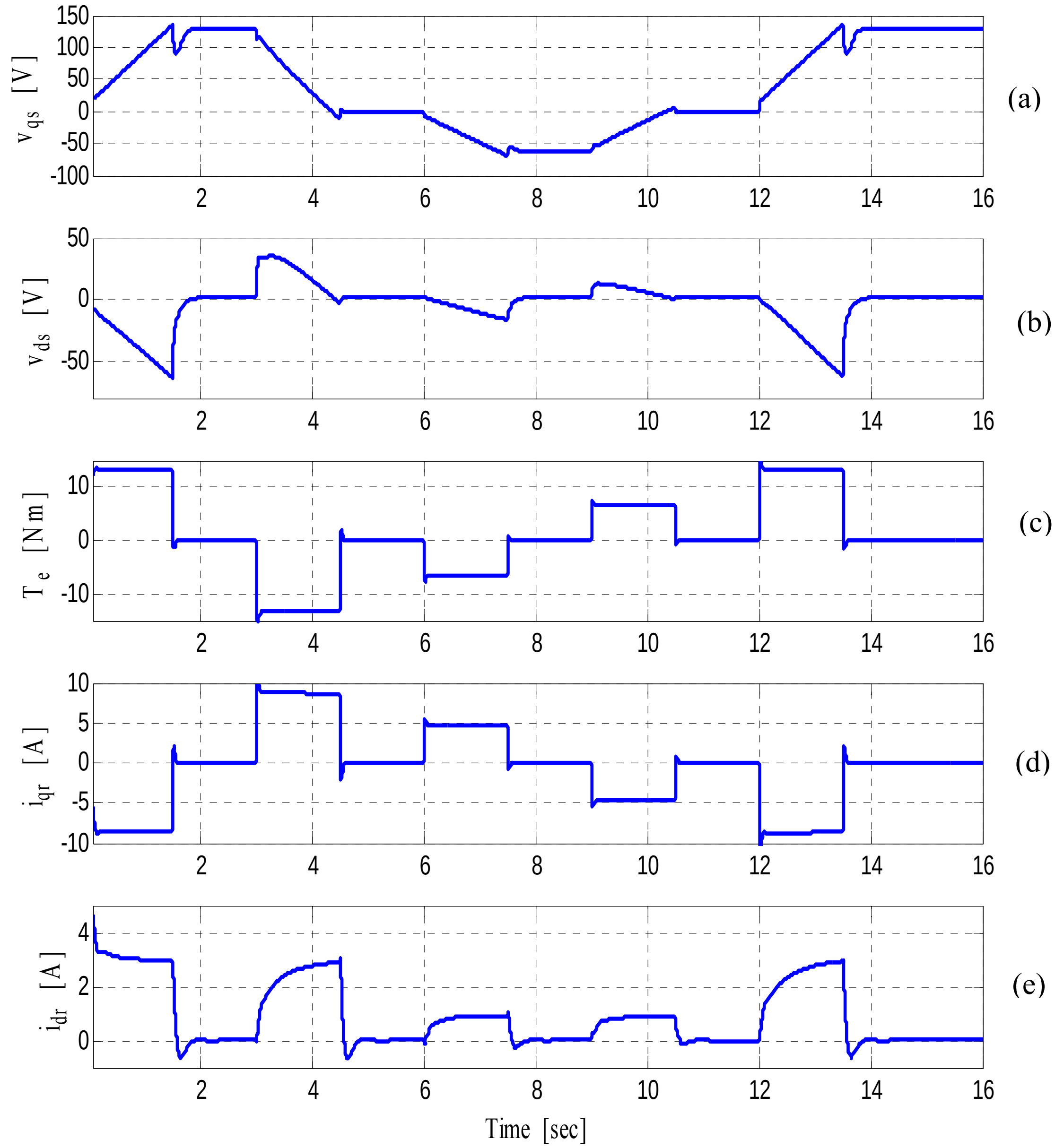

Figure 6.4 Controller simulation (a) stator q-axis voltage (b) stator d-axis voltage (c) Electromagnetic torque (d) rotor q-axis current (e) rotor d-axis current

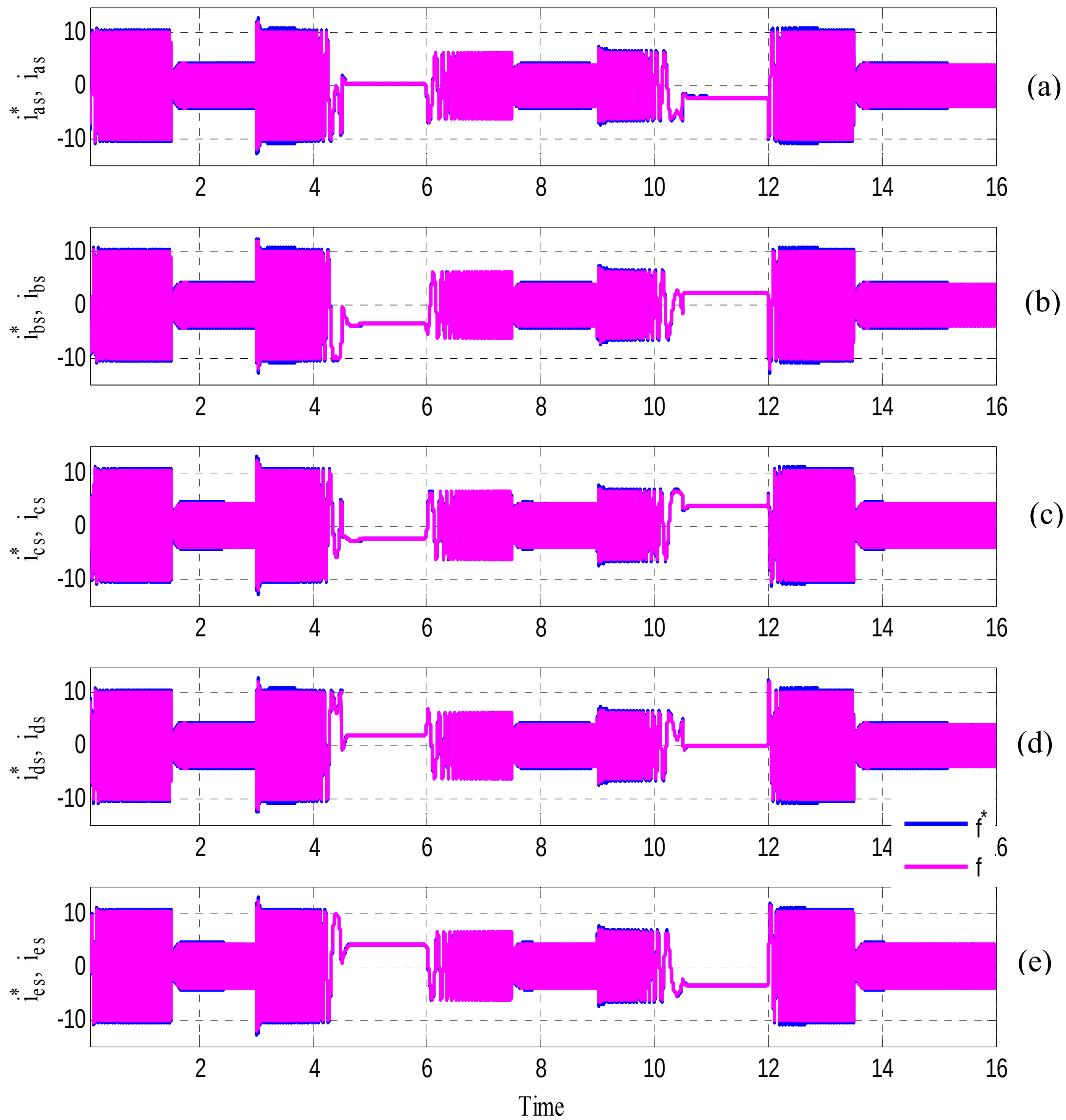

Figure 6.5 Stator reference and actual phase currents (a) stator phase ‘a’ current (b) stator phase ‘b’ current (c) stator phase ‘c’ current (d) stator phase ‘d’ current (e) stator phase ‘e’ current. (Magenta – actual phase currents, Blue - reference phase currents).

6.6 Conclusion

The vector control of the five-phase induction machine has been presented. Four controllers have been realized and different expressions for obtaining the controller parameters have been derived. Simulation results have been presented. A careful examination of the presented results show that the controller is working and it is possible to get the actual values of the stator and rotor variables.

The rotor reference d-axis flux was chosen to be 0.275 Wb, whereas the speed was ramped from 0 to 450 rad/sec for the rising part, then kept constant at 450 rad./sec, before it was ramped to 0 rad/sec for the falling part. The speed was then allowed to become negative after it was kept at 0 rad/sec for some time. Figure 6.4 (c) reveals the torque produced according to the commanded speed. The actual rotor speed in Figure 6.2 (d) tracked the reference rotor speed of figure 6.2 (e) effectively.

CHAPTER 7

CONVERTER RECONFIGURATION FOR IMPROVED EXTENDED SPEED RANGE OF MULTIPHASE INDUCTION MOTOR DRIVES

7.1 Introduction

One of the advantages of a multiphase machine apart from its tolerance is that it can be used in high speed applications. In general, the maximum speed of the machine is limited by the inverter voltage and current limits. High speed operation can be made possible by either employing an inverter with higher voltage or by reducing the counter emf value of the machine using field weakening techniques. Other techniques employed to achieve significant wider speed ranges include reducing the per phase equivalent impedance of the machine, pole amplitude and phase modulation by changing the number of poles. These techniques require additional semiconductor devices in the converter as well as special machine designs. An m-phase machine (where $m > 3$) can be connected in $\frac{m+1}{2}$ different ways. With these available alternatives, the speed range of an m-phase machine can be significantly increased. As the connection pattern changes from one to the other, the impedance of the machine seen by the inverter varies making it possible to achieve higher speeds before the converter rating voltage is reached. In such connection transitions different torque-speed characteristics are realized.

In this Chapter, the approach in reconfiguring the inverter in order to achieve wider speed range of operation for the multiphase induction machines is presented.

7.2 Multiphase Stator Winding Machine Connections

For an odd number of phases, the stator winding of a multiphase machine can be connected in $\frac{m+1}{2}$ different ways. The first two are the normal star connection and delta connection. The normal delta connection in this case is called the conventional delta. The remaining configurations are the alternate delta connections which are obtained buy changing the phase sequences.

In order to achieve the alternate connections, the machine windings are supposed to be connected in delta across the inverter legs. In this section, the peaks of the voltages across the phase windings of the five and seven five machines are calculated as examples. Since the machine is supplied through an inverter, it is easiest to implement the connection changeover from one delta configuration to the other by changing the modulation signals sent to the base drives of the inverter legs.

7.2.1 Five Phase Stator Winding Machine Connections

With the five-phase machine, there are three possible connections one star and two alternate delta connections.

Figure 7.1 (a) shows the schematic representation of a five phase stator winding connected in star configuration. Figures 7.1 (b) and (c) show the delta connections of the five phase stator winding of the induction machine in the conventional and alternate configurations, respectively. It is obvious that the difference between the configuration of

Figure 7.1 (b) and that of Figure 7.1 (c) is the phase sequence orientation, which will eventually result in different magnitudes of the peak voltages across the machine phase windings. The phase sequence for the delta connection of the five-phase machine are *abcde* and *acebd*.

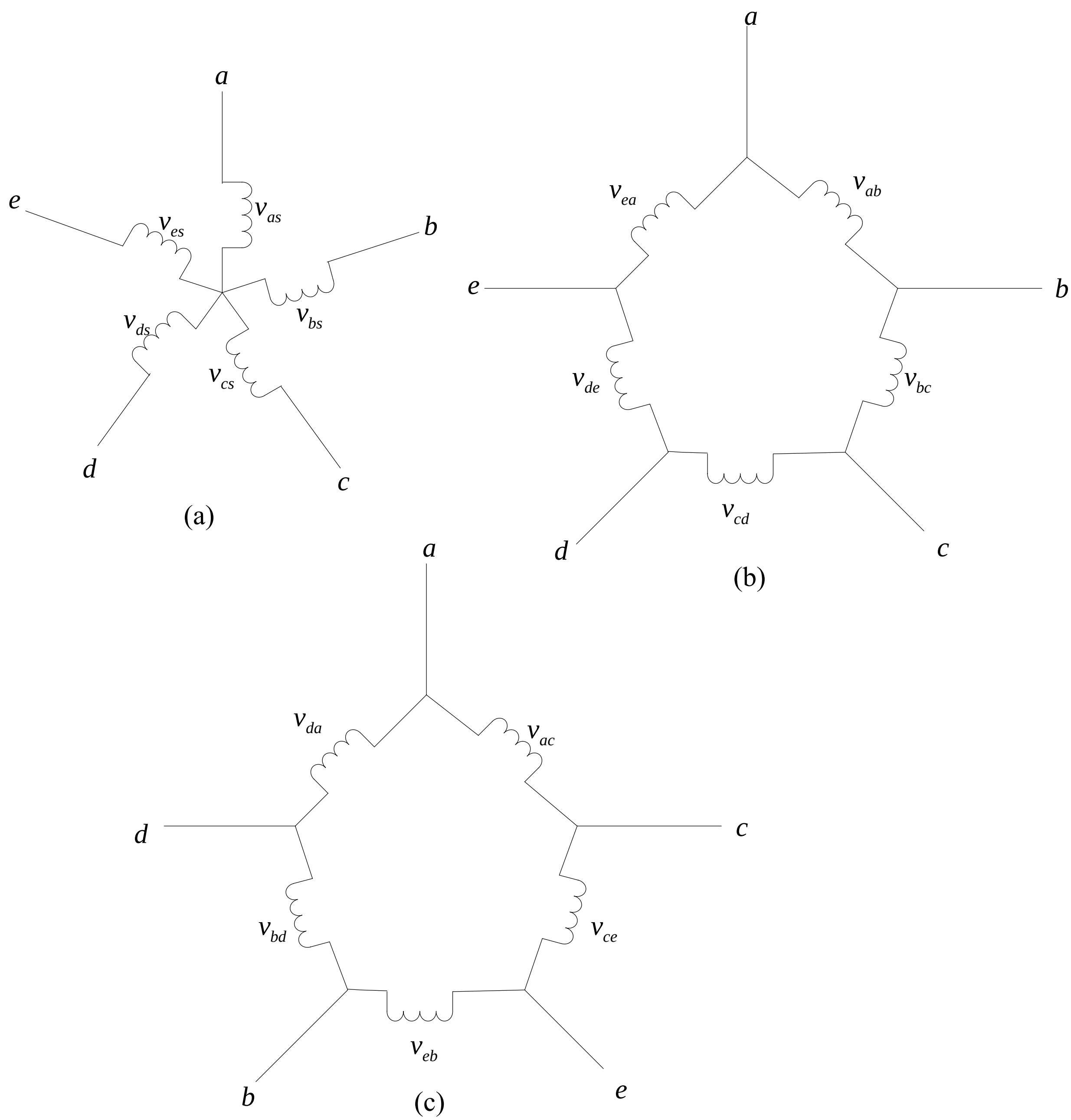

Figure 7.1 Different stator winding connections for a five-phase stator winding (a) star (b) normal (conventional) delta, *abcde* and (c) alternate delta, *acebd*.

7.2.2 Seven Phase Stator Winding Machine Connections

For the seven phase stator winding, there are four possible connections one star and three alternate delta connections, i.e. $\frac{7+1}{2}=4$ different connections. Whereas the star and normal delta connections have the same abcdefg phase sequence, the three alternate delta connections are obtained by changing the phase sequences alternately. The four connections for a seven phase stator winding are shown in Figures 7.2, 7.3, 7.4 and 7.5 for the star, conventional delta, alternate delta I, and alternate delta II, respectively.

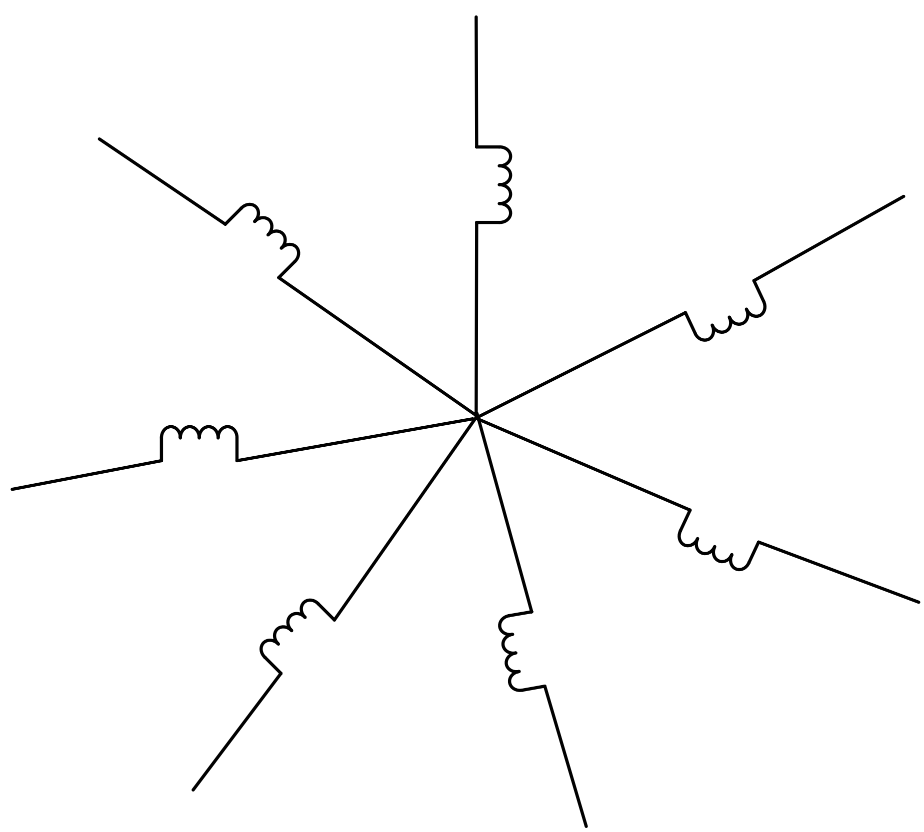

Figure 7.2 Seven phase stator winding in star connection.

For the seven phase machine there are *abcdefg*, *acegbdf*, and *adgcfbe* phase sequences for the three alternate delta connections as shown in Figures 7.3, 7.4 and 7.5, respectively.

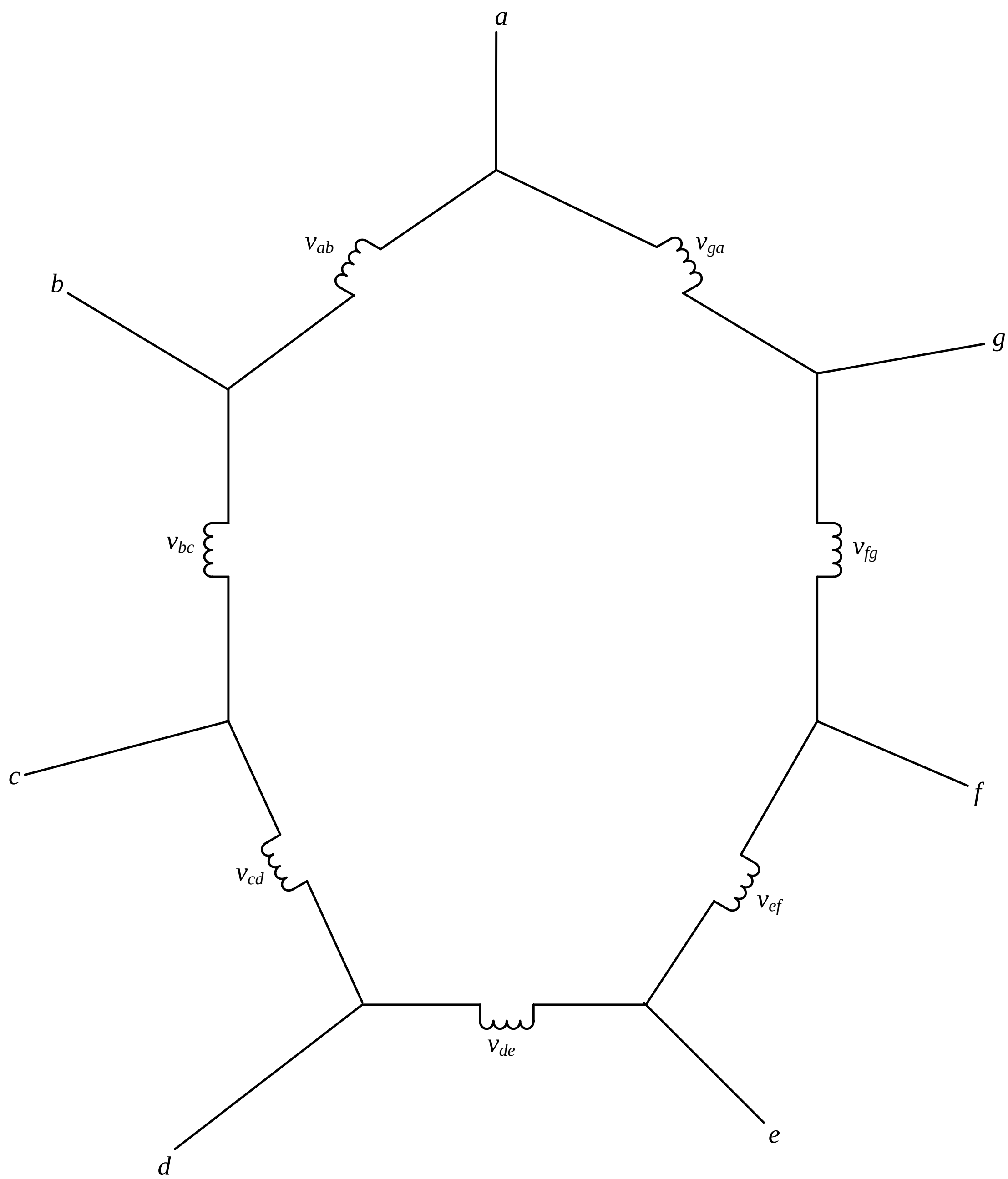

Figure 7.3 Seven phase stator winding in conventional delta (*abcdefg*) connection.

The peak of the phase voltage across each phase winding in Figure 7.3 is $0.8678V_m$

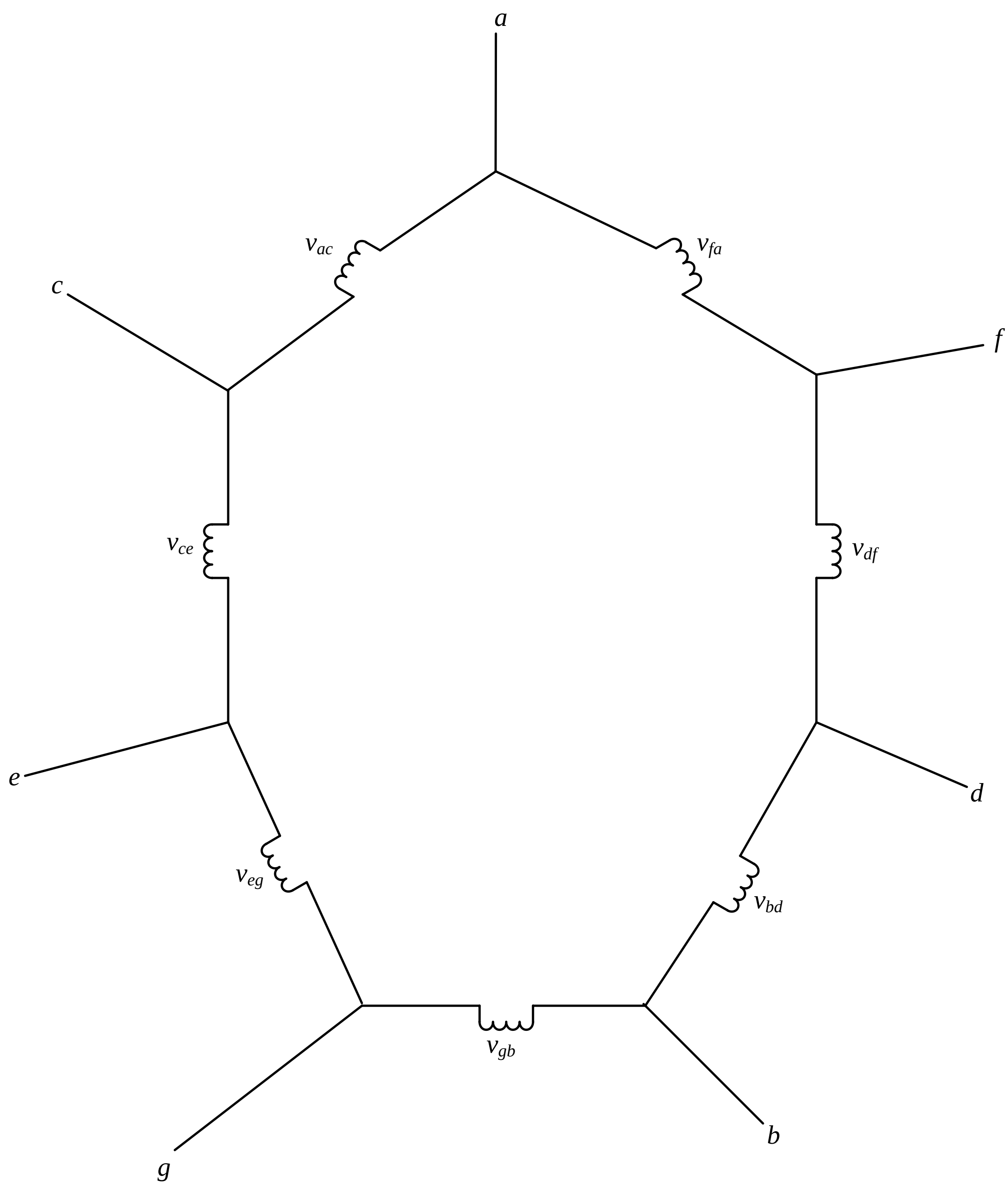

Figure 7.4 Seven phase stator winding in alternate delta (*acegbdf*) connection I.

The peak of the phase voltage across each phase winding in Figure 7.4 is $1.5637V_m$

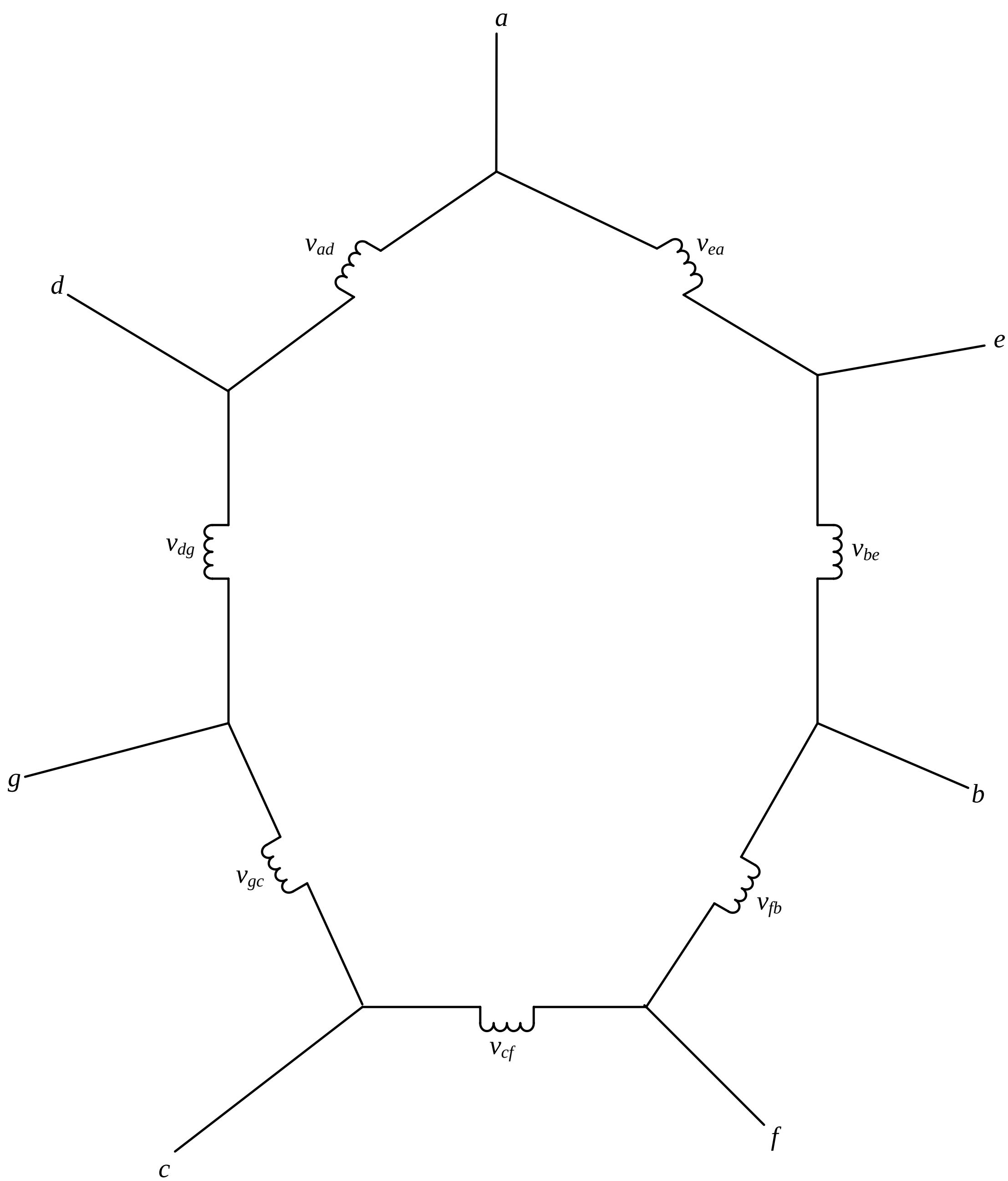

Figure 7.5 Seven phase stator winding in alternate delta (*adgcfbe*) connection II.

The peak of the phase voltage across each phase winding in Figure 7.5 is $1.9499V_m$

7.3 Converter Reconfiguration

If the m-phase machine is supplied through an m-leg inverter, the voltages across the machine phases change based on the winding connections. If the machine is star connected, then each phase voltage is equal to the inverter leg output voltage. For the other connections, each phase voltage is equal to the voltage difference between the two inverter legs to which the phase winding is connected. For the five-phase machine, the magnitude of the voltage across each phase winding will be $1.1756V_m$ and $1.902V_m$ for *abcde* and *acebd*,, respectively. Similarly for the seven–phase machine, the amplitudes of the voltages across each phase winding will be $0.8678V_m$, $1.5637V_m$ and $1.9499V_m$ for *abcdefg*, *acegbdf*, and *adgcfbe*,, *respectively*.

In general, for the alternate delta connections, the voltages across each phase winding are obtained as

$$V_{ij} = V_{mij} \cos(\omega t - \phi_{ij})$$

where $V_{mij} = V_m \sqrt{(\cos\phi_i - \cos\phi_j)^2 + (\sin\phi_i - \sin\phi_j)^2}$

V_m is the peak of the inverter-leg output voltage.

$$\phi_i,\ \phi_j = (k-1)\frac{2\pi}{m},\ k = 1, 2, \cdots, m$$

$$\phi_{ij} = \tan^{-1}\left(\frac{\sin\phi_i - \sin\phi_j}{\cos\phi_i - \cos\phi_j}\right),\ i \neq j,$$

$i,\ j = a,b,c,d,e$ for m = 5, $i,\ j = a,b,c,d,e,f,g$ for m = 7

The configurations with lower voltages are suitable for higher torque, lower speed range operation while those with higher voltages will give lower torques, high speed range operating points. Assume the phase angles of the inverter voltages shown in Figure 1(c) are $0, \frac{2\pi}{5}, \frac{4\pi}{5}, \frac{6\pi}{5}$ and $\frac{8\pi}{5}$ for legs *a*, *b*, *c*, *d*, and *e*, respectively; the magnitude of the machine winding phase voltage is $1.1756V_m$, which is equivalent to the configuration of Figure 1(a). If these angles are multiplied by a factor of 3, the magnitude of the voltage across each machine phase will be $1.902V_m$ which is equal to the magnitude of machine phase voltage for the *acebd* delta configuration of Figure 7.1(b). This connection can be realized through the phase angles of the modulation signals.

In general, given the modulation signals for the five legs of the star connection of the machine windings of the induction machine, the respective factors (k_i) with which the phase angles are multiplied by to obtain the i^{th} delta configuration are given by $k_i = odd(1, 3, \cdots, m-2)$, where $m(odd)$ is the number of phases and $i = 1, 2, 3, \cdots, \frac{m-1}{2}$. Thus by changing the phase angles of the modulation signals, as illustrated in Table 7.1 for a five-phase machine, an automatic changeover between the delta winding configurations without adding any mechanical or semiconductor switches are realized.

Figure 7.6 shows the phase windings of a five phase induction machine connected across the outputs of the voltage source five phase voltage source inverter in a conventional delta connection. Figure 7.7 shows the phase windings of a five phase induction machine connected across the outputs of the voltage source five phase voltage source inverter in an alternate delta connection.

Switching over from the connection in Figure 7.6 to that of Figure 7.7 would require physical switching between the windings. Instead of using a physical switch, the proposed approach requires one to change the modulation angle of the modulating signals for the respective legs and by so doing, the voltages across the windings in Figure 7.6 will be as if the windings are connected as shown in Figure 7.7.

Table 7.1 Modulation signals for star connection and changeover from delta connection I to delta connection II

Phase	Star connection (abcde-n)	Delta connection I (abcde)	Delta connection II (acebd)
a	$M\cos(\omega t+\delta)$	$M\cos(\omega t+\delta)$	$M\cos(\omega t+3\delta)$
b	$M\cos\left(\omega t-\frac{2\pi}{5}+\delta\right)$	$M\cos\left(\omega t-\frac{2\pi}{5}+\delta\right)$	$M\cos\left(\omega t-\frac{6\pi}{5}+3\delta\right)$
c	$M\cos\left(\omega t-\frac{4\pi}{5}+\delta\right)$	$M\cos\left(\omega t-\frac{4\pi}{5}+\delta\right)$	$M\cos\left(\omega t-\frac{12\pi}{5}+3\delta\right)$
d	$M\cos\left(\omega t-\frac{6\pi}{5}+\delta\right)$	$M\cos\left(\omega t-\frac{6\pi}{5}+\delta\right)$	$M\cos\left(\omega t-\frac{18\pi}{5}+3\delta\right)$
e	$M\cos\left(\omega t-\frac{8\pi}{5}+\delta\right)$	$M\cos\left(\omega t-\frac{8\pi}{5}+\delta\right)$	$M\cos\left(\omega t-\frac{24\pi}{5}+3\delta\right)$

where M is the magnitude of the modulation index and δ is the phase angle.

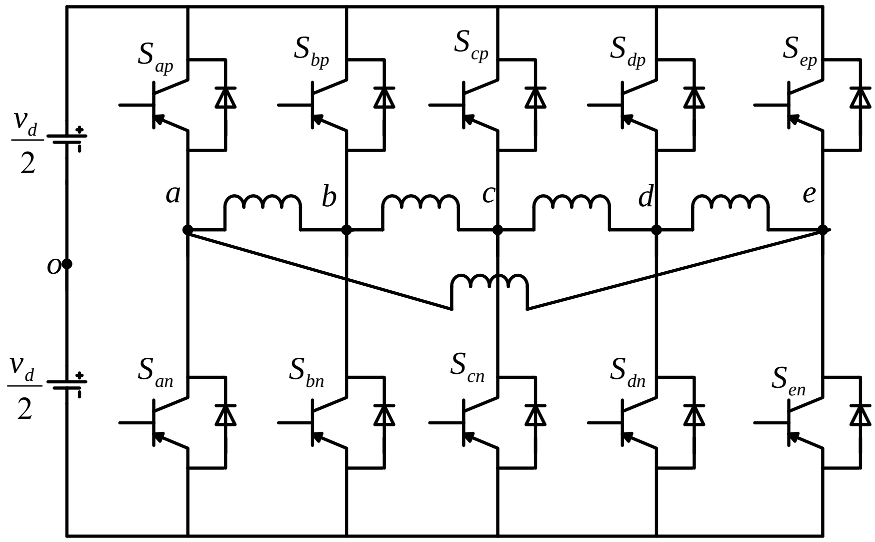

Figure 7.6 Five-leg inverter feeding a five-phase induction machine in abcde delta connection.

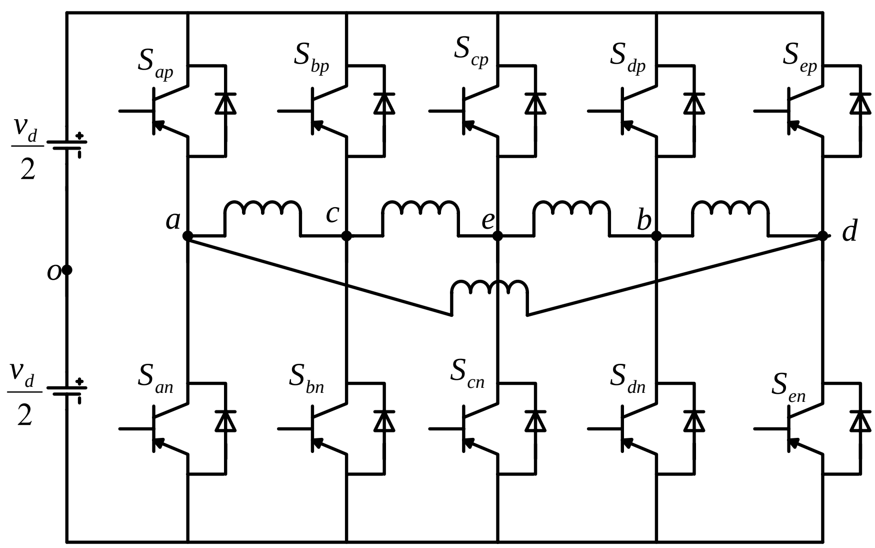

Figure 7.7 Five-leg inverter feeding a five-phase induction machine in acebd delta connection.

7.4 Rotor Reference Frame Vector Control

The induction machine equations represented in the qd synchronous reference frame are given by [7.1]

The stator voltage Equations are

$$
\begin{aligned}
v_{qs} &= r_s i_{qs} + p\lambda_{qs} + \omega\lambda_{ds} \\
v_{ds} &= r_s i_{ds} + p\lambda_{ds} - \omega\lambda_{qs}
\end{aligned}
\tag{7.1}
$$

The rotor voltage Equations are

$$
\begin{aligned}
v'_{qr} &= r'_r i'_{qr} + p\lambda'_{qr} + (\omega - \omega_r)\lambda'_{dr} \\
v'_{dr} &= r'_r i'_{dr} + p\lambda'_{dr} - (\omega - \omega_r)\lambda'_{qr}
\end{aligned}
\tag{7.2}
$$

The stator flux linkages are given by

$$
\begin{aligned}
\lambda_{qs} &= L_s i_{qs} + L_m i_{qr} \\
\lambda_{ds} &= L_s i_{ds} + L_m i_{dr}
\end{aligned}
\tag{7.3}
$$

The rotor flux linkages are given by

$$
\begin{aligned}
\lambda'_{qr} &= L_m i_{qs} + L'_r i'_{qr} \\
\lambda'_{dr} &= L_m i_{ds} + L'_r i'_{dr}
\end{aligned}
\tag{7.4}
$$

The electromagnetic torque is given by

$$
T_e = \frac{mPL_m}{4L_r}\left(\lambda'_{dr} i_{qs} - \lambda'_{qr} i_{ds}\right) \tag{7.5a}
$$

The rotor speed is

$$
p\omega_r = \frac{2J}{P}\left(T_e - T_L\right) \tag{7.5b}
$$

For rotor field oriented control [7.2] $\lambda'_{qr} = 0$ and $p\lambda'_{qr} = 0$. Therefore from (7.4) and (7.5)

$$i_{qr}^{'} = -\frac{L_m}{L_r} i_{qs} \tag{7.6}$$

$$T_e = \frac{mPL_m}{4L_r} \lambda_{dr}^{'} i_{qs} \tag{7.7}$$

At steady state the derivative of the peaks are zero. Therefore, since $v_{qr}^{'} = v_{dr}^{'} = 0$, then from (7.2)

$$i_{dr}^{'} = 0 \tag{7.8}$$

Substituting (7.6) and (7.8) into (7.3) results into

$$\lambda_{qs} = L_\sigma i_{qs} \tag{7.9a}$$

$$\lambda_{ds} = L_s i_{ds} \tag{7.9b}$$

where $L_\sigma = L_s - \frac{L_m^2}{L_r^{'}}$

Substituting (7.8) into (7.4), the following d-axis rotor flux Equation is obtained

$$\lambda_{dr}^{'} = L_m i_{ds} \tag{7.10}$$

Substituting (7.9) into (7.1) at steady state,

$$\begin{aligned} v_{qs} &= r_s i_{qs} + \omega L_s i_{ds} \\ v_{ds} &= r_s i_{ds} - \omega L_\sigma i_{qs} \end{aligned} \tag{7.11}$$

Substituting (7.6) and (7.10) into (7.2), the slip speed is obtained as

$$\omega_{sl} = \frac{r_r^{'} i_{qs}}{L_r^{'} i_{ds}} \tag{7.12}$$

where $\omega_{sl} = \omega - \omega_r$

7.4.1 Constant Torque Region

In this region, while the rotor flux producing current is kept constant, the speed increases from zero to base speed, as shown in Figure 7.9 during which the q- and d-axis currents are constant. The rated stator current is drawn under this condition. Under this condition, the phase machine winding voltage also increases from zero to the maximum allowable rated value. The torque is constant as depicted in Figure 7.10.

The constraints on the inverter voltage and currents are [7.2-7.5]

$$v_{qs}^2 + v_{ds}^2 \le V_s^2 \tag{7.13a}$$

$$i_{qs}^2 + iv_{ds}^2 \le I_s^2 \tag{7.13b}$$

V_s and I_s are the peak values of the inverter maximum allowable voltage and current. If the stator resistance drop is neglected, then the transition stator frequency from constant torque region to field weakening region I (when the machine phase voltage and current are rated values concurrently) is $\omega_1 = \dfrac{V_s}{\sqrt{L_s^2 i_{ds-rated}^2 + L_\sigma^2 \left(I_s^2 - i_{ds-rated}^2\right)}}$ (7.14)

where $i_{ds-rated}$ is the stator d-axis rated current at rated flux.

7.4.2 Field Weakening Region I

The stator qd voltages and currents are given by the equality constraint version of Equations (7.13) which still hold true in the field weakening region I. For this region of operation, the speed increases beyond base speed and the q- and d-axis stator currents vary with rotor speed. They are given in (7.15)

$$i_{qs} = \sqrt{\frac{\omega^2 L_s^2 I_s^2 - V_s^2}{\omega^2 L_s^2 - \omega^2 L_\sigma^2}} \tag{7.15a}$$

$$i_{ds} = \sqrt{\frac{V_s^2 - \omega^2 L_\sigma^2 I_s^2}{\omega^2 L_s^2 - \omega^2 L_\sigma^2}} \tag{7.15b}$$

The rotor speed increases until the voltage is no longer able to supply the rated current. Thus the current constraint in (7.13) does not hold any more, Figure 7.9. This is the point at transition from field weakening region I to field weakening region II which is discussed in the next subsection. That is, the phase voltage corresponds to the rated phase voltage but the phase current drawn by the motor is less than the rated phase current.

7.4.3 Field Weakening Region II

In field weakening region II, the current constraint no longer holds true. In this case there is not enough phase voltage from the source to supply the rated phase current. Therefore by using the torque optimization approach, the optimum q- and d-axis stator currents and slip speed can be obtained as

$$\frac{dT_e}{di_{qs}} = 0 \tag{7.16}$$

$$i_{qs-opt} = \frac{V_s}{\sqrt{2}\omega_{opt} L_\sigma} \tag{7.17a}$$

$$i_{ds-opt} = \frac{V_s}{\sqrt{2}\omega_{opt} L_s} \tag{7.17b}$$

The optimum value of slip speed is given by

$$\omega_{slip-opt} = \frac{r_r^{'} L_s}{L_r^{'} L_\sigma} \tag{18}$$

where ω_{opt} is the transition frequency between field weakening regions I and II given by

$$\omega_{opt} = \frac{V_s}{L_s L_\sigma I_s} \sqrt{\frac{L_s^2 + L_\sigma^2}{2}} \tag{7.19}$$

As the frequency increases beyond ω_{opt} the stator currents decrease as

$$i_{qs} = \frac{V_s}{\sqrt{2}\omega L_\sigma} \tag{7.20a}$$

$$i_{ds} = \frac{V_s}{\sqrt{2}\omega L_s} \tag{7.20b}$$

7.4.4 Current Controller design

Two controllers are required. The q-axis current controller and d-axis current controller. Using Equations (7.4) the rotor currents can be eliminated as follows

$$i_{qr}^{'} = \frac{1}{L_r^{'}}\left(\lambda_{qr}^{'} - L_m i_{qs}\right) \tag{7.21}$$

$$i_{dr}^{'} = \frac{1}{L_r^{'}}\left(\lambda_{dr}^{'} - L_m i_{ds}\right) \tag{7.22}$$

Substituting Equations (7.21) and (7.22) into Equations (7.3), stator flux linkages are given by

$$\lambda_{qs} = \left(L_s - \frac{L_m^2}{L_r^{'}}\right) i_{qs} + \frac{L_m}{L_r^{'}} \lambda_{qr}^{'} \tag{7.23}$$

$$\lambda_{ds} = \left(L_s - \frac{L_m^2}{L_r^{'}} \right) i_{ds} + \frac{L_m}{L_r^{'}} \lambda_{dr}^{'} \tag{7.24}$$

Substituting for the qd stator flux linkages from Equations (7.23) and (7.24) into Equations (7.1) gives the following results for the stator voltage Equations

$$v_{qs} = r_s i_{qs} + L_\sigma p i_{qs} + \omega_e L_\sigma i_{ds} + \frac{L_m}{L_r^{'}} p\lambda_{qr}^{'} + \omega_e \frac{L_m}{L_r^{'}} \lambda_{dr}^{'} \tag{7.25}$$

$$v_{ds} = r_s i_{ds} + L_\sigma p i_{ds} - \omega_e L_\sigma i_{qs} + \frac{L_m}{L_r^{'}} p\lambda_{dr}^{'} - \omega_e \frac{L_m}{L_r^{'}} \lambda_{qr}^{'} \tag{7.26}$$

Equations (7.25) and (7.26 can be re-written as

$$L_\sigma p i_{qs} = v_{qs} - r_s i_{qs} - \omega_e L_\sigma i_{ds} - \frac{L_m}{L_r^{'}} p\lambda_{qr}^{'} - \omega_e \frac{L_m}{L_r^{'}} \lambda_{dr}^{'} \tag{7.27}$$

$$L_\sigma p i_{ds} = v_{ds} - r_s i_{ds} + \omega_e L_\sigma i_{qs} - \frac{L_m}{L_r^{'}} p\lambda_{dr}^{'} + \omega_e \frac{L_m}{L_r^{'}} \lambda_{qr}^{'} \tag{7.28}$$

For a squirrel cage induction machine, the rotor voltages are zero, i.e. $v_{qr1}^{'} = 0$ and $v_{dr1}^{'} = 0$.

Therefore Equation (7.2) becomes

For the q-axis rotor voltage Equation

$$0 = \frac{r_r^{'}}{L_r}\left(\lambda_{qr}^{'} - L_m i_{qs}\right) + p\lambda_{qr}^{'} + \left(\omega_e - \omega_r\right)\lambda_{dr}^{'}$$

$$p\lambda_{qr}^{'} = -\frac{r_r^{'}}{L_r}\lambda_{qr}^{'} + \frac{r_r^{'} L_m}{L_r} i_{qs} - \left(\omega_e - \omega_r\right)\lambda_{dr}^{'} \tag{7.29}$$

For the d-axis rotor voltage Equation

$$0 = \frac{r_r^{'}}{L_r}\left(\lambda_{qr}^{'} - L_m i_{qs}\right) + p\lambda_{qr}^{'} + \left(\omega_e - \omega_r\right)\lambda_{dr}^{'}$$

$$0 = \frac{r_r^{'}}{L_r}\left(\lambda_{dr}^{'} - L_m i_{ds}\right) + p\lambda_{dr}^{'} - \left(\omega_e - \omega_r\right)\lambda_{qr}^{'}$$

$$p\lambda_{dr}^{'} = -\frac{r_r^{'}}{L_r}\lambda_{dr}^{'} + \frac{r_r^{'} L_m}{L_r} i_{ds} + \left(\omega_e - \omega_r\right)\lambda_{qr}^{'} \tag{7.30}$$

Substituting Equations (7.29) and (7.30) into Equations (7.25) and (7.26), respectively results into

$$L_\sigma p i_{qs} = v_{qs} - r_\sigma i_{qs} + \frac{r_r^{'} L_m}{L_r^{'2}}\lambda_{qr}^{'} - \omega_e L_\sigma i_{ds} - \omega_r \frac{L_m}{L_r^{'}}\lambda_{dr}^{'} \tag{7.31}$$

$$L_\sigma p i_{ds} = v_{ds} - r_\sigma i_{ds} + \frac{r_r^{'} L_m}{L_r^{'2}}\lambda_{dr}^{'} + \omega_e L_\sigma i_{qs} + \omega_r \frac{L_m}{L_r^{'}}\lambda_{qr}^{'} \tag{7.32}$$

where

$$L_\sigma = L_s - \frac{L_m^2}{L_r^{'}} \text{ and } r_\sigma = r_s + \frac{r_r^{'} L_m^2}{L_r^{'2}}.$$

Aligning the rotor flux linkage with the d-axis of the synchronous reference frame, the q-axis rotor flux linkage and its derivative are zero. Thus

$$\lambda_{qr}^{'} = 0 \tag{7.33}$$

$$p\lambda_{qr}^{'} = 0 \tag{7.34}$$

$$\lambda_r^{'} = \lambda_{dr}^{'} \tag{7.35}$$

where $\lambda_r^{'}$ is the rotor flux linkage.

Substituting Equations (7.33) - (7.35) into Equations (7.5a) and (7.29) – (7.32), results into

$$T_e = \frac{mP}{4}\frac{L_m}{L_r}\lambda_{dr}^{'} i_{qs} \tag{7.36}$$

$$0 = \frac{r_r^{'} L_m}{L_r} i_{qs} - (\omega_e - \omega_r)\lambda_{dr}^{'} \tag{7.37}$$

$$p\lambda_{dr}^{'} = -\frac{r_r^{'}}{L_r}\lambda_{dr}^{'} + \frac{r_r^{'} L_m}{L_r} i_{ds} \tag{7.38}$$

$$L_\sigma p i_{qs} = v_{qs} - r_\sigma i_{qs} - \omega_e L_\sigma i_{ds} - \omega_r \frac{L_m}{L_r^{'}}\lambda_{dr}^{'} \tag{7.39}$$

$$L_\sigma p i_{ds} = v_{ds} - r_\sigma i_{ds} + \frac{r_r^{'} L_m}{L_r^{'2}}\lambda_{dr}^{'} + \omega_e L_\sigma i_{qs} \tag{7.40}$$

Equation (7.37) yields the expression of the fundamental component of the slip frequency required for rotor field orientation control given by

$$(\omega_e - \omega_r) = \frac{r_r^{'} L_m}{L_r^{'}} \frac{i_{qs}}{\lambda_{dr}^{'}} \tag{7.41}$$

The input-output linearization method is used to design the control scheme of the 5-phase induction machine as follows [6.1]

Equations (7.39) and (7.40) can be re-arranged and written as

$$L_\sigma p i_{qs} + r_\sigma i_{qs} = v_{qs} - \omega_e L_\sigma i_{ds} - \omega_r \frac{L_m}{L_r^{'}}\lambda_{dr}^{'} = \sigma_{qs} \tag{7.42}$$

$$L_\sigma p i_{ds} + r_\sigma i_{ds} = v_{ds} + \omega_e L_\sigma i_{qs} + \frac{r_r^{'} L_m}{L_r^{'2}}\lambda_{dr}^{'} = \sigma_{ds} \tag{7.43}$$

where

σ_{qs} is the output of the q-axis current controller

σ_{ds} is the output of the d-axis current controller

The controller outputs are related to the reference and actual quantities as follows

For the fundamental components

$$\sigma_{qs} = K_{qs}\left(i_{qs}^{*} - i_{qs}\right) \tag{7.44}$$

$$\sigma_{ds} = K_{ds}\left(i_{ds}^{*} - i_{ds}\right) \tag{7.45}$$

where

K_{qs} is the transfer function of the controller for the q-axis stator current.

K_{ds} is the transfer function of the controller for the d-axis stator current,

From Equations (7.42) and (7.43), the fundamental components of the qd reference stator voltages are given by

$$v_{qs}^{*} = \sigma_{qs} + \omega_e L_\sigma i_{ds} + \omega_r \frac{L_m}{L_r^{'}} \lambda_{dr}^{'} \tag{7.46}$$

$$v_{ds}^{*} = \sigma_{ds} - \omega_e L_\sigma i_{qs} - \frac{r_r^{'} L_{m1}}{L_r^{'2}} \lambda_{dr}^{'} \tag{7.47}$$

where

v_{qs}^{*} is the q-axis reference stator voltage.

v_{ds}^{*} is the d-axis reference stator voltage.

i_{ds}^{*} is the d-axis reference stator current.

i_{qs}^{*} is the q-axis reference stator current.

The reference rotor flux linkage beyond the base speed is given by

$$\lambda_{dr}^{*} = a_4\omega_r^4 + a_3\omega_r^3 + a_2\omega_r^2 + a_1\omega_r + a_o \tag{7.48}$$

where

$a_o = 0.8940\ Wb$

$a_1 = -1.7325\ x\ 10^{-3}\ Wb \sec rad^{-1}$

$a_2 = 1.5065\ x\ 10^{-6}\ Wb \sec^2 rad^{-2}$

$a_3 = -6.05025 \ x\ 10^{-10} \ Wb\sec^3 rad^{-3}$

$a_4 = 9.1 \ x\ 10^{-14} \ Wb\sec^4 rad^{-4}$

The reference voltages are given by

$$v_{qs}^* = \sigma_{qs} + \omega_e L_\sigma i_{ds}^* + \omega_r^* \frac{L_m}{L_r} \lambda_{dr} \tag{7.49}$$

$$v_{ds}^* = \sigma_{ds} - \omega_e L_\sigma i_{qs}^* - r_r^{'} \frac{L_m}{L_r^2} \lambda_{dr} \tag{7.50}$$

The reference currents are given by

$$i_{dr}^* = \frac{\lambda_{dr}^*}{L_m} \tag{7.51}$$

$$v_{ds} = -\omega_e \lambda_{qs} \tag{7.52}$$

$$v_{ds} = -\omega_e \left(L_s i_{qs} + L_m i_{qr}^{'} \right) \tag{7.53}$$

$$\lambda_{qr}^{'} = L_m i_{qs} + L_r i_{qr}^{'} \tag{7.54}$$

$$\lambda_{qr}^{'} = 0 \tag{7.55}$$

$$i_{qr}^{'} = -\frac{L_m}{L_r} i_{qs} \tag{7.56}$$

$$v_{ds} = -\omega_e \left(L_s - \frac{L_m^2}{L_r} \right) i_{qs} \tag{7.57}$$

This gives the stator current as

$$i_{qs}^* = -\frac{v_{ds}^*}{\omega_e \left(L_s - \frac{L_m^2}{L_r} \right)} \tag{7.58}$$

If the actual q-axis stator current is greater than the rated q-axis current, then the reference current is given by

$$i_{qs}^{*} = \sqrt{I_s^2 - i_{ds}^{*}} \tag{7.59}$$

When the actual voltage exceeds the rated voltage, then the following Equations will generate the reference voltages

$$v_{qs}^{*} = \omega_e \lambda_{ds} \tag{7.60}$$

However, the d-axis rotor current, $i_{dr}^{'}$ is zero, i.e. $i_{dr}^{'} = 0$

$$\lambda_{ds} = L_s i_{ds} + L_m i_{dr}^{'} = L_s i_{ds} \tag{7.61}$$

$$\lambda_{dr} = L_m i_{ds} + L_r i_{dr}^{'} = L_m i_{ds} \tag{7.62}$$

$$i_{ds} = \frac{\lambda_{dr}}{L_m} \tag{7.63}$$

Therefore,

$$\lambda_{ds} = \frac{L_s}{L_m} \lambda_{dr} \tag{7.64}$$

$$v_{qs}^{*} = \omega_e \frac{L_s}{L_m} \lambda_{dr}^{*} \tag{7.65}$$

The reference speed is ramped at a slope of $300\, rad/\mathrm{sec}/\mathrm{sec}$.

Figure 7.8 shows the block diagram for extended speed range operation of a five phase induction motor drive.

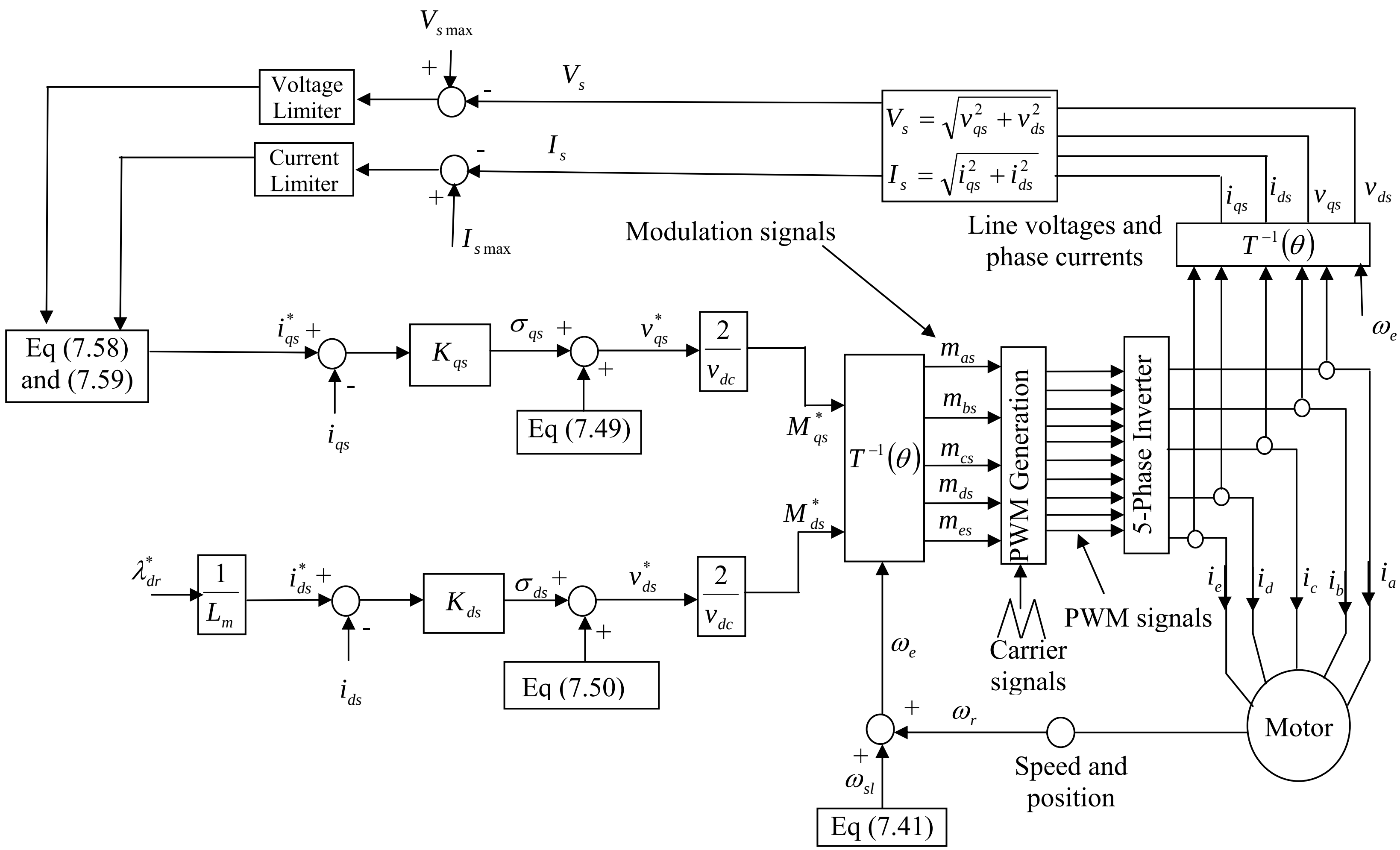

Figure 7.8 Control Block Diagram for extended speed range operation of the five-phase induction motor drive

7.5 Steady-State Results

Steady-state results for the five-phase induction machine in different stator winding configurations are presented in this section. Figure 7.9 and Figure 7.10 show the steady-state results for different stator winding connections. It can be seen that the base speeds depend on the type of winding connection. Also with connections that have higher magnitudes of the phase winding voltage, result in lower torque values but with an extended speed range.

Assuming the voltage across the machine phase winding during star configuration is 1 per unit (p.u.), then when the winding is connected in conventional delta (Figure 7.1(a)), the peak voltage across the machine phase winding is 1.1765 p.u, whereas for the alternate delta connection (Figure 7.1(b)) the peak voltage across the machine's phase winding is 1.902 p.u. In Figure 7.10, it has been clearly shown that for the delta connection with a phase peak voltage of 1.902 p.u., the torque in the high speed range is higher than that for the other delta and star connections. Thus in high speed applications, relatively high torque can be obtained by changing the voltages across the machine winding as it has been presented in section 7.2.

In Figure 7.10, when the machine winding is star connected, higher torque is obtained during the constant torque operation region until the speed is 1 p.u., at a point which field weakening region I starts. At a rotor speed of about 2 p.u., the torque due to the conventional delta connection is higher than those of the other two connections, and therefore the converter has to switch from star connection to delta connection until at appoint when the torque produced due to the alternate delta connection is greater than the other two connections. Thus at a rotor speed of about 2.4 p.u. the changeover from conventional delta to alternate delta will take place.

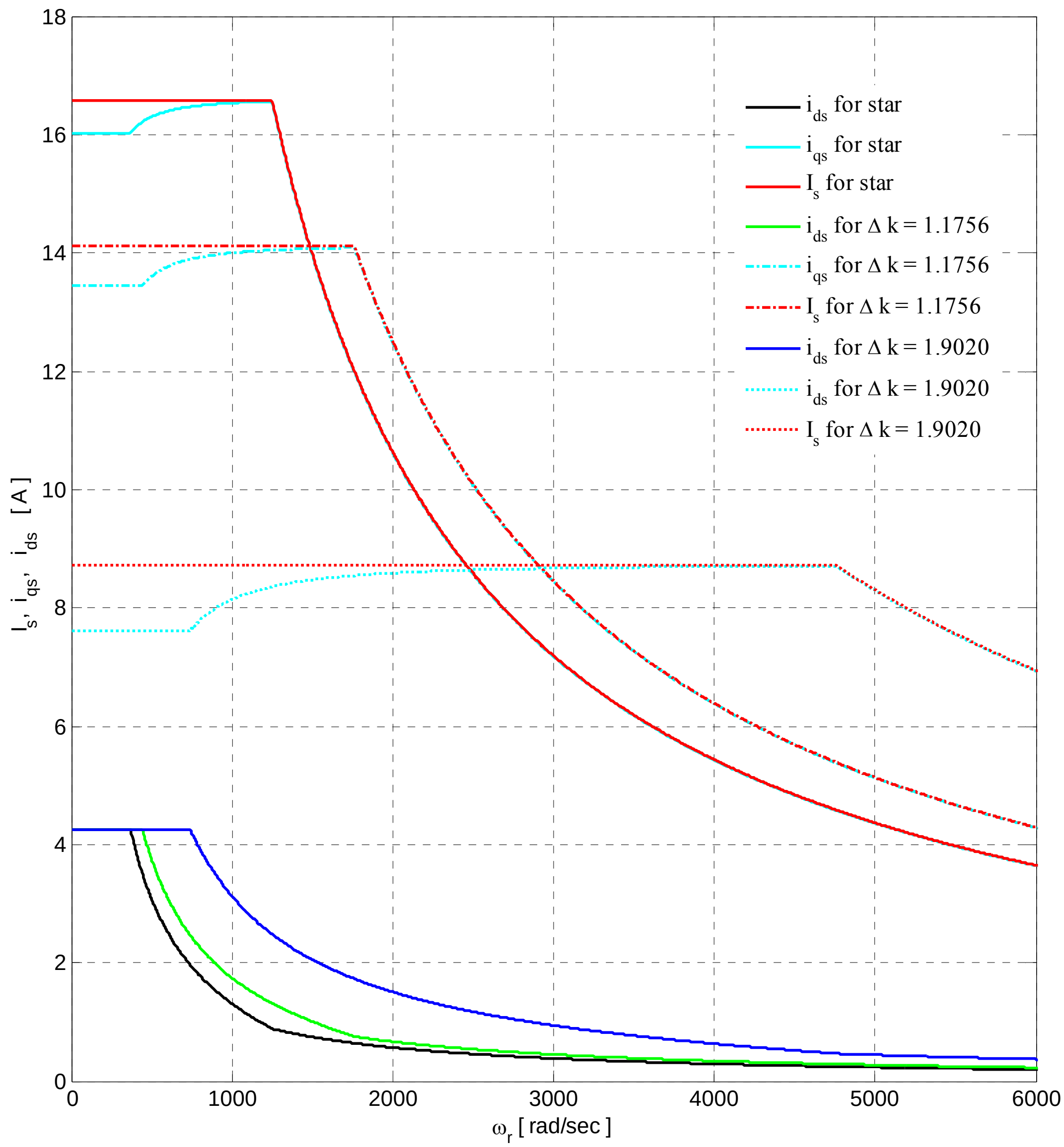

Figure 7.9 Stator peak, q-axis and d-axis currents as functions of rotor speed for the three different connections of the five-phase induction motor.

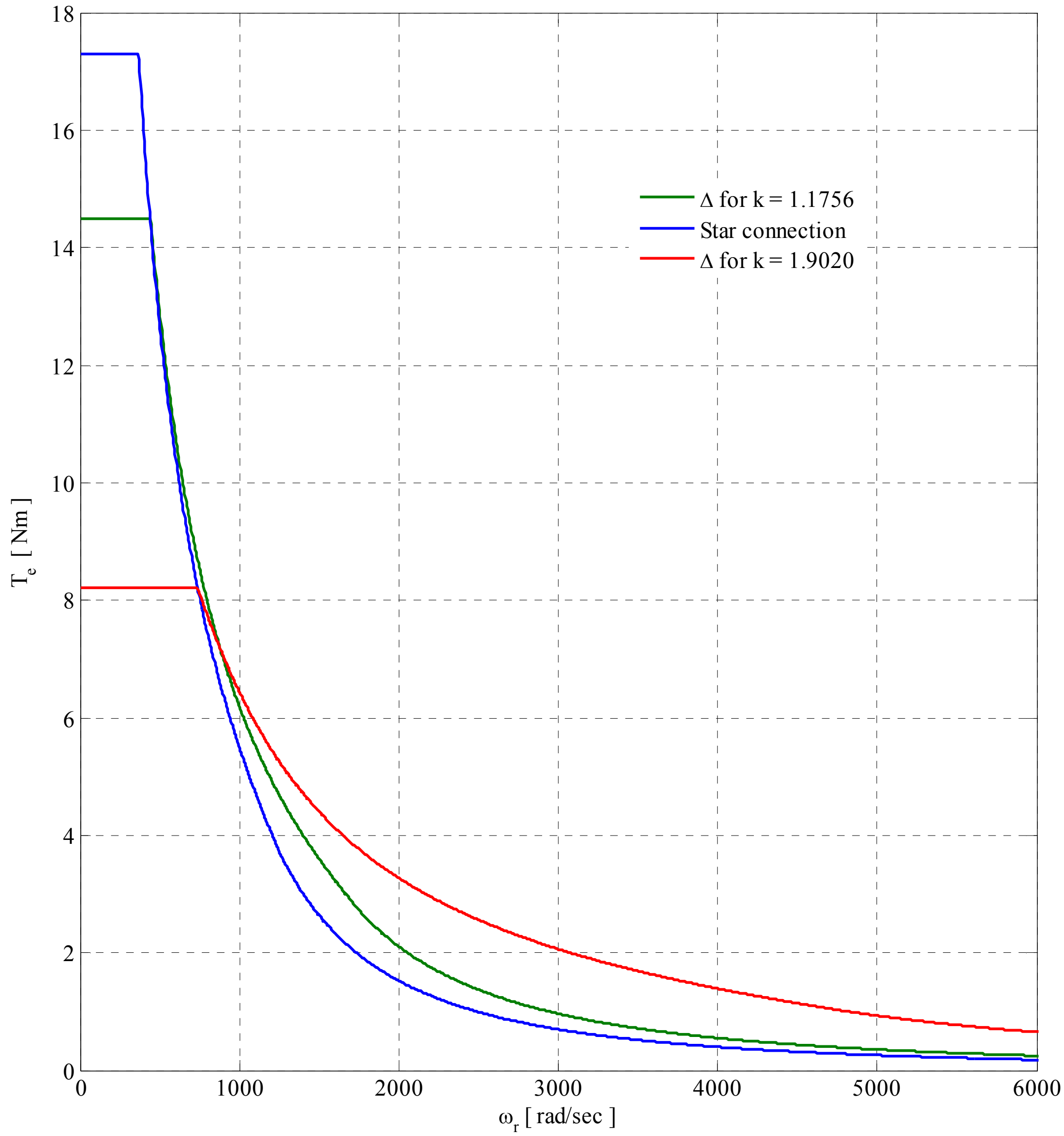

Figure 7.10 Torque as a function of rotor speed for the three different connections of the five-phase induction motor.

7.6 Control Simulation Results

Figure 7.11 shows the simulation results for rotor field oriented control of a five-phase induction machine for varying speed commands in which the actual rotor speed closely follows the command rotor speed. The reference d-axis rotor flux linkage is 0.4574 Wb. Figure 7.12 shows the electromagnetic torque and both the actual and reference rotor speed. Figure 7.12 also shows the simulation results for the field weakening control. It can be observed that before base speed (i.e. 1 p.u.), the torque is approximately constant and as the speed increases, the torque and the flux are gradually reduced.

At about 2 p.u. speed, the machine winding connection is changed from star to delta configuration until the speed is about 2.4 p.u. when changeover from conventional delta to alternate delta occurs. It is important to note that during field weakening operation, the reference d-axis rotor flux linkage is given by Equation (7.48).

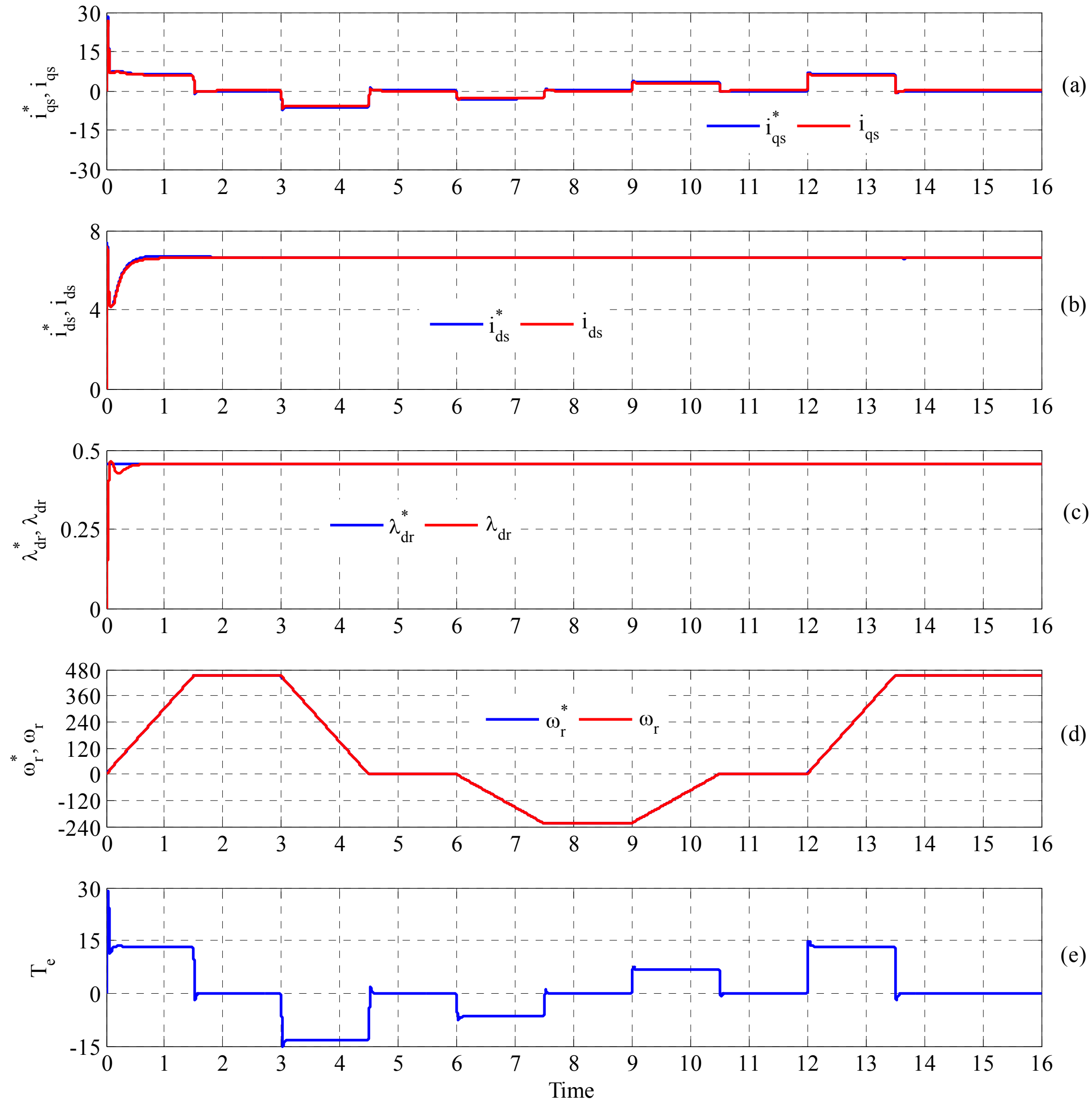

Figure 7.11 Simulation for the speed controlled five-phase machine, (a) actual and reference q-axis stator currents (b) actual and reference d-axis stator currents (c) actual and reference d-axis rotor flux linkages (d) actual and reference rotor speed and (e) electromagnetic torque.

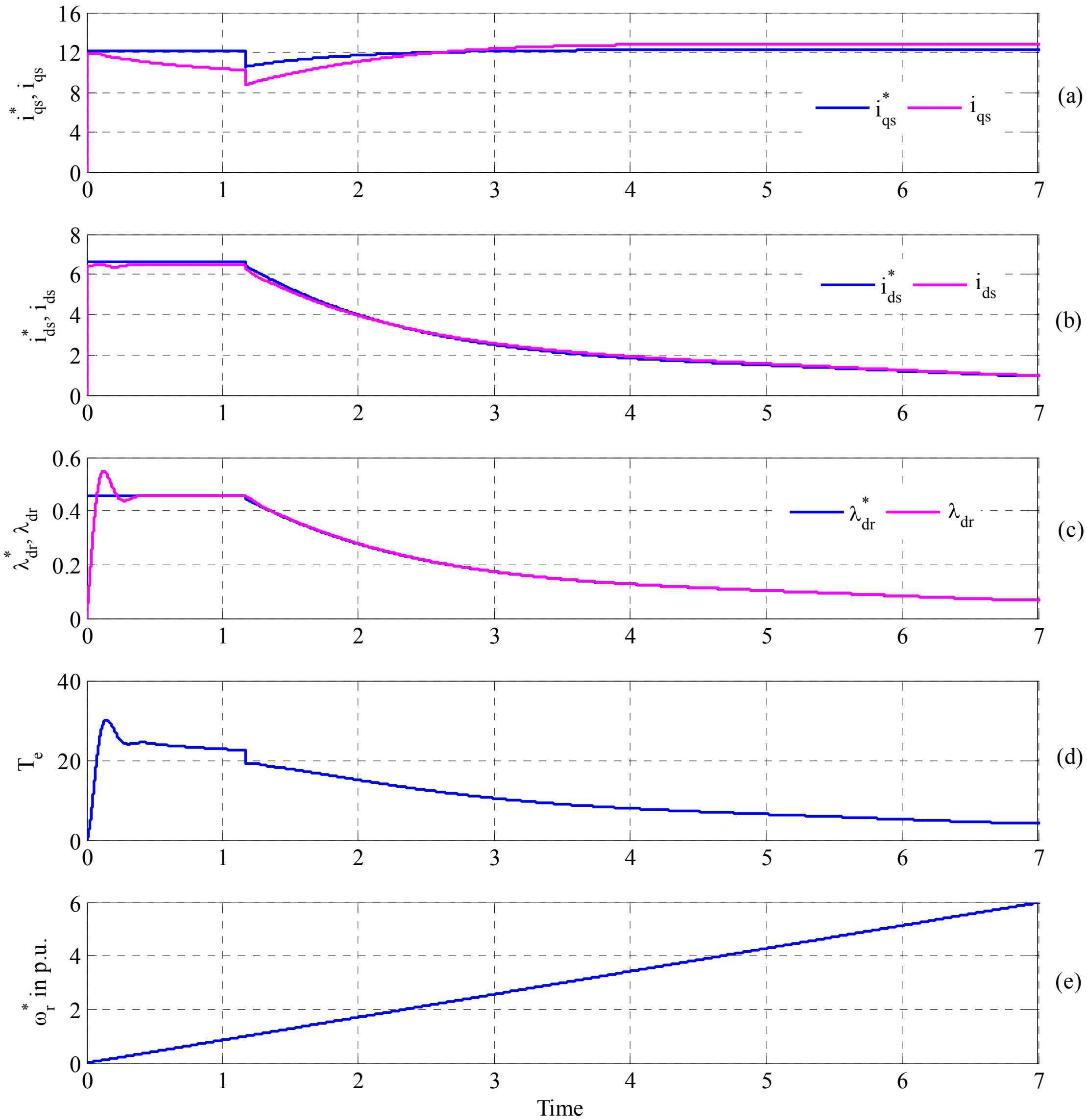

Figure 7.12 Simulation for the speed field weakening control of a five-phase machine, (a) actual and reference q-axis stator currents (b) actual and reference d-axis stator currents (c) actual and reference d-axis rotor flux linkages (d) electromagnetic torque and (e) reference rotor speed.

7.7 Conclusion

In this Chapter, the approach to reconfigure the inverter in order to achieve wider speed range of operation for the multiphase machines has been presented. The multiphase machines offer extended range speeds of operations when connected in different delta schemes across the inverter output phases. By changing the phase angles of the modulation signals, changeover connection from one delta configuration to the other is achieved. The higher the voltage across the machine phase winding, the higher the speed range and lower the operating torque point. Steady state and simulation results for the rotor flux oriented control have been presented and clearly show that it is possible to operate at higher speeds with a relatively high torque when other connections of the stator windings of the multiphase machine are explored.

CHAPTER 8

CONCLUSIONS AND FUTURE WORK

8.1 Introduction

A complex stationary reference frame transformation has been analyzed. It can be used to transform variables of the multiphase system into complex quantities and thus eliminating the time variation. This eases the process of computation and its also simplifies the expressions. Three kinds of transformed variables have been discusses. The forward rotating complex variable, the backward rotating complex variable which are conjugate o s the forward rotating ones and the zero sequence components. The zero sequence component is a real quantity. Therefore for any system with odd number of phases, there are $\frac{m-1}{2}$ forward rotting complex vectors and $\frac{m-1}{2}$ backward rotating vectors. Whereas for the case when the number of phases are even, there exist two zero sequence component. The second one occurring at $\frac{m}{2}$. Using the complex reference frame, expressions for determining the real and reactive power have bee derived. These Equations are such that one can compute the power by using the actual machine variables (current and voltage). The reference frame of transformation used in this Thesis obeys power invariance. Therefore, one can obtain the actual values of the real and reactive powers by using the transformed variables without any need of using a multiplying factor. The obtained expressions are good for calculating the power of the multiphase systems and can be applied in any mode of operation, healthy as well as fault operations, as long as the natural variables are known.

A five-phase induction machine has been modeled. The winding function method is used to calculate the self and mutual inductances in the stator windings and the rotor circuits, with constant air gap in which the space harmonics of the stator windings and rotor circuits are accounted for. A n x n complex variable reference frame transformation is carried out to simplify computation of the currents, voltages and torque equations. Computer simulation results of the no-load starting transient have been shown with the response of the machine for a change in the load torque. This approach has made it possible to calculate the rotor bar currents.

A five-phase carrier based PWM (Pulse Width Modulation) induction motor drive has been presented. The induction machine windings have been connected in alternate ways to increase the torque produced by the machine. A third harmonic voltage component has been injected to detect the ability of a five phase machine to contribute a third harmonic torque component to the fundamental torque component.

The dynamics of a five phase induction motor under open phase faults has been considered. Using stationary reference frame and harmonic balance technique, circuit based models have been used to analyze the open phase, two adjacent phases and two non-adjacent phase faults.

A voltage source converter has been reconfigured for the purpose of operating the induction motor at high speeds.. It investigates the possibilities of operating a multi-phase induction motor drive in field weakening region under optimum torque production. Computer simulation results for the current controllers have shown to agree with those found in several literature. The advantage of this approach is that torque can be optimized during field weakening regions I and II by employing proper means of changing over from one winding connection to the other, for the available delta configurations. For the five phase induction machine considered in this work, there are two different delta connections, conventional delta (with the peak voltage across the machine phase winding of 1.1756 p.u.) and the alternate delta (with the peak voltage across the machine phase winding of 1.902 p.u.).

8.2 Suggestions for Future Work

Extension of the investigation of five phase induction machines and multiphase systems still has many areas to be accounted for. One of the areas of research is how to control the machine under open phase faults, as well as short-circuited turns. The modeling of the machine using the winding function approach can lead to a controller design, which could command the required current to reduce the high phase currents that occur because of faults.

The modulation strategy using space vector approach is currently attracting attention from researchers especially on how to utilize the dc link voltage fully in all sectors for multiphase machine control.

REFERENCES

[1.1] J. R. Fu and T. A. Lipo, “Disturbance Free Operation of a Multiphase Current Regulated Motor Drive with an Opened Phase,” IEEE Transactions on Industry Applications, vol. 30, No. 5, pp. 1267-1274, 1994.

[1.2] Levi, E. “Multiphase Electric Machines for Variable-Speed Applications,” IEEE Transactions on Industrial Electronics, vol. 55, No. 5, pp. 1893-1909, May 2008.

[1.3] Williamson, S. and Smith, A. C., “Pulsating Torque and Losses in Multiphase Induction Machines,” IEEE Transactions Industry Applications, vol. 39, No. 4, pp. 986–993, July/August 2003.

[1.4] Abbas, M. A., Christen, R., and Jahns, T. M., “Six-Phase Voltage Source Inverter Driven Induction Motor,”IEEE Transactions on Industry Application, vol. IA-20, No. 5, pp. 1251-1259, September/October 1984.

[1.5] Pavithran, K. N., Parimelalagan, R. and Krishnamurthy, M. R., “Studies on inverter-fed Five-Phase Induction Motor Drive,” IEEE Transactions on Power Electronics, vol. 3, No. 2, pp. 1177-1184, 1988.

[1.6] Lyra, R. O. C. and Lipo, T. A., “Torque Density Improvement I a Six-phase Induction Motor with Third Harmonic Current Injection,” IEEE Transactions on Industrial Applications, vol. 38, No. 5, pp. 1351-1360, September/October 2002.

[1.7] Singh, G. K., Nam, K., and Lim, S. K., “A Simple Indirect Field-oriented Control Scheme for Multiphase Induction Machine,” IEEE Transactions on Industrial Electronics, vol. 52, No. 4, pp. 1177-1184, August 2005.

[1.8] Bojoi, R. Levi, E., Farina, F., Tenconi, A., and Profumo, F, “Dual Three-phase Induction Motor Drive with Digital Current Control in the Stationary Reference Frame,” IEE Proc. Electr. Power Appl., 2006, vol. 153, No. 1, pp. 129-139, 2006.

[1.9] Kianinzhad, R., Nahid, B., Betin, F., and Capolino G. A., “A new field orientation Control of dual three phase induction machines,” In Proc. IEEE ICIT, pp. 187-192, Hammamet, Tunisia, 2004.

[1.10] Pereira, L., Scharlau, C. C., Pereira, L. F. A., and Haffner, J. F., “Model of a five-phase induction machine allowing for harmonics in the air-gap field, Part II: Transformation of coordinates and d-q models,” in Proc. IEEE IECON, pp. 1682-1687, Busan, Korea, 2004.

[1.11] Pereira, L., Scharlau, C. C., Pereira, L. F. A., and Haffner, J. F., “General model of a five-phase induction machine allowing for harmonics in the air-gap field,” IEEE Transactions on Energy Conversion, vol. 21, No. 4, pp. 891-899, December, 2006.

[1.12] Figuora, J., Cros, J., and Viarouge, P., "Generalized transformations for polyphase phase modulation motors," IEEE Transactions on Energy Conversion, vol. 21, No. 2, pp. 332-341, June, 2006.

1.13] Camillis, L., de Matuonto, M., Monti, A., and Vignati, A., "Optimizing Current Control Performance in Double Winding Asynchronous Motors in Large Power Inverter Drives," IEEE Transactions on Power Electronics, vol. 16, No. 5, pp 676-685, September 2001.

[1.14] Williamson, S. and Smith, A. C., "Pulsating Torque and Losses in Multiphase Induction Machines," IEEE Transactions on Industry Applications, vol. 39, No. 4, pp. 986–993, July/August 2003.

[1.15] X. Xu and D. W. Novotny, "Selection of the flux reference for induction machine drives in the field weakening region," IEEE Transactions on Industry Applications, vol. 28, pp. 1353–1358, Nov./Dec. 1992.

[2.1] L. Parsa and H. A. Toliyat, "Fault-tolerant five-phase permanent magnet motor drives," Proceedings of IEEE Ind. Applications Soc. Annual Meeting IAS, Seatle, USA, 2004, pp. 1048 – 1054.

[2.2] David C. White and Herbert H. Woodson, "Electromechanical Energy Conversion," John Wiley & Sons, Inc. 1959.

[2.3] D. Casadei, F. Milanesi, G. Serra, A. Tani and L. Zarri, "Space Vector Modulation Based on a Multidimensional Approach for Multiphase Inverters with an Odd Number of Phases," Conference Record of IEEE Power Electronics Specialists Conference, June, 15-19 2008, Rhodes, Greece.

[2.4] Gan Dong,"Sensorless and Efficiency Optimized Induction Machine Control with Associated PWM Modulation Schemes," PhD Dissertation, Tennessee Tech University, December 2005.

[3.1] Luis Alberto Pereira, Cesar Cataldo Scharlau, Luis Fernando Alves Pereira and Jose Felipe Haffner, "General Model of a Five-Phase Induction machine Allowing for Harmonics in the Air Gap Field," IEEE Transactions on Energy Conversion, vol. 21, No. 4, pp. 891-899, December, 2006.

[3.2] Hamid A. Toliyat, "Analysis and Simulation of Five-Phase Variable-Speed Induction Motor Drives Under Asymmetrical connections," IEEE Transactions on Industrial Electronics, vol. 13, No. 4, pp.748-756, July, 1998.

[3.3] H. A. Toliyat, L. Y. Xue and T. A. Lipo, "A five-phase reluctance motor with high specific torque," IEEE Transactions on Industrial applications, vol. 28, pp. 659-667, May/June 1992.

[3.4] H. Xu, H. A. Toliyat, and L. J. Petersen, "Five-phase induction motor drives with DSP-based control system," IEEE Transactions on Power Electronics, vol. 17, No. 4, pp. 524-533, July 2002.

[3.5] Zhiqiao Wu, "An investigation of dual stator winding induction machines," PhD Dissertation, Tennessee Tech University, 2006.

[3.6] Z. Wu, O. Ojo, "Coupled-circuit-model simulation and air-gap calculation of a dual-stator-winding induction machine," IEE Pro.-Electr. Power Appl. Vol. 153, No. 3, pp. 387-400, May 2006.

[3.7] Leila Parsa, Hamid A. Toliyat, "Five-Phase Interior Permanent-Magnet motors with Low Torque Pulsation," IEEE Transactions on Industrial Applications, vol. 43, No.1, pp. 40-46, January/February 2007.

[3.8] M. G. Say, "The Performance and design of Alternating Current Machines Transformers, Three-phase induction motors and Synchronous machines," CBS Publishers and Distributors, Third Edition.

[3.9] Alexander S. Langsdorf, "The Theory of Alternating-current Machinery," McGraw-Hill Boo Company, Inc., New York and London, 1937.

[4.1] Olorunfemi Ojo, "The generalized Discontinuous PWM Scheme for Three-Phase Voltage source Inverters," IEEE Transactions on Industrial Electronics, vol. 51, No. 6, pp. 1280-1289, December, 2004.

[4.2] Olorunfemi Ojo, "ECE 7620 Adjustable Speed Drives," Lecture notes, Fall 2006.

[5.1] Luis Alberto Pereira, Cesar Cataldo Scharlau, Luis Fernando Alves Pereira and Jose Felipe Haffner, "Genaral Model of a Five-Phase Induction machine Allowing for Harmonics in the Air Gap Field," IEEE Transactions on Energy Conversion, Vol. 21, No. 4, pp. 891-899, December, 2006.

[5.2] Emil Levi, "Multiphase Electric Machines for Variable-Speed Applications," IEEE Transactions on Industrial Electronics, Vol. 55, No. 5, pp. 1893-1907, May 2008.

[5.3] A. Consoli and T. A. Lipo, "Orthogonal Axis Models for Asymmetrically Connected Induction Machines," IEEE Transactions on Power apparatus and Systems, Vol. PAS-101, No. 12, December 1982.

[5.4] Gojko M. Joksimović and Jim Penman, "The Detection of Inter-Turn Short Circuits in the stator Windings of Operating Motors," IEEE Transactions on Industrial Electronics, Vol. 47, No. 5, pp. 1078-1084, October 2000.

[5.5] Xiaoping Tu, Louis-A. Dessaint, Mohammed El Kahel and Alpha O. Barr, "A New Model of synchronous machine Internal Faults Based on Winding Distribution," IEEE Transactions on Industrial Electronics, Vol. 53, No. 6, pp. 1818-1828, December 2006.

[5.6] Hyung-Min Ryu, Ji-Woong Kim and Seung-Ki Sul, "Synchronous-Frame Current Control of Multi-phase Synchronous Motor under Asymmetric Fault Condition Due to Open Phases," IEEE Transactions on Industrial Applications, Vol. 42, No. 4 pp. 1062-1070, July/August 2006.

[5.7] Leon Chua, Charles A. Desoer and Ernest S. Kuh, "Linear and Nonlinear Circuits," McGraw-Hill Book Company, 1987.

[5.8] Obasohan I. Omozusi, "Dynamics and Control of a Battery Inverter Single-Phase Induction Generator System," MS Thesis, Tennessee Tech University, 1998.

[6.1] Fernando Briz, Alberto Diez, Michael W. Degner, and Robert D. Lorenz, "Current and Flux Regulation in Field-Weakening Operation," IEEE Transactions on Industry Applications, vol. 37 No. 1, January/February 2001.

[6.2] Tae-Suk Kwon, and Seung–Ki Sul, "Novel Antiwindup of a Current regulator of a Surface-Mounted Permanent-Magnet Motor for Flux-Weakening Control," IEEE Transactions on Industry Applications, vol. 37 No. 1, September/October 2006.

[6.3] Olorunfemi Ojo, Madhani Vipin and Ishwar Bhat, "Steady-State Performance Evaluation of Saturated Field Oriented Induction Motors," IEEE Transactions on Industry Applications, vol. 30 No. 6, November/December 1994.

[6.4] Lecture Notes, ECE 6380 Nonlinear Auto Control, Tennessee Tech University, Spring 2006.

[7.1] Paul C. Krause, Oleg Wasynczuk and Scott D. Sudhoff, "Analysis of Electric Machinery and Drive Systems," IEEE Press, Piscataway, NJ, Second Edition, 2002.

[7.2] D. W. Novotny and T. A. Lipo, "Vector Control and Dynamics of AC Drives," Clarendon Press Oxford, 1996.

[7.3] Sang-Hoon Kim and Seung-Ki Sul, "Maximum Torque Control of an Induction Machine in the Field Weakening Region," IEEE Transactions on Industrial Applications, Vol. 31, No. 4, pp. 787 – 794, July/August 1995.

[7.4] Michele Monona, Luca Zarri, Angelo Tani, Giovanni Serra and Domenico Casadei, "Stator flux Vector control of Induction Motor Drive in the Field Weakening Region" , IEEE Transactions on Power Electronics, Vol. 23, No. 2, pp. 941 – 949, March 2008.

[7.5] Horst Grotstollen and Josef Wiesing, “Torque Capability and Control of a Saturated Induction motor Over a wide range of Flux Weakening,” IEEE Transactions on Industrial Electronics, Vol. 42, No. 4, pp. 374 – 381, August 1995.

VITA

Sosthenes Francis Karugaba was born in Muleba District, Kagera Region, Tanzania. He received his BSc. Electrical Engineering from the University of Dar es Salaam, Tanzania, in 1999. In Fall 2006, he joined Tennessee Technological University and is a candidate for Master of Science Degree in Electrical Engineering.

PUBLICATIONS

Conferences

1. Sosthenes Karugaba, Olorunfemi Ojo and Michael Omoigui ," Switching Function Based Modeling of Flying Capacitor DC-DC Converters," Conference Record of IEEE Power Electronics Specialists Conference, June, 15-19 2008, Rhodes, Greece.
2. Sosthenes Karugaba, Ge Wang, Olorunfemi Ojo, and Michael Omoigui, "Dynamic and Steady-State Operation of a Five Phase Induction Machine with an Open Stator Phase," accepted for presentation at the NORTH AMERICAN POWER SYMPOSIUM 2008 Conference, September 28 - 30, 2008, Calgary, Canada.
3. Michael Omoigui, Olorunfemi Ojo and Sosthenes Karugaba," Analysis of Multi-Terminal Unified Power Flow Controller for Power Transfer," accepted for presentation at the NORTH AMERICAN POWER SYMPOSIUM 2008 Conference, September 28 - 30, 2008, Calgary, Canada.